(NASA-CR-124473) INSULATION COMMONALITY ASSESSMENT (PHASE 1). VOLUME 2: SECTION 7.0 THROUGH 16.0 (North American Rockwell Corp.) ~~584~~ 586 p HC $31.25 CSCL 22B

N74-10798

Unclas
G3/31 21646

SD72-SA-0157-2

INSULATION COMMONALITY ASSESSMENT

(PHASE I)

VOLUME II - SECTION 7.0 THROUGH 16.0

1 FEBRUARY 1973

Contract NAS7-200

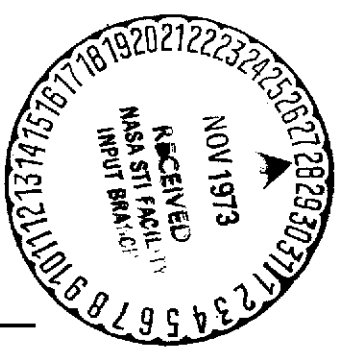

C. J. Schroeder
Task Manager
Launch Vehicles Engineering

Space Division
North American Rockwell

SD72-SA-0157-2

INSULATION COMMONALITY ASSESSMENT

(PHASE I)

VOLUME II - SECTION 7.0 THROUGH 16.0

1 FEBRUARY 1973

Contract NAS7-200

C. J. Schroeder
Task Manager
Launch Vehicles Engineering

Space Division
North American Rockwell

FOREWORD

This report documents the work performance by North American Rockwell Corporation through its Space Division in fulfillment of a Task Authorization entitled "Insulation Commonality Assessment," sponsored by the National Aeronautics and Space Administration's George C. Marshall Space Flight Center, Huntsville, Alabama. The work performed under Contract NAS7-200 in accordance with Task Authorization 2026-TA-48 by members of the Structural Systems, Flight Dynamics, and Manufacturing organizations of the Space Systems and Applications Division. Contributions to the efforts also were made by the Division's Safety, Quality Assurance, Reliability, and Laboratories and Test Organizations.

The period of performance extended from April 24, 1972, through February 1,1973. The NASA Technical Monitor was Dr.J.M. Stuckey, S&E-ASTN-MNM.

The report is printed in two volumes. Volume I contains Sections 1.0 through 6.0 and Volume II contains Sections 7.0 through 16.0 and the appendix.

PRECEDING PAGE BLANK NOT FILMED

CONTENTS

PRECEDING PAGE BLANK NOT FILMED

ILLUSTRATIONS

TABLES

7.0 THERMAL PERFORMANCE ANALYSIS

This section provides the designer of insulation systems and components with a ready reference to the basic principles of heat transfer, methods of heat transfer analysis, and practical application of these principles and methods in the design of insulation systems and components. The practical applications presented in Subsection 7.3 are discussions of pertinent analyses used to determine the thermal performance characteristics of the insulation systems considered in Section 6.0. Special thermal calculations are presented in Subsection 7.4 These are intended to be of a general type that would be of special interest and would be nearly directly applicable for new designs.

The basic principles of heat transfer are presented in this section in order to make this document more complete and to provide an easy reference for the formulas and relationships involved. This material, expecially that covered in Subsection 7.1, is intended to provide the reader who may not have recently utilized knowledge of heat transfer, with a brief "refresher" on the subject as it applies to insulation.

7.1 BASIC HEAT TRANSFER PRINCIPLES

Whenever a temperature gradient exists within a system, or when two systems at different temperatures are brought into contact, energy is transferred. The process by which this energy transfer takes place is known as heat transfer. Heat energy in transit cannot be measured or observed but the effects it produces can be observed and measured. Consider an insulation cryogenic storage tank containing liquid hydrogen. It is postulated that heat energy flows from the relatively hot external environment through the insulation into the stored LH_2, where some of the LH_2 is converted to vapor. The observed and measurable effects resulting from the heat transfer are the temperature distribution through the insulation and the rate of vapor generation from the bulk liquid. Determination of the quantity of heat transferred into the LH_2 or of the rate of heat transfer through the insulation requires application of basic principles and laws formulated by observation, experimentation, and analysis.

7.1.1 Relation of Heat Transfer to Thermodynamics

From an engineering viewpoint, the determination of the rate of heat transfer at a specified temperature difference is the key problem. A detailed analysis is needed to estimate the size, the feasibility, and the cost of equipment necessary to transfer a specified amount of heat in a given amount of time. For example, the successful operation of combustion chamber walls in rocket engines during engine firing depends upon the ability to remove heat continuously at a rapid rate from a surface. The problem is predict thermal performance characteristics and define the assumptions and idealizations.

7.1.2 Modes of Heat Transfer

Heat transfer occurs classically by one or more of the following modes: conduction, convection, and radiation. Definitions of each of these modes, excerpted from "Principles of Heat Transfer" by F. Kreith, are presented in the following paragraphs. (This book is published by International Textbook Company and is recommended for those requiring more detailed information.)

7.1.2.1 Conduction

Conduction is a process by which heat flows from a region of higher temperature to a region of lower temperature within a medium (solid, liquid, or gaseous) or between different mediums in direct physical contact. In conduction heat flow, the energy is transmitted by direct molecular communication without appreciable displacement of the molecules. According to the kinetic theory, the temperature of an element of matter is proportional to the mean kinetic energy of its constituent molecules. The energy possessed by an element of matter by virtue of the velocity and relative position of the molecules is called internal energy. Thus, the more rapidly the molecules are moving, the greater will be the temperature as well as the internal energy of an element of matter. When molecules in one region acquire a mean kinetic energy greater than that of molecules in an adjacent region, as manifested by a difference in temperature, the molecules possessing the greater energy will transmit part of their energy to the molecules in the lower-temperature region. The transfer of energy could take place by elastic impact (e.g., in fluids) or by diffusion of faster-moving electrons from the higher to the lower-temperature regions (e.g., in metals). Irrespective of the exact mechanism, which is by no means fully understood, the observable effect of heat conduction is an equalization of temperature. However, if differences in temperature are maintained by addition and removal of heat at different points, a continuous flow of heat from the hotter to the cooler region will be established.

Conduction is the only mechanism by which heat can flow in opaque solids. Conduction is also important in fluids, but in nonsolid mediums it is usually combined with convection, and in some cases with radiation also.

7.1.2.2 Radiation

Radiation is a process by which heat flows from a high-temperature body to a body at a lower temperature when the bodies are separated in space, even when a vacuum exists between them. The term "radiation" is generally applied to all kinds of electro-magnetic-wave phenomena, but in heat transfer only those phenomena which are the result of temperature and can transport energy through a transparent medium or through space are of interest. The energy transmitted in this manner is termed radiant heat.

All bodies emit radiant heat continuously. The intensity of the emissions depends on the temperature and the nature of the surface. Radiant energy travels at the speed of light (186,000 mps) and resembles phenomenologically the radiation of light. In fact, according to the electromagnetic theory, light and thermal radiation differ only in their respective wave-lengths.

Radiant heat is emitted by a body in the form of finite batches, or quanta, of energy. The motion of radiant heat in space is similar to the propagation of light and can be described by the wave theory. When radiation waves encounter some other object, their energy is absorbed near its surface. Heat transfer by radiation becomes increasingly important as the temperature of an object increases and follows the absolute temperature to the fourth power relationship. In engineering problems involving temperatures approximating those of the atmosphere, radiant heating may often be neglected.

7.1.2.3 Convection

Convection is a process of energy transport by the combined action of heat conduction, energy storage, and mixing motion. Convection is most important as the mechanism of energy transfer between a solid surface and a liquid or a gas.

The transfer of energy by convection from a surface whose temperature is above that of a surrounding fluid takes place in several steps. First, heat will flow by conduction from the surface to adjacent particles of fluid. The energy thus transferred will serve to increase the temperature and the internal energy of these fluid particles. Then the fluid particles will move to a region of lower temperature in the fluid where they will mix with, and transfer a part of their energy to, other fluid particles. The flow in this case is of fluid as well as energy. The energy is actually stored in the fluid particles and is carried as a result of their mass motion. This mechanism does not depend for its operation merely on a temperature difference and therefore does not strictly conform to the definition of heat transfer. The net effect, however, is a transport of energy, and since it occurs in the direction of a temperature gradient, is also classified as a mode of heat transfer and is referred to as heat flow by convection.

Convection heat transfer is classified according to the mode of motivating flow into free convection and forced convection. When the mixing motion takes place merely as a result of density differences caused by temperature gradients, we speak of natural, or free, convection. When the mixing motion is induced by some external agency, such as a pump or a blower, the process is called forced convection.

The effectiveness of heat transfer by convection depends largely upon the mixing motion of the fluid. Consequently a study of convective heat transfer is predicated on a knowledge of the characteristics of the fluid flow.

7.1.3 Basic Laws of Heat Transfer

To analyze heat transfer problems, the physical laws and relations which govern the various mechanisms of heat flow must be investigated. This subsection presents the basic equations governing each of the three heat transfer modes.

7.1.3.1 Conduction

The defining relation for heat transfer by conduction was proposed by the French scientist, J. Fourier, in 1822. It states that q_k, the rate of heat flow by conduction is a material, is equal to the product of the following three quantities:

K, the thermal conductivity of the material

A, the area of the section through which heat flows by conduction, to be measured perpendicularly to the direction of heat flow.

dT/dX, the temperature gradient at the section

To write the heat conduction equation in mathematical form, a sign convention must be adopted. The direction of increasing X is specified to be the direction of positive heat flow. Then, since according to the second law of thermodynamics heat will automatically flow from points of higher temperature to points of lower temperature, heat flow will be positive when the temperature gradient is negative (Figure 7.1.3.1-1). Accordingly, the elementary equation for one-dimensional conduction in steady state is written

$$q_k = -KA \frac{dT}{dX}$$

For the simple case of steady-state heat flow through a plane wall, the temperature gradient and the heat flow do not vary with time and the cross-sectional area along the heat-flow path is uniform. The variable in the equation can be separated and the resulting equation is

$$\frac{q_k}{A} \int_0^L dX = - \int_{T_{HOT}}^{T_{COLD}} K dt$$

The limits of integration are shown in Figure 7.1.3.1-2, where the temperature at the left-hand face (X = 0) is uniform at T_{HOT} and the temperature at the right-hand face (X = L) is uniform at T_{COLD}.

If K is independent of T, the following expression for the rate of heat conduction through the wall is obtained upon integration:

$$q_K = \frac{AK}{L} (T_{HOT} - T_{COLD}) = \frac{\Delta T}{L/AK}$$

In the equation ΔT, the temperature difference between the higher temperature T_{HOT} and the lower temperature T_{COLD}, is the driving potential which causes the flow of heat. The expression L/AK is equivalent to a thermal resistance which the wall offers to the flow of heat by conduction. The reciprocal of the thermal resistance is referred to as the thermal conductance. The concepts of resistance and conductance are helpful in the analysis of thermal systems where several heat transfer modes occur simultaneously. Most insulation systems transfer heat primarily by conduction.

7.1.3.2 Radiation

The quantity of energy leaving a surface as radiant heat depends on the absolute temperature and the nature of the surface. A perfect radiator or black body emits radiant energy from its surface as a rate q_r given by

$$q_r = \sigma A_1 T_1^4 \text{ Btu/hr}$$

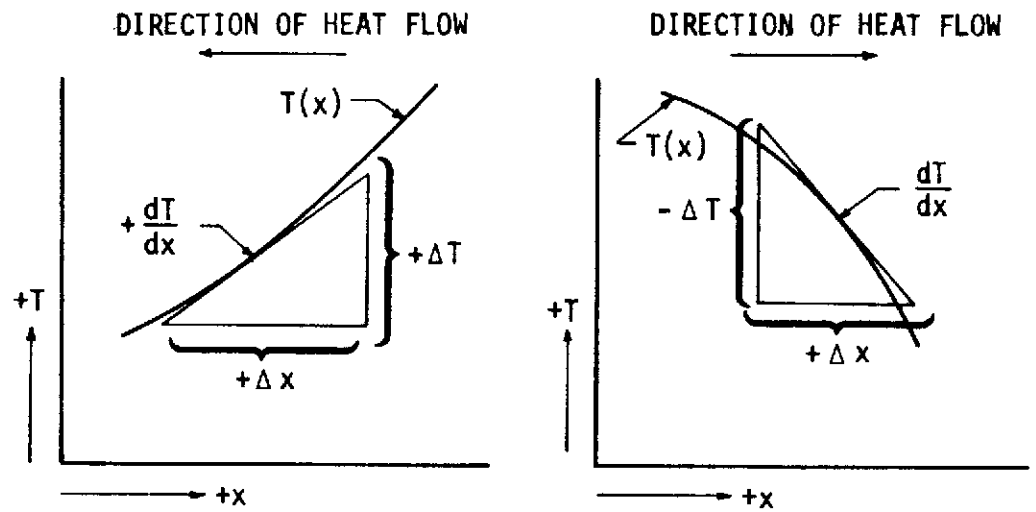

Figure 7.1.3.1-1. Sign Convention for Conduction Heat Flow

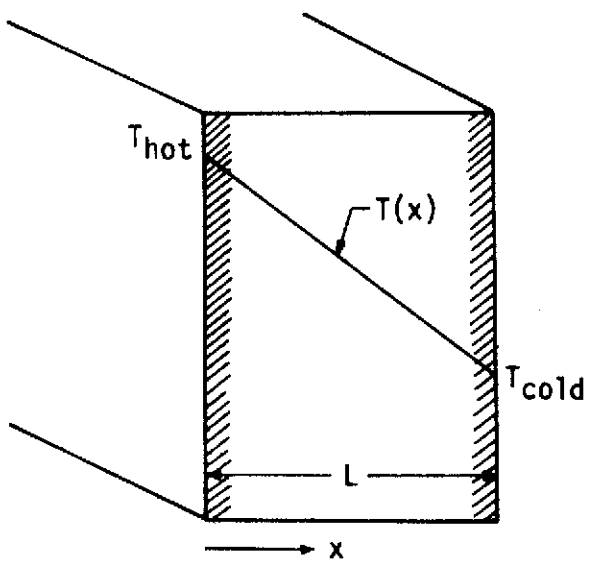

Figure 7.1.3.1-2. Temperature Distribution for Steady-Stage Conduction Through a Plane Wall

where A_1 is the surface area in sq ft., T_1 is the surface temperature in degrees Rankine (R), and σ (the Stefan-Boltzman constant) is a dimensional constant with a value of 0.1714×10^{-8} Btu/hr-sq ft-R^4.

Any black-body surface above a temperature of absolute zero radiates heat at a rate proportional to the fourth power of the absolute temperature. While the rate of emission is independent of the conditions of the surroundings, a net transfer of radiant heat requires a difference in the surface temperature of any two bodies between which the exchange is taking place. If the black body radiates to an enclosure which completely surrounds it and whose surface is also black (i.e., absorbs all the radiant energy incident upon it), the net rate of radiant heat transfer is given by

$$q_r = \sigma A_1 \ (T_1^4 - T_2^4)$$

where T_2 is the surface temperature of the enclosure in degrees Rankine.

Real bodies do not meet the specifications of an ideal radiator but emit radiation at a lower rate than black bodies. If they emit, at a temperature equal to that of a black body, a constant fraction of black-body emission at each wavelength, they are called gray bodies. The net rate of heat transfer from a gray body at a temperature T_1 to a black surrounding body of T_2 is

$$q_r = \sigma \ A_1 \epsilon_1 \ (T_1^4 - T_2^4)$$

where ϵ_1 is the emissivity of the gray surface and is equal to the ratio of emission from the gray surface to the emission from a perfect radiator at the same temperature.

If neither of two bodies is a perfect radiator and if the two bodies possess a given geometrical relationship to each other, the net heat transfer by radiation between them is given by

$$q_r = \sigma \ A_1 \ F_{1-2} \ (T_1^4 - T_2^4)$$

where F_{1-2} is a modulus which modifies the equation for perfect radiators to account for the emissivities and relative geometries of the actual bodies.

In many engineering problems, radiation is combined with other modes of heat transfer. The solution of such problems can often be simplified by using a thermal conductance K_r, or a thermal resistance R_r, for radiation. The definition of K_r is similar to that of K_k, the thermal conductance for conduction. If the heat transfer by radiation is written

$$q_r = K_r \ (T_1 - T_2^1)$$

the conductance is given by

$$K_r = \frac{\sigma \ A_1 \ F_{1-2} \ (T_1^4 - T_2^4)}{T_1 - T_2^1} \text{ Btu/hr-R}$$

and the unit thermal conductance for radiation $\bar{h}_r$ by

$$\bar{h}_r = \frac{K_r}{A_1} = \frac{\sigma F_{1-2} (T_1^4 - T_2^4)}{T_1 - T_2} \text{ Btu/hr-ft}^2\text{-R}$$

where T_2 is any convenient reference temperature whose choice is often dictated by the convection equation, which will be discussed next. Similarly, the thermal resistance for radiation is

$$R_r = \frac{T_1 - T_2}{\sigma A_1 F_{1-2} T_1^4 - T_2^4)} \text{ hr-ft}^2\text{-R/Btu}$$

7.1.3.3 Convection

The rate of heat transfer by convection between a surface and a fluid may be computed by the relation

$$q_c = \bar{h}_c A \Delta T$$

where

q_c = rate of heat transfer by convection, Btu/hr

A = heat transfer area, ft^2

ΔT = Difference between the surface temperature T_s and a temperature of the fluid T_∞ (usually far away from the surface), °F

$\bar{h}_c$ = Average unit thermal convective conductance, Btu/hr°F-ft^2

The relation expressed by the equation was originally proposed by Isaac Newton in 1701. Newton observed that the temperature of a hot iron bar decreased at a rate proportional to the temperature difference between the iron bar and the air blown past it. In 1701, however, the difference between "heat" and "temperature" was not understood. When the relation between heat and temperature was finally resolved, later investigators reformulated Newton's observation into its present equation form.

Engineers have used this equation for many years, even though it is a definition of $\bar{h}_c$ rather than a phenomenological law of convection. The evaluation of $\bar{h}_c$ is very difficult because convection is a complex phenomenon. The numerical value of $\bar{h}_c$ in a system depends on the geometry of the surface, the velocity and physical properties of the fluid, and often the temperature difference ΔT. Since these quantities are not necessarily constant over a surface, $\bar{h}_c$ may also vary from point to point. For this reason, it is necessary to distinguish between a local and an average convective heat transfer coefficient. The local coefficient is defined by

$$d_{q_c} = \bar{h}_c \, dA \, (T_s = T_\infty)$$

while the average coefficient $\bar{h}_c$ can be defined in terms of the local value by

$$\bar{h}_c = \frac{1}{A}\int_A h_c \, dA$$

For engineering applications, the average values are of most interest. The usual technique in heat-transfer analysis is to define a thermal conductance K_c for convective heat transfer as

$$K_c = \bar{h}_c A$$

and the thermal resistance to convective heat transfer R_c as

$$R_c = \frac{1}{\bar{h}_c A}$$

The analysis of the convection phenomenon is more difficult than for either conduction or radiation. The heat transfer and the fluid flow are interrelated. This necessitates the solution of two problems instead of one. First, the nature of the fluid flow must be established. When the flow is understood, then the manner in which the heat transfer occurs can be studied. Much experimental work has been done to evaluate convective heat-transfer phenomena.

The nature of the fluid flow can be described in accordance with several classification schemes. The most important classifications are those which separate laminar and turbulent flows and those which distinguish free and forced convection.

Table 7.1.3.3-1 summarizes the dimensionless groupings of fluid properties which are commonly used in fluid flow and heat transfer problems. The name, symbol, and significance of each of the different groupings are given. The use of these groupings to classify fluid flow phenomenon will be presented later. The terms used in the dimensionless groups in Table 7.3.3.3-1 are:

1. u = Fluid velocity $\simeq$ ft/sec.
2. x = Significant dimension, (e.g., distance from leading edge, body diameter, etc) $\simeq$ ft.
3. ρ = Fluid density $\simeq$ slugs/ft^3 = $\frac{\text{lbf - sec}^2}{\text{ft}^4}$
4. μ = Fluid viscosity $\simeq \frac{\text{lbf - sec}}{\text{ft}^2} = \frac{\text{slug}}{\text{sec-ft}}$ (where 1 slug - 32.174 lbm)
5. g = Acceleration due to gravity $\simeq$ ft/sec^2
6. $\beta = 1/v \left(\partial v/\partial T\right)_p \simeq \frac{1}{R^\circ}$ where v = volume $\simeq$ ft^3
7. h = Convective - heat-transfer coefficient $\simeq$ Btu/hr °R-ft^2
8. k = Conductive - heat-transfer coefficient $\simeq$ Btu/hr °R-ft

9. gc = Gravitational constant $\simeq {}^{\text{slug-ft}}/_{\text{lbf-sec}}$ = dimensionless

10. Cp = Specific heat at constant pressure $\simeq {}^{\text{Btu}}/_{\text{lbm-°R}}$

The dimensionless groups in Table 7.1.3.3-1 are used to present fluid flow and heat transfer data in a form which can be used by analysts and designers. For example, consider the heat transfer from a heated horizontal cylinder in free convection. When an experiment is run, the data available from the tes are the cylinder surface area, the cylinder surface temperature, the heat input into the cylinder, and the ambient air temperature. That is, q, A, Ts, TF, and x are obtained by measurement. The experimenter uses a table of Properties of Air and determines K, ρ, Cp, and μ. He then computes $h = q/A(Ts-Tf)$ and reports his results in terms of the derived dimensionless moduli:

$$\frac{hD}{K} = \text{Function of} \left| \frac{g\rho^2 B\Delta TD^3}{\mu^2}, \frac{\mu C_p}{K} \right|$$

The results of experiments by different investigators have been gathered over many years, and it has been possible to show these results on a common graph. Standard heat transfer reference books present Nusselt modulus versus the Grashof-Prandtl modulus product for the heat transfer from heated horizontal cylinders and other configurations of engineerin interest. These graphs and curve-fit equations are used to make heat transfer calculations.

Table 7.1.3.3-1. Summary of Heat Transfer Dimensionless Groups

SYMBOL	GROUP	NAME	SIGNIFICANCE
Re	$ux\rho/\mu$	REYNOLDS MODULUS	INSURES THAT FOR GEOMETRICALLY SIMILAR SYSTEMS THE RATIO OF VISCOUS TO INERTIA FORCES IS THE SAME IN THE TWO SYSTEMS AND THEREFORE THE FLOW PATTERNS WILL BE THE SAME
Gr	$g\rho_\infty^2 \beta\Delta Tx^3/\mu^2$	GRASHOF MODULUS	IN PURE FREE CONVECTION, THE NATURE OF THE FLOW IS DETERMINED BY THE GRASHOF MODULUS
N_u	hx/k	NUSSELT MODULUS	DESCRIBES THE RELATION BETWEEN THE HEAT TRANSFER AND THE TEMPERATURE GRADIENT IN THE FLUID AT THE SURFACE
Pr	$\mu C_p/k$	PRANDTL MODULUS	IF THE FLUID FLOWS ARE THE SAME IN TWO SYSTEMS, THE PRANDTL MODULUS MUST BE THE SAME IF THE TEMPERATURE FIELDS ARE TO BE THE SAME
x IS THE "SIGNIFICANT DIMENSION", SUCH AS HEIGHT, LENGTH, THICKNESS, ETC., AS APPLICABLE			

Free convection is defined as that convection which occurs when the fluid movement is brought about by density changes in the fluid which produce bouyancy forces.

The Grashof modulus (Gr) is the dimensionless ratio which characterizes free convection fluid flow and heat transfer. Physically, Gr represents the ratio of bouyant to viscous forces in the flow near a surface. At small values of Gr ($<10^8$), the viscous forces dominate and the fluid moves in a streamlined motion called laminar flow. At large values of Gr ($> 10^{10}$), the bouyant forces dominate and the fluid flow is disrupted by randomly moving whirls and eddies. This type of fluid motion is called turbulent flow. Between Gr = 10^8 and Gr = 10^{10}, a mixed or transition flow exists. For analysis purposes, a Grashof modulus of 10^9 is the accepted point of transition from laminar to turbulent flow.

Figure 7.1.3.3-1, which is reproduced from Reference 35, shows the correlation of experimental data for free-convection heat transfer from vertical plates. Predictive equations for the heat transfer conductance in both the laminar and turbulent flow regimes are shown for reference. The predictive equation has the form

$$\overline{Nu}_L = aG_{R_L}{}^{b} P_R{}^{c}$$

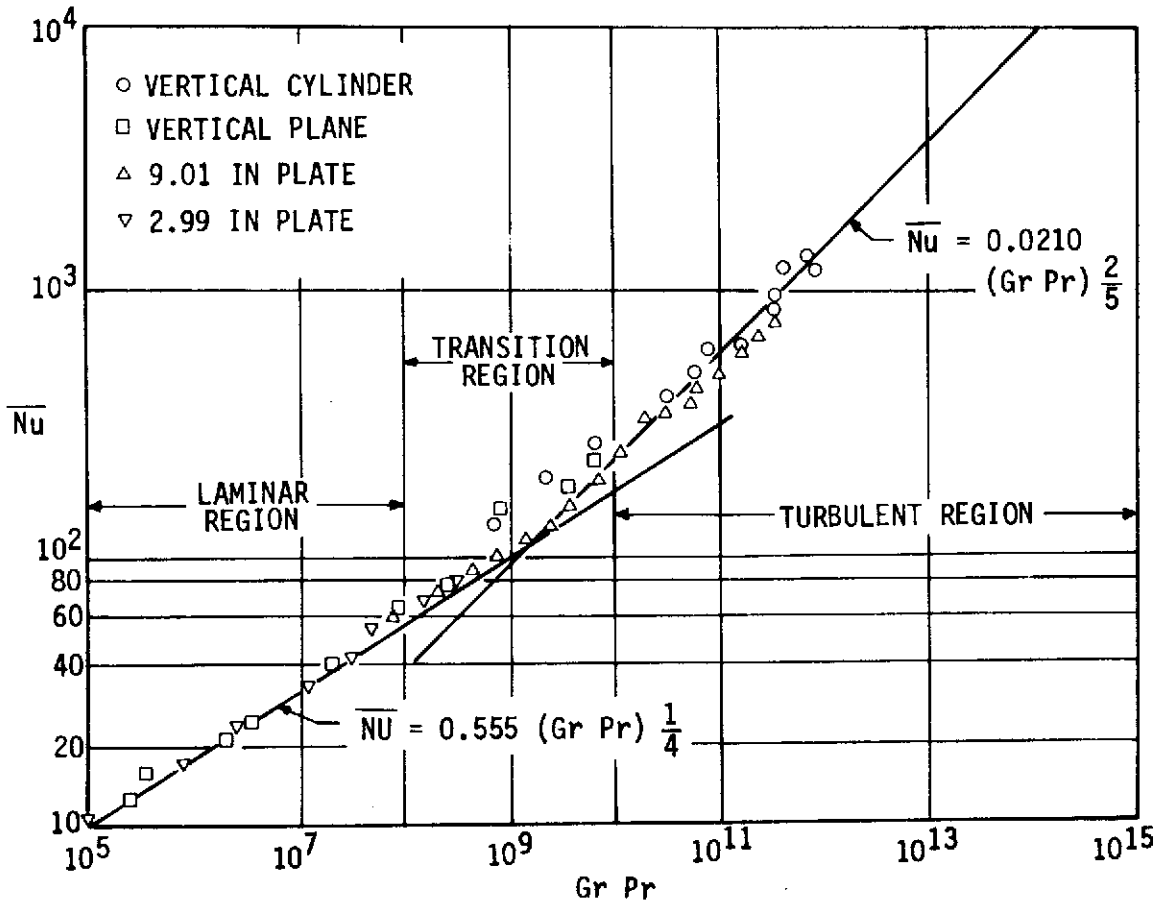

Figure 7.1.3.3-1. Correlation of Data for Free-Convection Heat Transfer From Vertical Plates and Cylinders

where a, b, and c are determined experimentally. For most free convection process, b = c; so that the Gr_L*P_R product becomes the abscissa of graphical presentations. For laminar flow, the exponent b is 1/4, while b is 1/3 or 2/5 for turbulent flow. Table 7.1.3.3-2 presents some predictive equations for free convection heat transfer from vertical plates and other simple geometries in both laminar and turbulent flow. The laminar flow equation is presented before the turbulent flow equation for each geometry.

When an order-of-magnitude estimate for the convective heat transfer conductance is needed, the following equation is useful:

$$Nu_L = 0.13\ (GR_L*P_R)^{1/3}$$

Table 7.1.3.3-2. Free Convection Corrections

FC	PAST A CYLINDER	
	$\overline{Nu}_D = .468\ (GR_d*P_R)^{1/4}$	$10^3 < GR_D < 10^7$
FC	PAST A SINGLE VERTICAL SURFACE	
	$\overline{NU}_L = .61\ (GR_L*P_R)^{14}$	$10^3 < GR_L < 10^7$
	$.726\ (GR*P_R)^{1/4}$	$10^8 < GR < 10^{10}$
FC	PAST A HORIZONTAL SURFACE (FACE UP)	
	$\overline{Nu}_L = .825\ (GR*PR)^{1/4}$	
	(FACE DOWN)	
	$\overline{Nu}_L = .413\ (GR_L*PR)^{1/4}$	$10^3 < GR < 10^7$
	(SPHERE)	
	$\overline{Nu}_D = .84\ (GR_D*PR)^{1/4}$	$10^3 < GR < 10^7$

Using the properties of air at atmospheric temperature and pressure, this equation reduces to

$$\overline{h}_c = 0.19\ (\Delta T)^{1/3}$$

Note that the length L actually cancels. A detailed analysis, however, requires use of the more accurate correlations. The General Thermal Analyzer Computer Program, discussed in the next subsection uses curve-fit data points rather than the correlations.

Forced convection is defined as that convection which occurs when the fluid movement relative to the surface is caused by a force other than bouyancy. Examples of forced convection flow are the flow through pipes and the flow over flat plates.

The Reynolds modulus (RE) is the dimensionless ratio which characterizes forced convection fluid flow and heat transfer. Physically, RE represents the ratio of inertia to viscous forces in the flow near the surface. At small values of RE, the fluid moves in a streamlined motion when the viscous forces dominate. As the RE increases above a critical value, the flow is distrupted by randomly moving whirls and eddies. The critical RE where the laminar-to-turbulent transition occurs is unique for each geometric configuration. The critical RE is 2000 for flow-through pipe while it is 5×10^5 for flow over a flat plate.

Table 7.1.3.3-3 presents correlations of experimental data for predicting average thermal conductances in forced convection for selected geometries. The predictive equations are presented in the form:

$$\overline{Nu_L} = a\ RE_L^{\ b}\ PR^c$$

where a, b and c are experimentally determined. Where available, the laminar flow equation is given before the turbulent flow equation. The equations presented predict $\overline{h}_c$ within $\pm$ 20 percent. The effect of this error on overall heat leak through an insulation system depends on the physical and geometrical properties of other system components.

7.2 COMPUTATIONAL TECHNIQUES

The heat transfer computer programs available at SD to support insulation design are described briefly in this subsection.

7.2.1 General Thermal Analyzer (XF0014)

This is a digital computer program which solves diffusive processes with emphasis on the transfer of heat and flow of fluids; but it is not restricted to these phenomena. The program solves transient or steady-state potentials for multidimensional physical systems using explicit finite difference approximation procedures. In addition, a variety of related variables, auxiliary functions, and parameters are available to aid in problem solution; their use is limited mainly by the ingenuity of the user.

Table 7.1.3.3-3. Forced Convection Correlations

OVER FLAT PLATE

$$\overline{Nu}_L = 0.664\ RE_L^{1/2} P_R^{1/3}$$

$$\overline{Nu}_L = 0.036\ RE_L^{0.8} P_R^{1/3}$$

INSIDE TUBE AND DUCTS

$$\overline{NU}_D = 1.86\ \left(RE_D P_R D/L\right)^{1/3} \left(\mu_b/\mu_s\right)^{0.14}$$

$$\overline{NU}_D = 0.023\ RE_D^{0.8} PR^{1/3}$$

CYLINDER IN CROSS FLOW

$$\overline{NU}_D = \left[0.35 + 0.56\ RE^{0.5}\right] P_R^{1/3}$$

SPHERE IN CROSS FLOW

$$\overline{NU}_D = 0.37\ RE_D^{0.6}$$

Because the General Thermal Analyzer is a dynamic program, it has undergone an impressive history of growth and change. The program was originally intended to be used in thermal analysis, but its capabilities have been expanded so greatly by continually increasing user requirements that it may not be used to solve a wide variety of problems.

The program solves diffusive processes and is currently being used in many projects (for example, Apollo and Saturn programs). Heat, electricity, mass diffusive processes; therefore, with the auxiliary variables and subroutine addition capability, the potential areas of General Thermal Analyzer application are many.

7.2.1.1 General Energy Balance

The General Thermal Analyzer program considers an energy balance over a finite interval of time, where all parameters other than the variable being evaluated are held constant.

The basic energy balance characteristics of the program enable it to be used in the solution of widely varying types of phenomena. Thus, in a system:

Energy Supplied = Energy Stored + Energy Removed

This equation represents the first law of thermodynamics.

7.2.1.2 Energy Transfer

Energy may be transferred in the form of work, heat, electricity, bulk fluid flow, momentum, mass diffusion, etc. In terms of heat, the second law of thermodynamics declares that energy is transferred as heat only by virtue of a negative temperature gradient (that is, heat always flows in the direction of diminishing temperature). The phenomenon of transfer of heat by conduction may be represented by Fourier's Law. For the one-dimensional case,

$$q/A = -k \frac{\partial T}{\partial X}, \text{ where } k > 0$$

The negative sign is introduced in order that the positive direction of the flow of heat should coincide with the positive direction of X. Thus, the heat flux transported is proportional to the temperature gradient.

7.2.1.3 Diffusive Processes

The transfer of heat is analogous to other transport phenomena. In order for any transport process to occur, there must be: (1) a suitable carrier, and freedom to move, (2) a potential difference between two points of the system.

Thus, any phenomenon in which the flux transported is proportional to a potential gradient may be represented by a form similar to the above equation. Table 7.2.1-1 contains a selected list of the many analogous forms of this potential flow law and gives some of the diffusive processes that may be solved by the program. The units for the program are historically in terms of heat and fluid flow but the user may substitute the appropriate analogous units for the diffusive process in which he is interested.

7.2.1.4 Energy Storage

The quantity of the charge (entity being transported) required to raise the potential difference by one unit is termed the conductance (in mechanical systems), or capacitance (in thermal or electrical systems). If heat is the only mode of energy transfer, then the enthalpy change is proportional to the stored heat. Hence, from the general energy balance equation, the energy transfer and energy storage terms may be described as an equation in terms of heat.

$$\frac{\partial T}{\partial \theta} = \alpha\left(\frac{\partial^2 T}{\partial X^2} + \frac{\partial^2 T}{\partial Y^2} + \frac{\partial^2 T}{\partial Z^2}\right)$$

Table 7.2.1-1. Analogous Transport Phenomena

Flux Transported		Potential		Constant of Proportionality			
Name	Symbol	Name	Symbol	Name	Symbol	Equation	Name
Heat	$\frac{q}{A}$	Temperature	T	Thermal conductivity	k	$\frac{q}{A} = -k\frac{\partial T}{\partial X}$	Fourier's Law
Electricity	$\frac{I}{A}$	Voltage	E	Conductance	$\frac{1}{R}$	$\frac{I}{A} = -\left(\frac{1}{R}\right)\frac{\partial E}{\partial X}$	Ohm's Law
Mass (by diffusion)	J	Concentration	C_m	Diffusivity	D	$J = -D\frac{\partial C_m}{\partial X}$	Fick's First Law
Momentum	U	Velocity	V	Viscosity	μ	$U = -\mu\frac{\partial V}{\partial X}$	Newtonian Fluid Law
Fluid (bulk flow)	$\dot{W}$	Pressure	P	Flow conductance	K_f	$\dot{W} = -K_f\frac{\partial P}{\partial X}$	Modified Fanning Equation

where

$$\alpha = \frac{k}{\rho(C_p)} = \text{thermal diffusivity}$$

This equation, commonly known as the Fourier equation, represents a form of the diffusion equation in terms of heat parameters.

7.2.1.5 Approximation Methods

Analytical solutions to the Fourier equation for the nonlinear thermal systems usually encountered in practice become prohibitively complex. Practical solutions require the methods of numerical approximations.

The Fourier equation is approximated by breaking the system into nodes connected by a network of thermal elements. The physical properties are lumped together for each node and thermal element of the network. This lumped parameter method enables the user to synthesize a complex thermal network from the available repertoire of thermal elements: conductances, radiation conductances, capacitance, cathode followers or directional conductance, and heat fluxes to the nodes. Two types of nodes are used: interior and boundary nodes. The boundary nodes are differentiated by not assigning a capacitance to them. The temperature of the boundary nodes are inputs to the program. More thermal elements or special calculations can be generated by the user with the variables block and communication linkages provided by the program.

The lumped parameter method reduces the system to a set of simultaneous differential equations and algebraic equations (for interior nodes of zero capacitance). Considering a given node (i), we obtain the differential equation:

$$C_i \frac{dT_i}{\partial\theta} = \sum_{j=1}^{P} K_{ji} (T_j - T_i) + \sum_{j=1}^{P} R_{ji} (T_j^4 - T_i^4) + \sum_k Q_k$$

Notice that if the nodal capacity is zero, this equation becomes an algebraic equation which can be solved by an iteration technique. If the derivative $\left(\frac{dT_i}{d\theta}\right)$ is approximated by the difference $\left(\frac{\Delta T_i}{\Delta\theta}\right)$, the above differential equation can be reduced to a difference equation. Notice that such an approximation is made for the finite and alternating direction options provided by the program.

7.2.2 Two-Dimensional Transient Heat Conduction Program (XF0012)

This program, which is written in FORTRAN IV for use on the IBM S/360, was developed to compute the temperature histories of complex body geometries in two dimensions. The program includes both charring and subliming ablation, and phase change options. The input to the program defines the geometry of the physical system, material properties, and boundary conditions. Output is in the form of temperature histories at discrete points. The Crank-Nicolson finite difference technique is used to integrate the heat equation and the Gauss-Seidel iteration process with relaxation is used to solve the implicit system of linear equations.

7.2.3 Space Vehicle Thermal Environment (XF0001)

This program computes the thermal flux of direct sunlight, planet-reflected sunlight, and planet radiation incident on a set of surface elements of a space vehicle whose position and attitude are given functions of time. This program was developed to compute the thermal environment encountered by multi-surfaced vehicles in orbit about any of the nine planets, moon, or sun. The physical model of orbital motion employed by the program is an isolated dynamic system consisting of the planet, a satellite, and the sun. It is assumed the planet has a uniform spherical shape, has no atmosphere, and is a diffuse reflector of the solar spectrum. Orbital data required as input to the program include orbital altitude, angle between orbit plane and sun (β), position at which the satellite crosses the equator traveling from south to north, and in the case of elliptical orbits, the semi-major and semi-minor axes. The program uses these orbital parameters to describe the position of the space vehicle relative to the planet and sun for a complete orbit including planetary shadow effects. As output, this program will provide a complete orbital history of the radiant energy incident upon each satellite surface due to direct solar radiation, planetary reflected solar radiation, and earth emission radiation. If desired, the program will also determine the transient temperature history of the satellite surfaces for the complete orbit.

7.2.4 CONFAC I AND II

These programs compute the radiant-interchange geometric configuration and form factors which are used in radiative heat transfer and illumination analyses. CONFAC I was originally developed to provide a rapid and accurate means of computing configuration factors. The source of radiant flux may be any general plane polygon, and the receiver may be any general plane or nonplanar polygon. CONFAC II was developed to extend the capability of CONFAC I to compute configuration factors between a general plane polygon and a sphere or other irregular shaped solid.

The configuration factor is defined as the fraction of radiant energy streaming from a diffusely emitting surface incident upon one surface. The radiant flux leaving the opaque differential surface, dA_1, will stream with uniform intensity I_1 into the hemispherical space above the surface. This is illustrated in Figure 7.2.4-1. In the space above dA_1, a second opaque differential surface dA_2 intercepts a faction of the energy seen through the solid angle dw_{12}. The fraction of radiant energy which leaves dA and is incident upon dA_2 can be expressed as:

$$F\,(d_1,\ d_2) = \frac{I,\ \mathrm{Cos}\ \theta_1\ \mathrm{Cos}\ \theta_2\ dA_1\ dW_{1-2}}{I_1,\ dA_1}$$

This definition of configuration factor, however, is applicable only when differential areas are involved. Actual engineering problems are concerned with surfaces having finite areas. This situation requires that the equation be integrated over the areas involved. The defining equation for the configuration factor between two finite areas can be expressed as:

$$A_1\ F_{(1,2)} = \int_{A_1} \int_{A_2} \frac{\mathrm{Cos}\ \theta_1\ \mathrm{Cos}\ \theta_2}{\pi R_{12}^2}\ d_{A_2} d_{A_1}$$

CONFAC II is a digital computer program which provides a rapid and accurate means for determination of configuration factors. The basic equation is integrated by a simple numerical procedure based upon the Nusselt sphere concept. The radiant source (surface 1) may be any general plane polygon; the receiver (surface 2) may be any arbitrarily oriented plane or solid figure, or combination of plane and solids. The detailed procedures for surface coordinate input data are given in SID65-1043-1. Eight classes of data entry are possible. Of these, only the data entry for Class 1 -- Plane Polygon will be discussed.

This program requires the following input data:

1. Coordinate data, Class 1 - Plane Polygons - x, y, z coordinates of the vertices of planar polygonal surfaces (up to 17 surfaces with 100 defining points may be given).

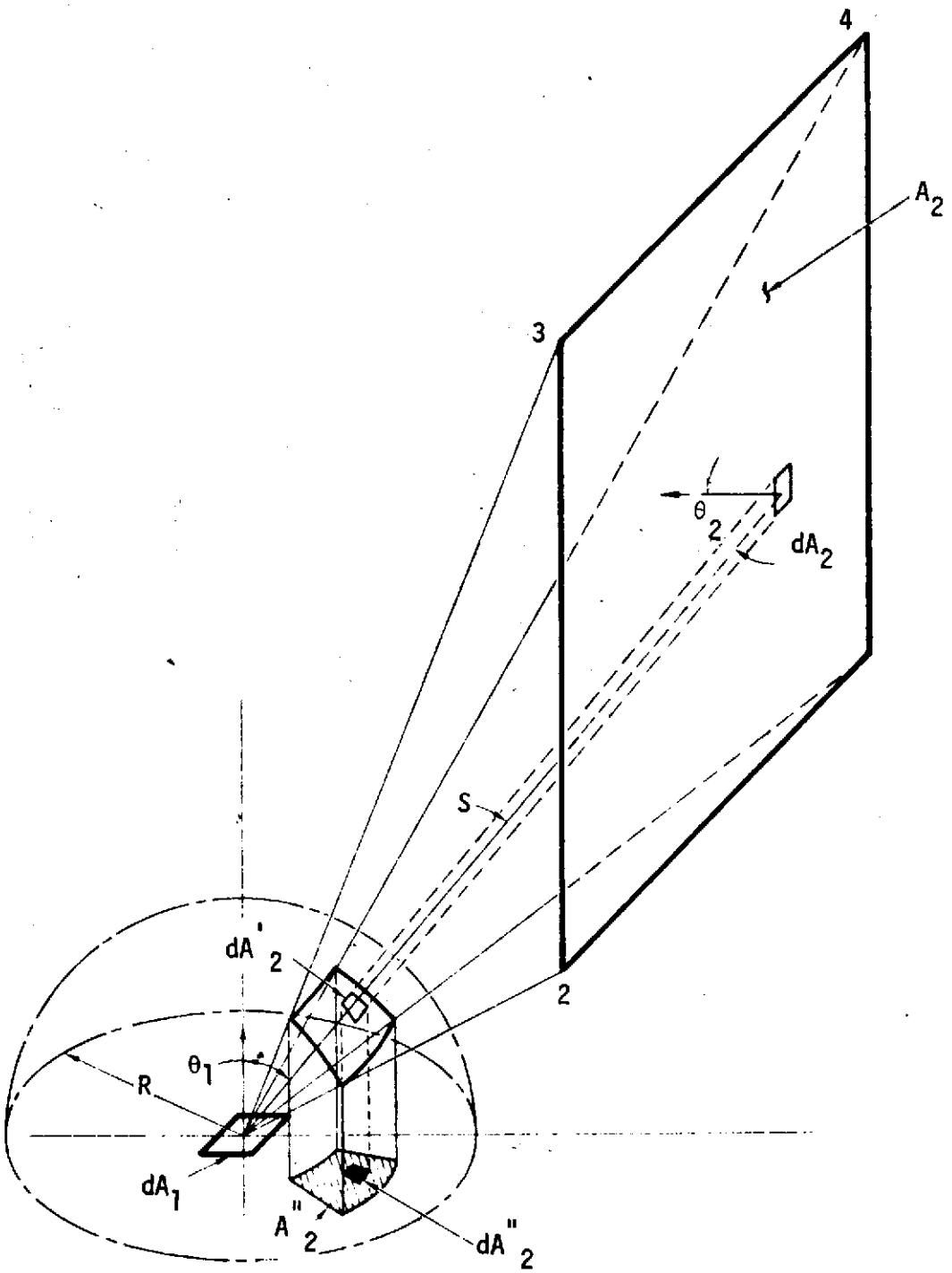

Figure 7.2.4-1. Nusselt Geometrical Relationships

2. Identification of emitting and receiving surfaces for which factors are desired. If the factors to all surfaces are desired, a GROUPRUN command may be substituted for the individual factor requests.

3. Data determining the number of horizontal and vertical increments into which a planar surface is to be subdivided. If no such data input is given, the program assumed 24 vertical and 24 horizontal divisions.

The basic output from this program consists of:

1. Configuration factor

2. Area over which the point configuration factors were computed.

3. The product $F(kj) - A_K$

4. The area A_k

5. The area A_j

The output of CONFAC II is a listing of the FA product for each surface-pair in a specified group of surfaces. When the participating surfaces are ideal radiators, the FA products can be used directly in a radiant heat transfer analysis. However, most engineering surfaces have emittances less than ideal. This requires that a more complex analysis be made to account for interreflections between surfaces. A measure of the net radiant transfer is the FA product.

Two approaches are commonly used in heat transfer analysis to determine FA values. One approach is to input the FA products and surface properties directly into a thermal network in the form of a radiosity network (SID63-1397). The other approach is to use intermediate program, such as Radiation Interchange Program, to determine FA from the surface properties and the FA products. The resulting FA products are than input directly into the thermal network.

CONFAC II was used extensively in the calculation of configuration factors between the J-2 engines and the rigid heat shield and flexible curtain. Details of this study are presented in Subsection 7.3.3.

7.2.5 Radiation Interchange Program (XF0016)

This program calculates the radiation interchange factors for a radiation network and prints out the FA products for the entire network. The program solution for the interchange is based on Hottel's method for diffuse radiation in gray enclosures, and utilizes as input data surface areas, geometric view factors, and emissivities, and determines by matrix solution the radiation interchange factors.

7.2.6 Real Surface Radiation Interchange Factor Program (XF0028)

This program computes thermal and solar F radiation interchange factors among surfaces having any combination of the following properties: (1) diffuse

emittance and reflectance, (2) diffuse emittance, specular reflectance; (3) diffuse emittance, components of diffuse or specular reflectance; and (4) directional emittance and bidirectional reflectance.

7.3 THERMAL ANALYSIS

7.3.1 Cryogenic Storage

The important thermal performance characteristics used in the design of an insulation system for a cryogenic storage tank on a launch vehicle are external surface temperature, heat transfer rate, and accumulated heat transfer for a typical mission. The maximum and minimum temperatures are needed to select materials and to evaluate structural capability. The heat transfer rate is needed to determine propellant boiloff and to select ground support equipment. The accumulated or mission heat transfer is needed to evaluate overall system and engine performance.

The thermal design characteristics presented here are calculated for a typical S-II flight which consists of a ground hold phase and launch phase. The natural environments for hot and cold day and nominal day ground hold conditions are defined in Section 4.1. The induced environments during launch are defined in Section 4.2. The application of these environmental criteria and of other analytical techniques in thermal performance calculations is presented in Section 7.0. A tabulation of thermal properties is presented in Section 12.0.

The temperature of liquid hydrogen at atmospheric pressure is -423 F. This is far below the temperature at which the nitrogen in the air will liquify (-323 F) against the cold side wall. During such liquification the rate of heat transfer to the hydrogen is so excessive that it would be nearly impossible to even fill the tank. For this reason the gas must be in retained, restrained, or excluded or, as discussed in the following section, the air may be replaced with helium during ground operations since the liquification point for helium is below the temperature of liquid hydrogen.

7.3.1.1 Helium Purged, Foam-Filled, Honeycomb

The insulation discussed in this section is also discussed and illustrated in Paragraph 6.1.1.1. The manner of presentation follows the normal thermal analysis. This is presented as a nearly complete section even though it may repeat some of the material previously presented.

a. Statement of Problem: Determine insulation surface temperature, heat rate to LH_2, and total accumulated heat to LH_2 for the 1.6-inch helium-purged LH_2 tank sidewall insulation during ground hold, S-IC boost, and S-II boost utilizing the following aerodynamic heating trajectories:

   1. Design trajectory $\alpha \neq 0$

   2. Design trajectory $\alpha \neq 0$

   3. Nominal trajectory $\alpha \neq 0$

Determine the LH_2 boiloff rates as a function of wind speed and the sidewall insulation K/X during a hot and cold day prelaunch environment at MILA.

Determine LH_2 tank structural and GH_2 temperatures during tank preconditioning, propellant loading, static firing, and S-II boost for hot day conditions. In addition, the LH_2 boiloff rate during tanking and hold is to be determined for hot and cold day conditions.

b. Methodology and Analysis: Discussed in this subsection are the LH_2 configuration, the sidewall insulation thermal model, the method of determining sidewall heat leak to LH_2, aerodynamic heating trajectories, ground hold boiloff analysis, and the LH_2 structural temperature.

1. Description of LH_2 Tank: The LH_2 tank of the S-II vehicle consists of a 33-foot diameter cylindrical section, a forward bulkhead, and a common bulkhead with the LOX tank. The tank is designed to hold approximately 150,000 pounds of usable liquid hydrogen propellant at engine ignition. The S-II Model Specification (SID61-361) requires that the LH_2 tank be insulated so that the LH_2 boiloff rate does not exceed 6 percent/hour. Therefore, an analytical prediction is needed to determine that this requirement is satisfied.

   The LH_2 tank insulation configuration is illustrated in Figure 7.3.1.1-1 with emphasis on the joints. For analysis purposes, the tank insulation system was divided into five major sections. The analysis reflects the latest vehicle design. The major sections are the J-joint, sidewall, common bulkhead, forward skirt, and the forward dome. These sections are defined as follows:

   (a) J-Joint: By definition, the J-joint (V7-313102) extends from Station 299.4 on the LH_2 tank sidewall to the intersection of the sidewall and the common bulkhead at Station 297, and to Station 317.6 on the common bulkhead.

   Two major design changes have occurred in the J-joint section. One is the removal of the CRES insulation internal to the LOX tank and the other is the extension of the common bulkhead phenolic honeycomb core to Station 296.2, replacing the glass cloth insulation. As a result of these two changes, the heat leak through the J-joint section into the LH_2 is increased.

   (b) Sidewall: Figure 7.3.1.1-2 illustrates the type of insulation which is employed on the sidewall of vehicles S-II-1 through -7. Basically, the insulation consisted of a helium-purged, polyurethane foam-filled phenolic honeycomb core. This insulation system extended from Station 324.5 to Station 816.6.

   (c) Common Bulkhead: The common bulkhead section is defined as that area of common bulkhead not included in the J-joint definition. Sandwiched between the fore and aft sheets of the common bulkhead is the helium-purged phenolic honeycomb core insulation.

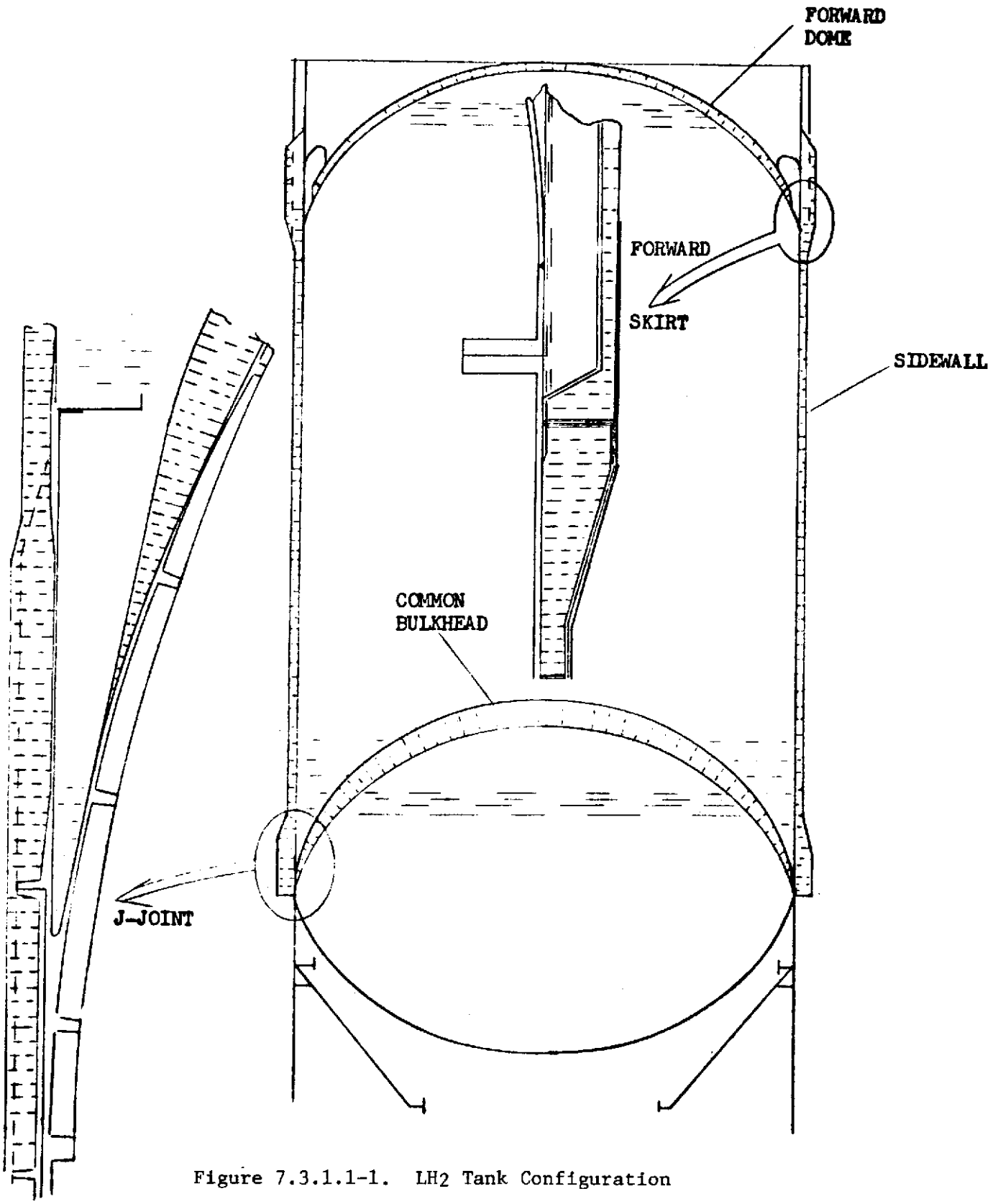

Figure 7.3.1.1-1. LH_2 Tank Configuration

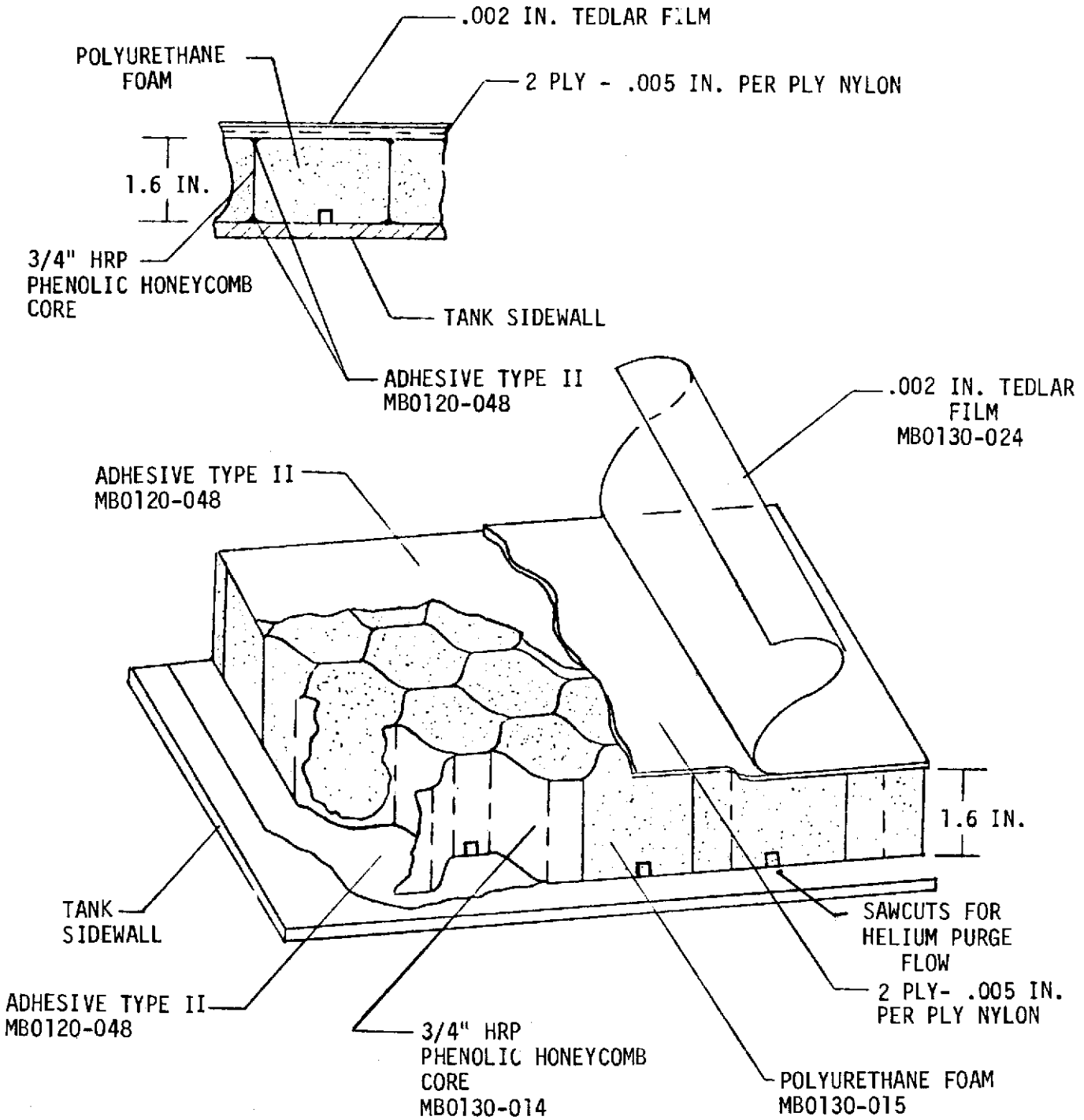

Figure 7.3.1.1-2. 1.6-Inch Thick Helium-Purged Insulation

(d) Forward Skirt: The forward skirt heat leak area extends from Station 819 on the LH_2 tank sidewall to the tangent point of the forward dome and the sidewall at Station 823. Reference V7-532196 presents the sidewall insulation design incorporated in this section.

(e) Forward Dome: The forward dome includes all of the forward bulkhead to the tangent point of the forward skirt and the sidewall at Station 823. The insulation on the forward dome consists of a helium-purged, polyurethane foam-filled phenolic honeycomb core. A portion of the forward dome, from Station 823 to 830, is not insulated.

(f) Others: In addition to the heat leak due to the major tank sections, heat (leak) enters the LH_2 tank from the LH_2 recirculation system, the J-2 engine pumps, and other miscellaneous sources. Also classified under miscellaneous heat leaks are the LH_2 fill and drain valve and the bolts which thread into the LH_2 tank.

(1) LH_2 Recirculation System: SID62-141 describes the LH_2 recirculation system design and operation. LH_2 is pumped through the vacuum jacketed LH_2 bypass lines and vacuum jacketed LH_2 feed lines to the LH_2 pumps on the J-2 engines. Then the LH_2 is manifolded and returned to the LH_2 tank via the vacuum jacketed return line. There are portions of this system, such as flanges, which are not insulated.

(2) J-2 Engines' LH_2 Pumps: The bottom portion of the J-2 engines' LH_2 pumps is not insulated. Therefore, a considerable heat leak is realized in this area. From tests conducted by Rocketdyne and DACo, the heat leak is estimated to be 10 Btu/second per engine.

(3) Miscellaneous: The system tunnel, LH_2 feed line fairings, LH_2 return line fairing, and LH_2 fill and drain valve fairing are attached to the vehicles by metal bolts which are threaded directly into the LH_2 tank. Likewise, the LH_2 fill and drain valve is attached directly to the LH_2 tank sidewall. As a result, a thermal short exists between the ambient and the LH_2, through which heat is flowing.

2. Description of Sidewall Insulation Thermal Model and Information Obtained: The insulation composite shown in Figure 7.3.1.1-2 was divided into ten sections representing the foam-filled honeycomb, one section representing the nylon phenolic cover and outer adhesive layer, and one section representing the aluminum tank wall. The thermal network representing the insulation composite (shown in Figure 7.3.1.1-3) was analyzed on a 7094 digital computer program to determine heat rates into the LH_2 and total heat into the LH_2

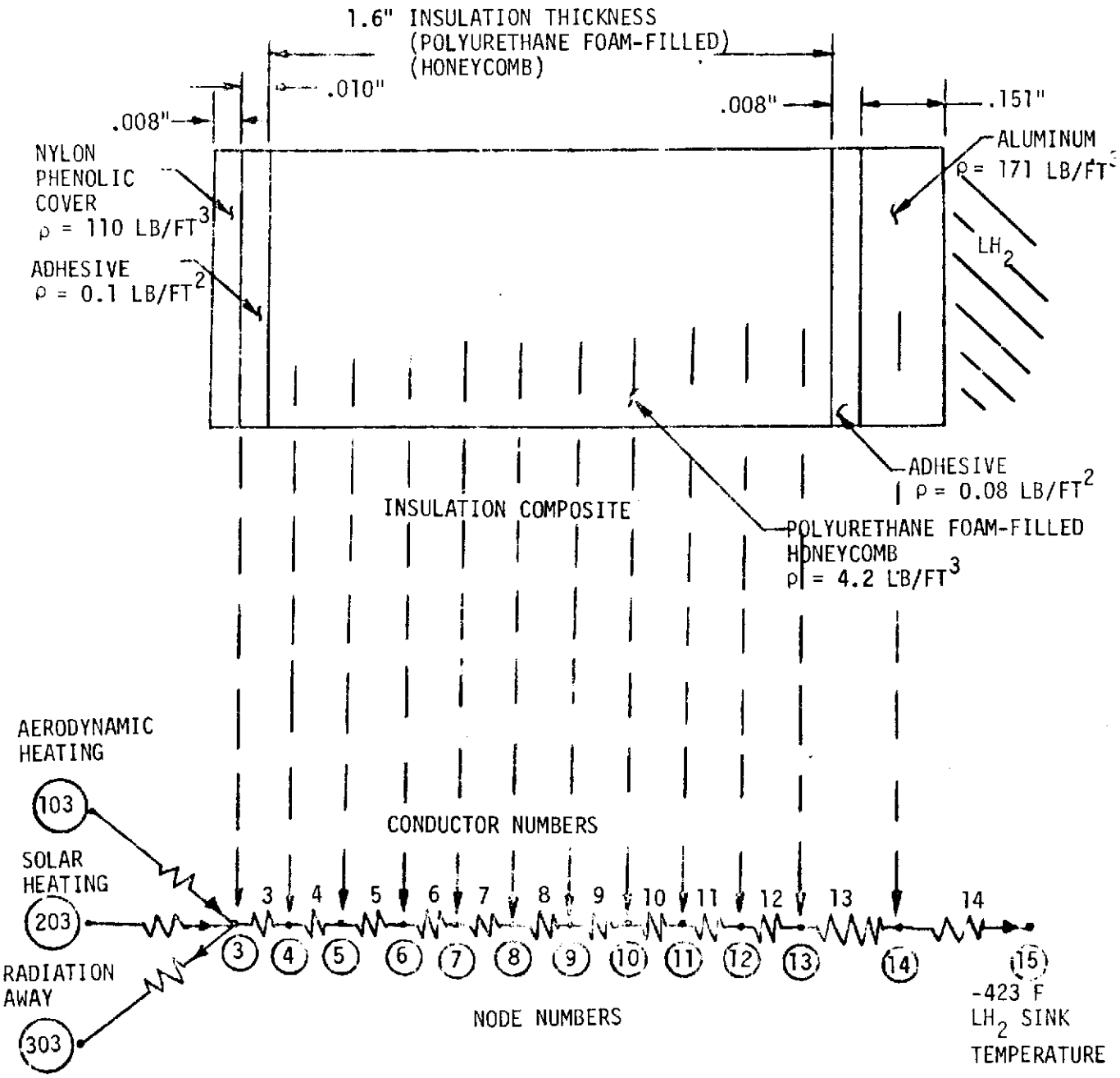

Figure 7.3.1.1-3. Electrical Analog Circuit

during ground hold and S-IC/S-II boost. Temperature profiles through the insulation also were computed. The capacitance of nodes 3 through 13 were varied with local node temperature by utilization of existing insulation material specific heat data versus temperature (Figure 6.1.1.3-1). The capacitance of node 14 was varied with temperature by utilization of aluminum specific heat information and theoretical Debye relationships at LH_2 temperatures. Node 15 was held at -423 F representing an infiniite LH_2 sink temperature.

Conductor number 14 represents the turbulent natural convection heat transfer coefficient between the LH_2 and the aluminum tank wall. Conductor 14 was computed from a turbulent natural convection heat transfer relationship. Conductors 3 through 13 were varied with temperature by means of curve 2 obtained from helium-purged insulation test data.

3. Method of Determining Sidewall Heat to LH_2: The total heat to the LH_2 through the LH_2 tank side wall was tabulated by summing the heat through conductor 14 for a square-foot section during 90 seconds of ground hold, 155 seconds of S-IC boost, and 394 seconds of S-II boost for a no-engine-out case, and 493 seconds of S-II boost for a one-engine-out case. The net heat to the LH_2 from the sidewall of the LH_2 tank was determined by multiplying the accumulated heat per square foot through conductor 14 during ground hold to 50 seconds into S-II boost by 4550 square feet of sidewall area (Station 297 to Station 823). After 50 seconds of S-II boost, the LH_2 liquid level will reach the cylindrical portion of the LH_2 tank and the sidewall area exposed to LH_2 is reduced. The total heat computed by integrating the product of the heat rate through conductor 14 times the effective wetted sidewall area versus time.

4. Description of Aerodynamic Heating Trajectories: The LH_2 tank sidewall insulation surface temperature versus time, heat rate to LH_2 versus time, and total accumulated heat to LH_2 versus time were determined for three aerodynamic heating trajectories.

   The first trajectory given in SID63-498, Section 3, is a design trajectory including angle of attack. This trajectory will produce the highest aeroheating rates (SID63-498, Section 7, page 9) of the three. The other two trajectories were studied to make certain that the first was the most severe.

   The aerodynamic heating trajectory was chosen as a most severe heating condition and the analysis is based directly on these trajectory values with no factor of safety. In general, there is a factor applied to the numbers obtained for stress using a loads trajectory. No attempt is made to determine simultaneous temperature and stress.

5. Ground Hold LH_2 Boiloff Parametric Analysis: The apparent thermal conductivity, K, of the sidewall insulation for either set of vehicles is not definitely known. Therefore, a parametric analysis of the heat leak into the LH_2 is conducted with the sidewall insulation K/X as one of the parameters.

A minimum of K of 0.2 $\frac{\text{Btu-in}}{\text{hr-ft}^2\text{-°F}}$ for an X of 0.8 inch is postulated. At the other extreme, a maximum K of 1.0 $\frac{\text{Btu-in}}{\text{hr-ft}^2\text{-°F}}$ might be obtained, or a K/X of 1.25 $\frac{\text{Btu}}{\text{hr-ft}^2\text{-°F}}$ for an X of 0.8 inch. Therefore for completeness sake, the analysis is conducted with K/X varying from 0.25 to 3.0 $\frac{\text{Btu}}{\text{hr-ft}^2\text{-°F}}$.

The LH_2 tank sidewall exposes the greatest cross-sectional area through which heat is transferred into the LH_2. The amount of heat transferred through the sidewall is directly influenced by the external heat transfer coefficient, which is a function of the wind speed. Hence, the wind velocity is another parameter in the analysis and is allowed to vary from 5 to 45 mph. For a given sidewall insulation K/X and a given wind speed, the amount of heat transferred to the LH_2 is influenced by the ambient temperature. Therefore, the analysis considers the effect of a hot and cold day environment.

6. LH_2 Tank Structural Temperatures: The maximum temperature gradients (dT/dX) and structural temperatures versus time is required for the LH_2 tank of all vehicles during preconditioning, propellant loading, and detanking so that maximum induced stresses may be determined. The maximum temperature gradients (dT/dX) in the LH_2 tank structure will occur on the vehicle with the smallest tank wall or sidewall insulation thickness under hot day conditions. Since the S-II-T vehicle had the thinnest insulation, it was analyzed for tank preconditioning, propellant loading, and static firing. The conditions considered with respective case number are summarized in Table 7.3.1.1-1.

Table 7.3.1.1-1 Structural dT/dX

Condition	S-II-T	Information Given
Preconditioning Hot Day	Case 1 (Figure 7.3.1.1-8)	Maximum structural dT/dX and GH_2 temperatures versus time.
Propellant Loading Hot Day	Case 2a (Figures 7.3.1.1-9 and -10)	Maximum structural dT/dX, GH_2 temperatures and maximum LH_2 boiloff versus time.
Propellant Loading Cold Day	Case 2b (Figure 7.3.1.1-11)	Minimum LH_2 boiloff versus time.
Static Firing Hot Day	Case 3 (Figures 7.3.1.1-11 and -12)	Maximum structural dT/dX and GH_2 temperatures versus time

c. Assumptions: The pertinent assumptions used in the analysis to determine the thermal performance characteristics of the 1.6-inch helium-purged, foam-filled honeycomb, and other S-II insulation systems are listed below.

1. Natural Environment:

   (a) Hot Day:

      (1) Ambient temperature is 99 F, (SID 614-473-1).

      (2) External heat transfer coefficient versus wind speed is determined from two and is presented in Figure 7.3.1.1-4.

   (b) Cold Day:

      (1) Ambient temperature is 28 F (SID 61-473-1).

      (2) External heat transfer coefficient versus wind speed is determined from twenty and is presented in Figure 7.3.1.1-4.

2. Induced Environment:

   (a) Aeroheating - Three trajectories, basic smooth-skin heating:

      (1) Design trajectory $\alpha \neq 0$

      (2) Design trajectory $\alpha = 0$

      (3) Nominal trajectory $\alpha = 0$

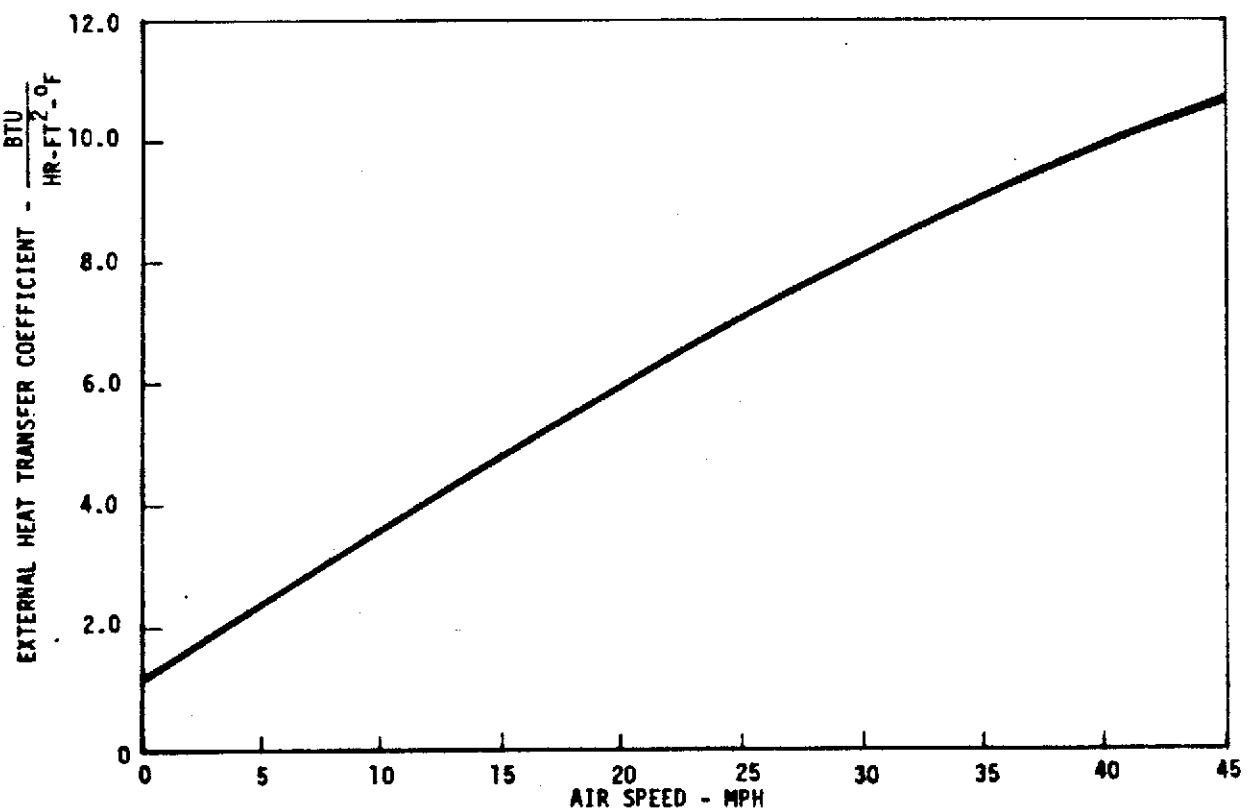

Figure 7.3.1.1-4. External Heat Transfer Coefficient Versus Wind Speed

The heating rates during the boost operation varies over the surface of the vehicle. In addition, S-II LH_2 tank sidewall insulation is affected by many protuberances. The sidewall surface has therefore been divided into sections so that the thermal histories may be determined for each area.

(b) Protuberance Factors:

(1) S-II LH_2 tank sidewall insulation protuberance regions (Figure 7.3.1.1-5)

(2) Details of protuberance - factors versus time (Figures 7.3.1.1-6 and -7)

(3) The details of the locations and references are provided in Table 7.3.1.1-2. For convenience, the resulting temperatures are also shown on the table.

(4) The basic heating rate information is presented in Table 7.3.1.1-3 for:

A. 90 seconds pressurized ground hold

B. 155 seconds S-IC boost

C. 395 seconds S-II boost

3. Propellant Loading:

(a) S-II-1, -2, and -3 are loaded with 930,000 pounds of propellant.

(1) LH_2 level is at Station 875.25.

(2) LOX level is at Station 359.17.

(b) S-II-4, -5, and -6 are loaded with 970,000 pounds of propellant.

(1) LH_2 level is at Station 899.62.

(2) LOX level is at Station 369.62.

4. Preconditioning Flow Conditions:

(a) Flow rate - 4 pounds/second GH_2

(b) Purge temperature - 400°F

(c) Flow introduced through LH_2 fill line

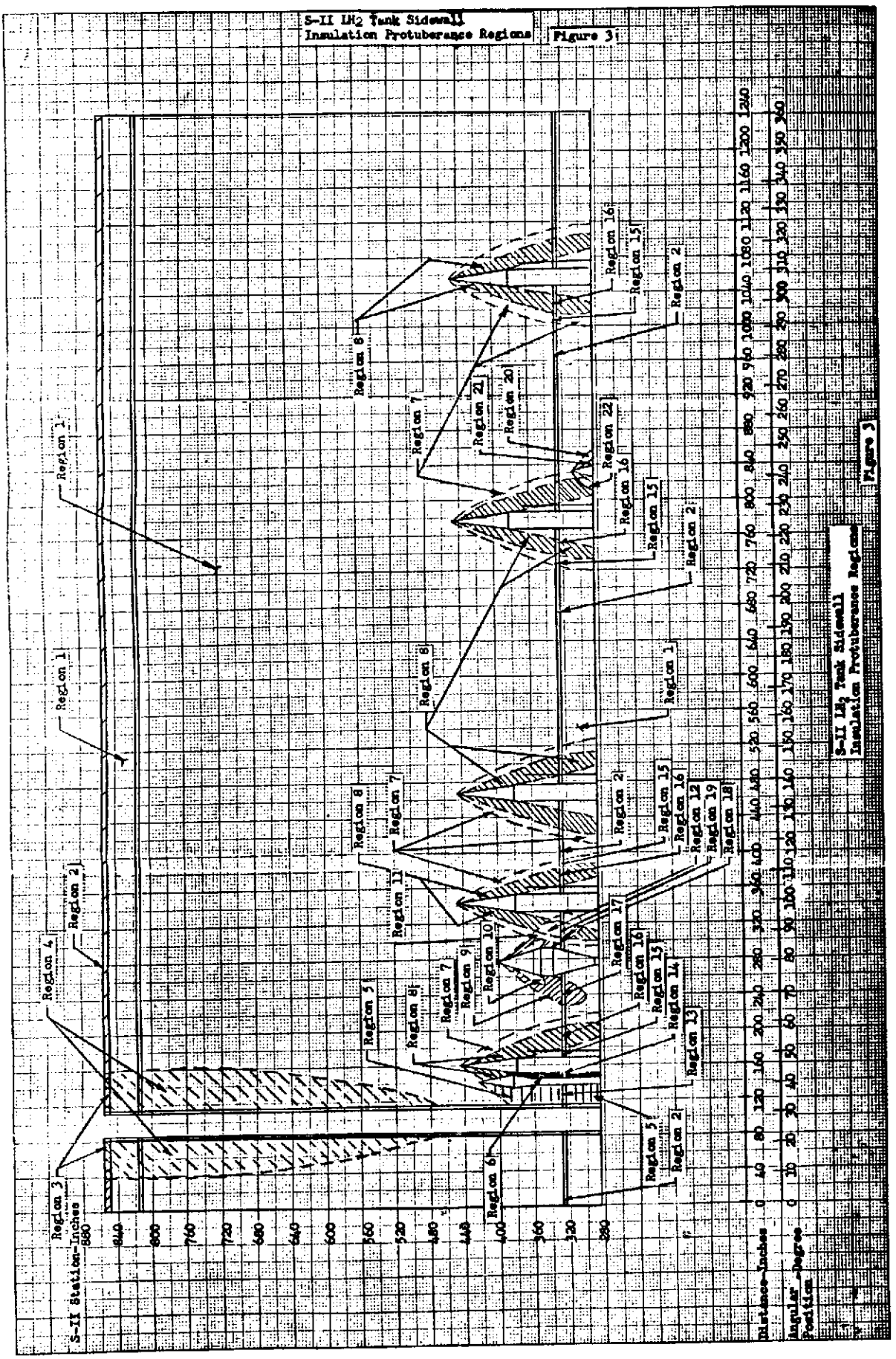

Figure 7.3.1.1-5. LH_2 Tank Sidewall Insulation Protuberance Regions

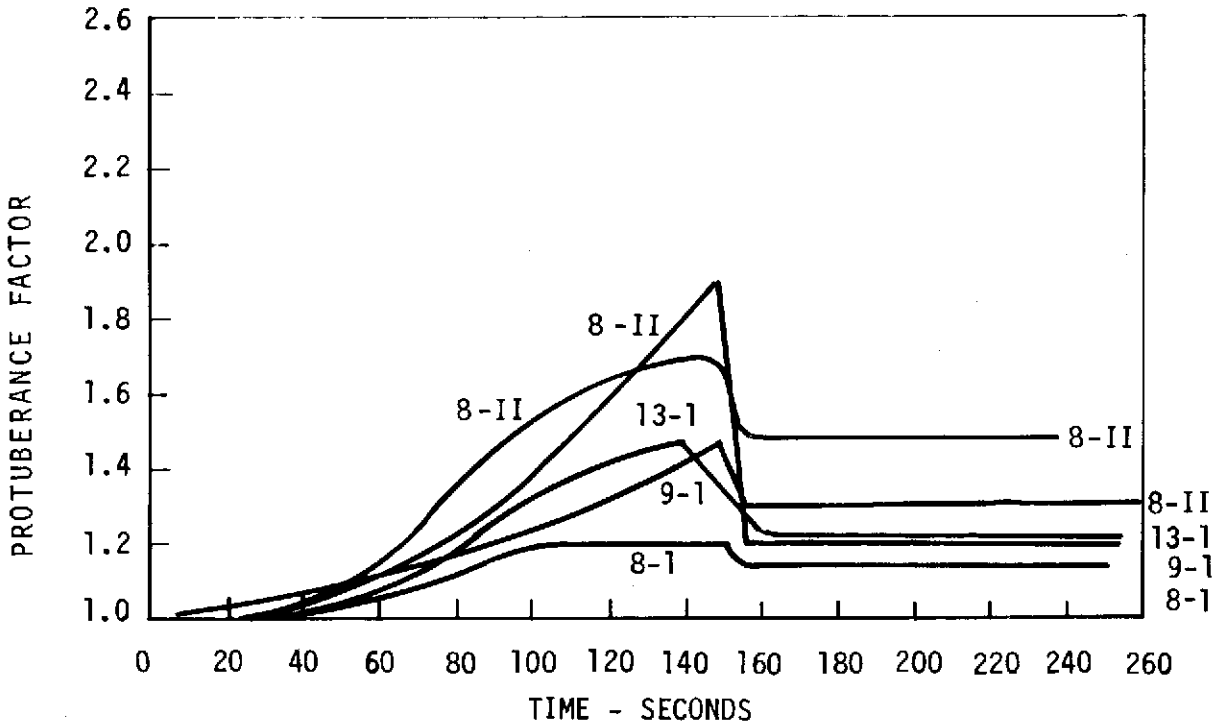

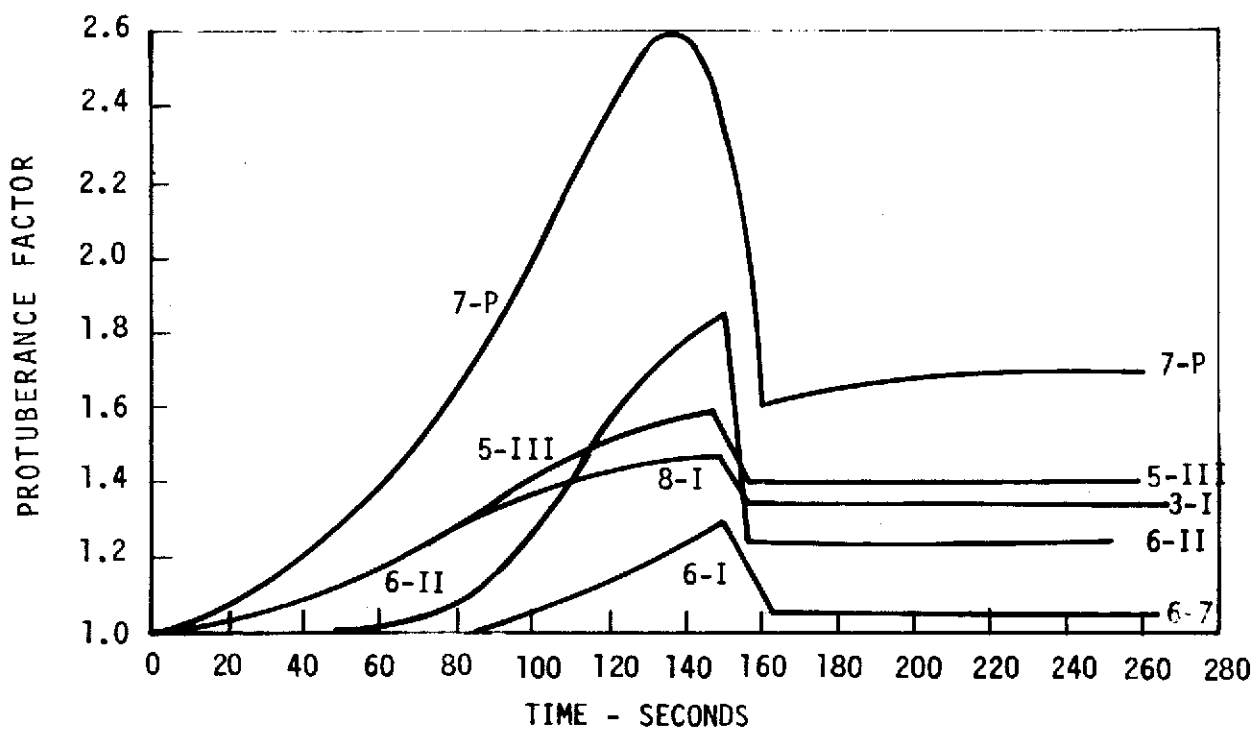

Figure 7.3.1.1-6. Protuberance Factors - LH_2 Tank Insulation

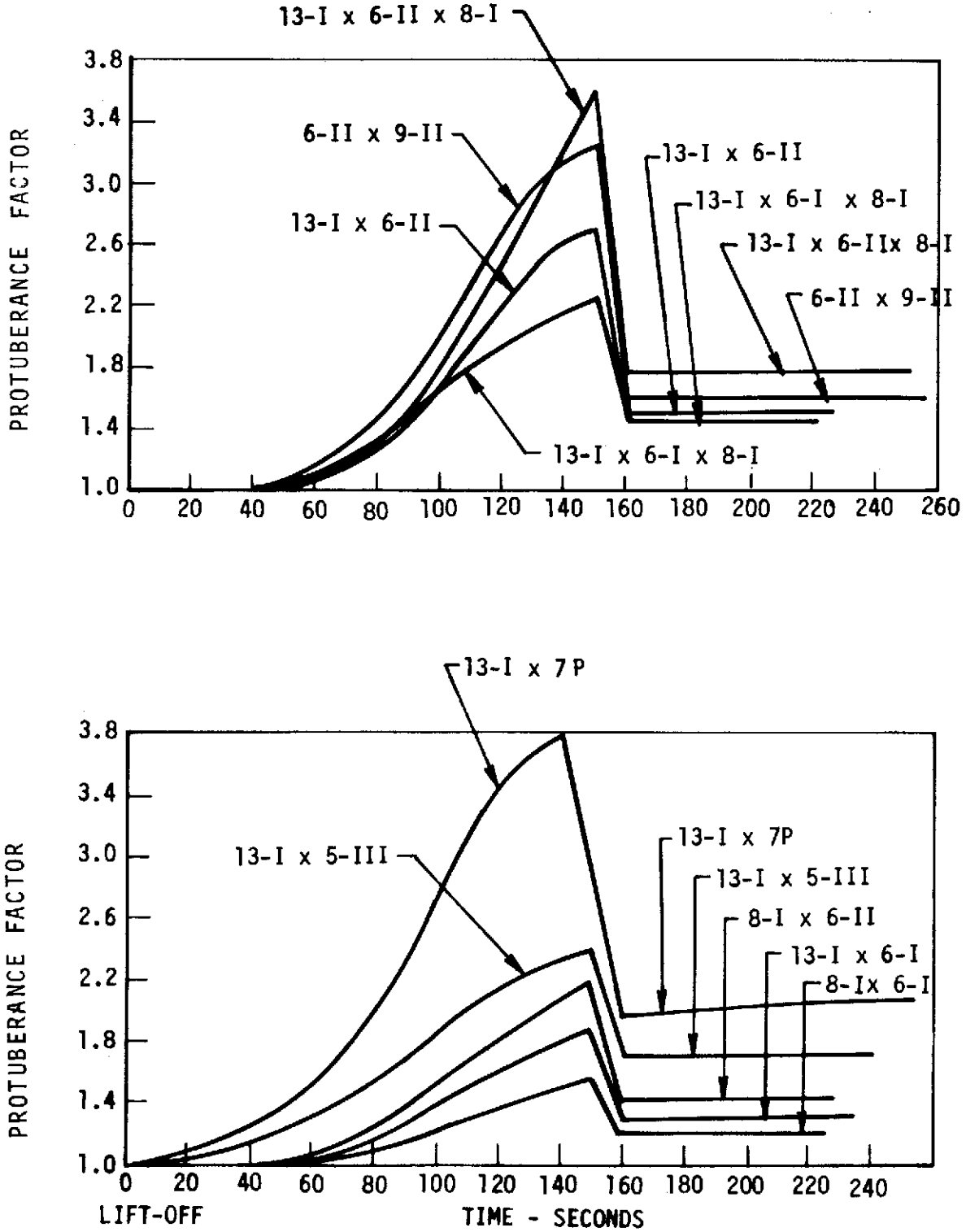

Figure 7.3.1.1-7. Protuberance Factors - LH_2 Tank Insulation

Table 7.3.1.1-2. Details of Protuberance Locations, References, and Maximum Temperatures

REGION	PROTUBERANCE FACTOR NO.	MAXIMUM TEMPERATURE °F 1.6 2.0	REFERENCE	PROTUBERANCE SOURCE
1.	NONE	375	SID63-498 PG. 7-9 (BASIC)	NONE
2.	13-I	458	SID63-498 PG. 8-107	15° RAMP
3.	13-I x 5-I	560	SID63-408 PG. 8-107 S-II/SI64-1095 (REGION I)	15° RAMP SYSTEMS TUNNEL
4.	5-I	460	S-II/SI64-1095 (REGION I)	SYSTEMS TUNNEL
5.	5-III	483	S-II/SI64-1095 (REGION III)	SYSTEMS TUNNEL/LH_2 FEED LINE FAIRING
6.	7-P	598	S-II/SI64-747	LH_2 FEED LINE AND LH_2 RECIRCULATION RETURN LINE FAIRINGS
7.	6-I	411	S-II/FT64-536 (REGION I)	LH_2 FEED LINE AND/OR ULLAGE ROCKET FAIRING
8.	6-II	491	S-II/FT64-536 (REGION II)	LH_2 FEED LINE AND/OR ULLAGE ROCKET FAIRING
9.	8-I	416	S-II/SI64-758 (REGION I)	LH_2 FILL AND DRAIN VALVE FAIRING
10.	8-II	494	S-II/SI64-758 (REGION II)	LH_2 FILL AND DRAIN VALVE FAIRING
11.	8-I x 6-I	455	S-II/SI64-758 (REGION I) S-II/FT64-536 (REGION I)	LH_2 F/D VALVE FAIRING LH_2 FEED LINE FAIRING
12.	8-I x 6-II	540	S-II/SI64-758 (REGION I) S-II/FT64-536 (REGION II)	LH_2 F/D VALVE FAIRING LH_2 FEED LINE FAIRING
13.	13-I x 5-III	577	SID63-498 PG. 8-107 S-II/SI64-1095 (REGION III)	15° RAMP SYSTEM TUNNEL
14.	13-I x 7P	698	SID63-498 PG. 8-107 S-II/SI64-747	15° RAMP LH_2 FEED LINE AND RECIRCULATION LINE FAIRING
15.	13-I x 6-I	499	SID63-498 PG. 8-107 S-II/FT64-536 (REGION I)	15° RAMP LH_2 FEED LINE AND/OR ULLAGE ROCKET FAIRING
16.	13-I x 6-II	586	SID63-498 PG. 8-107 S-II/FT64-536 (REGION II)	15° RAMP LH_2 FEED LINE OR ULLAGE ROCKET FAIRING

Table 7.3.1.1-2. Details of Protuberance Locations, References, and Maximum Temperatures (Sheet 1 of 2)

REGION	PROTUBERANCE FACTOR NO.	MAXIMUM TEMPERATURE °F 1.6 2.0	REFERENCE	PROTUBERANCE SOURCE
17.	13-I x 8-I	504	SID63-498 PG. 8-107 S-II/SI64-758 (REGION I)	15° RAMP LH_2 FEED LINE OR ULLAGE ROCKET FAIRING
18.	13-I x 6-I x 8-I	547	SID63-498 PG. 8-107 S-II/FT64-536 (REGION I)	15° RAMP LH_2 FEED LINE OR ULLAGE ROCKET FAIRING
19.	13-I x 6-II x 8-I	638	SID63-498 PG. 8-107 S-II/FT64-536 (REGION II)	15° RAMP LH_2 FEED LINE OR ULLAGE ROCKET FAIRING
20.	9-I	453	S-II/SI64-758 (REGION I) S-II/FT64-582 (REGION I)	LH_2 F/D VALVE FAIRING LOX VT VALVE FAIRING
21.	9-II	500	S-II/FT-64-582 (REGION II)	LOX VT VALVE FAIRING
22.	6-II x 9-I	590	S-II/FT64-536 (REGION II) S-II/FT64-582 (REGION I)	LH_2 FEED LINE FAIRING LOX VT VALVE FAIRING

Table 7.3.1.1-3. Basic Heat Rate Versus Time

TIME IN SECONDS	HEAT TRANSFER RATE IN BTU/SEC/FT^2 FOR VARIOUS SURFACE TEMPS IN °F						
	-260°	-160°	-60°	40°	140°	240°	340°
0	1.07	.793	.026	.0098	-.0068	-.32	-.597
10	1.07	.793	.026	.0098	-.111	-.32	-.597
20	1.45	.923	.026	.0098	-.225	-.523	-.792
30	2.30	1.364	.705	.0098	-.351	-.792	-1.192
40	2.80	1.770	.912	.0098	-.465	-1.038	-1.558
50	3.40	2.111	1.089	.0098	-.535	-1.210	-1.816
60	3.70	2.304	1.206	.278	-.533	-1.253	-1.905
70	3.60	2.323	1.278	.397	-.372	-1.056	-1.675
83	3.10	2.180	1.408	.751	.173	-.339	-.803
90	2.40	1.775	1.223	.750	.334	-.037	-.373
100	2.20	1.754	1.366	1.033	.738	.472	.229
110	1.80	1.546	1.311	1.096	.905	.729	.569
120	1.40	1.255	1.115	.987	.873	.771	.672
130	1.05	.950	.875	.806	.742	.681	.624
140	.72	.692	.655	.619	.584	.552	.521
150	.55	.476	.459	.442	.426	.409	.393
155	.85	.750	.721	.693	.665	.639	.613
160	.70	.523	.504	.485	.446	.448	.430
172	.30	.207	.201	.194	.187	.181	.174
180	.20	.104	.101	.098	.095	.091	.088
187	.1	.049	.048	.047	.045	.044	.042
196	.05	.023	.022	.022	.021	.021	..020
204	.02	.011	.011	.010	.010	.010	.010
228	.003	.002	.002	.002	.002	.002	.002
268	0	0	0	0	0	0	0
650	0	0	0	0	0	0	0

5. LH_2 Fill Rate - Propellant Loading:

   (a) 1000 gpm to 5% liquid level

   (b) 10000 gpm to 93% liquid level

   (c) 1000 gpm to 100% liquid level

6. Static Firing and S-II Boost LH_2 Drain Rate:

   (a) 395 pounds/second for five engines

   (b) 395 seconds duration

7. Static Firing and S-II Boost LOX Drain Rate:

   (a) 1970 pounds/second for five engines

   (b) 395 seconds duration

8. LH_2 and LOX Tank Pressurization Gas Flow: 2.5 pounds/second GH_2, 6 pounds/second GOX.

9. Heat flux through the J-2 engines' LH_2 pumps is 36,000 Btu/hour per engine.

10. No ice or frost formation on the sidewall insulation.

11. Mission Timeline:

   (a) Ground hold - 90 seconds

   (b) S-IC boost - 155 seconds.

   (c) S-II boost.

      (1) 394 seconds for the no-engine-out case.

      (2) 493 seconds for the one-engine-out case.

12. LH_2 Tank Sidewall Insulation:

   (a) Composite densities and thicknesses

   (b) Insulation thermal conductivity Figure 7.3.1.1-8)

   (c) Cover Cp versus temperature

   (d) Foam and honeycomb Cp versus temperature

   (e) Nominal thickness - S-II-T = 0.8-inch helium purged foam filled honeycomb

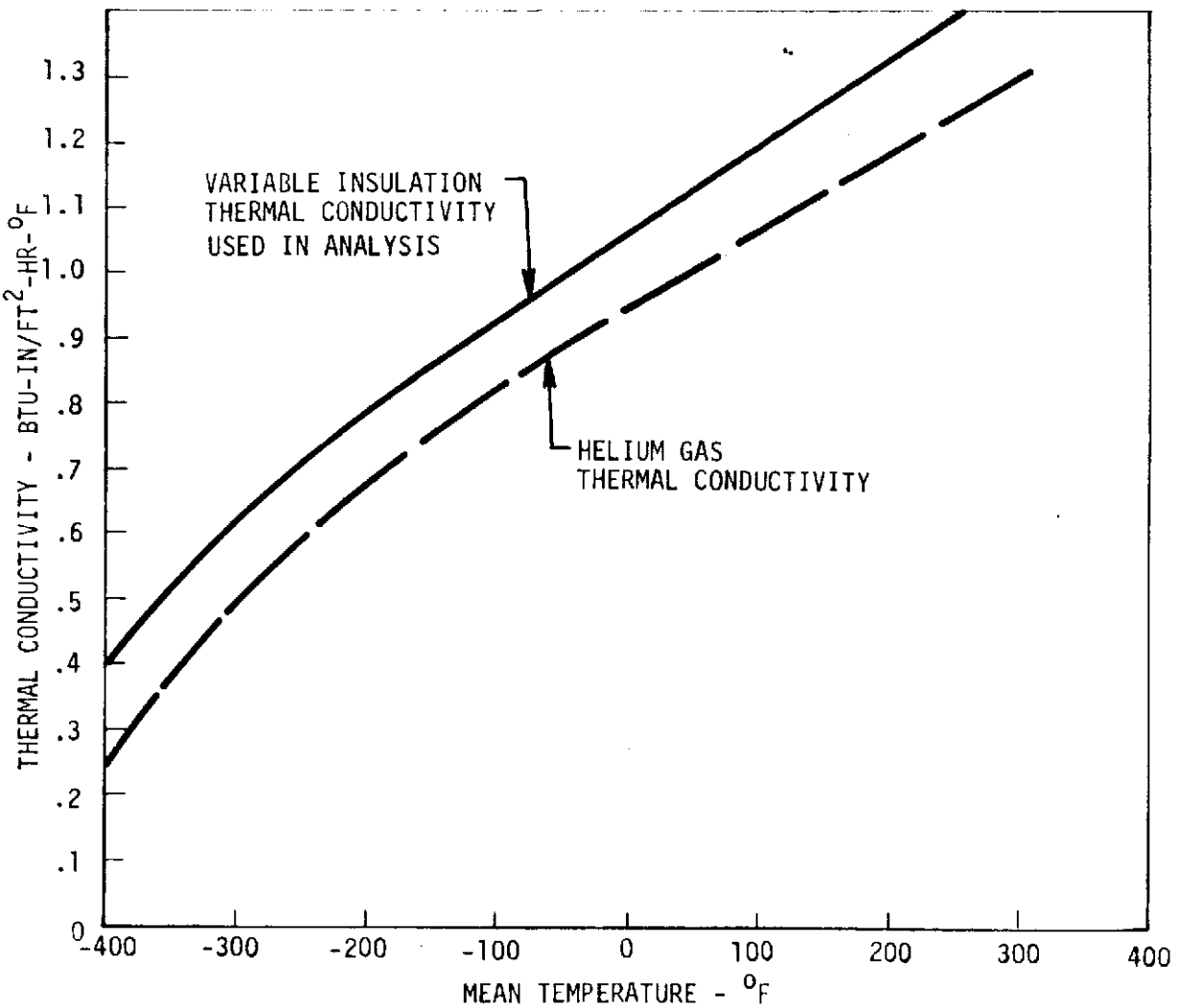

Figure 7.3.1.1-8. Insulation Thermal Conductivity Versus Mean Temperature

13. LH_2 Tank Sidewall Structure:

(a) Minimum aluminum skin thickness

1. Minimum aluminum skin thicknesses

2. S-II-4 -0.125 inch

(b) LH_2 tank sidewall - typical cross section (Figure 7.3.1.1-2)

(c) Aluminum Cp versus temperature

(d) Minimum LH_2 tank sidewall skin thickness

14. LH_2 Tank Forward Bulkhead Insulation:

    (a) Composite densities and thicknesses (Figure 7.3.1.1-3)

    (b) Insulation thermal conductivity

    (c) Cover Cp versus temperature

    (d) Foam and honeycomb Cp versus temperature

    (e) Nominal thickness - 0.5 inch

15. LH_2 Tank Forward Bulkhead Structure:

    (a) Bulkhead skin thickness versus station - S-II-T and S-II-2

    (b) Aluminum Cp versus temperature

16. Common Bulkhead Insulation:

    (a) Composite densities (4.1 lb/ft^3)

    (b) Insulation thermal conductivity

d. Results and Conclusion:

1. External Surface Temperature:

The minimum external surface temperature of the basic 1.6-inch helium-purged, foam-filled honeycomb insulation on the S-II LH_2 tank sidewall occurs on a cold day. The predicted minimum temperature is -160 F for basic sidewall areas when they are covered by a layer of frost. However, panel edges which experience convective cooling from below by the chilled helium purge gas may have lower minimum temperatures (see detail A of Figure 6.1.1.1-1). For example, surface temperatures as low as -240 F were observed under the rubber doubler type closeouts used on S-II. The expected temperature for a nominal day environment is -160 F.

The maximum insulation external surface temperature which occurs during boost is influenced by boost trajectory, angular position on vehicle, and local protuberance heating. The effect of different boost trajectories is discussed in this section.

(a) Design Trajectory $\alpha \neq 0$ (Trajectory A):

Figure 7.3.1.1-9 presents insulation surface temperature, heat rate to LH_2 and total accumulated heat to LH_2 versus time for the design trajectory incorporating angle of attack. The maximum insulation surface temperature and total accumulated heat to LH_2 at liftoff, end of S-IC boost, and end of S-II boost are also presented in Figure 7.3.1.1-9. For comparison with

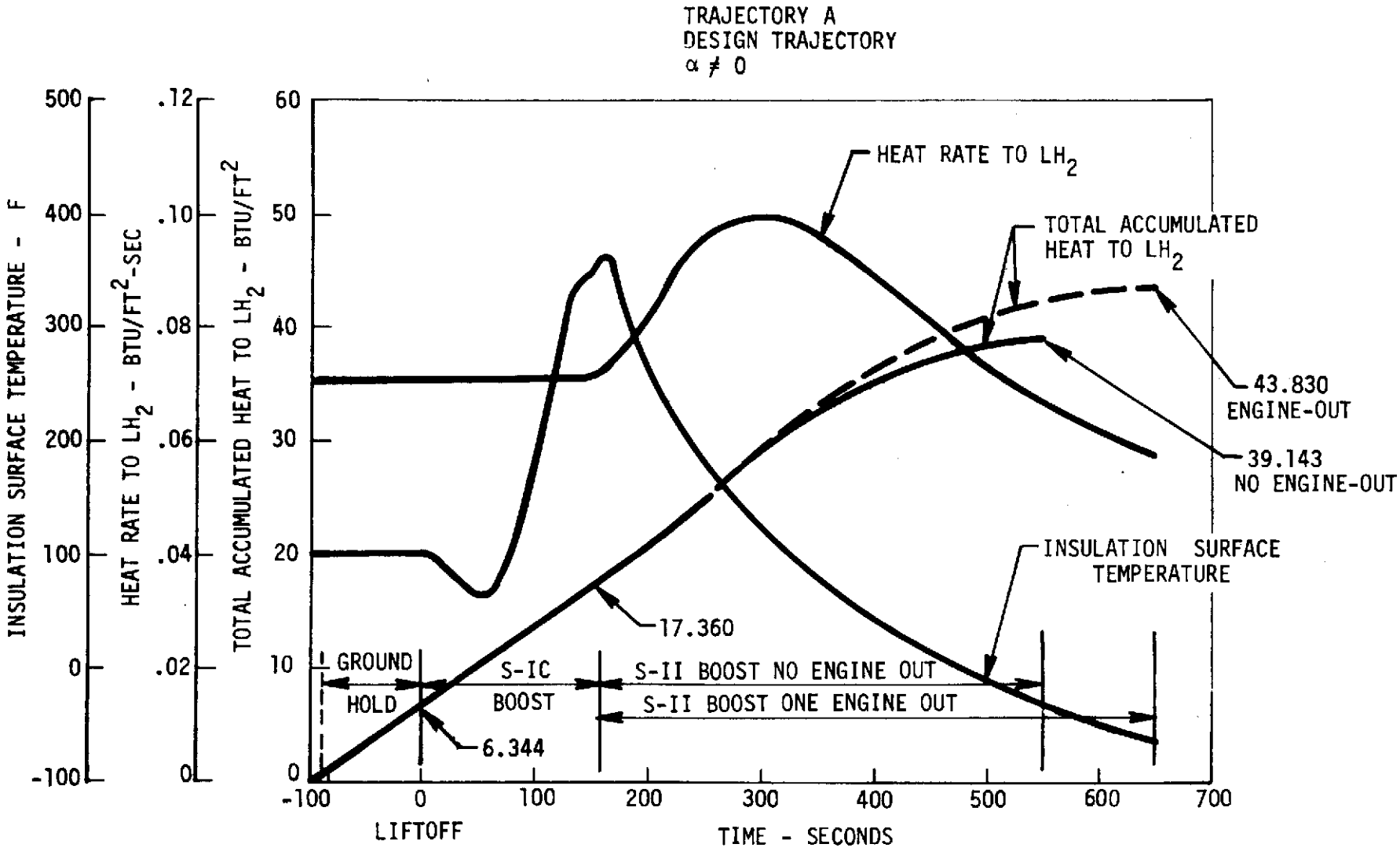

Figure 7.3.1.1-9. Q_{Total}, Q_{Rate}, $T_{Surface}$ Versus Time for Trajectory A (Hottest)

similar data obtained for other trajectories, Figure 7.3.1.1-10 is presented. The maximum insulation surface temperature was found to be 364 F and the maximum heat rate to LH_2 to be 0.1 Btu/ft^2-sec. The total accumulated heat to LH_2 for the no-engine-out case was found to be 178,000 Btu/4550 ft^2 (39.143 Btu/ft^2), and 199,000 Btu/4550 ft^2 (43.830 Btu/ft^2) for the one-engine-out case.

(b) Design Trajectory α = 0 (Trajectory B):

Figure 7.3.1.1-11 presents insulation surface temperature, heat rate to LH_2, and total accumulated heat to LH_2 versus time for the design trajectory without angle of attack. The maximum insulation surface temperature and total accumulated heat to LH_2 at liftoff, end of S-IC boost, and end of S-II boost are presented in Figure 7.3.1.1-10 for comparison with similar data obtained for the other trajectories shown.

The maximum insulation surface temperature was found to be 313 F and the maximum heat rate to LH_2 0.092 Btu/ft^2-sec. The total accumulated heat to LH_2 for the no-engine-out case was found to be 171,500 Btu/4550 ft^2 (37.710 Btu/ft^2), and 191,000 Btu/4550 ft^2 (42.040 Btu/ft^2) for the one-engine-out case.

(c) Nominal Trajectory α = 0 (Trajectory C):

Figure 7.3.1.1-12 presents insulation surface temperature, heat rate to LH_2, and total accumulated heat to LH_2 versus time for the nominal trajectory without angle of attack. The maximum insulation surface temperature and total accumulated heat to LH_2 at liftoff, end of S-IC boost, and end of S-II boost are presented for comparison with similar data obtained for other trajectories in Figure 7.3.1.1-10. The maximum insulation surface temperature was found to be 266 F and the maximum heat rate of LH_2 0.086 Btu/ft^2-sec. The total accumulated heat to LH_2 for the no-engine-out case was found to be 167,000/4550 ft^2 (36.661 Btu/ft^2) and 185,500 Btu/4550 ft^2 (40.735 Btu/ft^2) for the one-engine-out case.

The influence of local protuberance heating was considered for the 22 regions identified in Figure 7.3.1.1-5. Region 1 is the basic sidewall. The protuberance sources, the reference used for each source, and the maximum temperature for each region are tabulated in Table 7.3.1.1-2. The maximum temperature of 698 F occurs in region 14 approximately 150 seconds after launch (see Figures 7.3.1.1-13, 7.3.1.1-14, and 7.3.1.1-15).

The external surface temperature at the point of maximum dynamic pressure (max q) has important structural implications. At max q, which occurs at 85 seconds, the basic sidewall insulation temperature is 120 F. This is for the hottest trajectory of Figure 7.3.1.1-9. For the nominal trajectory of Figure 7.3.1.1-11 the temperature at max q will be 95 F.

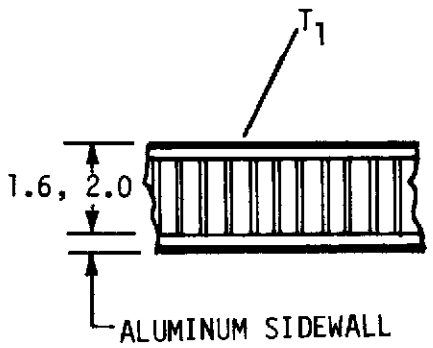

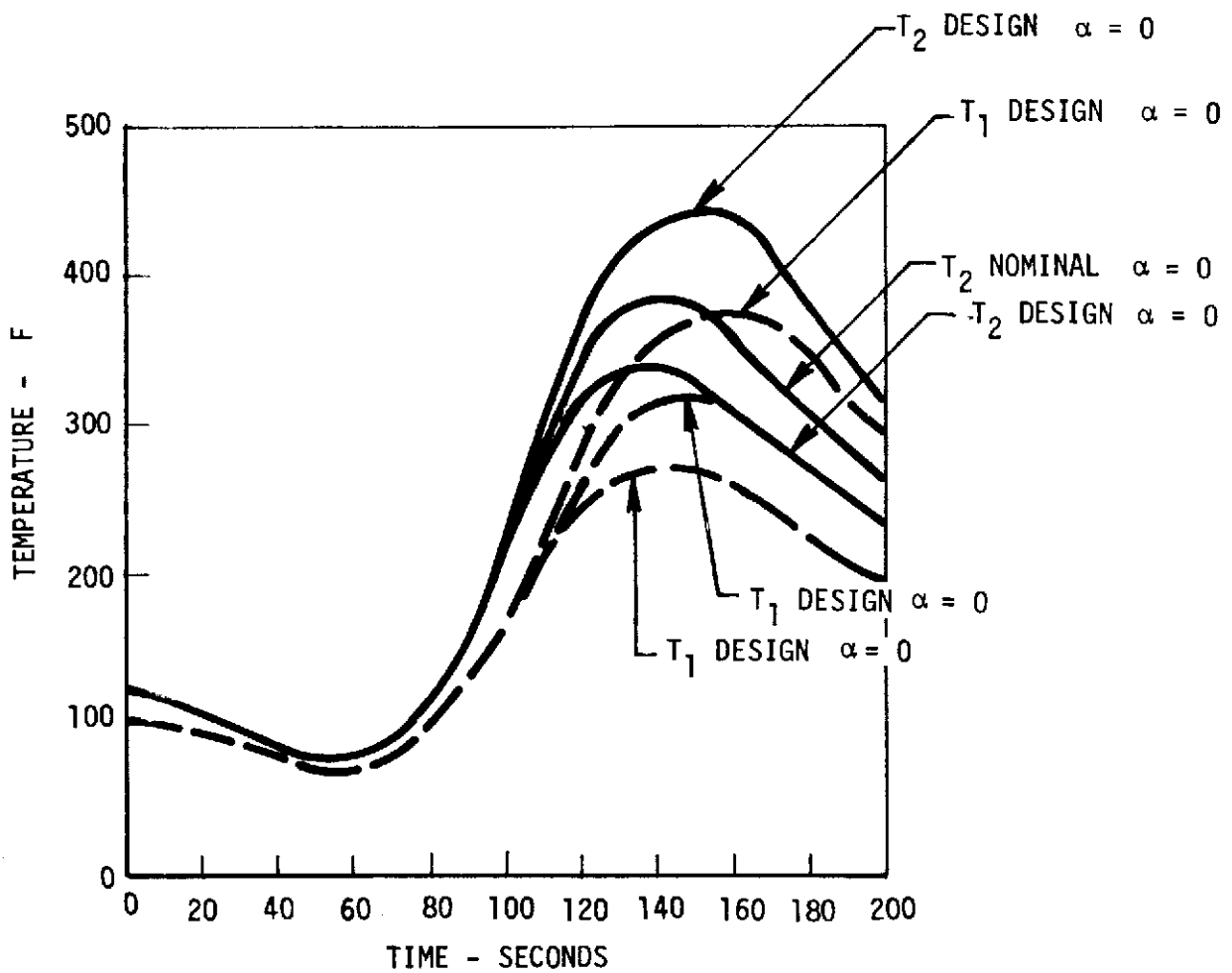

Figure 7.3.1.1-10. LH_2 Tank Sidewall Insulation Surface Temperature Effect of Aerodynamic Heating Trajectory

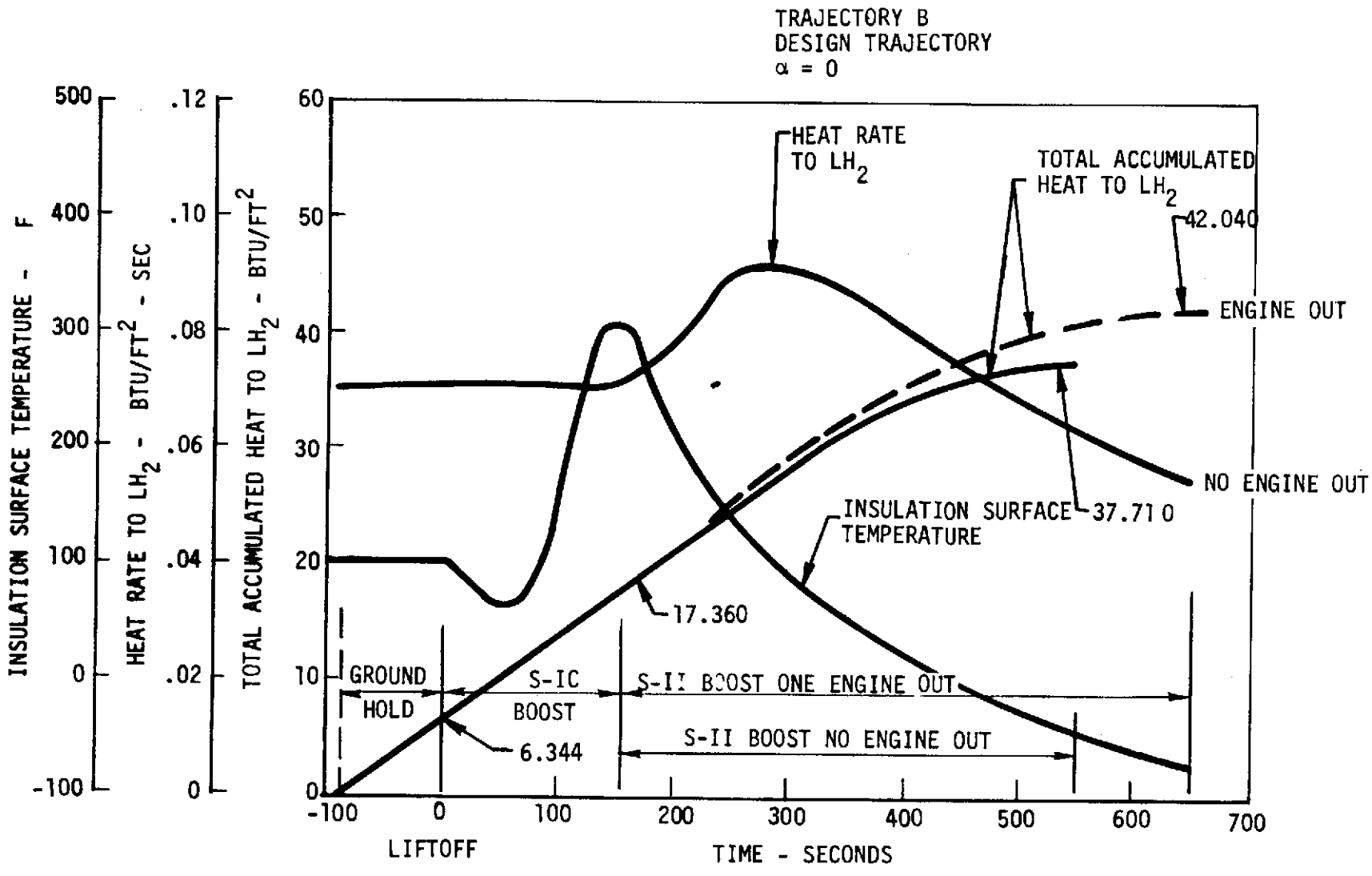

Figure 7.3.1.1-11 Q_{Total}, Q_{Rate}, $T_{Surface}$ Versus Time for Trajectory B (Nominal)

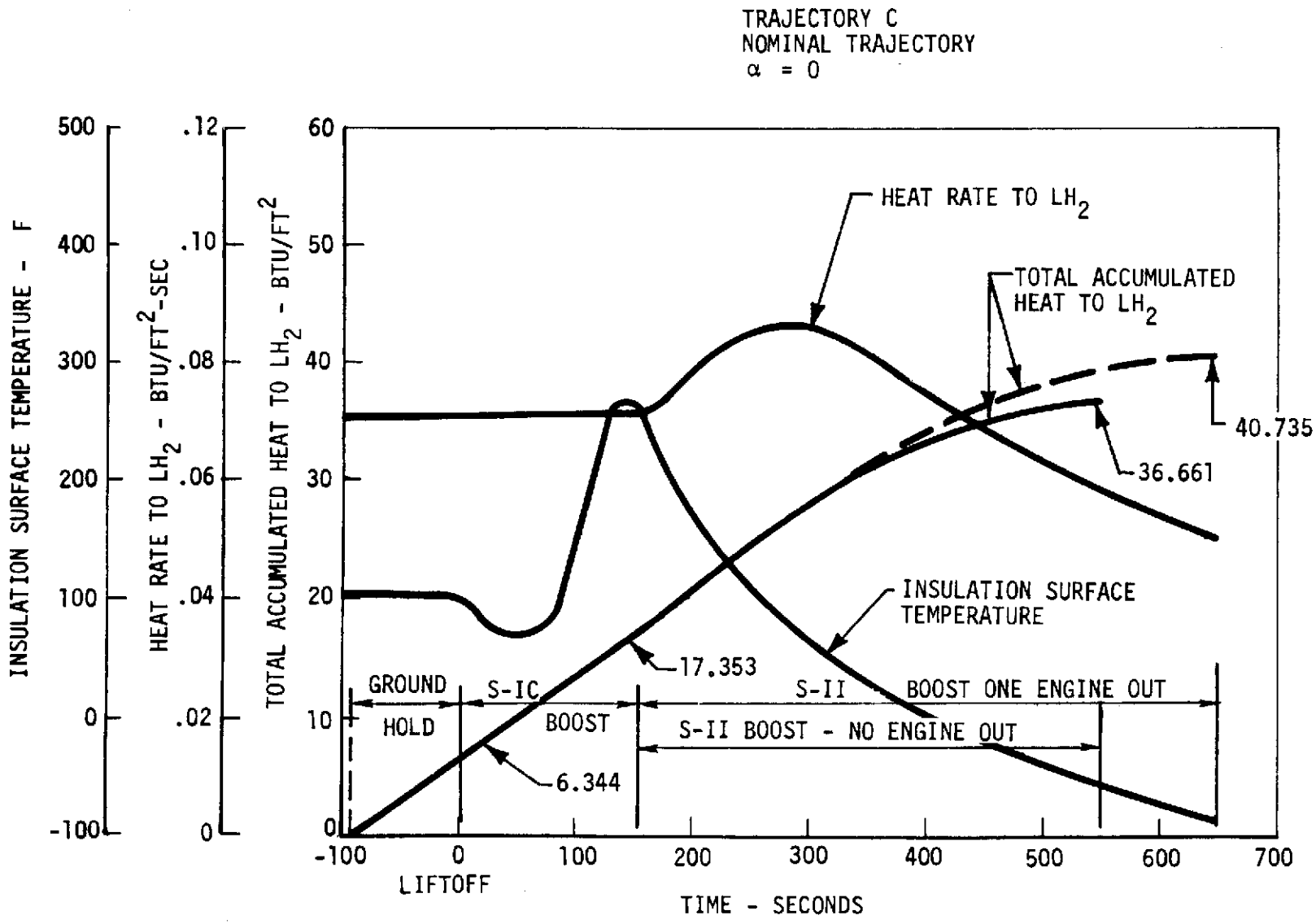

Figure 7.3.1.1-12 Q_{Total}, Q_{Rate}, $T_{Surface}$ Versus Time for Trajectory C (Coldest)

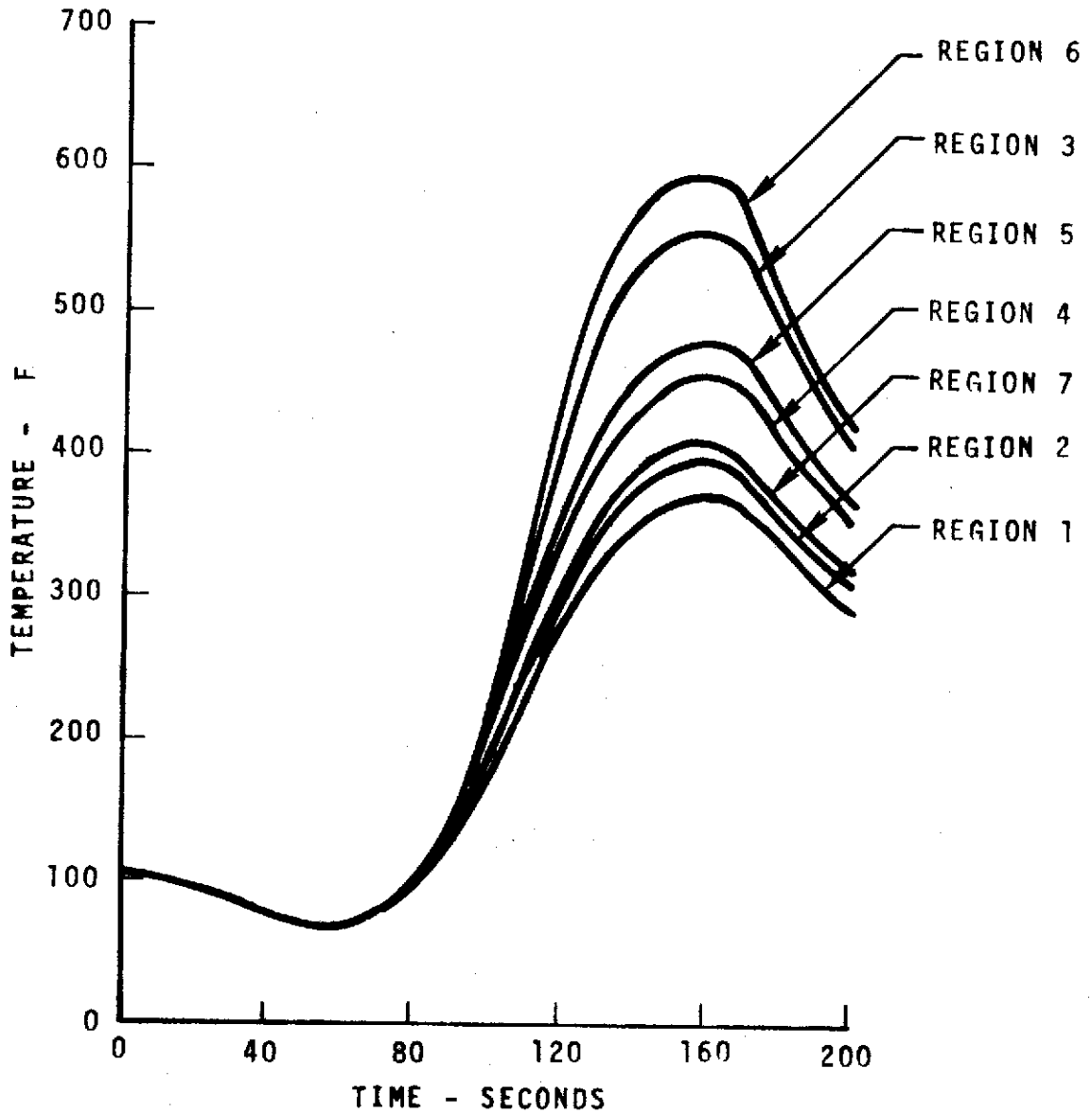

Figure 7.3.1.1-13. 1.6- and 2.0-Inch Foam Insulation Time-Temperature Histories (Regions 1-7)

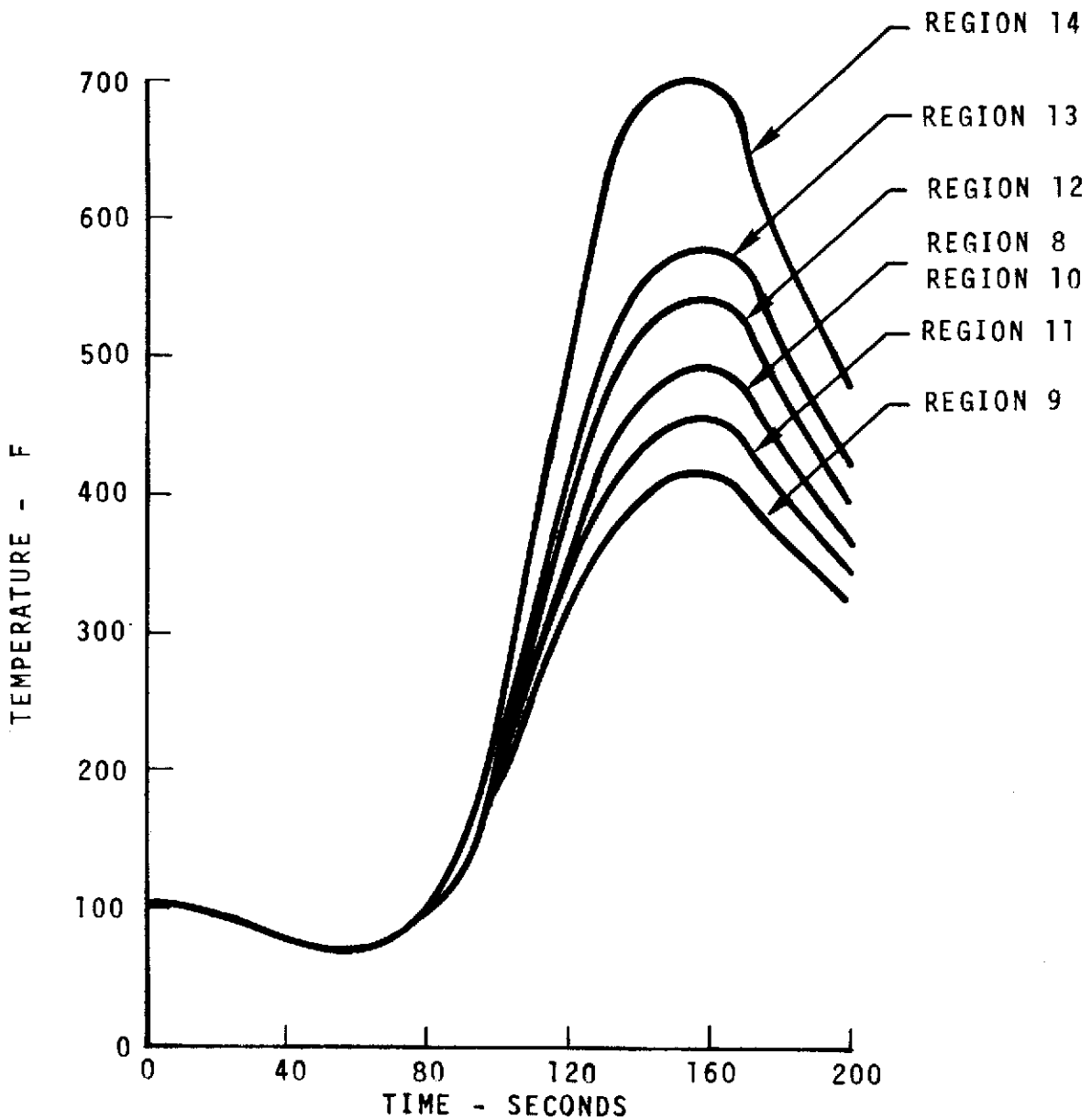

Figure 7.3.1.1-14. 1.6- and 2.0-Inch Foam Insulation Time-Temperature Histories (Regions 8-14)

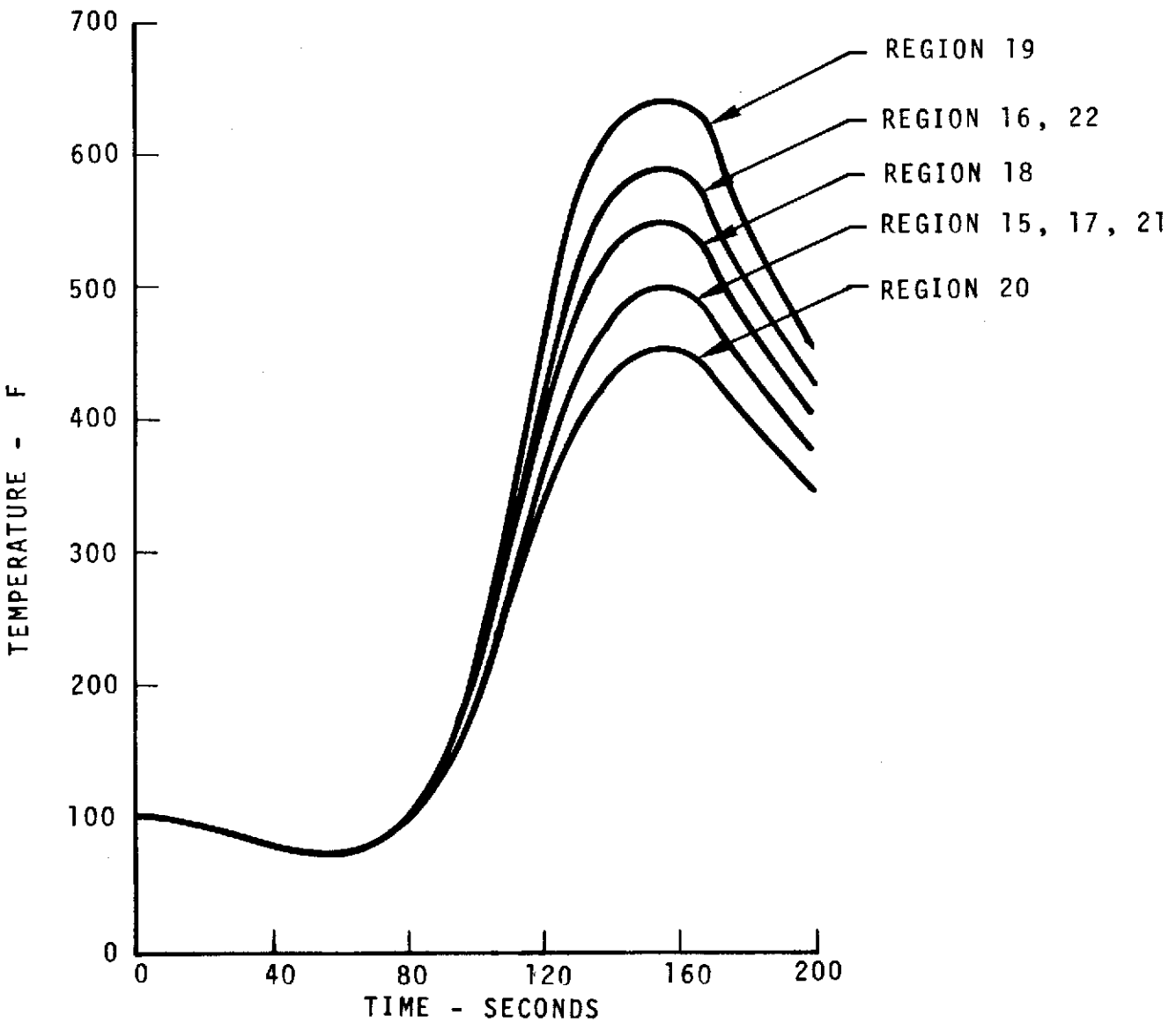

Figure 7.3.1.1-15. 1.6- and 2.0-Inch Foam Insulation Time-Temperature Histories (Regions 15-22)

The maximum and minimum temperatures of 1.6-inch, helium-purged foam-filled honeycomb for an orbital environment have not been computed.

The comparison of the maximum surface temperatures and total accumulated heat to the LH_2 for the aerodynamic trajectories are shown in Table 7.3.1.1-4.

2. Heat Transfer Rate to LH_2:

The predicted nominal day heat transfer rate through the 1.6-inch, helium-purged, foam-filled honeycomb as installed on S-II is 0.07 Btu/sec-ft^2. This heat rate is equivalent to 1.3 pounds/hr-ft^2 of saturated LH_2 boiloff. The total S-II LH_2 tank boiloff rate based on actual experience was less than the allowable of 6 percent per hour. Of this total, approximately 75 percent is due to the basic sidewall insulation.

The predicted maximum heat transfer rate of 0.09 Btu/sec-ft^2 during boost occurs approximately 300 seconds after liftoff. This is illustrated in Figure 7.3.1.1-11 where boost temperature, heating rate, and accumulated heat versus time are presented. Note that the point of maximum heating rate lags the maximum temperature by approximately 150 seconds.

Table 7.3.1.1-4. Comparison of Maximum Insulation Surface Temperature and Total Accumulated Heat to LH_2 for Three Aerodynamic Trajectories

	TRAJECTORY (A) (DESIGN $\alpha \neq 0$)	TRAJECTORY (B) (DESIGN $\alpha = 0$)	TRAJECTORY (C) (NOMINAL $\alpha = 0$)
MAXIMUM INSULATION SURFACE TEMPERATURE, ^{o}F	364 F	313 F	266 F
TOTAL ACCUMULATED HEAT TO LH_2 BTU/FT^2			
GROUND HOLD (90 SECONDS)	6.344	6.344	6.344
S-IC BOOST (155 SECONDS)	17.364	17.360	17.353
S-II BOOST (NO ENGINE (394 SECONDS) OUT)	39.143	37.710 (3.67% LESS)*	36.661 (635% LESS)*
S-II BOOST (ONE ENGINE (493 SECONDS) OUT)	43.830	42.040 (4.10% LESS)*	40.735 (7.08% LESS)*

* PERCENTAGES REFERENCED TO TRAJECTORY (A) VALUES

Tabulated in Table 7.3.1.1-5 are the heat fluxes through the J-joint, common bulkhead, forward skirt, forward dome, LH_2 recirculation system, J-2 engine LH_2 pumps, and miscellaneous items for vehicles S-II-1 through 6. The total heat flux of these items for S-II-4, -5, and -6 is greater than that for S-II-1, -2, and -3. This is because of the increase in the wetted area, a result of the greater propellant loading of the S-II-4, -5 and -6.

Table 7.3.1.1-5. Heat Flux into LH_2 Excluding That Through Sidewall Insulation

Source	S-II-1, -2, and -3		S-II-4, -5, and -6	
	Hot Day (Btu/hr)	Cold Day (Btu/hr)	Hot Day (Btu/hr)	Cold Day (Btu/hr)
J-Joint	63,200	62,400	63,200	62,400
Common Bulkhead	9,600	9,600	9,700	9,700
Forward Skirt	29,600	14,240	29,600	14,240
Forward Dome	182,600	58,800	311,400	143,800
LH_2 Recirculation System	10,000	10,000	10,000	10,000
J-2 Engines' LH_2 Pumps	180,000	180,000	180,000	180,000
Miscellaneous	33,200	30,800	33,200	30,800
Total	508,200	365,840	637,100	450,940

Figure 7.3.1.1-16 presents the sidewall heat flux versus the sidewall insulation K/X and wind speed for a hot day condition, respectively. From this figure it is apparent that the lower the K/X value, the less effect the wind speed has on the heat flux. Also, it is noted that for a given K/X, the difference in the sidewall heat flux between a 5 to 15 mph wind is greater than it is between a 35 and 45 mph wind.

Figure 7.3.1.1-17 illustrates the total LH_2 boiloff rates and topping rates versus the sidewall insulation K/X and wind speed for a hot day condition. This is for a given wind speed and for a K/X less than about 1.25 $\frac{\text{Btu}}{\text{hr-ft}^2\text{-°F}}$ ($K = 0.28 \frac{\text{Btu-in.}}{\text{hr-ft}^2\text{-°F}}$). Thus, for the hot day high wind speed conditions, the LH_2 boiloff rate is 5.8 percent per hour. In constrast, the expected minimum sidewall insulation K/X for vehicles S-II-4, -5, and -6 (if double seal insulation were used) is 0.25 $\frac{\text{Btu}}{\text{hr-ft}^2\text{-°F}}$ ($K = 0.2 \frac{\text{Btu-in.}}{\text{hr-ft}^2\text{-°F}}$) resulting in a boiloff rate of 4 percent per hour for the same environmental conditions.

3. Accumulated Heat Transfer to LH_2: A nominal S-II mission consists of 90 seconds of ground-hold, 155 seconds of S-IC boost, and 351 seconds of S-II boost. For S-II, the accumulated sidewall heat transfer is 150,130 Btu and the accumulated total of all sources if 198,780 Btu. These values represent a point-design condition. For each new

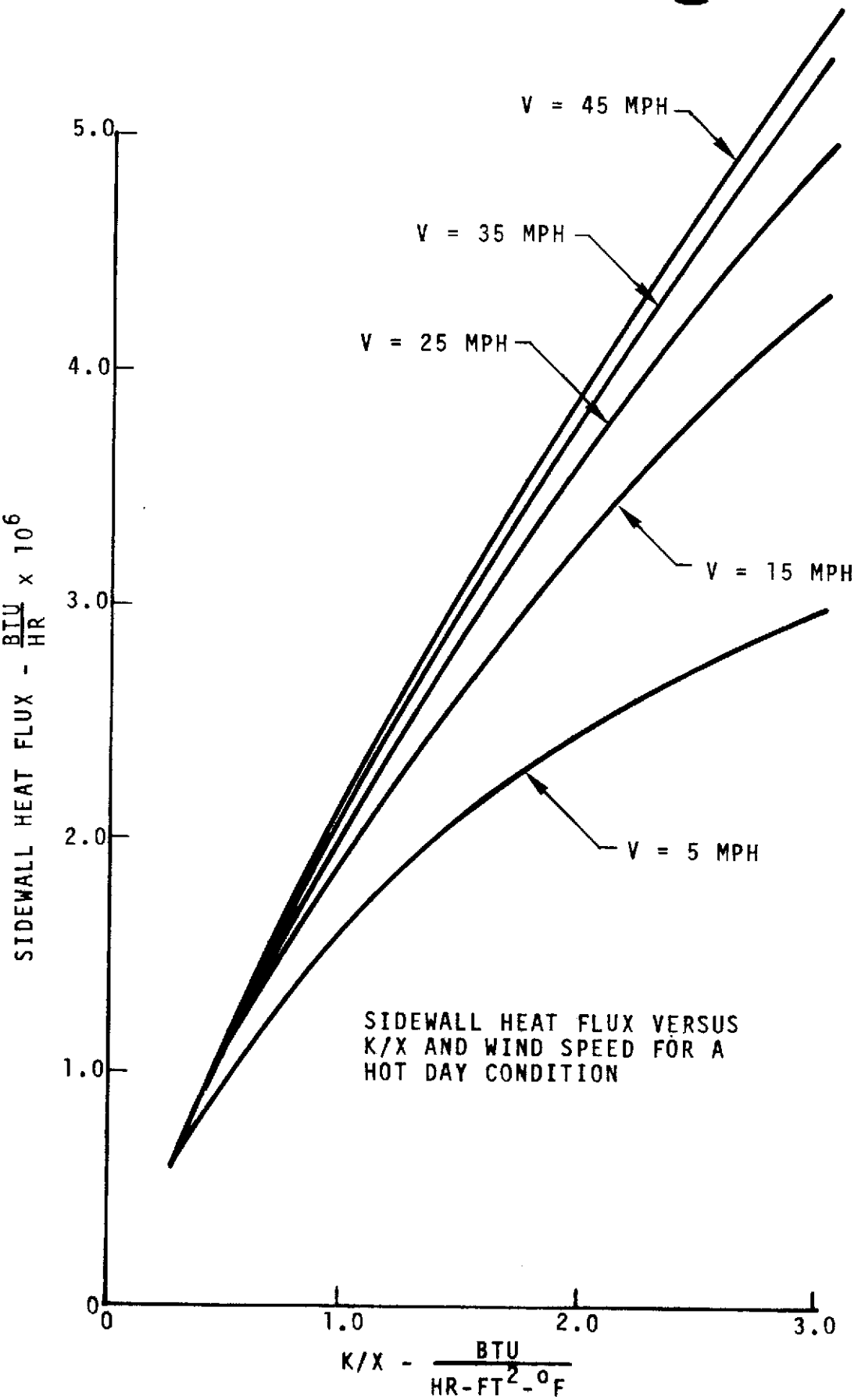

Figure 7.3.1.1-16. Sidewall Heat Flux Versus K/X and Wind Speed for Hot Day Condition

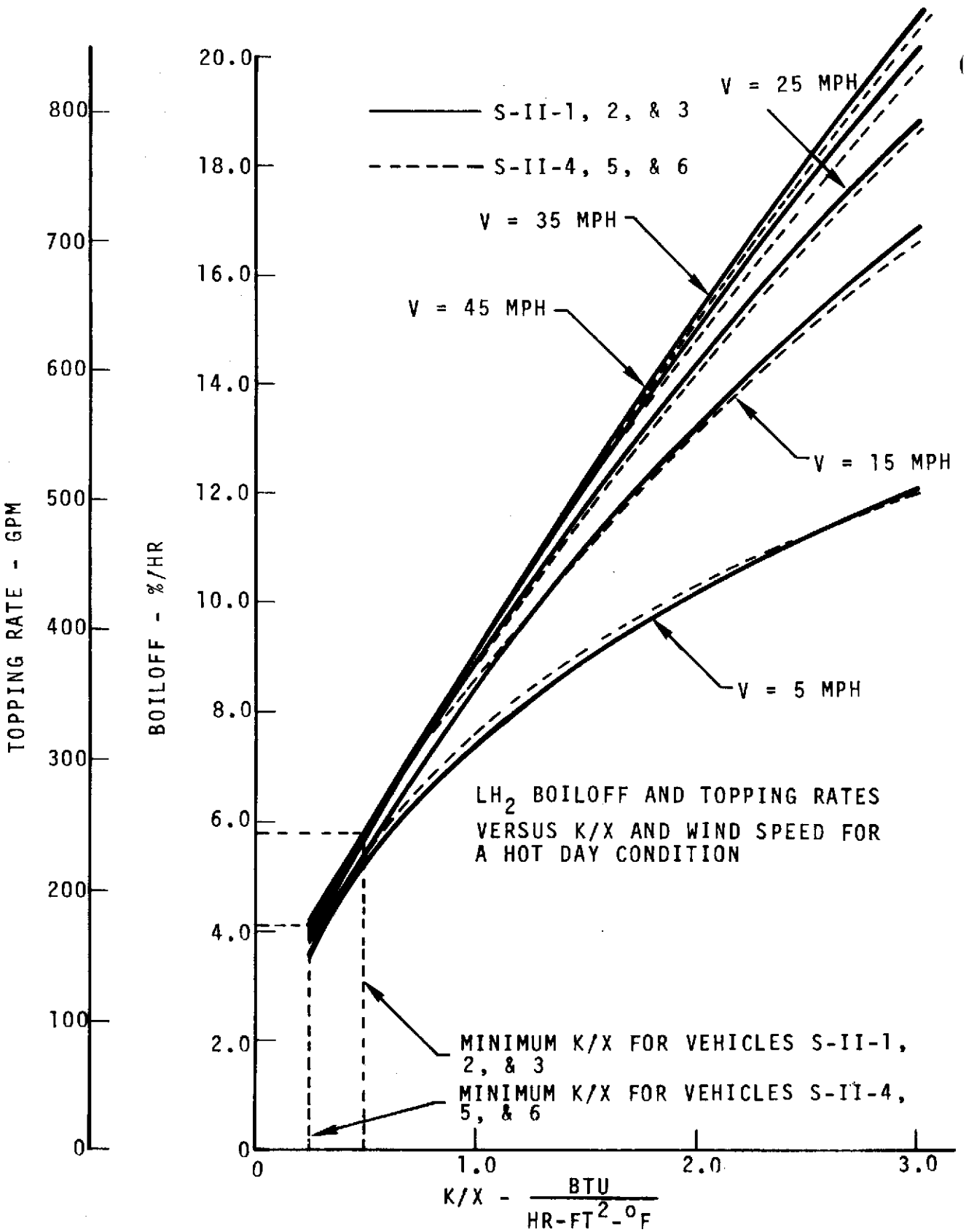

Figure 7.3.1.1-17. LH_2 Boiloff and Topping Rates Versus K/X and Wind Speed for Hot Day Condition

trajectory new calculations must be performed. Therefore, a parametric analysis for design purposes might be desired. Such an analysis would be of value only for this particular design, thus may not be of general interest.

4. Other Thermal Performance Parameters: Maximum temperature gradients and structural temperatures during preconditioning, propellant filling, and detanking have important structural implications. The maximum temperature gradients in the LH_2 tank structure of S-II will occur on the vehicle with the smallest tank wall and sidewall insulation thickness under hot day conditions. Typical temperature history for the S-II-4 stage are presented in Figures 7.3.1.1-13 through 7.3.1.1-15.

   (a) LH_2 Tank Preconditioning (Figures 7.3.1.1-18 and -20) Cases I and II: Figure 7.3.1.1-18 presents LH_2 tank structural and GH_2 temperatures versus S-II station versus time for S-II-T. Figure 7.3.1.1-19 indicates that the LH_2 tank structure temperature between Stations 315 and 330 lags behind the major portion of the tank during chilldown because of the greater skin thickness in this area. In general, the S-II-4 LH_2 tank structure chills down more rapidly than the S-II-T structure due to the smaller skin thickness. The LH_2 tank GH_2 temperatures do not differ appreciably for the S-II-T and S-II-4 vehicles.

   (b) LH_2 Tank Propellant Loading (Figures 7.3.1.1-19 and -20): Figures 7.3.1.1-19 and -20 present LH_2 tank structural and GH_2 temperatures versus S-II station versus time for S-II-T. The maximum LH_2 tank structure dT/dX occurs at Station 325 (240 F/6 inches), the warmest spot in the tank below the LH_2 fill line. Portions of the LH_2 tank above the LH_2 fill line are chilled below -160 F by the LH_2 boiloff gas before the liquid level reaches these stations. The forward bulkhead LH_2 tank sidewall juncture at Station 820 is chilled to below -350 F before the LH_2 liquid level reaches that point.

   The GH_2 temperatures for S-II-T and S-II-4 are similar, except that the GH_2 temperatures near the end of fill for S-II-T are slightly lower than S-II-4 because of the higher heat transfer boiloff for S-II-T.

   (c) Static Firing (Figures 7.3.1.1-21 and -22: Figures 7.3.1.1-21 and -22 present LH_2 tank structural and GH_2 temperatures versus S-II station versus time for S-II-T with similar information for S-II-4. Figure 7.3.1.1-21 indicates that the LH_2 tank structure will exceed the pressurization gas temperature of -250 F and reach a maximum temperature of -220 F at the end of static firing. The pressurization gas heats the structure to -250 F and the heat leak from the external ambient allows the structure to warm to -220 F. The S-II-T sidewall structure reaches a maximum wall temperature of -220 F while the S-II-4 sidewall structure only warms to -235 F because of the better sidewall insulation on S-II-4.

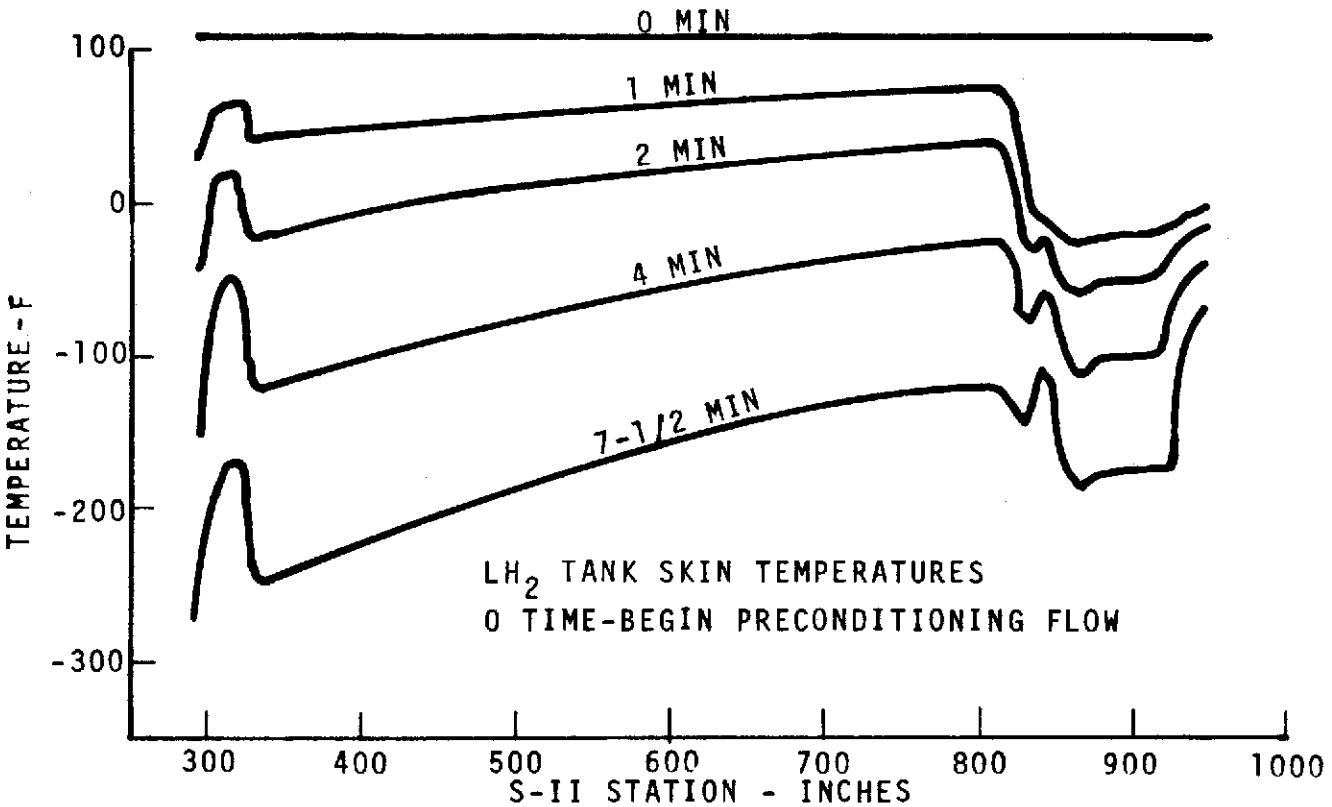

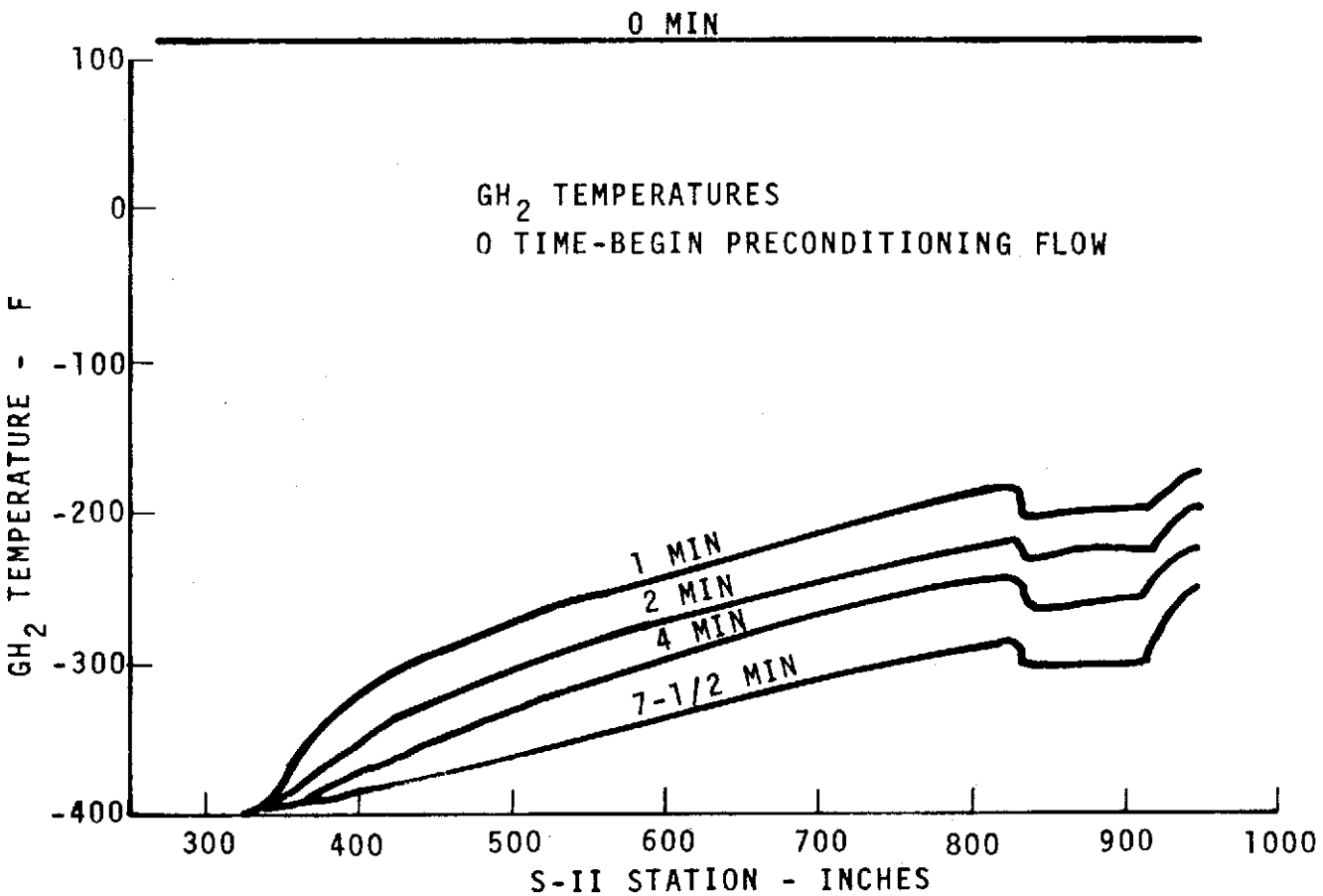

Figure 7.3.1.1-18. Case 1 S-II-T Preconditioning LH_2 Tank Structural and GH_2 Temperature

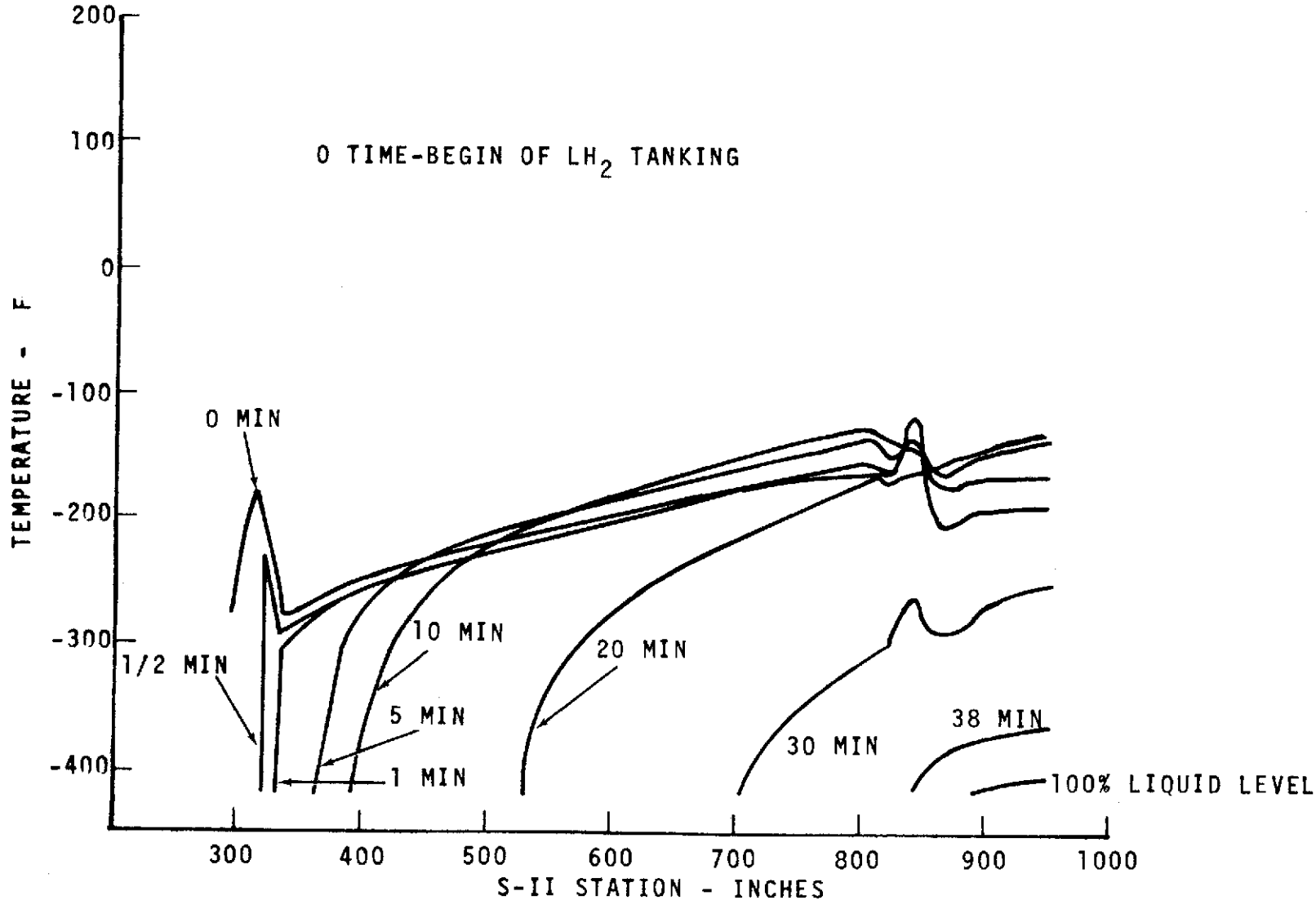

Figure 77.3.1.1-19 Case 2A S-II-T Propellant Loading LH_2 Tank Structural Temperature

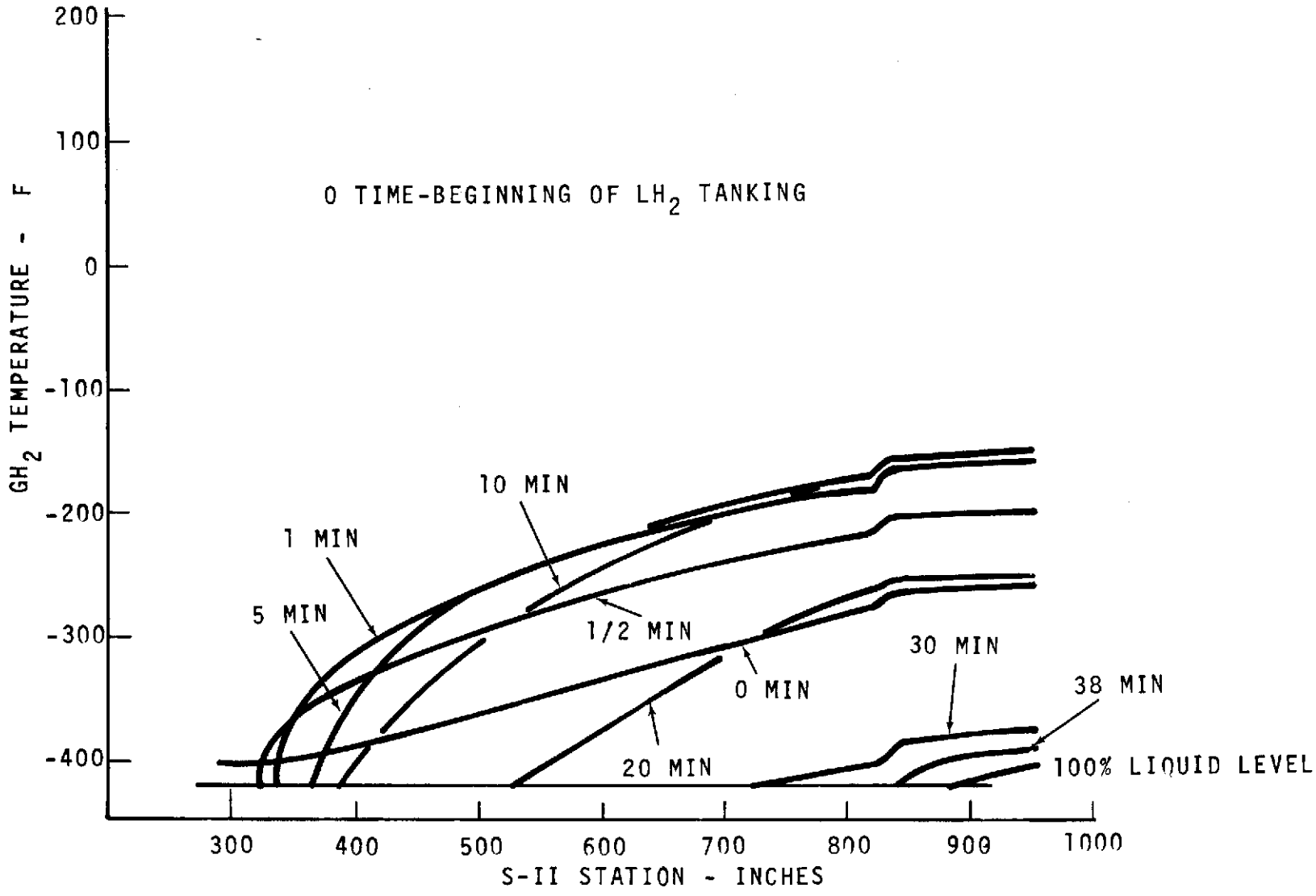

Figure 7.3.1.1-20. Case 2A S-II-T Propellant Loading LH_2 Tank GH_2 Temperature

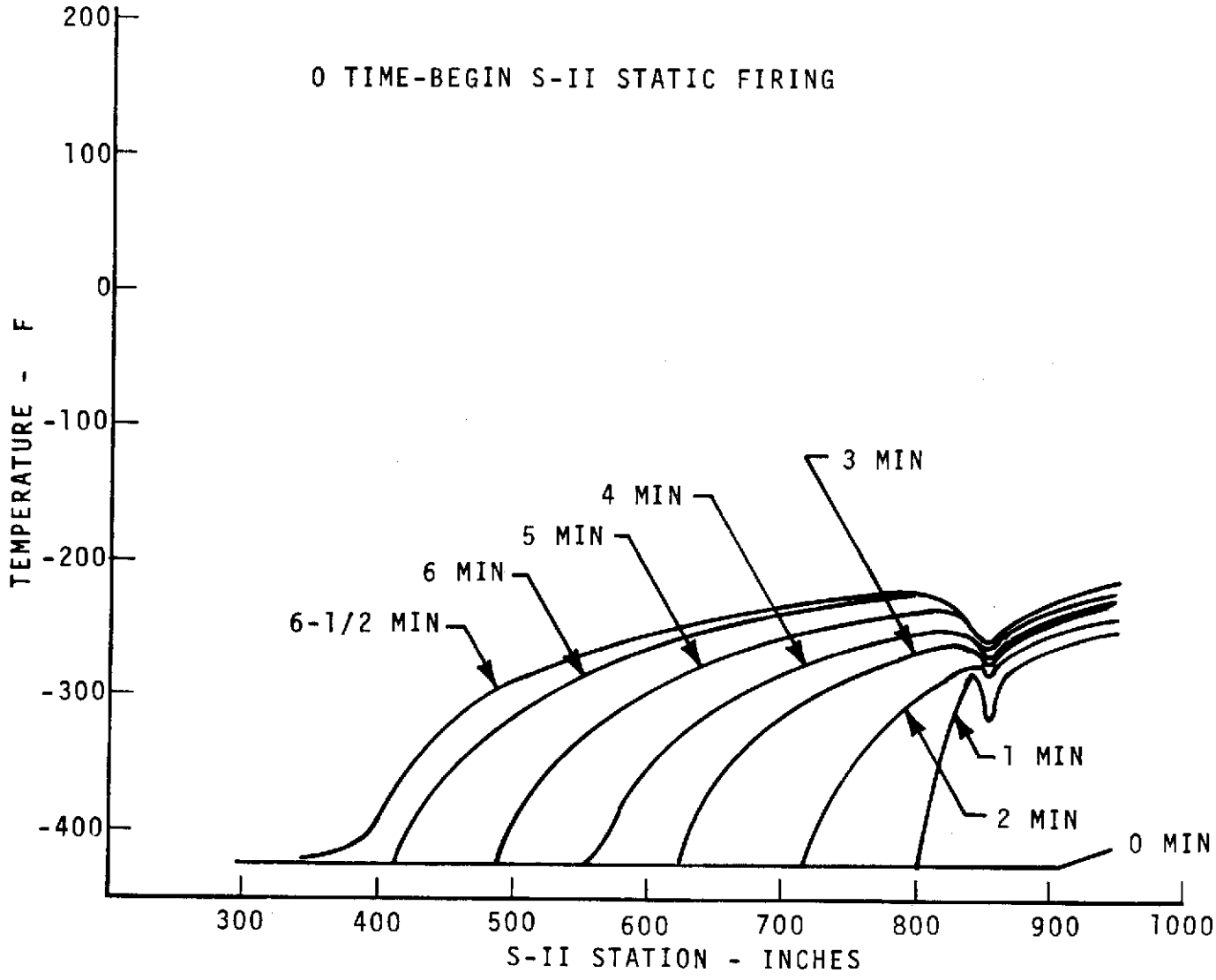

Figure 7.3.1.1.21. Case 3 S-II-T Static Firing LH_2 Tank Structural Temperature

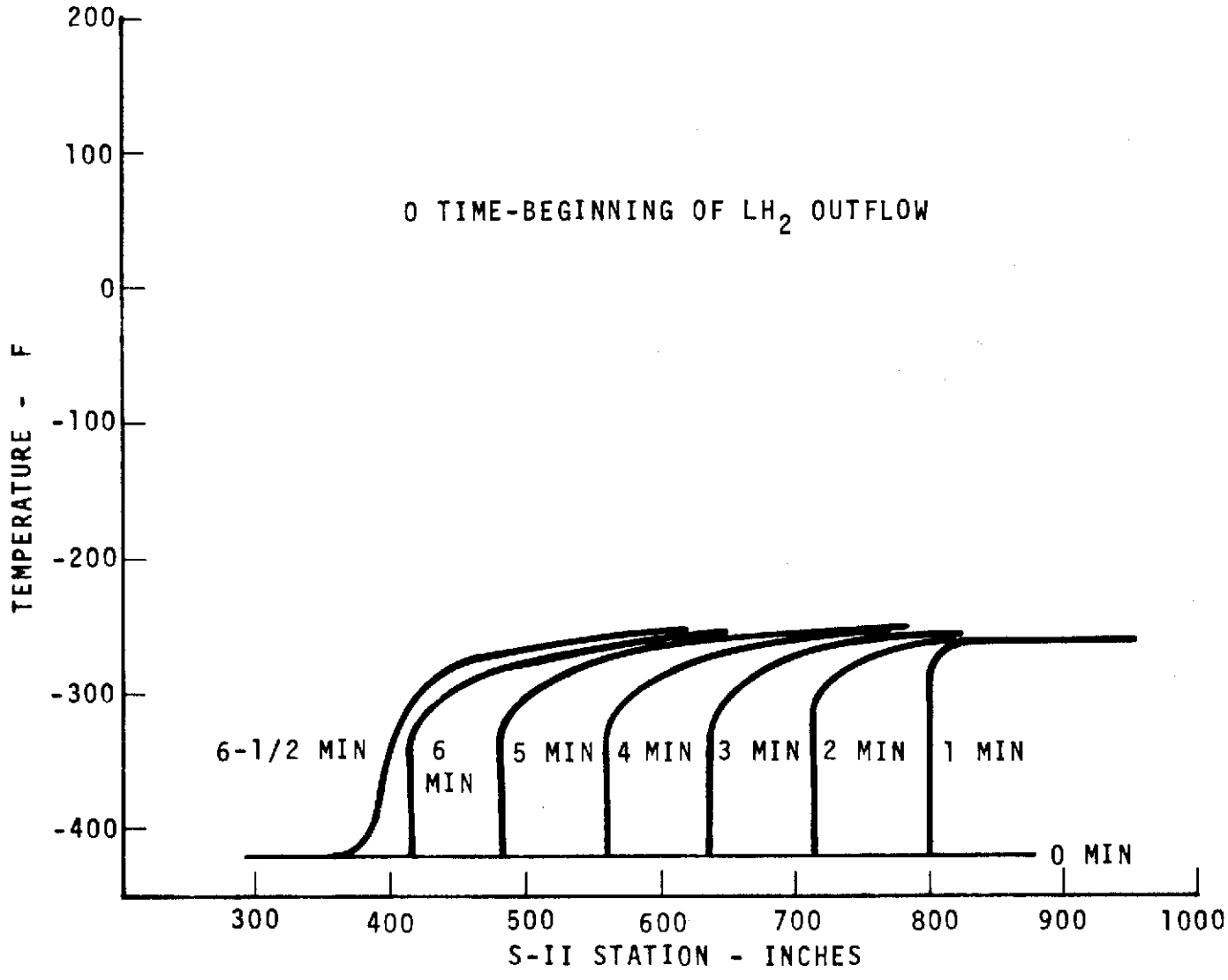

Figure 7.3.1.1-22. Case 3 S-II-T Static Firing LH_2 Tank GH_2 Temperature

The inflection points in the structural temperature curves are due primarily to forward bulkhead and forward skirt insulation configurations, rather than structural skin thickness. Since the LH_2 tank forward bulkhead is uninsulated from Stations 821 to 830, the forward bulkhead will warmup more rapidly when uncovered by LH_2 than from Stations 830 to 866, where it is insulated. Above Station 866 the forward bulkhead is insulated, but the external environment is warmer than below Station 866 because of the close-out which separates the warmer GN_2 above from the colder helium below. This results in warmer forward bulkhead skin temperatures above Station 866.

Figure 7.3.1.1-22 indicates that LH_2 tank GH_2 temperatures do not exceed -250 F. The S-II-4 GH_2 temperatures are slightly lower than the S-II-T temperatures because of the better LH_2 tank side-wall insulation.

7.3.1.2 Evacuated Honeycomb

The thermal performance characteristic of this insulation design is the relatively high heat transfer rate across the S-II common bulkhead from LOX to LH_2. The S-II point design analysis for this insulation is presented in a study where the total heat leak to LH_2 through the common bulkhead and total heat to LOX from all sources are determined. For analysis the common bulkhead is divided into three sections: forward, J-joint, and equatorial. The evacuated honeycomb design is represented by the forward section. Analyses of the other two sections are also presented for completeness.

a. Statement of Problem: Determine the heat transfer rate into or out of the gas or the liquid oxygen in the LOX tank through the common bulkhead during a 186-second prelaunch LOX tank pressurization hold and through S-IC and S-II boost.

b. Methodology: The heat transfer rate was computed for a 710-second S-II mission time which includes 186 seconds for preluanch LOX tank pressurization hold, the period from an initiation of the LOX tank pressurization to liftoff, 150 seconds of S-IC boost, and 374 seconds of S-II boost. The analysis reflects the latest stage structure and tank design and the latest propellant loading and tank depletion rate for S-II-4 and subsequent stages.

   Major areas that affect the heat transfer to the LOX in the LOX tank are the common bulkhead, aft bulkhead, and components of four systems which are associated with the LOX tank: the LOX tank pressurization system, the LOX feed system, and LOX recirculation system, and the LOX fill and drain system.

   The following paragraphs present a detailed discussion of the heat transfer through the common bulkhead.

   The common bulkhead forms an upper half of the LOX tank shell structure, separating the LOX tank from the LH_2 tank. The helium purged phenolic

glass-cloth honeycomb core, sandwiched between the fore and aft aluminum facing sheets, acts as insulation between the LOX and LH_2 in the tanks. Evacuation of the helium gas in the honeycomb core to at least 3 psia prior to liftoff further reduces the heat transfer between the onboard propellants. A reduction of the honeycomb core thickness in the vicinity of the J-joint allows a relatively high heat transfer across this local area. It should be noted that in the common bulkhead area forward to the J-joint, heat is transferring away from the LOX and into the LH_2, resulting in a negative heat transfer with respect to the LOX The following describes the complicated heat transfer phenomena across the three sections of the common bulkhead (refer to Figure 7.3.1.2-1).

1. Common Bulkhead Forward Section: The forward section extends from Station 317.63 to the LOX tank-full level at approximately Station 370. The majority of this section of the common bulkhead is well insulated with a 4.75-inch thick, helium-gas-purged, 3/16-inch-cell phenolic glass honeycomb core. As previously discussed, a negative heat transfer with respect to the LOX tank exists in this section.

2. J-Joint Section: The J-joint section is defined as the section aft of the previoulsy mentioned forward section to the aft end of the J-joint (Station 296.7). This section includes a 6.75-inch-long segment of the common bulkhead that has the thinnest honeycomb core of $^{+0.25}_{-0.03}$ inch.

   Because of the extremely thin honeycomb core used in this section, high heat transfer is experienced across this area in a negative direction with respect to the LOX in the LOX tank. The nominal honeycomb core thickness (0.08 inch) was assumed for calculation purposes.

3. Common Bulkhead Equatorial Section: The equatorial section includes the area between the aft end of the J-joint (Station 296.7) and the LOX tank equator (Station 284). This section is enclosed in the bolting ring which utilizes an external insulation of polyurethane foam.

   Major heat sources affecting the heat transfer through this section are: (1) external ambient, (2) solar radiation, (3) earth emission, and (4) aerodynamic heat during boost. The external ambient considered in the analysis is the KSC hot day ambient. The solar radiation and the earth emission imposed on the insulation external surfaces are determined from the values stated in Reference 53. The current predicted aerodynamic heat transfer rates are used (Table 7.3.1.1-3).

c. Results (Overall Heat Transfer Rates of the Common Bulkhead): Referring to Figure 7.3.1.2-2, the overall heat transfer rate through the common bulkhead, shown by the heavy solid line, has negative values until approximately 255 seconds after liftoff. At this time the LOX level is about midway down the J-joint section. During this period, as shown by the additional curves presented in Figure 7.3.1.2-2, there is an increasing positive heat transfer rate into the LOX from the equatorial area. This increase is offset, however, by the combined negative heat transfer rate through the forward and J-joint sections.

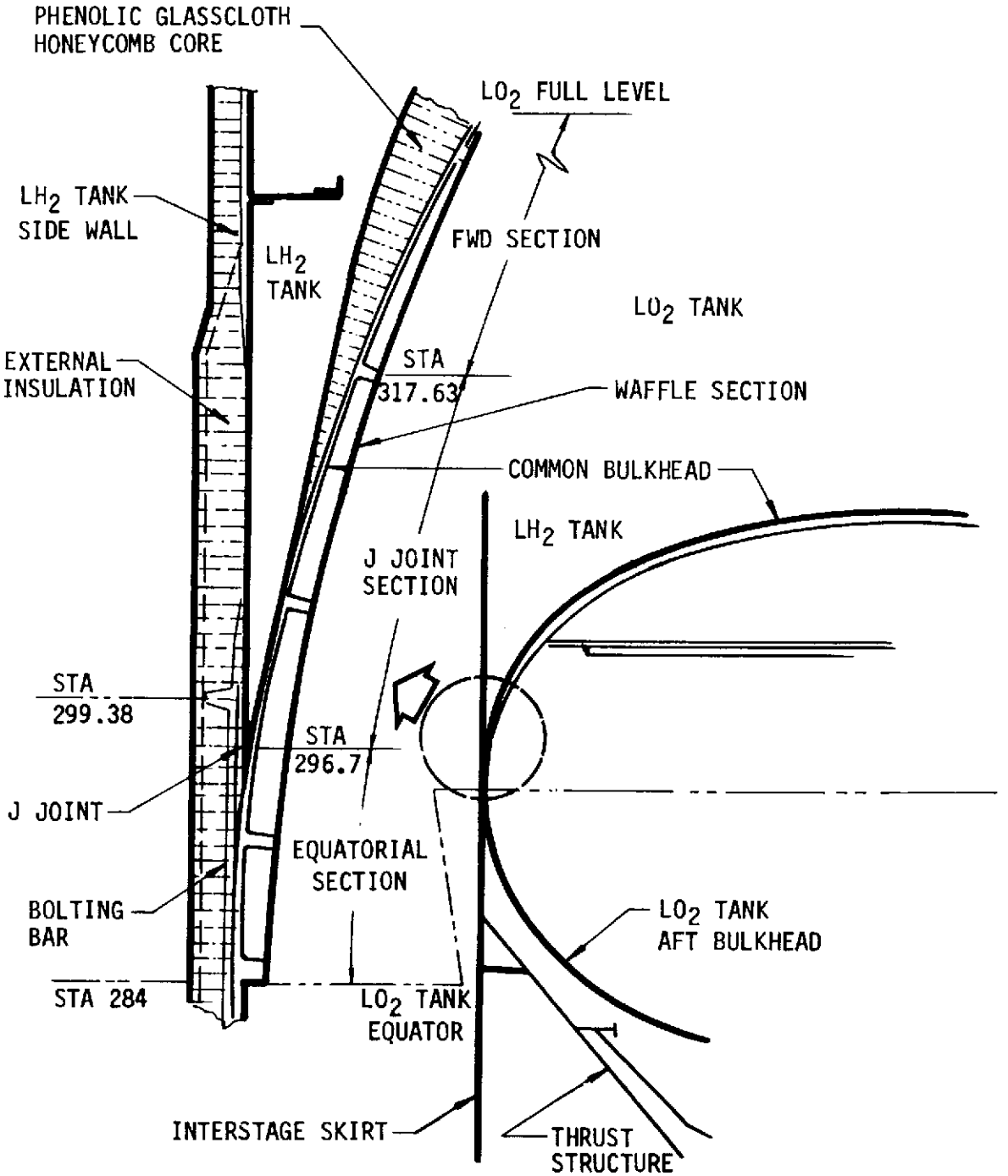

Figure 7.3.1.2-1. LO_2 Tank and Associated Stage Structures

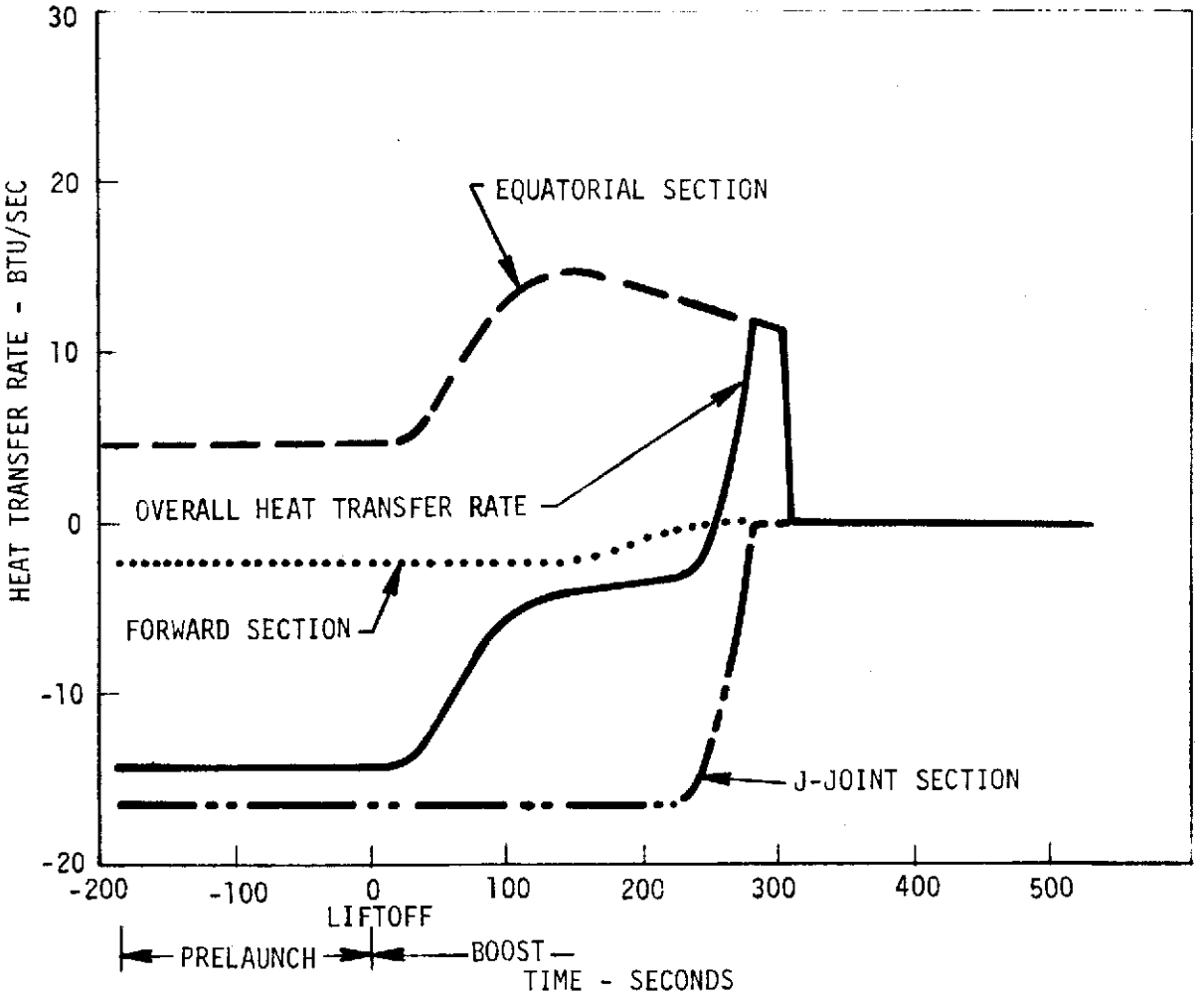

Figure 7.3.1.2-2. Heat Transfer Rates Through Common Bulkhead

This combined negative heat transfer rate vanishes, however, as the LOX level passes below the J-joint. The overall heat transfer rate than coincides with the positive heat transfer rate through the equatorial section. This also vanishes as the LOX level drops below the LOX tank equator.

7.3.1.3 Helium-Purged, Foam-Filled Honeycomb Mechanically Attached Over Bonded Foam Blocks (Forward Skirt Insulation)

The supporting analysis to determine the thermal performance characteristics of this insulation system assumed that the S-II forward skirt insulation was an extension of the basic sidewall insulation. Representative insulation and structural temperatures, ground-hold and launch heating rates to LH_2, and accumulated heat transfer for a typical S-II mission are presented in Paragraph 7.3.1.1, the LH_2 tank thermal study.

The foam-filled honeycomb system as used on S-II was purged with helium. The thermal conductivity of helium was used in the analysis to represent the conductivity of the foam.

7.3.1.4 Spray-on Foam

The thermal performance characteristics of spray-on foam insulation are: the transient temperature distribution during launch, the ground-hold heat transfer rate, and the accumulated heat leak to the LH_2 during ground-hold, S-IC boost, and S-II boost. The S-II design analyses are based on a 0.75-inch thickness of 2 lb/ft^3 density foam.

a. Statement of problem: Determine the insulation temperature distribution, heat transfer rate to LH_2, and total accumulated heat to LH_2 for the 0.75-inch LH_2 tank sidewall spray-on foam insulation during ground hold, S-IC boost, and S-II boost. The data are to be based on the design $\alpha = 0$ aerodynamic heating trajectory. Determine the LH_2 stratification conditions resulting from the imposed heat fluxes.

b. Methodology: The phenomenon of thermal stratification of a liquid under pressure is a direct result of the heat flux distribution. In the case of the S-II LH_2 tank, the majority of the input heat flux is through the sidewall. As a result, the heat flux is transported up the sidewall by the natural convection currents, establishing a thermal stratum. The temperature gradient in the stratum may be such that a portion of the LH_2 pumps, cannot be used. This results in a weight penalty from the LH_2 residual engine shutdown. During ground hold under ambient pressure, the heat leak to the LH_2 is dissipated in LH_2 boiloff which determines the LH_2 boiloff which determines the LH_2 topping-off rate. This analysis will aid in predicting the extent of thermal stratification in the LH_2 and determine the maximum hydrogen boiloff rate.

The heat leak into the LH_2 is through five major sections and two systems of the S-II. Referring to Figure 7.3.1.1-1, the major sections are the J-joint, common bulkhead, forward skirt, forward dome, and tank sidewall. The two systems are the LH_2 recirculation system and the J-2 engine LH_2 pumps. Other sources of heat leak, classified as miscellaneous heat leaks, are the LH_2 fill and drain valve and bolts which thread into the LH_2 tank.

The analysis reflects the latest vehicle design and propellant loading for S-II-8 and subs. The design configurations and assumptions are discussed in the following paragraphs.

1. Design Configuration:

   (a) J-Joint: By definition, the J-joint extends from Station 299.4 on the LH_2 tank sidewall to the intersection of the sidewall and the common bulkhead.

   (b) Common Bulkhead: The common bulkhead section is defined as that area of the common bulkhead not included in the J-joint definition. Sandwiched between the fore and aft aluminum facing sheets of the common bulkhead is the helium-purged, phenolic honeycomb core insulation. The common bulkhead is evaculated to a pressure of 3 psia or less before liftoff to reduce the heat transfer between the LOX tank and LH_2 tank.

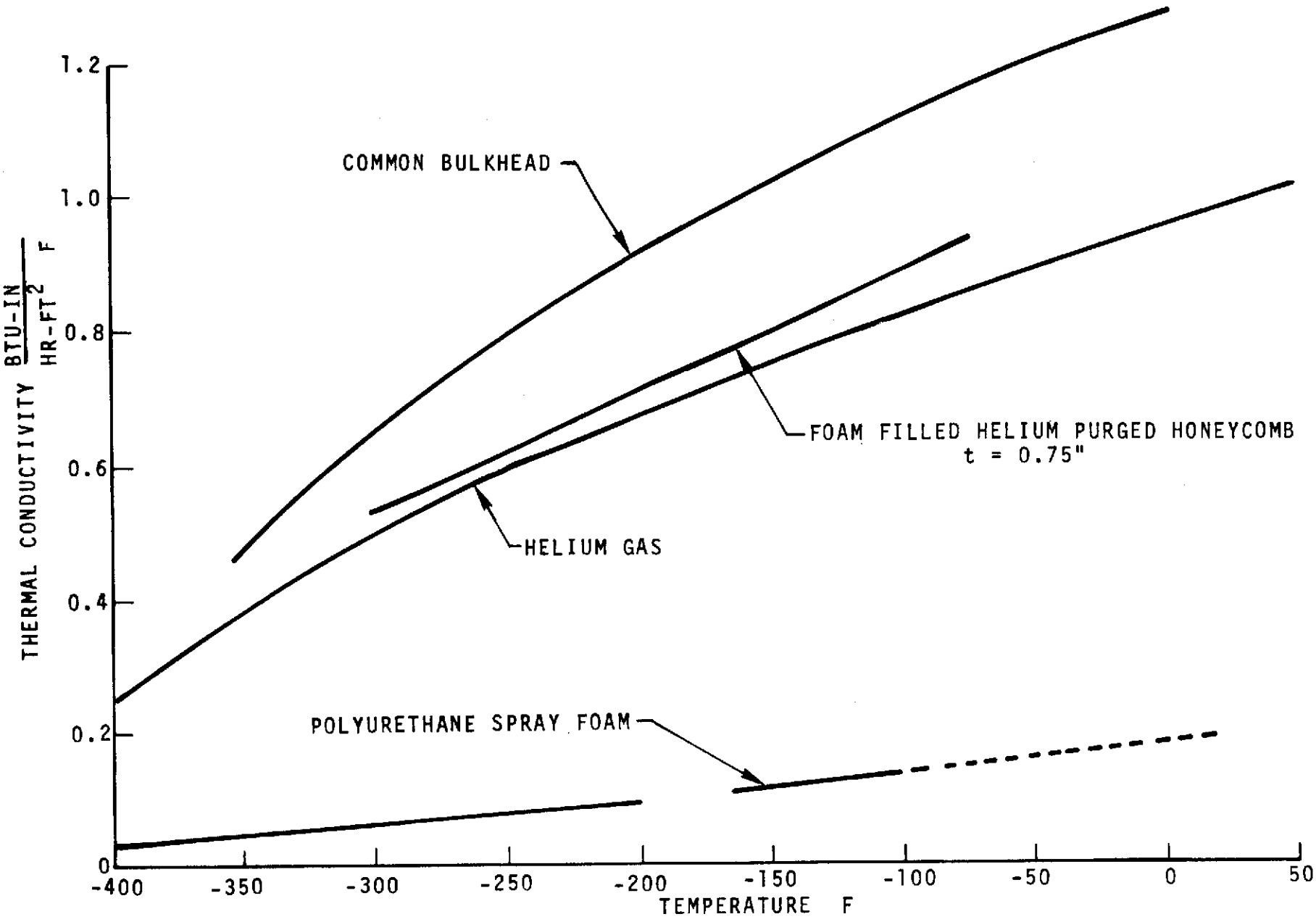

Figure 7.3.1.4-1. LH_2 Tank Insulation Thermal Conductivities

(c) Forward Skirt: The forward skirt from Station 819 on the LH_2 tank sidewall to the tangent point of the forward bulkhead and the sidewall at Station 823 is in close contact with the LH_2 tank. For S-II-8 and subs, the forward skirt is insulated with polyurethane spray foam.

(d) Forward Dome: The forward dome includes all of the forward bulkhead to the tangent point of the forward skirt and the sidewall at Station 823. The insulation on the forward dome on stages S-II-1 through -5 consists of a helium-purged, polyurethane foam-filled phenolic honeycomb. Insulation on S-II-6 and subs consists of polyurethane spray foam. The spray foam surface is sealed with a wet layup of nylon cloth and polyurethane resin.

(e) LH_2 Recirculation System: LH_2 is pumped from the LH_2 tank through the vacuum jacket LH_2 bypass lines and vacuum-jacketed LH_2 feed lines to the LH_2 pumps on the J-2 engines. Then the LH_2 is manifolded and returned to the LH_2 tank via the vacuum-jacketed return line.

(f) J-2 Engines' LH_2 Pumps: The bottom portion of the J-2 engines' LH_2 pumps are not insulated. Therefore, a considerable heat leak is realized in this area. From tests conducted by Rocketdyne and DACo., the heat leak is estimated to be 10 Btu/sec per engine.

(g) Miscellaneous: The system tunnel, LH_2 feed line fairings, LH_2 return line fairing, and LH_2 fill and drain valve fairing are attached to the vehicles by metal bolts which are threaded directly into the LH_2 tank. Likewise, the LH_2 fill and drain valve is attached directly to the LH_2 sidewall.

(h) Sidewall Insulation: This insulation system extends from Station 324.5 to Station 816.6. The sidewall insulation on stage S-II-8 and subs is 0.75-inch polyurethane spray foam. The outside surface of the spray foam is sealed with a coating of "Chemseal" polyurethane resin which in turn is coated with "dynatherm", a white vinyl paint (Figure 6.1.1.4-1).

. Propellant Loading and Mixture Ratio:

(a) Propellant Loading: The propellant loading for vehicles S-II-4 and subs is 970,000 pounds. The corresponding LH_2 level for the pressurized ground hold condition is at Station 880.

(b) Programmed Mixture Ratio: The effect of programmed mixture ratio (PMR) is considered in this analysis. The S-IC boost time used for the analysis was 155 seconds. The boost time for S-II is composed of 280 seconds with 5.5 oxidizer/fuel ratio and 93 seconds with 4.7 oxidizer/fuel mixture ratio.

(c) Insulation Thermal Conductivity: Thermal conductivities, k values, for the sidewall and forward dome foam filled helium purged honeycomb, the common bulkhead, spray foam, and helium gas are given in Figure 7.3.1.4-1.

The insulation composite shown in Figure 7.3.1.4-2 was divided into five sections representing the spray-on foam, one section representing the outer surface layer, and one section representing the aluminum tank wall. The heat flow path between sections or nodal temperatures was represented by equivalent conductances. The resulting thermal network representing the insulation composite was analyzed on a digital computer to determine nodal temperatures, heat rates to LH_2, and total heat into the LH_2 during ground hold and S-IC/S-II boost.

The total heat to the LH_2 through the LH_2 tank sidewall was determined by summing the heat through a square foot section during 90 seconds of ground hold, 155 seconds of S-IC boost, and 394 seconds of S-II boost. The net heat to the LH_2 from the tank sidewall was determined by multiplying the accumulated heat per square foot during ground hold through 50 seconds into S-II boost by the tank sidewall area. After 50 seconds of S-II boost, the LH_2 liquid level will reach the cylindrical portion of the LH_2 tank and the sidewall area exposed to LH_2 is reduced. The total heat to the LH_2 from 50 seconds of S-II boost to the end of S-II boost was computed by integrating the product of the heat rate times the effective wetted sidewall area versus time.

c. Assumptions:

1. Natural Environment (ambient temperatures is 99 F during ground hold):

(a) Hot Day:

(1) External heat transfer coefficient is $10 \frac{Btu}{hr\text{-}ft^2\text{-}^\circ F}$; corresponds to a wind speed of 45 mph

(2) Solar heating

(3) Radiation to ambient

(b) Nominal Day:

(1) Same as hot day above except external heat transfer coefficient is 1 Btu/hr-ft^2-°T.

2. Induced Environment: Aerodynamic design heating trajectory with $\alpha = 0$ is obtained from Figure 4.2.2.3-1.

3. Propellant Loading: S-II-4 and subs are loaded with 970,000 pounds of propellant.

(1) Ground hold pressurized LH_2 level is at Station 880.

NOTE: PT'S 1 THRU 7 ARE NODE LOCATIONS
USED IN TEMPERATURE ANALYSIS

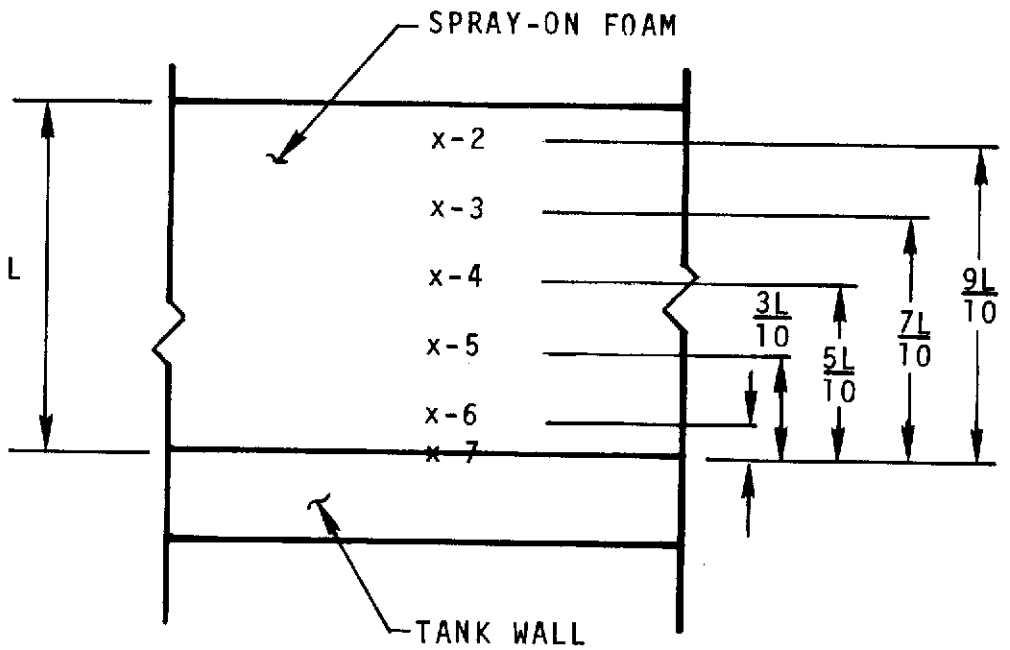

L = DEPTH OF FOAM

P_T (NODE)	DISTANCE FROM TANK WALL TO P_T IN FOAM			
	L = 1.0"	L = 0.75"	L = .50"	L = 0.25"
1	1.00	0.750	0.50	0.250
2	0.90	0.675	0.45	0.225
3	0.70	0.525	0.35	0.175
4	0.50	0.375	0.25	0.125
5	1.30	0.225	0.15	0.075
6	0.10	0.075	0.05	0.025
7	0	0	0	0

Figure 7.3.1.4-2. Foam Insulation Node Location

(2) Ground hold pressurized LOX level is at Station 368.35.

4. Times for which heat leak is calculated:

   (a) Ground hold - 90 seconds

   (b) S-IC boost - 155 seconds

   (c) S-II boost - 373 seconds

5. Heat flux through the J-2 engines' LH_2 pump is 36,000 $\frac{Btu}{Hr}$ per engine (10 Btu/second).

6. No frost or ice formation on the sidewall insulation.

7. Heat transfer from the LH_2 tank ullage gas to the LH_2 is neglected.

8. Heat conducted from the non-wetted LH_2 tank sidewall down the sidewall into the LH_2 is n eglected.

9. LH_2 Tank Insulation:

   (a) Sidewall (area is 4480 square feet) S-II-8 and subs -0.75-inch polyurethane spray foam:

      (1) Emissivity is 0.9.

      (2) Solar absorptivity is 0.3.

      (3) Specific heat is 0.3 $\frac{Btu}{lb\ °F}$

      (4) Density is 2.0 lb/ft^3, density of the seal coat was considered negligible.

      (5) Apparent thermal conductivity versus temperature is presented in Figure 7.3.1.4-1.

   (b) Forward Dome.

   (c) Common Bulkhead, S-II-1 and subs:

      (1) The insulation is 4.75-inch-thick helium-purged phenolic honeycomb core.

      (2) Apparent thermal conductivity versus temperature is presented in Figure 7.3.1.4-1. Also, at the end of S-II boost, the thermal conductivity of the insulation is 75 percent of the value at liftoff.

      (3) Specific heat is 0.18 $\frac{Btu}{lb_m-°F}$ at -100 F and varies with temperature

      (4) Density is $\frac{lb_m}{Ft^3}$

d. Results and Conclusions: Predicted transient temperatures at different points through the 0.75-inch-thick spray-on foam insulation system on the S-II-8 sidewall is presented in Figure 7.3.1.4-3. The maximum external surface temperature of 568 F occurs approximately 140 seconds after lift-off (time zero).

Predicted LH_2 boiloff rates for hot day and nominal day ground hold conditions are presented in Table 7.3.1.4-1. The predicted hot day LH_2 boiloff rate is approximately 2.4 percent of full load per hour. The accuracy of the LH_2 boiloff rate prediction has been verified by S-II testing. A comparison of predicted versus experimental boiloff rates is presented in Figures 7.3.1.4-4 and 7.3.1.4-5, and is discussed below.

The experimental estimates of LH_2 boiloff rate were determined from liquid level (fine mass system) sensor data recorded at the Mississippi Test Facility (MTF) during the S-II-8 cryoproof test and the S-II-9 static firing test. The average experimental LH_2 boiloff rate of 1.84 percent per hour for S-II-8 and 2.2 percent per hour for S-II-9 compare favorably with the predicted LH_2 boiloff rate of 2.1 percent per hour for nominal day conditions. The increased LH_2 boiloff rate of S-II-9 is due primarily to a higher environment temperature during testing. These test results indicate a good correlation between analysis and experiment and, thereby, verify theoretical thermal conductivity values in the predictive analyses.

The expected temperatures in certain sections reach values that are above the allowable temperature of the foam for the maximum or design heating trajectory. The values are shown on Figure 7.3.1.4-3. This design trajectory is more severe than would be expected for a flight condition. The analysis assumed that there was no paint as a heat absorber and protector and the heating rates that were provided are believed to be conservative. It was also determined that a melting or degradation of the foam would require more time at higher temperatures than was available in the boost trajectory for the non-reusable vehicle. A study was made to determine the effects from any possible erosion. The results are shown in Figure 7.3.1.4-6. It is apparent that even if the foam were to erode during boost it would not adversely affect the flight.

Table 7.3.1.4-2 lists the heat leak from various sources for S-II-8 and subsequent vehicles. The total mission heat leak into LH_2 is 88,250 Btu. This total represents a substantial reduction in total heat leak from the approximately 200,000 Btu predicted for S-II-1 through S-II-7. Approximately 60 percent of the total, or 52,240 Btu, is through the sidewall insulation.

7.3.1.5 Spray-On Foam Plus Foam Blankets

The thermal performance characteristics of this insulation system are presented assuming that the system is applied to a structural skirt protruding from a tank containing LOX which is subjected to both groundhold and launch environments. The S-II point design analyses determine the heat leak into LOX through the equatorial section of the common bulkhead.

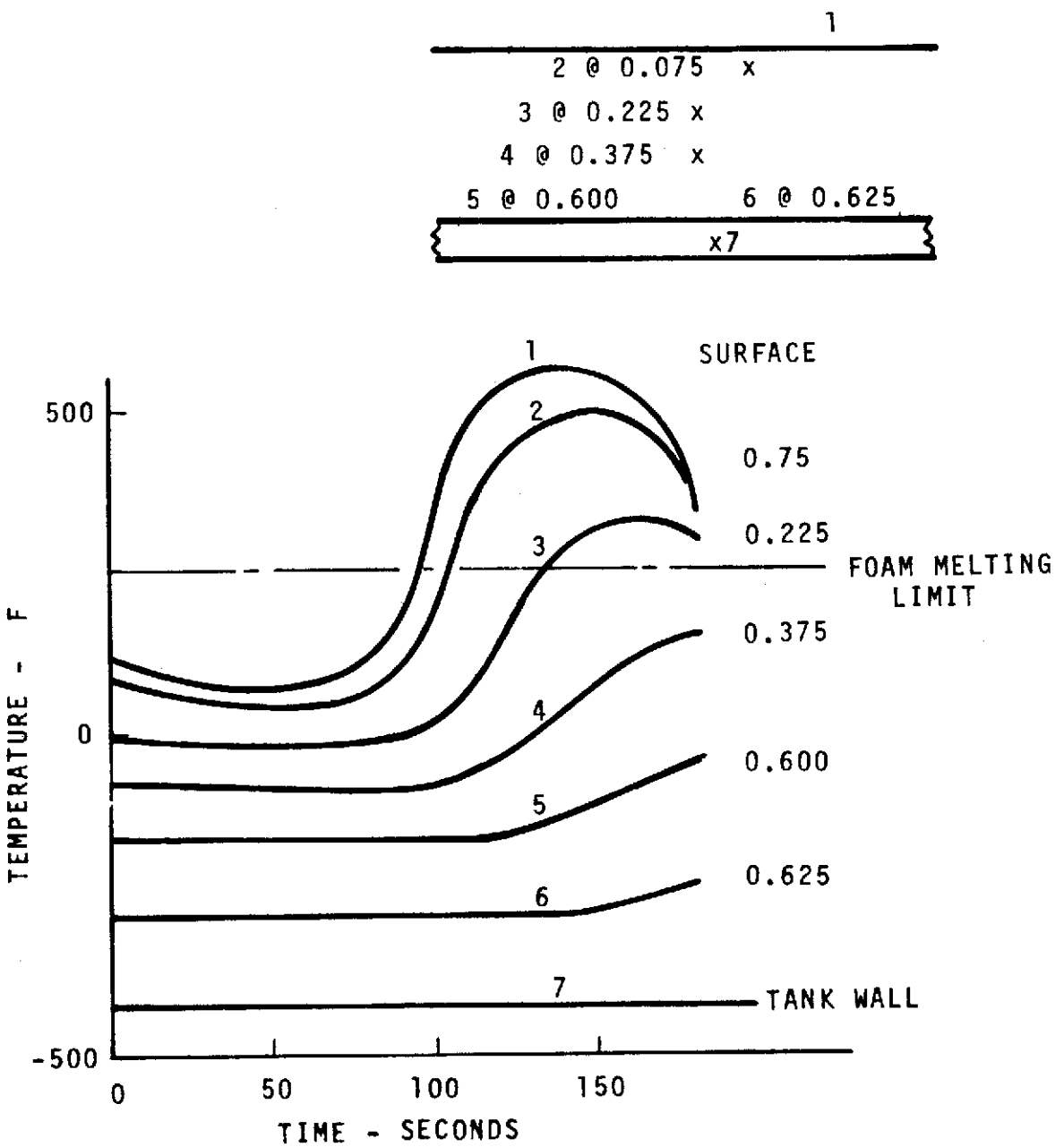

Figure 7.3.1.4-3. Predicted Transient Temperature Through 0.75-Inch Spray-on Foam Insulation

Table 7.3.1.4-1. LH_2 Boiloff During Ground Hold

SPRAY-ON FOAM

	S-II-1, 2, 3	S-II-4, 5	S-II-6, 7	S-II-8 AND SUBS
TOTAL LH_2 ABOARD LBS	153,000	158,500	158,500	158,500
	HOT DAY CONDITIONS			
HEAT LEAK RATE BTU/HR	1,585,000	1,610,000	1,460,000	710,000
BOILOFF RATE LBS/HR	8,330	8,450	7,680	3,740
PERCENTAGE OF TOTAL LH_2 PER HR.	5.4	5.3	4.8	2.4
	NOMINAL DAY CONDITIONS			
HEAT LEAK RATE BTU/HR	1,422,000	1,442,000	1,253,000	644,000
BOILOFF RATE LBS/HR	7,490	7,600	6,610	3,490
PERCENTAGE OF TOTAL LH_2 PER HR.	4.9	4.8	4.2	2.1

NOTE:

1) THIS TABLE PROVIDES COMPARATIVE INFORMATION AND IS PROVIDED HERE FOR COMPLETENESS. ONLY THE COLUMN FOR S-II-8 AND SUBS APPLIES TO THIS SECTION

2) CONFIGURATION CHANGES:

a) HELIUM PURGE HONEYCOMB FOR S-II-1 THRU -7
b) LARGER PROPELLANT LOADING AT S-II-4
c) SPRAY FOAM ON FWD BULKHEAD AT S-II-6

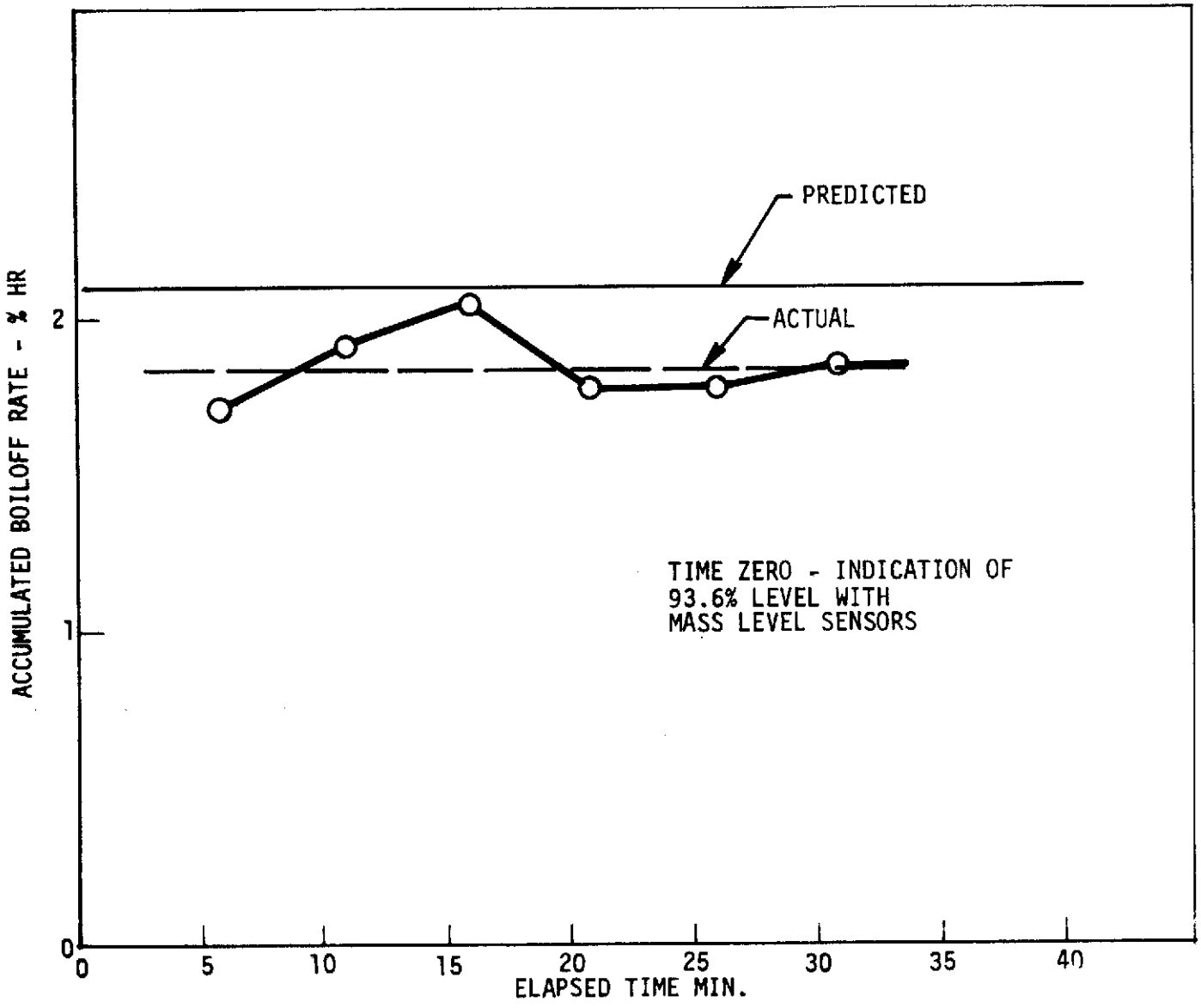

Figure 7.3.1.4-4. Predicted and Experimental LH_2 Boiloff Rates for S-II-8 Cryoproof Test

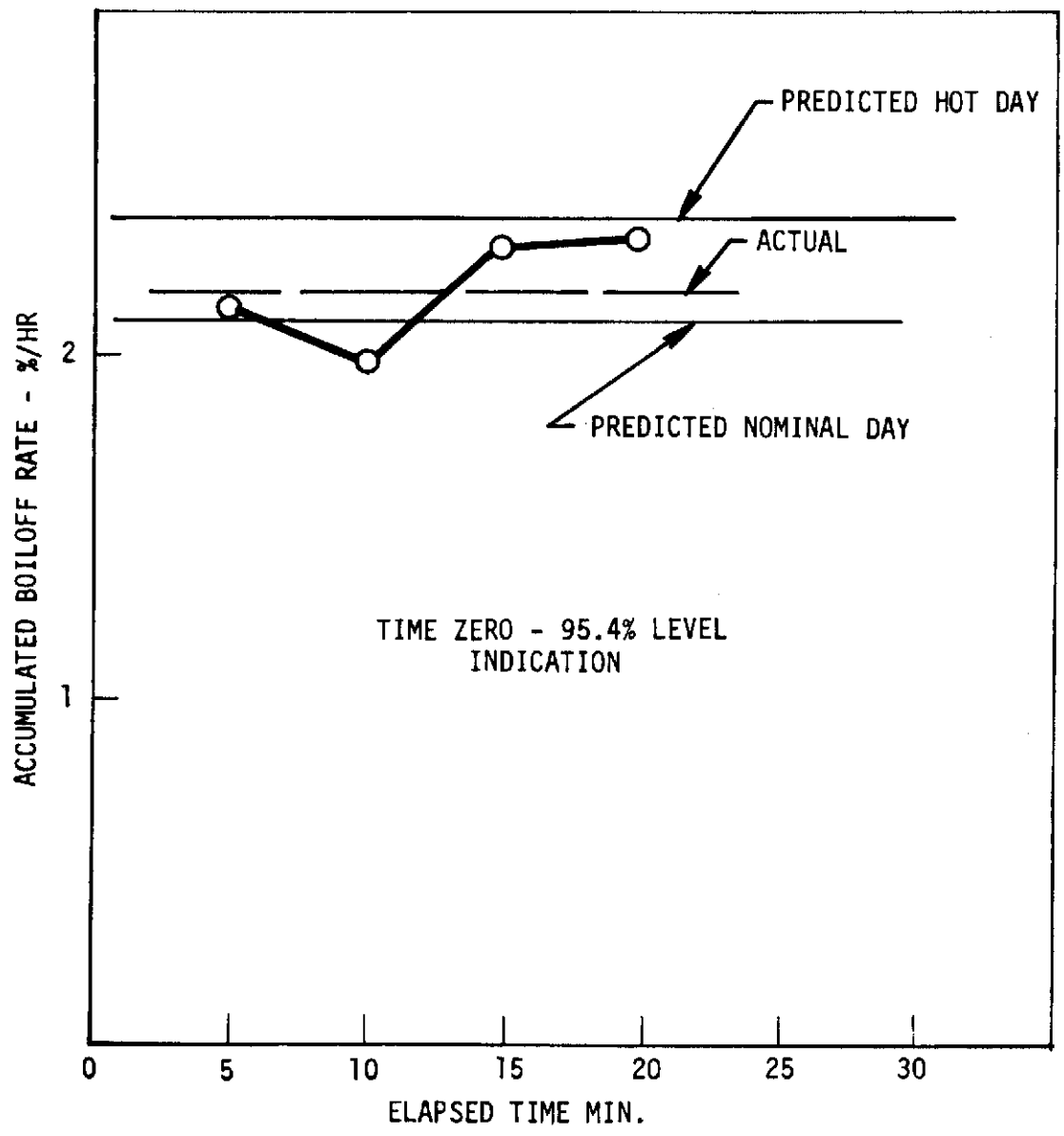

Figure 7.3.1.4-5 Predicted and Experimental LH_2 Boiloff Rates for S-II-9 Static Firing

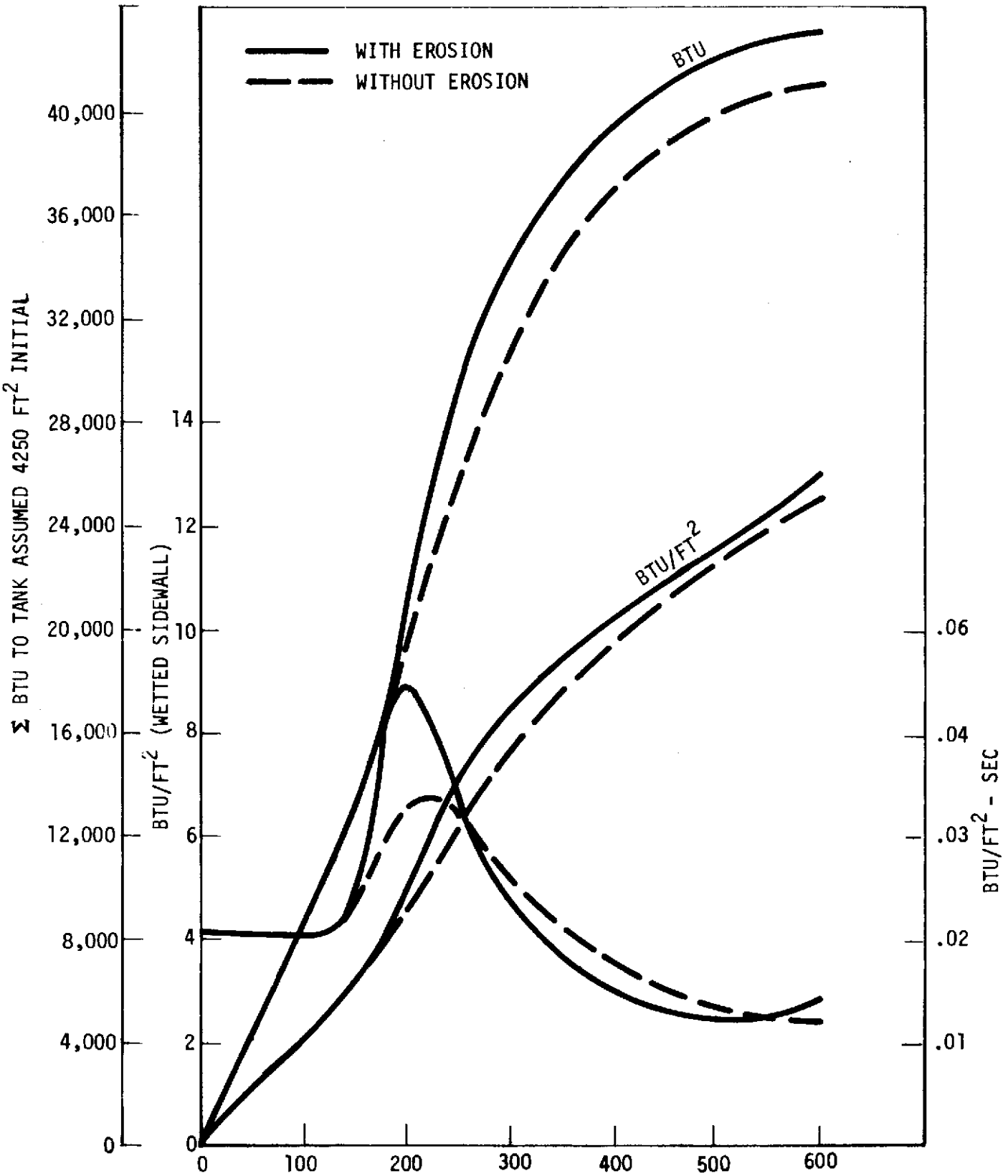

Figure 7.3.1.4-6. 0.75-Inch Spray Foam Heat Leak With and Without Erosion

Table 7.3.1.4-2. Heat Leak Into LH_2

	SIDE WALL	"J" JOINT	COMMON BLKHD.	FWD SKIRT	FWD DOME	LH_2 RECIRC. SYSTEM	J-2 ENGINES LH_2 PUMPS	MISC.	TOTAL
S-II-1, 2, AND 3									
GROUND HOLD	26,430	1,580	240	740	5,040	250	4,500	830	39,610
S-IC BOOST	45,790	2,730	410	1,210	8,680	350	7,750	1,550	68,470
S-II BOOST	77,910	7,800	950	370	2,520	—	—	1,150	90,700
TOTAL	150,130	12,110	1,600	2,320	16,240	600	12,250	3,530	198,780
S-II-4 AND 5									
GROUND HOLD	26,430	1,580	240	740	5,580	250	4,500	830	40,150
S-IC BOOST	45,790	2,730	410	1,210	9,610	350	7,750	1,550	69,400
S-II BOOST	85,020	8,180	1,195	370	2,790	—	—	1,235	98,790
TOTAL	157,240	12,490	1,845	2,320	17,980	600	12,250	3,615	208,340
S-II-6 AND 7									
GROUND HOLD	26,430	1,580	240	740	900	250	4,500	830	35,470
S-IC BOOST	45,790	2,730	410	1,210	1,540	350	7,750	1,550	61,330
S-II BOOST	85,020	8,180	1,195	370	450	—	—	1,235	96,450
TOTAL	157,240	12,490	1,845	2,320	2,890	600	12,250	3,615	193,250
S-II-8 AND SUBS SPRAY-ON FOAM									
GROUND HOLD	8,710	1,580	240	740	900	250	4,500	830	17,750
S-IC BOOST	14,980	2,730	410	1,210	1,540	350	7,750	1,550	30,520
S-II BOOST	28,550	8,180	1,195	370	450	—	—	1,235	39,980
TOTAL	52,240	12,490	1,845	2,320	2,890	600	12,250	3,615	88,250

NOTE:

1) THIS TABLE PROVIDES COMPARATIVE INFORMATION AND IS PROVIDED HERE FOR COMPLETENESS. ONLY THE COLUMN FOR S-II-8 AND SUBS APPLIES TO THIS SECTION.

2) CONFIGURATION CHANGES:

a) HELIUM PURGE HONEYCOMB FOR S-II-1 THRU S-II-7
b) LARGER PROPELLANT LOADING AT S-II-4
c) SPRAY FOAM ON FWD BULKHEAD AT S-II-6

a. Statement of Problem: Determine the heat transfer rates and total accumulated heat transfer into the LOX tank through the common bulkhead and Cylinder #1/bolting ring during a 186-second prelaunch LOX tank pressurization hold and through S-IC/S-II boost for stage S-II-4 and subs.

b. Methodology and Analysis: The heat transfer rate to LOX in the LOX tank is needed to support the design and evaluation of the propellant and LOX tank pressurization systems and to predict the resulting LOX losses from boiloff. The heat transfer was computed for a 710-second S-II mission time which includes:

186 seconds - Preluanch/LOX tank pressurization hold

150 seconds - S-IC boost

374 seconds - S-II boost

The prelaunch ground hold period extends from vent valve closing (initiation of LOX tank pressurization) to liftoff and differs from other ground-hold periods when the vent valve is open. The analysis reflects the latest stage structure and tank design and the latest propellant loading and tank depletion rates for stage S-II-4 and subs.

The major areas of the LOX tank that affect heat transfer into the LOX are the common bulkhead, aft bulkhead, and components of four associated systems. The common bulkhead forms the upper half of the LOX tank shell structure, separating the LOX tank from the LH_2 tank. The common bulkhead is divided into three sections for analysis purposes (see Figure 7.3.1.2-1). The forward section extends from Station 317.63 forward to the LOX tank full level at approximately Station 370. The majority of this section is insulated with evacuated honeycomb, as discussed previously. The J-joint section is defined as the section aft of the forward section to the aft end of the J-joint (Station 296.7). This section includes a 6.75-inch segment of the common bulkhead with the thinnest honeycomb core and the highest heat transfer rate from LOX to LH_2. The equatorial section includes the area between the aft end of the J-joint (Station 296.7) and the LOX tank equator (Station 284). This section is enclosed by the Cylinder #1 bolting ring which utilizes polyurethane foam as external insulation.

The major heat sources affecting heat transfer through the equatorial section of the common bulkhead are the external ambient, solar radiation, earth emission, and aerodynamic heating. The KSC hot day environment is defined in Paragraph 4.1.1.2. The launch environment used is the maximum aerodynamic heating trajectory for the LOR mission shown in Figure 4.2.2.3-1. The effective thermal conductivity of this insulation system is identical to that given for the spray-on foam given in Figure 6.1.4.3-1.

c. Results and Conclusions: The computed heat transfer rate history through the bolting ring and equatorial section of the common bulkhead is presented in Figure 7.3.1.5-1. The heat transfer rate of 4.3 Btu/sec during prelaunch LOX tank pressurization hold is equivalent to a heat flux of approximately 140 Btu/hr/ft^2. The maximum heat flux of 550 Btu/hr/ft^2 (16.8 Btu/sec) during launch occurs approximately 150 seconds after liftoff.

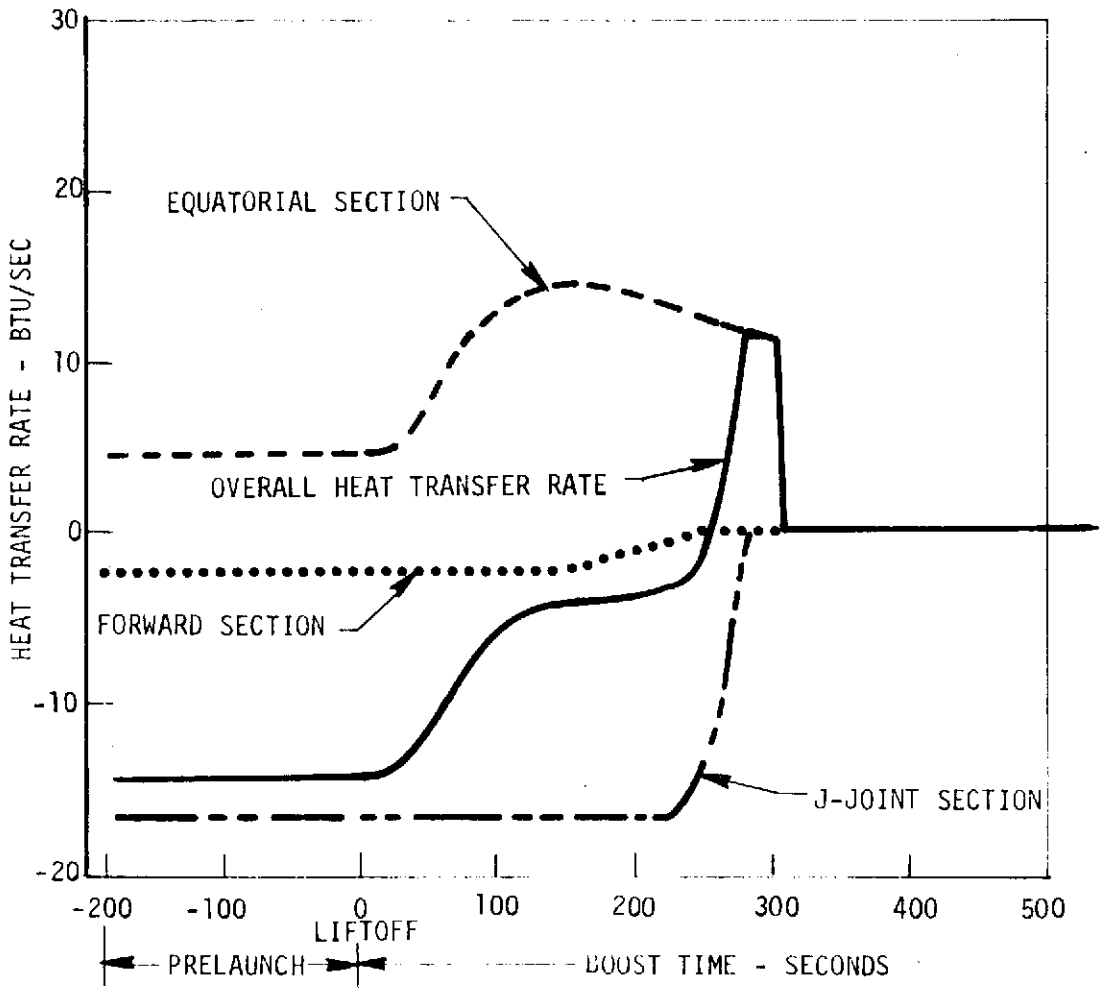

Figure 7.3.1.5-1. Heat Transfer Rates Through Common Bulkhead

The total accumulated heat leak to LOX throughout the nominal S-II mission is approximately 4500 Btu, or 41 Btu/ft^2.

For comparison, the overall heat transfer rate and the component heat rates through the forward and J-joint sections are presented also in Figure 7.3.1.5-1. It is interesting to note that the net heat transfer rate to LOX is negative.

7.3.1.6 Pour Foam Performance

Analysis for pour foam is the same as spray-on foam (see Paragraph 7.3.1.4).

7.3.1.7 Pour Foam Block Performance

Analysis for pour foam blocks and blankets is the same as that listed for spray-on foam (see Paragraph 7.3.1.4).

The actual performance of the spray-on foam and the blocks are expected to be slightly different only by the effect of bonding material at the edges as compared to a thicker rind. These differences are below the level of analysis as performed.

7.3.1.8 Cork

In areas of high aerodynamic heating due to multiple protrusion and interference effects, cork has been bonded to the foam surface to prevent possible foam erosion. In these areas, the bondline temperatures during S-IC boost are required to remain below 200 F. The cork thickness assumed the analyses was 1/4 inch.

The predicted temperatures determined are based on the maximum design conditions. Temperatures were predicted using a one-dimensional analog network thermal model for use with the general thermal analyzer digital computer program. Modes of heat transfer considered were solar radiation, aerodynamic heating, radiation from surface, and conduction through the insulation; ablation effects were neglected. Initial temperatures at liftoff were predicted based on hot day design ground conditions.

The following cork properties were assumed: solar absorptivity of 0.3, emissivity of 0.8, specific heat of 0.5 Btu/lb-°F, density of 30 lb/ft^3, and thermal conductivity of 0.05 Btu/ft-hr-°F. The properties for foam (spray-on and pour) are listed in the foam section.

In Figures 7.3.1.8-1 through 7.3.1.8-4 the regions affected by aerodynamic heating are illustrated. Figure 7.3.1.8-5 shows typical foam surface temperature histories that would result without cork protection. Figure 7.3.1.8-6 presents the cork surface and bondline temperature histories in the regions of high aerodynamic heating.

Since the affected regions include various insulating configurations, Table 7.3.1.8-1 presents temperature data for all S-II insulation combinations for each region. From the table, it is seen that 0.25-inch cork protection will keep most bondline temperatures below 200 F during S-IC boost as required. There are three small regions in the vicinity of the LH_2 recirculation line which would exceed a bondline temperature of 200 F before 200 seconds of S-IC/S-II boost. The total area encompassed by these regions is less than 5 square feet. Therefore, even if the cork were to debond in these areas and the foam underneath were melted, the resulting heat leak is well within tolerances.

In addition to the above analysis, a comparison was made using assumed cork densities of 8 and 30 lb./ft^3 with and without a 0.02-inch fiberglass phenolic cover. The cork thickness assumed was 0.25 inch in all cases. Figure 7.3.1.8-7 shows the temperature histories for the cork-form bondline and the surface temperatures of the fiberglass cover for both 8 and 30 lb./ft^3 cork. Figure 7.3.1.8-8, without the fiberglass cover, shows the cork surface and cork-foam bondline temperature histories for the 8 and 30 lb./ft^3 cork. Also shown in Figure 7.3.1.8-8 is the maximum bondline temperatures for various thicknesses of 30 lb./ft^3 cork. This analysis was performed using the interference heating

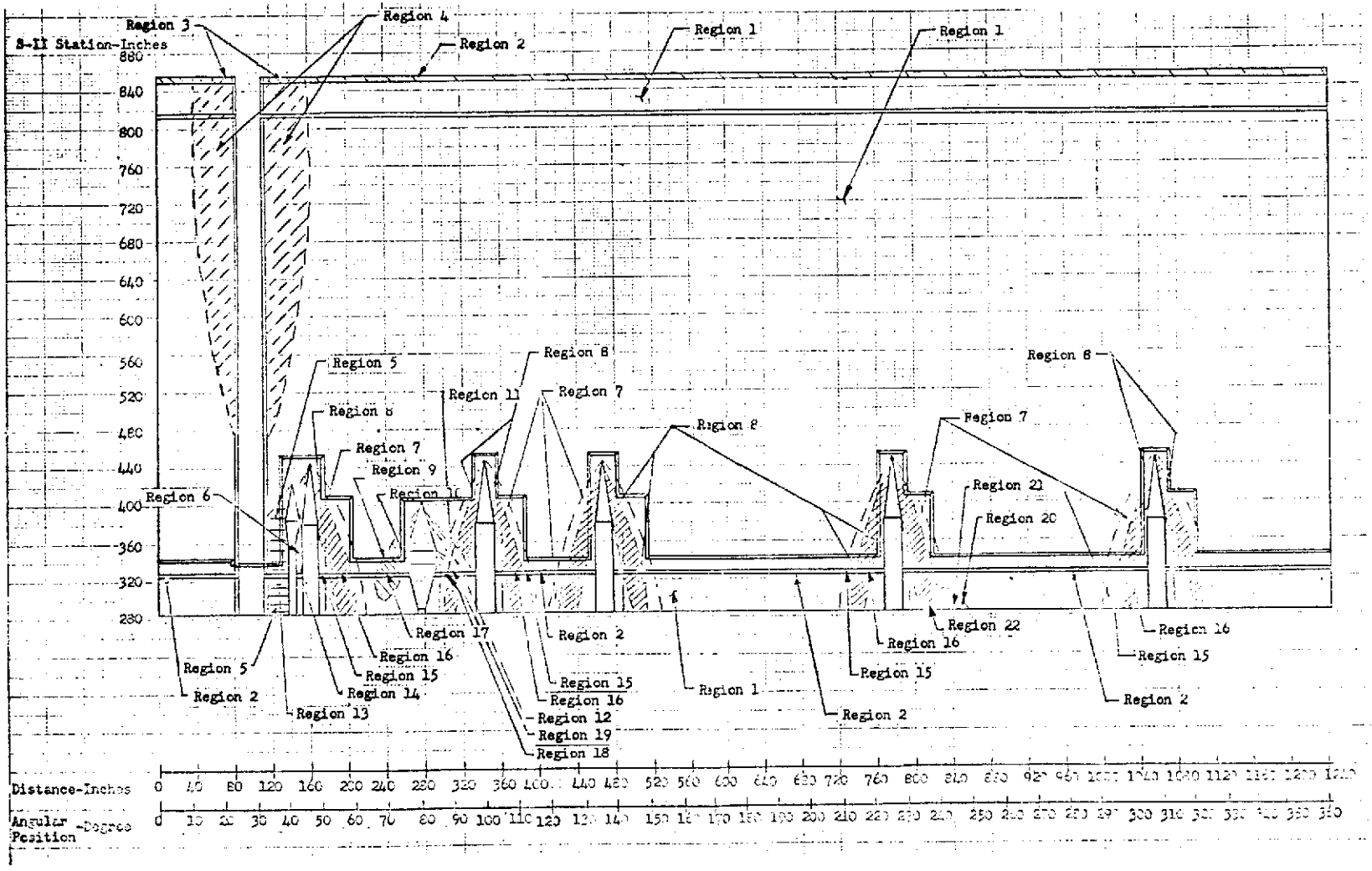

Figure 7.3.1.8-1. LH_2 Tank Sidewall Insulation Protuberance Regions

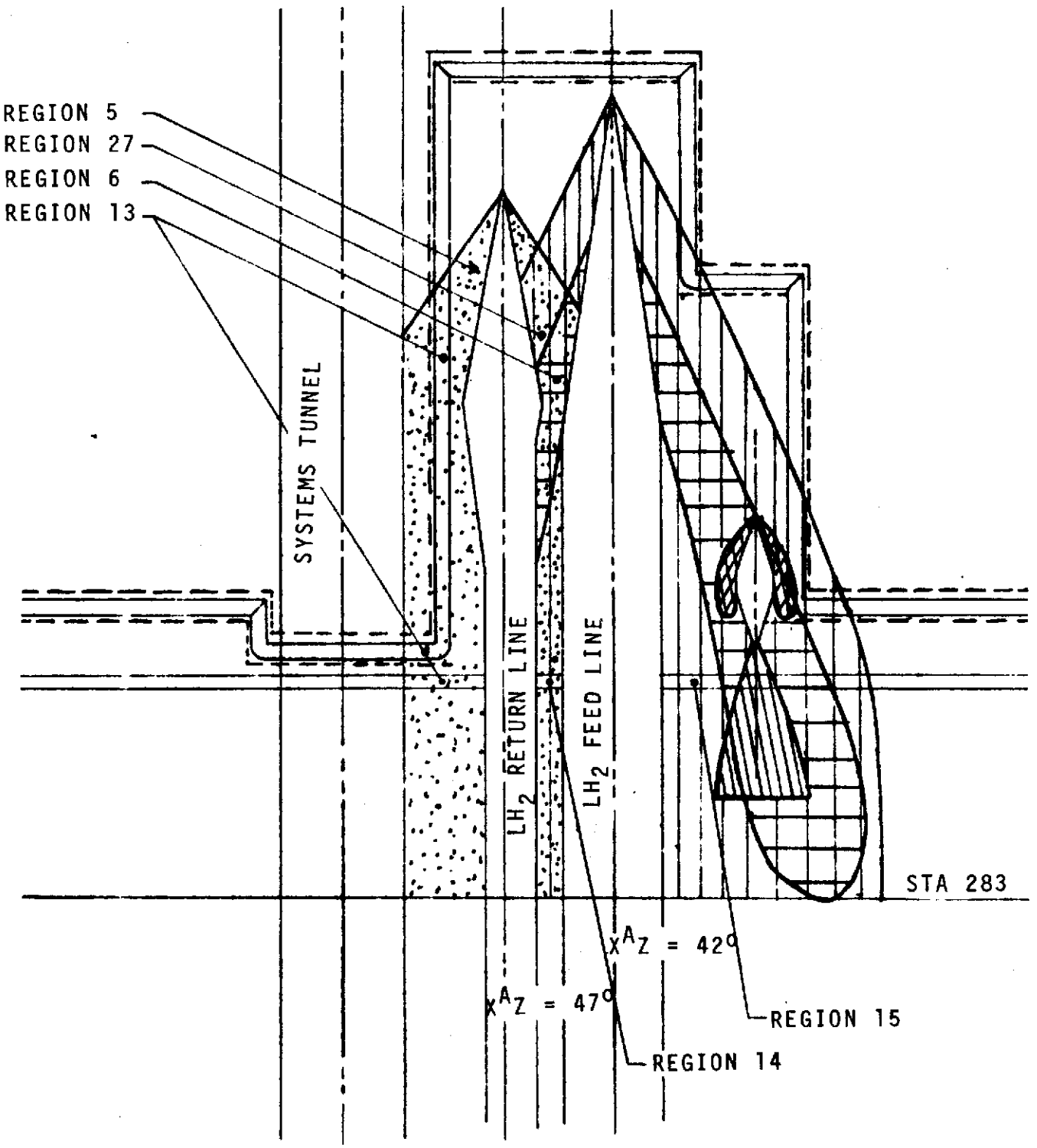

Figure 7.3.1.8-2. Surface Regions Influenced by Interference Heating

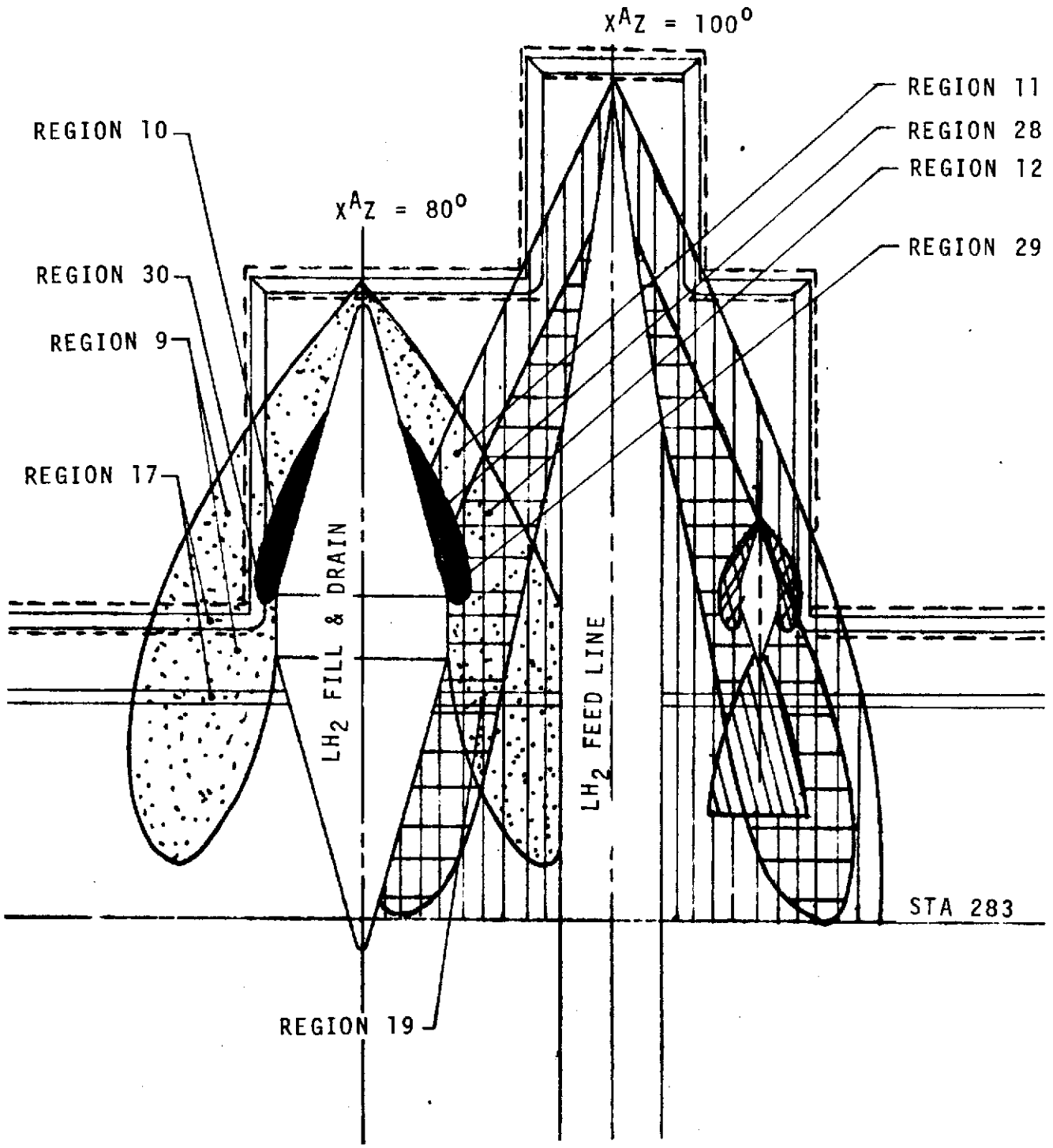

Figure 7.3.1.8-3. Surface Regions Influenced by Interference Heating

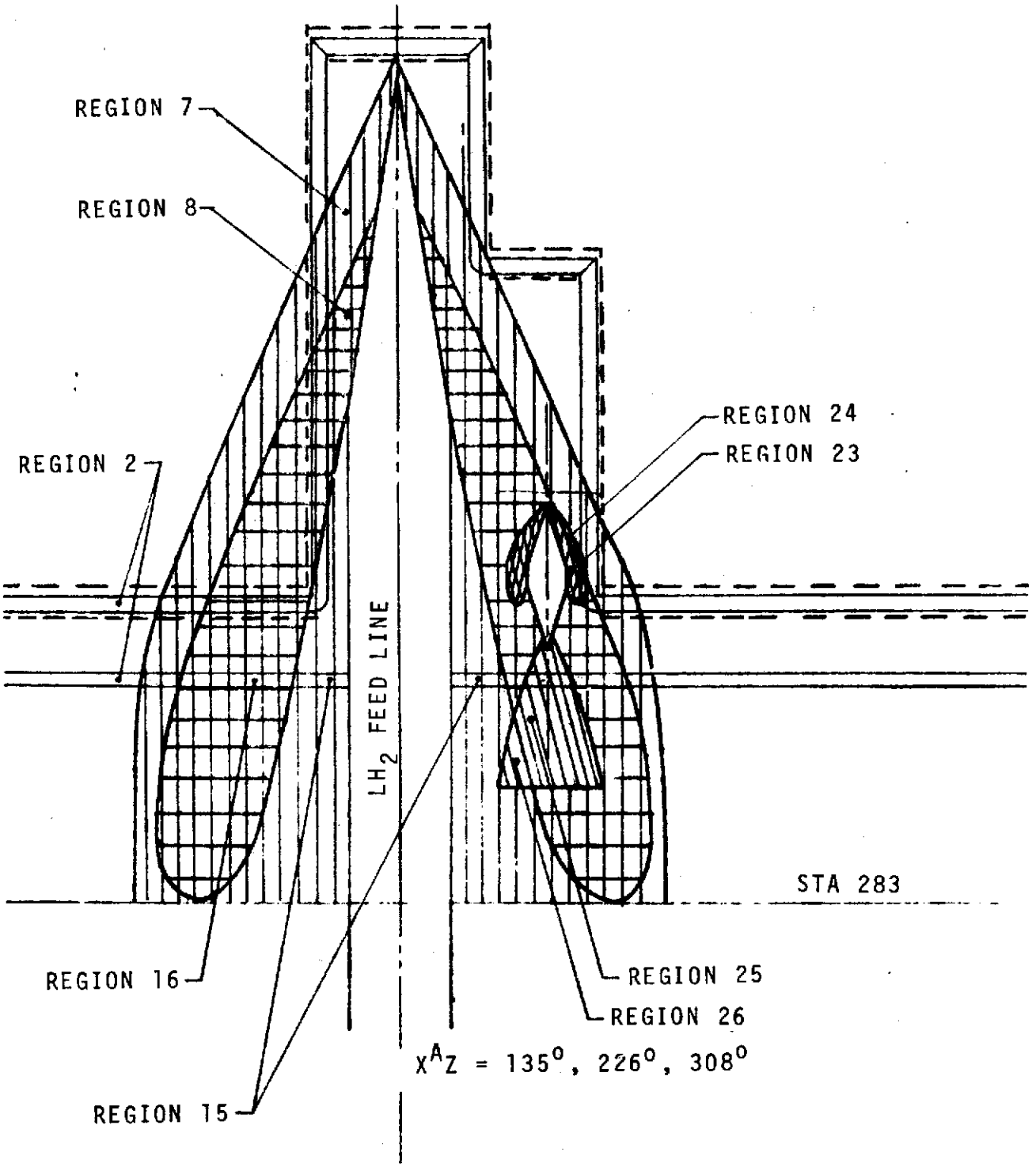

Figure 7.3.1.8-4. Surface Regions Influenced by Interference Heating

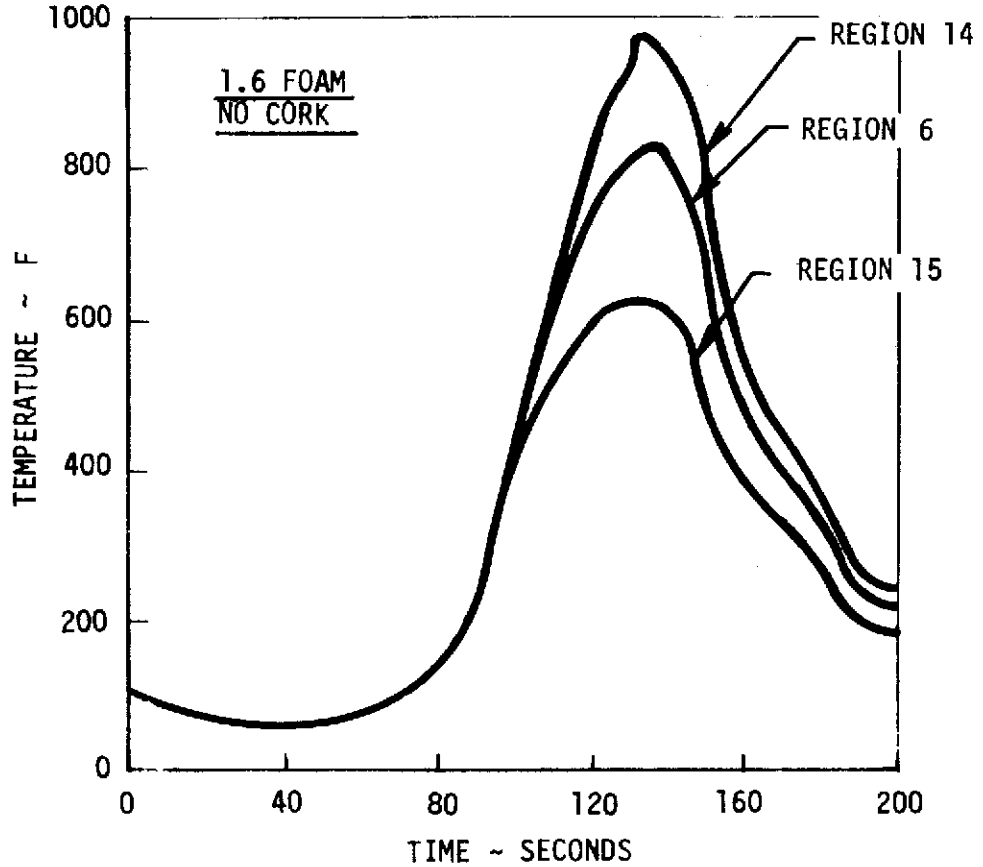

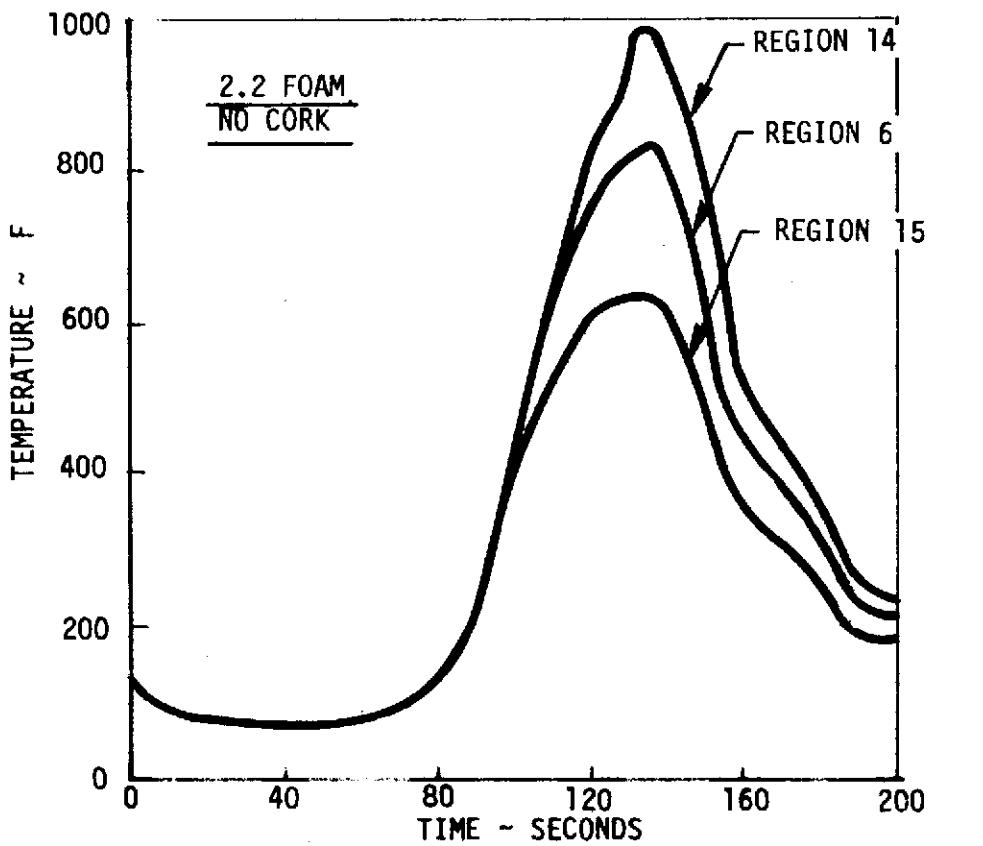

Figure 7.3.1.8-5. LH_2 Tank Sidewall Spray Foam Insulation Temperature History

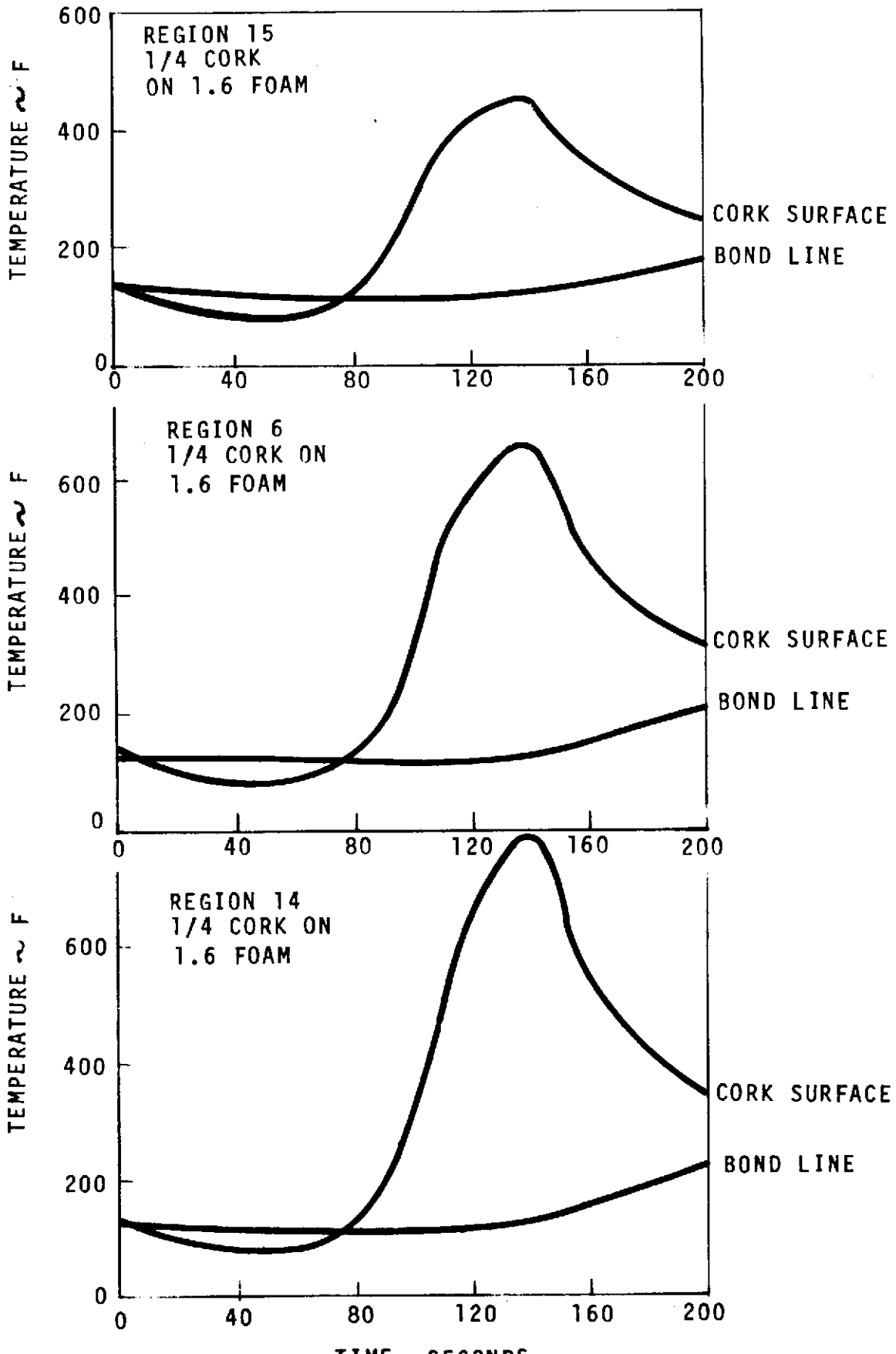

Figure 7.3.1.8-6· Typical Time-Temperature History-Cork Surface and Bond Line

Table 7.3.1.8-1 LH_2 Tank Sidewall Insulation Protuberance Regions

REGION	PF	3/4 FOAM				1.6 FOAM				2.2 FOAM			
		T_1	T_2	T_{150}	T_{200}	T_1	T_2	T_{150}	T_{200}	T_1	T_2	T_{150}	T_{200}
1	1.0	518	324	92.4	121.6	525	334	122	150	530	335	130	159
2	1.55	605	399.4	95.8	135.4	610	408	126	164	620	408	133	172
3	2.195	680	471	99.1	149	685	480	129	178	690	479	137	186
4	1.416	586	384	95	133	590	393	125	162	600	393	133	170
5	3.221	760	560	102.8	164.5	765	568	132	193	770	565	140	200
6	4.068	850	629	105	175	860	630	135	203	865	632	142	212
7	1.2	550	351	93	126	553	360	123	155	560	360	130	163
8	1.72	625	416	96	137	630	425	126	167	635	424	134	174
9	1.2	550	355	94	128	555	365	124	157	560	365	132	165
10	1.64	616	412	97	138	620	421	127	167	627	420	134	175
11	1.44	590	384	95	132	595	394	125	162	605	393	133	170
12	2.065	665	455	98	145	670	463	128	174	680	462	136	182
13	4.92	892	668	107	184	900	699	136	212	910	696	144	221
14	6.29	981	746	109	195	990	794	139	223	995	791	146	232
15	1.86	645	432	97	141	650	442	127	170	655	440	134	178
16	2.66	725	510	100	154	735	524	130	183	740	523	137	191
17	1.86	645	437	98	142	650	445	127	171	655	444	135	179
18	2.232	683	472	99	148	690	484	129	177	700	483	136	185
19	3.264	770	555	102	162	775	572	132	191	785	571	139	199
20	1.388	581	378	95	132	590	387	125	161	595	387	132	169
21	1.700	625	415	96	138	630	424	126	167	635	423	134	175
22	2.38	694	484	99	150	700	497	129	179	710	497	136	187
23	2.1798	678	466	98	146	685	474	128	175	690	473	136	183
24	1.51	600	393	95	134	605	402	125	163	610	402	133	171
25	2.707	728	517	101	156	735	524	130	184	740	522	138	192
26	1.877	650	438	98	143	655	446	127	171	660	445	135	179
27	3.213	770	557	102	163	780	576	132	192	785	575	140	200
28	2.104	670	460	98	146	675	469	128	175	680	469	136	183
29	3.034	750	542	102	160	760	552	131	189	765	551	139	197
30	2.797	728	519	101	157	735	527	131	186	740	525	139	195
31	1.05	530	332	93	123	535	342	123	152	540	343	130	160

PF = PROTUBERANCE FACTOR AT 130 SECONDS FROM LIFTOFF

T_1 = FOAM SURFACE TEMPERATURE (F) FOR NOTED FOAM THICKNESS AND NO CORK

T_2 = CORK SURFACE TEMPERATURE (F) FOR NOTED FOAM THICKNESS AND 1/4 CORK

T_{150} = CORK BONDLINE TEMPERATURE (F) FOR NOTED FOAM THICKNESS AT 150 SECONDS FROM LIFTOFF

T_{200} = CORK BONDLINE TEMPERATURE (F) FOR NOTED FOAM THICKNESS AT 200 SECONDS FROM LIFTOFF

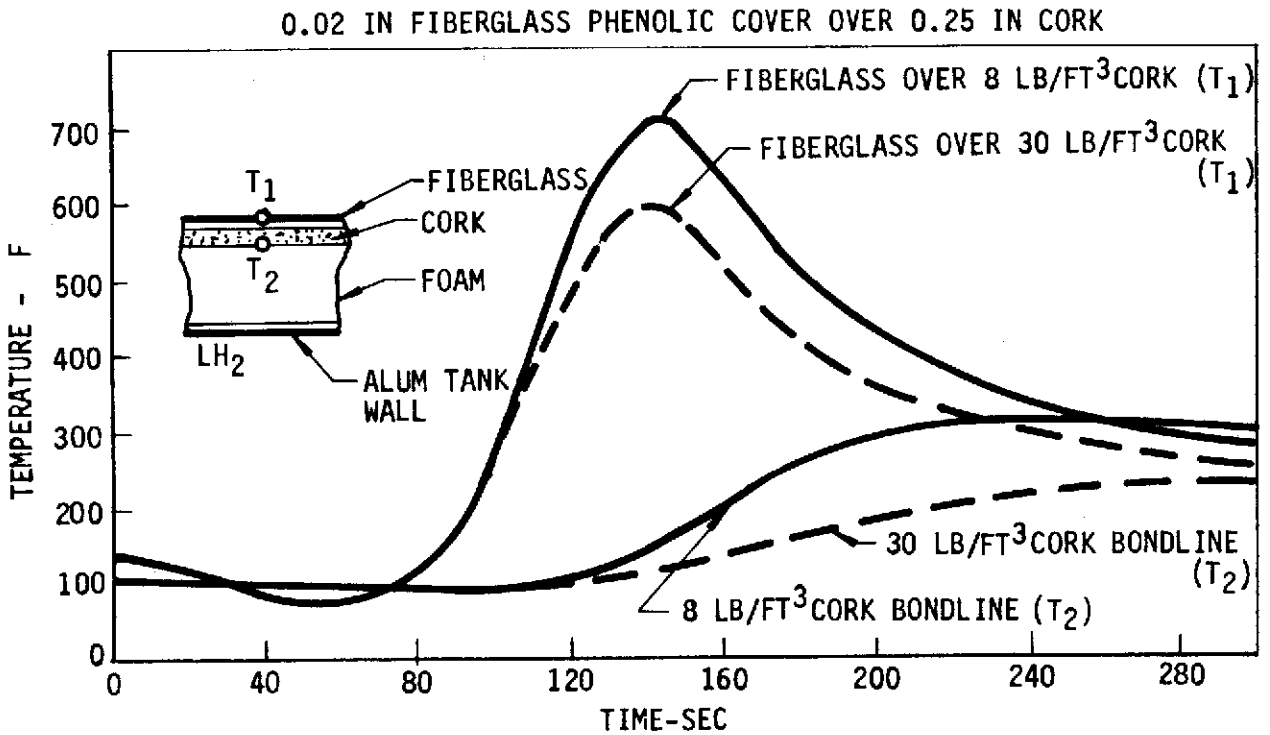

Figure 7.3.1.8-7. Fiberglass on Cork on Foam Insulation-Maximum Design for Region 6

obtained in region 6 as seen in Figure 7.3.1.1-1. The only area where cork is mechanically attached is between the systems tunnel flanges and the tank wall. There was no specific analysis for this design. The purpose of the cork is to prevent any erosion on the foam adjacent to the flanges. A temperature history of this system tunnel is shown in Figure 7.3.1.8-9. The heat flux through the fastener is 12 Btu/hr./bolt. It is not known what effect this has on the temperature gradients through the cork and foam. The heat pulse to the tank wall would not occur until after completion of S-II firing; thus the effect in no way jeopardizes the mission.

7.3.1.9 Polyimide Erosion Barrier

This insulation is made of 0.19-inch-thick polyimide honeycomb barrier mechanically attached over the basic foam insulation surface. The analysis of this insulation concept was conducted with and without an assumed radiation barrier in the polyimide honeycomb. Sketches of the insulation concepts and the attach point designs are shown in Figure 7.3.1.9-1.

Peak temperatures were calculated for the basic heating regions, and for typical single and multiple protuberance regions. The predicted peak temperatures are tabulated in Figure 7.3.1.9-1. The nodal numbers correspond to the locations shown on the accompanying sketches. On the INT-21 configuration, the S-II stage is exposed to a higher aerodynamic heating than the current Saturn V configuration. The higher aerodynamic heating is due to a payload protuberance

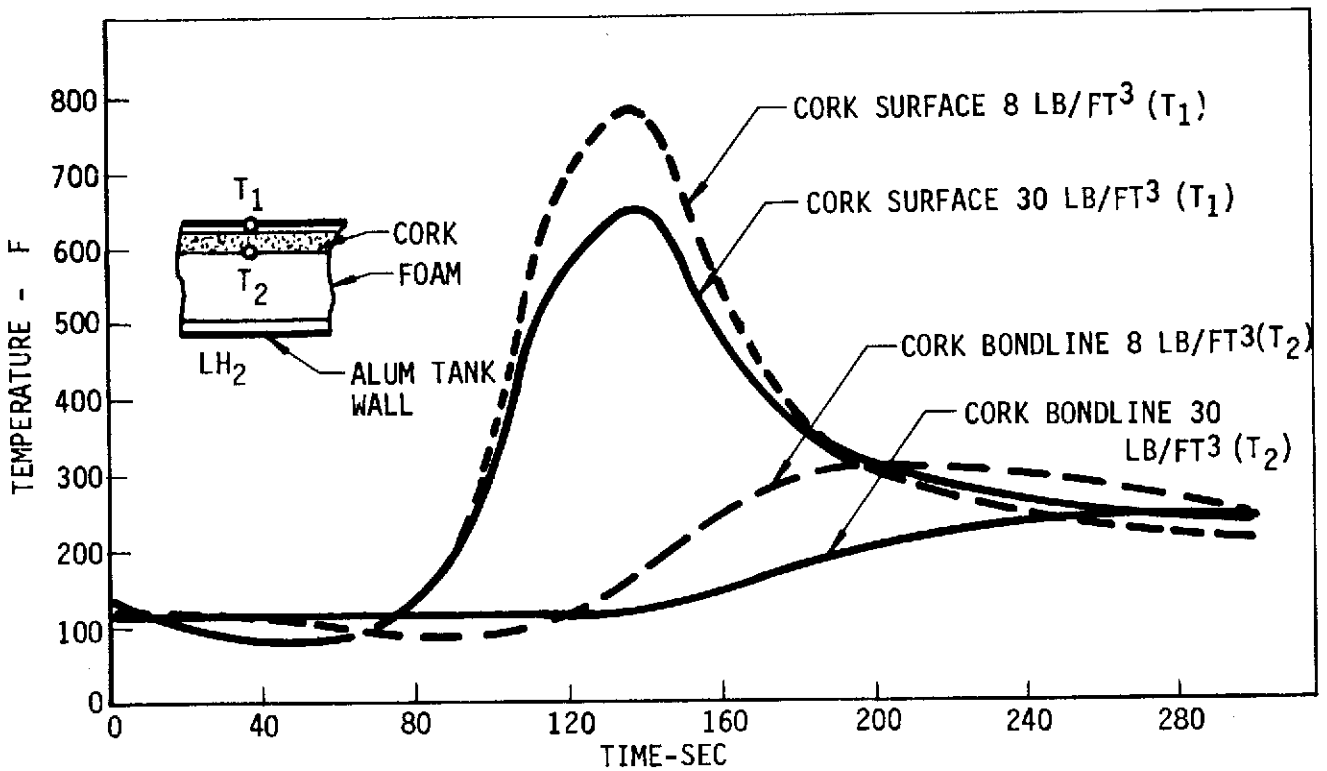

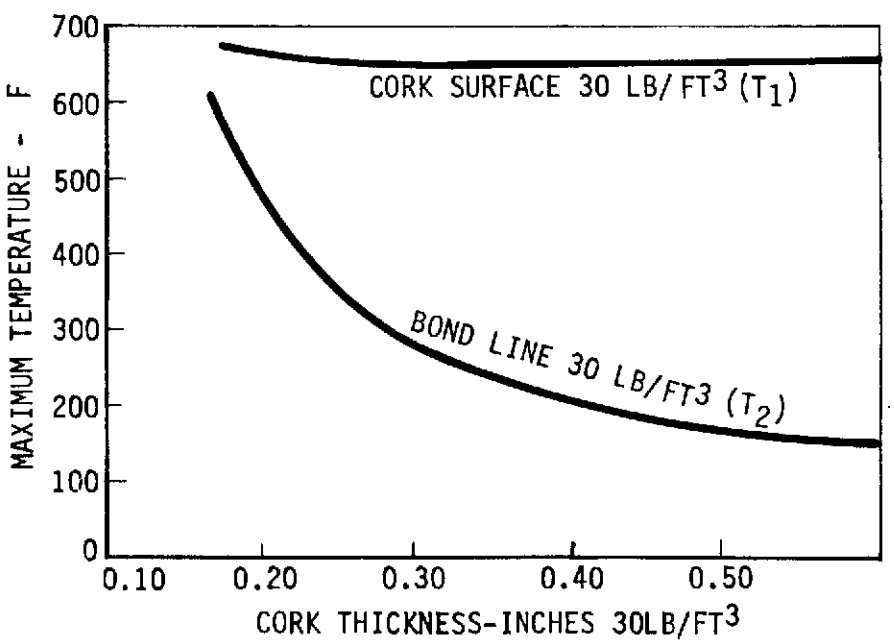

Figure 7.3.1.8-8· Cork on Foam Insulation-Maximum Design for Region 6

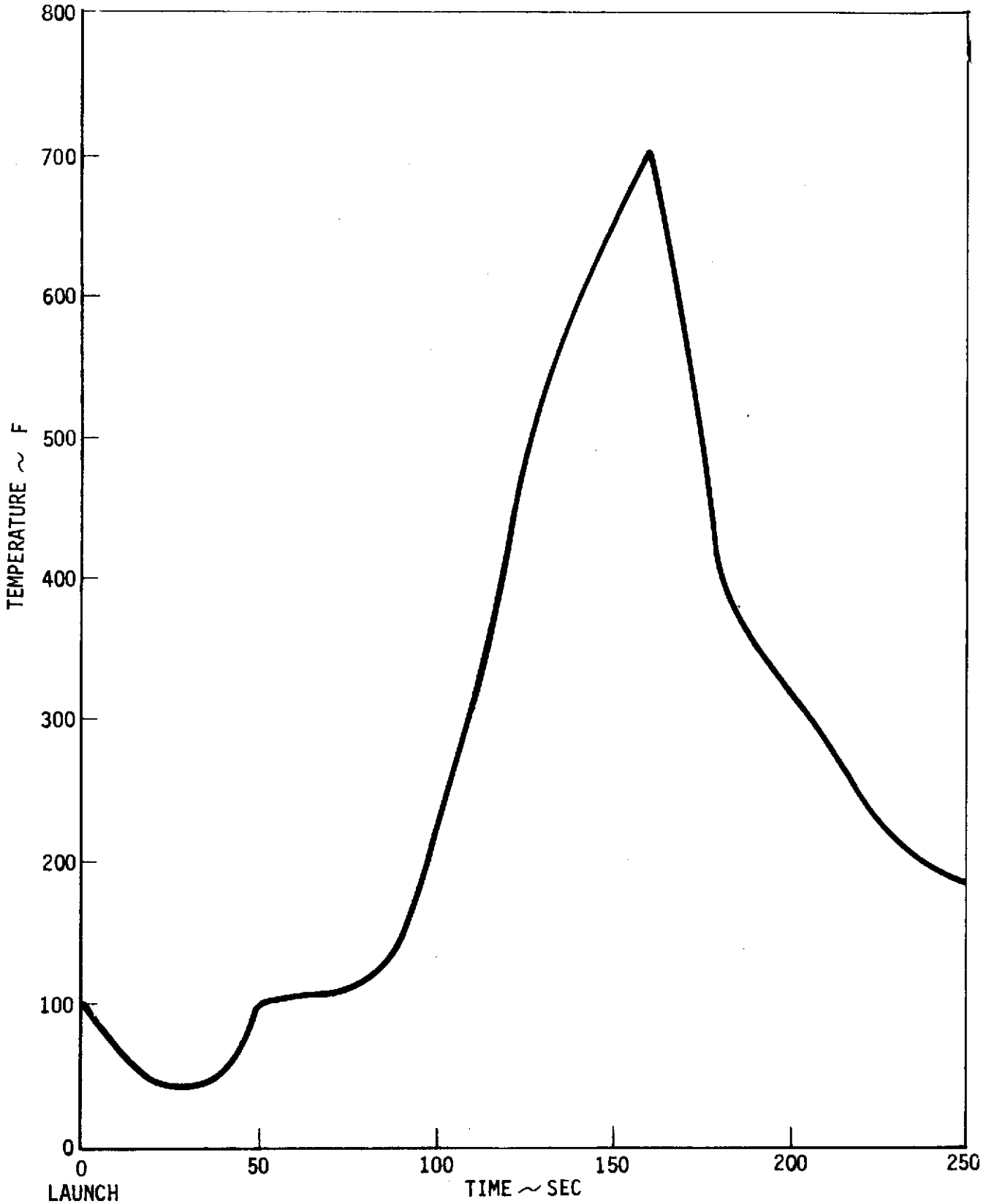

Figure 7.3.1.8-9· System Tunnel Spring-Loaded Fastener

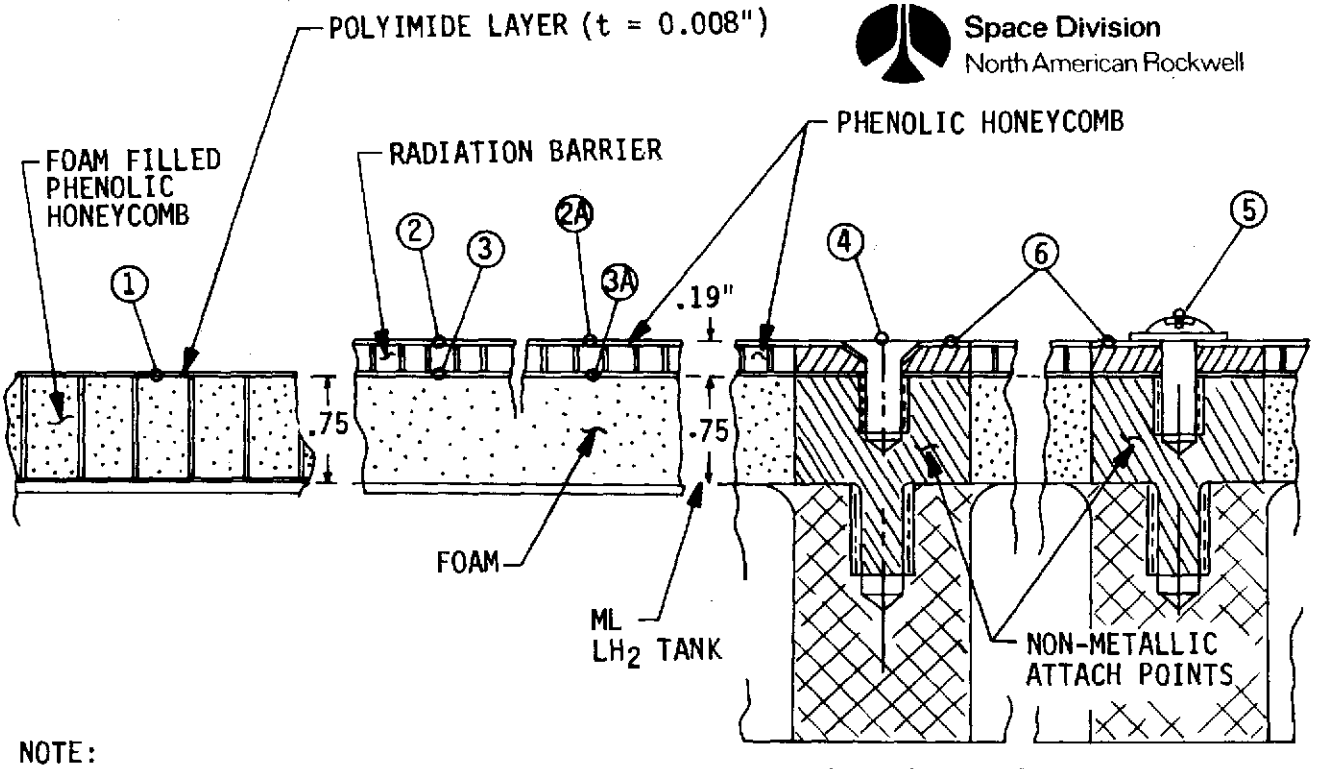

NOTE:

1. SATURN V BASIC DESIGN AERODYNAMIC HEAT RATES ARE USED
2. EXTERNAL SURFACE EMISSIVITY = 0.9, AND SOLAR ABSORBTIVITY = 0.3
3. (1) AERODYNAMIC HEATING RATE MULTIPLYING FACTORS DUE TO MDAC SPACE STATION PROTUBERANCES. FOR AREAS WHERE THESE MULTIPLYING FACTORS ARE APPLICABLE, SEE FIGURE 2
4. (2) SATURN V BASIC DESIGN PROTUBERANCE FACTORS ARE USED FOR S-II SINGLE AND MULTIPLE PROTUBERANCE REGIONS. SEE FIGURE 2 FOR THE PROTUBERANCE REGIONS
5. (3) R.B. (RADIATION BARRIER) K EQUIVALENT TO AIR WAS ASSUMED

		POLYIMIDE LAYER ON FOAM FILLED PHENOLIC HC	PHENOLIC HONEYCOMB BARRIER ON FOAM				FLAT HEAD TIE-DOWN BOLT	ROUND HEAD TIE-DOWN BOLT	NON-METALLIC ATTACH POINTS
			WITH R.B. (3)	NO R.B.	WITH R.B. (3)	NO R.B.			
CASE	NODAL NUMBER	①	②	②A	③	③A	④	⑤	⑥
1	BASIC x MF = 1.0	444	421	373	184	292	-53	70	86
2	BASIC x MF = 1.8 (1)	557	540	486	249	407	4	168	178
3	BASIC x MF = 2.0 (1)	581	565	510	262	431	17	190	200
4	TYPICAL SINGLE PROTUBERANCE REGION 1 (2)	641	626	574	295	494	34	237	248
5	TYPICAL SINGLE PROTUBERANCE REGION 2 (2)	609	590	535	275	455	20	205	214
6	TYPICAL MULTIPLE PROTUBERANCE REGION 3 (2)	686	675	634	322	552	53	281	291

Figure 7.3.1.9-1 INT-21 Proposed Insulation Temperatures

effect on the S-II stage. The payload protuberance multiplying factors (MF) are presented in Figure 7.3.1.9-2. Case 2 peak temperatures are for MF = 1.8 region, while those of Case 3 are for MF = 2.0 region. Case 1 peak temperatures are for the current S-II basic design aerodynamic heating rates. S-II fairing wake regions result in higher peak temperatures because of an additional local protuberance heating. Typical single protuberance and multiple protuberance regions are shown in Figure 7.3.1.9-2, details A and B, respectively. The peak temperatures for these regions are presented as Cases 4, 5, and 6 in Figure 7.3.1.9-1.

The maximum peak temperature predicted for the insulation concepts is 675 F, which is well below the 900 F maximum design target temperature. It should be noted that these predicted peak temperatures are based on the present S-II basic design aerodynamic heating rates and local protuberance factors. However, it is anticipated that the final INT-21 heating rates will be similar to the heating rates used in this analysis.

7.3.1.10 Multilayer Insulation - Flow-Through Purge

The analysis which was used to predict the thermal performance characteristics of the NARSAM-2 type multilayer insulation system is presented in the final report of the Cryo Storage Thermal Improvement Study (SD 71-263) involving a NASA/MSFC supplied 105-inch diameter LH_2 tank. The essential features of that study are presented in the following paragraphs.

a. Tank Heat Transfer Analysis: The purpose of the tank heat transfer analysis is to predict bulk LH_2 heating rates and tank and MLI temperature distributions for the imposed test conditions. Two important transient test sequences are considered: LH_2 fill and launch ascent to orbit.

b. Thermal Model Assumptions:

   1. The 105-inch diameter test tank consists of two hemispherical heads separated by a short cylindrical section. Protruding from the top of the tank is a fill and vent pipe referred to as the neck penetration. It consists of a nominal three-inch schedule 40 pipe which provides for filling the tank with LH_2 and a concentric six-inch schedule 40 pipe which permits venting the LH_2 boiloff gas through a flow meter and provides structural support of the tank to the spider beam. The outer surface of the tank and the neck penetration is insulated with NARSAM-2 MLI. The termination point of NARSAM on the neck penetration is 11.5 inches above the bimetallic joint (Figure 7.3.1.10-1). The test tank also incorporates a purge manifold under the MLI and an outer purge bag for insulation conditioning and associated instrumentation.

      An energy balance schematic for the 105-inch diameter test tank during thermal performance testing is shown in Figure 7.3.1.10-1. The major heat transfer terms shown are radiation and conduction through the MLI composite, conduction from the spider beam to the bare spool through support connections, radiation from the environment to the exposed surfaces of the bare spool, and convection cooling of neck penetration and tank wall above the LH_2 level by the vented boiloff gas from the

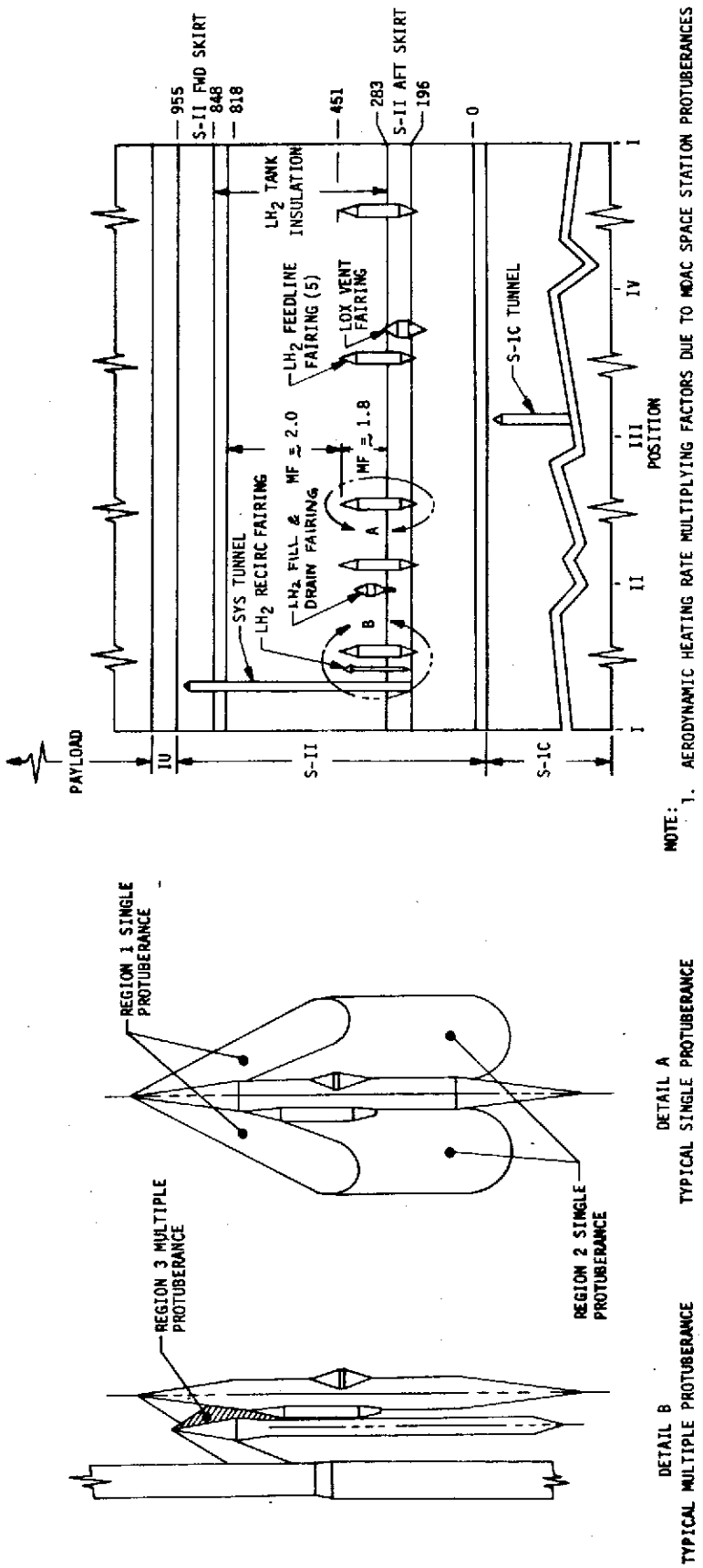

Figure 7.3.1.9-2. S-II Stage Fairing Arrangement

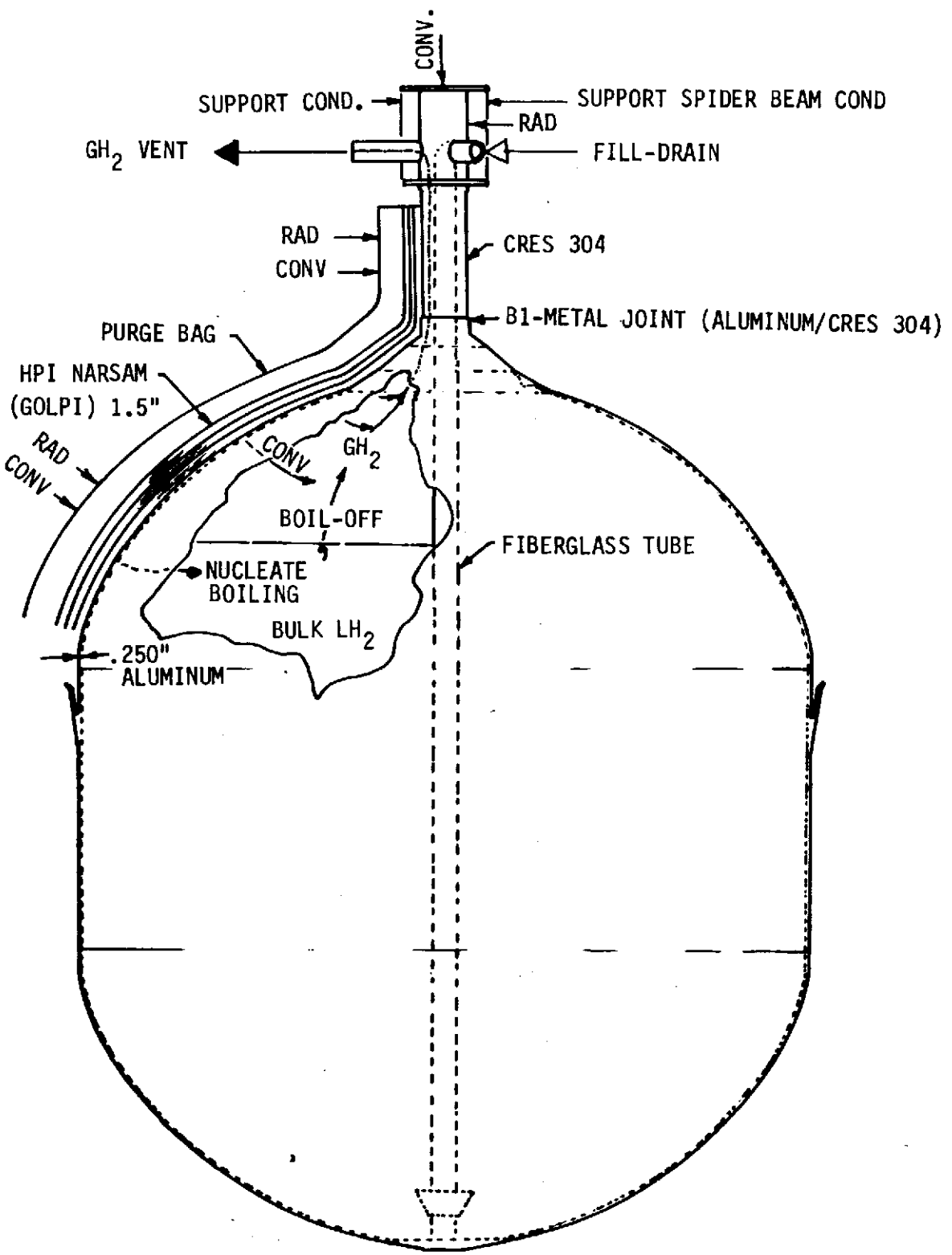

Figure 7.3.1.10-1· Energy Balance Schematic for 105-Inch Diameter Tank Installed With NARSAM-2

bulk LH_2 in the tank. The total heat leak from all sources above the LH_2 level, minus the convective cooling, produces a delta heat leak which increases LH_2 boiloff that due to the heat leak through the MLI below the LH_2 level.

Heat transfer through NARSAM and other MLI composites involves the simultaneous interaction of radiation, solid conduction, gas conduction, and convection. Because of the complex structure of MLI composites these separate components of heat transfer are not strictly additive; however, a reasonable approximation is obtained by assuming that these components are additive and then adjusting the results by multiplying each term by an experimentally determined coefficient.

For long-term space applications, an MLI composite is evacuated to a low pressure. Numerous investigators have found that gas conduction and convection in an evacuated MLI composite can be neglected when compared to radiation and solid conduction. By using standard curve-fitting techniques, NR has developed the following universal equation for the effective thermal conductivity of different MLI composites reported in the literature for NARSAM-2:

$$K_{EFF} = K_c N^{-A} \left(\frac{T_h + T_c}{2}\right) + \frac{K_r}{N} \frac{F_e + \tau}{1 - \tau} (T_h^2 + T_c^2)(T_h + T_c)$$

The coefficients K_c and K_r and the exponent A are determined analytically from flatplate calorimeter test data. NARSAM-2, as installed on the tank, consists of 30 layers of in-specification material and 60 layers of out-of-specification material. The values of K_c, K_r, A, and F_e used in this study are listed in Table 7.3.1.10-1.

Table 7.3.1.10-1. Constants for K_{EFF} Equation

	K_c	K_r	A	F_e
In-Specification	2.05×10^{-16}	1.2×10^{-10}	4.75	0.0415
Out-of-Specification	2.05×10^{-16}	1.47×10^{-10}	4.75	0.0580

For an installed layer density of 60 layers per inch and 2 percent perforation area, the effective thermal conductivity of NARSAM-2 is:

$$K_{EFF} = 0.285 \times 10^{-7} (T_h + T_c) + 1.283 \times 10^{-5} \sigma (T_h^2 + T_c^2) (T_h + T_c)$$

A representative value of K_{EFF} for a surface temperature of 530 R and LH_2 cold wall is 3.7×10^{-5} Btu/hr-ft°F when the effects of posts, joints, gas conduction, and other heat shorts are neglected. The actual value of K_{EFF} used in the thermal model is calculated by standard thermal analyzer techniques. The first term on the right-hand side of the first equation represents solid conduction and becomes a curve entry for a temperature-dependent thermal conductivity. The other term

represents radiation. The function $K_r (F_e + \tau)/ N (1 - \tau)$ when divided by MLI thickness becomes an equivalent script F factor in the thermal analyzer entry.

NR has extended the application of the basic equation to actual MLI installation where the ideal thermal performance is degraded due to joints and posts. The degradation of installed NARSAM-2 thermal performance due to joints is accounted for by increasing the radiation term of the basic equation. The detailed calculation of joint heat leak for both the in-specification and out-of-specification material is presented in Section 3.1.2.2 of SD 71-263. The correction increased the radiation by approximately 10 percent.

The degradation of NARSAM-2 thermal performance by posts is accounted for by a solid conductor connected between the inner and outer MLI surface temperatures and parallel to the MLI conductors defined by the basic equation. The 156 fiberglass posts are distributed to different nodal locations according to the distribution in Figure 7.3.1.10-2. The thermal conductivity of Type R fiberglass reinforced phenolic was obtained from SD 712-363. The post area is 5.28×10^{-5} square feet and its length is 1.5 inches. The approximate heat leak is 0.055 Btu/hr. per post.

During ground-hold and launch-to-orbit phases of vehicle operation, energy will be transferred through MLI composites by gas conduction in addition to radiation and solid conduction. Ordinary gas conduction occurs during ground-hold because the gas pressure between MLI layers is near atmospheric pressure. The variation in thermal conductivity of atmospheric pressure helium gas with temperature is nearly linear between ambient and cryogenic temperature.

During launch to orbit, a typical MLI composite will evacuate itself to the low pressure corresponding to orbital operation. The gas conduction mechanism at orbital pressures differs from ordinary conduction at atmospheric pressure. Gas molecules rarely collide, thus an individual gas molecule travels across the space between MLI layers without exchanging energy (free molecular regime). An analysis of the energy transferred by molecular conduction is presented in SD 71-263.

The following result, which applies to parallel plates and concentric cylinders and spheres, was obtained:

$$Q/A = F_a \, GP \, (T_h - T_c)$$

where G is an equivalent conductivity coefficient defined by

$$G = \frac{\gamma+1}{\gamma-1} \left(\frac{g_c R}{8\pi MT}\right)^{1/2}$$

and F_a is the accommodation coefficient factor defined by

$$\frac{1}{F_a} = \frac{1}{a_1} + \frac{1}{a_2} - 1$$

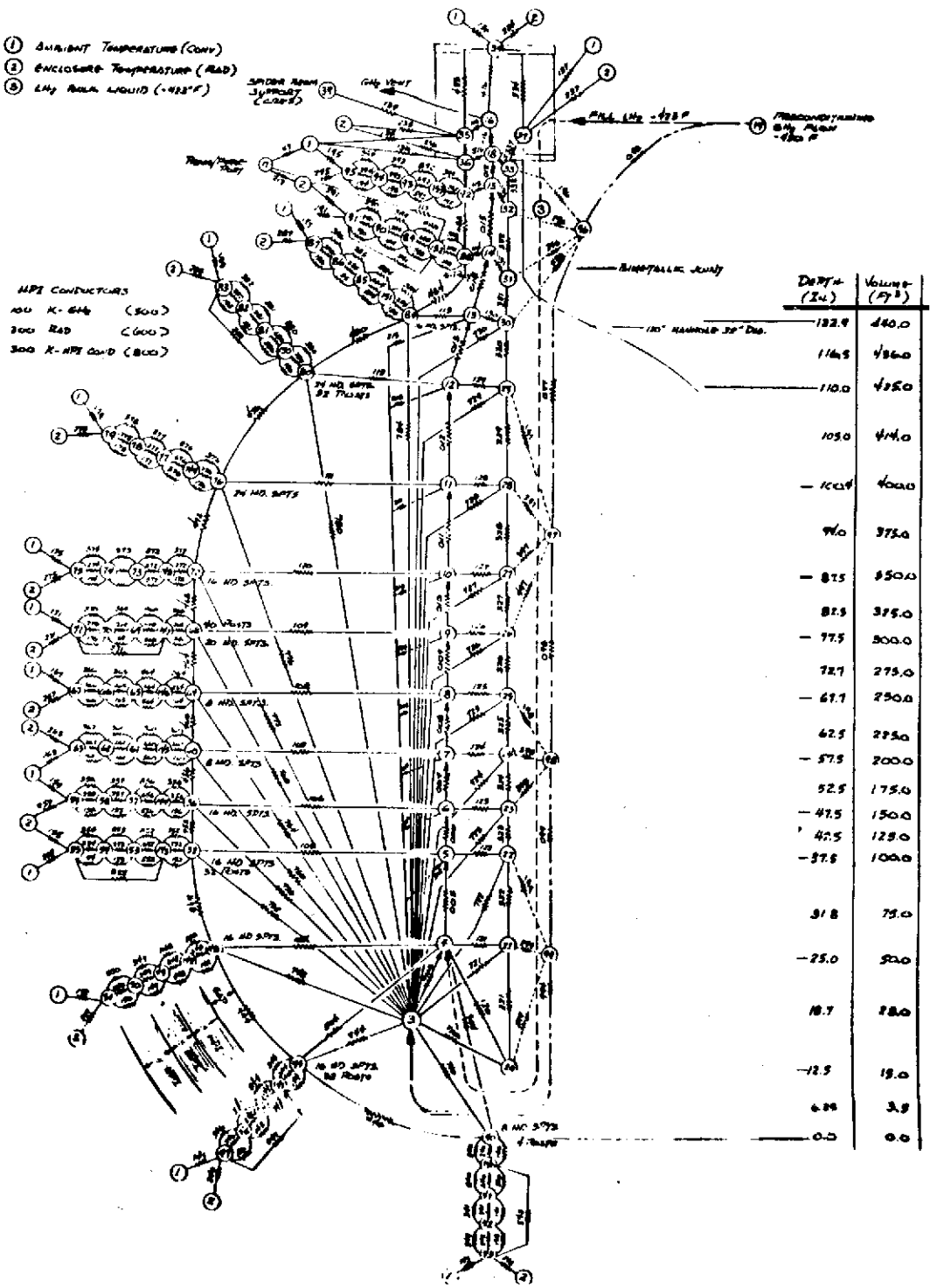

Figure 7.3.1.10-2. Fill-Transient Thermal Model for NARSAM-2 Installed on 105-Inch Diameter Tank

NR has extended this result to include the effects of multiple layers, variable pressure, and temperature-dependent properties. When more than two participating surfaces are involved, the geometry laws used in radiation can be applied. Applying the summation technique for adding radiation conductances in series, the following gas conduction result is obtained:

$$Q/A = F_a \frac{GP}{N} (T_2 - T_1)$$

The use of N in the summation instead of N-1 or N+1 as other authors have obtained is a matter of computational convenience. It is expected that this term will be multipled by an experimental coefficient when evaluating the effective thermal conductivity of MLI composites and that layer density will be an important variable.

Published thermal conductivity data for common gases suggests that K is relatively constant at high pressure where continuum effects predominate and that K varies linearly with pressure at low pressures where free molecule effects predominate. NR uses the following expression to evaluate pressure dependent thermal conductivity values:

$$\frac{1}{K} = \frac{1}{K_\infty} + \frac{\bar{N}}{F_a GP}$$

The expression reduces to the proper limiting values at the pressure extremes, reasonably predicts the effective K in the transition flow regime between the continuum and free molecule flow regimes, and is easy to program for thermal analyzer calculations.

The effect of temperature-dependent properties on effective thermal conductivity is accounted for by evaluating the last equation at different temperatures in the cryogenic range. The resulting K values are input to the thermal analyzer as bivariable curves with temperature as the independent variable and pressure as the parameter.

The equivalent network shown as Figure 7.3.1.10-2 was prepared to calculate heat leak and temperature distributions. The temperature distribution through NARSAM was represented by four nodes: one at the LH_2 tank surface and interior nodes at the one-third points. The energy transfer between nodes is represented by three parallel conductors; one each for radiation, solid conduction, and gas conductivity. The effects of lateral conduction parallel to laminations of MLI have been neglected.

2. Spider Beam and Neck Penetration: The function of the spider beam is to support the 105-inch tank during test operations. The beam conducts heat to the bare spool portion of the neck penetration through attach bolts and support connections. This node was represented by a single solid conduction type conductance which is connected between a fixed

environmental temperature boundary and the bare spool temperature. The boundary is located 12 inches from the bare spool and the equivalent conductance has a contact area of 14.4 square inches. No attempt was made to perform a detailed thermal analysis of the spider beam because of the complex configuration factors associated with the radiation calculations. An error assessment was made, however, to determine the limits of analysis error in predicting heat leak to bulk LH_2.

The bare spool region of the neck penetration has surfaces which are exposed to the chamber wall and other warm surfaces. No attempt was made to calculate configuration factors. Instead, the bare spool was assumed to be a small object inside a large enclosure. The resulting shape-emittance factor for this net radiant exchange is simply the emittance of the bare spool. The basic case analysis assumes an emittance of 0.4. However, other cases were analyzed where emissivity was allowed to assume different values.

A simple mass flow model is used to calculate convection cooling of the neck penetration and the tank wall above the LH_2 level. Boiloff of saturated LH_2 occurs at the exposed surface of the bulk fluid, and the resulting flow through the ullage space and neck annulus is uniform and predictable. This assumption requires that no secondary convection currents be set up at the ullage space that will influence fluid flow or heat transfer, and that boiloff from the superheated layer next to the tank wall mixes with the bulk fluid. The LH2 boiloff gas flow is allowed to rise in temperature because of convection at the pipe wall. Gas temperature nodes are selected adjacent to wall node locations. The heat transfer between the hot tank walls and the flowing gas is turbulent natural convection on a vertical surface. The equivalent conductance is calculated internally by the thermal analyzer and has a value of approximately 1.0 Btu/hr-ft^2°F. A check calculation was made to determine if laminar forced convection should be used. The calculated values of the equivalent conductance for laminar forced convection was negligibly small compared to natural convection. The thermal analyzer uses the following steady-state heat balance to predict the gas node temperatures:

$$\dot{w}\, C_p\, (T_{j-1} - T_j) + h\, A\, (T_i - T_j) = 0$$

The subscript j refers to fluid nodes and the subscript i refers to wall nodes. The specific heat of GH_2 (C_p) was allowed to vary with temperature.

Results and Conclusions:

1. LH_2 Fill-Transient: The thermal network shown in Figure 7.3.1.10-2 was used to predict tank and MLI transient temperature distribution

and resulting heat leak to LH_2 and LH_2 boiloff during the LH_2 fill sequence. The following initial conditions were assumed:

Chamber temperature	520 R
Chamber pressure	760 torr
Tank temperature	520 R
MLI purge gas	Helium
LH_2 fill rate	35 lb./min.
LH_2 quantity, when full	1,950 lb.

The LH_2 fill analysis was run for different LH_2 fill rates. An LH_2 fill rate of 35 pounds per minute results in minimum propellant consumption. Therefore, this case was selected for display purposes. The approximate fill time is 62 minutes and the total fill quantity is 2,160 pounds. After approximately 12 minutes, the LH_2 boiloff rate is stablized at 3.75 pounds per minute (230 pounds per hour) (Figure 7.3.1.10-3.) The approximate time for the tank skin temperature to stabilize is 100 minutes after the start of LH_2 fill (Figure 7.3.1.10-4). The neck temperature under the MLI (node 92) is the last temperature to stabilize. A steady-state temperature distribution through NARSAM is achieved quickly for the insulation sections below the final fill level (Figure 7.5.1.10-5). For the upper dome section, which is above the LH_2 level, approximately 75 minutes are required for stabilization (Figure 7.3.1.10-6). Approximately 75 minutes are required for the ullage gas temperature and the neck temperature at the exit port to stabilize (Figure 7.3.1.10-7).

Figure 7.3.1.10-8 presents the MLI temperature distribution during LH_2 fill with the insulation initially evacuated. As shown, the stabialization time is approximately 53 hours for the inner MLI layer. By contrast, the stabilization time for the LH_2 fill with the chamber at atmospheric pressure is approximately 1.5 hours (Figures 7.3.1.10-5 and 7.3.1.10-6). Clearly, the LH_2 fill sequences should be performed with the chamber initially at atmospheric pressure.

2. Tank Launch-Ascent to Orbit Transient: The thermal network shown in Figure 7.3.1.10-2 was used to predict tank and MLI transient distributions and resulting heat leak to LH_2 and LH_2 boiloff during the simulated launch ascent to orbit sequence. The following initial conditions were assumed:

Chamber Temperature	520°R
Chamber pressure	760 torr
MLI purge gas	Helium

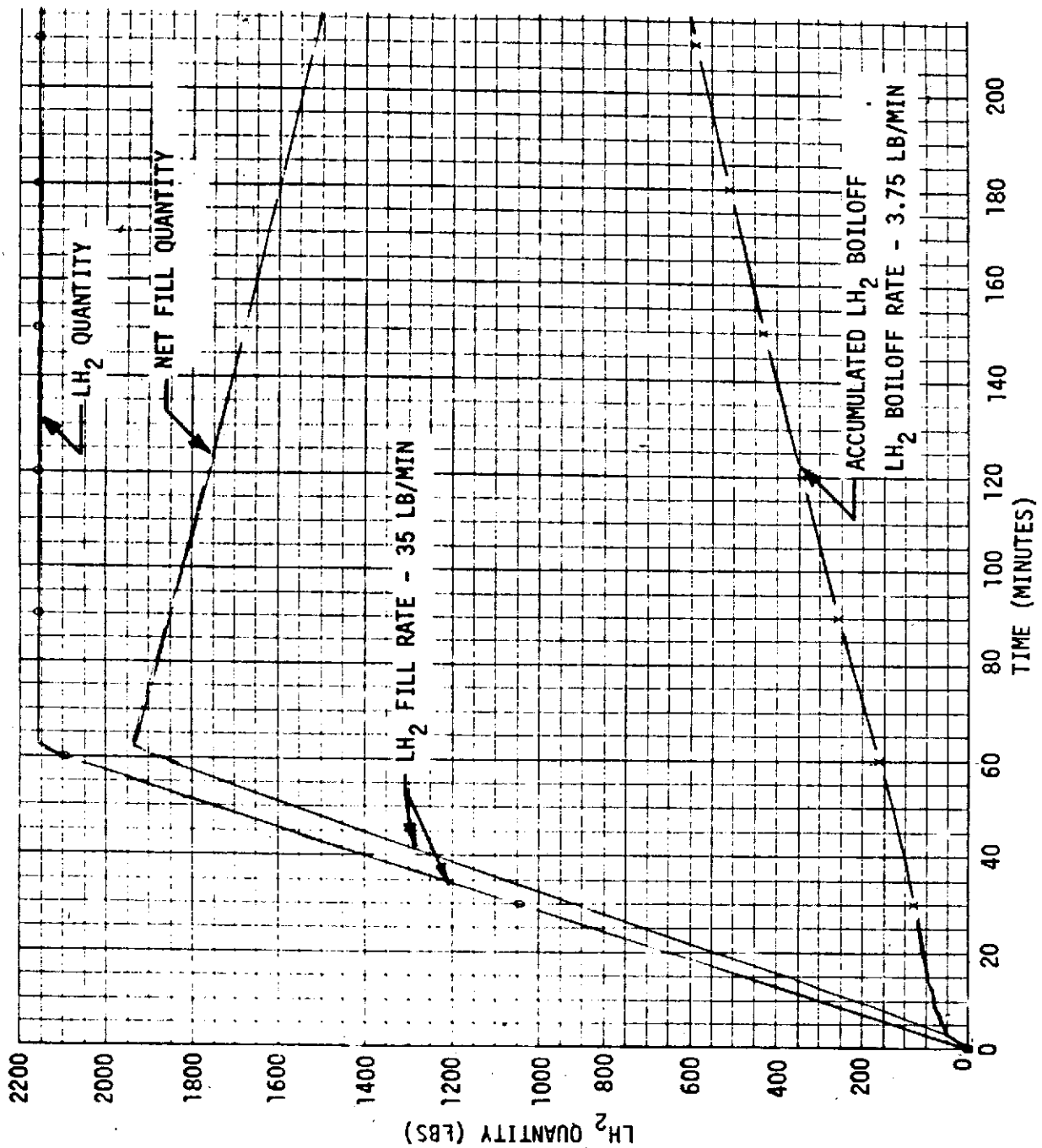

Figure 7.3.1.10-3. LH_2 Quantity as a Function of Fill Time

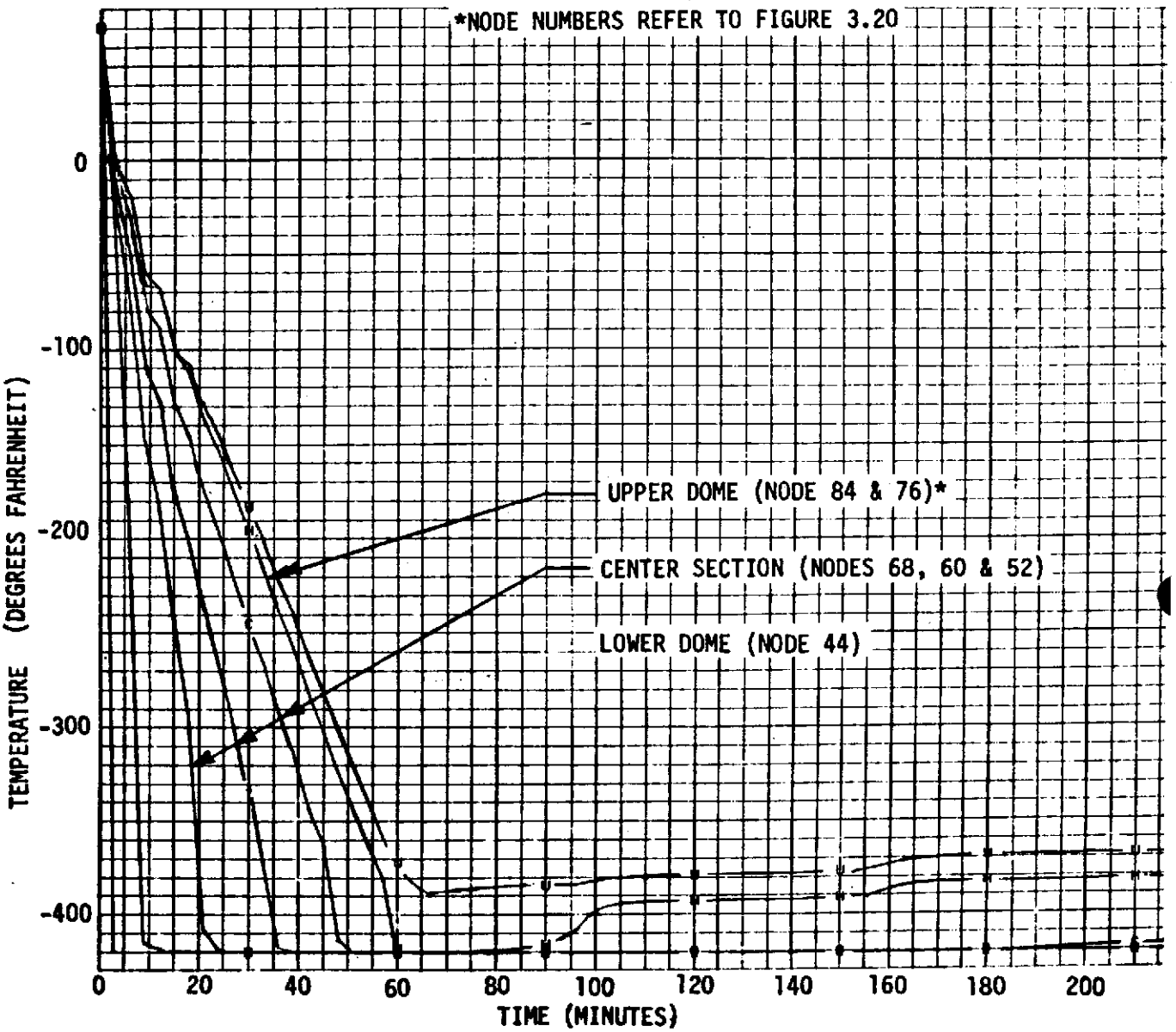

Figure 7.3.1.10-4. Tank Skin Temperatures as a Function of Fill Time

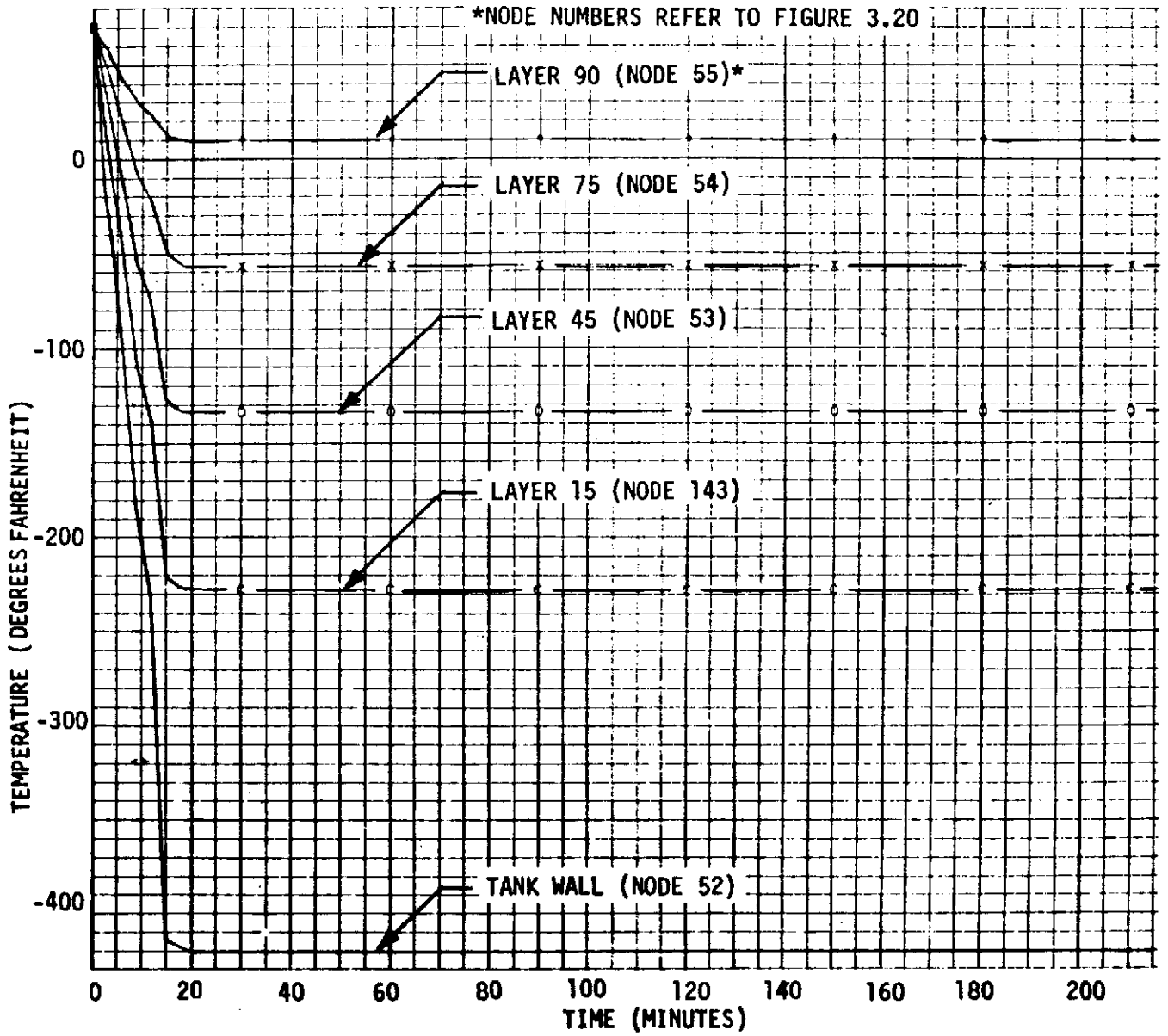

Figure 7.3.1.10-5. Temperature Distribution Through NARSAM-2 Insulation as a Function of Fill Time

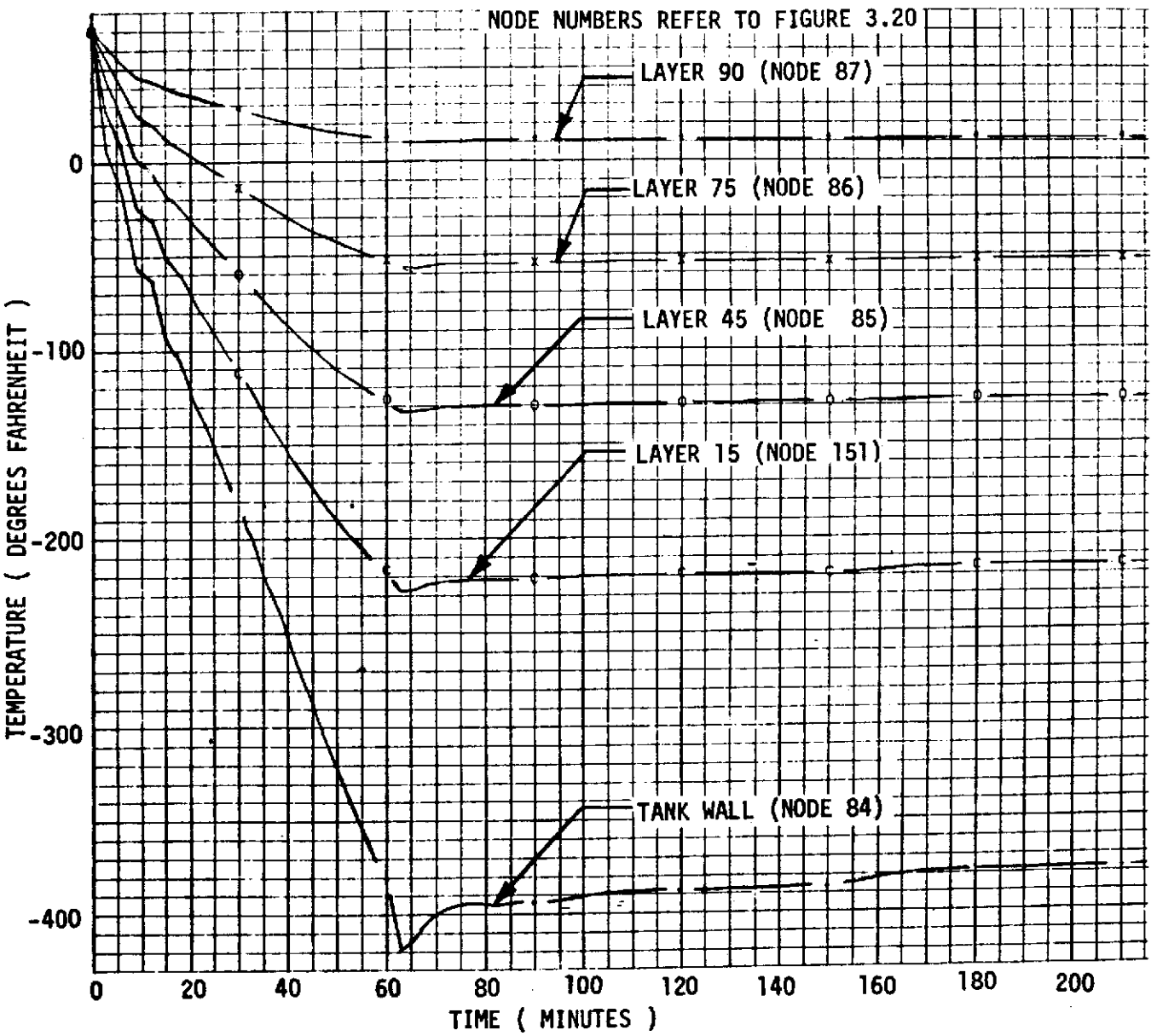

Figure 7.3.1.10-6. Temperature Distribution Through NARSAM-2 Insulation as a Function of Fill Time (Upper Dome Section)

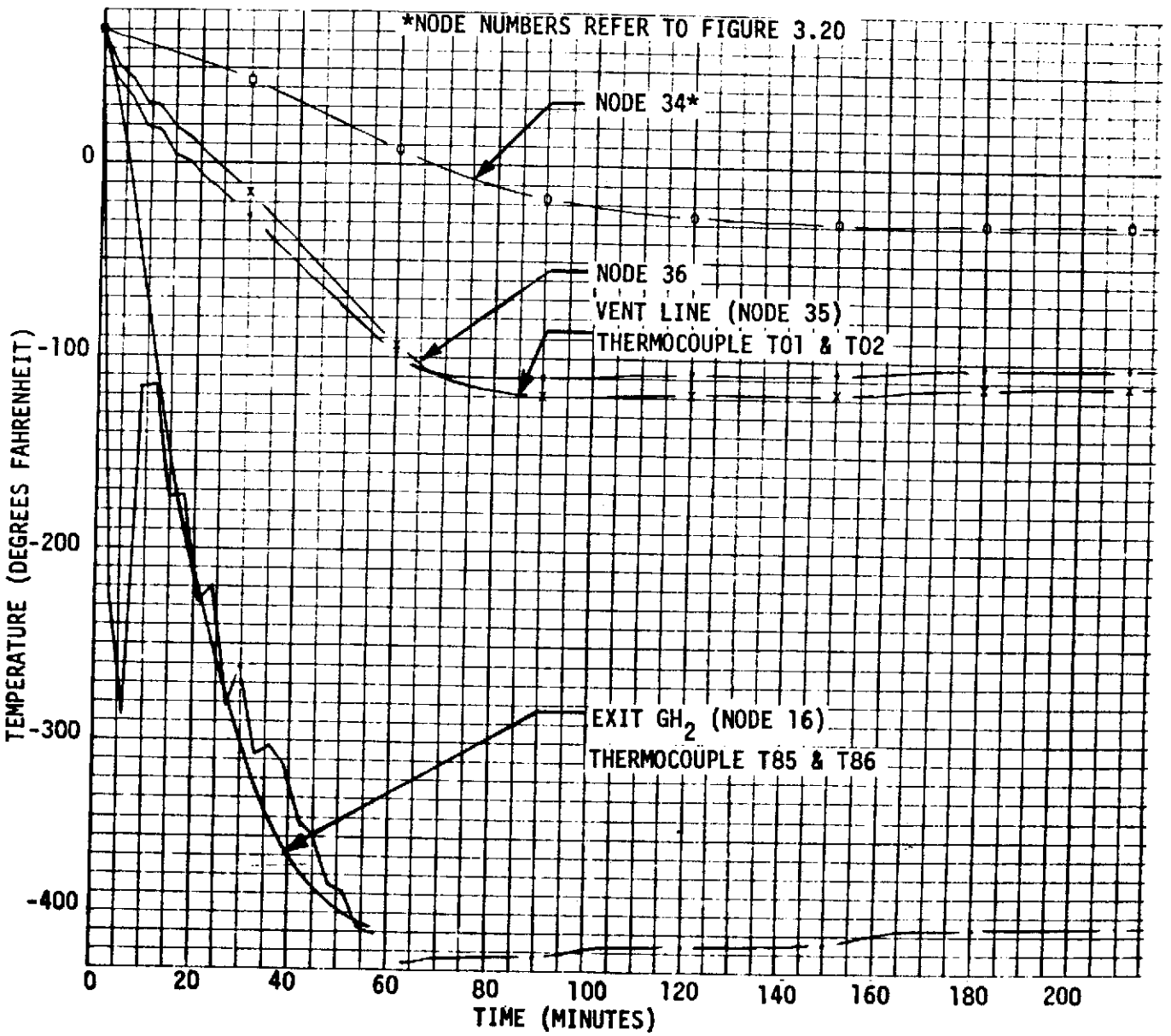

Figure 7.3.1.10-7. Ullage Gas as a Function of Fill Time

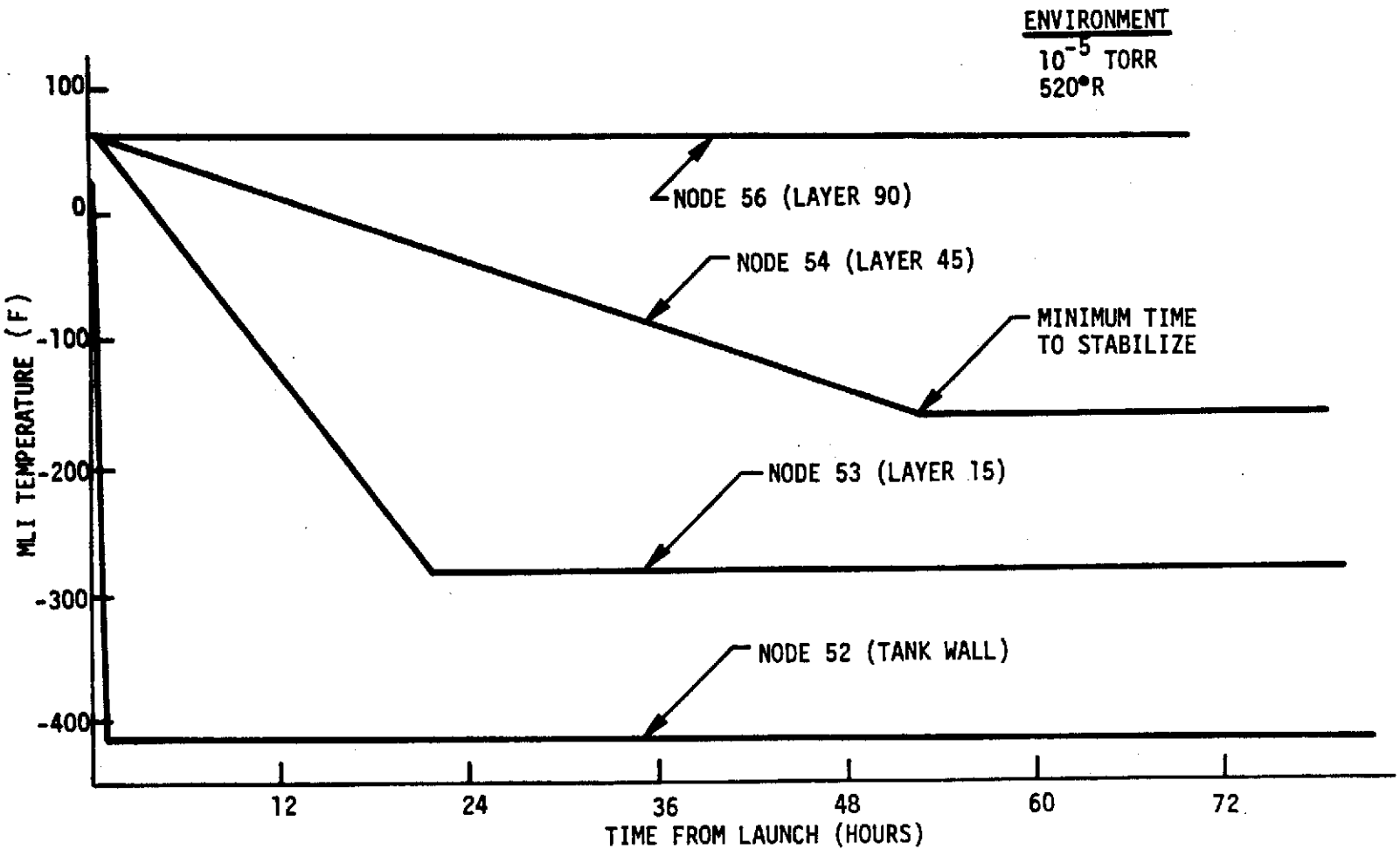

Figure 7.3.1.10-8. Transient Temperature Distribution Through NARSAM-2 During LH_2 Fill With Insulation Evacuated

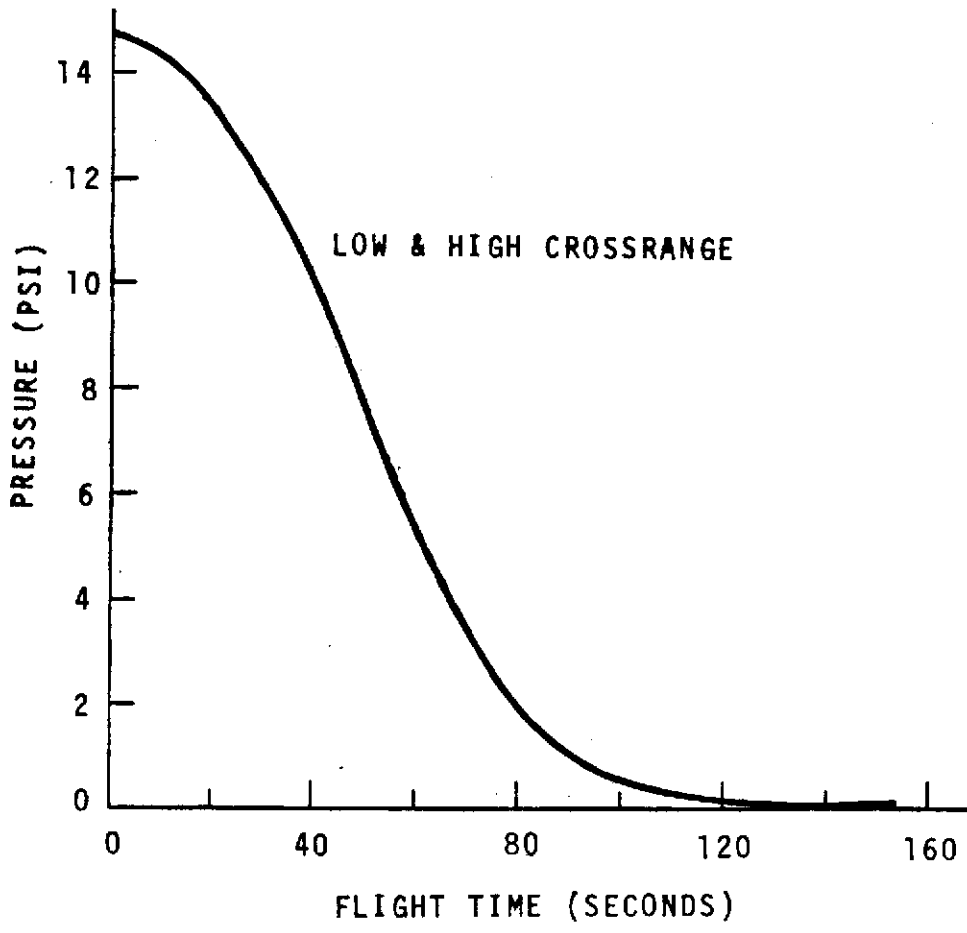

Figure 7.3.1.10-9. Tank Compartment Internal Pressure-Time History During Ascent

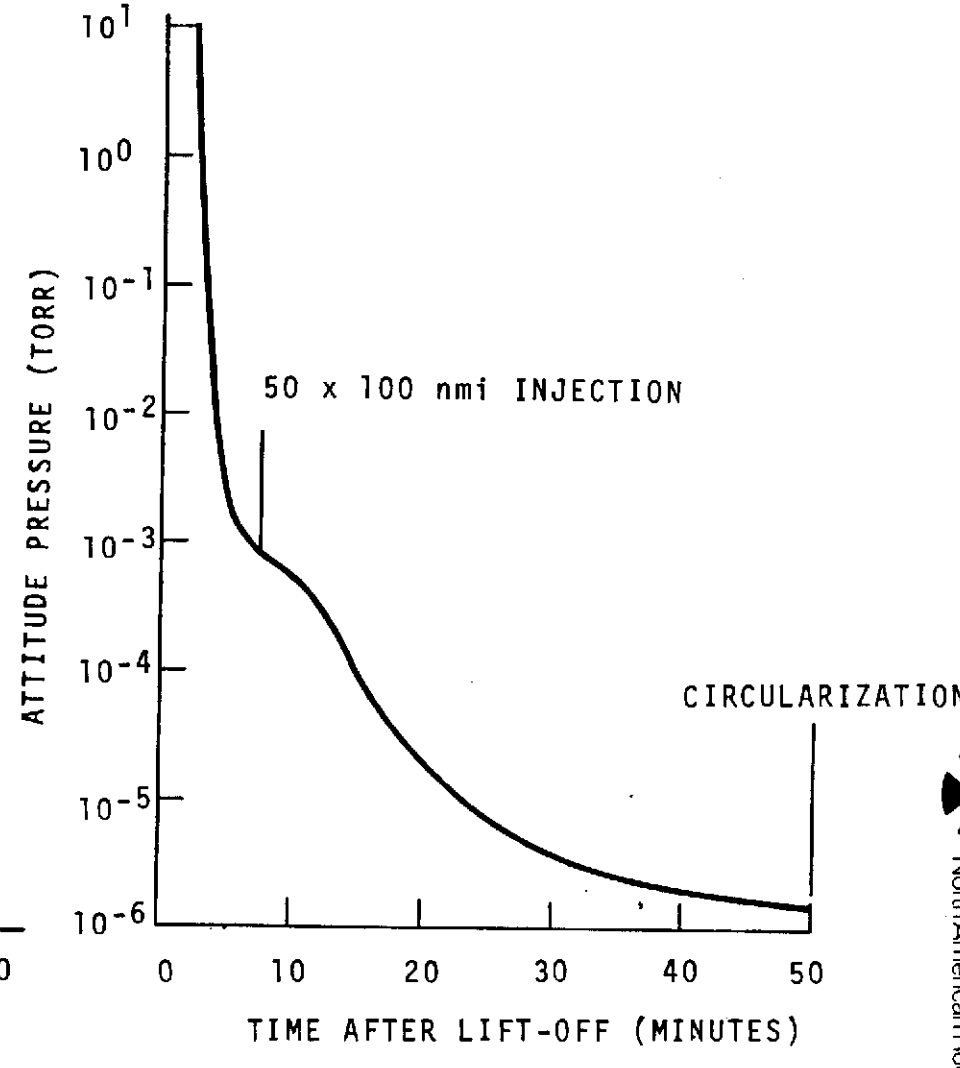

Figure 7.3.1.10-10. Tank Compartment Internal Pressure-Time History During Ascent, Vacuum Regime

LH_2 quantity 1,950 lb.

No topping

The analysis assumes that the transient pressure profile shown in Figure 7.3.1.10-9 and 7.3.1.10-10 is uniformly distributed through the MLI at any instant. The final chamber and MLI pressure is assumed to be 10^{-5} torr. Results are presented in Figures 7.3.1.10-11 through 7.3.1.10-15.

The ascent profile is a pressure profile simulating the boost trajectory of the application model tank compartment. The ascent profile will simulate the predicted profile (Figures 7.3.1.10-9 and 7.3.1.10-10; however, the vacuum chamber facility limits will most likely prevent a continuous pumping capacity at pressures lower than 10^{-6} torr. Coupled with the ascent profile is the long-term outgassing profile in which the outgassing from the insulation will continue over a period which could run into two or three days of continuous outgassing at pressures higher than the desired 10^{-4} torr for insulation thermal performance. The ascent pressure profile is essentially achieved when an elliptical orbit of 50 x 100 nautical miles is reached approximately eight minutes after launch. The continued long-term outgassing profile is part of an extension of the ascent profile reflecting a much longer period for low insulation pressures to be achieved.

7.3.1.11 Thermal Performance of Multilayer Insulation, Flow-By Purge

The thermal analysis of this insulation is essentially the same as for the flow-through purge presented in Paragraph 7.3.1.10.

7.3.1.12 Thermal Analysis of Meteoroid Protection System

The detailed thermal analysis of the meteoroid protection system has been documented in SD 71-245-4 and SD 72-SA-0042-3. The results of the analysis are indicated in Figure 6.1.12.3-1 and 6.1.12.3-2. Because of the extent of the analysis and the application to specific trajectories it is not repeated here.

The thermal operation of a meteoroid protective system during orbital flight is based alsmost entirely on heat transfer through the insulation by radiation and the heat leak through the supports are calculated in the normal way.

Particular attention should be paid to the ground, boost, and early orbit conditions with the associated cryopumping, frost formation, venting, and outgassing. These will affect the conductivity during early orbit.

7.3.2 Cryogenic Transfer

7.3.2.1 Vacuum-Jacket Propellant Lines

The important thermal performance characteristic of this insulation system is the overall heat transfer rate from the external environment to the cryogenic propellant flowing in the line. S-II point design performance for both LOX

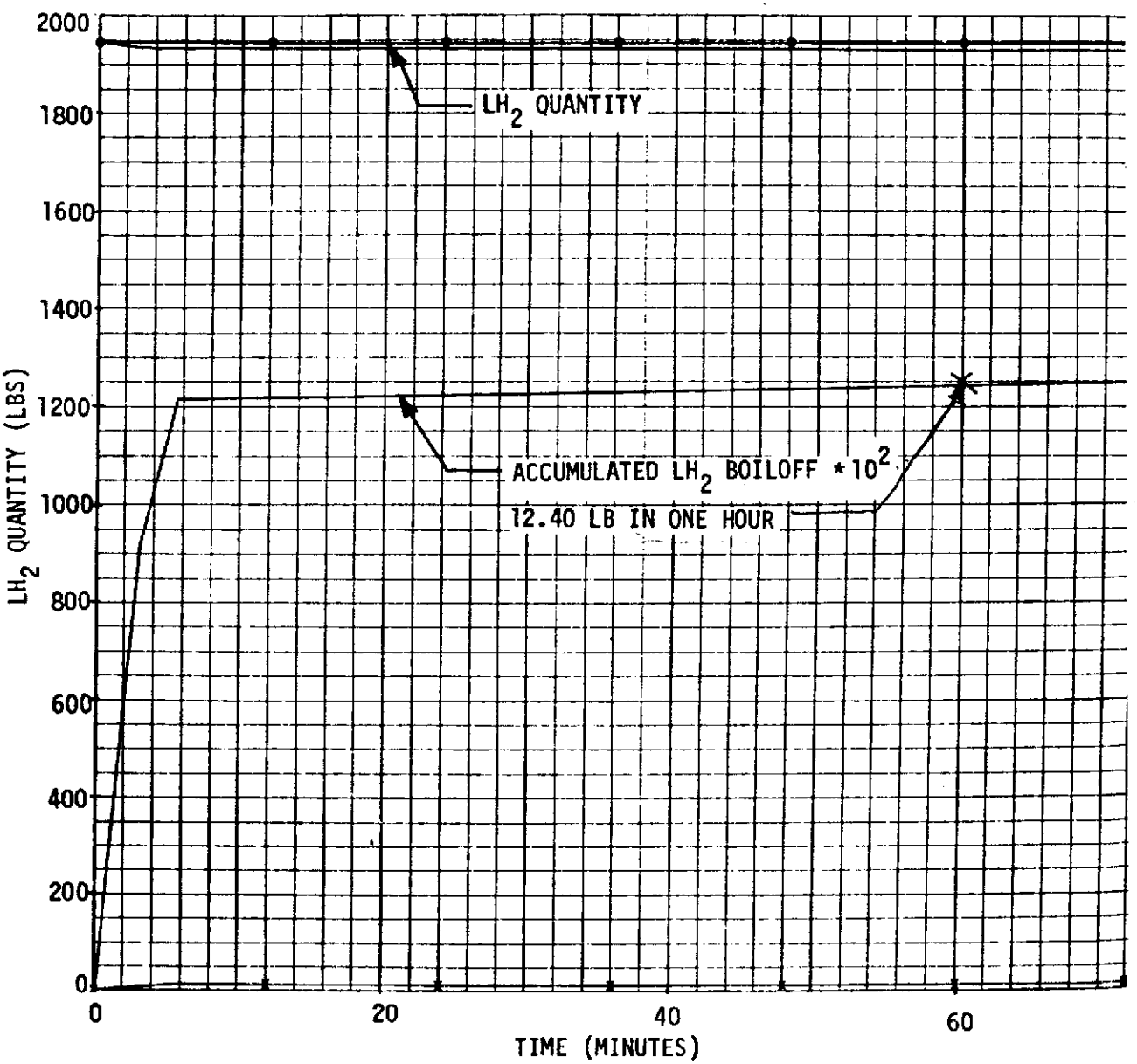

Figure 7.3.1.10-11. LH_2 Boiloff Rate During Launch Ascent to Orbit

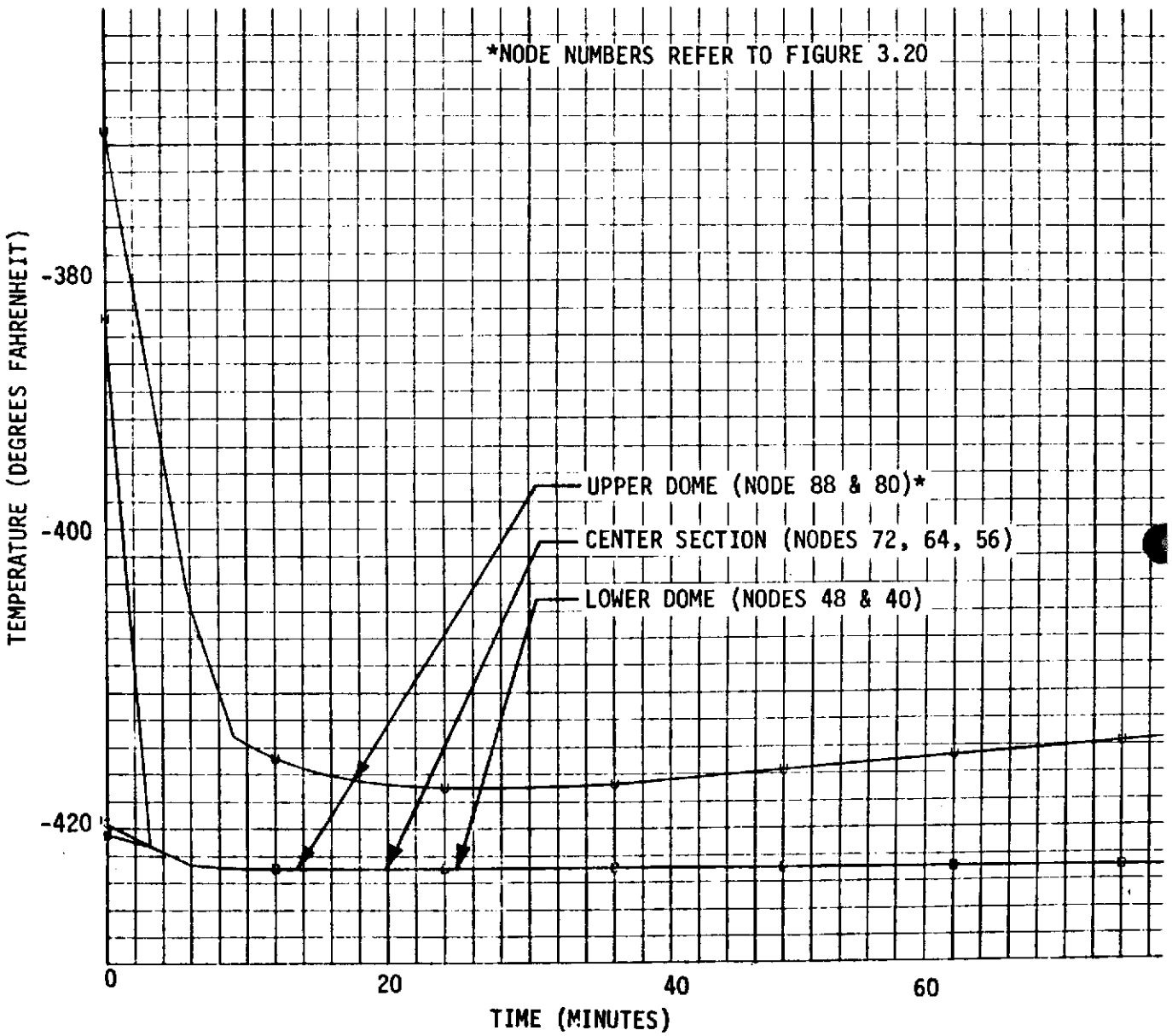

Figure 7.3.1.10-12. Tank Skin Temperature During Simulated Launch Ascent to Orbit

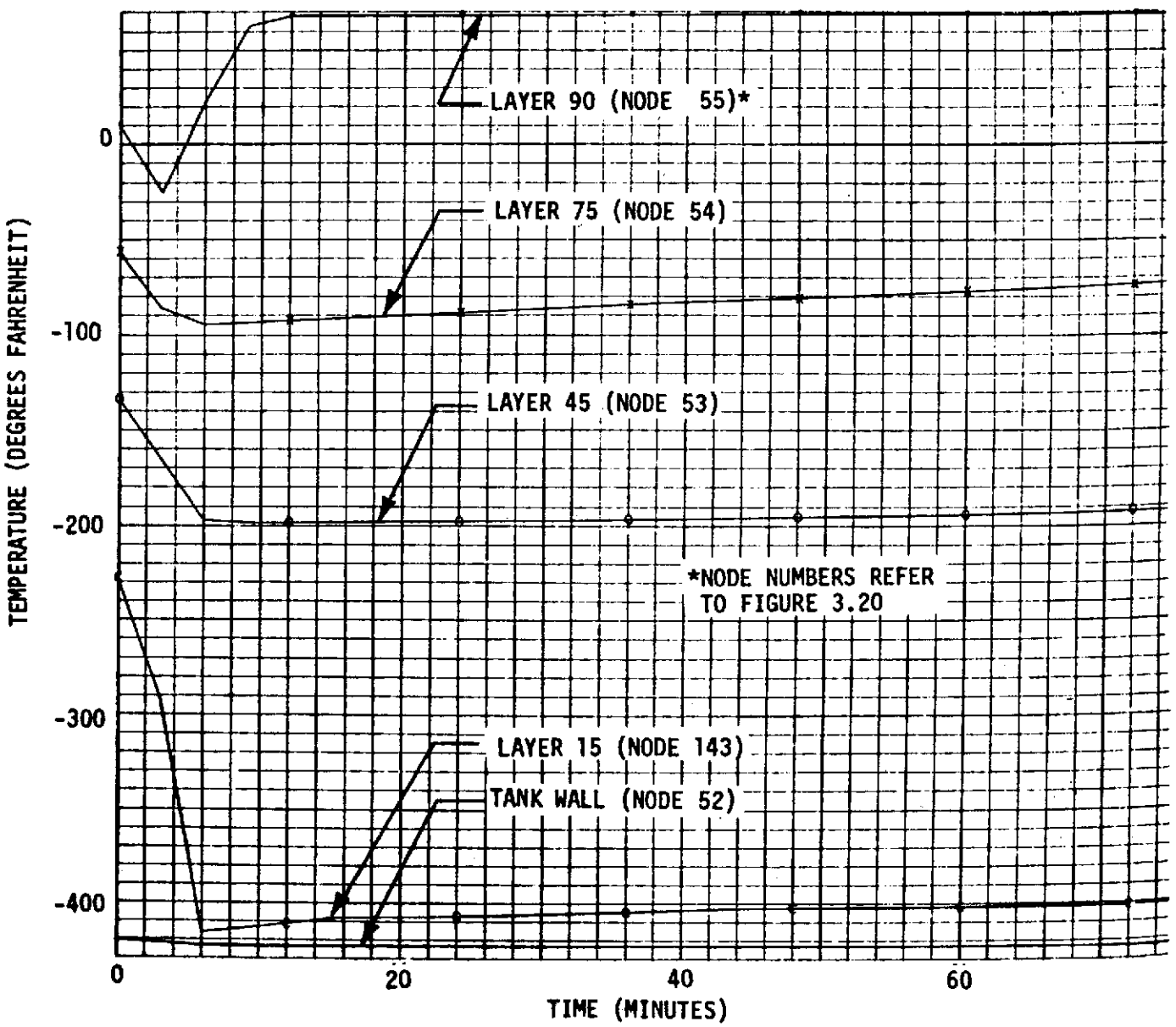

Figure 7.3.1.10-13. Temperature Distribution Through NARSAM-2 Insulation During Simulated Launch Ascent or Orbit (Center Section)

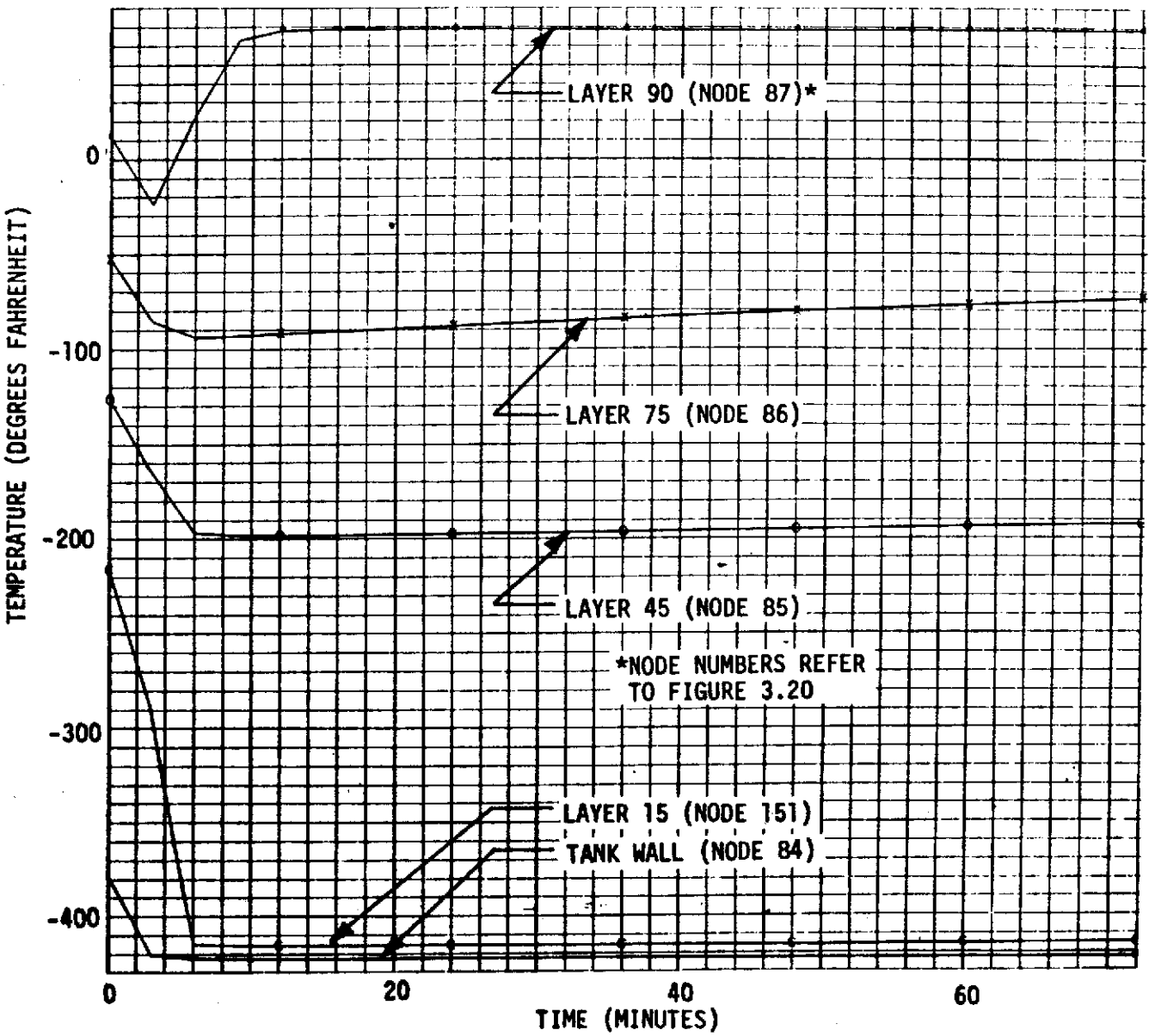

Figure 7.3.1.10-14. Temperature Distribution Through NARSAM-2 Insulation During Simulated Launch Ascent to Orbit (Upper Dome Section)

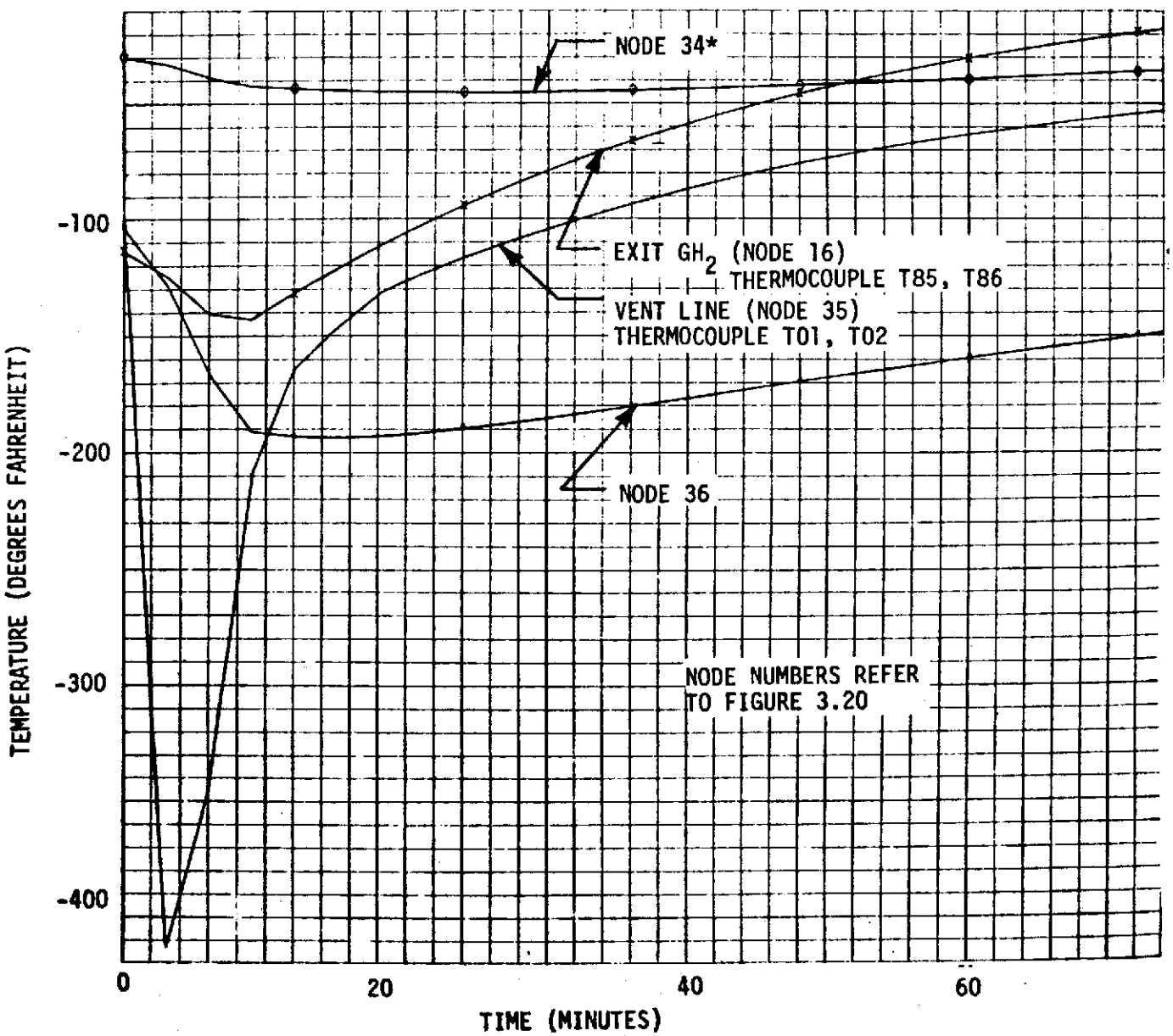

Figure 7.3.1.10-15. Ullage Gas Temperature as a Function of Time During Simulated Launch Ascent to Orbit

and LH_2 lines was specified in the S-II Vehicle Model Specification and vendor calculations show that the "as received" lines meet the specified requirements with adequate margin. However, subsequent S-II storage and operational procedures have resulted in degraded thermal performance due to loss of vacuum and caused marginal fluid conditions for S-II ignition. Several studies were initiated to determine improved procedures for better operational performance. The essential features of analyses as they relate to vacuum jacket performance are presented for completeness.

Heat is transferred across the annular space of the vacuum-insulated LH_2 feed and recirculation lines by radiation from the hot outer jacket to the cold inner wall, by gaseous conduction through the residual gas in the annular space, and by solid conduction through spacers and instrumentation bosses.

The radiant-heat transfer rate between the two surfaces is given by the expression

$$Q = F_e A_1 \sigma (T_2^4 - T_1^4)$$

For LH_2 lines, the pressure carrier is enclosed by the outer jacket. Surface 1 refers to the enclosed surface (pressure carrier) and Surface 2 refers to the enclosure (jacket). The emissivity factor for diffuse radiation between concentric cylinders is given by

$$F_e = \left[1/e + (A_1/A_2) (1/e_2 - 1) \right]^{-1}$$

Radiation heat exchange across the vacuum jacket depends upon surface emittances and temperatures and the spacing between the surfaces. The emittance (0.15) of the warm enclosing surface is assumed constant. The emittance of the LH_2 cooled inner wall, however, depends on the surface properties of the solid deposits formed by cryopumping. The following assumptions are available:

1. The solid deposit is completely transparent, and the emittance of the surface is identical to the emittance of the metal wall ($e, \simeq 0.061$).

2. The emittance of solid deposit is identical to ice ($e, \simeq 0.9$).

3. The effective value of emittance for the solid deposit cold wall combination is some intermediate value ($e, \simeq 0.3$).

Measurements were made to determine the absorbtance of CO_2 deposits on cold surfaces. Four combinations of well-polished copper wall and black wall surfaces were considered. For cryodeposit thicknesses greater than 1 mm, the absorbtance of well-polished surface is increased, and the absorbtance value of 0.3 appears to be good to use for a cryodeposit on a well-polished cold surface. Since emittance equals absorbtance for many materials, an effective emittance value ($e, \simeq 0.3$) was selected for Assumption 3. The cold wall surface temperature of 40 R was selected to represent LH_2 temperatures. The radiant heat transfer calculations presented in Figure 7.3.2.1-1 were made over a range of possible warm wall temperatures and the three emittance-coefficients shown. The recommended curve to use is labeled ($F_e = 0.1$) where

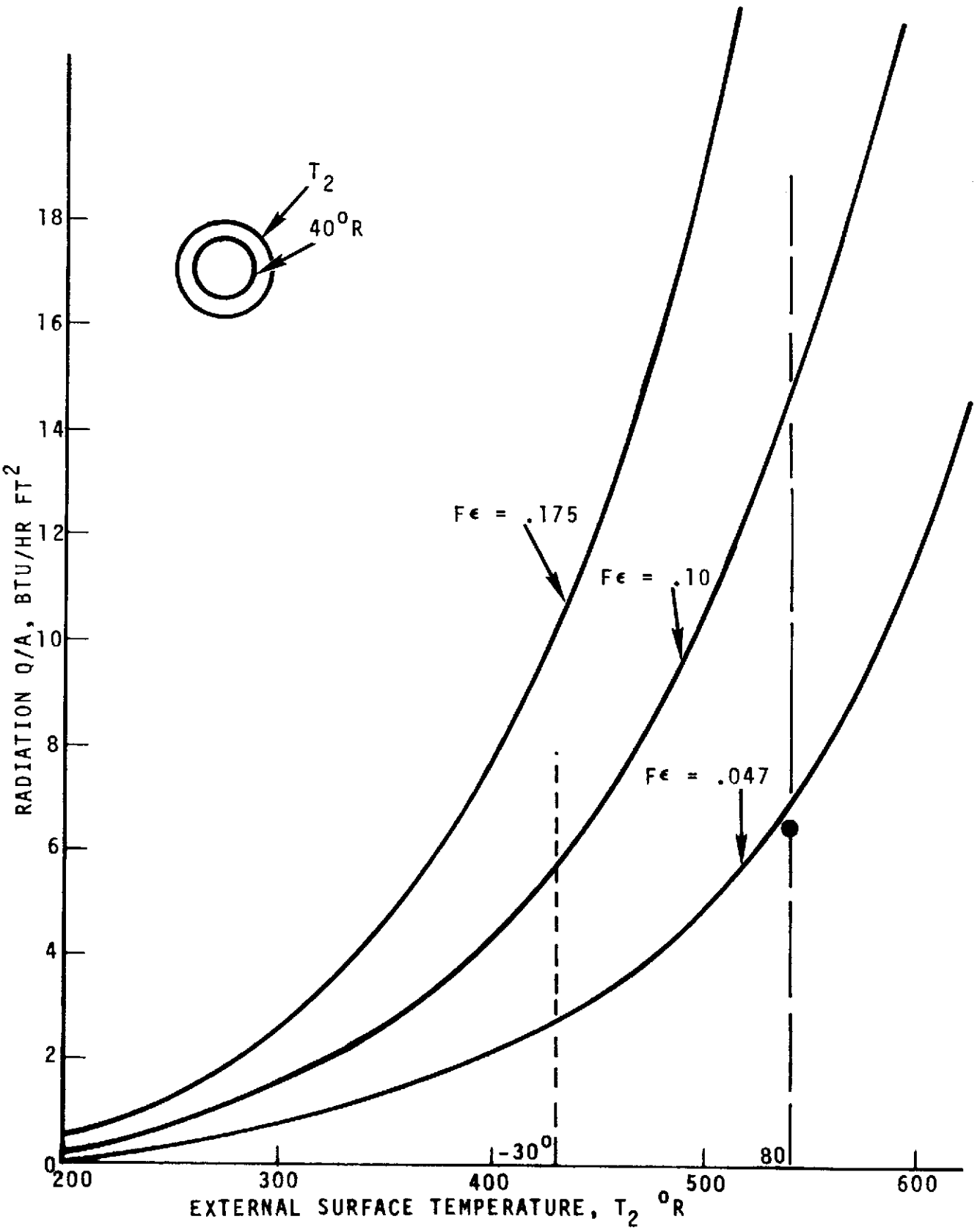

Figure 7.3.2.1-1. LH_2 Recirculation System Vacuum Jacket Performance

radiant heat transfer rates are 14.4 and 5.5 Btu/hr.-ft.^{2} for 80 and -30 F surface temperatures, respectively. The vendor who manufactured the S-II LH_2 feedlines assumed a cold wall emittance of 0.048 and neglected any emittance change due to frozen gas deposition in his design calculations. Therefore, the calculated radiant heat flux of 6.4 Btu/hr.-ft.^{2} is somewhat optimistic. The value is shown on Figure 7.3.2.1-1 for reference. In addition to heat transferred by radiation, energy is transmitted by gaseous conduction through the vacuum space in the jacket. If the pressure of the gas is low enough so that the mean free path of the gas molecules is greater than the distance between the two surfaces, the type of conduction differs from the usual continuum-type conduction at ambient pressure. For ordinary conduction with constant thermal conductivity, there is a linear temperature gradient within the medium transmitting heat. On the other hand, for free molecular conduction, the gas molecules rarely strike each other, thus, an individual gas molecule travels across the gas space without transferring energy to other gas molecules.

The technique for determination of heat transfer by free molecular conduction is presented in most textbooks. The essential features of these analyses as they apply to the current discussion are presented for completeness. Consider two concentric tubes maintained at T_1 and T_2, respectively, as shown in Figure 7.3.2.1-2. A gas molecule collides with the cold surface at T_1 and transfers some energy to the surface. Since the molecule does not remain on the surface long enough to establish thermal equilibrium, in general, it will leave with a kinetic energy corresponding to a somewhat higher temperature than T_1, say T_1'. This molecule at T_1' travels across the vacuum space and collides with the warm surface at T_2. Again, the molecule generally does not remain on the surface long enough to establish thermal equilibrium; therefore, it leaves the warm surface with a kinetic energy corresponding to a temperature somewhat less than T_2, say T_2'. The degree of approach to thermal equilbrium upon collision is expressed by the accommodation coefficient as defined

$$a = \frac{\text{Actual Energy Transferred}}{\text{Maximum Possible Energy Transfer}}$$

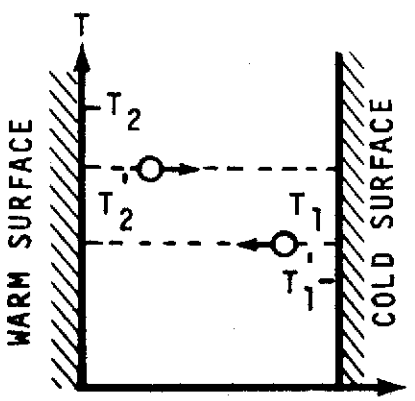

Figure 7.3.2.1-2. Gas Molecule "Temperatures" for Free Molecular Conduction

The accommodation coefficient depends on the specific gas surface combination in addition to the surface temperature.

For concentric cylinders, only a fraction (A_1/A_2) of the molecules emitted from Surface 2 will strike Surface 1. Therefore, the accommodation coefficients for the surfaces in Figure 7.3.2.1-2 are

$$a = \frac{T_2' - T_1'}{T_2' - T_1} \quad \text{cold surface}$$

$$a_2 = \frac{T_1' \; A_1/A_2 + T_2' \; (1 - A_1/A_2) - T_2'}{T_1' \; A_1/A_2 + T_2' \; (1 - A_1/A_2) - T_2} \quad \text{warm surface}$$

From the accommodation coefficient definitions, expressions for wall temperature can be determined. After some algebra, the temperature difference between the warm and cold surfaces may be written:

$$T_2 - T_1 = \left[\frac{1}{a_1} + \frac{A_1}{A_2}\left(\frac{1}{a_2} - 1\right)\right] \quad (T_2' - T_1') = \frac{T_2' - T_1'}{Fa}$$

where F_a is the accommodation coefficient factor which has exactly the same form as the emissivity factor.

The total change in energy per unit mass of the molecules striking the wall is the sume of the change in internal energy (C_vT) of the molecule as it is attached to the surface plus the change in kinetic energy (1/2 RT) of the molecules moving normal to the surface. Thus,

$$\Delta e = \frac{1}{2} \; \frac{\gamma+1}{\gamma-1} \; F_a \; R \; (T_2 - T_1)$$

From kinetic theory of gases, the mass flow rate of molecules per unit area is proportional to the product of gas density (ρ) and mean gas molecule velocity ($\bar{v}$):

$$\frac{\dot{m}}{A_1} = \frac{1}{4} \rho \bar{v} = \frac{1}{4}\left(\frac{P}{RT}\right)\left(\frac{8 \; g_c \; RT}{\pi}\right)^{1/2} = P \left(\frac{g_c}{2\pi \; RT}\right)^{1/2}$$

Reference 45 recommends that the temperature T used in the above equation be the temperature of the gauge used to measure the pressure of the gas. For S-II applications, the gauge temperature is identical to the vacuum jacket outer wall temperature. The energy transferred by molecular conduction may now be determined:

$$\frac{Q}{A} = \frac{\dot{m}}{A} \Delta e = \frac{\gamma+1}{\gamma-1} \left(\frac{99_c \; R}{8\pi MT}\right)^{1/2} F_a \; P \; (T_2 - T_1)$$

For convenience in the analysis of LH_2 vacuum-jacketed line, this equation is written in the following simplified form:

$$\dot{Q} = G\ F_a\ P\ A_1\ (T_2 - T_1)$$

where

$$G = \frac{\gamma+1}{\gamma-1}\left(\frac{g_c R}{8\pi MT}\right)^{1/2}$$

The quantity (G) is a function of individual gas properties, and has a unique value for each gas species. Computed values of G for the different gas constituents of air are presented in Table 7.3.2.1-1 for assumed gauge temperatures of 80 F and -30 F.

Table 7.3.2-1-1. Gas Conduction Parameters for Vacuum Jacket Thermal Analysis

	Free Molecule - Transition						Continuum Transition	
	G(ft/sec.-°R)		PD (μ - in.)		C (μ - in.)		PD (μ - in.)	
Component	T = 80	T = -30	T = 80	T = -30	T = 80	T = -30	T = 80	T = -30
N_2	2.18	2.44	6.6	4.9	-	-	198	147
He	4.11	4.61	19.5	15.1	71.0	54.7	585	453
A	1.30	1.46	-	-	-	-	-	-
Ne	1.84	2.03	13.8	10.3	51.6	39.4	414	309
H_2	7.95	8.91	12.0	9.4	14.9	10.9	360	282

For free molecular conduction to occur, the mean free path of the gas molecules must be larger than the spacing between the two surfaces. The Knudsen number (KN) is the criterion used to check this condition, and is given by:

$$KN = \frac{\lambda}{D} = \frac{\mu}{PD}\left(\frac{\pi RT}{2\ g_e M}\right)^{1/2}$$

The accepted standard for free molecular conduction is when KN is greater than 0.3. Since the viscosity of most gases varies at T0-54n (where 0 17 1/2) the mean free path varies inversely with pressure and is proportional to T. The free molecular conduction component is of heat transfer in vacuum-insulated lines may be made negligible compared to the radiation component of heat transfer by reducing the gas pressure to low values. Computed values of the PD product for the different gas components of air are presented in Table 7.3.2.1-1 for assumed gauge temperatures of 80 F and -30 F.

For KN less than 0.01, the usual form of gas conduction occurs. The thermal conductivity of gases in the continuum flow regime is tabulated in standard heat transfer references. The technique for calculating heat transfer is the following expression:

$$\dot{Q} = K\, A_1\, (T_2 - T_1)/D$$

As the gas pressure approaches atmospheric, gas conduction is supressed and natural convection in enclosed spaces prevails. An adequate discussion of this heat transfer mode is presented in most references. Since convection is not expected in S-II vacuum-jacketed lines, no further discussion is required.

Between the limits $(0.1 < KN < 0.3)$, a mixture of free molecular conduction in the usual form occurs. The defining relationship for heat transfer in the transition region is the usual heat conduction equation. However, the following special definition of thermal conductivity is required:

$$\frac{K}{K^{\infty}} = \left| 1 + \frac{C}{PD} \right|^{-1}$$

where

K = Thermal conductivity in transition region

K = Thermal conductivity in continuum region

P = Gauge pressure

D = Spacing between the warm and cold surfaces

C = A parameter defined by the relation:

$$\lim_{P \to 0} \frac{K}{K^{\infty}} = \frac{PD}{C}$$

The lower limiting condition for heat transfer in the transition flow region is the point where free molecular flow controls, thus

$$\dot{Q} = G\, F_a\, P\, A_1\, \Delta T = (K/D)\, A_1\, \Delta T$$

The parameter C, therefore, may be determined by the following expression:

$$\lim_{P \to 0} \frac{K}{K^{\infty}} = \frac{GF_a\, PD}{K^{\infty}} = \frac{PD}{C}$$

which implies that

$$C = \frac{K^{\infty}}{GF_a}$$

Computed values of C for the different gas components of air are presented in Table 7.3.2.1-1 for assumed gauge temperatures of 80 F and -30 F.

The above equation can be rewritten in a form which is more convenient for thermal analyzer calculations.

$$\frac{1}{K} = \frac{1}{K\infty} + \frac{1}{GF_{\alpha}PD}$$

By considering a section of pipe located away from the thermal shorts, solid conduction may be omitted from the analysis. The emittance coefficient (0.1) for the radiation from the passivated stainless steel outer wall to the cryopumped-gas solid deposit on the cold wall was calculated in Reference 45. For one square foot of external vacuum jacket surface, the heat transfer rate across the annular space is

$$(Q/A)_1 = GF_aP\ (T_{surf} - T_o) + 0.1\ \sigma\ (T_{surf}^4 = T_o^4)$$

where T_o equals the temperature of the cryogenically cooled wall.

Heat is transferred to the surface of the vacuum-jacket-insulated LOX feed lines by radiation from the surroundings and by convection from the environment. The effective radiation temperature of the surroundings is assumed equal to the ambient temperature. An emittance coefficient (0.9) for passivated stainless steel pipe is assumed. Turbulent natural convection on a vertical cylinder is assumed. For one square foot of external vacuum-jacketed surface, the heat transfer rate into the vacuum jacket is

$$(Q/A)_E = 0.19\ \sigma\ (T_{amb}^4 - T_{surf}^4) + 0.19\ (T_{amb} - T_{surf})^{4/3}$$

Heat is transferred across the annular space of the vacuum insulated lines by radiation from outer jacket to the cold inner wall, by gaseous conduction through the residual gas in the annular space, and by solid conduction through the material.

For steady state, $(Q/A)_E$ must equal $(Q/A)_I$. A graphical technique is the most convenient method of solution. Figure 7.3.2.1-3 plots solutions of the equation for $(Q/A)_E$ for ambient temperatures of -40, 0, -40 and 80 F over a range of surface temperatures from -200 F to 80 F. Figure 7.3.2.1-3 also plots solutions to the second term of the right-hand side of equation $(Q/A)_I$ over the same range of surface temperatures. The intersection of these curves represents the ambient temperature and surface temperature combination to be expected when a hard vacuum is present in the annular space of the LOX lines. Note, however, that the difference between the external heat input and the radiation across the annular space for a given surface temperature is the heat transfer due to gas conduction through the residual gases in the annular space. For example, measured ambient temperature adjacent to a LOX feedline is 80 F and the vacuum jacket surface temperature is 40 F. From Figure 7.3.2.1-3, the heat transfer rate from the environment is 0.0094 Btu/sec.-ft.^{2} and the heat transfer rate by radiation across the vacuum jacket is 0.0026 Btu/sec.-ft.^{2}. The difference

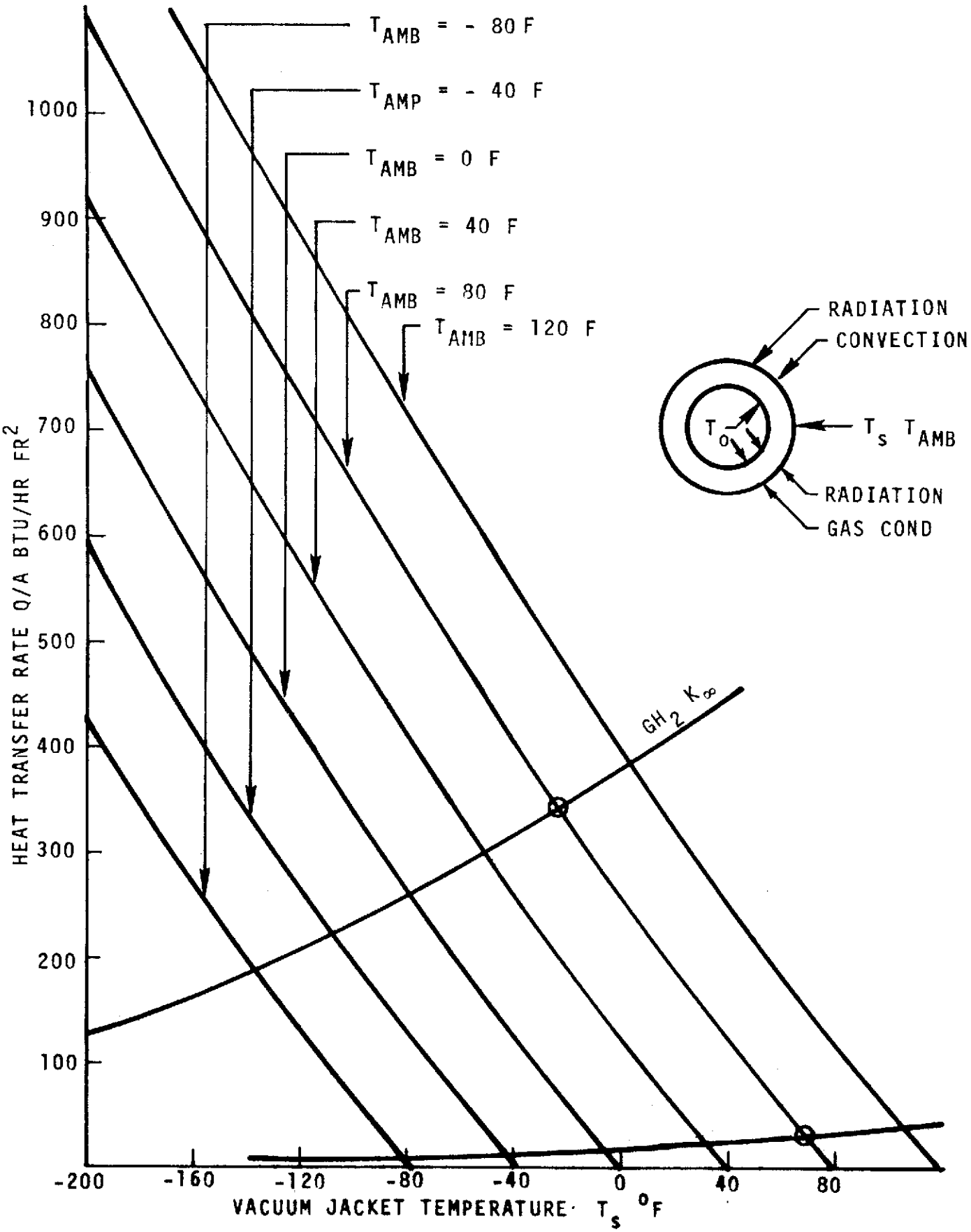

Figure 7.3.2.1-3. Vacuum Jacket Performance

(0.0068 Btu/sec.-ft.^{2}), therefore, is the gas conduction heat transfer rate. By comparison, had gas conduction been negligible, the surface temperature would have been 65 F and the corresponding heat transfer rate would have been only 0.0032 Btu/sec.-ft^2.

7.3.2.2 Vacuum Jacket With Multilayer Insulation

The heat transfer into various propellant ducts and lines is particularly important in determining engine start capability. The total surface area is small compared to the surface area of the tanks; however, the configuration is such that a majority of the total loss may come from such special lines. An example of this overall analysis is presented in Subsection 7.4.3.

The heat transfer for typical vacuum-jacketed lines has been calculated and is presented in Figure 7.3.2.2-1. The analysis was prepared assuming that the exterior surface was at zero F. The heat leak for a vacuum-jacketed line was found to be 10^{-2} Btu/hr.-ft. for a 4-inch line. This assumed that the vacuum jacket was evacuated to 10^{-5} torr. This rate is so hight that it would not be usable for long-term operation in space; thus the use of MLI was investigated. The results are shown in Figure 7.3.2.2-1 in which the rate was shown to be 4.5×10^{-4} Btu/hr.-ft. for the same size line with one inch of MLI.

The heat transfer through the MLI is particularly sensitive to the gas in the surrounding volume. The effects are shown in Figure 7.3.2.2-2 as copied from "Thermal Insulation Systems, A Survey," NASA SP-5027. There is sufficient long-time leakage of hydrogen through the metal wall of lightweight pipes so that the pressure in a vacuum jacket would rise about 10^{-3} torr; thus, for orbital conditions, the MLI must be vented. The curves and analysis as shown in Figure 7.3.2.2-1 assumed a gas pressure of less than 10^{-5} torr in the MLI.

7.3.2.3 Glass Fiber Batting Encased in CRES Sheet

a. Statement of Problem: The following thermal analysis was required in support of the design of the S-II stage LOX feed and recirculation system:

   1. Prediction of LOX temperature histories during unpressurized and pressurized ground-hold, and from liftoff through S-II ignition.

   2. Determination of heat transfer rates to individual system components.

   3. Determination of insulation requirements to minimize heat leak into the feed system.

      (a) Pre-molded insulation for LOX sump, prevalves, and center engine feedline.

      (b) Vacuum-jacketed insulation for outboard engine feedlines.

      (c) Premolded fiberglass insulation for engine components.

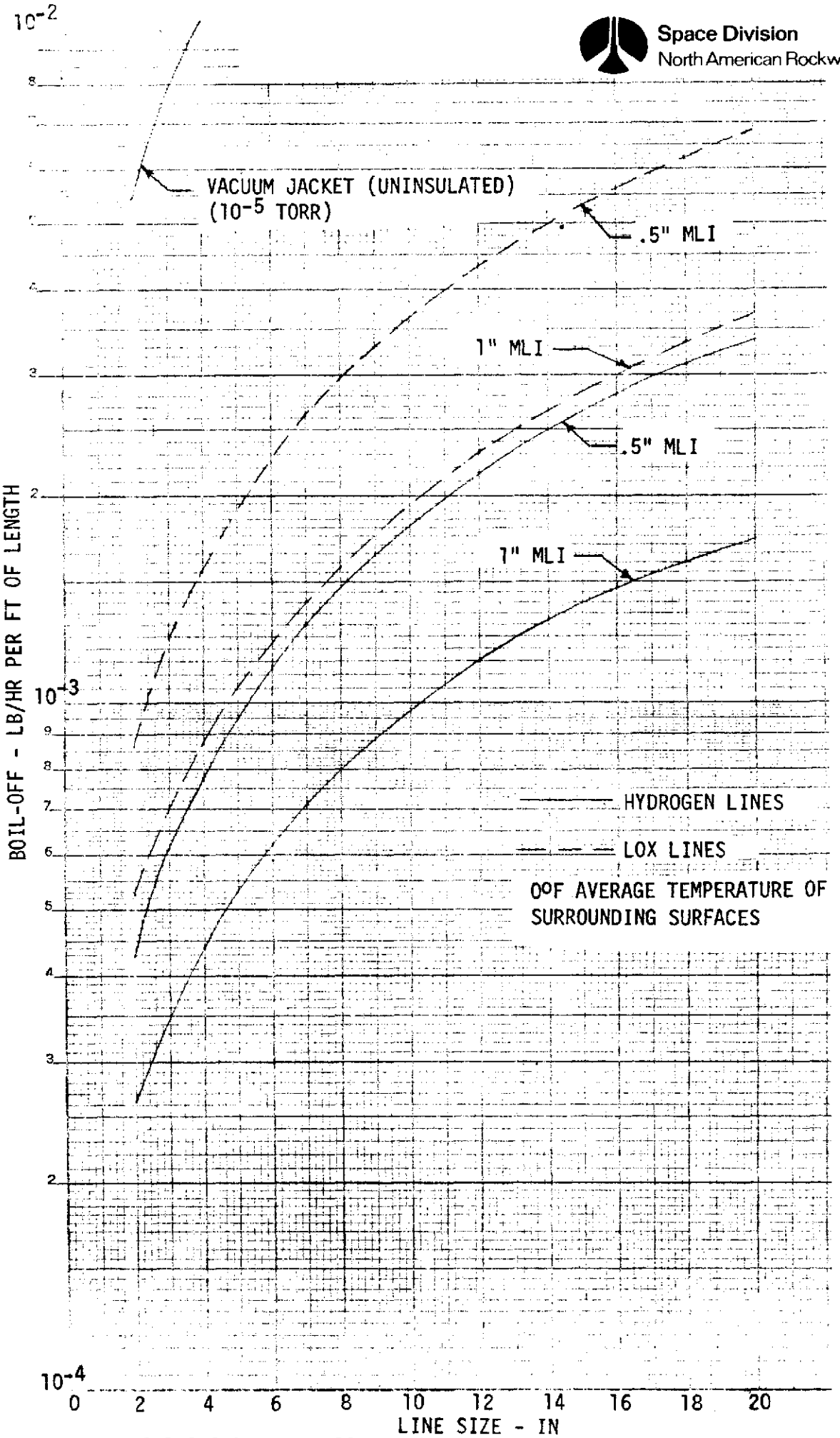

Figure 7.3.2.2-1. Propellant Line Heat Leak by Radiation - Orbit

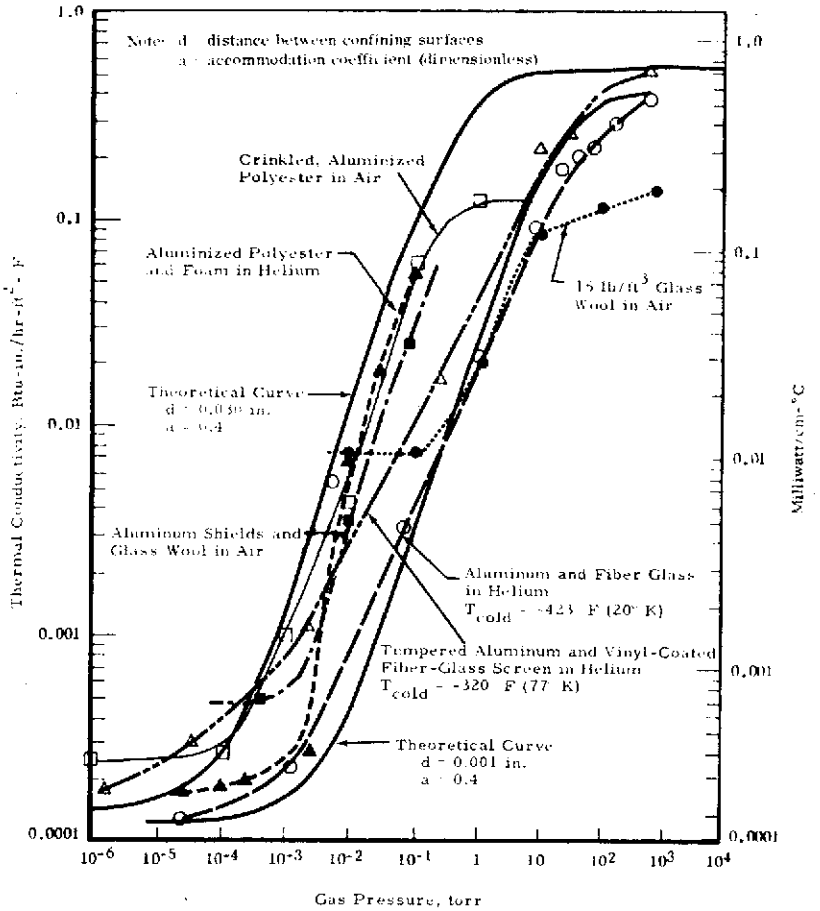

Figure 7.3.2.2-2. Effect of Gas Pressure on Thermal Conductivity

These problems were analyzed simultaneously as components of a single system.

b. Description of LOX Recirculation System: The LOX feed and recirculation system is shown schematically in Figure 7.3.2.3-1. One purpose of this system is to precondition the stage and engine LOX systems by removing heat from the feed ducts and pumps prior to engine start. This is achieved by recirculation of LOX by natural convection through the feed duct, engine pump, and gas generator bleed circuit of each engine, and then by return lines back to the LOX tank. The pre-valves and return line valves are opened prior to LOX tanking to allow the recirculation flow. The driving force for recirculation is provided by the density difference between the fluid in the feed ducts and the warmer, less-dense fluid in the uninsulated return lines.

A second purpose of this system is to assure that the J-2 engine LOX inlet temperature conditions are within specified limits at engine start. The design requirement is that the LOX pump discharge liquid temperature be a minimum of 3 F colder than the saturation temperature for a given LOX pump discharge total pressure. The required engine start box envelope is presented in Figure 7.3.2.3-2. The saturation temperature corresponding

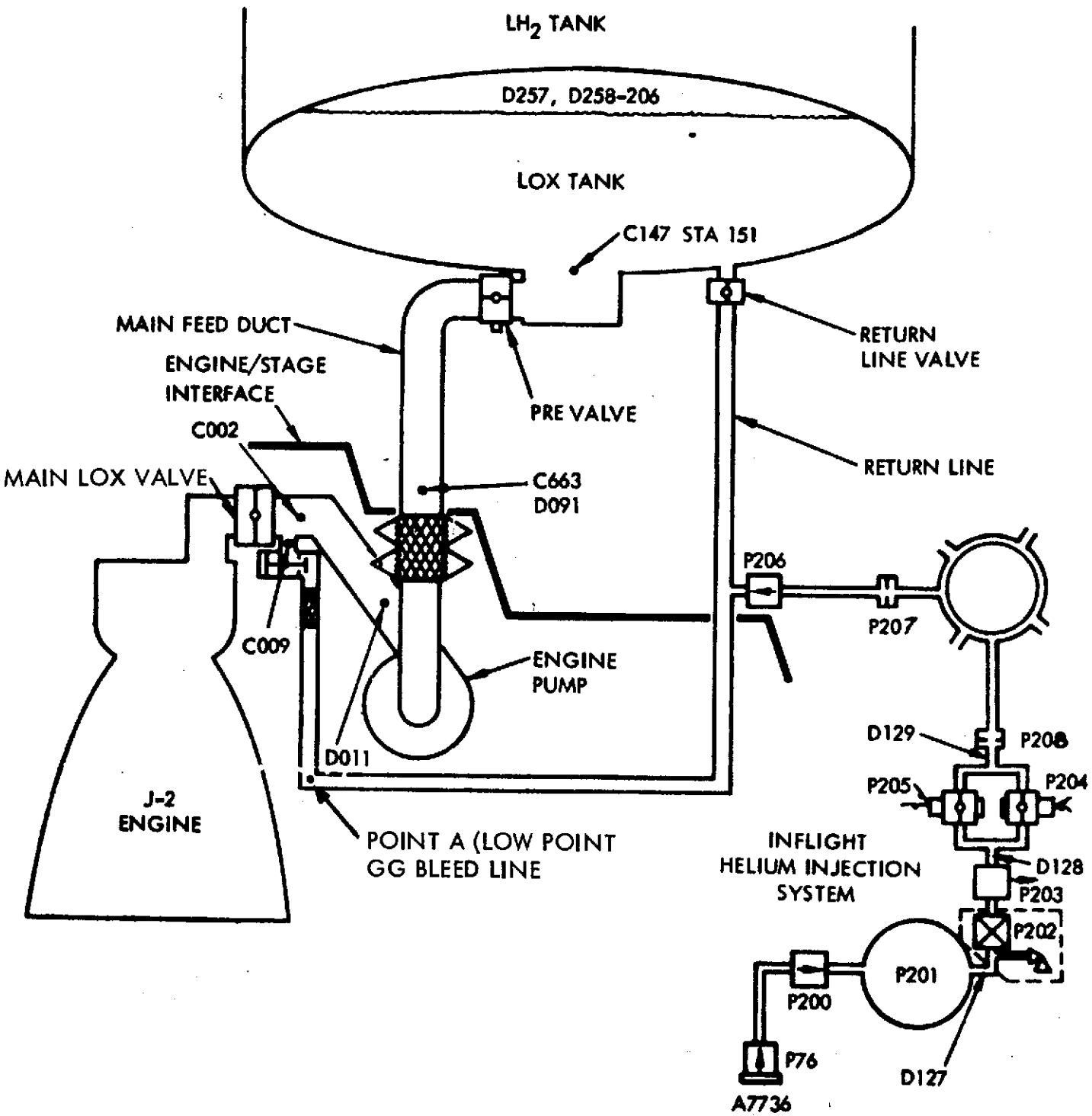

Figure 7.3.2.3-1. LOX Recirculation System Schematic

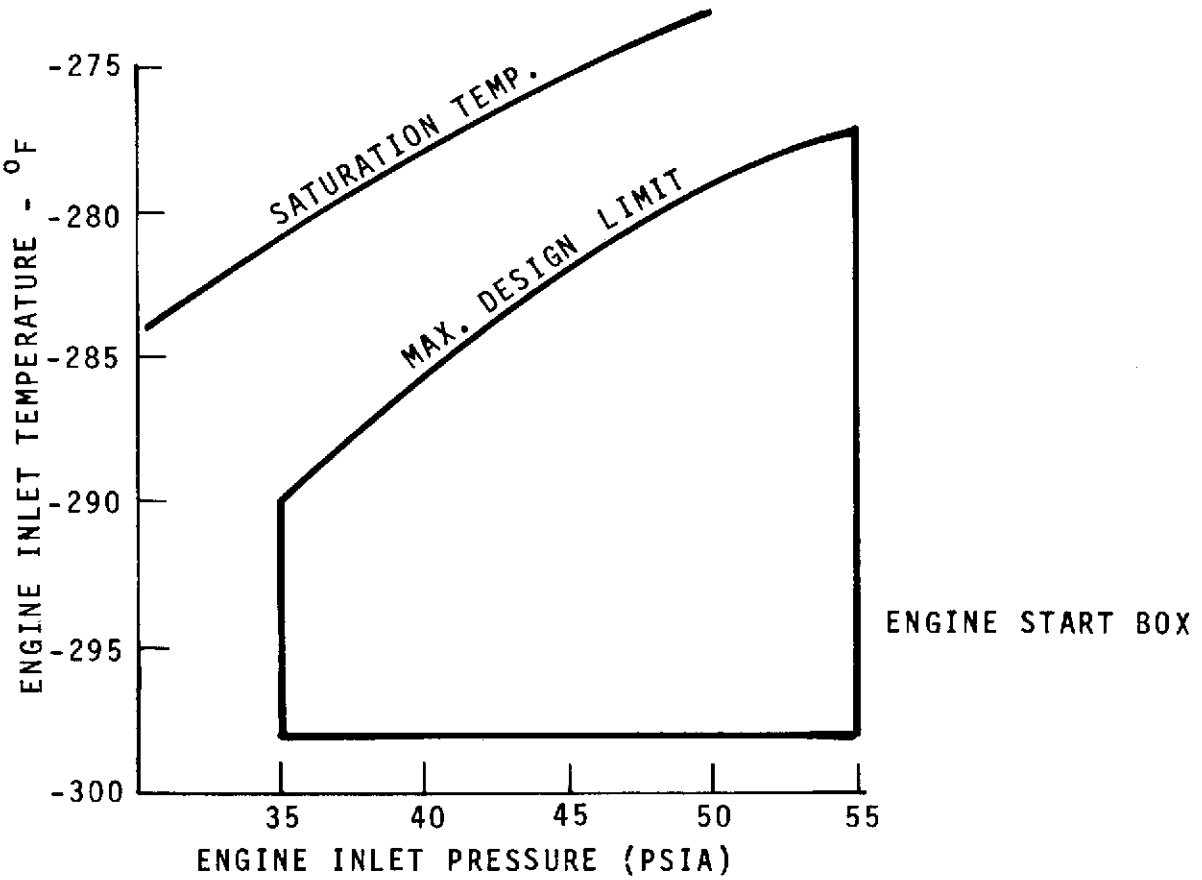

Figure 7.3.2.3-2. LH_2 Recirculation System Performance

to the different fluid pressure is presented for comparison. To assure satisfactory inflight engine start conditions, the stage portion of the system is vacuum-jacket insulated and the engine portion upstream of the gas generator bleed line low point (Point A, Figure 7.3.2.3-1) is insulated with fiberglass batting. The remaining portion of the engine piping and the individual return lines are uninsulated. To further assure satisfactory performance, the recirculation driving force is increased by injecting ambient helium gas into the bottom of the return lines to decrease the return line fluid density. The helium is injected into the recirculation system beginning 30 minutes prior to liftoff. Helium injection is maintained throughout S-IC boost and terminated 1.2 seconds prior to S-II engine start.

c. Methodology and Analysis: The insulation requirements for the LOX sump, pre-valves, and center engine feed line were determined by test and analysis. Tanking test data for battleship and early S-II flight vehicles revealed marginal LOX pump discharges temperatures at simulated liftoff conditions. A preliminary analysis of the S-II stage LOX recirculation system design revealed that the LOX sump and the pre-valves for each engine feed line were uninsulated and that the vacuum-jacket insulation for the center engine feed line had been removed due to manufacturing difficulties. Each of these uninsulated components is exposed to a relatively warm interstage environment. A further analysis of the S-II engine LOX system design revealed that the inlet bellows, volute, and high pressure duct of the LOX

pump were likewise uninsulated and exposed to the interstage environment. Obviously, the marginal LOX pump discharge temperature (LPDT) was due to excessive heat leak through these components. As a result, S-II Engineering decided to minimize heat leak and to reduce the LPDT to more acceptable levels by insulating specified components of the LOX feed and engine systems. The insulation of engine components was referred to the engine supplier.

The thermal performance characteristics of the LOX feed and recirculation system is reflected by the levels of fluid temperature and pressure at designated points in the flow system. A detailed thermal model was prepared to predict these characteristics. Seventeen fluid nodes were used to represent the LOX temperatures and additional nodes were used to represent piping and insulation components. The heat flux paths were represented by conductances between appropriate nodes.

The pre-formed insulation selected for stage components is shown schematically in Figure 6.2.3.1-1. The insulation consists basically of a fiberglass-type batting material enclosed by an inner and outer CRES foil sheet (3 mils thick) which serves as a moisture barrier. A parametric analysis was used to determine the required insulation thickness. An effective thermal conductance of 0.3 Btu/hr.-°F-ft.^{2} reduces the prevalve body temperature adjacent to the LOX to approximately the temperature of nearby components of the outboard engine feedlines, and, therefore, was selected for design purposes. The batting material has a thermal conductivity of 0.3 Btu-in./hr.-°F-ft.^{2} at ordinary room temperature. The minimum thickness requirements, therefore, is 1.0 inch, except for flanges, where 0.5 inch minimum is permitted.

Insulation for the LOX pump inlet bellows, pump volute, and high-pressure duct was provided by the engine supplier. A premolded polyurethane foam is applied to the inlet bellows and the high-pressure duct. The LOX pump volute is insulated with wrapped fiberglass batting covered by a sensitized aluminum tape and sealed with RTV. Supplier calculations (provided by Rocketdyne) indicate that this insulation reduces the heat leak attributable to these components approximately 50 percent. The insulation for the inlet bellows, however, may not provide the desired thermal protection. Because of requirements that axial movement be permitted, a two-piece construction was used. A 0.090-inch gap between the inner and outer section of insulation is large enough to permit a convective flow of warm environment gases between the insulation shell and the bellows surface. The presence of convective heating under the insulation together with the convoluted heat transfer surface make the bellows a difficult component to model thermally. An effective insulation (say K/X = 0.3 Btu/hr.-F-ft.^{2}) which completely encapsulates the bellows can reduce the overall heat transfer rate by 80 percent compared to natural convection with no insulation. The resulting LOX temperature rise due to this heat leak would also be reduced by 80 percent. Some Battleship test data, however, indicate that no reduction in LOX inlet temperature is experienced as a result of applying insulation to the inlet bellows.

d. Assumptions:

1. Interstage Environment:

(a) Ambient temperature is 0 F initially and varies with time.

(b) Natural Convective heating.

(c) Radiation from environment; effective radiation temperature assumed equal to environment.

2. Insulation:

(a) Vacuum jacket:

(1) Emissivity is 0.9, but varies with temperature.

(2) Gas conductivity varies with temperature.

(3) Solid conduction through spacers and instrumentation bosses.

(b) Premolded fiberglass insulation:

(1) Emissivity is 0.15, surface corresponding to the exterior stainless steel casing. (3 mils thick) at room temperature and varies with temperature.

(2) Thermal conductivity is 0.29 Btu-in./hr.-F-ft.^{2} at room temperature and varies with temperature.

(3) Specific heat is 0.3 Btu/lb.-°F at room temperature and varies with temperature.

(4) Mechanical joints are properly closedout so that convection beneath the insulation adjacent to LOX piping may be neglected.

(5) No frost or ice formation on insulation surface.

(c) Fluid Thermodynamics:

(1) Forced convective heating in boundary layer adjacent to pipe wall.

(2) Nucleate boiling in boundary layer adjacent to pipe when wall temperature is greater than fluid saturation temperature.

(3) No net vapor generation as subcooling causes local condensation.

(4) Homogeneous fluid assumptions used to compute local density, momentum change, and frictional loss properties for LOX-GHe mixture.

(5) Momentum change coefficients and equivalent lengths for valves and pipe fittings were obtained from standard text books.

(6) Fluid flow is turbulent.

(7) Helium injection flow rate is 0.002 lb./sec. at an injection pressure of 100 psia and environmental temperature.

(8) Ullage pressure in LOX tank varies with time.

(9) Local acceleration of fluid during S-I boost varies with time.

e. Results and Conclusions: LOX recirculation system and individual component heat transfer rates for a typical outboard engine feedline and the center engine feedline are summarized in Tables 7.3.2.3-1 and -2 respectively. The uninsulated heat leak totals are approximately 8.4 and 6.0 Btu/sec and center engine feedlines, respectively. Insulation reduces these totals to 4.2 and 2.9 Btu/sec. Analysis indicates the outboard engine heat leak could be further reduced by an evacuated double wall construction of the inlet bellows instead of externally applied fiberglass block insulation. However, the present insulation systems permit the LOX pump discharge temperatures to meet the desired engine start requirements.

The glass fiber batting is an effective insulation for reducing heat leak to LOX through the pre-valve from 0.322 to 0.026 Btu/sec. The overall heat flux through the insulation system is approximately 82 Btu/hr.-ft.^{2}. However, it should be noted that good thermal performance requires that the seams and joints of the insulation be sealed to prevent a convective flow of hot environmental gasses under the insulation.

7.3.2.4 Glass Fiber Batting - Tape-Wrapped

The supporting analysis for this insulation system is presented in Paragraph 7.3.2.3. The substitution of tape wrapping for the CRES sheet does not change the thermal performance characteristics of either the insulation system or the LOX feed and recirculation system where the insulation is used.

7.3.2.5 Pour Foam

The supporting analysis to determine the thermal performance of pour foam on cryogenic transfer lines is the same as that given for spray-on foam in Paragraph 7.3.2.6.

7.3.2.6 Spray-on Foam (Feed Lines)

On the S-II, the vacuum jacket is the prime insulation system for cryogenic transfer lines. However, the end flanges, valves, and other piping components of early S-II stages were uninsulated. The AS-501 flight and static firing test results indicated that insufficient LH_2 engine inlet NPSH margin existed for S-II inflight engine start. Since a large percentage of the heat absorbed

Table 7.3.2.3-1. Outboard Engine Feedline Heat Leak Summary

Component	Area ($ft.^2$)	Heat Transfer (Btu/sec.)	
		Insulation	Uninsulated
Pre-valve	1.142	0.026	0.322
Vacuum Jacket Feedline	14.835	0.086	0.450
Inlet Bellows	21.800	1.815	3.630
LOX Pump Volute	7.854	0.210	1.370
High Pressure Duct (Including MOV)	2.182	0.050	0.360
Subtotal		2.187	6.132
G.G. Bleed Line (Including Valve) (Insulated)	2.615	0.130	0.433
G.G. Bleed Line (Uninsulated)	2.382	0.395	0.395
Return Line (Including Valve)	8.822	1.470	1.470
Total		4.182	8.430

Table 7.3.2.3-2. Center Engine Feedline Heat Leak Summary

Component	Area ($ft.^2$)	Heat Transfer (Btu/sec.)	
		Insulation	Uninsulated
Pre-valve	1.140	0.026	0.322
Feedline	9.070	0.200	1.670
LOX Pump Volute	7.854	0.210	1.370
High Pressure Duct (Including MOV)	2.182	0.050	0.360
Subtotal		0.486	3.722
GG Bleed Line (Including Valve) ((Insulated) to PTA)	2.615	0.130	0.433
GG Bleed Line (Uninsulated)	2.382	0.395	0.395
Return Line	8.822	1.470	1.470
Total		2.481	6.020

by LH_2 passes through uninsulated flanges and fittings, the following study was performed to determine the total feed line heat leak to LH_2 and to evaluate the reduced feed line total heat leak when specified heat leak sources are insulated with spray-on foam.

a. Statement of Problem: Determine the heat leak to LH_2 through specified feed line piping components and the reduced feedline total heat leak to be achieved by insulating these heat leak sources.

b. Methodology and Analysis: The following components are considered adaptable to insulation with spray-on foam:

Bypass support bracket

Valve interface flange (line side)

Pre-valve flanges

Pre-valve operator

LH_2 feed line gimbal (center engine only)

Stage interface flange

c. Assumptions: The following assumptions were used in preparing this analysis:

1. Miscellaneous Heat Sources: The results of a previous study indicate that the decrease in heat leak achieved by applying insulation to instrumentation bosses is neglibible and that the standoffs are components of the vacuum jacket structure and are not adaptable to insulation.

2. Environmental Conditions:

Turbulent natural convection

No air condensation on cryogenic surfaces

Ambient temperature = 100 F

3. Thermal conductivity of spray-on foam:

K = 0.06 Btu/Hr-Ft F → Btu-in/hr-Ft -F

4. Insulation thickness = 0.3 inch

d. Results and Conclusions: The heat leak into the LH_2 feed and recirculation lines due to the various sources is summarized in Tables 7.3.2.6-1 and 7.3.2.6-2 for an outboard engine and the center engine, respectively. The results presented indicate that approximately 90 percent of the heat leak absorbed by LH_2 is due to flanges and fittings. The remaining 10 percent is due to radiation across the vacuum jacket. Insulating the specified items reduces the heat leak to those items by 90 percent and reduces the overall

Table 7.3.2.6-1. Miscellaneous Heat Leak Summary - Outboard Engine Feed Line

Component	Heat Leak (Btu/hr.)	
	Insulated	Uninsulated
Bypass Support Bracket	137	956
Valve Interface Flange (Line Side)	21.7	308.0
Pre-valve Flanges	42.3	628.0
Pre-valve Operator	25	252.0
Stage/Engine Interface Flange	21.7	310
Subtotal	247.7	2454
Other Sources*		
Standoffs	426	426
Bosses	367	367
Subtotal	1040.7	3247
LH_2 Recirculation Pump*	1735	1735
LH_2 Recirculation Line*		
Vacuum Jacket	23	23
Instrumentation Bosses (4)	142	142
Spacers (3)	171	171
Flanges (2)	520	520
Subtotal	856	856
Total Heat Leak	3631.7	5838

*No Insulation

Table 7.3.2.6-2. Miscellaneous Heat Leak Summary - Center Engine Feed Line

Component	Heat Leak (Btu/hr.)	
	Insulated	Uninsulated
Bypass support bracket	137.0	956.0
Valve Interface Flange (Line Side)	21.0	308.0
Pre-valve Flanges	42.3	628.0
Pre-valve Operator	25.0	252.0
Gimbal	161.8	2480.0
Stage/Engine Interface Flange	21.7	310.0
Subtotal	409.5	4934.0
Other Sources*		
Standoffs	426.0	426.0
Bosses	367.0	367.0
Subtotal	1202.5	5727.0
LH_2 Recirculation Pump*	1735	1735
LH_2 Recirculation Line*		
Vacuum Jacket	23	23
Instrumentation Bosses (4)	142	142
Spacers (3)	171	171
Flanges (2)	520	520
Subtotal	856	856
Total Heat Leak	3793.5	8318.0

*No Insulation

heat leak by 38 percent for the outboard engine feed lines and by 54 percent for the center engine feed line. The difference in heat leak savings is due to a gimbal joint in the center engine feed line. Qualification tests of the S-II-4 stage, where the specified components were insulated with spray-on foam, verify that an overall heat leak reduction of approximately 50 percent was achieved.

For the S-II, insulating bare flanges and fittings was the most expedient procedure for reducing heat leak. For future vehicles, the use of vacuum-insulated fittings should be considered.

Fluid thermal properties have a strong temperature dependence on cryogenically cooled surfaces. This condition makes prediction of the boundary layer convective conductance difficult. This analysis assumed a value of 4.0 Btu/hr.-°F-ft.^{2}. The resulting overall heat leak to LH_2 Btu/sec. with the specified items uninsulated and approximately 1.05 Btu/sec. insulated. Figure 7.3.2.6-1 shows the fluid temperature rise in the feed line as a function of LH_2 flow rate. For a flowrate of 0.6 lb./sec., the LH_2 temperature rise is 1.6 F uninsulated and 0.8 F insulated.

The effects of reduced ambient temperature and aerodynamic heating under the fairing upon the heat leak to LH_2 were investigated. A reduction in ambient temperature to 0 F reduces the overall heat leak to LH_2 less than 5 percent. The increase in heat leak due to boost aerodynamic heating is negligible.

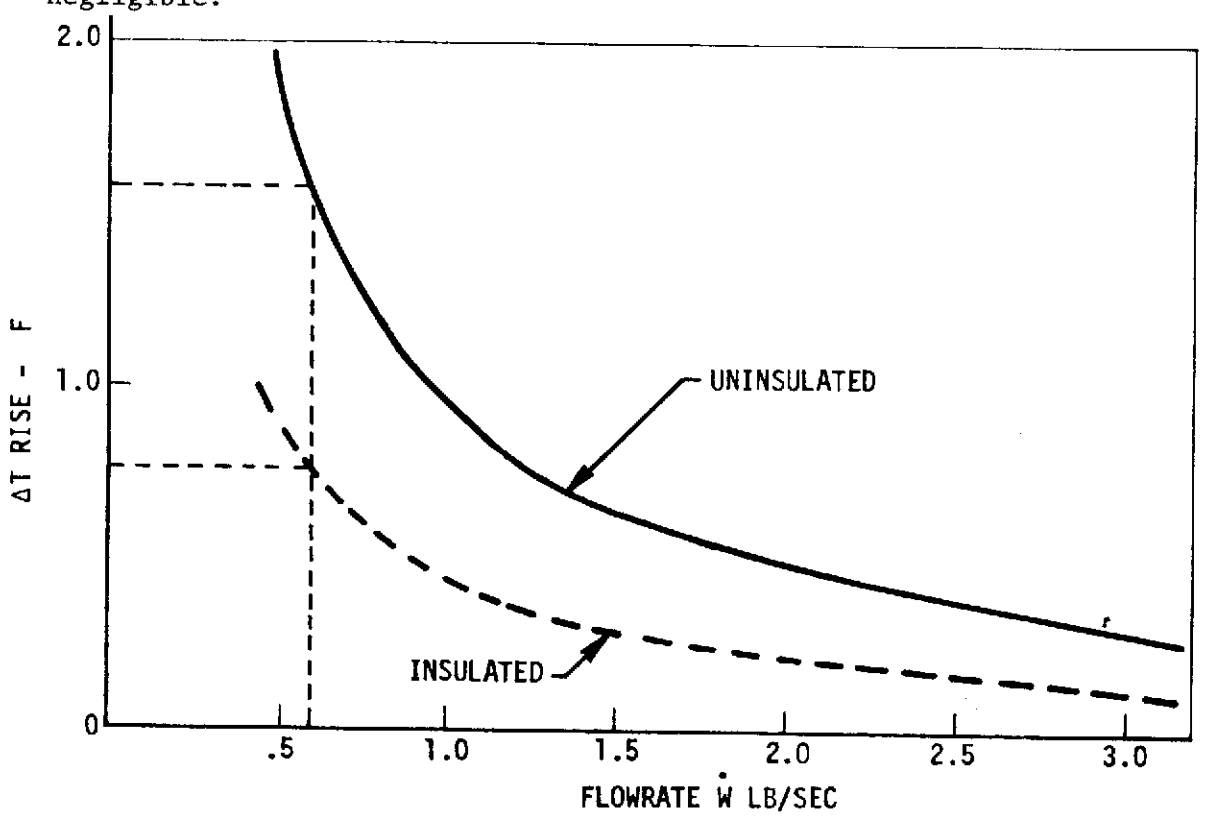

Figure 7.3.2.6-1. LH2 Recirculation System Performance

7.3.3 High Temperature Systems

7.3.3.1 Heat Resistant Phenolic (HRP) Honeycomb Rigid Heat Shield

For analysis purposes the rigid heat shield was dividied into zones as shown in Figures 7.3.3.1-1 and 7.3.3.1-2. Radiant heat configuration factors were determined for each zone and all other zones including the engines and space. A general heat transfer analysis computer program was then used to determine temperatures for all heat shield zones. Heat transfer modes used in the analysis were convective (from the recirculating hot exhaust gases), radiant (from the engine plumes), radiation interchange (between all heat shield zones, nozzles, and space) and conduction (through the heat shield).

The thermal properties used in the analysis are listed in Table 7.3.3.1-1. Except for the thermal conductivity, these properties were based on static thermal properties laboratory tests. The thermal conductivity of the filled honeycomb was determined based on the results of a rigid shield 48 x 48 inch structure-thermal vibration test and is considerably higher than values determined during static thermal tests. It is believed that the vibration in the 48 x 48 inch test agitated the micro-balloon filler within the HRP honeycomb and thus increased the thermal conductivity.

Temperatures for the various zones are shown in Figure 7.3.3.1-3 and Table 7.3.3.1-2. Figure 7.3.3.1-4 is a typical temperature history for zone R-10 that was subjected to heating rates resulting from a dual actuator failure condition. Table 7.3.3.1-2 provides temperatures for each zone for both dual and single actuator failure cases and for an outboard engine-our failure case. The aft surface temperatures are given at the time of PMR reduction and at end of S-II boost; the center and forward laminate temperatures are supplied at end of S-II boost only. Figure 7.3.3.1-4 and 7.3.3.1-5 present heat shield temperatures for the engine-out failure case. The engine-out failure case has the longest heating period and results in the highest temperatures.

Figure 7.3.3.1-4 presents the temperature history of the rigid heat shield splice plates. The 3/16-inch gap (maximum value) between honeycomb sections exposes a portion of the plate to base heating, resulting in significant temperature gradients across the plate. Figure 7.3.3.1-5 shows the temperature history of the heat shield support.

7.3.3.2 Silica Mat Rigid Heat Shield

The temperature response for this analysis was provided by the Heat Shield Aft Laminate Parametric Study. The pertinent data are shown in Figure 7.3.3.2-1. For an assumed convective heating rate of 20 Btu/ft.^{2} sec, a radiative heating rate of 1 Btu/ft.^{2}-sec., and recovery temperature of 2325 F, the aft face temperature of the heat shield is found to be approximately 1600 F. To obtain this value based on available parametric data required extrapolating the two recovery temperature (2000 F and 2500 F) curves out to a convective heating rate of 20 Btu/ft.^{2} sec. This indicates a shortage of data. But the nature of the curves provides justification. Pertinent parametric data for future use are presented in Figures 7.3.3.2-2 through 7.3.3.2-5.

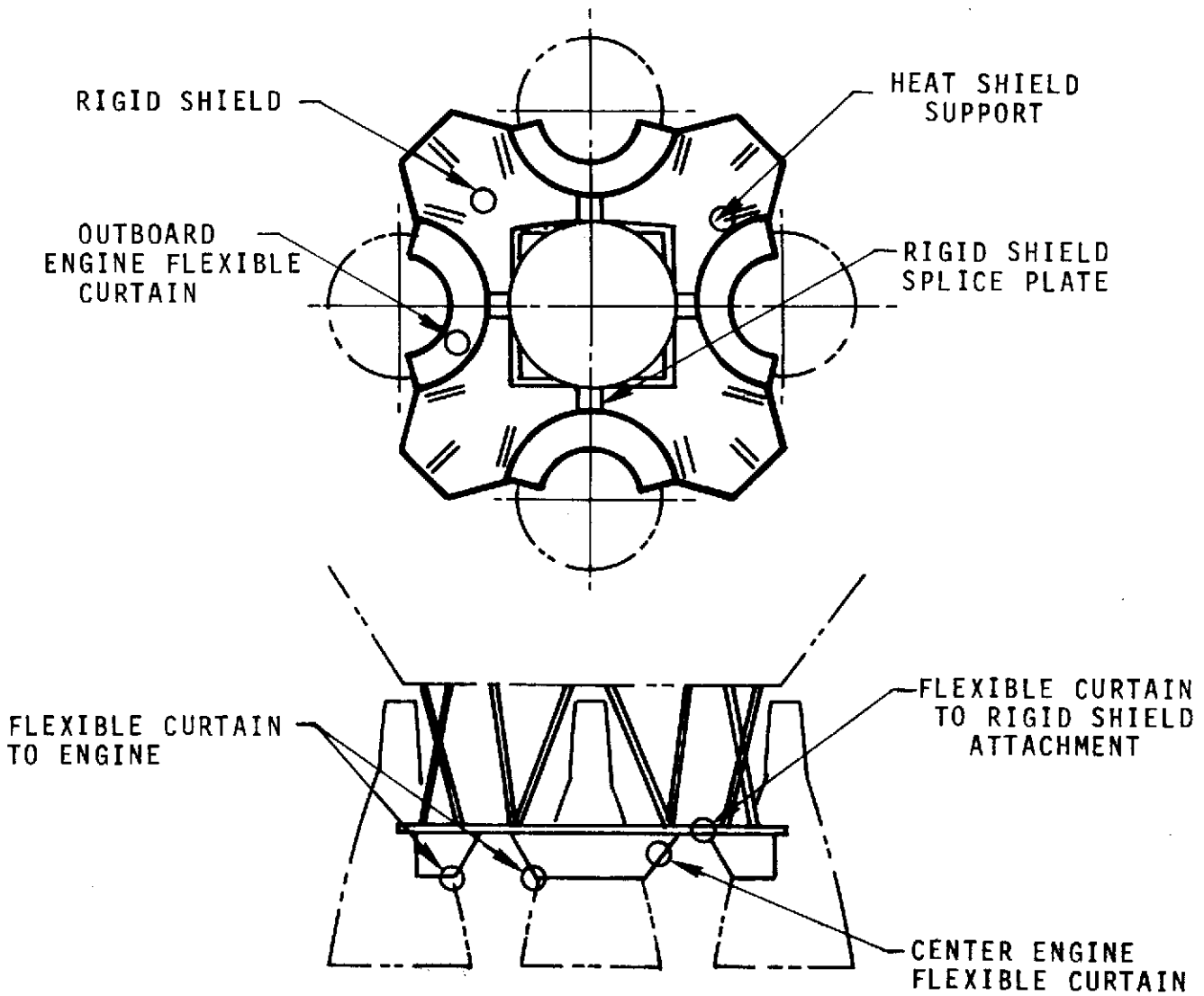

Figure 7.3.3.1-1. Base Heat Shield

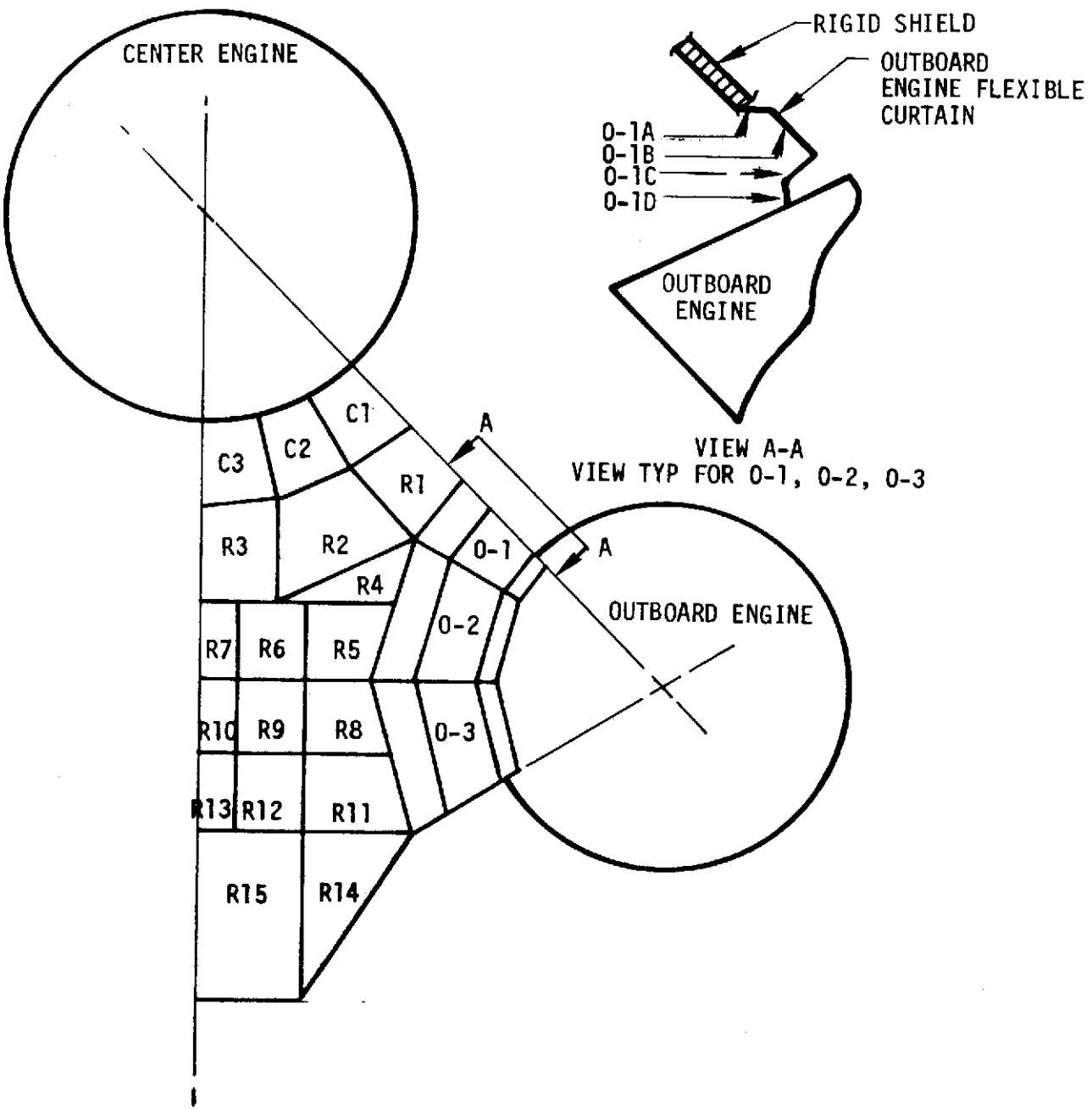

Figure 7.3.3.1-2· Heat Shield Thermal Model

Table 7.3.3.1-1. Material Thermal Properties

MATERIAL	THERMAL CONDUCTIVITY $\left(\frac{\text{BTU-FT}}{\text{FT}^2\text{-HR-}^\circ\text{F}}\right)$	SPECIFIC HEAT $\left(\frac{\text{BTU}}{\text{LB - F}}\right)$	DENSITY $\left(\frac{\text{LB}}{\text{FT}^3}\right)$	EMISSIVITY
HIGH SILICA OR FIBERGLASS PHENOLIC LAMINATE		0.13 @ -100 F 0.6 @ 2000 F	105.	0.85
FIBERGLASS PHENOLIC HONEYCOMB FILLED WITH SILICA MICRO-BALLOONS	0.066 @ -200 F 0.070 @ 400 F 0.088 @ 800 F 0.310 @ 2000 F	0.13 @ -100 F 0.6 @ 2000 F	6.2	
FIBERGLASS PHENOLIC HONEYCOMB NOT FILLED	0.02 @ 0 F 0.52 @ 2000 F	0.13 @ -100 F 0.6 @ 2000 F	2.2	
HIGH SILICA BATT	0.017 @ -100 F 0.022 @ 450 F 0.033 @ 800 F 0.064 @ 2000 F	0.13 @ -100 F 0.6 @ 2000 F	12.	
HIGH SILICA CLOTH		0.13 @ -100 F 0.6 @ 2000 F	65.	0.5
EPOXY FILLER	0.12	0.20	75.	
ALUMINUM	75.	0.20	171.	0.35
CRES STEEL	7. @ -200 F 10.5 @ 600 F 15.5 @ 2000 F	0.12	500	0.35

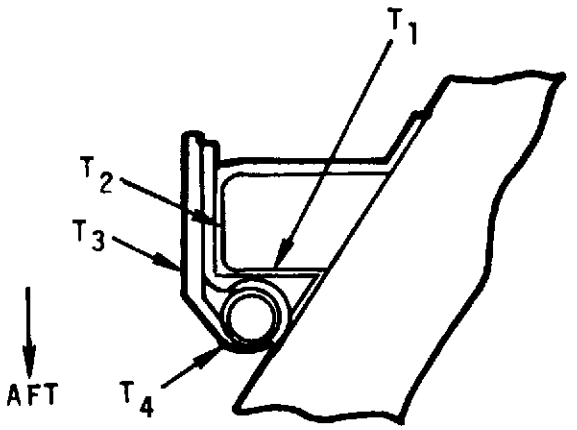

NOTE: HEATING RATES FOR OUTBOARD ENGINE OUT

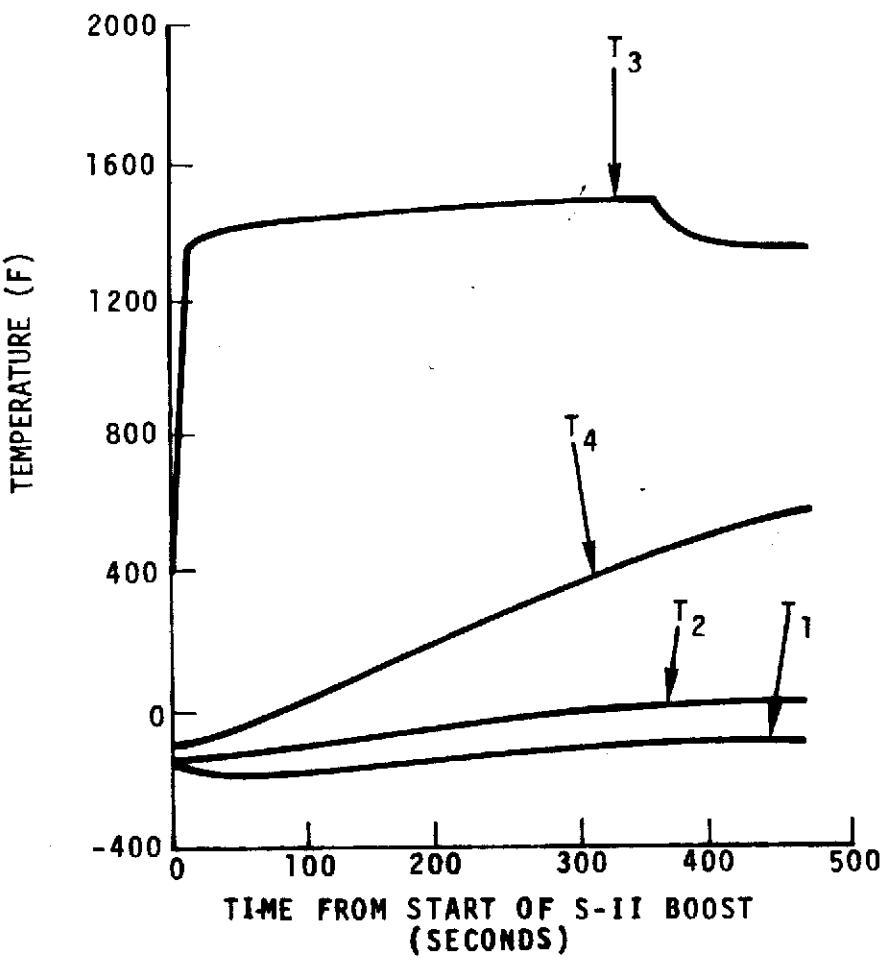

Figure 7.3.3.1-3· Flexible Curtain to Engine Attachment Temperature History

Table 7.3.3.1-2. Rigid Heat Shield Temperatures

	TEMPERATURE °F											
	DUAL ACT. FAILURE (NOMINAL)				SINGLE ACTUATOR FAILURE				OUTBOARD ENGINE OUT			
	AT PMR REDUCT.	AT END S-II BOOST			AT PMR REDUCT.	AT END S-II BOOST			AT PMR REDUCT	AT END S-II BOOST		
SECT.	T_1	T_1	T_2	T_3	T_1	T_1	T_2	T_3	T_1	T_1	T_2	T_3
R-1	1265	1164	432	256	1249	1151	425	255	1236	1135	503	297
R-2	1160	1069	382	244	1431	1317	528	287	1311	1205	549	316
R-3	1269	1168	436	257	1519	1399	585	304	1341	1232	569	322
R-4	1176	1084	389	246	1435	1321	531	287	1334	1225	561	322
R-5	1260	1160	433	254	1469	1351	558	290	1454	1337	646	349
R-6	1341	1233	475	269	1560	1444	612	314	1505	1384	675	369
R-7	1392	1280	507	277	1535	1413	596	308	1428	1312	626	346
R-8	1283	1181	441	260	1466	1349	550	294	1467	1348	648	359
R-9	1412	1298	519	281	1560	1437	612	314	1548	1425	706	382
R-10	1472	1353	553	292	1544	1421	602	309	1454	1337	642	354
R-11	1240	1141	417	253	1386	1275	502	276	1431	1316	626	342
R-12	1416	1302	519	283	1511	1391	580	304	1550	1425	707	381
R-13	1470	1351	553	292	1512	1392	581	303	1450	1333	640	353
R-14	1235	1135	418	254	1262	1161	434	259	1410	1295	613	343
R-15	1356	1247	487	272	1377	1265	500	276	1410	1295	615	342

T_1 - TEMPERATURE AFT LAMINATE

T_2 - TEMPERATURE CENTER LAMINATE

T_3 - TEMPERATURE FORWARD LAMINATE

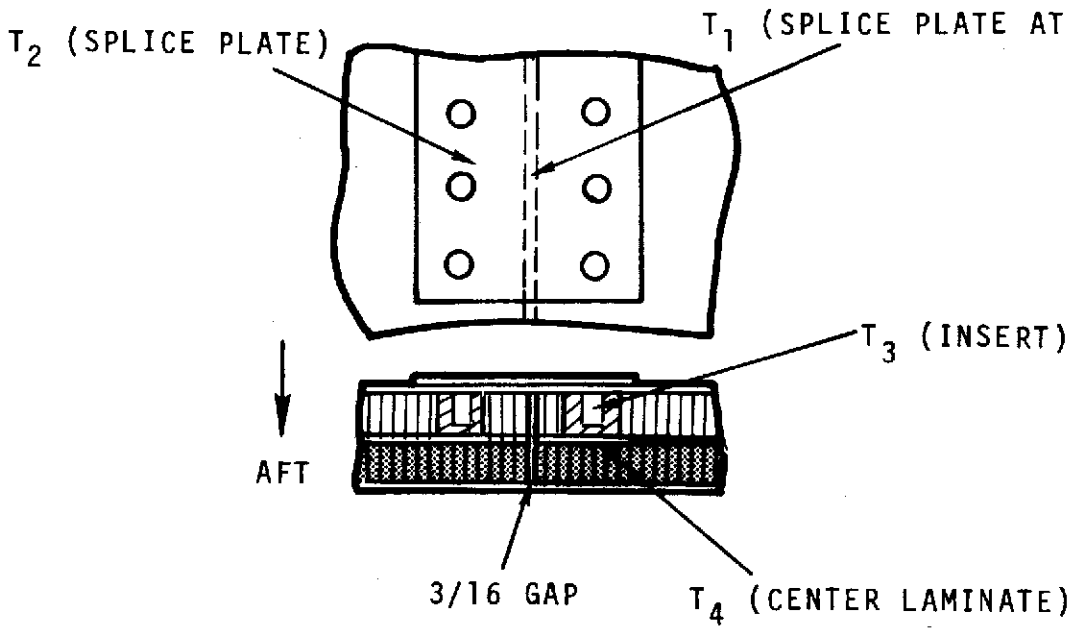

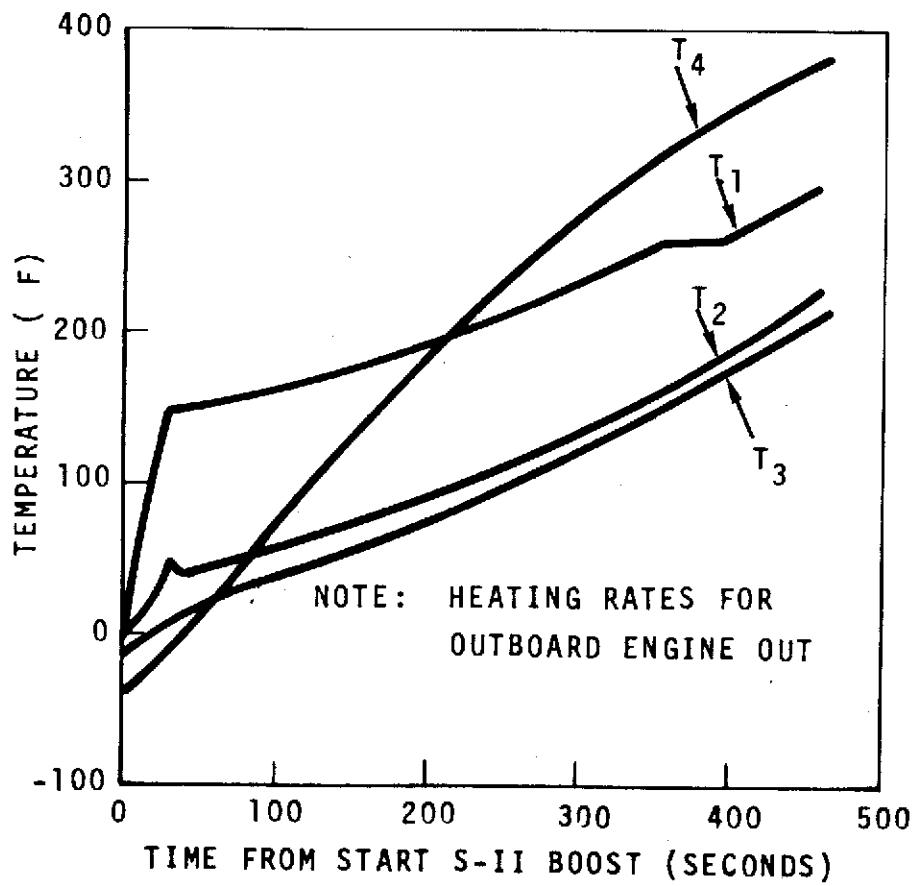

Figure 7.3.3.1-4· Temperature History - Rigid Shield Splice Plate

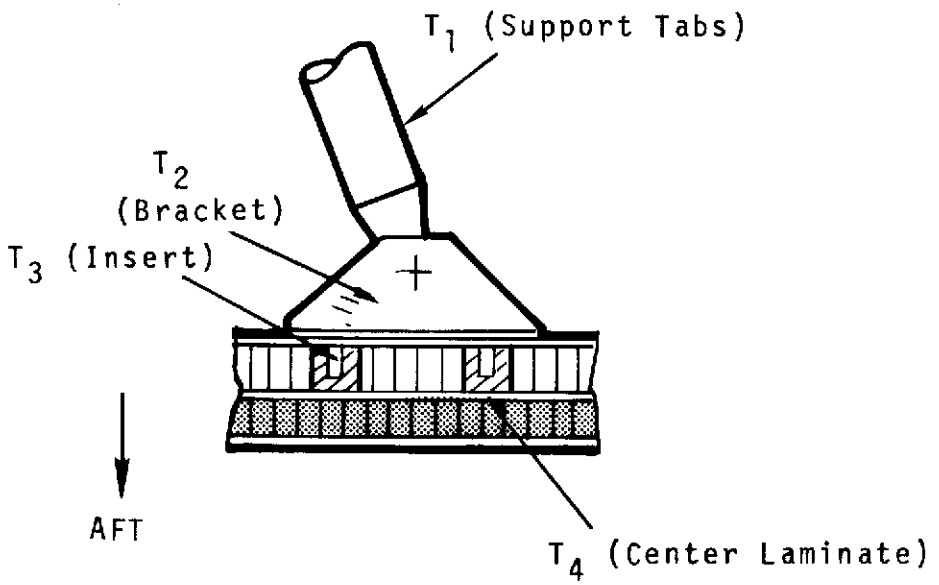

NOTE: HEATING RATES FOR OUTBOARD ENGINE OUT

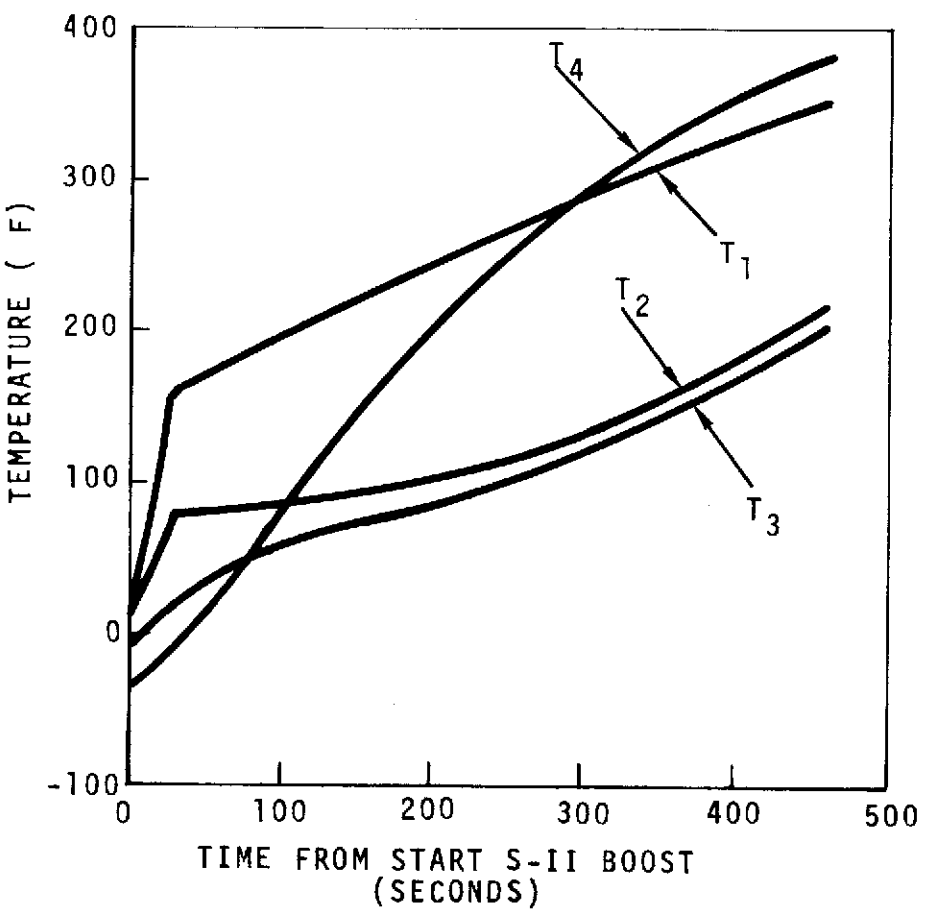

Figure 7.3.3.1-5. Temperature History - Heat Shield Support

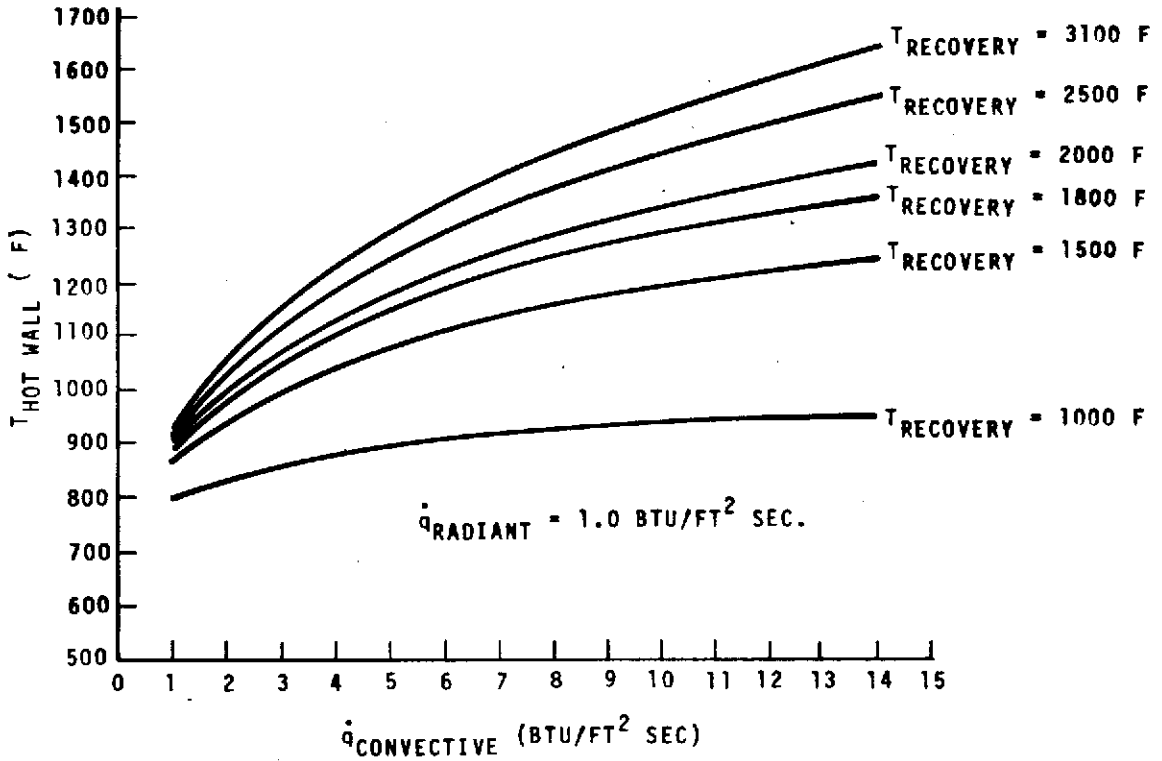

Figure 7.3.3.2-1. Predicted Heat Shield Temperatures q̇ Radiant = 1.0

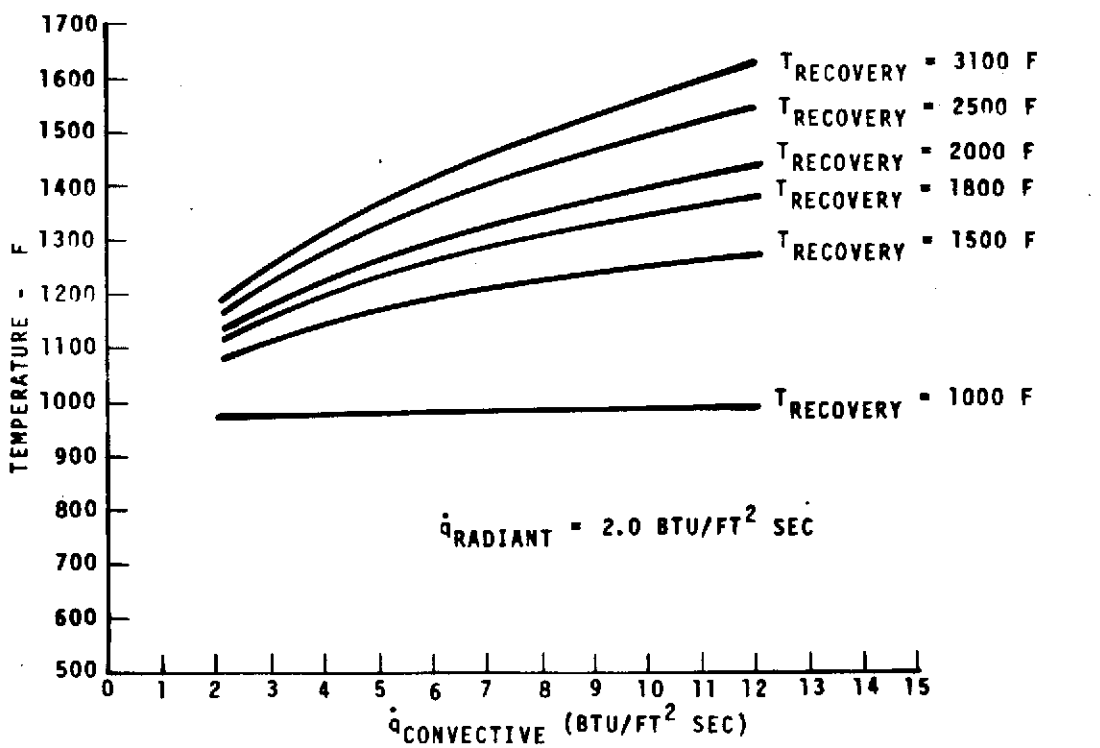

Figure 7.3.3.2-2. Predicted Heat Shield Temperatures q̇ Radiant = 2.0

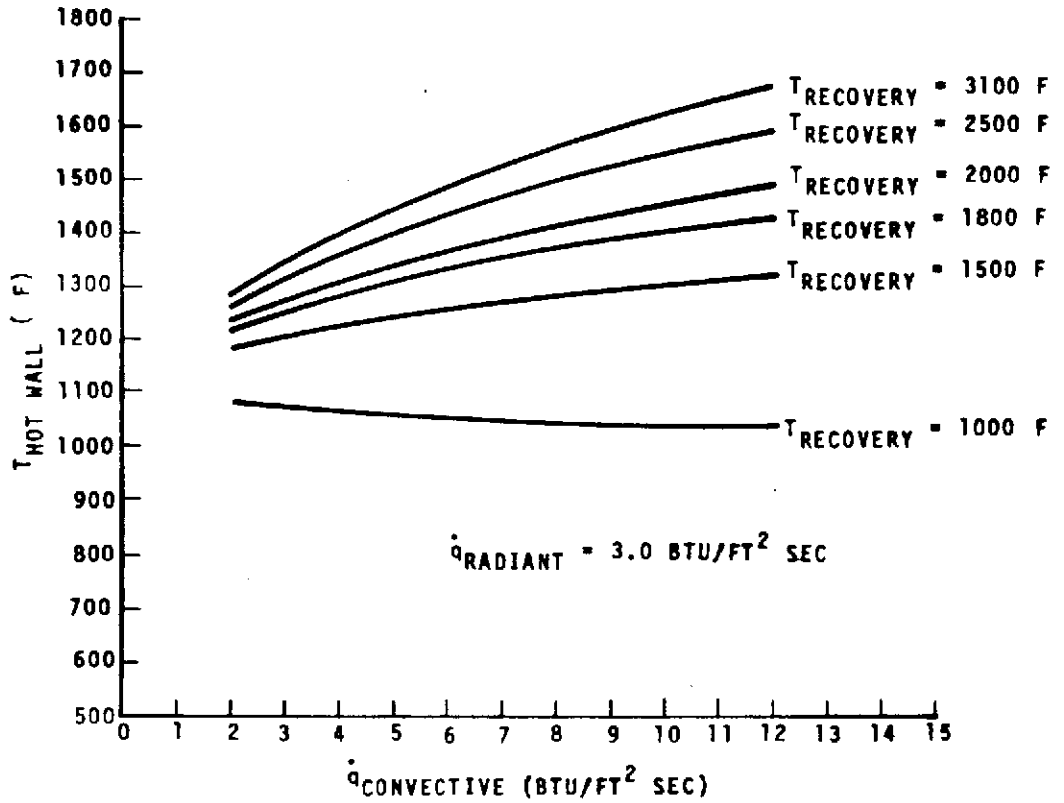

Figure 7.3.3.2-3. Predicted Heat Shield Temperatures $\dot{q}$ Radiant = 3.0

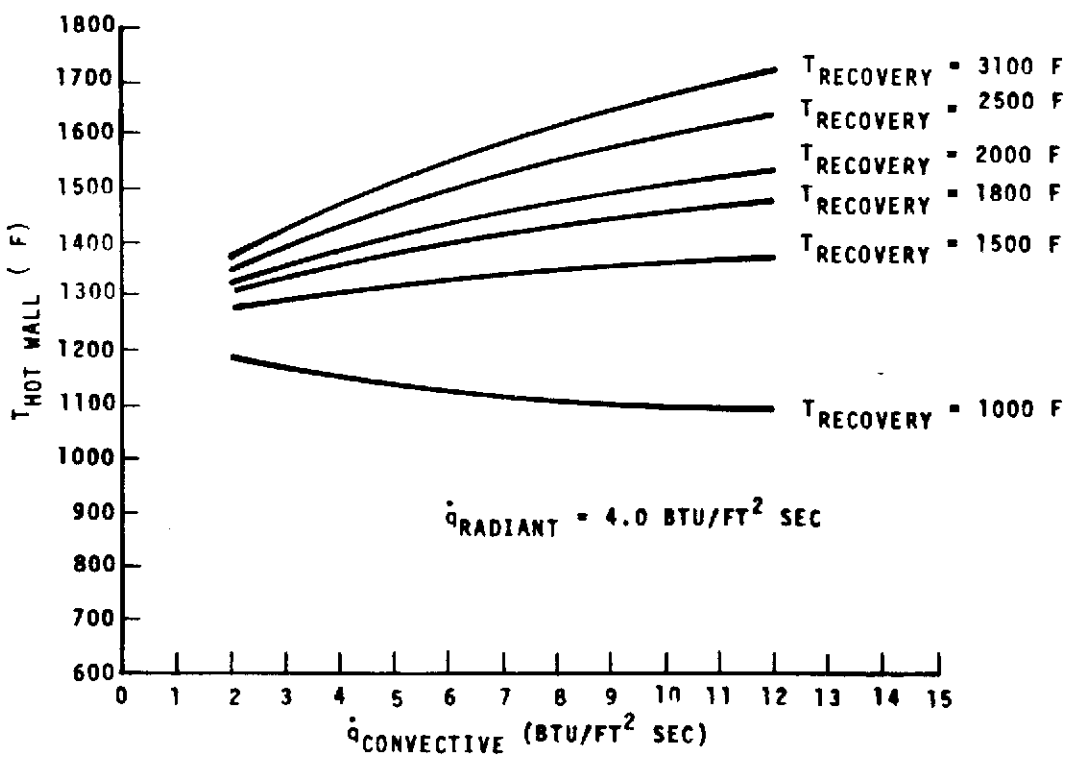

Figure 7.3.3.2-4. Predicted Heat Shield Temperatures $\dot{q}$ Radiant = 4.0

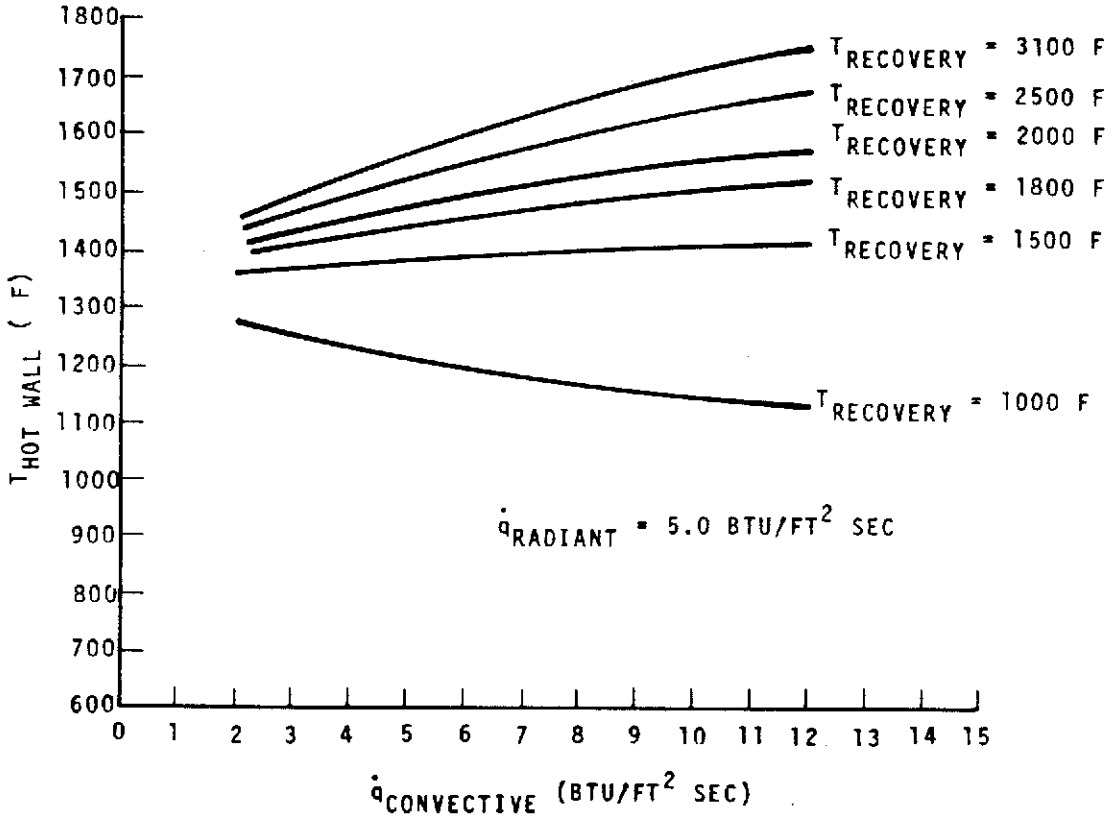

Figure 7.3.3.2-5. Predicted Heat Shield Temperatures $\dot{q}$ Radiant = 5.0

7.3.3.3 HRP Honeycomb, Glass/Polyimide Facing Sheet Heat Shield

A parametric thermal study of high temperature resistant laminates was made and provided the temperature response data employed in this analysis. The worst-case convective heating rates during S-II boost on the vertical surfaces and cover were approximated to be 10.0 and 8.0 Btu/ft.^{2}-sec, respectively. The radiant heating rate assumed was 2.0 Btu/ft.^{2}-sec. Maximum shield temperatures were obtained from the parametric data in Figure 7.3.2.3-2 assuming that the gas recovery temperature of the base heating return flow gas is 2325 F. The maximum temperatures thus predicted during S-II boost are 1460 F for the vertical sides and 1410 F for the cover. This analysis does not include any heating due to direct plume impingement from the J-2 engines. The estimated heating and recovery temperature ranges for this condition are 80 to 150 Btu/ft.^{2}-sec. and 3500 F to 4500 F, respectively. This environment results in heat shield temperatures between 2350 F and 3250 F. Therefore, further analysis should be made to correct the potential problem. Additional typical corrections would be to apply high temperature insulation, such as an ablator, to the areas that would be affected by the exhaust plume of the auxiliary propulsion system (APS) or to move the APS forward to avoid the impingement. There are no direct data shortages involved; however, the expected temperatures exceed the allowable temperatures in the as-prepared configuration.

7.3.3.4 Heat Shield Flexible Curtain

The analysis of the temperature response of the flexible curtain was performed in the same manner as that for the rigid heat shield in Section 7.3.3.1. The curtain is located as shown in Figure 7.3.3.1-1 and was sectioned into zones as shown in Figure 7.3.3.1-2. Using a computer program, radiant heating configuration factors were determined from each zone to all other zones, including the engines and space. A general heat transfer analysis computer program was then used to determine temperature responses for all flexible curtain zones. Heat transfer modes used in the analysis were convective (from recirculating hot exhaust gases), radiant (from the engine plumes), radiation interchange (between all heat shield zones, nozzles and space), and conduction (through the curtain).

The thermal properties and densities used in this analysis are listed in Table 7.3.3.1-1. Temperatures for the various flexible curtain zones are shown in Figure 7.3.3.4-1 and Table 7.3.3.4-1. Figure 7.3.3.4-2 represents typical temperature histories for Zones 0-1A and C-1 corresponding to heating rates which occur in the event of a dual actuator failure. Table 7.3.3.4-1 provides temperatures for each curtain zone's exterior surface which result from the base heating environments occurring during dual and single actuator failure cases and for an engine-out failure case. Temperatures are given at the time of propellant mixture ratio reduction and at the end of S-II boost. Figure 7.3.3.4-2 presents a temperature history for various flexible curtain zones for an outboard engine-out failure case. Figure 7.3.3.4-3 is a temperature history of the flexible curtain attachment to the rigid shield, again for an outboard engine-out failure case. The insert to which the aluminum angle is bolted is not shown, but its temperature will not exceed T_3. The outboard engine-out failure case heating rates were used in the foregoing analysis because this failure mode represents the longest heating duration and results in the highest temperatures.

Pertinent parametric data for future use in predicting flexible heat shield temperatures are shown in Figures 7.3.3.4-4 through 7.3.3.4-9. Assumptions for these data are: radiant plume heating rate equal to 1.0 Btu/ft.^{2}-sec., absorbitivity equal to 0.5, and emissivity equal to 0.5

7.3.3.5 High Silica Fabric and Batting Flexible Heat Shield

Assumptions made for analyzing the flexible curtain during boost of the S-II for the Skylab mission are: emissivity of curtain equal to 0.5, recovery gas temperature equal to 2325 F, radiant heating rate of 1.0 Btu/ft.^{2}-sec, center and outboard convective heating rates of 7.7 Btu/ft.^{2}-sec and 13.3 Btu/ft.^{2}-sec, respectively. The flexible curtains are assumed to be made of refrasil composite material.

The convective heating rates indicated are 20 percent higher than the rates supplied by NASA. This was to account for wrinkles in the curtain. The maximum flexible curtain temperatures predicted based on the above assumptions were 1520 F for the center engine and 1760 F for the outboard engines. The thermal environments assumed in the foregoing analysis are for a on-engine-out failure case.

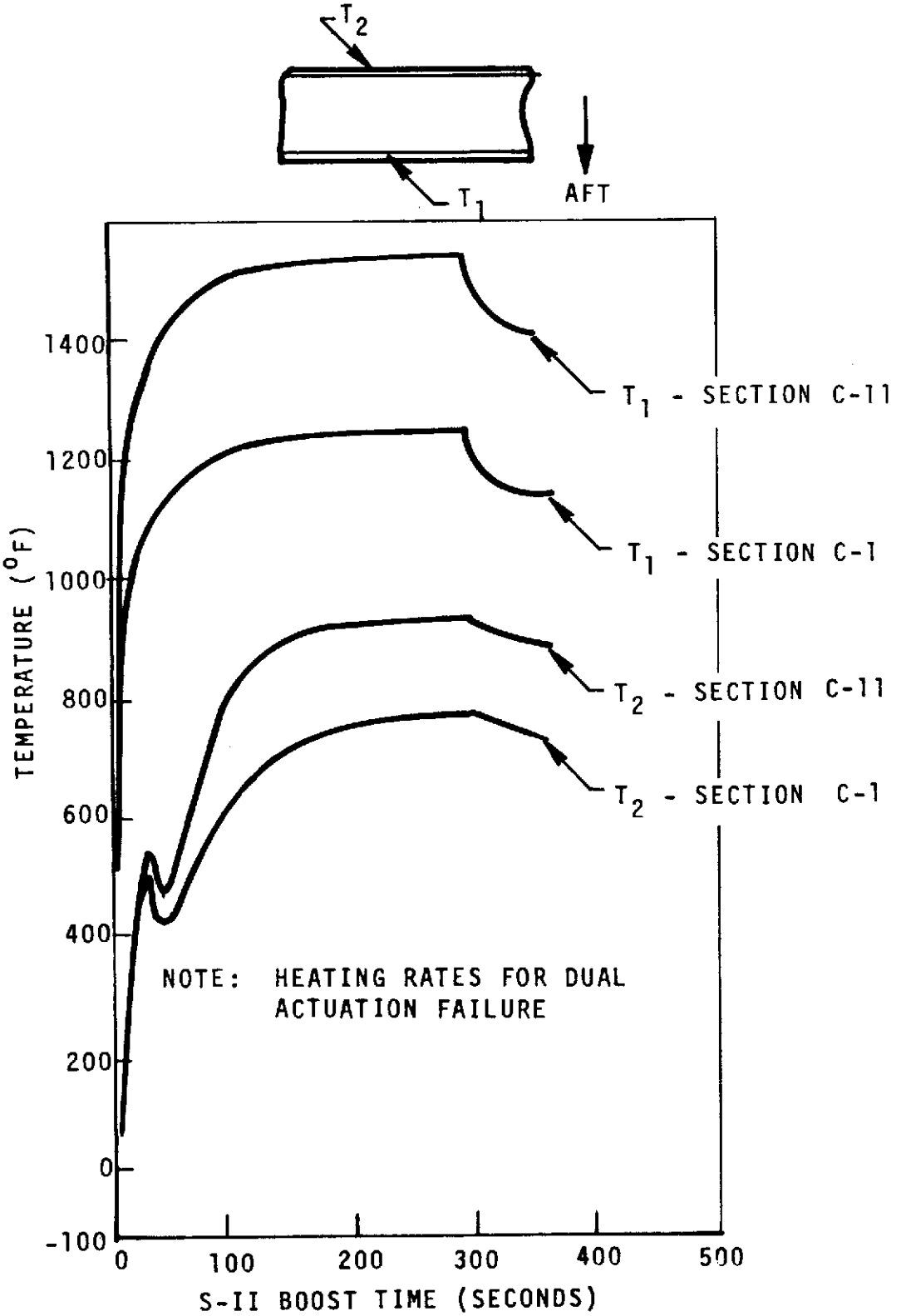

Figure 7.3.3.4-1· Typical Flexible Curtain Sections

Table 7.3.3.4-1. Flexible Curtain Temperatures

	DUAL ACTUATOR FAILURE TEMP.				SINGLE ACTUATOR FAILURE TEMP.				ENGINE OUT TEMPERATURE			
	AT PMR REDUCT.		AT END S-II BOOST		AT PMR REDUCT.		AT END S-II BOOST		AT PMR REDUCT.		AT END S-II BOOST	
SECT.	T_1	T_2	T_1	T_2	T_1	T_2	T_1	T_2	T_1	T_2	T_1	T_2
C-1	1247	774	1142	726	1361	837	1247	784	1351	829	1236	772
C-2	1232	766	1128	719	1416	867	1298	811	1370	839	1254	782
C-3	1239	769	1135	722	1450	886	1329	828	1405	858	1286	799
0-1A	1542	930	1417	876	1566	923	1339	834	1616	962	1480	901
0-1B	1415	867	1297	810	1448	888	1327	828	1553	932	1422	872
0-1C	1458	941	1337	892	1498	910	1374	908	1599	1000	1464	946
0-1D	1431	931	1314	883	1459	944	1340	895	1568	989	1437	935
0-2A	1367	841	1252	787	1483	902	1360	844	1552	932	1421	871
0-2B	1390	853	1274	799	1437	878	1316	822	1526	920	1397	859
0-2C	1396	915	1281	867	1414	923	1298	875	1527	971	1399	918
0-2D	1416	924	1300	876	1454	942	1335	983	1553	982	1423	929
0-3A	1279	792	1171	742	1456	889	1334	831	1521	917	1392	856
0-3B	1240	771	1134	722	1346	829	1232	775	1395	853	1276	794
0-3C	1219	831	1118	791	1323	880	1212	835	1391	910	1274	858
0-3D	1302	870	1195	828	1411	922	1295	874	1472	947	1349	894

T_1 - AFT SURFACE TEMPERATURE

T_2 - FORWARD SURFACE TEMPERATURE

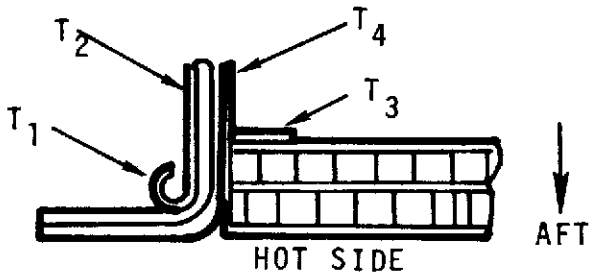

NOTE: HEATING RATES FOR OUTBOARD ENGINE OUT

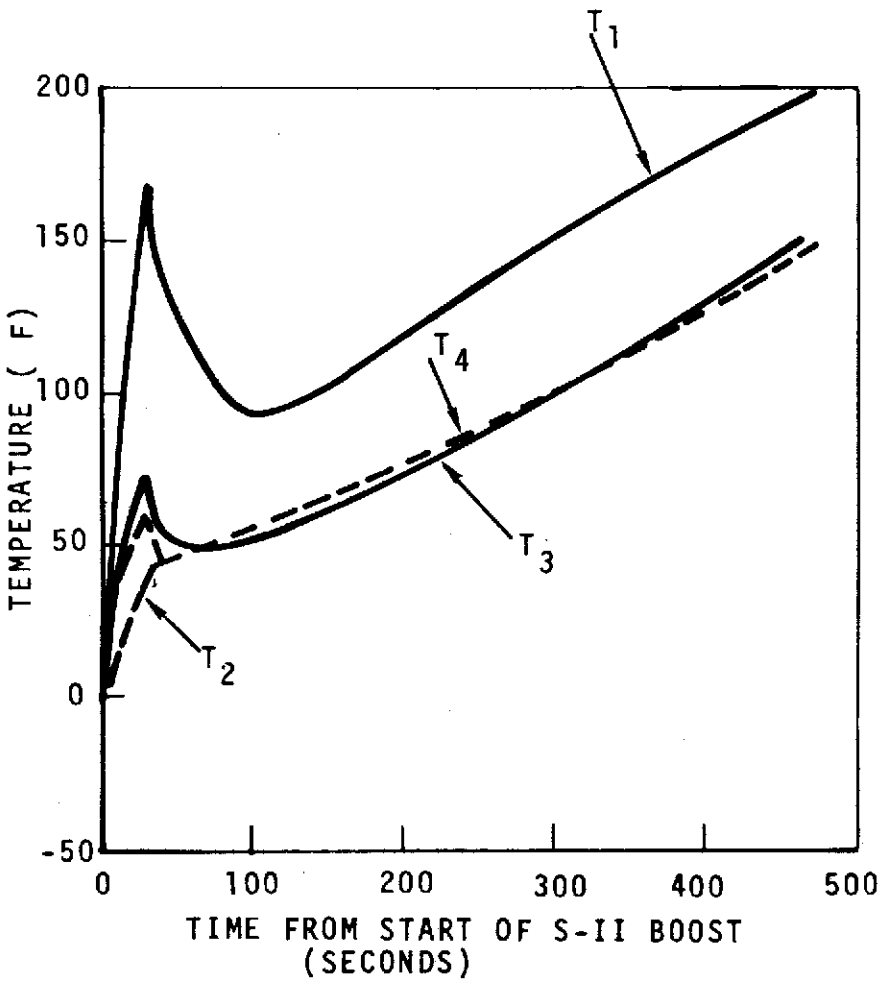

Figure 7.3.3.4-2. Temperature History - Flexible Curtain to Rigid Shield Attachment

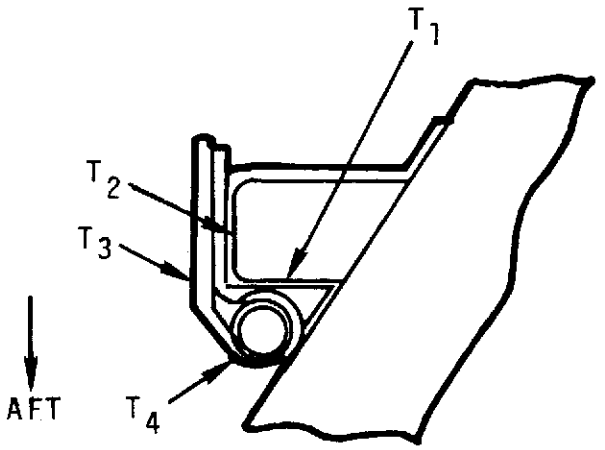

NOTE: HEATING RATES FOR OUTBOARD ENGINE OUT

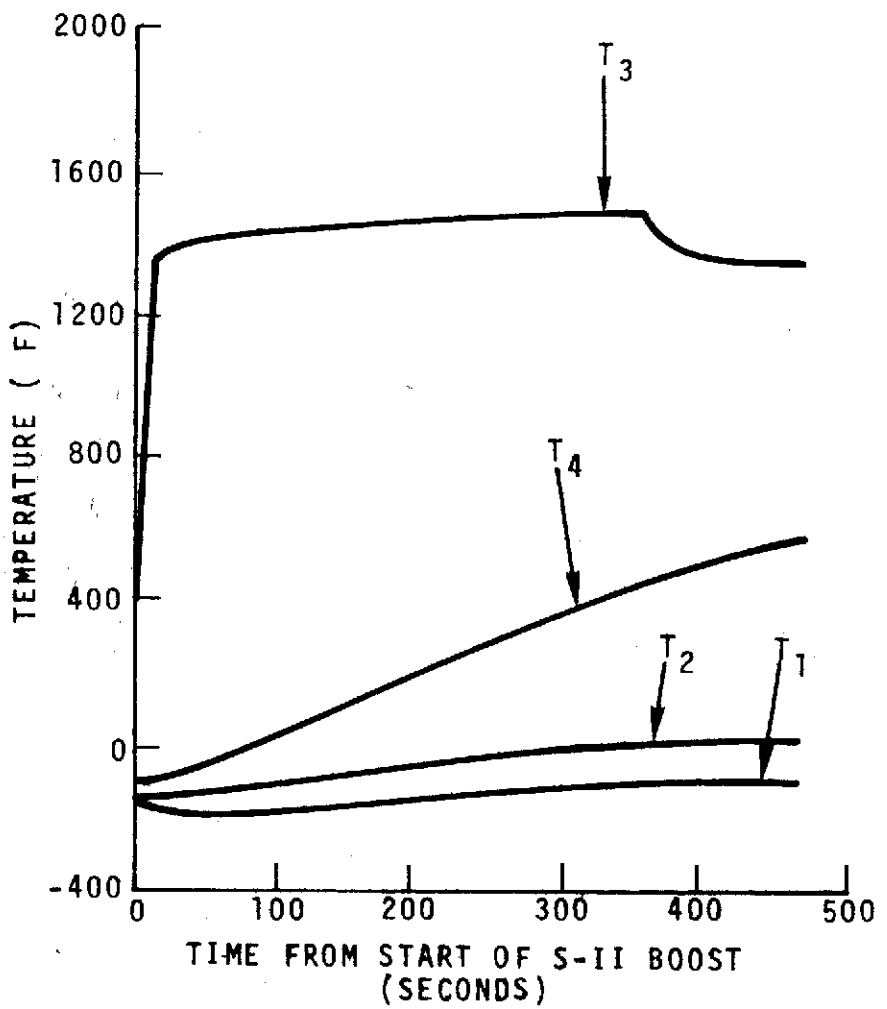

Figure 7.3.3.4-3· Flexible Curtain to Engine Attachment Temperature History

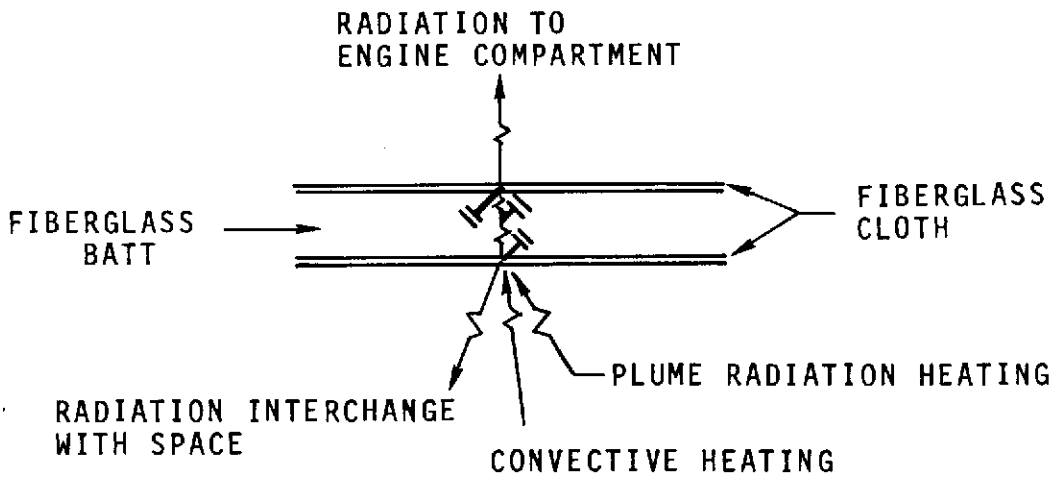

Figure 7.3.3.4-4. Thermal Model of Flexible Curtain

7.3.3.6 Bonded Cork

Aft skirt and interstage structures of the S-II stages are exposed to aerodynamic and solar heating during S-IC/S-II boost. Interstage structures also are exposed to exhaust plume heating during the first 30 seconds of S-II boost. Established structure temperature limits for S-II-4 through -15 are 235 F during S-IC boost and 500 F for the interstage during the first 30 seconds of S-II boost.

To maintain the structure temperature within the required limits, external cork insulation MB 0130-020 Type I is bonded to the structure as shown in Figure 7.3.3.6-1. In addition, internal skin and frame surfaces are protected by Korotherm insulation MB 0130-074 as indicated in Figure 7.3.6.3-1. Structure in the aft skirt and in the interstage of stage S-II-11 through -15 are heavier than those of S-II-4 through -10. Therefore, the thickness of cork required at a given location differs between the earlier and later series of S-II stages.

The insulation and structure section selected as the thermal model is shown in Figure 7.3.3.6-1. The aft skirt and interstage layout together with the aerodynamic heating protuberance zones are shown in Figure 7.3.3.6-2.

The thermal model is a one-dimensional analog network suitable for use with a general digital computer program. Materials and dimensions are those called out in the drawings listed in Figure 7.3.6.3.-1. Modes of heat transfer considered are aerodynamic, solar and base heating, conduction in materials, sensible heat, and radiation to space and to internal structures.

Aerodynamic heating rates used in this study are those of Paragraph 4.3.3.1, which are based on real gas effects. These aerodynamic heating rates are lower than used in previous analyses which were based on ideal gas effects. Protuberance zones and factors are those of the main stage and were altered in this study to reflect ullage rocket fairing removal at four of the previous eight positions.

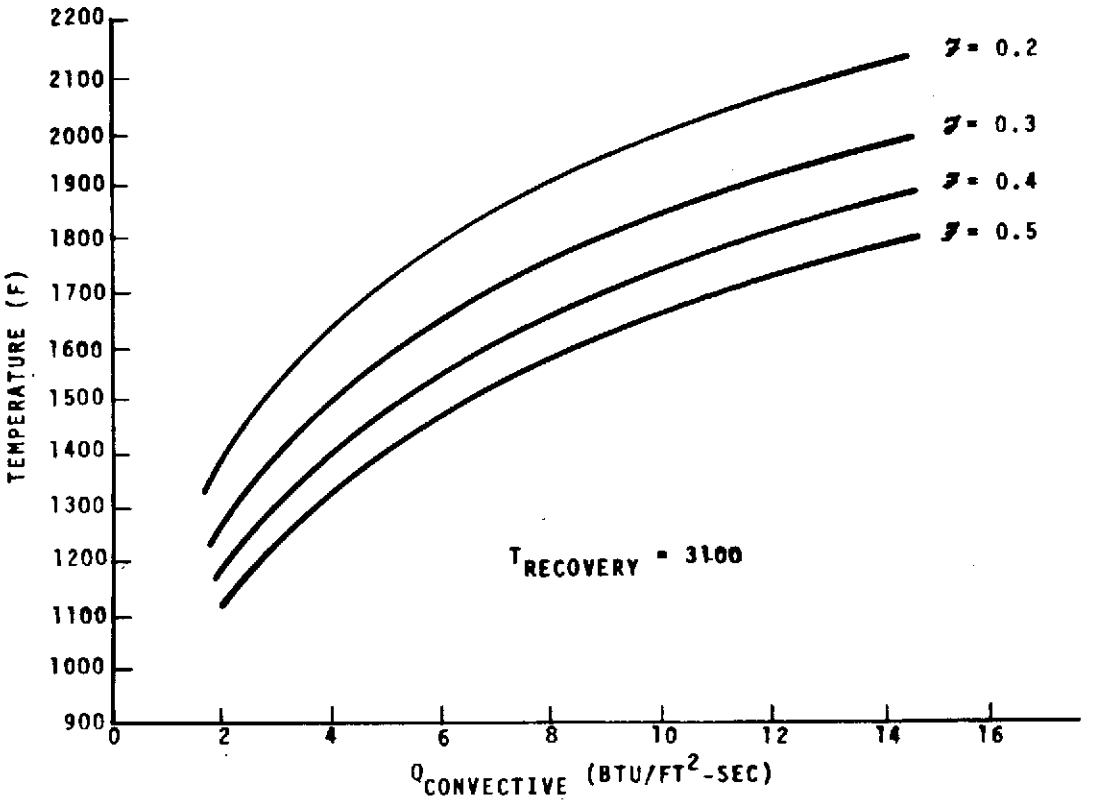

Figure 7.3.3.4-5. Maximum Flexible Curtain Temperatures Versus Convective Heating and Radiation to Space

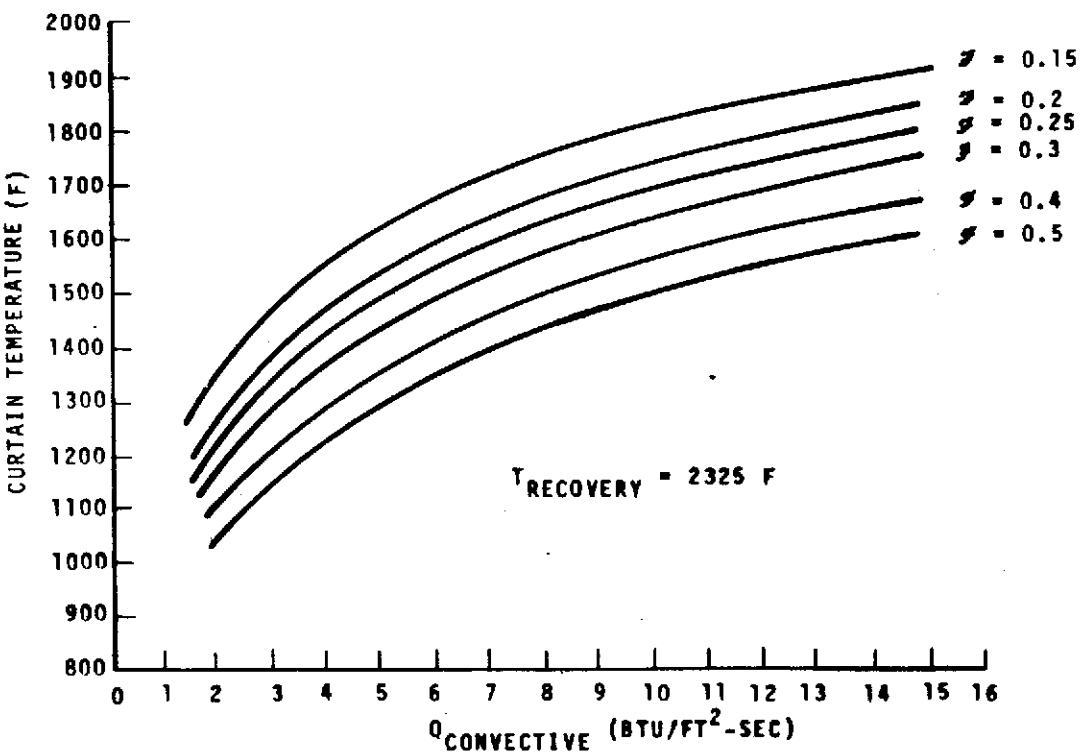

Figure 7.3.3.4-6. Maximum Flexible Curtain Temperatures Versus Convective Heating and Radiation to Space

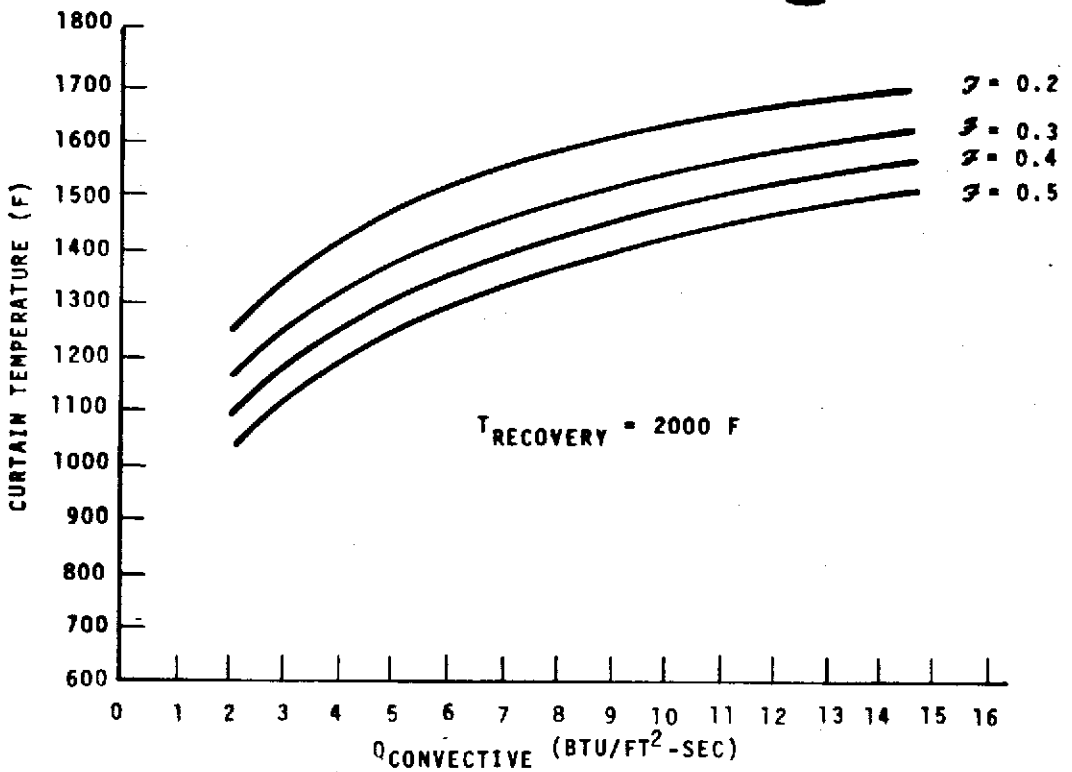

Figure 7.3.3.4-7. Maximum Flexible Curtain Temperatures Versus Convective Heating and Radiation to Space

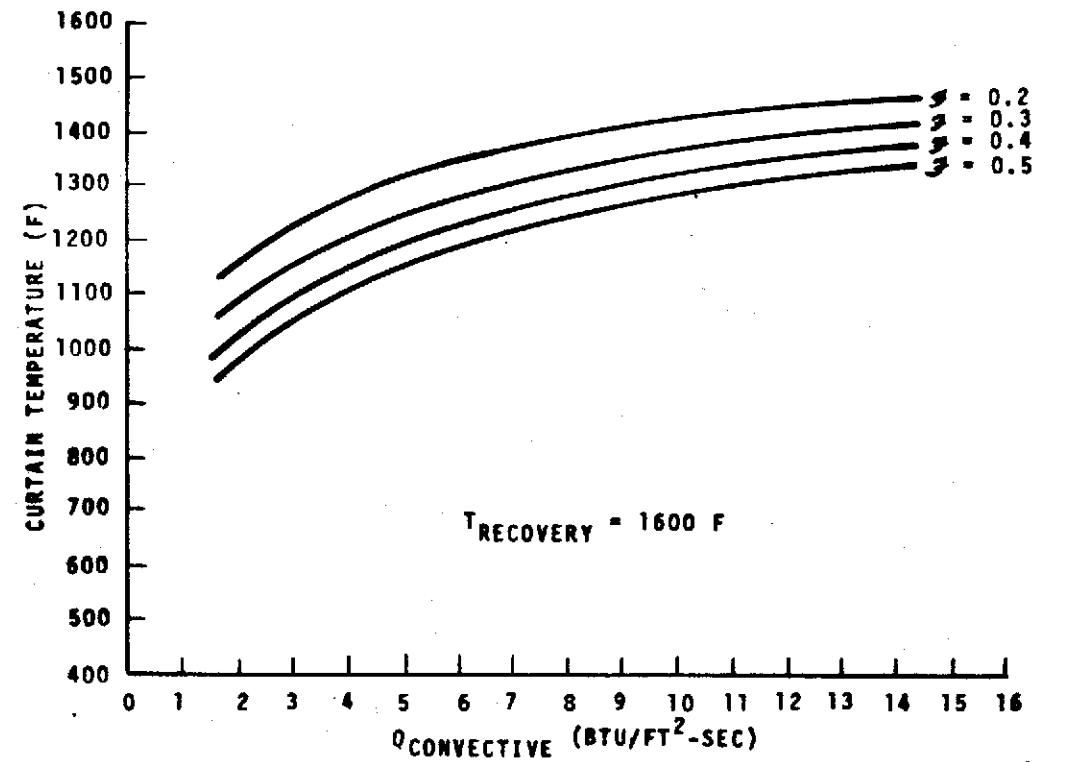

Figure 7.3.3.4-8. Maximum Flexible Curtain Temperatures Versus Convective Heating and Radiation to Space

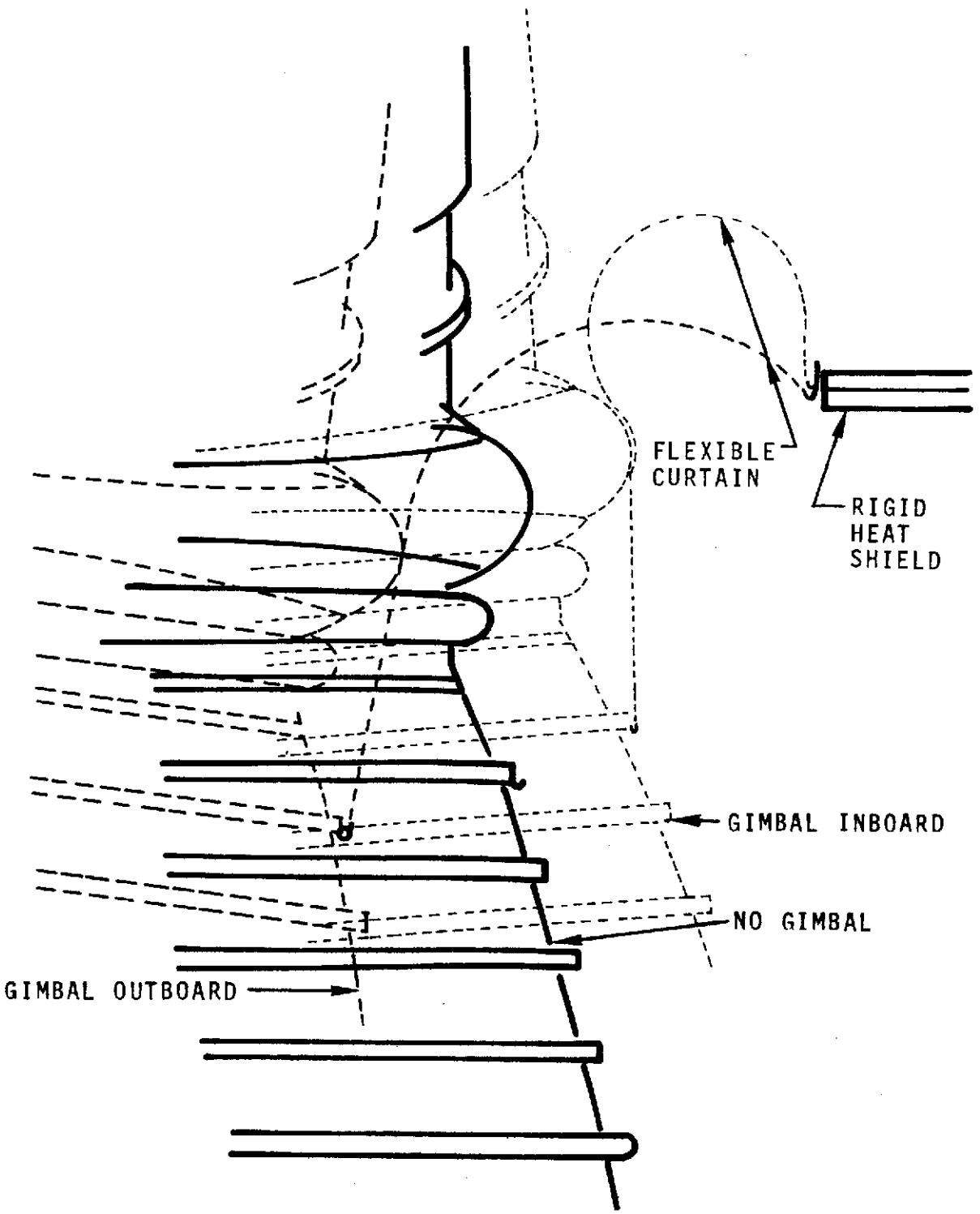

Figure 7.3.3.4-9. J-2 Engine Heat Shield Cross-Section

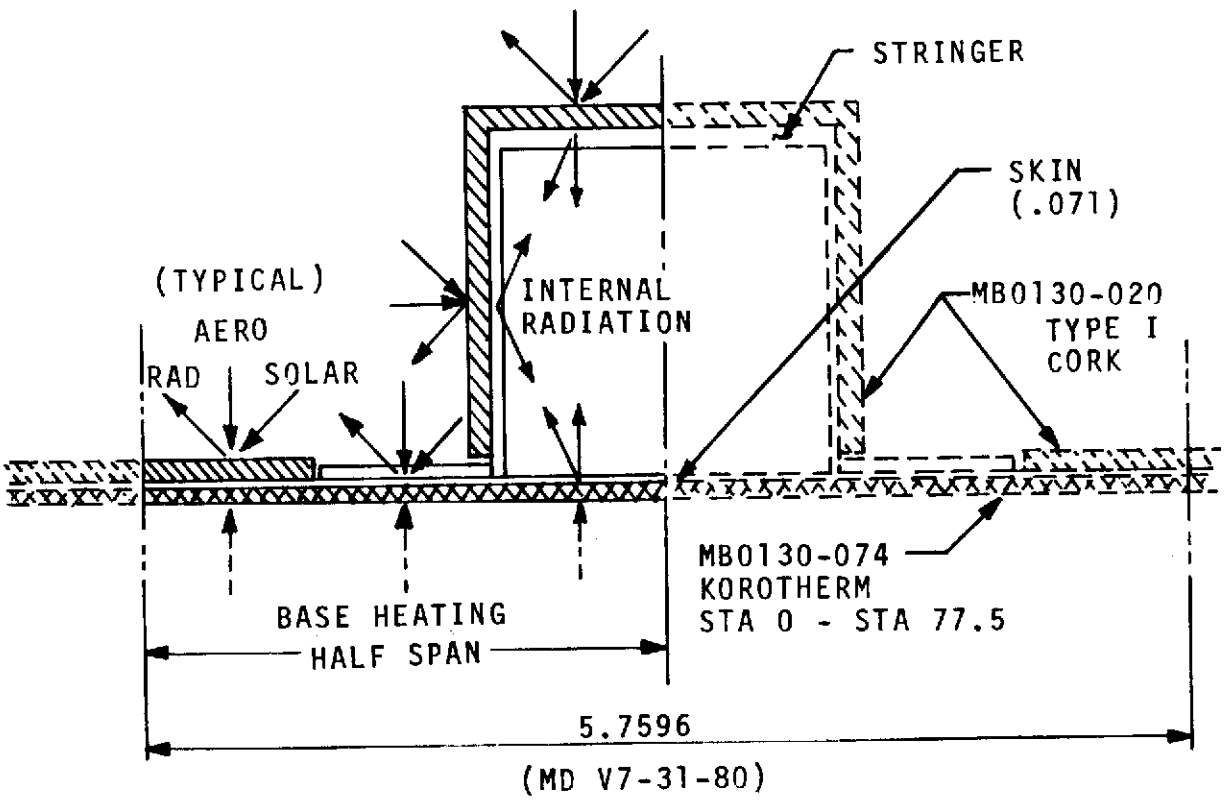

	S-II-4 THRU 10		S-II-11 & SUBS
STRINGER			
STA 196 TO STA 283	V7-315757		V7-315551
STA 0 TO STA 196	V7-317974		V7-317974-3
STA -23 TO STA 0		V7-317996	
EXTERNAL CORK INSULATION			
STA -23 TO STA 196	V7-317957		V7-531320 (S-II-11 THRU 13)
STA 196 TO STA 283		V7-315007 (S-II-4 THRU 14)	
INTERNAL KOROTHERM INSULATION			
STA 0 TO STA 77.5		V7-531104	

Figure 7.3.3.6-1. S-II-4 Through -15 Skirt and Interstage Thermal Model

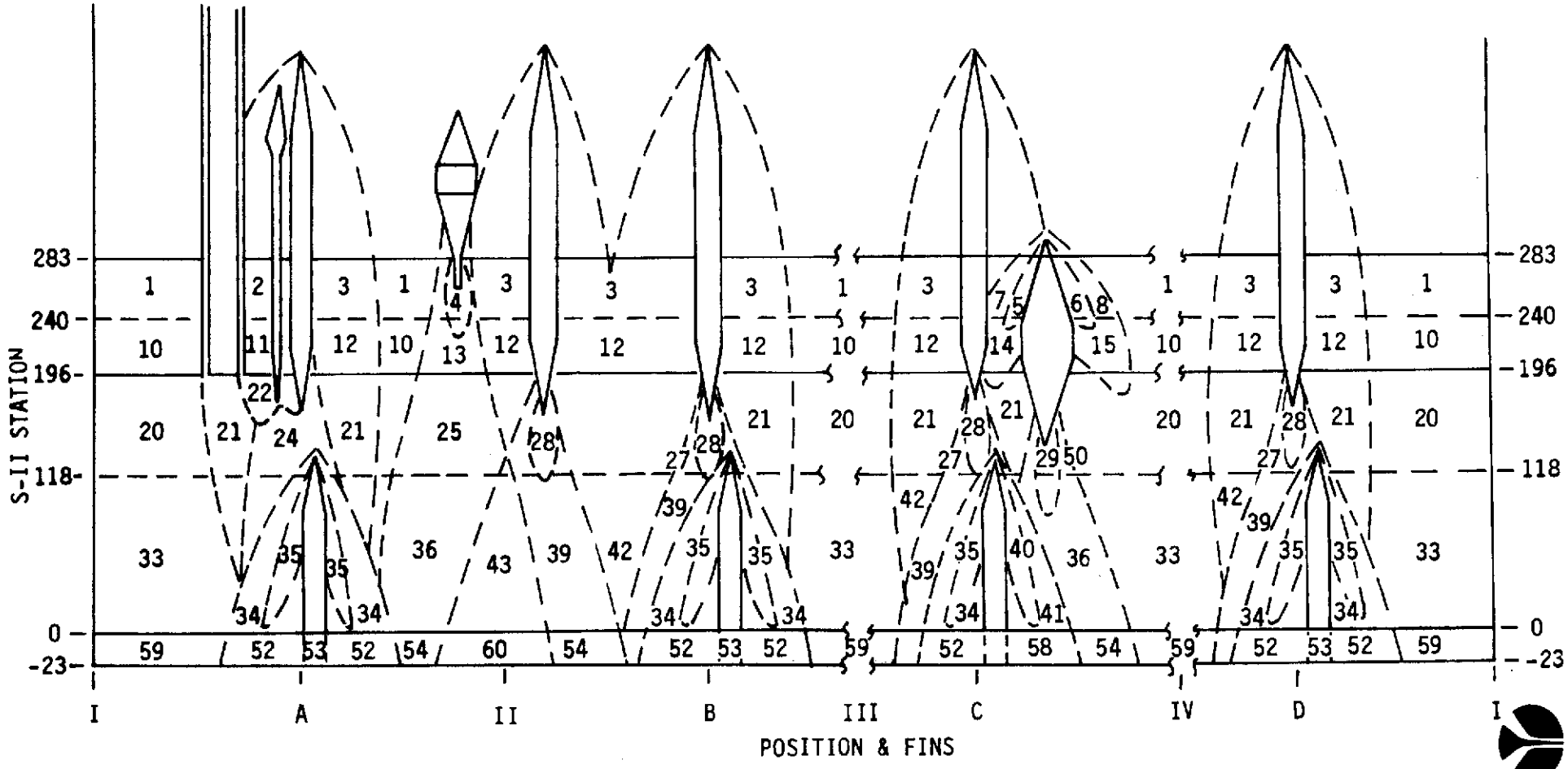

Figure 7.3.3.6-2. S-II Protuberance Regions on Sidewall

a. Assumptions:

1. Solar radiation: 438 Btu/hr. F-ft.^{2}

2. Nominal dimensions are used to evaluate heat conductance and capacitance.

3. Material Properties:

Density (lb./ft.^{3})	Conductivity (Btu/hr.-F-ft.)	Specific Heat (Btu/lb.-F)
Aluminum 171	68 (@ 80 F)	0.199 (@ 80 F)
Cork (MB 0130-020 Type I)		
30	0.05	0.5
Korotherm (MB 0130-074)		
55	0.12	0.54

4. External Surfaces:

Emissivity = absorptivity = 0.8

5. Initial Temperature:

Sta. 240 to Sta. 283, 0 F

Sta. -23 to Sta. 240, 80 F

b. Results: Structure temperatures of S-II-4 through -10 and of S-II-11 through -15 are tabulated in Tables 7.3.3.6-1 and -2. The tabulation includes protuberance zone, station, present cork insulation thickness, initial temperature, and temperature at end of S-IC boost. In addition, the required cork thickness is included in Table 7.3.3.6-2 for stages S-II-11 through -15. The reduction in aerodynamic heating rates from ideal to real gas effects result in the external insulation in many zones being either not required or less than presently specified for the heavier S-II-11 through -15 structure.

Structure temperature histories of the two series of S-II stages are similarly presented in Figures 7.3.3.6-3 and -4. Figure 7.3.3.6-5 shows the maximum interstage temperature versus station at the end of S-II boost (180 seconds) for both the S-II-4 through -10 configuration and S-II-11 through -15 configuration.

c. Conclusions:

1. Maximum aft skirt and interstage structure temperatures of the S-II-4 through -15 vehicles are below 235 F during S-IC boost (150 seconds) and are below 500 F during S-II boost (180 seconds).

Table 7.3.3.6-1. S-II-4 Through -10 Aft Skirt and Interstage Structure Temperature at End of S-IC Boost

——— , DASH LINE MEANS NONE

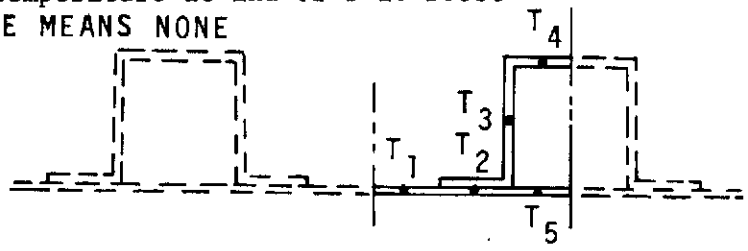

ZONE	STATION	PRESENT CORK THICKNESS (INCHES)	INITIAL TEMP. (°F)	TEMPERATURE AT END OF S-IC BOOST (°F)				
				T_1	T_2	T_3	T_4	T_5
	STA 273 - STA 283							
1		--	0	141	135	141	139	130
2		.07	0	195	180	156	133	160
3		--	0	151	143	150	147	137
4		.05	0	165	154	144	130	142
5		.03	0	166	155	151	140	142
6		.03	0	154	144	140	131	133
7		.03	0	149	139	136	127	129
8		.03	0	138	130	127	119	121
	STA 240 - STA 273							
1		--	0	165	160	170	158	155
2		.07	0	230	218	194	143	194
3		--	0	177	170	183	167	164
4		.05	0	195	186	177	142	171
5		.03	0	197	187	187	156	173
6		.03	0	182	174	173	147	162
7		.03	0	176	168	168	142	157
8		.03	0	164	157	156	134	147
	STA 196 - STA 240							
10		.02	80	203	199	205	205	190
11		.125	80	228	222	194	171	202
12		.02	80	215	210	218	217	200
*13		.05						
14		.05	80	216	209	212	205	195
15	(CONTINUED)	.03	80	220	215	221	218	203

*NOT REQUIRED IN UMBILICAL AREA

Table 7.3.3.6-1. S-II-14 Through -10 Aft Skirt and Interstage Structure Temperature at End of S-IC Boost (Cont)

ZONE	STATION	PRESENT CORK THICKNESS (INCHES)	INITIAL TEMP. (^{o}F)	TEMPERATURE AT END OF S-IC BOOST (^{o}F)				
				T_1	T_2	T_3	T_4	T_5
	STA 118 - STA 196							
20		.04	80	205	198	200	192	187
21		.04	80	217	210	211	202	196
22		.125	80	185	181	161	145	165
24		.06	80	216	208	205	193	193
25		.06	80	225	217	213	200	201
27		.06	80	216	208	205	193	193
28		.06	80	228	219	215	201	202
29		.09	80	226	219	204	185	200
30		.09	80	191	185	176	163	171
	STA 0 - STA 118							
33		.04	80	186	180	182	176	171
34		.06	80	226	217	214	200	201
35		.06	80	235	232	227	211	214
36		.04	80	221	214	215	206	201
39		.06	80	195	188	187	177	176
40		.125	80	220	216	184	162	194
41		.125	80	206	201	175	156	183
42		.06	80	181	175	175	166	164
43		.06	80	230	221	217	203	205
	STA 23 - STA 0							
52		.06	80	231	221	223	215	207
53		.06	80	226	216	219	211	202
54		.04	80	222	212	223	220	203
57		.125	80	217	212	181	164	191
58		.125	80	222	217	185	168	196
59		.04	80	186	179	189	188	173
60		.06	80	235	225	227	218	210

Table 7.3.3.6-2. S-II-11 Through -13 Aft Skirt and Interstage Structure Temperature at End of S-IC Boost

-----DASH LINE MEANS NONE

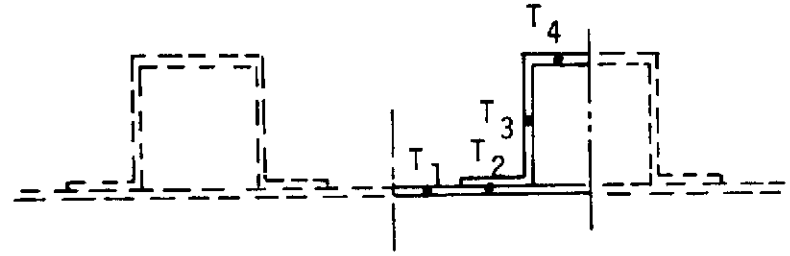

ZONE	STATION	CORK THICKNESS (INCHES) PRESENT	CORK THICKNESS (INCHES) REQD	INITIAL TEMP (^{o}F)	TEMPERATURE AT END OF S-IC BOOST (^{o}F) T_1	T_2	T_3	T_4	T_5
	STA 240 - STA 283								
1		--	--	0	142	135	145	137	132
2		.07		0					
			.04	0	228	214	202	166	195
3		--	--	0	152	144	155	146	140
4		.05		0	223	212	228	215	207
			--	0					
5		.03		0	202	189	207	191	183
			--	0					
6		.03	--	0	186	176	191	178	171
7		.03	--	0	180	169	184	171	164
8		.03	--	0	167	159	171	160	154
	STA 196 - STA 240								
10		.02		80	195	189	189	187	180
			--	80	212	206	212	213	197
11		.125	.125	80	216	211	177	160	189
12		.02		80	207	200	199	198	189
			--	80	226	218	225	226	208
*13		.05	.05	80	234	223	217	209	208
14		.05		80	207	198	193	187	183
			.03	80	225	216	214	210	202
15		.03	.03	80	211	204	202	199	192
	STA 118 - STA 196								
20		.04		80	197	189	181	170	176
			--	80	235	225	226	217	214
21		.04		80	209	199	191	177	185
			.02	80	230	220	216	203	205
22		.09		80	199	191	172	153	174
			.07	80	235	226	213	198	210
24		.09		80	186	178	162	146	163
			.04	80	231	220	213	199	206
25		.06		80	217	206	193	176	190
			.05	80	230	218	208	191	203

*NOT REQUIRED ON UMBILICAL AREA

Table 7.3.3.6-2. S-II-11 Through -13 Aft Skirt and Interstage Structure Temperature at End of S-IC Boost (Cont)

ZONE		CORK THICKNESS (INCHES)		INITIAL TEMP. (^{o}F)	TEMPERATURE AT END OF S-IC BOOST (^{o}F)				
		PRESENT	REQD		T_1	T_2	T_3	T_4	T_5
	STA 118 - STA 196								
27		.09		80	186	178	162	146	163
			.04	80	231	221	213	198	205
28		.09		80	195	187	170	168	150
			.05	80	233	222	210	191	203
29		.125		80	196	190	161	141	172
			.08	80	234	222	202	180	204
30		.125		80	167	162	149	142	127
			.04	80	235	226	209	189	208
	STA 0 - STA 118								
33		.04		80	179	172	162	166	157
			--	80	209	201	191	201	194
34		.09		80	194	185	170	168	151
			.05	80	230	218	208	191	202
35		.09		80	206	197	180	177	157
			.06	80	233	221	205	185	202
36		.125		80	159	154	143	137	124
			.02	80	235	225	221	199	199
39		.06		80	189	180	167	171	158
			.01	80	235	225	224	213	212
40		.125		80	212	207	185	170	146
			.110	80	235	225	193	171	204
41		.125		80	199	193	174	162	141
			.100	80	228	222	197	177	203
42		.06		80	176	168	156	160	149
			--	80	222	213	201	214	205
43		.16		80	164	161	148	134	119
			.05	80	235	224	212	203	207

Table 7.3.3.6-2. S-II-11 Through -13 Aft Skirt and Interstage Structure Temperature at End of S-IC Boost (Cont)

ZONE		CORK THICKNESS (INCHES)		INITIAL TEMP.	TEMPERATURE AT END OF S-IC BOOST (^{o}F)				
		PRESENT	REQD	(^{o}F)	T_1	T_2	T_3	T_4	T_5
	STA 23 - STA 0								
52		.09	.06	80 80	209 231	201 221	187 223	192 215	180 207
53		.09	.06	80 80	204 226	197 216	182 219	188 211	177 202
54		.09	.04	80 80	187 222	180 212	169 223	175 220	167 203
57		.16	.125	80 80	202 217	202 212	180 181	162 164	143 191
58		.16	.125	80 80	208 222	206 217	185 185	165 168	146 196
59		.06	--	80 80	175 212	168 205	160 230	173 235	170 200
60		.16	.06	80 80	183 235	181 225	165 227	151 218	136 210

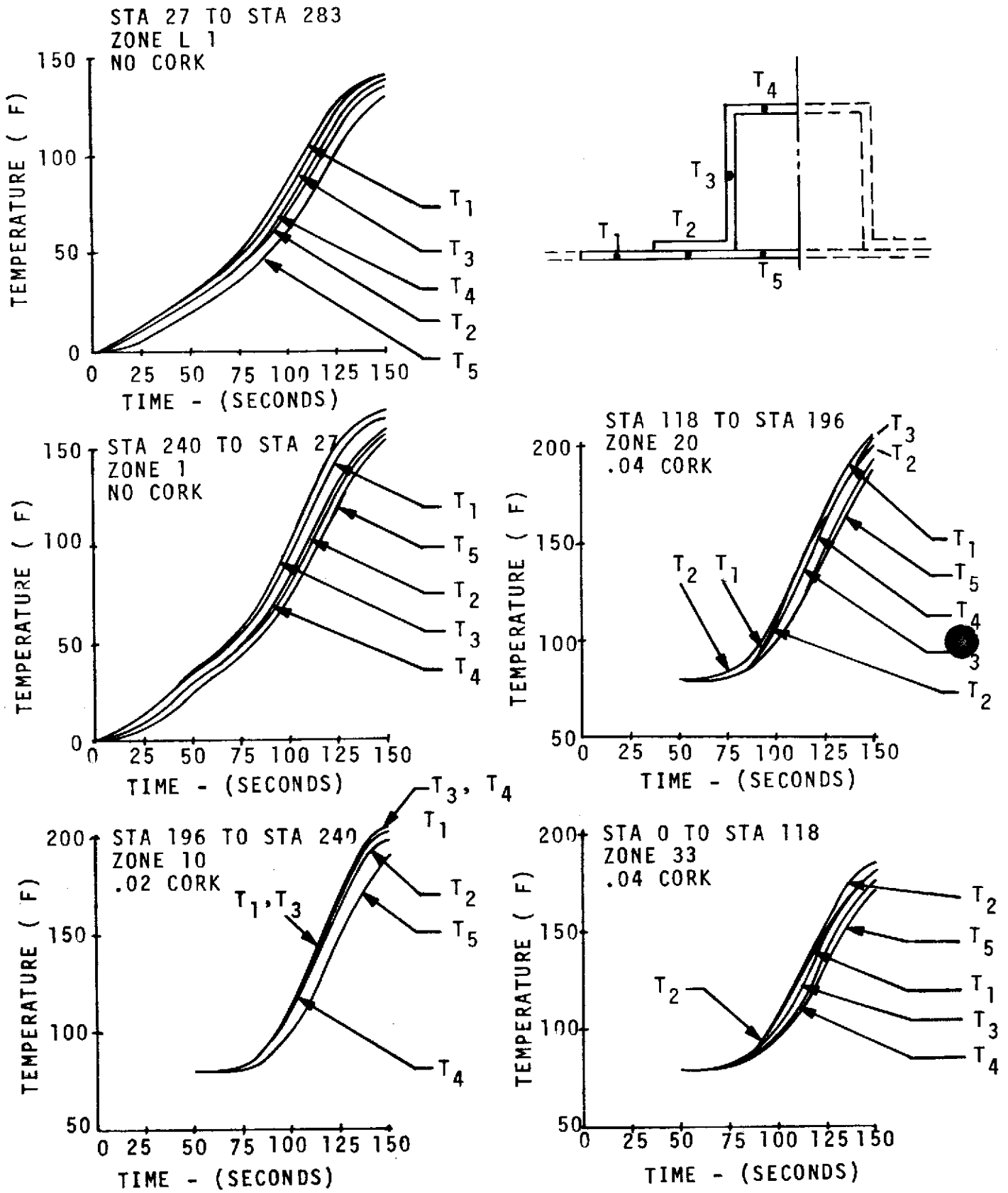

Figure 7.3.3.6-3. S-II-4 Through -10 Aft Skirt and Interstage Structure Temperature Histories

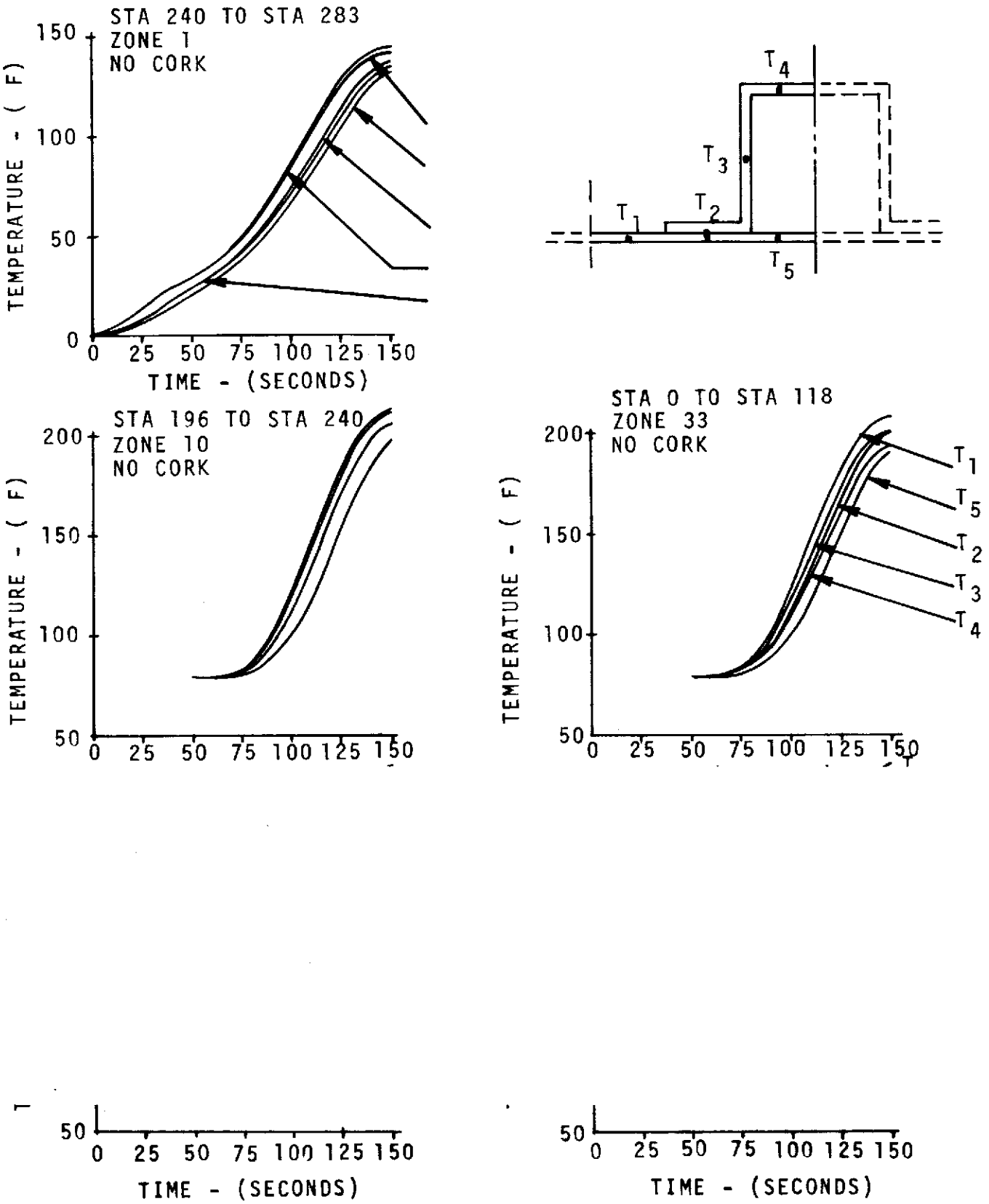

Figure 7.3.3.6-4. S-II-11 Through -13 Aft Skirt and Interstage Structure Temperature Histories

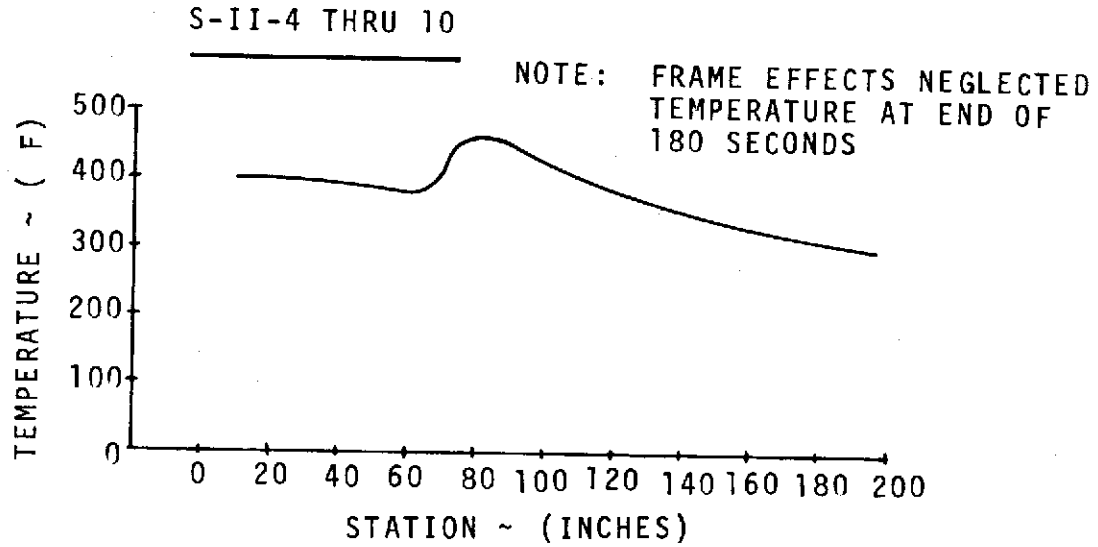

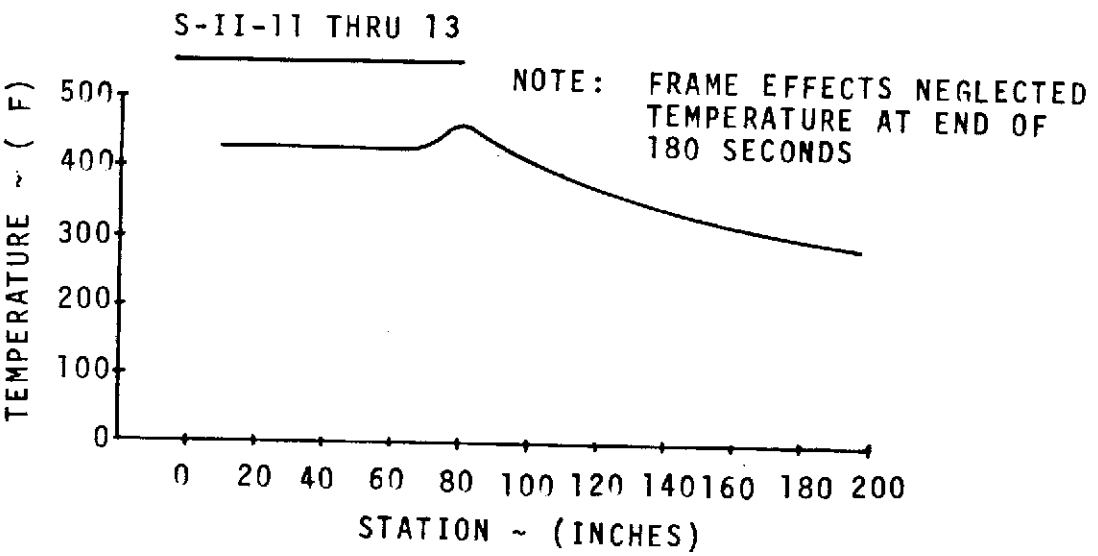

Figure 7.3.3.6-5. S-II-4 Through -13 Interstage Maximum Temperatures

2. Present external and internal insulation concepts of S-II-4 through -10 are adequate to maintain aft skirt and interstage structure temperatures within the established limits during S-IC/S-II boost.

3. Present insulation concepts of S-II-11 through -15 are more than adequate to maintain structure temperatures within the established limits. External cork insulation specified for many regions of the aft skirt and interstage structure could be reduced or deleted for any follow-on effort.

Another example of a thermal analysis of a bonded cork insulation system is presented in Paragraph 7.3.3.7, which gives an analysis of the use of bonded cork to insulate the S-II stage thrust cone web frame located at Station 196 for S-II-6 and subs. The 196 web frame is subjected to base heating throughout S-II boost. The use of bonded-cork rather than RTV which was employed on S-II stages 1 through -5 is shown in Paragraph 7.3.3.7 to provide adequate thermal protection at nearly a 60 percent weight saving.

7.3.3.7 RTV

An analysis made to determine the temperature of the uninsulated S-II thrust cone web frame at Station 196 revealed that this structure, which is subjected to base heating throughout S-II boost, reached a maximum temperature of 720 F, exceeding the maximum allowable temperatures from stress considerations. The analysis presented in the following paragraphs was conducted to determine the adequacy of: (1) insulating this structure on stages S-II-1 through -5 with 1/4-inch-thick room temperature vulcanizing (RTV) rubber, and (2) insulating this structure on S-II-6 and subs with 1/4-inch-thick bonded cork. Both approaches are shown to be adequate; however, the cork is considerably less dense and represents an approximate 60 percent weight saving over RTV.

The thermal properties of the materials used in the following analysis are given in Table 7.3.3.7-1.

Table 7.3.3.7-1. Thermal Properties of Materials Used on 196 Web

Material	Density ($lb./ft.^3$)	Thermal Conductivity (Btu-ft./$ft.^2$-hr-F)	Specific Heat (Btu/lb.-F)
Aluminum	173	75	0.19
CRES	500	10	0.10
Cork (Type 1)	30	0.042	0.5
RTV	80	0.12	0.3

The base heating environment in the activity of the 196 web frame varies with angular position due to the asymmetric reverse flow of hot exhaust gases resulting from the mutual impingement of the J-2 rocket exhaust plumes. The

heating environment also varies with time because of the effect of the presence of the interstage for the first 30 seconds of S-II boost and the change in engine mixture ratio which occurs after 350 seconds of S-II boost. These variations in convective and radiative base heating rates are defined in SID 61-473-1.

The transient temperature response of the 196 web frame was determined with the aid of the General Thermal Analyzer Program, based on the foregoing thermal properties and base heating environment. A sketch of the 196 web station coated with 1/4-inch-thick RTV is presented, together with the web structure's transient temperature response during S-II boost in Figure 7.3.3.7-1. This figure also shows temperatures of the brackets and surface temperatures of the RTV insulation during S-II boost. Temperatures of these same locations, for the RTV coated web, versus thrust cone angle, θ, are shown in Figure 7.3.3.7-2 for three times: 30 seconds, 350 seconds, and 467 seconds after start of S-II boost.

For stage S-II-6 and subs, a cork (Type 1) insulation is used for the thermal protection of the web during S-II boost. The cork is 1/4-inch-thick and is pre-cut into pieces which fit between the web lightening holes. Between the sections of the cork where the brackets fit, RTV is spread to cover the lower portions of the brackets. This RTV is also about 1/4-inch thick.

Temperatures of typical locations on the 196 web with cork insulation during S-II boost are shown in Figure 7.3.3.7-3. This figure also includes temperatures of the brackets and surface temperatures of the cork during S-II boost. Figure 7.3.3.7-4 shows temperatures of these same locations versus thrust cone angle θ at three different times: 30 seconds, 350 seconds, and 467 seconds after start of S-II boost. The temperatures of the web insulated with RTV gradually increased to 445 F at the end of S-II boost (467 seconds) except at the lip of the web where temperatures rose to 475 F after 30 seconds of boost. The temperatures of the lip dropped below 380 F by 70 seconds after start of S-II boost and then gradually increased to 445 F by 350 seconds and finally dropped to 430 F by 467 seconds.

The temperatures of the web decreased on an average of 100 F between 0 and 36-degree thrust cone angles. This is because of decreased heating rates with increased thrust cone angle as shown in SID 61-473-1.

The temperatures of the web insulated with cork followed the same pattern as those insulated with RTV. The temperatures of the insulated web gradually increased with time from start of S-II boost to approximately 480 F as a maximum. Temperatures of the uninsulated lip of the web rose to 480 F after 30 seconds from start of boost but dropped to 360 F by 100 seconds and finally increased to 450 F at the end of S-II boost.

The maximum surface temperature of the cork was 640 F after 30 seconds from start of S-II boost. This surface temperature dropped rapidly to 400 F by 50 seconds and then gradually increased to 480 F at the end of S-II boost.

The maximum RTV surface temperature rose to 395 F after 30 seconds from start of S-II boost, dropped below 270 F by 50 seconds and gradually rose to 425 F by the end of S-II boost.

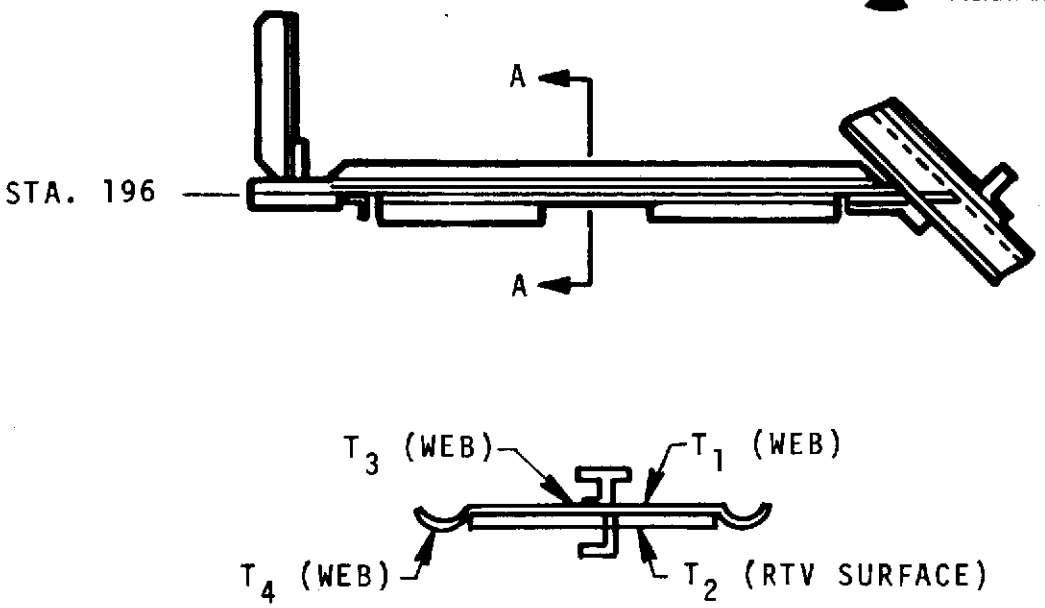

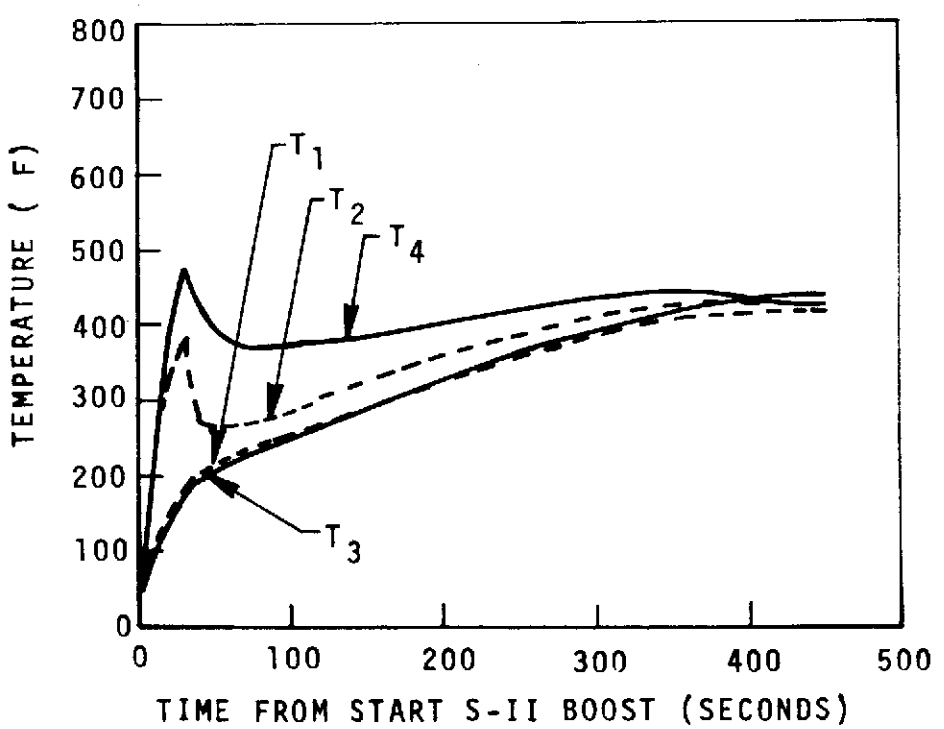

Figure 7.3.3.7-1. Temperatures of 196 Web Midway Between Engines (RTV Insulation)

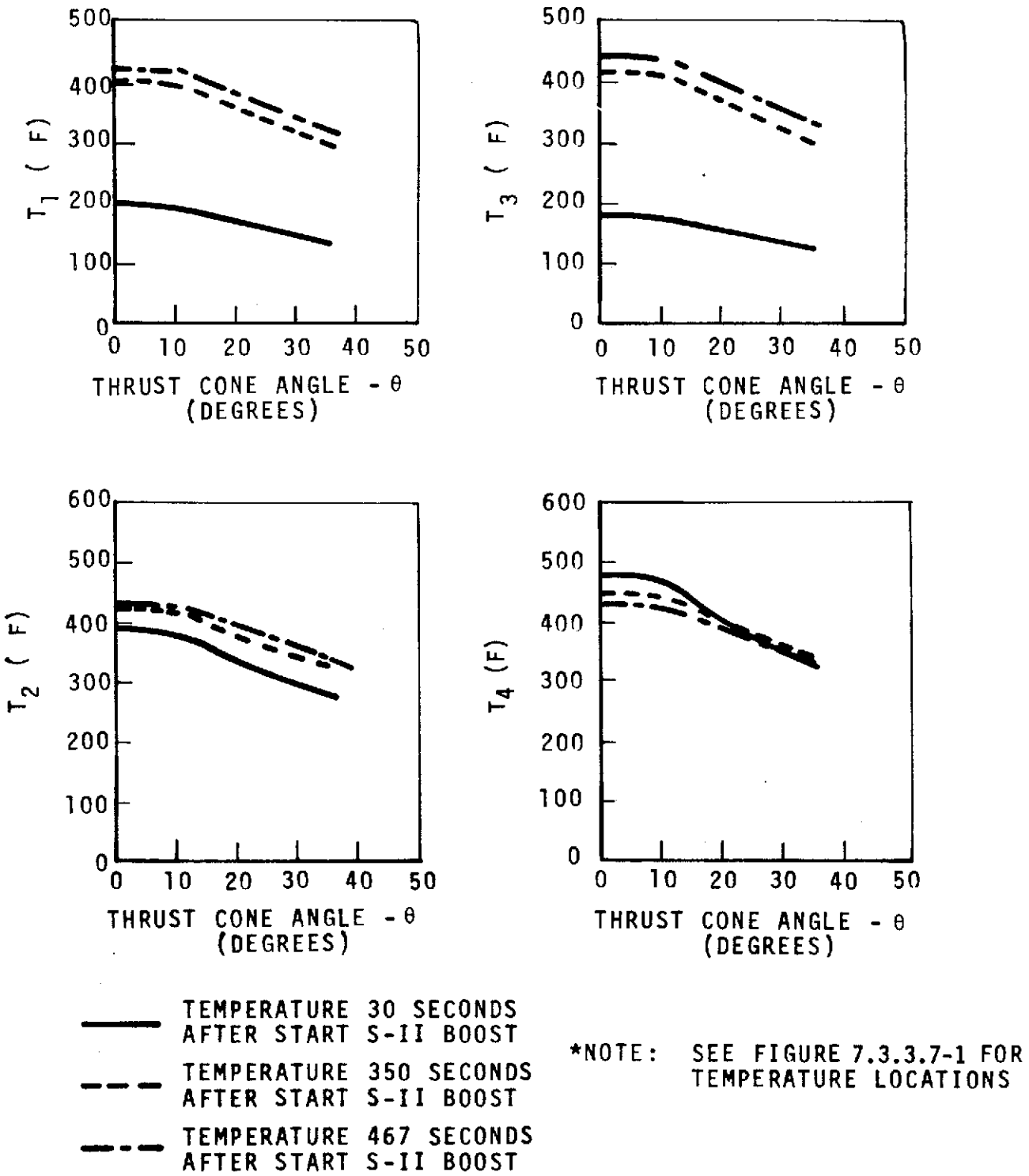

Figure 7.3.3.7-2. Temperature of 196 Web Versus Thrust Cone Angle for RTV Insulation

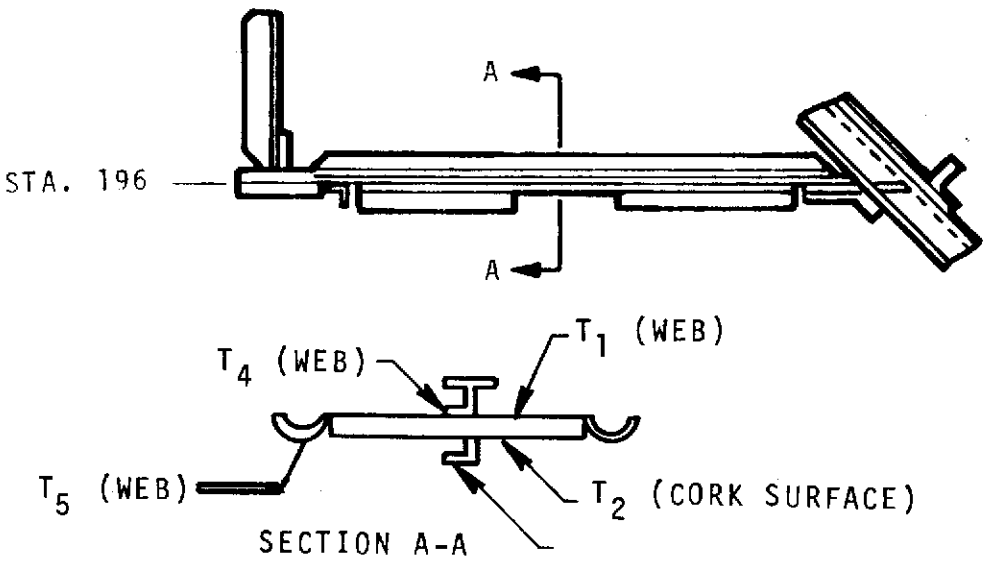

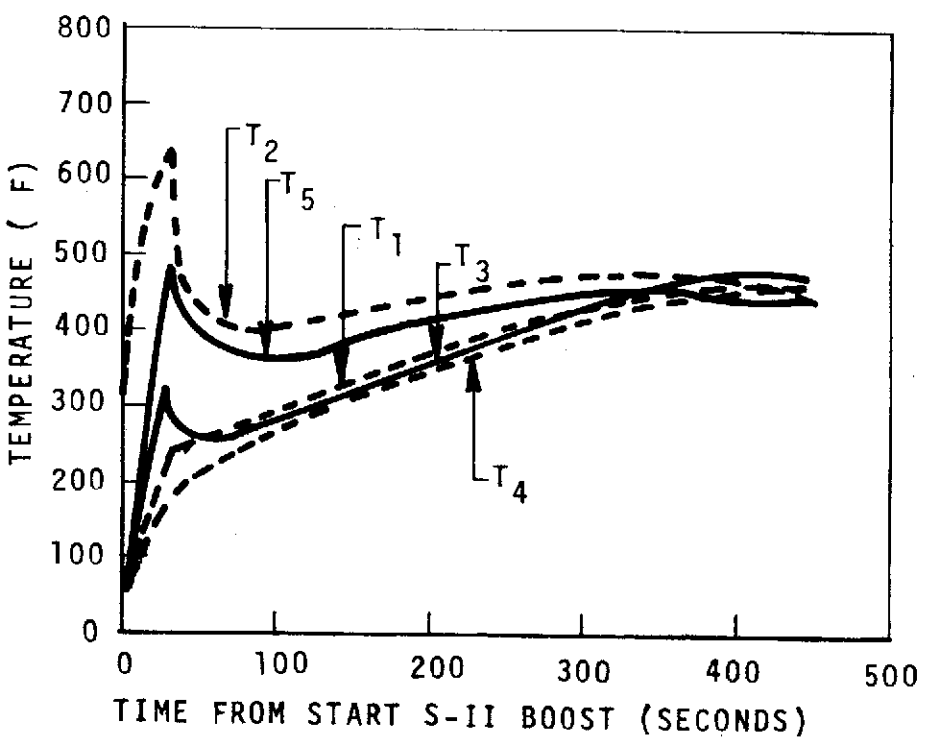

Figure 7.3.3.7-3. Temperatures of 196 Web Midway Between Engines (Cork Insulation)

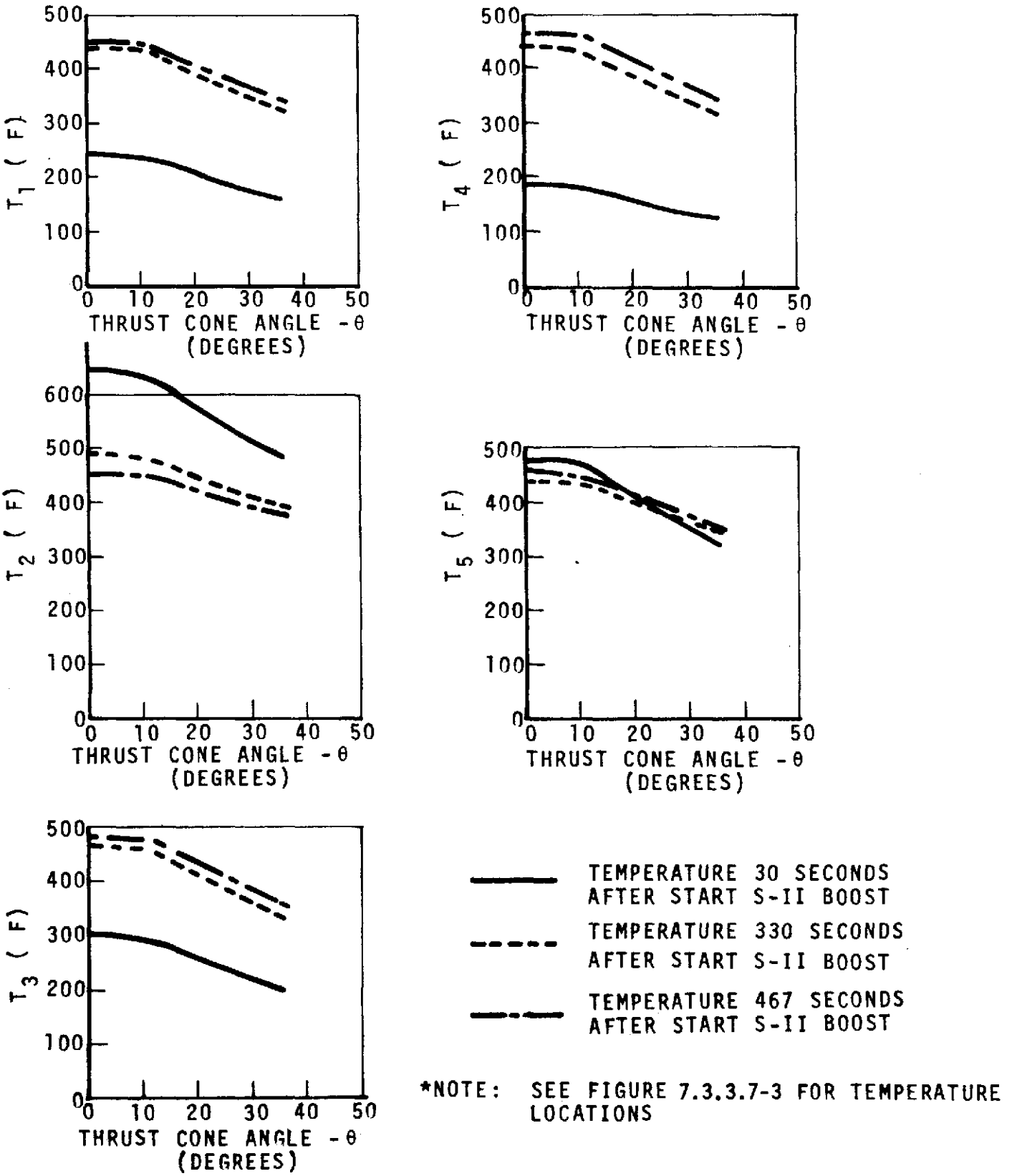

Figure 7.3.3.7-4. Temperature of 196 Web Versus Thrust Cone Angle (θ) For Cork Insulation

The surface temperature of the RTV stays considerably lower than the surface of the cork temperatures. This is because the lower thermal conductivity of the cork tends to hold the heat out to the surface of the cork and the cork has a lower heat capacity than that of the RTV.

7.3.3.8 Korotherm Coating

A thermal performance analysis was performed to determine the transient temperature response during S-IC and S-II boost of the cork-and Korotherm-protected S-II aft skirt and interstage structures. This analysis is presented in Paragraph 7.3.3.6. The Korotherm is essentially a zero capacity layer and will have the same temperature as the exterior layer of cork.

7.3.4 Miscellaneous Systems

7.3.4.1 Bonded Cork (Protection of Avionics Equipment)

S-II avionics equipment housed within aft equipment containers located in the engine compartment is subjected to base heating throughout S-II boost. The base heating rates assumed for the cover, sides, and ends of the containers are listed in Table 7.3.4.1-1. The heating rates used for the bottom of the mounting base were assumed to be 10 percent of the convective heating rates specified in Table 7.3.4.1-1, with radiant heating assumed to be zero. These base heating rates are in agreement with those of the S-II Environmental Data Book (SD 61-473-1).

The cover and sides of containers 206A31, 206A84, 206A85, 208, 209, 210, 211, 212, 213, and 214 and the battery cover for container 207A1 are insulated with 0.625-inch of 8-lb./ft.^{3} cork (per MB0130-020, Type II) located inside the 0.060-inch fiberglass structural wall.

Table 7.3.4.1-1. Base Heat Rates

TIME FROM LIFTOFF (SEC)	CONVECTIVE HEATING (BTU/FT^2-SEC)	RADIATIVE HEATING (BTU/FT^2-SEC)
0 - 150	0	0
150 - 180	2.80	0.240
180 - 500	0.16	0.050
500 - 617	0.12	0.038

A cover for the components on the container 207 mounting shelf (container 207A2) is also required. The cover is constructed of 0.060-inch fiberglass and requires internal insulation to limit heat transfer to the equipment inside.

The ends of each container, except container 207, are presently insulated with 0.25 inch of 30-lb/ft^3 cork insulation (per MB0130-020, Type I) located behind fiberglass structural wall. The higher density cork was used on the ends in order to provide additional mechanical capability associated with access to connectors and other components located on the ends.

All containers, except containers 207A1, 207A2, and 211, are insulated with 0.25 inch of 8-lb/ft^3 cork insulation (per MB0130-020, Type II) located externally beneath the aluminum honeycomb mounting bases as shown in Figure 7.3.4.1-1. This insulation was originally installed for protection during ground hold in a tanked condition to prevent heat loss from the containers. Container 211 has 0.50 inch of 8-lb/ft^3 cork inside the 0.060-inch fiberglass base. Container 207 has no insulation on the mounting base. A maximum mounting base temperature of 125 F is required for all containers.

The thermal properties of the materials considered in the study are given in Table 7.3.4.1-2.

Table 7.3.4.1-2. Material Properties

MATERIAL	THERMAL CONDUCTIVITY (BTU/FT-HR- F)	SPECIFIC HEAT (BTU/LB- F)	DENSITY (LB/FT^3)
FIBERGLASS	0.07 AT 0 F 0.214 AT 1300 F	0.182 AT 0 F 0.325 AT 610 F	110
CORK (MB0130-020, TYPE I)	0.04	0.40	30
CORK (MB0130-020, TYPE II)	0.020 AT 0 F 0.023 AT 140 F 0.029 AT 287 F	0.46 AT 0 F 0.46 AT 150 F 0.60 AT 275 F	8
ALUMINUM HONEYCOMB CORE	1.00 AT 0 F 1.30 AT 175 F 1.63 AT 283 F 2.56 AT 465 F	0.22	4.4
ALUMINUM	84	0.22	171

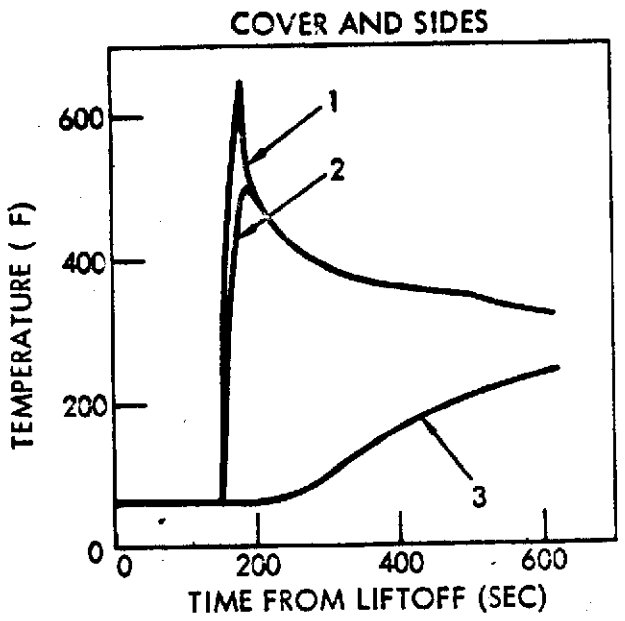

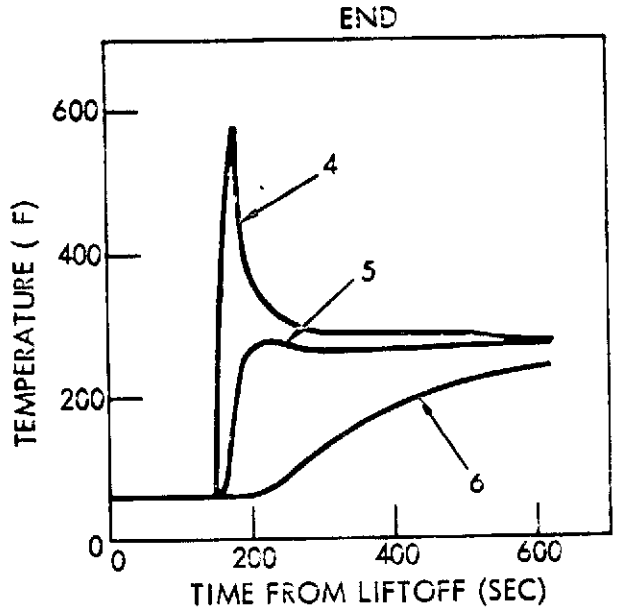

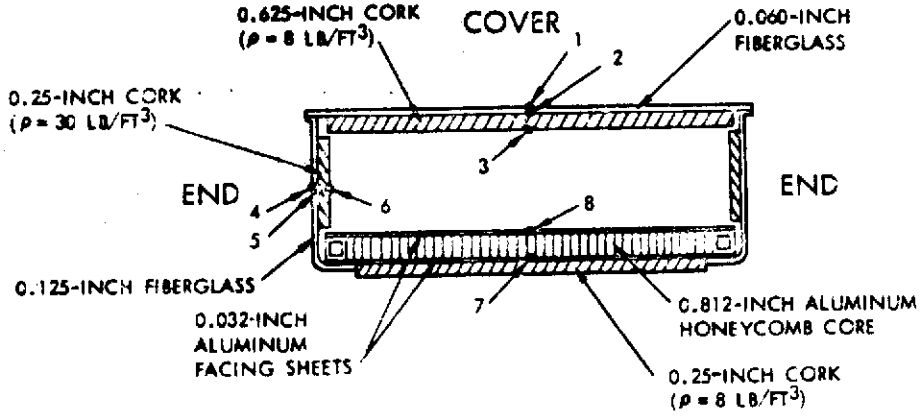

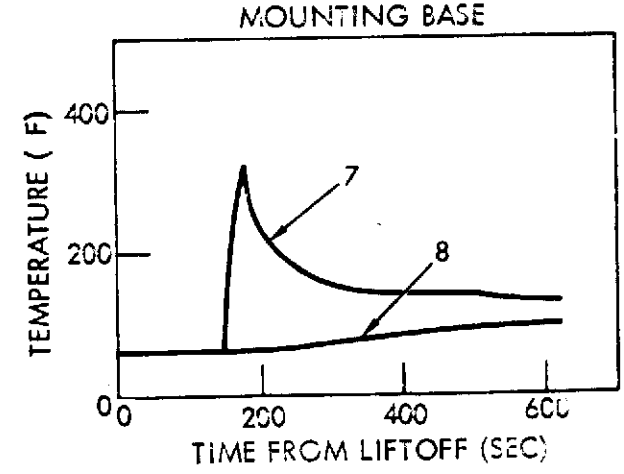

Figure 7.3.4.1-1. Temperature Histories of Aft Equipment Containers (Except Containers 207, 211, and 207A2)

Results of the temperature prediction study of the various insulation configurations are shown in Figure 7.3.4.1-1 and 7.3.4.1-2. The predicted internal wall temperatures for both the cover and side configuration of 0.060-inch fiberglass and 0.625-inch 8-lb/ft^3 cork and end configuration of 0.125-inch fiberglass and 0.25-inch 30-lb/ft^3 cork reached a maximum of approximately 240 F at the end of a one-engine-out boost, as shown in Figure 7.3.4.1-1. This is 40 F higher than the design requirement of 200 F used in previous studies. A supplementary analysis was conducted to determine the effect of increase in internal wall temperature of the covers, sides, and ends from 200 to 240 F. Since the containers have vent holes which allow leakage of gas to the interstage, it was assumed that there would not be sufficient gas remaining in the containers at the beginning of S-II boost to make convection heat transfer significant. Therefore, heat transfer from the container cover and sides to the components will be entirely by radiation. Conduction to the mounting base was not considered, since base temperatures never exceed the temperature limits of the components.

The internal wall temperature history of the cover, shown in Figure 7.3.4.1-1, was used as the heat source. The upper surface and all four sides of each component were assumed to be exposed to radiation from the container cover. The largest temperature increase for any component was 18 F at the end of a one-engine-out boost, assuming an initial component temperature of 60 F. At the end of a no-engine-out boost, the largest temperature increase was 11 F. The component for which these increases are predicted is the relay unit in container 209. A temperature history of the relay unit is shown in Figure 7.3.4.1-3.

The study showed that the maximum mounting base temperatures will be satisfied for all containers with the present insulation design. The temperature historie for the mounting base configuration with 0.25 inch of external 8-lb/ft^3 cork insulation and aluminum honeycomb are shown in Figure 7.3.4.1-1. Temperature histories for the mounting bases of containers 207 and 211 are shown in Figure 7.3.4.1-2.

The results of this study show that a maximum internal wall temperature of 240 F will not overheat the components and that an increase in insulation thickness for the cover, sides, and ends is not required.

The cover for container 207A2 employed 0.25 inch of 8-lb/ft^3 cork (per MB0130-020, Type II) located behind the 0.060-inch fiberglass structural wall. The internal wall temperature reached a maximum of 390 F during S-II boost, as shown in Figure 7.3.4.1-2. Assuming a component temperature of 60 F, component emissivity of 0.5, and component-to-cover geometric view factor of 0.5, a heat transfer rate of 0.054 Btu/ft.^{2}-sec was calculated for a typical component inside container 207A2 when the cover is at 390 F. This heat transfer rate is low enough not to require a cover; so it can be concluded that the internal wall temperature of the cover can reach 390 F and not cause damage to the components inside.

7.3.4.2 MLI and Fibrous Glass/Silicone Resin Binder

A thermal analysis was conducted (SD 70-687) to establish the feasibility of a thermal control system to protect the S-II stage avionics equipment during an

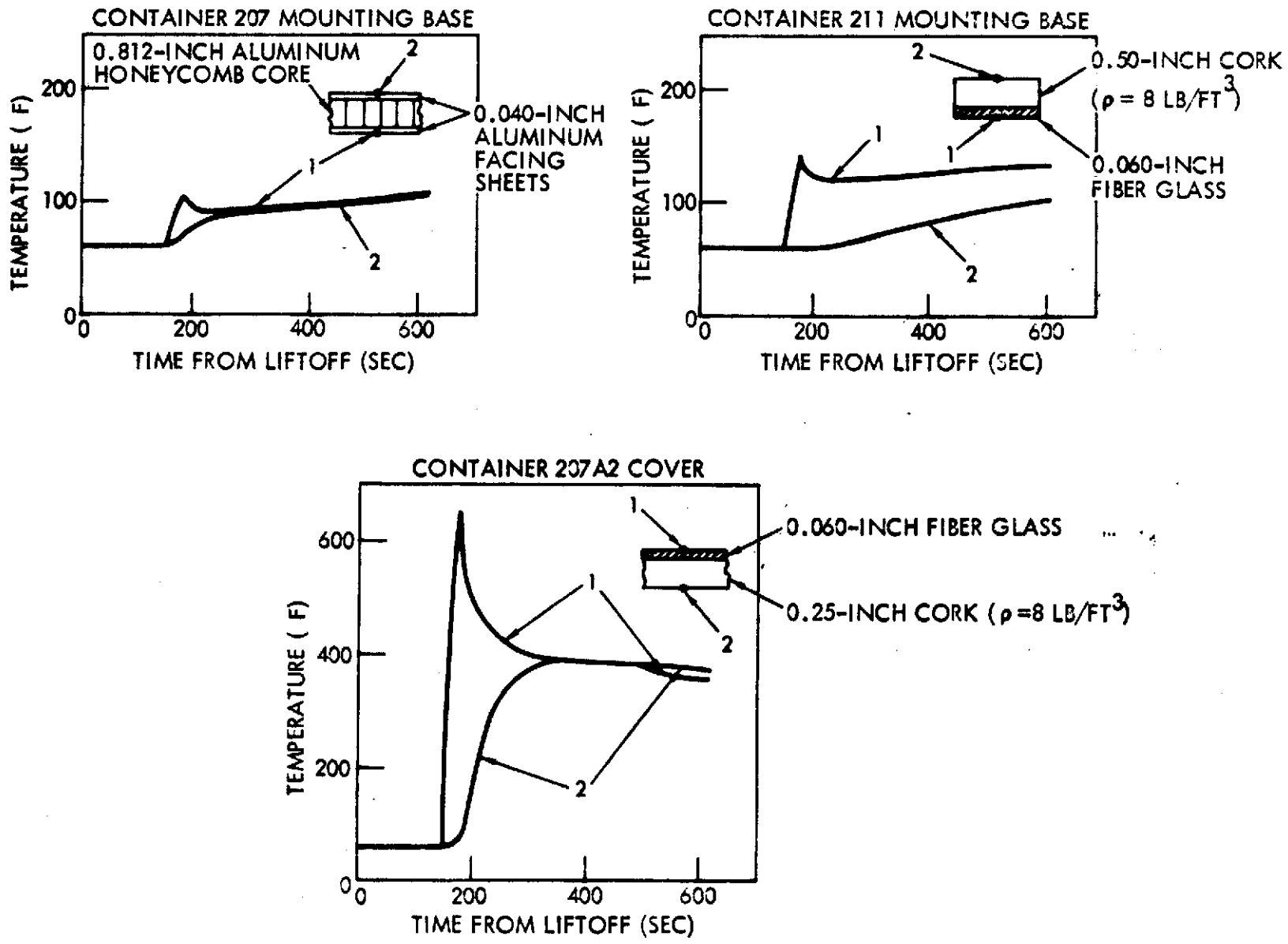

Figure 7.3.4.1-2. Temperature Histories of Aft Equipment Containers 207, 211, and 207A2

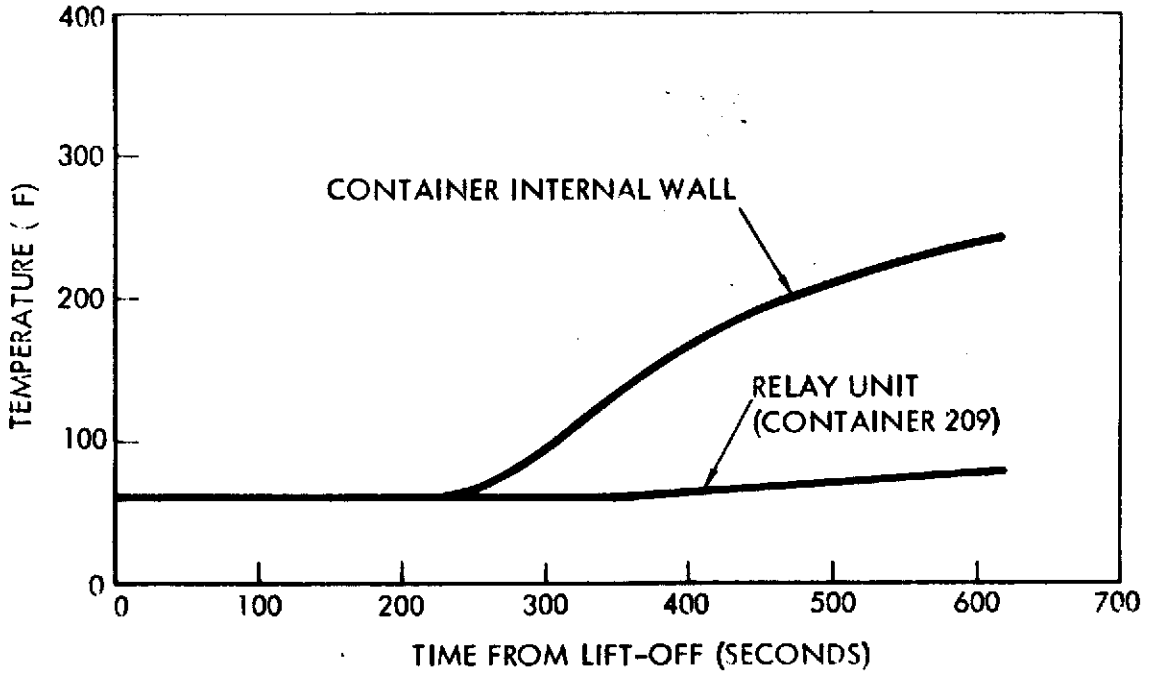

Figure 7.3.4.1-3. Temperature History of Typical Component

INT-21 mission. That analysis is summarized in this subsection. The avionics equipment is located in the aft and forward equipment containers on the S-II stage. The thermal analysis was to establish the prelaunch, launch and orbital environments affecting the avionics equipment during orbital missions of S-II derivatives and to determine design requirements which will allow the avionics equipment to operate under these conditions:

This study was conducted based on the following guidelines:

a. The avionics equipment is classified into equipment used up to the end of S-II boost, up to auxiliary propulsion system burn, and for the entire 24-hour mission.

b. The recommended thermal control system must be capable of maintaining the equipment operating temperature within the established limits for the required life of the equipment.

c. The thermal analysis was conducted for Space Station, Space Base, and Reusable Nuclear Stage (RNS) missions based on the following parameters:

   1. Space Station will be a direct ascent to a 270-nautical-mile orbit at an inclination of 55 degrees to the equator.

   2. Space Base and RNS will be in a 100- by 270-nautical-mile orbit for 5.3 hours and 18.7 hours in a 270-nautical-mile orbit at an inclination of 30 degrees.

d. The design solar orientation for all missions is a fixed vehicle Y axis perpendicular to the orbit plane (Y-POP) with nose forward in the direction of flight. Also included in the thermal studies was a solar orientation with vehicle -Z axis to the sun to determine the effect of solar orientation.

e. The angle between the orbit plane and sun (β angle) was varied between 0 and 80 degrees to determine the maximum and minimum orbital solar environment for each container.

f. The S-II stage orbital operation requires an attitude control system to maintain a fixed attitude. Thermal control depends on minimizing solar heating for containers with high equipment heat dissipation and maximizing solar heating for containers with lower equipment heat dissipation.

g. The study assumed that two extreme onboard environmental conditions could exist which would influence the container thermal environment. The first assumption was that the cryogenics would be completely vented immediately following boost. This could occur for the Space Station mission which is a direct ascent. For this maximum environmental condition, the LH_2 tank forward dome and LOX tank dome temperatures were conservatively estimated to vary between 0 and 100 F depending on the orbital heat load for the vehicle side under consideration. The other assumption was that cryogenics would remain onboard for the entire 24-hour mission. This condition could occur for the Space Base which is circularized at 5.3 hours and then vented. However, the venting rate has not been established and therefore cryogenics were assumed to remain onboard. For this minimum environmental condition, the LH_2 tank forward dome and LOX tank dome temperatures were assumed to be -165 F and -290 F, respectively.

The prime intent in developing a thermal control system was to eliminate the need for an active cooling system and to minimize the requirements for electrical heaters. The steps taken in the analysis of the selected system are:

a. Define avionics equipment and operating temperature ranges and heat dissipations of each piece of equipment.

b. Define equipment in each container and total equipment heat dissipation within each container.

c. Determine orbital solar environment around the vehicle represented by an eight-sided prism.

d. Locate containers on the vehicle depending on internal heat dissipation and external orbital solar environment.

e. Develop simplified thermal model of each container.

f. Conduct parametric thermal analyses of each container to optimize surface coatings and insulation thicknesses in order to achieve passive thermal control.

g. Establish electrical heater requirements.

a. Summary: A feasible thermal control system for the aft and forward containers of the avionics equipment was established. Tyis system will allow the equipment to operate in the predicted orbital thermal environment without exceeding its operating limits. Thermal models were developed for each container which included orbital solar heat loads and equipment heat dissipation. Surface coatings and insulations were varied to minimize the need for electrical heaters and eliminate the need for an active cooling system. The design of the system requires a vehicle attitude control system so as not to expose containers with high equipment heat dissipations to high solar heating and thus overheat the equipment.

Modifications to the existing aft containers include replacing the fiberglass covers with aluminum covers and applying Z-93 white inorganic thermal control coating to the external surface of the aluminum covers. The Z-93 coating is required to obtain a relatively low ratio of solar absorptivity (α) to infrared emissivity (ε) of approximately 0.16 while exposed to direct solar heating. Surface coatings required on other external surfaces of the aft containers and on internal surfaces are varied depending on solar heating and equipment heat dissipation. The internal insulation on the cover and fiberglass walls is a combination of Kapton and NRC-2. A layer of Kapton is required between the external wall and NRC-2 because of its performance at elevated temperatures of approximately 270 F experienced due to base heating during S-II boost. NRC-2 is used for the remainder of the insulation blanket because of its lower cost. TG 15000 insulation is used externally underneath the aluminum honeycomb mounting base because it is more compatible with the present container design. Insulation thickness varied between 1/8 and 1/2 inch depending on environmental conditions and equipment heating.

The basic construction of the fiberglass forward containers are not altered except for surface coating and insulation requirements. Containers with high internal heat dissipations require Thermatrol white paint, with a high emissivity of approximately 0.95, on external and internal surfaces to dissipate the internal heat, while containers with low heat dissipations require aluminum foil and aluminum silicone paint, with relatively low emissivities of approximately 0.10 and 0.28, respectively, NRC-2 internal insulation is used within the covers and walls of containers 221, "D" and "E", and TG 15000 is used externally underneath the base on all containers except container 223. Insulation thicknesses for the forward containers also vary between 1/8 and 1/2 inch. Container 223 requires no thermal control modification since it is only required through S-II boost.

None of the forward containers require electrical heaters. Aft containers 206A31, "B" and "C" will require electrical heaters when orbiting in the design Y-POP solar orientation. For a -Z to the sun orientation aft containers 207 and "B" would require heaters. All heaters are designed with thermal switches which activate the heaters at 8 F and turn the heaters off at 10 F.

b. Predicted Orbital Thermal Environment: The orbital thermal environments used in this study were generated utilizing the Space Division's Space Vehicle Thermal Environment Program.

To determine the incident orbital heat load around the vehicle, the vehicle was represented by an eight-sided prism for use with the orbital heating program as shown in Figures 7.3.4.2-1 and 7.3.4.2-2. The arrangement of vehicle sides for the Y-POP nose forward solar orientation is shown in Figure 7.3.4.2-1. In Figure 7.3.4.2-2 the arrangement of sides for the -Z axis to sun orientation is presented.

Table 7.3.4.2-1 gives the integrated incident radiation for a complete orbit for each of the eight vehicle sides as well as for the nose and

Table 7.3.4.2-1. Integrated Incident Radiation for Eight-Sided Prism (With Two Ends) In Orbit

SIDE	SUN VS ORBIT INCLINATION ANGLE-B	Y-POP NOSE FORWARD 100/210 nmi		-Z TOWARDS SUN 270 nmi	
		*SOLAR	EARTH EMITTED	*SOLAR	EARTH EMITTED
1	0°	79.8622	98.915	440.9463	38.6545
	40°	65.2903	98.915	461.5948	34.5405
	80°	48.8458	98.915	703.5586	30.5055
2	0°	214.6548	0	315.6166	33.8318
	40°	164.3048	0	338.1063	30.3604
	80°	37.0768	0	502.0234	32.5081
3	0°	177.3812	33.4336	20.7227	30.3105
	40°	142.5761	33.4336	30.7585	33.127
	80°	42.4089	33.4336	9.3219	38.253
4	0°	59.4537	74.4346	42.4909	33.7959
	40°	38.9037	74.4346	41.7118	38.5003
	80°	8.7836	74.4346	8.0711	35.2112
5	0°	22.7913	33.4336	54.669	38.5824
	40°	17.4466	33.4336	34.1742	34.4856
	80°	3.9411	33.4336	4.3887	30.4936
6	0°	154.5878	4.4912	42.4416	33.7809
	40°	9.3620	4.4912	17.6064	30.3546
	80°	0.5253	4.4912	1.3269	32.5502
7	0°	153.9719	33.4336	20.6726	30.3106
	40°	121.4950	33.4336	4.924	33.1737
	80°	40.0195	33.4336	0.3996	38.3247
8	0°	155.0423	4.4912	315.5948	33.8469
	40°	302.1195	4.4912	325.6763	38.5723
	80°	471.8127	4.4912	496.1491	35.2702
9	0°	23.1815	33.4336	24.2477	38.5306
	40°	290.6761	33.4336	18.5369	38.5306
	80°	670.5327	33.4336	4.1346	38.5305
10	0°	59.5514	74.4346	24.2342	38.8227
	40°	132.5509	74.4346	18.5744	38.8226
	80°	480.1972	74.4346	4.2446	38.8225

*SOLAR = SUM OF DIRECTED AND REFLECTED SOLAR RADIATION

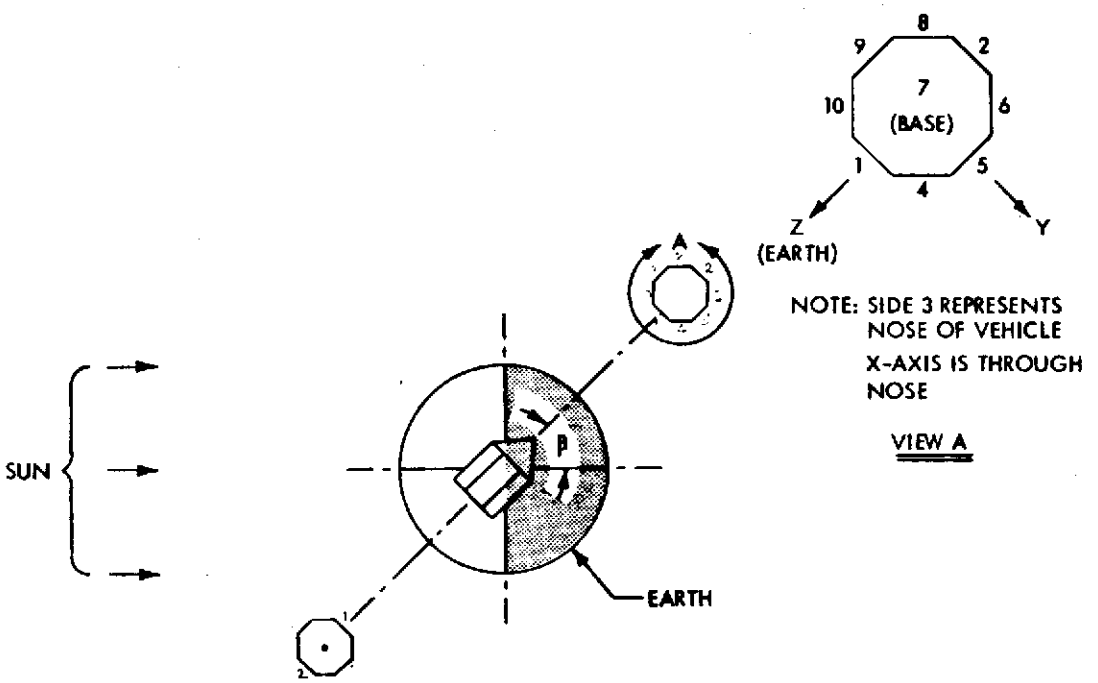

Figure 7.3.4.2-1. Y-POP Forward Solar Orientation

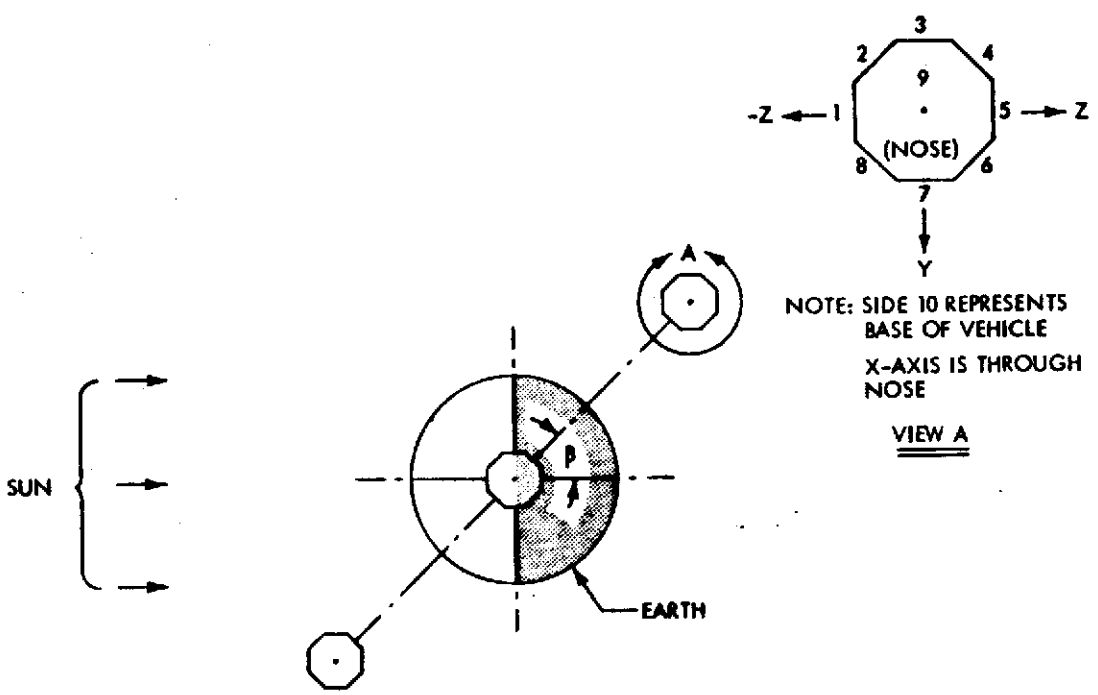

Figure 7.3.4.2-2. -Z Axis to Sun Solar Orientation

base of the vehicle. The combined sum of direct solar plus planetary reflected solar radiation is shown along with earth-emitted radiation for solar orientations of Y-POP nose forward and -Z axis to sun at β angles of 0, 40, and 80 degrees. From this table, the maximum and minimum incident orbital heat loads for each of the vehicle sides can be determined for the range of orbital parameters considered in this study.

Table 7.3.4.2-2 gives the vehicle side location for each of the containers for both Y-POP nose forward and -Z axis to sun orientations and also the orbital parameters which will create the maximum and minimum orbital heat loads for each container. For vehicle side locations, refer to Figures 7.3.4.2-1 and 7.3.4.2-2.

c. Surface Coatings - General: The selection of surface coatings depends on their usage. Equipment containers housing high heat-producing equipment should have internal and external coatings which provide high infrared emittance to all radiating surfaces to dissipate this heat by radiating to the cool surfaces of the LH_2 forward dome and the aft thrust cone.

Equipment containers housing low heat-producing equipment, which are not exposed to direct solar radiation, should have the internal surfaces coated with high reflective coating and the exterior surface coated with a low emittance coating for proper thermal control. Table 7.3.4.2-3 lists candidate surface coatings showing solar absorptivity and infrared emissivity.

To minimize the effect of solar heat input, surface coatings with relatively low α to ε ratio were investigated for application on the external surface of the thrust cone and the covers of the aft containers. On the Apollo program a white inorganic thermal control coating (Z-93 applied per specification MA018-022) has been successfully used for space radiators and other aluminum surfaces where specific thermal control was required. This coating is baked onto sand-blasted aluminum surfaces at a temperature of 270 F. The solar absorptivity (α) of this coating although increasing from 0.14 to 0.25 after 500 hours' exposure to 500 F will still maintain a relatively low α/ε ratio of 0.27. Another thermal control coating used on the Apollo program is an organic white coating identified as DC92-007 applied per specification MA0608-018. This coating exhibits more degradation than Z-93 when exposed to elevated temperatures, such as base heating, but appears to be useful for exterior coatings of the aft and forward container housings which have lower predicted temperatures. Another white coating considered in the study which appears acceptable for passive thermal control is Thermatrol. Thermatrol is the trade name for another thermal control coating which exhibits a very low α to ε ratio. Thermatrol is a white silicon paint which deteriorates only when exposed to ultraviolet radiation for a period in excess of 500 hours.

Table 7.3.4.2-2. Location of Container Versus B-Angle With High and Low Incident Orbital Heat Load

CONTAINER NO.	LOCATED ON SIDE Y-POP	-Z	B-ANGLE	HIGH ORBITAL HEAT LOAD	LOW ORBITAL HEAT LOAD
206A31	8	2	0° 80°	X	X
207	9	3	80° 80°	X	X
214	2	3	80° 80°	X	X
"A"	5	7	0° 80°	X	X
"B"	4	6	0°	X	X
225	5	7	0° 80°	X	X
"D"	1	5	0° 80°	X	X
210	2	1	80° 80°	X	X
209	5	7	0° 80°	X	X
"E"	5	7	0° 80°	X	X
"C"	6	8	80° 80°	X	X
"F"	4	6	0° 80°	X	X
221	4	6	0° 80°	X	X

Table 7.3.4.2-3. Surface Coatings Considered for Thermal Control Applications

THERMAL CONTROL APPLICATIONS		SURFACE COATINGS	SOLAR ABSORPTIVITY (α)	INFRARED EMISSIVITY (ϵ)	COMMENTS
EXTERNAL TO CONTAINER	INTERNAL TO CONTAINER				
USE FOR LOW EMITTANCE REQUIREMENTS (DO NOT USE WHEN EXPOSED TO HIGH SOLAR HEAT LOADS)	USE FOR LOW EMITTANCE OR LOW ABSORPTANCE REQUIREMENTS	ALUMINUM SHEET	.16 - .2	.06 - .10	USE WHEN < 750F
		ALUMINUM FOIL (MYSTIK 7402)	.12	.04	
		BERYLLIUM	.11 - .50	.10	
		INCONEL FOIL	.32 - .38	.11 - .13	
		INCONEL X FOIL	.18 - .66	.15	
USE FOR LOW SOLAR ABSORPTION & HIGH EMITTANCE REQUIREMENTS	USE FOR HIGH EMITTANCE OR HIGH ABSORPTANCE REQUIREMENTS	WHITE LACQUER (SHERWIN WILLIAMS)	.28	.86	α = .5, WHEN $\gtrsim$ 700F
		FULLER WHITE SILICONE PAINT	.25	.9	α = .6, WHEN $\lesssim$ 800F α = .6 FOR ULTRAVIOLET RADIATION
		OPTICAL SOLAR REFLECTOR ALUM. COATED	.1	.744 - .807	
		THERMATROL WHITE SILICONE PAINT	.16	.95	α = .32 FOR ULTRAVIOLET RADIATION UNAFFECTED BELOW + 650F
		S13 (ZnO/SILICONE)	.19 - .2	.79 - .87	
		S13G(ZnO/SILICONE)	.16 - .2	.84 - .86	
		Z93 (ZnO/K_2SiO_3)	.14	.91 - .97	α = .3 WHEN DETERIORATES REQUIRES ALUMINUM SURFACE AS BASE
		LPIOA ($ZnSiO_4/K_2SiO_3$)	.1 - .14	.87 - .91	
		HUGHES ($AlSiO_4/K_2SiO_3$)	.13 - .14	.88 - .91	
		DOW CORNING DC92-007	.192	.832	
USE FOR HIGH EMITTANCE REQUIREMENTS (DON'T USE WHEN EXPOSED TO HIGH SOLAR HEAT LOADS)	USE FOR HIGH EMITTANCE OR HIGH ABSORPTANCE REQUIREMENTS	BLACK LACQUER (SHERWIN WILLIAMS)	.93	.88	USE WHEN < 450F
		FULLER BLACK SILICONE PAINT	.89	.88	USE WHEN < 1070F
		ROKIDE C (CHROMIC ACID)	.82 - .9	.85 - .86	
		PLATINUM BLACK	.85 - .94	.8 - .9	
USE FOR LOW EMITTANCE REQUIREMENTS (DON'T USE WHEN EXPOSED TO HIGH SOLAR HEAT LOADS)	USE FOR LOW EMITTANCE OR LOW ABSORPTANCE REQUIREMENTS	FULLER ALUMINUM SILICONE PAINT (172-A-1)	.25	.28	
		FULLER ALUMINUM SILICONE PAINT (171-A-152)	.22	.24	
		ALUMINUM ACRYLIC PAINT	.38 - .52	.36 - .58	USE WHEN < 650F

The equipment containers located in the forward skirt area are not exposed to base heating or direct solar radiation. Therefore, any high infrared emittance coating should be adequate for the surfaces of the containers containing high heat-producing equipment.

Table 7.3.4.2-4 lists the recommended coatings for the interior and exterior surfaces of the forward and aft equipment containers.

Table 7.3.4-2-4. Recommended Container Surface Coatings

Stage Location	Container Surface	Container Internal Heat Load	Coating
Aft	Cover external	High or low	Z-93
Aft	Cover internal	High or low	Thermatrol or DC-92-007
Aft	Housing and bases internal	High	Thermatrol or DC-92-007
Aft	Housings and bases internal	Low	Fuller aluminum silicone paint
Aft	Housings and bases external	High	Thermatrol or DC-92-007
Aft	Housings and bases external	Low	Aluminum foil
Forward	External including covers	Low	Aluminum foil
Forward	External including covers	High	Thermatrol or DC-92-007
Forward	Internal including covers	Low	Fuller aluminum silicone paint
Forward	Internal including covers	High	Thermatrol or DC-92-007

d. Insulation: In selecting candidate insulations for passive thermal control in equipment containers care was taken to pick only those proven in application. This was done to eliminate the cost of developing fabrication and installation techniques. Also, the thermal analysis could be conducted with known thermal conductivity values, thus eliminating costly testing. Six insulations qualified as candidates. All six are currently being used on programs within the Space Division. Spray foam, foam-filled honeycomb, and cork insulations are used on S-II while NRC-2, Kapton, and TG15000 are used successfully on Apollo. The insulation selected for the aft containers must be capble of surviving the high temperatures associated with base heating during boost without degradation of its thermal characteristics.

Since the S-II stage will be in a vacuum environment during on-orbit operations, the selected insulation also must be capable of high performance in this environment.

The six candidate insulations were evaluated for maximum temperature limits and thermal conductivity under vacuum conditions. This evaluation (Table 7.3.4.2-5) shows that although cork has a reasonably high maximum temperature limits, it along with spray foam and foam-filled honeycomb were eliminated from further consideration because of their high thermal studies for NRC-2, Kapton, and TG15000 were based on design values used for Apollo.

Table 7.3.4.2-5. Insulations - Performance Evaluation

	NRC-2	Kapton	TG15000	Spray Foam	Foam-Filled Honeycomb	Cork
Vacuum Conductivity (Btu/hr.-ft.-°F)	2.5×10^{-4}	2.5×10^{-4}	5×10^{-4}	125×10^{-4}	175×10^{-4}	500×10^{-4}
Maximum Temperature Limit (°F)	250	700	900	250	250	700

The remaining three insulation candidates (NRC-2, Kapton, and TG15000) are:

1. NRC-2 is a high performance insulation manufactured by National Research Corporation, Cambridge, Mass. This material consists of aluminum deposited on a Mylar substrate sheet. Each sheet is 0.15 mil thick and is crinkled to reduce conduction. Insulation blankets are made by stacking these aluminized Mylar sheets to obtain the desired thickness.

   Handling and assembly must be done with great care to prevent dmmage. The insulation must be isolated from moisture because water removes aluminum from the Mylar shields and causes material outgassing, thereby degrading the required thermal properties. To prevent moisture, a dry gas purge is required during ground operations. The insulation must also be vented to prevent pressure buildup in the installed configuration due to the pressure differentials encountered during boost.

   NRC-2 is a low cost, off-the-shelf product, currently used on the Apollo program where its fabrication and installation is controlled by NR Specification MA0311-001. The fabrication and installation techniques have been developed and proven. It has low material cost. However, fabrication time is lengthy due to handling precautions. Its application is restricted to areas where the maximum temperature is below 250 F.

2. Kapton is a high-performance insulation material consisting of aluminum deposited on a Kapton substrate. Each sheet is 0.15 mil thick. The installation and fabrication requirements are similar to those of NRC-2. The thermal conductance of Kapton is similar to that of NRC-2. However, the effective performance temperature is much higher (700 F).

Kapton is a high-cost insulation as compared to NRC-2. It is an off-the-shelf product currently used on the Apollo program where its fabrication and installation are controlled by NR specification MA0311-0001.

3. TG15000 is an insulation material manufactured by the HITCO Corporation, Gardena, California. The material is a resin-bonded fiberglass manufactured to the desired thickness. The thermal conductivity of evacuated TG15000, although approximately twice that of NRC-2 or Kapton, is still considerably lower than insulations used on the S-II stage. The upper temperature limit for performance effectiveness is very high (900 F).

   TG15000 is a low-cost, off-the-shelf product. Fabrication and installation require no special technique. This insulation is used on the Apollo program where its fabrication and installation are controlled by NR Specification MA0311-0006. TG15000 is an insulation with proven space applications. It is easy to handle and install, has low material cost, and high upper temperature limit.

For the forward containers, use of NRC-2 inside the cover and walls and TG15000 external to the mounting base is recommended. Adequate handling and quality control procedures for installation of these materials are available from the Apollo program, where much experience with this type of insulation was gathered.

The aft containers are exposed to base heating during S-II boost, with preliminary values for LOR missions indicating a maximum predicted temperature of approximately 270 F. This is just above the temperature capability of NRC-2; therefore, it is recommended that internal to the cover and walls, a layer of Kapton be used with the remainder of the insulation blanket of NRC-2. The use of a minimum number of layers of Kapton reduces the cost significantly. This approach was successfully used on the Apollo program, and is recommended. TG15000 is recommended external to the mounting bases. The studies confirmed that high-performance insulation would be required for almost all container surfaces to minimize active thermal control requirements.

e. Equipment Container Thermal Models: Thermal models of the equipment containers are required to:

1. Determine the influence of orbital thermal environment on equipment.

2. Conduct parametric analyses to optimize surface coating and insulation selection.

3. Determine electrical heater requirements.

The modes of heat transfer used in preparation of the thermal models are shown in Figures 7.3.4.2-3 and 7.3.4.2-4 for typical forward and aft containers. To conduct the thermal analysis, preliminary thermal models were developed for:

1. Forward containers with vibration isolation mounts (similar to No. 225).

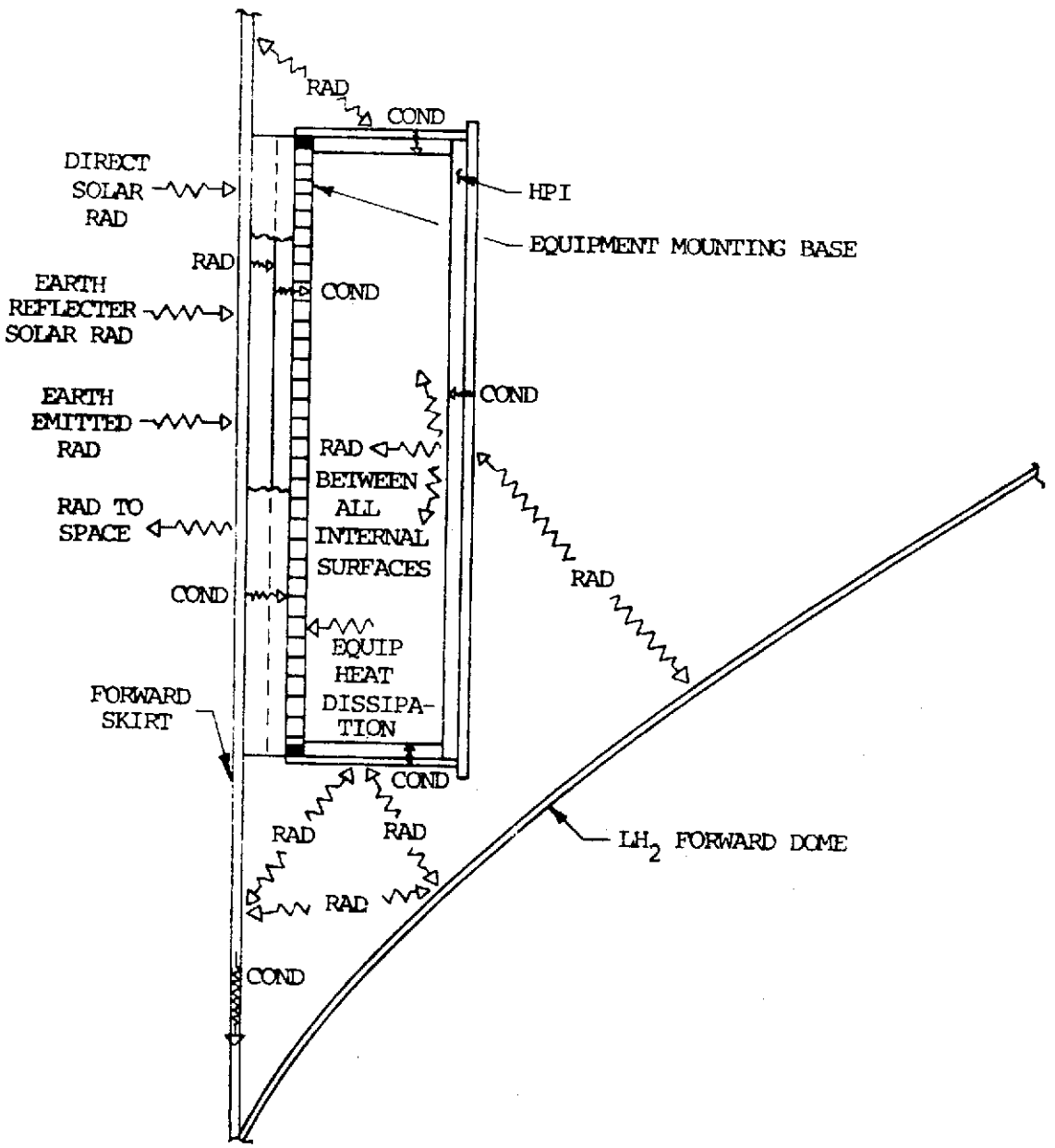

Figure 7.3.4.2-3. Modes of Heat Transfer for Typical Forward Container

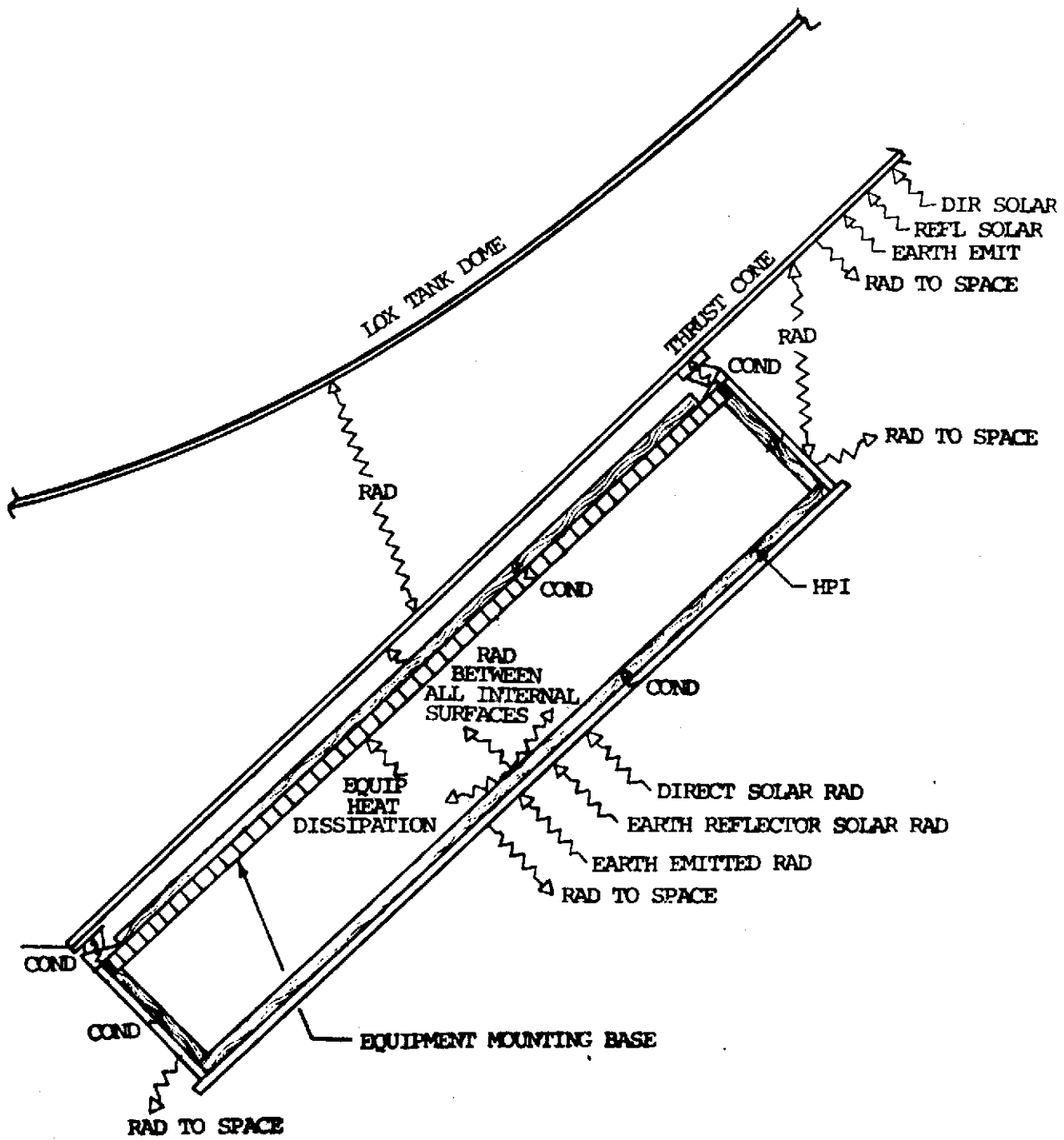

Figure 7.3.4.2-4. Modes of Heat Transfer for Typical Aft Container

2. Aft containers with vibration isolation mounts (similar to No. 210).

3. Aft containers with direct (hard) mounting (similar to No. 206A31) to the structure.

4. Aft containers with direct (hard) mounting to the structure (similar to No. 207).

5. Aft containers with direct (hard) mounting to the structure (similar to No. 214).

Thermal models developed for the containers included a honeycomb mounting base with outside insulation of TG15000, aluminum covers for aft containers, fiberglass covers for forward containers and side walls constructed of fiberglass, and NRC-2 or Kapton on the inside of covers and walls. Initially, the external coating assumed for the forward container covers and sides was aluminum foil with an internal coating of white paint to enhance radiation of radiative heaters. The external coating of the aft containers was assumed to be white paint with the internal coating the same as for the forward containers.

Modifications to the S-II-15 design for the directly mounted forward and aft avionics containers included changing the aluminum mounting brackets and aluminum rivets to CRES steel, and addition of fiberglass washers under bolt and rivet heads and between the mounting brackets and structure.

Figures 7.3.4.2-5 through 7.3.4.2-11 show typical forward and aft containers in the S-II-15 and preliminary passive thermal control configurations.

The thermal networks representing the containers and associated modes of heat transfer were generated for use with the General Thermal Analyzer Program. To prepare a problem for solution with the program, the physical system must be approximated by division into representative finite elements. Each element is assumed to be homogeneous and of uniform temperature throughout. The mass of each element is represented by a point or node at its geometric center. Each node is assumed to be connected to each other by one or more conducting paths. This method of network representation allows the physical system to be described by a set of simulteneous finite difference equations which can be solved using the IBM 360 computer.

Shown in Figures 7.3.4.2-12 and 7.3.4.2-13 are representative thermal networks for a typical forward container (225) and typical aft container (210). The networks represent a relatively simple thermal model of the containers in that individual nodes, identified by circles, represented a complete element of container construction or adjacent vehicle structure. Conductances, identified by squares, between nodes represented both radiation and conduction modes of heat transfer. The external surfaces nodes were assigned a pair of special "QDOT" conductances which facilitated the application of orbital heating fluxes obtained on punched cards from the orbital heating program. The direct solar and earth-reflected solar

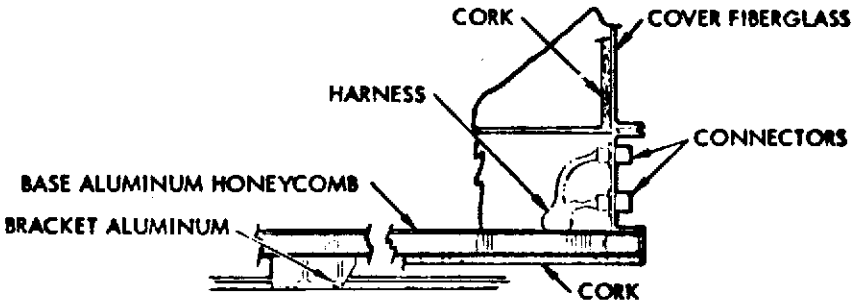

Figure 7.3.4.2-5 Section F-F in S-II-15 Configuration

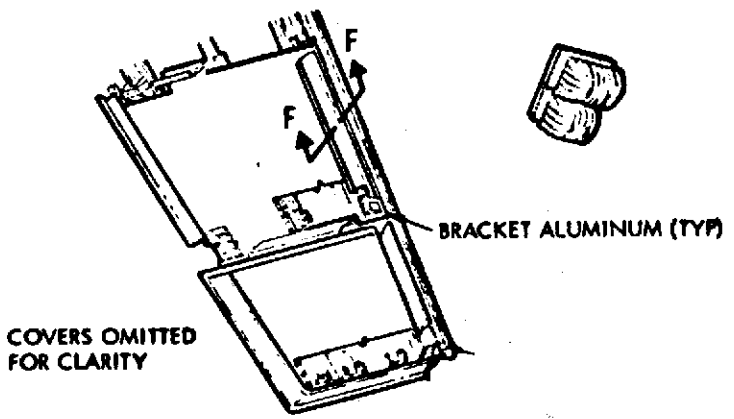

Figure 7.3.4.2-6 207 Container in S-II-15 Configuration

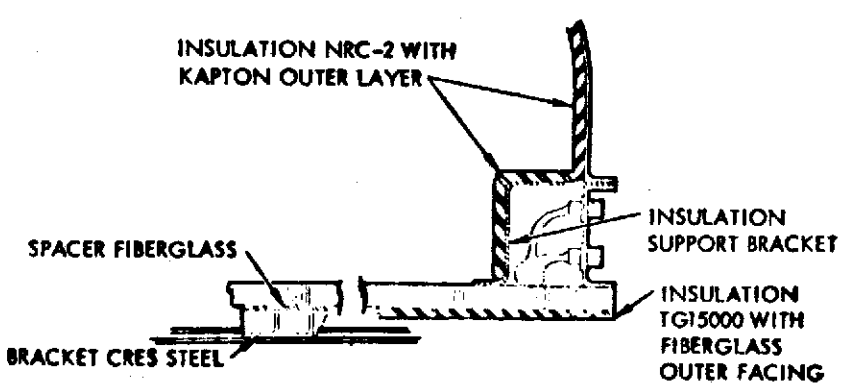

Figure 7.3.4.2-7. Section F-F Passive Thermal Control for Preliminary Configuration

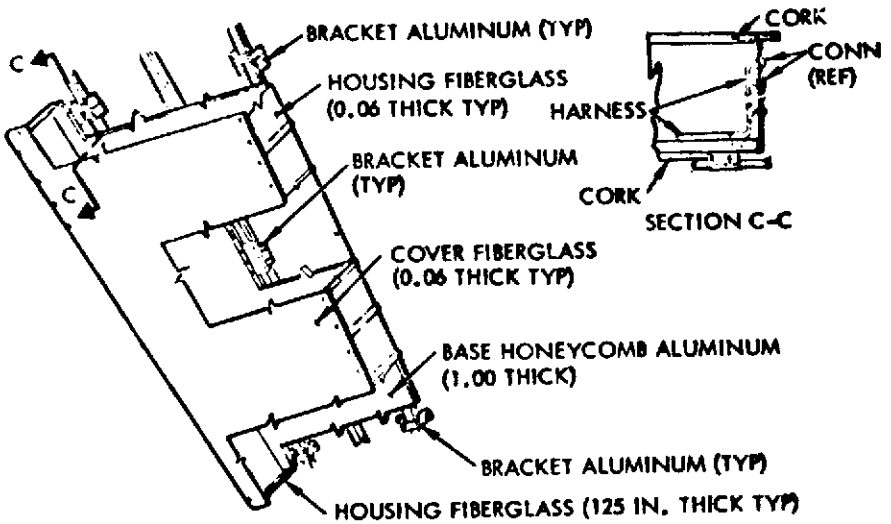

Figure 7.3.4.2-8. Containers 206A31 and 214 in S-II-15 Hard-Mounted Configuration

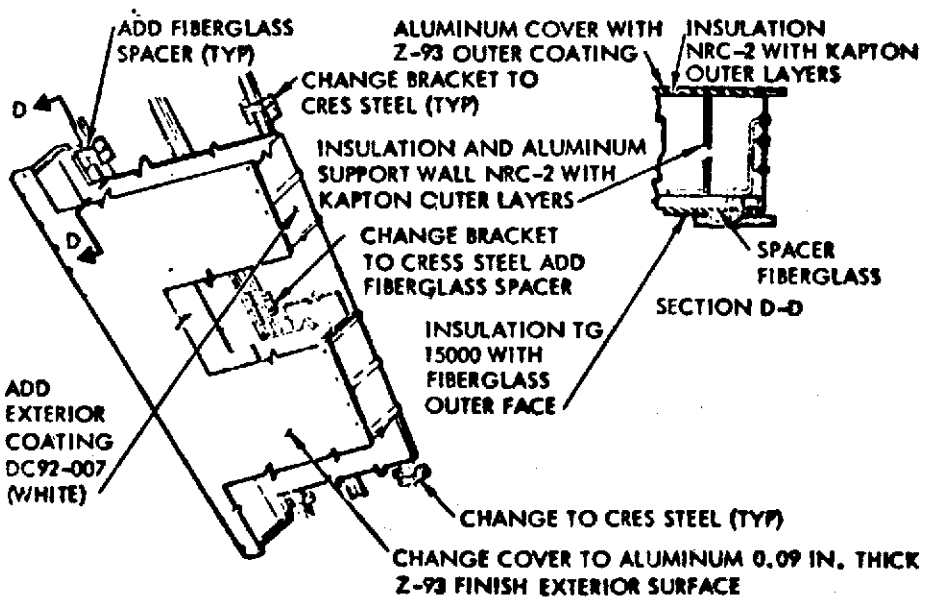

Figure 7.3.4.2-9. Passive Thermal Control for Containers 206A31 and 214 Preliminary Configurations

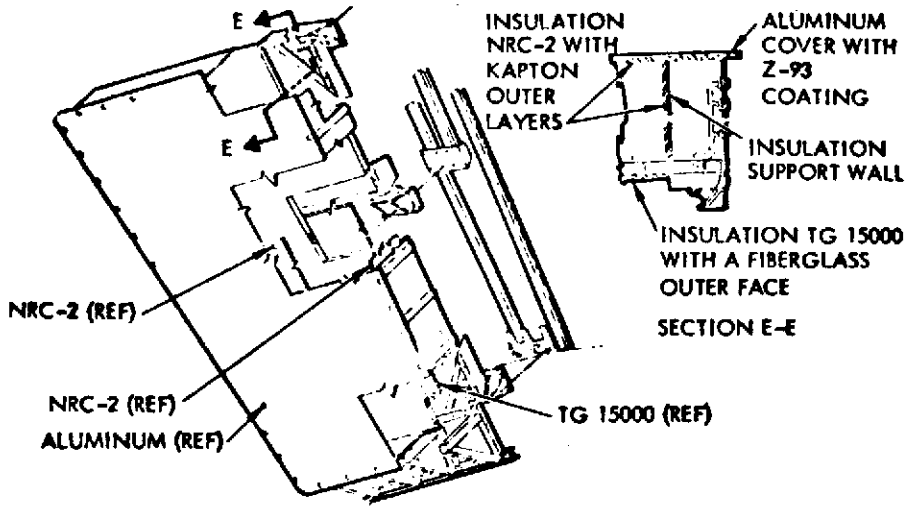

Figure 7.3.4.2-10. Containers 209 and 210 in Preliminary Passive Thermal Control Configuration

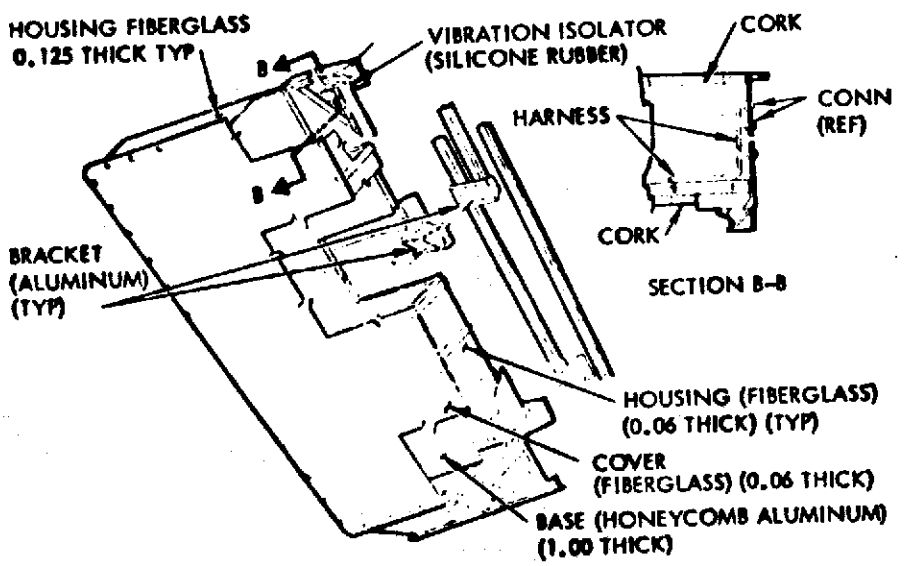

Figure 7.3.4.2-11. Containers 209 and 210 in S-II-15 Configuration

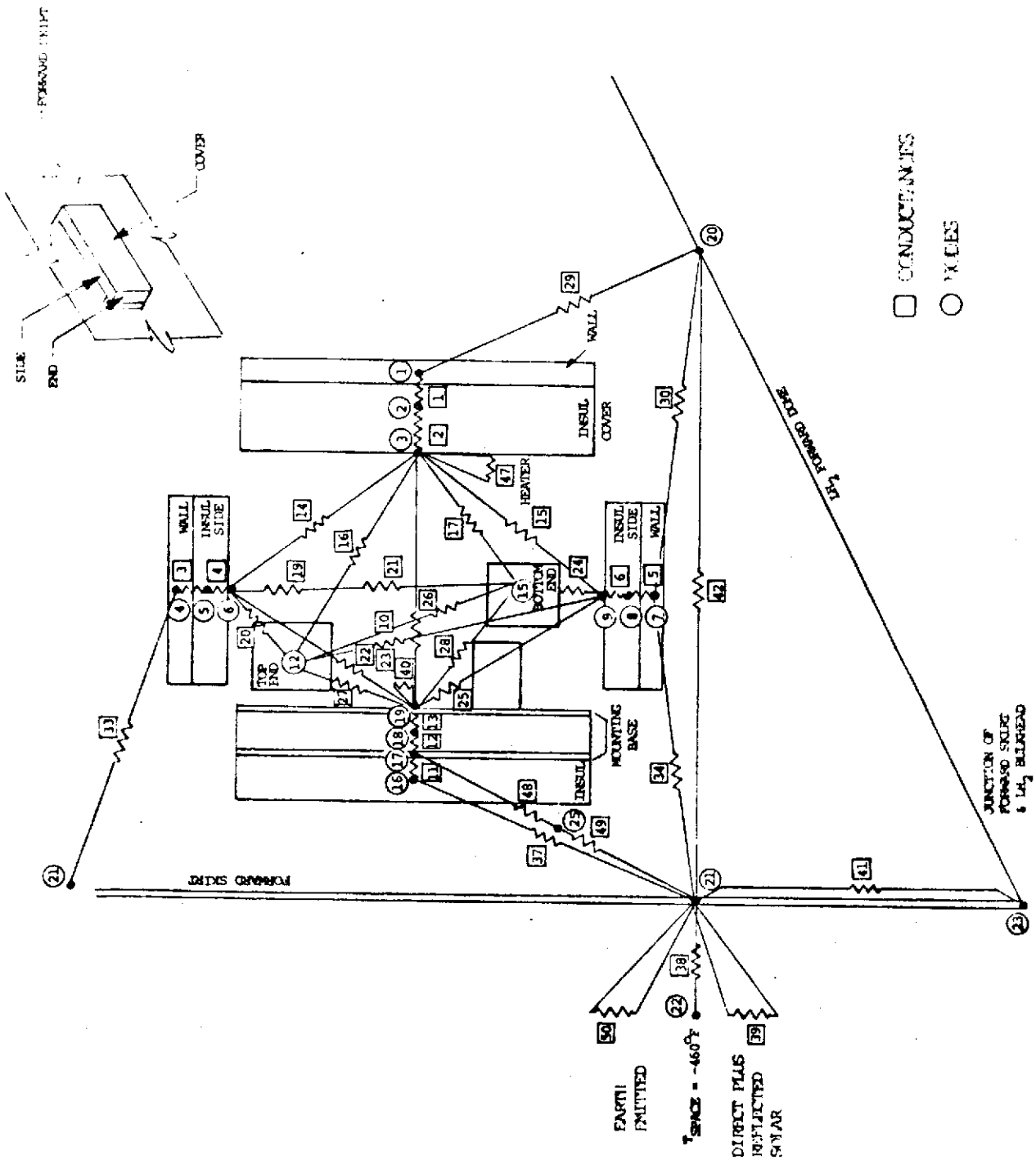

Figure 7.3.4.2-12. Forward Container Thermal Model Network

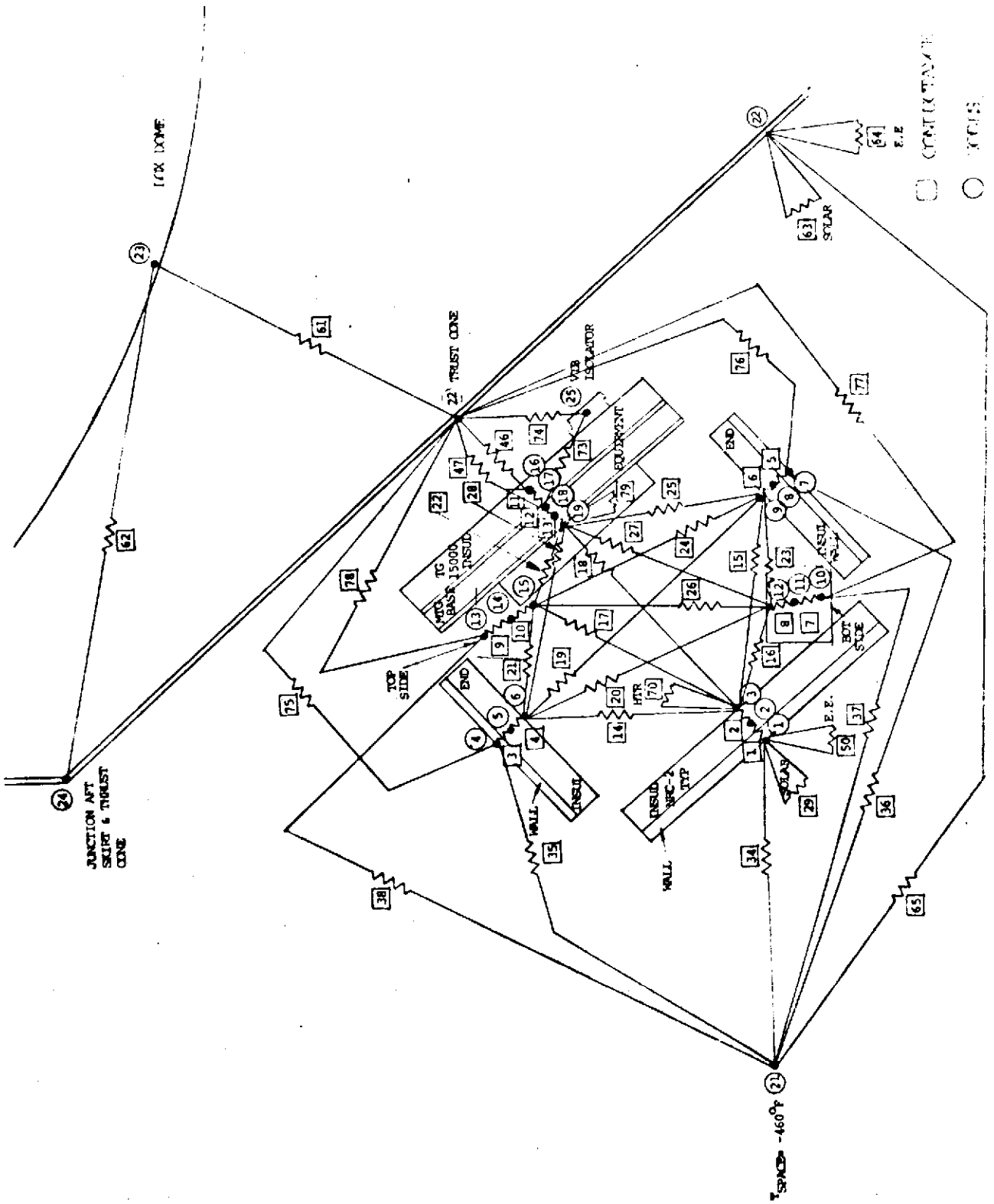

Figure 7.3.4.2-13. Aft Container Thermal Model Network

radiation in combined in the punched deck and are used in the Thermal Analyzer Program with the surface solar absorptivity (α) while the earth emission radiation is used with surface infrared emissivity (ε).

f. Preliminary Power Requirements: Since the equipment allocated to each container on the S-II stage was not identified during the early stages of this study, the original thermal models did not incorporate any internal heat dissipation. The only heat input to these early models consisted of the orbital heat load.

The original approach incorporated no special fixed attitudes or attitude control, and therefore, these early models were assumed to be located at the coldest and the hottest sides of the stage to determine an optimum passive thermal control design which would satisfy any orbital thermal environment, and also to establish any possible requirement for active thermal control to maintain the specified thermal environment.

The initial calculations based on these early preliminary models indicated requirements for large (500-watt) heaters for some of the directly mounted containers in addition to passive thermal control.

After the internal heat dissipation of the equipment placed in the various containers was determined, the preliminary thermal models were changed and updated to incorporate these internal heat loads. New calculations determined that the containers with high internal heat-dissipating equipment exceeded the permissible higher temperature limits. The thermal models of these containers were modified by reducing the insulation thickness and using surface coatings with high infrared emissivities to satisfy specified temperature limits. This effort resulted in individual application of passive thermal control devices for the containers and, therefore, it was required to delete general thermal control design considerations in order to eliminate the need for an active cooling system.

Calculations based on these changed assumptions still resulted in forward container 225 and aft container 214 exceeding their upper temperature limit for the maximum orbital heat load input with super-imposed equipment heat dissipation. The results of this phase of the study are shown in Table 7.3.4.2-6. Electrical heater requirements presented in the table were based on a switch turn-on setting of -40 F. The switch setting was lowered from +8 F to -40 F to demonstrate lower electrical heater requirements at the lower setting. However, it was determined that cost in requalification of equipment at lower temperatures would be excessive and +8 F was used in the remainder of thermal studies. The problem of exceeding maximum temperature limits could be solved in three basic ways:

1. Active attitude control of the stage to maintain these containers on a low orbital heat load side of the vehicle.

2. Removal of part of the high heat-dissipating equipment to other containers.

3. Active cooling by means of a cold plate or similar type of equipment.

Table 7.3.4.2-6. Preliminary Temperature Summary and Heating Requirements for Maximum and Minimum Orbital Heating - LH_2 and LOX at -165 F and -290 F for 16 Orbits (24 Hours)

CONTAINER NO.	MOUNTING	EQUIPMENT HTG IN WATTS	SPECIAL DESIGN FEATURES	TEMPERATURE OF BASE (EOMT)	ADDITIONAL HEATING IN WATTS	DUTY CYCLE
FORWARD 221	ISOLATOR	96	NO INSULATION ALL WHITE SURFACES FWD SKT = .9	+125°F MAX -1 F MIN	NONE	
223	DIRECT	2.5	.5" THICK INSULATION, ST. ST. FITTINGS WITH FIBER-GLASS WASHERS, ALL WHITE SURFACES. FWD SKT = .9	+128°F MAX -40°F MIN CYCL FROM 9th ORBIT ON	37	26%
225	ISOLATOR	290	NO INSULATION ALL WHITE SURFACES FWD SKT = .9	+152°F MAX -2° F MIN	NONE	
AFT 207	DIRECT	241	.5" THICK INSULATION, EXCEPT AT BASE .125" THICK INSULATION, ALL WHITE SURF-ACES, ST. ST. FITTINGS WITH FIBERGLASS WASHERS	+114°F MAX +50° F MIN	NONE	
209	ISOLATOR	209	.125" THICK INSULATION ALL WHITE SURFACES	+112°F MAX +20 °F MIN	NONE	
210	ISOLATOR	336	.125" THICK INSULATION ALL WHITE SURFACES	+117°F MAX +57 °F MIN	NONE	
214	DIRECT	426	.125" THICK INSULATION ALL WHITE SURFACES, ST. ST. FITTINGS WITH FIBERGLASS WASHERS	+148°F MAX	NONE	
206A31	DIRECT	14.5	.5" THICK INSULATION ALL WHITE SURFACES, ST.ST. FITTINGS WITH FIBERGLASS WASHERS	+104°F MAX -40 °F MIN CYCL FROM 5th ORBIT ON	50	10%

It was decided to use the first of these three solutions and add attitude control as a system requirement. In this manner, the high heat-dissipating equipment containers would be placed on relatively cold sides, and the low heat-dissipating equipment containers on comparatively hot sides. The use of attitude control for the stage along with addition of containers for INT-21 requirements were incorporated into the final thermal analysis requirements.

g. Operational Time Line Consideration in Thermal Control Design: During the initial phases of this study, the container environments and equipment temperature limits were established based on the S-II-15 configuration. Because orbital equipment operation had not been sufficiently defined at that time in the study, the thermal analysis did not incorporate any internal heat dissipation. The studies were conducted to develop a general container thermal control design which would satisfy the maximum and minimum orbital thermal environments for a 24-hour mission without benefit of attitude control. However, upon definition of container equipment heat dissipation, it was determined that maximum temperatures would be exceeded in containers 214 and 225, thus establishing the need for vehicle attitude control.

New operating time lines considering the measurement systems equipment were established in accordance with a new configuration which separated the equipment requirement into equipment operating through boost and SPS burn, and into equipment operating continuously for 24 hours of orbiting.

The equipment was repackaged in containers separating, as much as possible, equipment operating only through boost and APS burn and equipment requiring continuous operation. Containers with high heat-dissipating equipment were located at the colder areas of the stage, with regard to incident orbital heat loads. Thus, vehicle attitude control resulted in an important consideration for the overall thermal control system, eliminating a requirement for an active cooling system. The change in the equipment configuration from S-II-15 with UHF replacing VHF for the minimum instrumentation configuration necessitates the addition of six containers on the S-II stage.

The equipment container locations and the maximum and minimum total orbital heat loads on each side of the simulated eight-sided satellite for both the Y-POP and -Z axis attitudes are shown in Figures 7.3.4.2-14 and 7.3.4.2-15.

The initial thermal models for the equipment containers were changed to incorporate the selected thermal control system modifications including orbital thermal environments for specific container locations and revised container equipment allocations. Also, new thermal models were developed for the added containers. These thermal models were then used to determine surface coating and insulation requirements and establish electrical heater requirements.

The containers which are operative only through APS burn for the Space Base mission were assumed to be exposed to onboard environments which are influenced by cryogenics. It was assumed that for Space Station, these

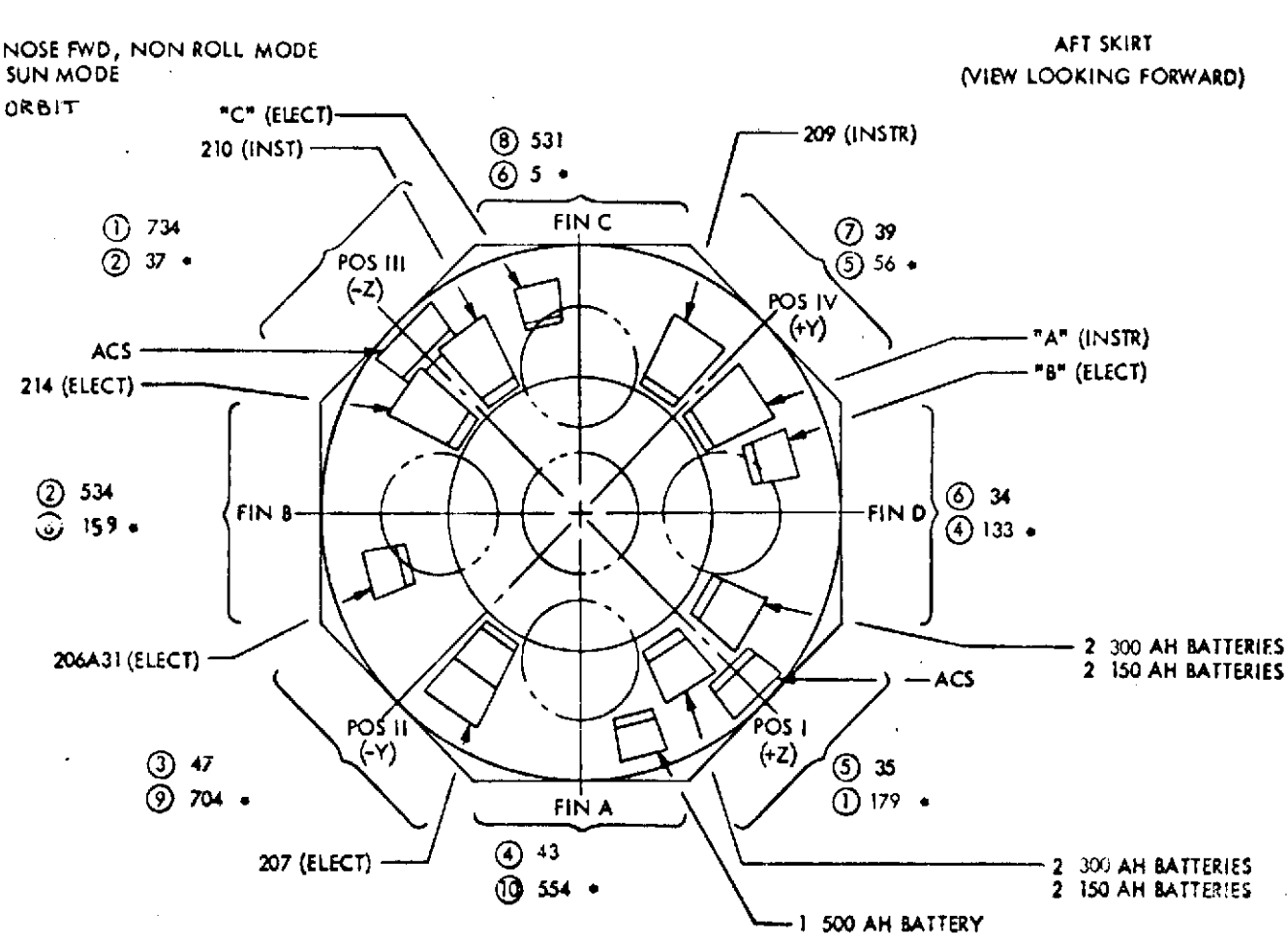

Figure 7.3.4.2-14. Aft Equipment Container Location Versus Maximum and Minimum Total Integrated Incident Radiation

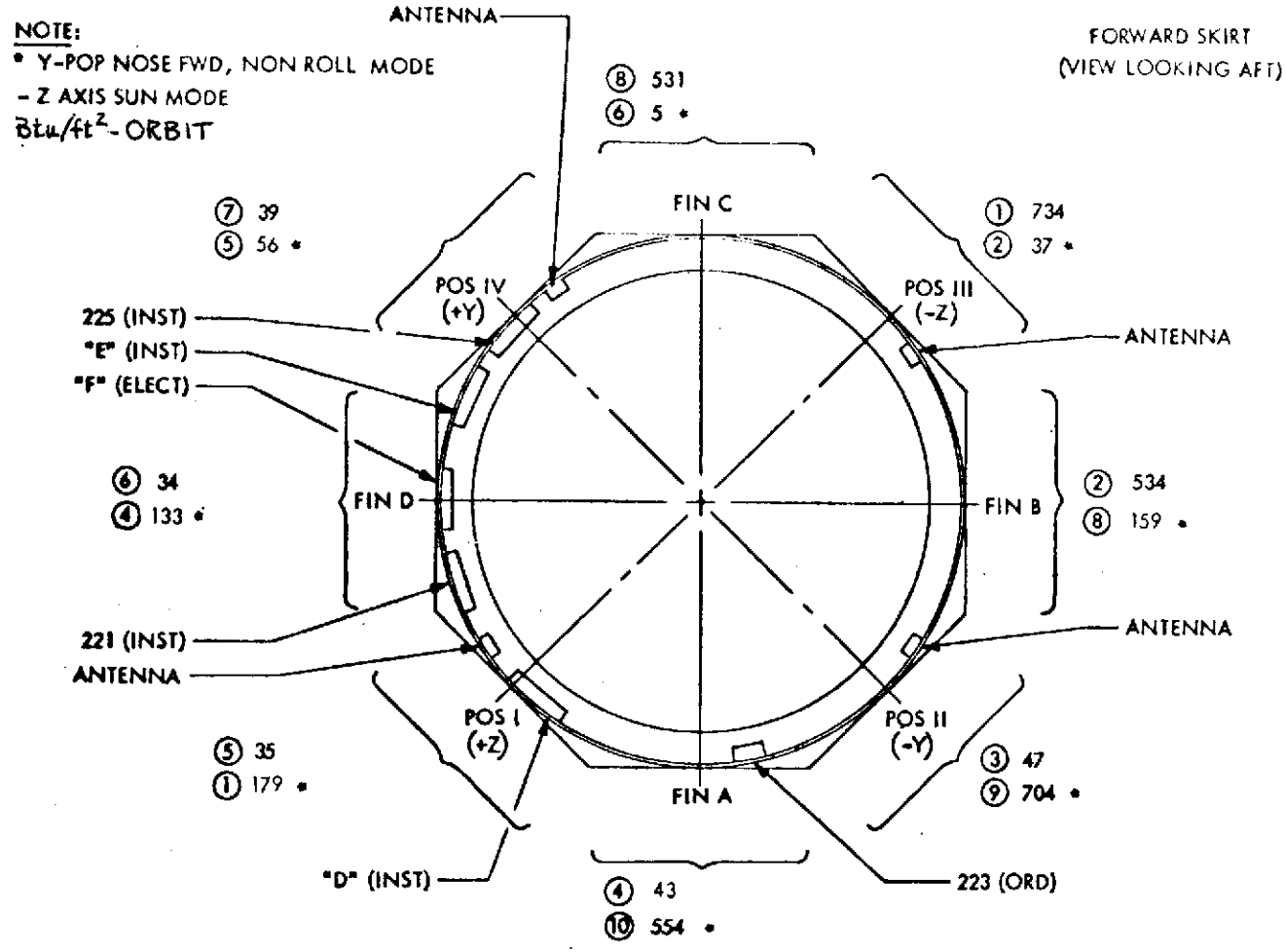

Figure 7.3.4.2-15. Forward Equipment Container Location Versus Maximum and Minimum Total Integrated Incident Radiation

containers would only be operative through S-II boost and therefore would not influence orbital thermal control design. The containers which are operative for the entire 24-hour missions of both Space Base and Space Station will require analysis assuming onboard environments which are influenced by cryogenics and by environments which have warmed up following propellant depletion. For Space Station, it was assumed that propellants would vent immediately following S-II boost and therefore onboard environments would be relatively warm for 24 hours. For this condition, the LH_2 tank forward dome and LOX tank dome was conservatively estimated to vary between 0 and 100 F depending on the orbital heat load for the vehicle side under consideration. The Space Base mission will have circularization at 5.3 hours and then vent the remaining propellants. However, the venting rates have not been established and therefore cryogenics were assumed to influence the onboard environment for the entire 24 hours. For this condition, the LH_2 tank forward dome and LOX tank dome were assumed to be -165 F and -290 F, respectively.

NRC-2 high-performance insulation was selected for the walls and covers of all containers with a layer of Kapton required to protect the NRC-2 from S-II boost heating in the aft containers. TG15000 was selected for base insulation of all containers.

The NRC-2 insulation is placed inside the container cover and on side and end walls, while the TG15000 insulation is attached to the outside of the honeycomb mounting base of each container. The thermal model for each container initially assumed the full 0.5-inch thickness of insulation to calculate temperatures using the appropriate equipment heat dissipations, orbital heat loads, and onboard thermal environments created by cryogenics or depletion of cryogenics. If th is calculation resulted in equipment temperatures beyond the specification limits, insulation thickness or surface coatings were changed to establish temperatures compatible with requirements. In this manner containers were equipped with insulation and coatings designed to maintain the required temperature throughout the mission without additional active cooling and possibly only with additional active heating. Several iterations with varying insulation thicknesses and varying coating types were required to obtain the desired result. The insulation thickness determined for each equipment container is shown in Tables 7.3.4.2-7 and 7.3.4.2-8.

h. Surface Coatings - Specific: The surface coatings used in the final calculations were tailored individually for each container to make the most of passive thermal control and minimize active thermal control requirements. For the covers of the aft containers Z-93 white inorganic thermal control coating is used to obtain a relatively low ratio of solar absorptivity and infrared emissivity of 0.16 while exposed to direct solar radiation. In general, the aft containers housing high heat-dissipating equipment require coatings with high emittances to dissipate the heat, and containers with low heat-dissipating equipment require coatings with low emittances to retain the heat within the containers. The surface coatings selected for use on internal surfaces of containers with high heat dissipation is Thermatrol, which will require a thin aluminum sheet inside the high-performance insulation for proper application to a rigid

Table 7.3.4.2-7. Design Requirements and Equipment Temperatures s

CONTAINER NO.	DIRECT MOUNTED	ISOLATOR MOUNTED	EQUIPMENT HEAT DISSIPATION IN WATTS	INSULATION THICKNESS IN INCHES	INSULATION ON ALL SURFACES	INSULATION ON BASE ONLY	CRES. ST. FITTINGS WITH FIBERGLAS WASHERS	SURFACE COATING: EXTERNAL ALUMINUM FOIL α = .2, ϵ = .1	SURFACE COATING: EXTERNAL THERMATROL α = .3, ϵ = .95	SURFACE COATING: COVER Z-93 α = .3, ϵ = .91	SURFACE COATING: INTERNAL AL. SILICONE PAINT α = .25, ϵ = .28	SURFACE COATING: INTERNAL THERMATROL α = .3, ϵ = .95	ATTITUDE & SIDE ** Y-POP NOSE FWD	ATTITUDE & SIDE ** -Z AXIS TO SUN	TEMPERATURE: TEMPERATURES WITH CRYOGENIC ENVIRONMENT	TEMPERATURE: TEMPERATURES WITH CRYOGENICS DEPLETED	ELECTRICAL HEATERS: POWER IN WATTS	ELECTRICAL HEATERS: DUTY CYCLE %	ELECTRICAL HEATERS: SWITCH ON +8 F, OFF +10 F
				INSULATION				SURFACE COATING					ATTITUDE & SIDE **		TEMPERATURE		ELECTRICAL HEATERS		
-225		X	366	.125		X			X			X	5		+108 F	*	0		
		X	186	.125		X			X			X	5		+ 76 F	+ 83 F	0		
		X	366	.125		X			X			X		7	+106 F	*	0		
		X	186	.125		X			X			X		7	+ 74 F	+ 80 F	0		
"D"		X	12	.5	X			X			X		1		+ 31 F	*	0		
		X	6	.5	X			X			X		1		+ 26 F	+ 92 F	0		
		X	12	.5	X			X			X			5	+ 15 F	*	0		
		X	6	.5	X			X			X			5	+ 9 F	+ 77 F	0		
"E"		X	11	.5	X			X			X		5		+ 17 F	*	0		
		X	11	.5	X			X			X			7	+ 14 F	*	0		
"F"		X	347	.125		X			X			X	4		+110 F	*	0		
		X	347	.125		X			X			X		6	+103 F	*	0		
221		X	108	.125	X				X			X	4		+ 68 F	*	0		
		X	108	.125	X				X			X		6	+ 57 F	*	0		
-206A31	X		8.5	.5	X		X		X	X		X	8		+ 8 F	+ 97 F	100	73	X
	X		8.5	.5	X		X		X	X		X		2	+ 20 F	+111 F	0		
207	X		16	.25	X		X		X			X	9		+ 64 F	+115 F	0		
	X		16	.25	X		X		X			X		3	+ 8 F	+105 F	150	58	X
209		X	162	.5	X				X	X		X	5		+ 53 F	*	0		
		X	162	.5	X				X	X		X		7	+ 51 F	*	0		
210		X	226	.125	X				X	X		X	2		+ 20 F	*	0		
		X	226	.125	X				X	X		X		1	+108 F	*	0		

Table 7.3.4.2-8. Design Requirements and Equipment Temperatures

CONTAINER NO.	DIRECT MOUNTED	ISOLATOR MOUNTED	EQUIPMENT HEAT DISSIPATION IN WATTS	INSULATION THICKNESS IN INCHES	INSULATION ON ALL SURFACES	INSULATION ON BASE ONLY	CRES ST. FITTINGS WITH FIBERGLAS WASHERS	ALUMINUM FOIL $\alpha = .2, \epsilon = .1$	THERMATROL $\alpha = .3, \epsilon = .95$	Z-93 $\alpha = .3, \epsilon = .91$	AL. SILICONE PAINT $\alpha = .25, \epsilon = .28$	THERMATROL $\alpha = .3, \epsilon = .95$	Y-POP NOSE FWD	-Z AXIS TO SUN	TEMPERATURES WITH CRYOGENIC ENVIRONMENT	TEMPERATURES WITH CRYOGENICS DEPLETED	POWER IN WATTS	DUTY CYCLE %	SWITCH ON $+8^{\circ}F$, OFF $-10^{\circ}F$
	INSULATION							EXTERNAL COVER INTERNAL SURFACE COATING					ATTITUDE & SIDE**		TEMPERATURE		ELECTRICAL HEATERS		
214	X		354	.125	X		X		X	X		X	2		$+59^{\circ}F$	*	0		
	X		354	.125	X		X		X	X		X		1	$+123^{\circ}F$	*	0		
A		X	172	.5	X				X	X		X	5		$+66^{\circ}F$	$+96^{\circ}F$	0		
		X	172	.5	X				X	X		X		7	$+61^{\circ}F$	$+94^{\circ}F$	0		
B	X		0	.5	X		X	X		X		X	4		$+8^{\circ}F$	$+39^{\circ}F$	150	30	X
	X		0	.5	X		X	X		X		X		6	$+8^{\circ}F$	$+15^{\circ}F$	150	65	X
C	X		0	.5	X		X	X		X		X	6		$+8^{\circ}F$	*	150	80	X
	X		0	.5	X		X	X		X		X		8	$+10^{\circ}F$	*	0		

*DENOTES THAT ALL OR PART OF EQUIPMENT IN THIS CONTAINER IS INOPERATIVE AFTER APS BURN FOR SPACE BASE OF S-II BOOST FOR SPACE STATION

**REFER TO FIGURES 7.3.4.1-17 AND 7.3.4.1-18 FOR DEFINITION OF SIDES

surface. Surface coatings required for external and internal surfaces of the aft containers are shown in Tables 7.3.4.2-7 and 7.3.4.2-8.

The forward containers having low heat-dissipating equipment were designed with low emissivity surface coatings. On the outside of these forward containers aluminum foil is used and inside a low emissivity coating is also applied over aluminum sheet. Fuller aluminum silicone paint was selected for this application. This combination resulted in the optimum passive thermal control with minimum active thermal control heating required. For foreard containers with high equipment heat dissipations, Thermatrol white paint with high infrared emissivity of 0.95 was selected for both external and internal surfaces. Surface coatings required for both external and internal surfaces of the forward containers are shown in Table 7.3.4.2-7.

i. Internal Heaters: The internal heaters used for active thermal control are applied to the inside of the cover of the containers. Heat is radiated to the equipment whenever the temperature of this equipment reaches + 8 F, and power to the heater is removed when the equipment temperature increases beyond + 10 F. The heater consists of redundant (for reliability) resistance wire elements embedded in a silicone rubber blanket.

The heaters proposed are of the same construction as the heaters currently used on the command and service modules (CSM) for Skylab. Installation of the heaters will be by bonding them to the substrate by means of an NR-qualifed adhesive, the same as used on CSM for Skylab.

Heaters of this identical design and construction have been successfully used on the lunar module reaction control system, on the G&N heating equipment for Apollo CSM, and now the heaters for the RCS and Service Propulsion System of the CSM for Skylab.

Each container was individually designed to achieve optimum passive thermal contaol using surface coatings and high performance insulation to minimize active heater requirements. The thermal analysis established that none of the forward containers would require electrical heaters. Aft containers 206A31, "B" and "C" will require electrical heaters when orbiting in the design Y-POP solar orientation. For a -Z to the sun orientation aft containers 207 and "B" would require heaters. All heaters are designed with thermal switches which activate the heaters at 8 F and turn the heaters off at 10 F. Typical power duty cycles for the 207 container during one orbit of operation are shown in Figure 7.3.4.2-16. Also shown in Figure 7.3.4.2-16 are the predicted temperature variations of the equipment mounting base corresponding to the cycling of the electrical heaters. The heater power demands and their duty cycles are shown in Table 7.3.4.2-9. For the Y-POP solar orientation, the maximum total power demand of the heaters when all three are operating simultaneously is 400 watts. The average total required based on the duty cycle demand is 238 watts between end of boost and APS burn for Space Base. For Space Station and for the period between APS burn and 24 hours for Space Base, the average total is 118 watts because container "C" is inoperative.

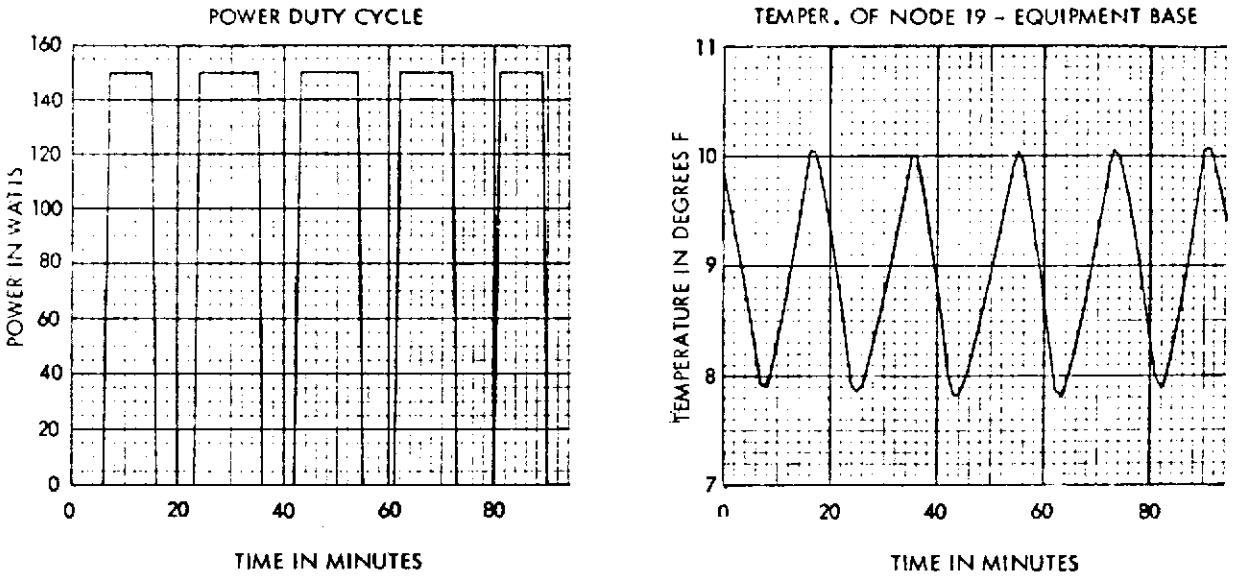

Figure 7.3.4.2-16. One-Orbit Power Duty Cycle, Container 207

j. Design Requirements Summary: Tables 7.3.4.2-7 and 7.3.4.2-8 contain a summary of the analytical calculations for all final configuration of the avionics containers. The type of mounting, equipment heat dissipation, insulation thickness, coating properties, attitude, and location of each container are given in this table. The calculated temperatures for the final container configurations are based on appropriate equipment heat dissipation, orbital thermal environments, and onboard cryogenic or non-cryogenic environments.

Tables 7.3.4.2-7 and 7.3.4.2-8 also show heater operation and duty cycles where calculations established the need for additional heating to maintain equipment within specified temperature limits.

The thermal control design requirements presented in Tables 7.3.4.2-7 and 7.3.4.2-8 were determined for each container individually taking into consideration the equipment heat dissipation, orbital thermal environment, and onboard environment for each specific container. Changes to design criteria such as equipment and heat dissipations, vehicle attitude control, and container stage location would require a reanalysis of the affected containers to verify thermal control requirements or establish new requirements.

7.3.4.3 Membrane Seal

The important thermal performance characteristics of this design are the temperature distribution of the forward skirt structure under the insulation and the resulting heat leak to LH_2. S-II point design analysis is presented in a study which determined these characteristics for the current design configuration and three reduced insulation configurations.

Table 7.3.4.2-9. Power Demand for Heaters

FWD CONTAINERS	Y-POP	-Z towards sun
221	None	None
225	None	None
D(225)	None	None
E(225)	None	None
F(225)	None	None
Aft Containers	Y-POP	-Z towards sun
206A31	100 Watts	None
209	None	None
207	None	150 Watts
210	None	None
214	None	None
A(210)	None	None
B(206A31)	150	150
C(206A31)	150	None
Max Total if all heaters go on at same time	400 Watts	300 Watts
Average (Duty Cycle)		
206A31	73 Watts (73%)	
207		86 Watts (58%)
B (206A31)	45 Watts (30%)	96 Watts (65%)
C(206A31)	120 Watts (80%)	
Average total (depending on Duty Cycle)	238 Watts	181 Watts

a. Statement of Problem: A study was made to determine thermal and structural effects on the S-II stage resulting from a reduction in insulation on the forward skirt. This subsystem presents the results of a thermal analysis to determine forward skirt temperature profiles, local heat leak into LH_2 and ground hold heating rate into LH_2. In this study, the present insulation configuration, three configurations with reduced insulation, and two purge gas conditions (helium and nitrogen) were considered. The membrane seal was the means developed to allow the use of helium as the gas in the J-joint area.

The forward skirt is the cyclindrical section from Station 818 to Station 955. It serves as the load-carrying structure between the aft interstage of the S-IVB and the LH_2 tank of the S-II stage. The forward skirt from Station 818 to the tangent point of the forward bulkhead at Station 823 is in close contact with the LH_2 tank. In the design for S-II-8 and subs, the skirt is spray-foam insulated between and inside the hat section stringers from Station 818 to Station 848. In addition, a 1/2-inch-thick spray foam blanket covers both the stringer caps and the insulation between stringers (Figure 7.3.4.3-1).

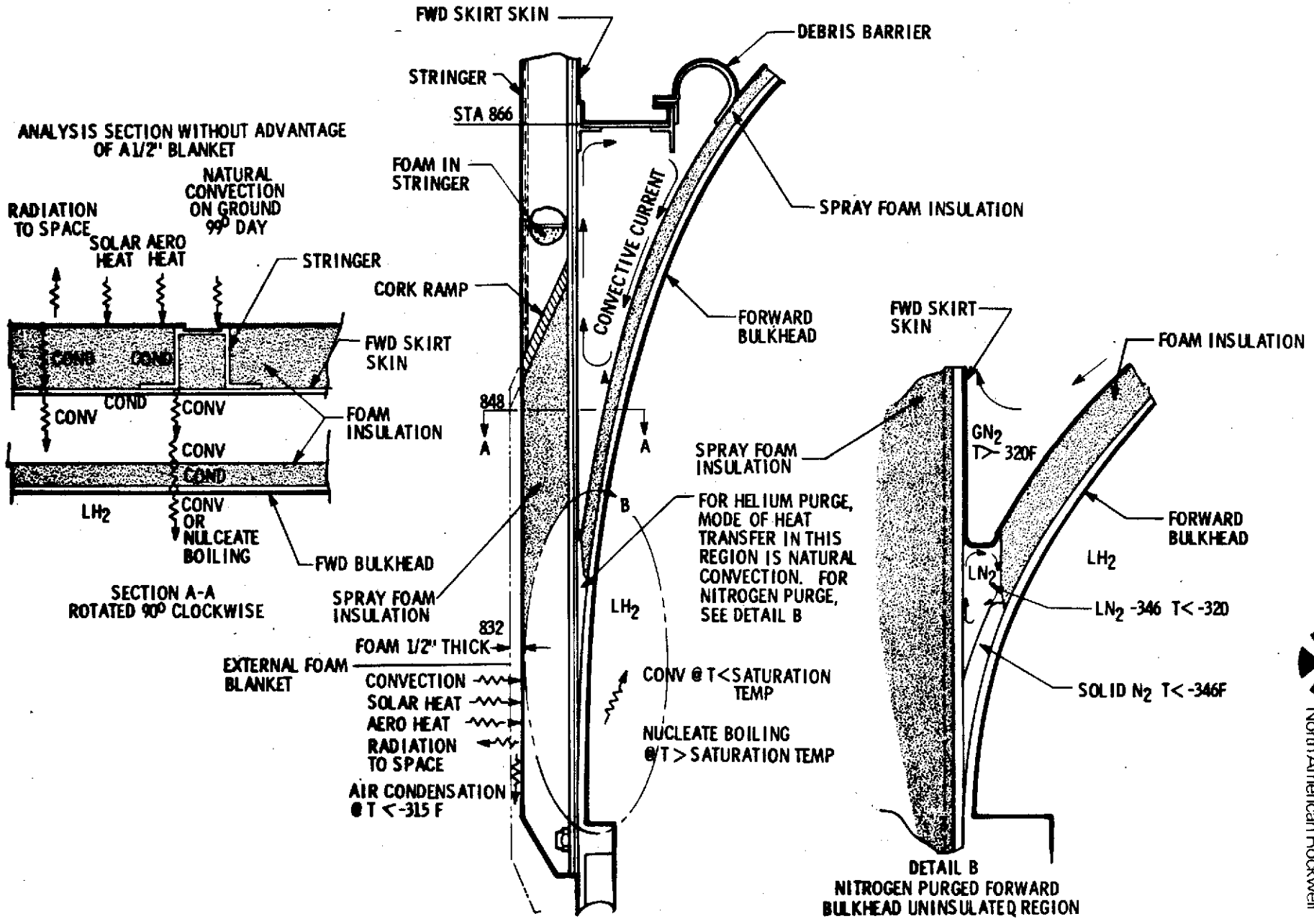

Figure 7.3.4.3-1. Modes of Heat Transfer

b. Methodology and Analysis: The following insulation configurations were analyzed to determine if some of the insulation could be removed from the vehicle:

1. Spray foam insulation up to Station 848 with external blanket removed.

2. Spray foam insulation up to Station 832 with external blanket removed.

3. No insulation at all on the forward skirt.

Each reduced insulation configurations was analyzed for both helium and nitrogen purge conditions. The present configuration for S-II-8 and subs has a helium purge in the enclosed region between the forward skirt and forward bulkhead below Station 866 (FBU helium purge system). If the helium purge were deleted, it would permit gaseous nitrogen from the S-II/S-IVB interstage to be exposed to this region. At LH_2 temperatures, nitrogen gas will liquefy and solidify in the FBU region (Figure 7.3.4.3-1). The forward bulkhead between Stations 823 and 832 is uninsulated (FBU).

Basic environment, structural configuration, and analytical procedures used in this study are the same with the following exceptions. MSFC aerodynamic design heating rates are used in lieu of CEI design heating rates. The evaluation of nitrogen boiling, condensation, and convection phenomena near the FBU and condensation of air on the stringer caps (Figure 7.3.1.3-1) required the development of a new methodology. A detailed discussion of the assumptions, analytical model, and computer techniques used is beyond the scope of this report.

c. Assumptions:

1. Natural Environment:

(a) Ambient temperature is 99 F during ground hold operation.

(b) External heat transfer conductance is $1.\frac{Btu}{hr.°f\text{-}ft.^2}$

(c) Solar heating.

(d) Radiation to environment.

2. Induced environment, MSFC aerodynamic design heating rates.

3. Insulation, polyurethane spray foam:

(a) Emissivity is 0.8

(b) Solar absorptivity is 0.3.

(c) Specific heat is 0.3 Btu/lb °F at room temperature and varies with temperature.

(d) Density is 2.0 lb/ft^3, density of the seal coat was considered negligible.

4. Propellant Loading: The propellant loading for S-II-4 and subs is 970,000 pounds. The corresponding LH_2 level for the pressurized ground hold condition is station 900.00

5. Programmed Mixture Ratio: The effect of programmed mixture ratio was incorporated. The S-IC boost time is 155 seconds. The boost time for S-II is composed of 280 seconds with 5.5 oxidizer/fuel ratio and 43 seconds with 4.3 oxidizer fuel ratio.

6. Internal convection processes occurring in the enclosed region between the forward skirt and forward bulkhead (Figure 7.3.4.3-1).

The innovative features required to evaluate conductances for the nitrogen convection process was to assume an equivalent natural convection conductance.

d. Results and Conclusions: The predicted hot day S-II forward skirt temperature profiles for ground hold, max $q\alpha$, and end of S-I boost were determined. Stringer temperatures, skin temperatures between stringers, and skin temperatures under stringers between S-II Stations 818 and 890 were determined for each specified time and insulation-purge gas case. A typical ground hold skin temperature profile shows that the skin temperature is below -400 F between Stations 818 and 827, that it rises rapidly above Station 827 to approximately 50 F at Station 860, and that it rises slowly to approximately 80 F above the Station 866 closeout. A typical stringer cap temperature is approximately -320 F between Stations 818 and 830. This extremely cold temperature will allow air from the external environment to condense. The skin temperature profiles do not change appreciably between ground hold and max $q\alpha$: however, the stringer cap temperature is increased to approximately 200 F between Stations 818 and 830. At the end of S-IC boost, the skin temperature above Station 855 is increased to approximately 160 F. The depression in the temperature at Station 866 is due to the additional mass of the closeout ring at that location. Predicted hot and cold day S-II forward skirt stringer cap temperature profiles in the region of the systems tunnel also were calculated. The cap temperatures for Stringers 46 through 50 at max $q\alpha$ and end of S-I boost were determined.

The predicted local heat leak into LH_2 through the forward skirt and bulkheat during a hot day ground hold, S-IC boost, S-II boost, and predicted hot day ground hold heating rates into LH_2 are presented in Table 7.3.4.3-1. Seven specified insulation purge gas configurations, including the present S-II-8 and subs design configuration (Case No. 7) are included. The present S-II-8 and subs design configuration accumulated heat leak into LH_2 due to all sources is predicted to be 88,250 Btu for a typical S-II mission from a previous study on the spray foam (Paragraph 7.3.1.4). The predicted pre-pressurization LH_2 boiloff corresponding to this heat leak is 2.1 percent per hour and has been verified by LH_2 boiloff tests. The accumulated local bulkhead leak into LH_2 of approximately 5000 Btu due to the forward skirt and bulkhead for the present S-II-8 and subs design configuration. When the insulation blanket is removed, the hat section stringers are exposed to the environment and obviously, a good thermal short for increased heat leak into LH_2 is provided. The allowable

Table 7.3.4.3-1. Heat Leak to Onboard LH_2

CASE NUMBER	INSULATION CONFIGURATION	HELIUM PURGE	$\dot{q}$ TO LH_2 DURING GROUND HOLD BEFORE TANK PRESSURIZATION	TOTAL Q TO LH_2 FROM T-90 SEC TO END OF S-II BOOST (T + 625 SEC)
1	SPRAY-FOAM INSULATION TO STA 848 BETWEEN STRINGERS ONLY. NO EXTERNAL BLANKET	NO	56,000 BTU/HR	36,000 BTU
2	SPRAY-FOAM INSULATION TO STA 832 BETWEEN STRINGERS ONLY. NO EXTERNAL BLANKET	NO	61,000 BTU/HR	49,000 BTU
3	COMPLETE ELIMINATION OF INSULATION	NO	656,150 BTU/HR	GREATER THAN 100,000 BTU
4	SPRAY-FOAM INSULATION TO STA 848 BETWEEN STRINGERS ONLY. NO EXTERNAL BLANKET	YES	68,000 BTU/HR	37,000 BTU
5	SPRAY-FOAM INSULATION TO STA 832 BETWEEN STRINGERS ONLY. NO EXTERNAL BLANKET	YES	76,900 BTU/HR	52,000 BTU
6	COMPLETE ELIMINATION OF INSULATION	YES	575,000 BTU/HR	GREATER THAN 100,000 BTU
7	SPRAY-FOAM INSULATION TO STA 848 WITH EXTERNAL BLANKET	YES	35,500 BTU/HR	5,000 BTU

increase of heat leak into LH_2 is determined by the LH_2 residual and by the temperature rise (ΔT) of the engine inlet fluid at S-II engine cutoff. The maximum allowable ΔT based upon NPSH requirements is 1.8 R; the design allowable ΔT is 1.6 R. For a minimum LH_2 residual of 1800 pounds, the maximum allowable local heat leak which can be absorbed by the LH_2 mass above Station 819 is 53,000 Btu and the design allowable heat leak is 40,500 Btu. The predicted local heat leak to the LH_2 mass above Station 819 for reduced insulation Case 1 is approximately 36,000 Btu and for Case 4 is approximately 37,000 Btu. Since these local heat leak accumulations are less than the design allowable, removal of the insulation blanket is acceptable from a thermodynamic view point. Removal of insulation above Station 832 results in the local heat leak exceeding the design value (40,500 Btu) for both the Case 2 nitrogen purge (49,000 Btu) and the Case 5 helium purge (52,000 Btu) condition, thus making removal of insulation above Station 832 unacceptable. Similarly, complete removal of the forward skirt insulation is unacceptable.

Removal of the external spray foam blanket exposes the cold stringer caps (approximately -320 F) to the ambient environment. At this temperature, air will condense on the stringer caps. A cursory investigation of the effects of liquid air on the insulation and other structure indicates that no problems or hazards are to be expected due to air liquefaction. This conclusion is based upon the following rationale. Liquefaction will cause liquid air to flow onto and over the insulation surfaces adjacent to the forward skirt stringers and to drip off the stringers onto objects below. Liquid air running over the adjacent insulation reduces the insulation surface temperature, the temperature gradient through the insulation, and the resulting thermal stress. From previous lab experience, liquid air is completely vaporized after falling 15 to 20 feet. The vaporized liquid is in an open area and, therefore, cannot buildup concentrations of oxygen. Also, no source of hydrogen is available in the area which the liquid air can contact prior to vaporization. For these reasons, there is no hazard associated with liquid air dripping off the stringers. It should be noted also that air condensation on the stringer caps is a major contributor to the high heat leak discussed in the previous paragraph.

7.4 SPECIAL THERMAL CALCULATIONS

There have been numerous special thermal calculations that have been prepared in conjunction with the analysis for S-II and for S-II applications. Some of these calculations and methods are included in this section so that they may be used for quick reference and preliminary design purposes.

7.4.1 Analytic Model for the Determination of the Thermal Conductivity of Closed Cell Foam Insulation

The closed-cell spray-foam insulation incorporates Freon 11 as the agent in the foaming action. The size of the cells varies with the temperature at foam formation. In this insulation, the important contributions to heat transfer are (1) conduction through the walls of the cells, (2) conduction across the gas within the cells, and (3) radiation from cell to cell within the foam composite and across a number of cells by transmission. Figure 7.4.1-1 is a

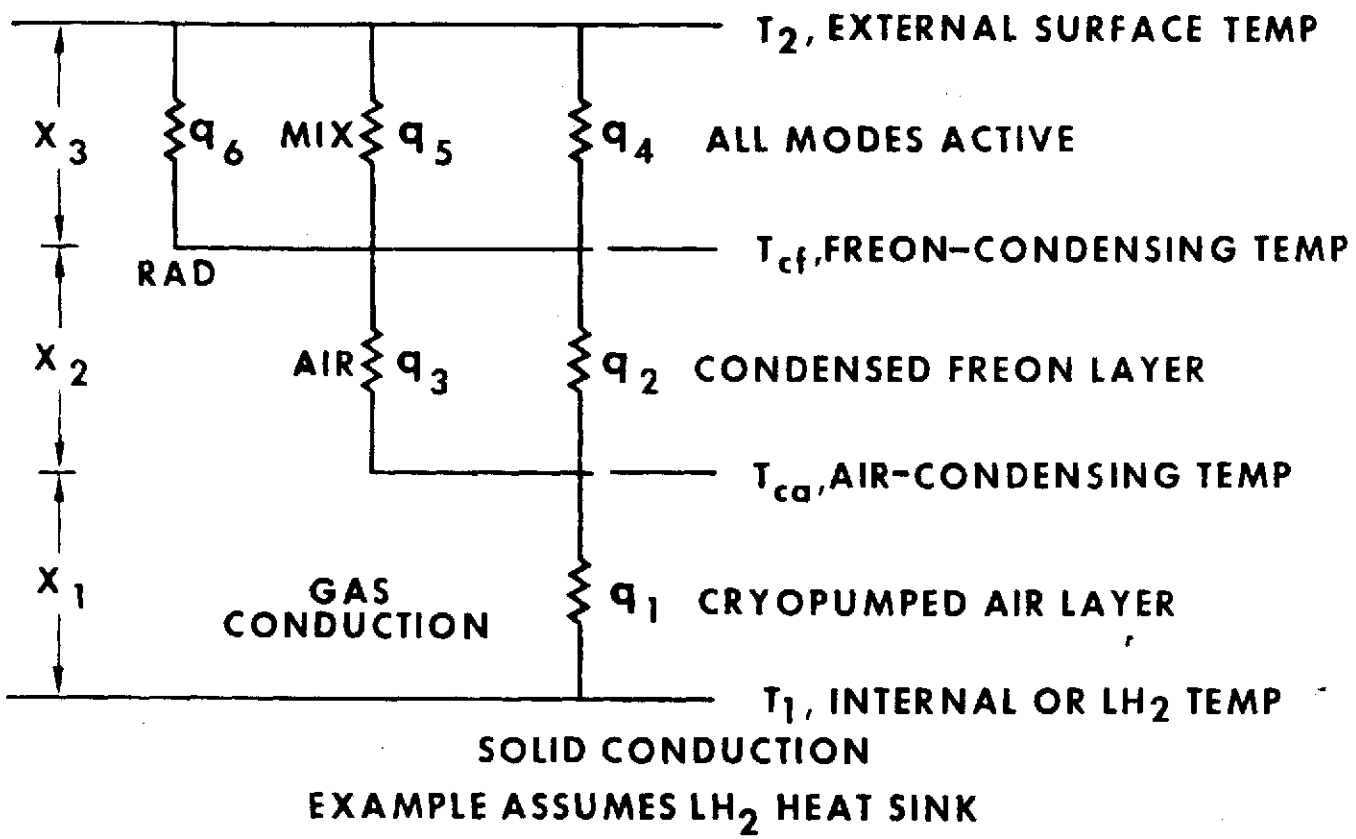

Figure 7.4.1-1. Heat Conduction Model for Foam Material (Steady State)

simplified description of the heat-conduction model. Initially, the gas within the foam is Freon. After the foam has been reacted and cured, however, the diffusion of air into the foam immediately begins to form a mixture. If the foam is exposed to helium then there will be a helium mixture in the cells. Figure 7.4.1-1 indicates that a cryopumped layer exists adjacent to the liquid-hydrogen cold wall. This is a high-vacuum layer in which gas conduction is not operative, and the primary mode of heat transport is by solid conduction in the cell walls. The model assumes that there is a discrete temperature at which air condenses (T_{ca}) and a discrete higher temperature at which Freon condenses (T_{cf}). Actually, neither of these is a discrete point but a range encompassing 50 to 100 F. This will be discussed in more detail later. The model assumes that between the air-condensing temperature and the Freon-condensing temperature, air is the active agent for gas conduction. Above the Freon-condensing temperature, the mole fraction of Freon will tend to reduce the gas conductivity below that of air. At temperatures over 200 F, radiation is a significant contributor to heat flow.

In this discussion, the first step will be to develop a solid-conduction contribution; the second will be to develop a diffusion model and apply it to the hypothetical air- and Freon-condensing temperatures. The third step will be to establish the Freon mole fraction and the heat conduction for mixtures of Freon and air. The fourth step will be to estimate the solid-radiation contribution. Finally, some test results will be compared with the results of the combined analytical model.

7.4.1.1 Solid Conduction

The first mode of heat transport is that of solid conduction within the cell walls. The polyurethane resin is an extremely disordered material. Its polymeric chains are not crystalline, which would cause increases in heat conduction at lower temperatures by means of lattice waves (phonons). As a result, the thermal conductivity will vary with temperature in an almost linear manner as with other plastic materials (Reference 37). In Reference 38, the thermal conductivity of a pure polyurethane resin, taken at approximately room temperature, is 0.917 Btu-in./hr.-ft.^{2}-°F. The density of the pure polyurethane resin is given in the same reference as 66 pounds per ft.^{3}. When the polyurethane is foamed to a low density, the solid contributions will be reduced, not only in solid cross-section due to the expansion, but also by the influence of a steric factor. The cells are dodecahedrons; as such, they elongate the distance and distort the cross-section through which heat must flow. This can be visualized more easily if the cells are presumed to be approximately cubic. In such a configuration, only two thirds of the cell wall material (four of the six sides) is effective in conducting heat in a given direction.

The solid-conductivity contribution to the effective conductivity, including all of the above-mentioned effects, can be stated:

$$K_{solid} = \frac{s\phi \int_{T_1}^{T_2} K_{res}\, dt}{T_2 - T_1} \qquad (7.4\text{-}1)$$

In this equation, the integration takes place from the inside to the outside temperature. The reason is indicated in Figure 7.4.1-1, where summation of the contribution across each of the three defined temperature regimes leads to the total contribution. The steric factor can lie between 2/3 and 1, but is nearer to 2/3 for the low-density closed-cell foam. The solidity ratio, ϕ. is the ratio of the final foam density to the initial resin density.

Figure 7.4.1.1-1 shows how resin conductivity varies as a function of foam density at constant mean temperature. The effect of variations in the steric factor is indicated. The solid-conduction factor is not a major contributor to heat conduntion in the foam insulation, except in the very thin cryopumped layer near the cold wall.

7.4.1.2 Diffusion Model

The next important contributor to heat transfer is gas conduction. The evaluation, however, presumes a knowledge of the mole fraction of each species, and the temperatures at which, thermodynamically, they condense.* Freon is considered

*The concept of a gas condensing implies that there are not sufficient molecules of one species to interact with other species, or that a vacuum is produced and gas conduction is negligible due to the free-molecule regime.

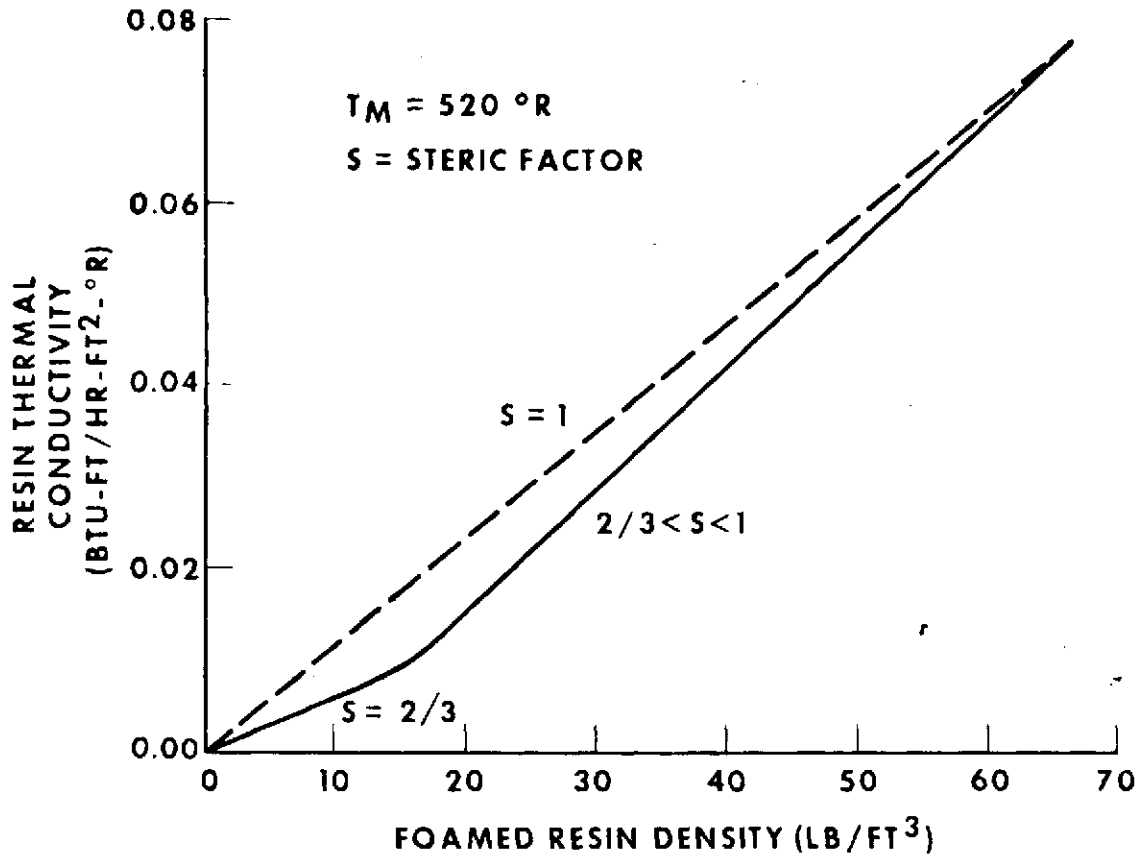

Figure 7.4.1.1-1. Resin Conductivity Versus Foam Density

the initial gas in the cells and retained at approximately 1-atmosphere pressure. The diffusion of air into the foam cells begins almost immediately after the foaming operation.

A mathematical model is used that describes the diffusion of gases within polymeric foams (Reference 39). The model chosen employs a three-dimensional array of cubes with walls uniform in thickness and permeable to gases. The solution obtained for the partial pressure of a gas as a function of distance and time was developed in terms of standard Fourier series coefficients of the well-known boundary value problem (Reference 40 includes a wide range of such solutions). In Reference 39, vacuum outgassing experiments were performed in order to provide empirical values of the average diffusion constant, D, for comparison with the analytically derived values from permeability measurements on polymeric films.

The earliest mathematical formulation of gas flow within a foam was based on a one-dimensional diffusion from an array of N layers of cubes. The solution permitted the N-linear homogeneous equations to be solved as functions of time and distance. However, if the number of cells traversed is greater than 20, the values for the Fourier coefficients can be easily obtained for the limiting case as N becomes infinite. For cells ranging in size from 1 to 10 mils, the number of layers would be on the order of a few hundred for a 1-inch-thick insulation. In the following equations, therefore, the gas transport is

considered as a diffusion process in a homogeneous medium characterized by an average diffusion constant. The Equation below is a solution to Fick's law for gas diffusion in a homogenous medium and represents the admission of air to the foam:*

$$P_{air} = 1 - \frac{4}{\pi}\sum_{n=0}^{\infty}\frac{(-1)^n}{2n+1}\cos\frac{(2n+1)\pi x}{2\ell}\exp\left[\frac{-(2n-1)^2\pi^2 D_1 t}{4\ell^2}\right] \quad (7.4\text{-}2)$$

Equation 7.4-3 is the same as 7.4-2 except it is in a form which converges more rapidly for very small values of the partial pressure:

$$P_{air} = \sum_{n=0}^{\infty}(-1)^n \operatorname{erfc}\frac{(2n+1)\ell - x}{2\sqrt{D_1 t}} + \sum_{n=0}^{\infty}(-1)^n \operatorname{erfc}\frac{(2n+1)\ell + x}{2\sqrt{D_1 t}} \quad (7.4\text{-}3)$$

The diffusion constants used for air are not well established in the test data. Data from Reference 39 indicate that the diffusion constant for a 2-lb.-per-ft.^{3} foam lies between 3.76×10^{-6} and 6.23×10^{-7} cm^2/sec. The lower results are in better agreement with both test results and predictions.

In most cryogenic thermal conductivity experiments, at least 20 to 30 days have elapsed after the foaming operation. This period includes 10 days for a complete cure, 5 days for trimming and closeout operations, and about 5 days for complete drying of the water-resistant coating. In a period of 20 days, with a diffusion constant of 5×10^{-7} cm.^{2}/sec. the partial pressure of air existing throughout the insulation is sufficient for it to be a controlling factor in the heat transport.

Equation 7.4-4 is similar to the previous two but represents the diffusion of Freon out of the foam insulation:

$$P_F = \frac{4}{\pi}\sum_{n=0}^{\infty}\frac{(-1)^n}{2n+1}\cos\frac{(2n+1)\pi x}{2\ell}\exp\left[-\frac{(2n+1)^2\pi^2 D_2 t}{4\ell^2}\right] \quad (7.4\text{-}4)$$

The Freon diffusion constant based on a rough measurement is on the order of 2×10^{-8} cm.^{2}/sec. Equation 7.4-5 sh ows how the mole fraction of Freon is determined in the insulation:

$$M_F = \frac{P_F(x,t)}{P_{air}(x,t) + P_F(x,t)} \quad (7.4\text{-}5)$$

*Reference 40 is the source for the solutions represented by Equations 7.4-2, 7.4-3, and 7.4-4, although the form differs somewhat from that of the solution in Reference 39.

The results of a preliminary calculation using the previously noted diffusion constants for air and Freon are shown in Figure 7.4.1.2-1. The insulation thickness is 3/4 inch, and the initial Freon concentration is assumed to be 1 atmosphere at 70 F. When a long period (e.g., two years) is involved, the Freon concentration is greatly diminished. This is degradation of the thermal performance, since the thermal conductivity of air is about two to three times larger than the thermal conductivity of Freon. Another factor that cannot be included here is the strong dependence of the diffusion constant upon the temperature at which the foam is stored. Data on the permeability of polymeric films have indicated (Reference 41) that the diffusion constant can triple between storage temperatures of 0 and 120 F. Below 0 F, after the Freon condenses out, air remains in the cells at partial pressures near the values for room temperature. A calculation of the mean free path of air in the foam indicates that for cell sizes between 1 and 10 mils, the partial pressure of air needs only to exceed approximately 1 torr for a continuum to exist. The vapor pressure of oxygen and nitrogen is approximately 1 torr at a temperature slightly 90 R (-370 F). Between liquid-hydrogen temperature and the air-condensing temperature, it is assumed that a cryopumped vacuum exists within the cells and that gas conduction does not contribute to heat transfer.

At the Freon triple-point pressure of 1 torr, a temperature of -160 F has been achieved. The Freon undergoes sharp mole fraction changes in the region above the triple-point temperature; these are not diffusion-related but thermodynamically induced by the Freon's saturation curve. For example, when the temperature within the insulation is -40 F, the pressure of Freon

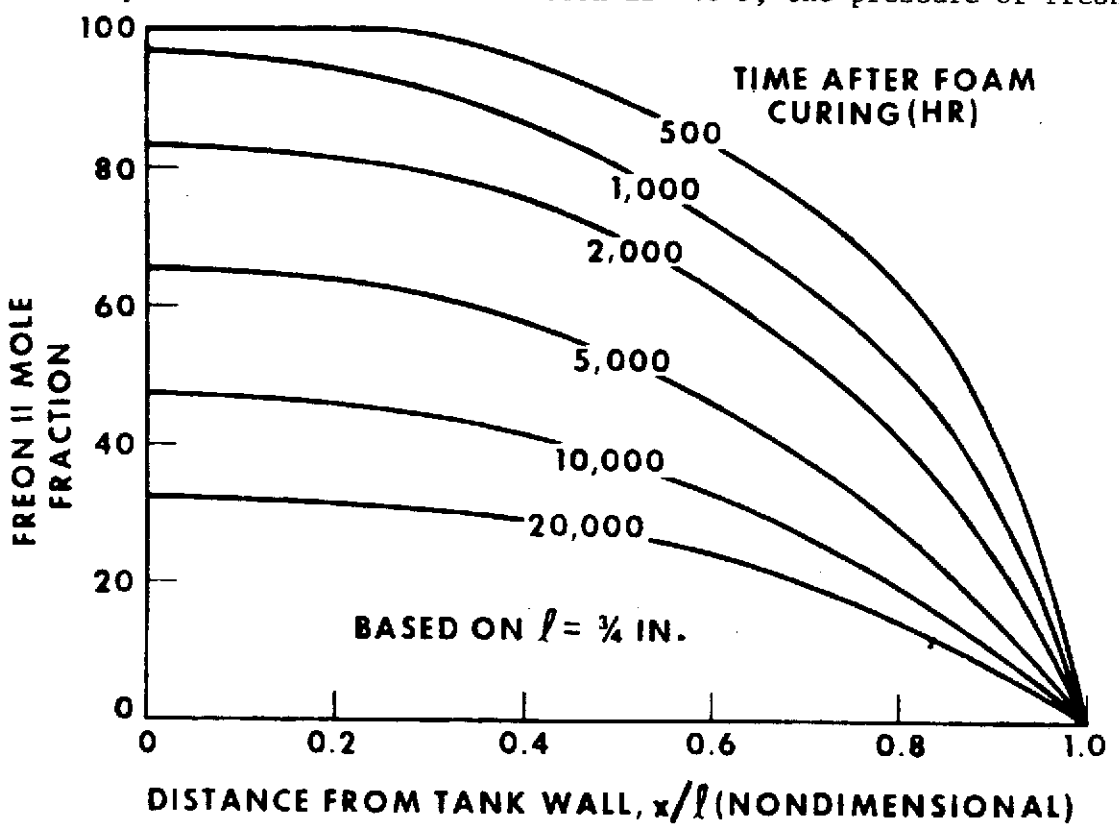

Figure 7.4.1.2-1. Freon Mole Fraction as a Function of Time and Distance

within the cells will have dropped from 1 atmosphere to 30 torr. Even at 0 F, the pressure would be only 130 torr. If air is assumed to be in the range of 400 to 760 torr, the mole fraction of air is clearly dominant in conduction (see next section). In order to simplify the analysis, the assumption is made that the Freon is essentially frozen out of the heat-transport property at a condensing temperature of 0 F.

7.4.1.3 Gas Conduction

The important contribution of gas conduction is determined by dividing the model into two separate temperature ranges (Figure 7.4.1-1). In the low-temperature range, between the air-condensing temperature (90 R) and the Freon-condensing temperature (450 R), the only significant influence is the thermal conductivity of air. In the high-temperature range, above the Freon-condensing temperature, the thermal conductivity of the gas is complicated by the presence of both air and Freon and by changes in concentration as functions of storage time and distance. In this study, the gases are assumed to be limited to mixtures of Freon 11 and air. Mixtures of water vapor and trace elements in air have been studied but are not significant to the heat transport. Reference 42 describes a computer program for obtaining the transport properties of polar and polyatomic gas mixture. The transport property theory employed is based on the exact Chapman-Enskog theory for dilute gases (dilute implies low pressures).

The thermal conductivity data for mixtures of Freon 11 and air are presented in Figure 7.4.1.3-1 for the temperature range 0 to 500 F. It can be seen from

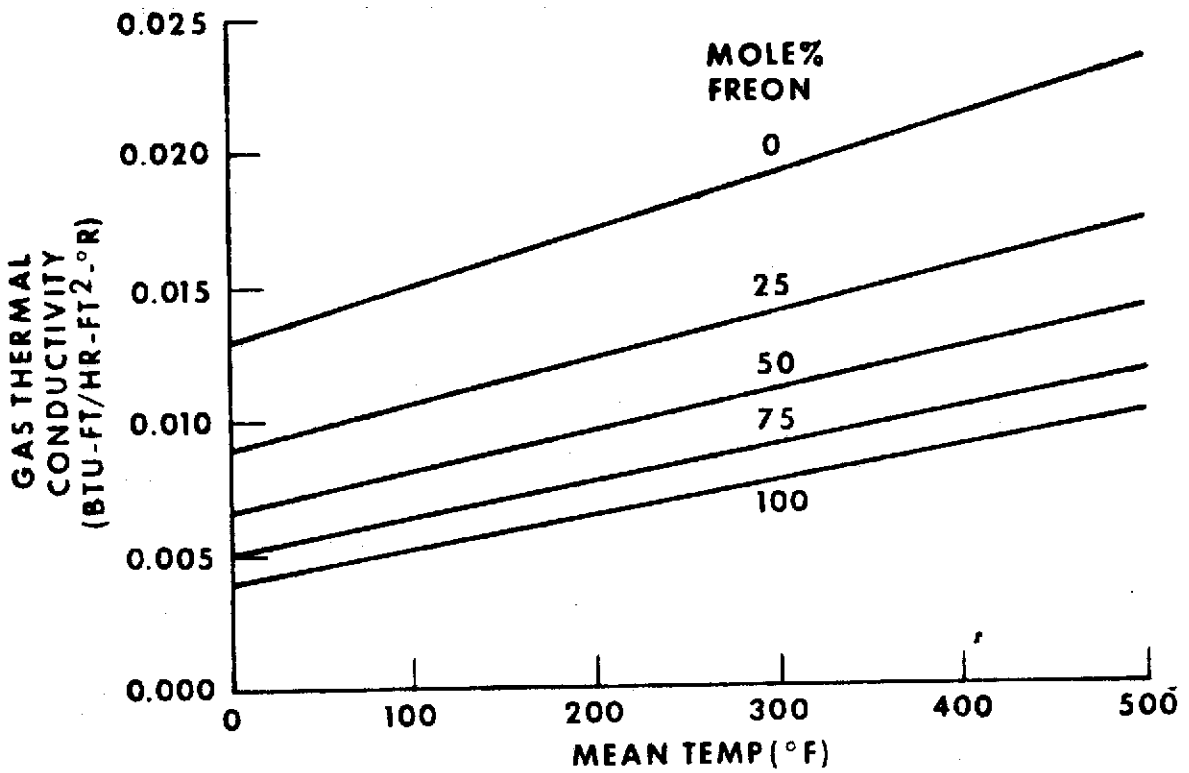

Figure 7.4.1.3-1. Gas Thermal Conductivity for Mixtures of Freon 11 and Air

the figure that Freon strongly influences the thermal conductivity of the mixture. The simple analytical model is described in Reference 41, which represents the gas-conduction contribution to the effective thermal conductivity of the insulation.

$$\bar{K}_{gas} = \frac{1 - \phi}{T_2 - T_1} \left[\int_{T_{da}}^{T_{cf}} K_{air} dt + \int_{T_{cf}}^{T_2} K_{mix} dt \right] \qquad (7.4\text{-}6)$$

This equation employs air as the prime component from -370 to approximately 0 F. Above this temperature, the mixture thermal conductivity depends on the diffusion shown in Figure 7.4.1.2-1 that establishes the mole fraction of Freon as a function of time and distance. If the insulation is exposed to normal atmospheric-temperature air for long periods, the thermal conductivity will approach the condition where air is the controlling factor in the gas-conduction expression throughout the insulation.

7.4.1.4 Radiation

The transfer of heat by radiation within solids is extremely complex and involves simulteneous transmission, absorption, and re-radiation. The radiation incident upon solids can be absorbed completely or partially, even selectively, depending on the characteristics of the solid material. Reference 43 is an excellent review of this subject and has been used in this study to postulate one approach to the determination of the effect of radiation on the effective conductivity of the foam insulation. Generally speaking, the foam is optically thick; that is, direct transmission of radiation through a faily thick specimen cannot be measured. However, Reference 43 presents a method for establishing the radiative conductivity of solids that permits use of measured values of specific absorptivity. In an experiment performed with a spectrophotometer, a range of monochromatic sources was used, with the foam placed between the energy source and the detector (Reference 44). The foam was selectively sliced to reduce thickness until, at approximately 0.025 inch, the direct transmission was measured as about 10 percent. This result is rather difficult to interpret because scattering processes are at work, together with absorption, to reduce the intensity of the collimated beam. Equation 7.4.1.7 describes the radiation contribution to the effective conductivity of the foam material as based upon the method discussed in Reference 43.

$$\bar{K}_{rad} = \frac{\int_{T_{cf}}^{T_2} 4\sigma T^3 dt}{T_2 - T_1)\lambda} = \frac{N\sigma T_2^{\,3}}{\lambda} \qquad (7.4.1\text{-}7)$$

N in Equation 7.4.1-7 is an integrating constant which must lie between a minimum value of 2 and a maximum of 8. The value of 2 applies only at the low end of the temperature scale; at the high end of the temperature scale, the value 8 is more generally correct.

In 1913, W. Nusselt studied the apparent thermal conductivity of gas-filled powders and fibrous materials. His equation employs a series-parallel combination of solid conduction across the fibers with gas conduction and radiation between the fibers (Reference 45). Nusselt's result for the radiation-conductivity contribution reduces to an equation very similar to 7.4.1-7; however, the mean diameter of the powder or fibers must be replaced by the diameter of the cells in the foam, and his void fraction must be replaced by the solidity ratio of the foam. Equation 7.4.1-8 is the expression developed by Nusselt and adapted for radiation-conductivity contribution in foam:

$$\bar{K}_{rad} = \frac{4\sigma Tm^3 \delta}{\phi} \qquad (7.4.1\text{-}8)$$

The estimated radiation contribution to the foam thermal conductivity is shown in Figure 7.4.1.4-1. It can be seen in this figure that the contribution of radiation becomes significant above 200 F. At temperature below 0 F, the simple model ignores the contribution of radiation to the effective thermal conductivity.

7.4.1.5 Summation of Heat-Conduction Contributions

The summation of the individual thermal conductivities will produce the effective thermal conductivity:

$$\bar{K}_{ef} = \bar{K}_{solid} + \bar{K}_{gas} + \bar{K}_{rad} \qquad (7.4.1\text{-}9)$$

The result provides a basis for a more refined conputation. The simple model can be evaluated with the assumption that the gas-conduction contribution is entirely derived from air, Freon, or some arbitrary mixture. In automatic computer programs, it is frequently necessary to insert a curve of thermal conductivity as a function of temperature only. For one of the earliest computations for boost heating on the Saturn V second stage, it was assumed that the full degradation of air had been achieved, and the air limiting curve was used as shown in Figure 7.4.1.5-1. The bottom curve in this figure represents the Freon limiting case where no diffusion of air has taken place.

A more exact solution will not be described for determining the thermal conductivity of the foam with varying Freon mole fraction. First, to simplify the computation up to the Freon-condensing temperature, it is possible to establish an effective conductivity as a function of temperature directly. The first step in the calculation is to assume a value of effective conductivity lying between the limits shown in Figure 7.4.1.5-1. It is then possible to make a direct calculation of the distance across the cryopumped layer and the condensed Freon layer:

$$\frac{x_1 + x_2}{\ell} = \frac{s\phi \int_{T_1}^{T_{cf}} K_{res}\,dt + (1 - \phi)\int_{T_{ca}}^{T_{cf}} K_{air}\,dt}{K_{ef}\,(T_2 - T_1)} \qquad (7.4.1\text{-}10)$$

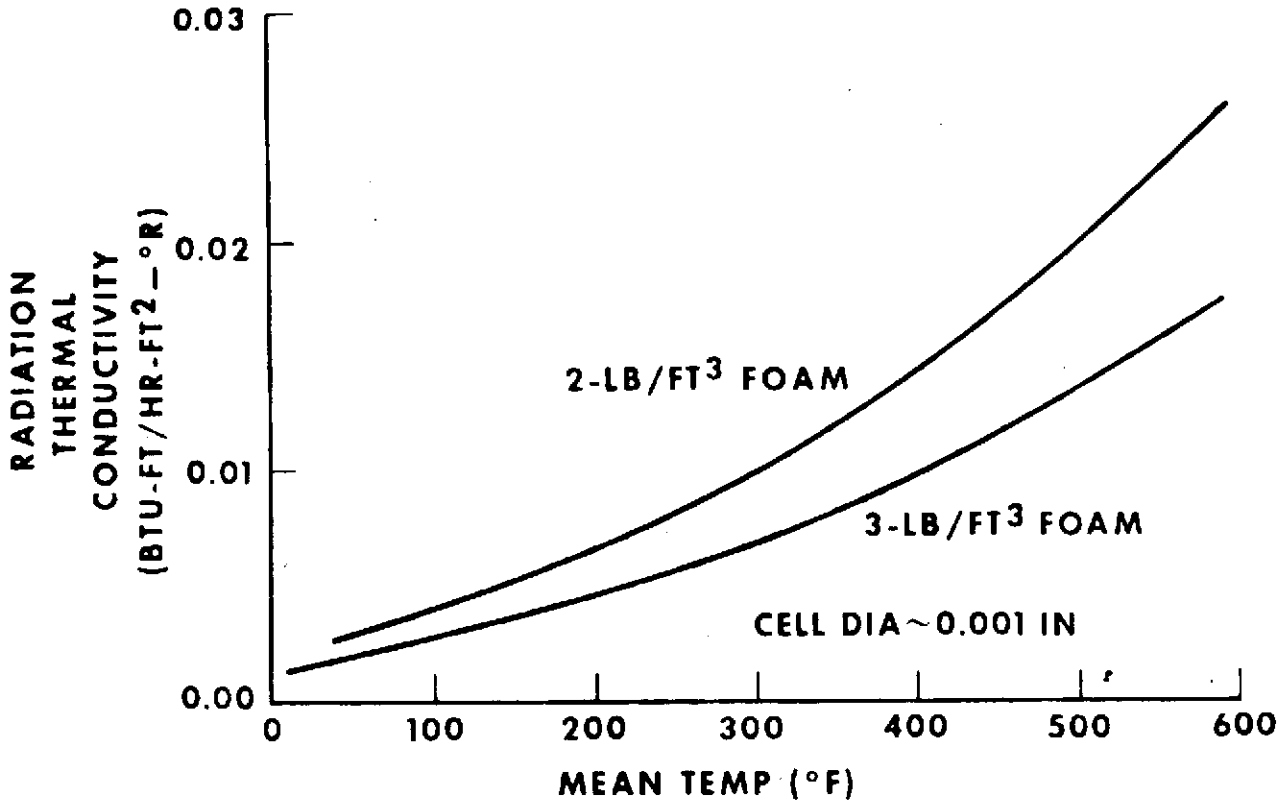

Figure 7.4.1.4-1. Radiation Conductivity Versus Mean Temperature

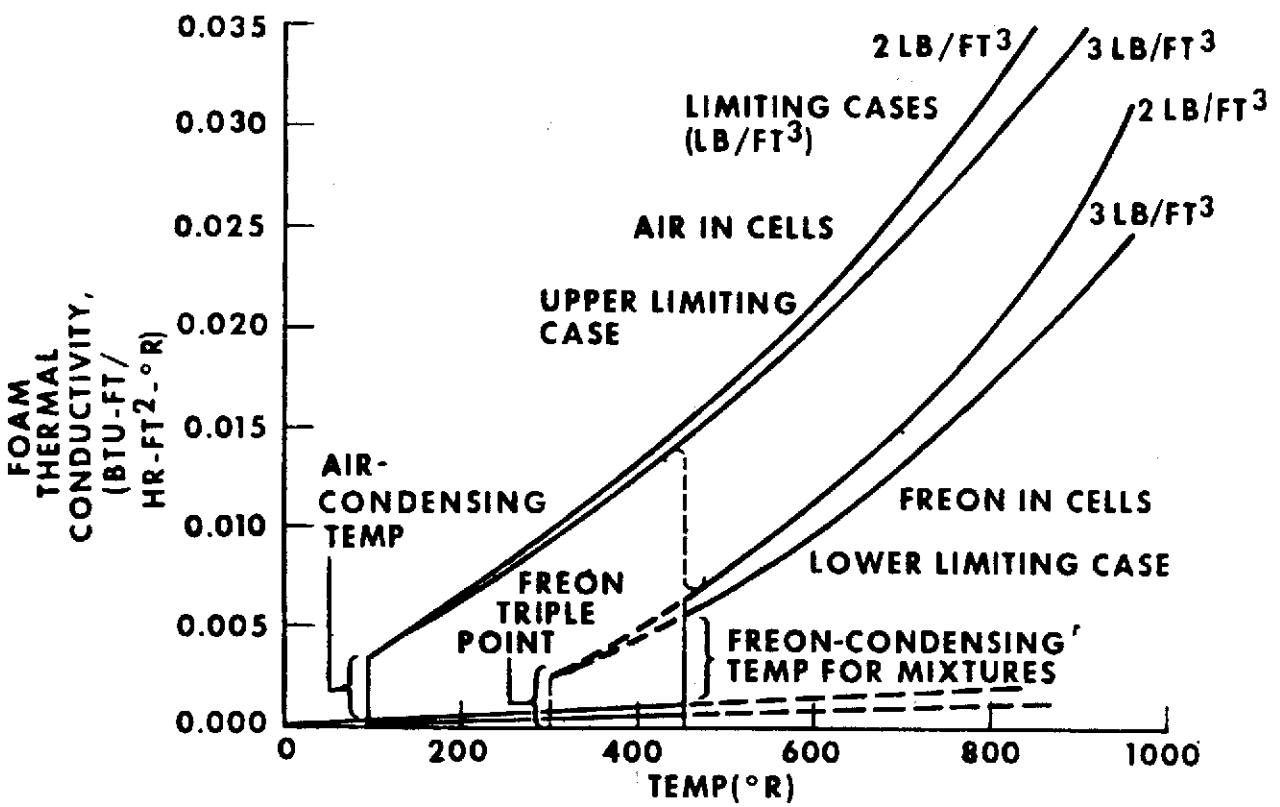

Figure 7.4.1.5-1. Limiting Cases of Foam Thermal Conductivity for Air and Freon in Cells

Starting at the point in the insulation where the Freon-condensening temperature is achieved, it is possible to use Figure 7.4.1.2-1 to obtain the spatial distribution of the mole fraction from the point x_3 to the outside boundary. The next step is to perform a numerical integration of thermal conductivity for the gas mixture to the outside boundary temperature:

$$\int_{T_{cf}}^{T_2} K_{mix}\,dt = \sum_{n=0}^{i} K_{mix}(M,T)\Delta T: \quad \begin{matrix} M = M(x) \\ T = T(x) \end{matrix} \qquad (7.4.1\text{-}11)$$

The third step is to sum the effective conductivity over all modes as shown in Equation 7.4.1-9 and then repeat this calculation until the assumed effective conductivity equals the solution. All of the methods discussed thus far apply strictly to the solution of steady-state problems. They should not be applied to transient problems without careful consideration. The solutions for the limiting cases of air and Freon (Figure 7.4.1.5-1) are directly usable in a transient calculation since thermal conductivity is only a function of temperature.

7.4.1.6 Comparison of Test Results

A comparison of the present analysis with test data is shown in Figure 7.4.1.6-1. The test data for the low-temperature tests were obtained using guarded tanks with liquid hydrogen; standard guarded hot plate apparatus was used for the above-ambient tests. The curve for low-temperature behavior, on the left in Figure 7.4.1.6-1, is based on a liquid-hydrogen cold-side temperature. Some scatter is evident in the test; this is a result of the method used to heat or cool the foam to achieve a range of temperatures. In repeated tests of the 2-pound density foam without auxiliary surface temperature modification, the results were very close to each other and the analysis curve (see box containing four data points). The curve on the right in Figure 7.4.1.6-1, based on an estimated Freon mole fraction after 500 hours of exposure, is plotted for the actual thermal conductivity as a function of temperature rather than effective thermal conductivity since all three modes are acting essentially in parallel. The shift in the thermal conductivity in the temperature range between -100 and 0 F was described earlier in this discussion as the transition that takes place in the gas-conduction term as Freon vaporizes.

The S-curve behavior shown in Figure 7.4.1.6-2 (Reference 46) is typical of thermal conductivity results in the Freon-condensing range. The tests were made in a vacuum over approximately 15 F temperature differentials. The fact that Freon appears to condense between +30 and -30 F is a further indication that the assumed Freon-condensing temperature of 0 F is a valid estimate.

Tests were also conducted on an 8-foot-diameter spray-foam insulated tank. The purpose of the tests was to improve confidence in the performance of spray-foam insulation under repeated cryogenic cycling. Thermal analyses were performed in conjunction with boiloff and experimental thermal gradient data to evaluate the effective thermal conductivity of the insulation. The calculated thermal conductivity, based upon the experimental temperature gradient at the

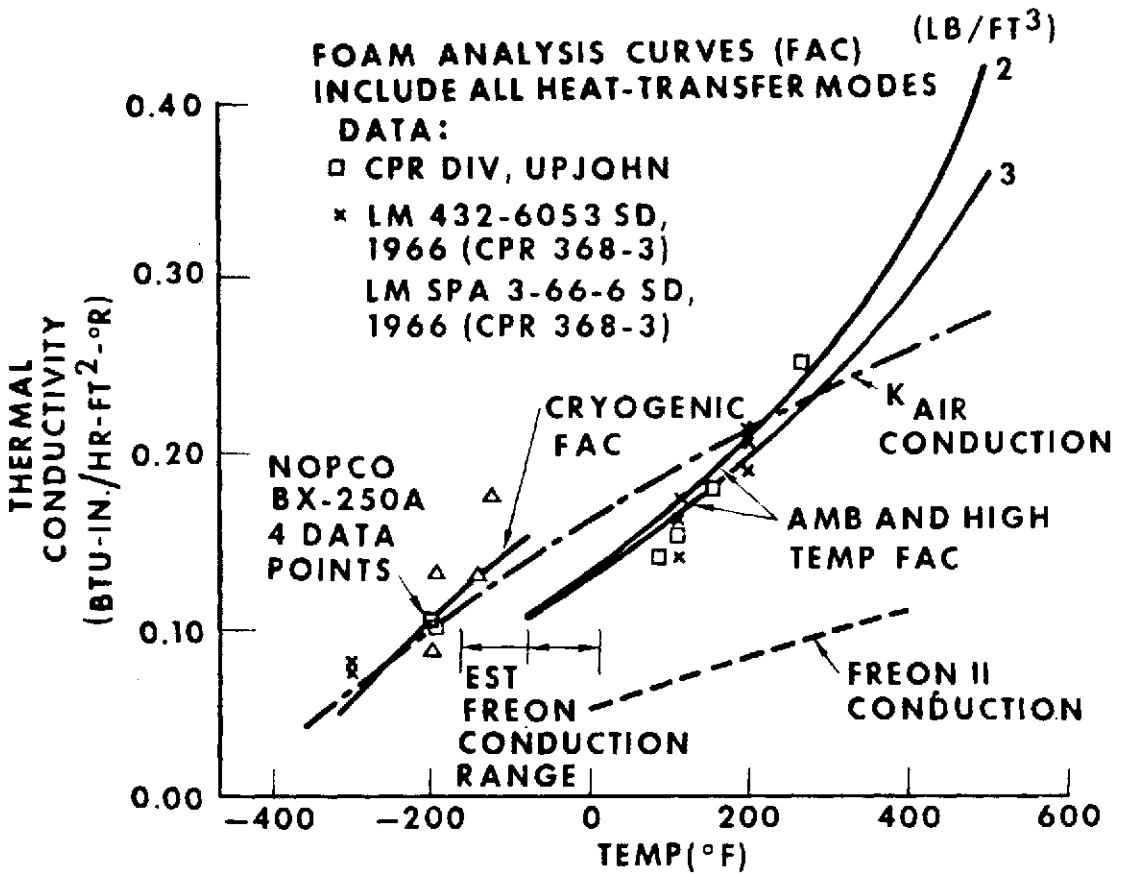

Figure 7.4.1.6-1. Comparison of Analysis Method With Foam Test Data

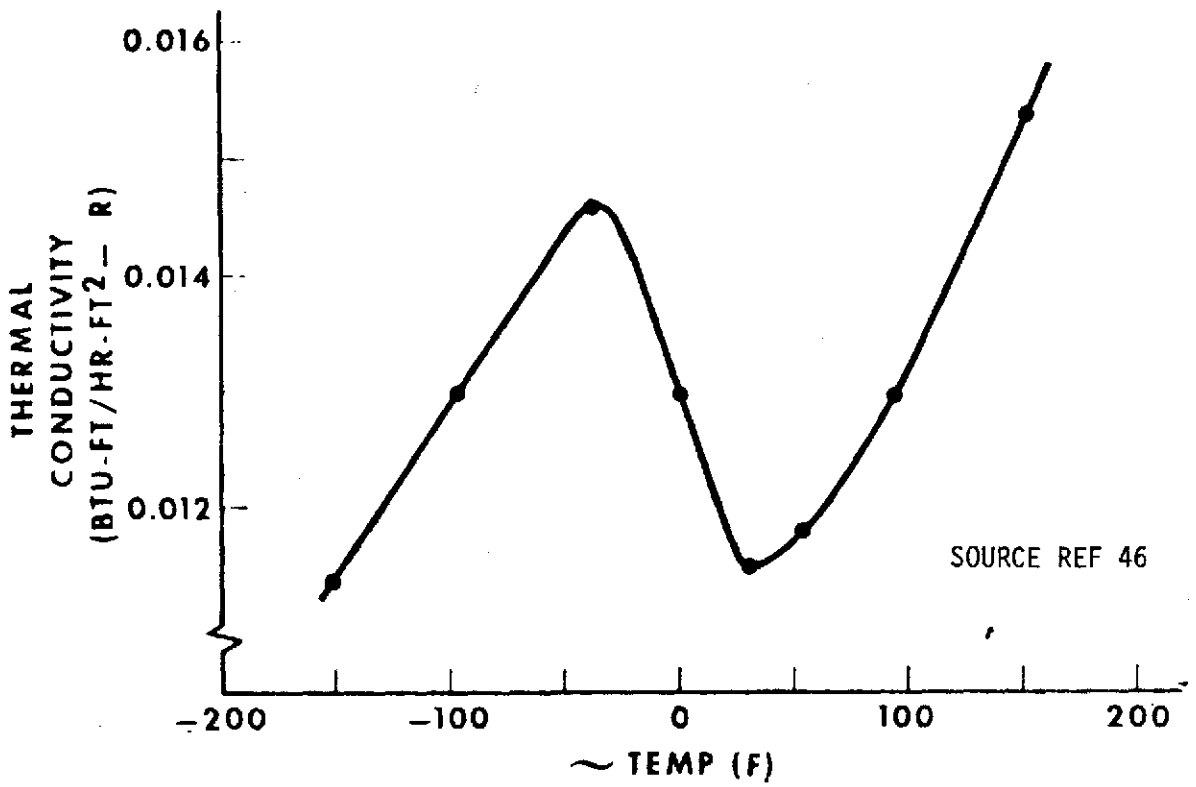

Figure 7.4.1.6-2. Thermal Conductivity of Polyurethane Foam Taken Over Small Temperature Intervals

surface, was 0.162 Btu-in./hr.-ft.^{2}-°F, compared to a theoretical value of 0.15 obtained from this study. The effective thermal conductivity based upon the overall temperature difference is 0.122 Btu-in./hr.-ft.^{2}-°F, compared to a theoretical value of 0.112 for the same temperature range.

The temperatures at several points were calculated as shown in Figure 7.4.1.6-3. Measured valves are also shown.

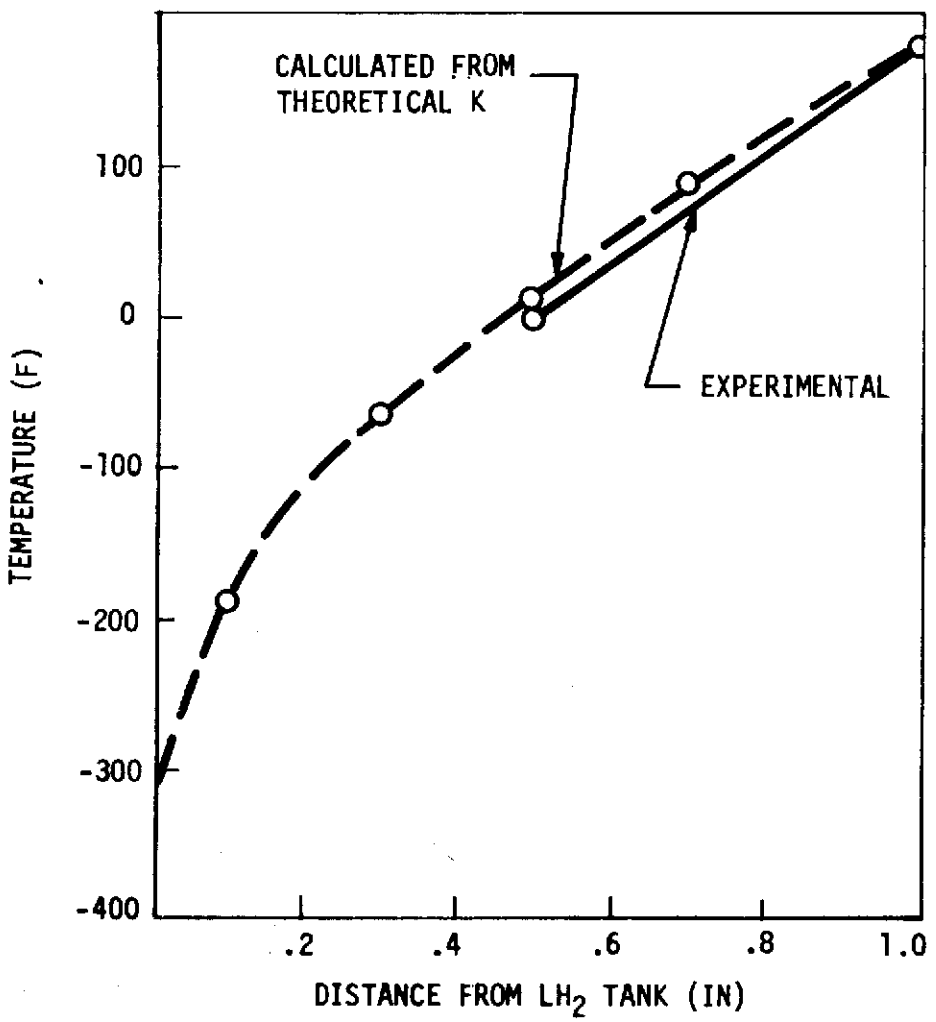

Figure 7.4.1.6-3. Spray-Foam Insulation Temperature Profile - MDC Tank No. 1

7.4.1.7 Conclusion

A method has been developed and experimentally verified that permits the analytical determination of the thermal conductivity of closed-cell foam insulation. The method accounts for the effect of gas diffusion and condensing, as well as the dependence of thermal conductivity on mole fraction and temperature. It is concluded that this method is valid for engineering analysis of steady-state heat flow in foam insulation and may be used to determine the long-term degrading effects of diffusion of atmospheric species.

7.4.2 Heat Exchange Through Support Areas by Conduction and Radiation

This study provides a graphical relationship between heat leak and the design of posts or struts for high-performance, well-insulated LH_2 and LOX tanks. Figures and examples are presented which can be utilized to determine the amount of heat which can be transmitted from the outside of a dewar type LH_2 or LOX tank to the inside by conduction and radiation.

These figures and the calculations associated with this effort are intended as an aid in the design of the tanks and insulation in the vicinity of the supports. The details of a particular installation and variations in thermal properties, installation, and insulation can cause variations from the values as presented. For these reasons, these graphs should be used for preliminary estimates only and not for the finalization of total heat leak values.

7.4.2.1 Penetration Heat Leak Into the Wall of Insulated Cryogenic Tank

A parametric study for preliminary design use was made of the heat leak by conduction through penetration (posts, struts, wires, tubing, etc.) into well-insulated liquid hydrogen and LOX tanks. This is illustrated in Figure 7.4.2.1-1. Figures 7.4.2.1-2 and -3 show the heat leak as a function of the size of the part, the material, and the temperature of the outer shell in the range of -200°F to 200 F. The abscissa of the graphs is A/X, where A is the cross-sectional area of the heat-conducting part in square feet and X is the length of the part in feet. The ordinate, Q, is the heat leak of one part or unit in Btu/hr. Four materials, aluminum, CRES, titanium, and fiberglass for different external wall temperatures (T_2) are identified on the graphs. The curves are applicable to conduction only and do not include radiation heat loss from the insulated tank surface which may be present in the vicinity of the penetration, radiation within the penetration, or radiation interchange between the external surface of the strut and the tank insulation and outer shell.

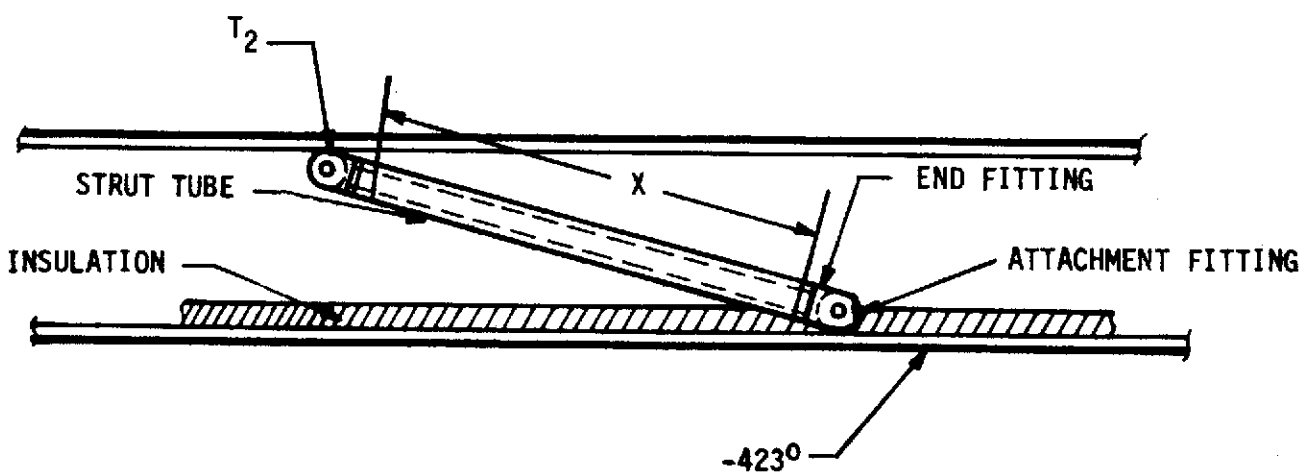

Figure 7.4.2.1-1. Example of Hydrogen Tank Penetration Heat Loss

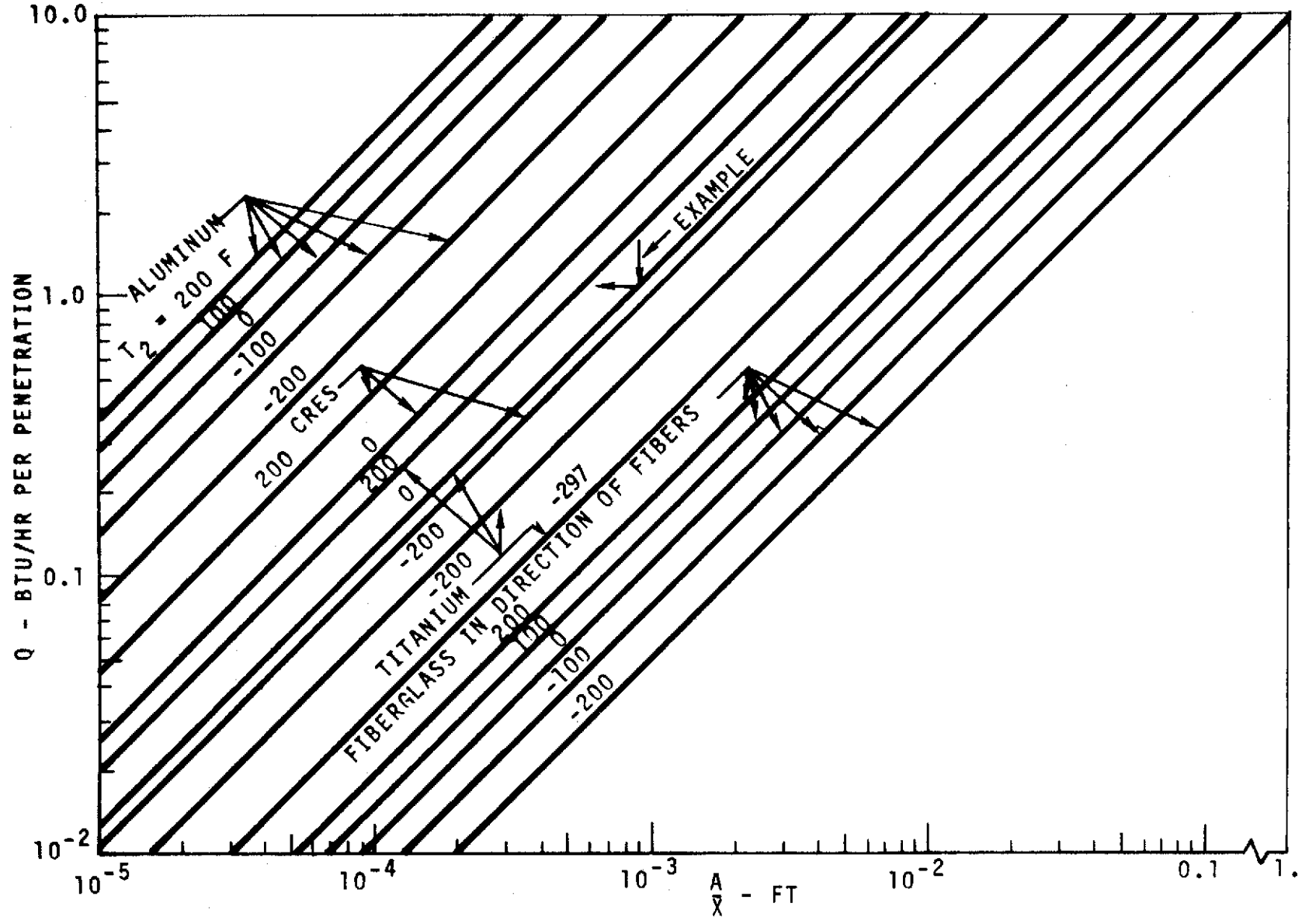

Figure 7.4.2.1-2. Hydrogen Tank Penetration Heat Loss

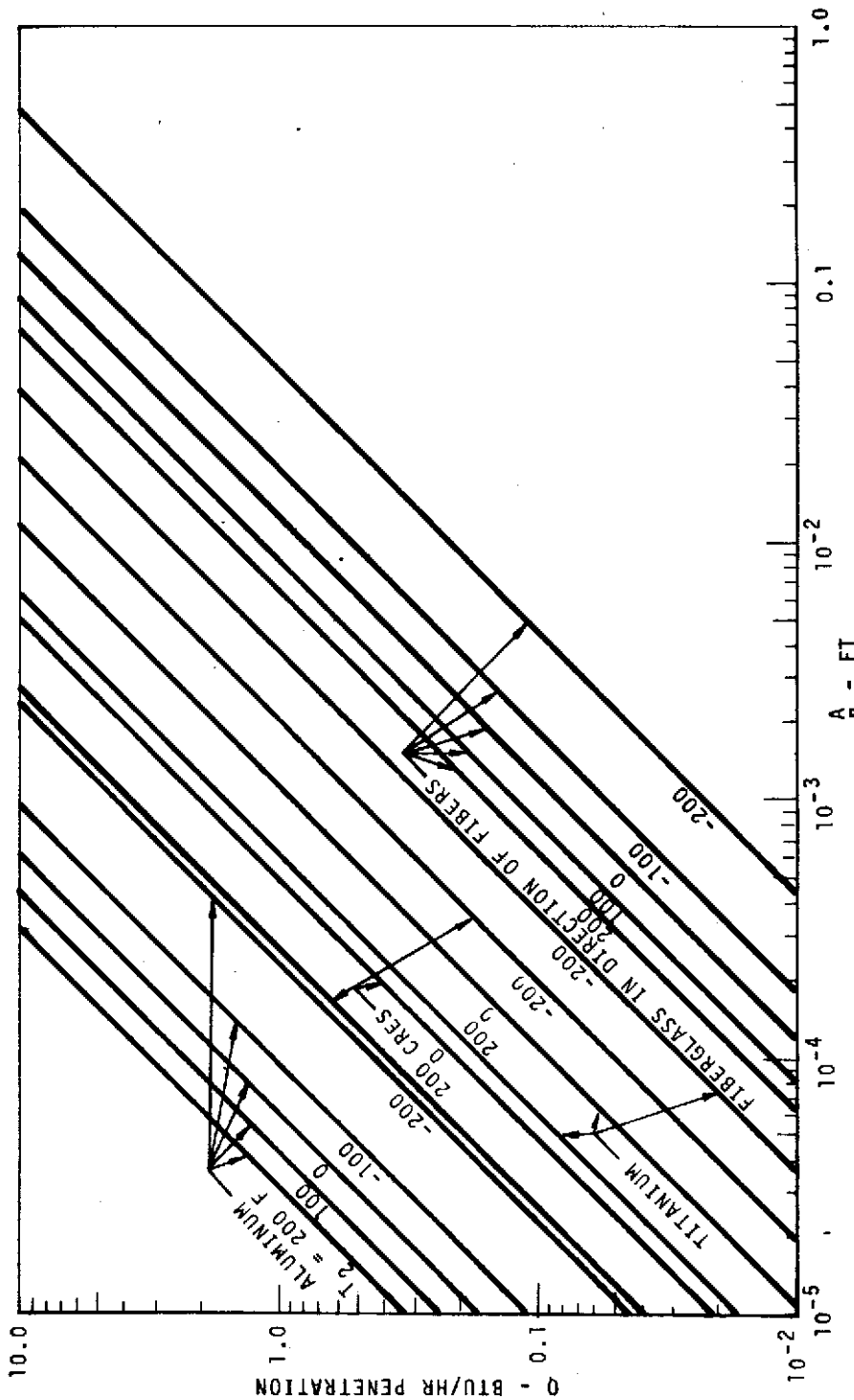

Figure 7.4.2.1-3. LOX Penetration Heat Loss

The following paragraphs present a typical example of how to use the curve to determine a penetration heat leak.

a. Problem: Determine the heat leak by conduction through eight struts connecting the outer shell to the inner shell of a liquid hydrogen tank as shown in Figure 7.4.2.1-1.

b. Assumptions:

1. Strut material: titanium

2. Outer shell temperature (T_2) - 0 F

3. Strut configuration consists of attach fitting, end fitting, and tube as shown in Figure 7.4.2.1-1. The heat conduction of the attachment and end fittings is high because of the large cross-sectional area and short length; therefore, it is assumed that the temperatures at the ends of the tube are equal to the temperatures of the inner and outer shells.

4. Tube outside diameter: 1.25 inches = D_2

5. Tube inside diameter: 1.17 inches = D_1

6. Length of tube: 14 inches = 1.167 feet = X

c. Solution:

1. $\text{Area} = A = \frac{\pi (D_2^2 - D_1^2)}{4} = (0.7854)\ (1.25^2 - 1.17^2)$

$$A = 0.1522 \text{ in.}^2 = 0.001057 \text{ ft.}^2$$

2. $\frac{A}{X} = \frac{0.001057}{1.167} = 0.000906 = 9.06 \times 10^{-4}$ ft.

3. On Figure 7.2.41-2, read down at 9.06×10^{-4} to the T_2 of the titanium (0° F) curve and across:

Q_S = 1.1 Btu/hr. for one strut.

4. Q_t = (8) (1.0) = 8.8 Btu/hr for 8 struts by conduction.

d. Comments: The penetration heat leak of the titanium strut may be reduced by reducing the outside diameter or wall thickness of the tube or by increasing the length of the tube. Another possible way of reducing the heat leak would be to use a material of lower thermal conductivity for the tube, such as fiberglass. However, the need for a larger cross-sectional area and or shorter length to meet structural requirements may tend to have an adverse effect on the extent of the reduction of the heat leak.

7.4.2.2 Heat Leak Into Cryogenic Tanks by Radiation to Uninsulated Areas

A parametric study for preliminary design use was made of the heat transfer by radiation from an external warmer surface to a locally uninsulated area of a liquid hydrogen and a LOX tank. This is illustrated by Figure 7.4.2.2-1. Figures 7.4.2.2-2 and -3 show the heat leak as a function of the radiation interchange factor and the temperature of the external surface in the range of -200 F to 200 F. The ordinate of the graphs, Q/A_1, is the heat leak in Btu/hr.-ft.^{2}. A_1 is the area of the uninsulated cryogenic tank wall. The abscissa is the nondimensional radiation interchange factor, F_{1-2}, which is defined as follows:

$$F_{1-2} = \frac{1}{\frac{1}{\varepsilon_1}-1 + \frac{A_1}{A_2}\left(\frac{1}{\varepsilon_2}-1\right) + \frac{1}{F_{1-2}}}$$

where

ε_1 = Emissivity of the tank wall, non-dimensional

ε_2 = Emissivity of the warmer external surface.

A_1 = Area of uninsulated tank wall, square feet.

A_2 = Area of the warmer external surface, which A_1 "sees" in square feet, as defined in Figure 7.4.2.2-2.

F_{1-2} = Geometric view factor, A_1, with respect to A_2; it is nondimensional and is defined in Figure 7.4.2.2-2.

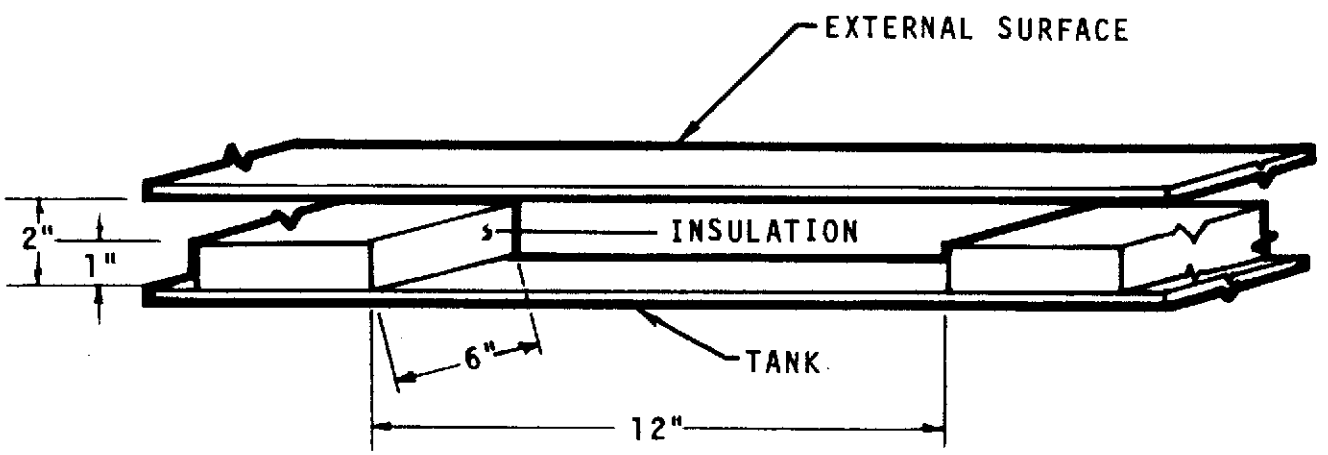

Figure 7.4.2.2-1. Example of Radiation Heat Leak to an Uninsulated Area of a Hydrogen Tank

The following values of emissivity for the expected unpolished clean tank surfaces are recommended for preliminary design:

Material	Emissivity
CRES	0.12
Aluminum	0.10
Titanium	0.12

The curves of Figures 7.4.2.2-3 and -4 are applicable only to heat transfer by radiation from the external surface to the uninsulated area of the tank.

Radiation between the uninsulated area of the tank and a mechanical part, such as a strut, and the insulation on the perimeter of the uninsulated area are not included. The heat loss by conduction of the mechanical part is not included. The following is a typical example of the application of Figures 7.4.2.2-2, -3, and -4 to the estimation of the radiation interchange factor and the heat loss by radiation from an uninsulated area of a hydrogen tank.

a. Problem: Determine the heat loss by radiation from an uninsulated area of a liquid hydrogen tank to a warmer external surface as shown in Figure 7.4.2.2-1.

b. Assumptions:

1. Material of tank and external surface, aluminum.

2. $T_2 = 0°F$, external surface temperature.

3. $\varepsilon_1 = \varepsilon_2 = .10$, emissivity of aluminum.

4. An uninsulated area of the tank which is typical of a strut installation with dimensions as follows (Figures 7.4.2-2-1 and -2).

a_1 = 6 inches = 0.5-foot width of uninsulated area.

b_1 = 12 inches = 1-foot length of uninsulated area.

c = 1 inch - thickness of insulation.

d = 2 inch = distance between tank and external surface.

c. Solution:

1. $A_1 = a_1, b_1$, Figure 7.4.2.2-2

$A_1 = (0.5)\ (1.) = 0.5$-square foot area of uninsulated part of tank.

2. $A_2 = a_1\ b_1 \left[4 \left(\frac{d}{c}\right)^2 - 4\left(\frac{d}{c}\right) + 1\right]$

$A_2 = (.5)\ (1.) \left[4 \left(\frac{2}{1}\right)^2 - 4\left(\frac{2}{1}\right) + 1\right] = 4.5$ square feet, area of external surface "seen" by A_1.

3. F_{1-2}, geometric view factor, Figure 7.4.2.2-2.

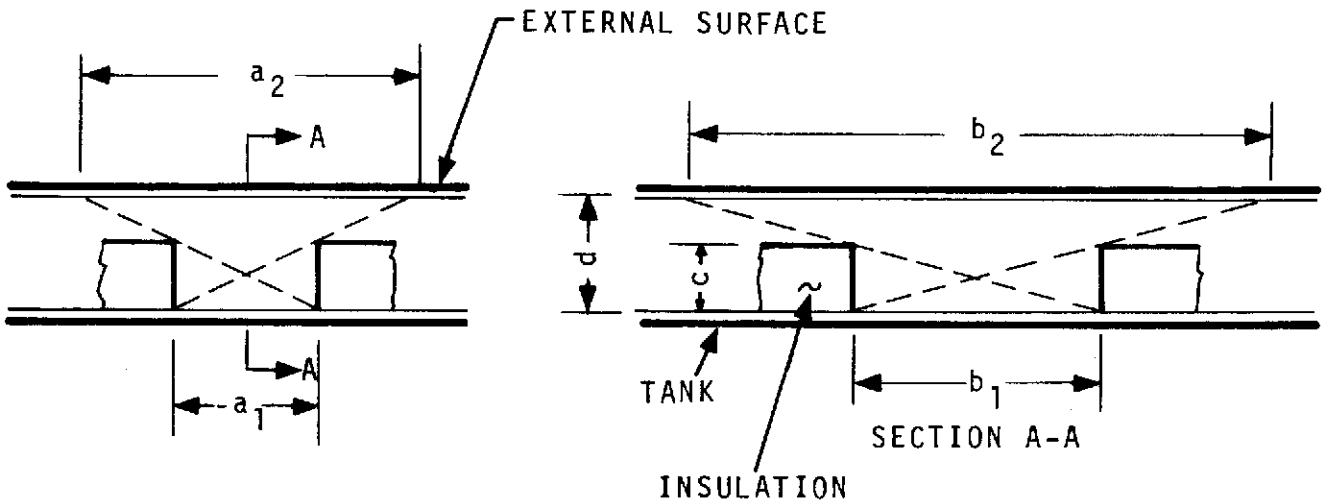

RECTANGULAR UNINSULATED TANK AREA

$A_1 = a_1 b_1$ = RADIATION AREA OF TANK, FT^2

$A_2 = a_2 b_2$ = RADIATION AREA OF EXTERNAL SURFACE "SEEN" BY A_1, FT^2

$$A_2 = a_1 b_1 \left[4\left(\frac{d}{c}\right)^2 - 4\,\frac{d}{c} + 1 \right], \; FT^2$$

CIRCULAR UNINSULATED TANK AREA

D_1 = DIAMETER OF UNINSULATED TANK, FT

$A_1 = .785\, D_1^{\,2}$, FT^2

$$A_2 = .785\, D_1^{\,2} \left[4\left(\frac{d}{c}\right)^2 - 4\,\frac{d}{c} + 1 \right], \; FT^2$$

GEOMETRIC VIEW FACTOR

F_{1-2} = GEOMETRIC VIEW FACTOR, A_1 WITH RESPECT TO A_2, NON-DIMENSIONAL, AS PLOTTED ON FIG. 5-18, PAGE 221 OF PRINCIPLES OF HEAT TRANSFER B F. KREITH

STEP 1 - FIND VALUE OF ABSCISSA: RATIO FOR RECTANGULAR $A_1 = \frac{a_1}{c}$; RATIO FOR CIRCULAR $A_1 = \frac{D_1}{c}$

STEP 2 - READ UP FROM VALUE OF ABSCISSA TO CURVE 1, 2, 3, OR 4 AND OVER TO THE ORDINATE SCALE AND READ F_{1-2}

Figure 7.4.2.2-2. Calculation of View Factor

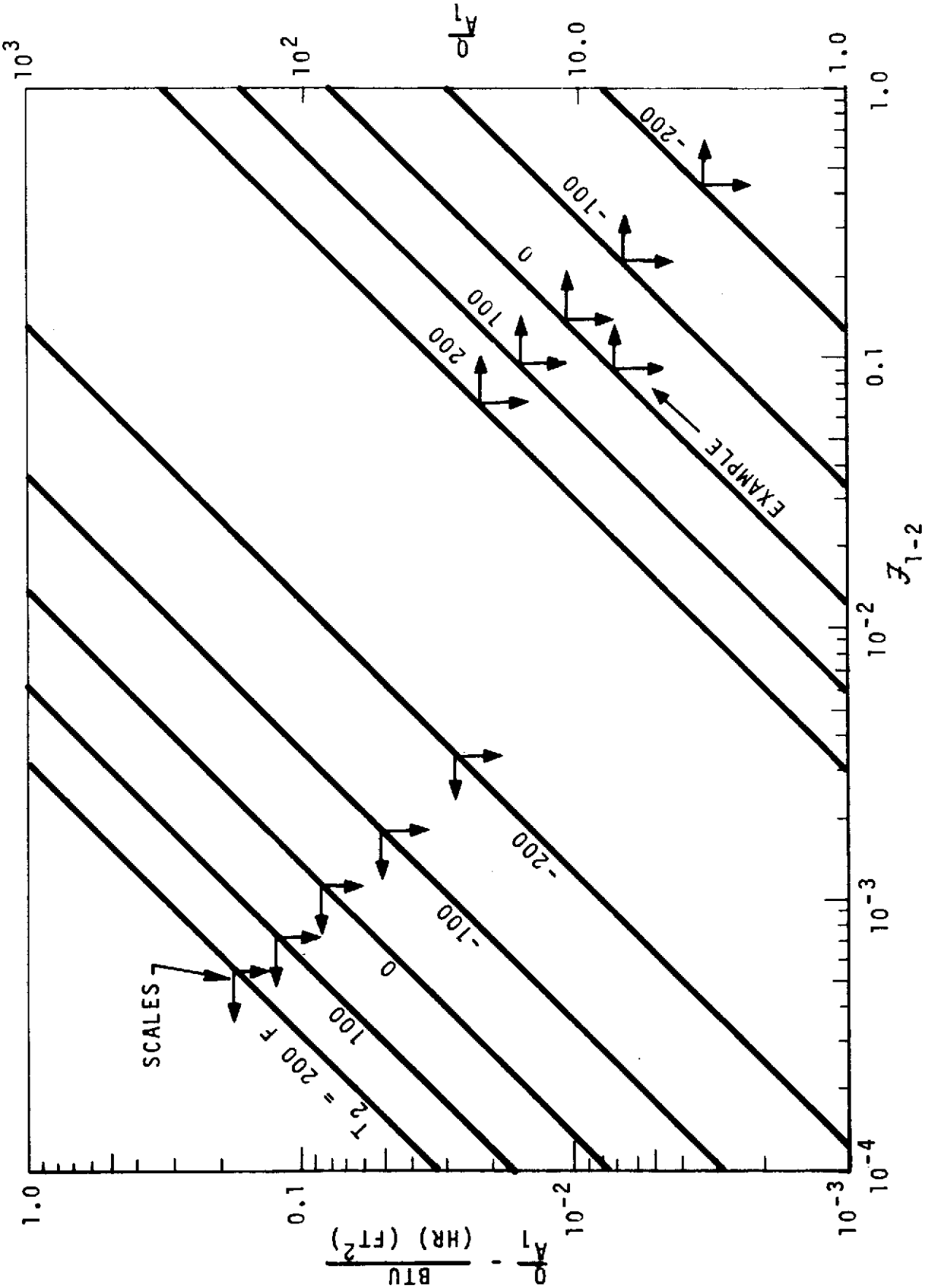

Figure 7.4.2.2-3. Hydrogen Tank Radiation Heat Loss From Insulation Gap

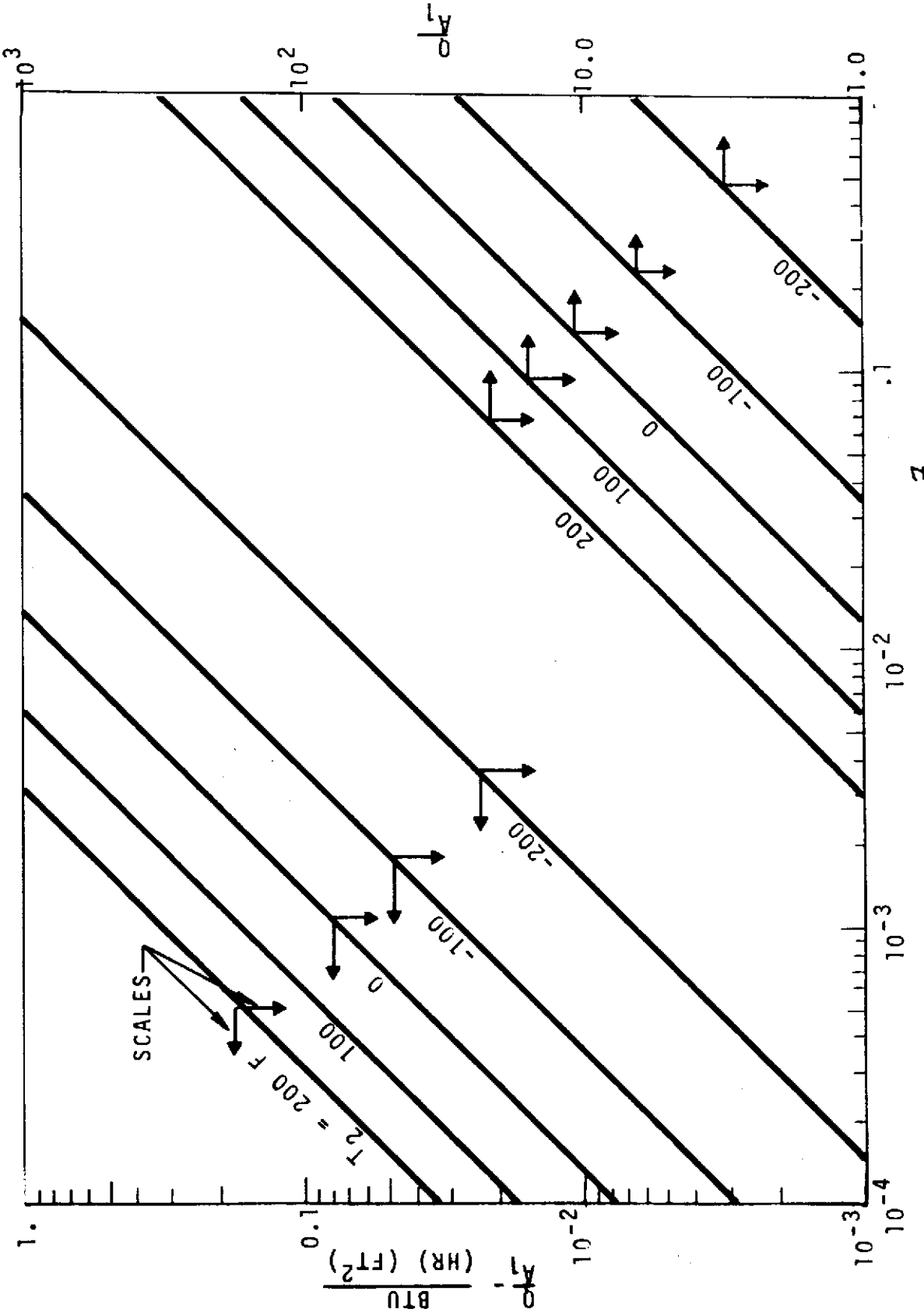

Figure 7.4.2.2-4. LOX Tank Radiation Heat Loss From Insulation Gap

Estimate the percentage coverage of the larger area that may be "seen" by the smaller area. This could be "guessed" to be about 70 percent or 0.70. For more exact procedures, follow steps 3.1 through 3.3 below.

3.1 $\frac{a_1}{c} = \frac{6}{1} = 6.$, the value of the abscissa of Figure 5-18 in Reference 35.

3.2 $\frac{b_1}{a_1} = \frac{12.}{6} = 2.$, dimension ratio of A_1, which identifies curve number 3 of Figure 5-18 of Kreith to be the applicable curve.

3.3 On Figure 5-18 of Kreith read up at 6 to curve number 3 and over to the ordinate scale, readings:

$$F_{1-2} = 0.77$$

4. Find F_{1-2}, the radiation interchange factor:

$$F_{1-2} = \frac{1}{\frac{1}{\varepsilon_1} - 1 + \frac{A_1}{A_2}\left(\frac{1}{\varepsilon_2} - 1\right) + \frac{1}{F_{1-2}}}$$

$$F_{1-2} = \frac{1}{\frac{1}{0.1} - 1 + \frac{0.5}{4.5}\left(\frac{1}{0.1} - 1\right) + \frac{1}{0.77}}$$

$$F_{1-2} = \frac{1}{10 - 1 + .111\ (10 - 1) + 1.3} = \frac{1}{11.3} = 0.0885 - 8.85 \times 10^{-2}$$

5. On Figure 7.4.2.2-3, read down at 8.85×10^{-2} to the T_2 curve of and over to the right, reading:

$$\frac{Q}{A_1} = 6.8 \text{ Btu/hr.-ft.}^2$$

6. $Q = 6.8A_1 = (6.8)\ (0.5) = 3.4$ Btu/hr., heat leak by radiation to the uninsulated tank area from the external surface.

d. Comments: The radiation heat leak may be reduced by reducing the area and emissivity of the uninsulated tank. Lowering the emissivity from 0.10 to 0.08 by polishing would result in a 18 percent lower heat leak. Polishing the external surface would have negligible effect.

7.4.3 Example of an Integrated Thermal Analysis

The individual analysis of the various parts of a complete thermal analysis have been presented in various portions of this report. The information from individual sections must be combined in order to make a comprehensive and meaningful analysis and report of the overall subject for a particular vehicle. An example analysis is the "Design and Systems Analysis of a Chemical Interorbit Shuttle" SD 72-SA-042 (May 1972), pages 272 through 319. This analysis shows the overall system approach, effect of solar attitude, optimum weight/boil-off relationships, and the effectiveness of a combined thermodynamic vent, LOX cooling, structure cooling, and instrumentation system thermal control system.

8.0 STRUCTURAL PERFORMANCE ANALYSIS

8.1 INTRODUCTION

Insulation systems generally utilize organic materials which exhibit mechanical property behavior significantly different from metals. This section presents the analytical methods which have been developed to allow meaningful structural analyses of insulation systems which utilize organic materials.

8.2 GENERAL

In general, the primary function of an insulation system is to provide thermal protection; it is not intended to be a primary load-carrying structure. However, since the insulation system is normally bonded or mechanically attached to the primary structure, it is required to match the strains and deflections of the primary structure, and therefore significant stresses are introduced into the system.

It has been determined that organic materials do not behave in the same elastic manner as metals. All organic materials investigated to date behave in a visco-elastic manner. This means that standard cryogenic test methods and analytical structural evaluation must be altered to allow design analytical predictions for organics. In solving this problem, a new cryogenic test method called monostrain testing has been developed to enable the measurement of organic mechanical properties in a uniaxial strain field. These properties are then used in standard stress analysis equations to support detail design.

Materials must be elastic or repeatable to enable mathematical analysis. Metals are elastic up to the proportional limit and may be accurately analyzed by conventional structural analysis methods. Metals follow Hooke's law within the elastic limit:

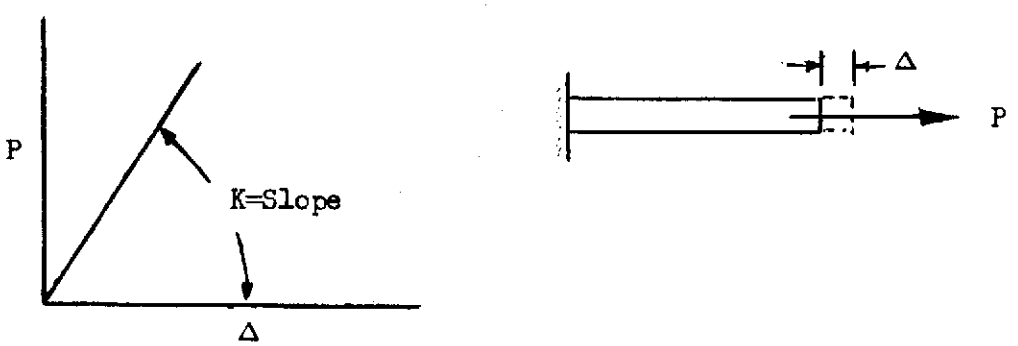

(8-1)

where

$P = K\Delta$

P = Forces (pounds)

Δ = Deflection (inches)

Organic materials (such as foam) are visco-elastic. Visco-elastic materials require time to return to original length after loading.

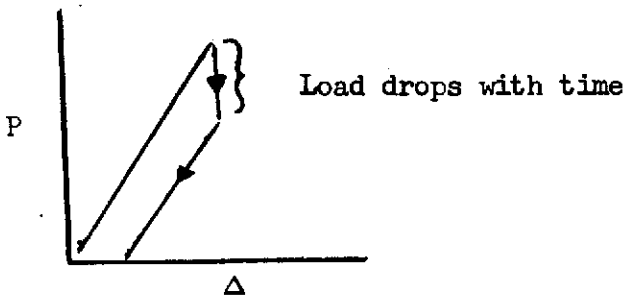

Therefore, organics require different analytical evaluations than metals. The thermal stresses caused by differential expansions or contractions cannot be predicted by the standard constants known as Young's modulus of elasticity (E) or the free contraction constant (α).

To determine the physical behavior of organics, the monostrain technique was devised. This was necessary since all previously known test techniques gave material properties when the organic was actually in a combined stress state rather than a uniaxial state of stress. To clarify this, if an organic material was bonded to end blocks in order to apply force and chilled to the test temperature, the temperatures would cause thermal stresses before the external force is applied. If the organic specimen was short in relation to the overall test specimen length, the stiff metallic end blocks restrained the relatively limber organic from free strain. The resultant physical properties such as modulus of elasticity, tensile strength, and shear modulus displayed considerable scatter, thereby precluding their use in practical analytical structural evaluation. This problem was overcome by fabricating 1-inch wide strips of the organic, 27 inches long. The bonded metallic end reinforcements were then short compared to the organic length, thereby greatly minimizing the thermal stress and end effect.

The monostrain test technique was utilized to evaluate the stress-strain relationship of organics at cryogenic temperature. The simple 1-inch wide strip of foam 27 inches long was inserted in a test machine. The specimen length was fixed at room temperature and held constant as the test temperature was lowered. As the specimen tried to contract, increasing forces were generated so that a load versus temperature curve was developed. In acknowledgement of the visco-elastic behavior of the foam, time was allowed to develop the slow chill curve. It was found that the curve was repeatable during numerous cycles. By dividing the thermal load curve by the specimen area, a uniaxial stress versus temperature curve was generated. An attempt was made to duplicate the force at any temperature analytically by using Young's modules and the free contraction constant:

$$P = E \alpha \Delta T A \qquad (8\text{-}2)$$

where

A	=	Cross-sectional area of specimen (square inches)
ΔT	=	Change in temperature (F)
α	=	Coefficient of free thermal contraction (in/in - F)
E	=	Young's modulus of elasticity

It was found that this yielded errors as high as 100 percent. To allow accurate prediction of the thermal stress, new constants were determined by tests. The first is called the thermo-elastic modules (E_T) which replaces Young's modulus. The second is called the thermo-elastic contraction $\left(\frac{\Delta L}{L}\right)_T$. The thermal stress caused by organic material contraction is designated thermo-stress (σ).

The thermo-elastic modulus is obtained by utilizing the monostrain constant length test. The specimen is locked at room temperature in the test fixture so that the specimen length remains constant. The specimen is then chilled to the first incremental temperature. The force caused by the thermal stress in the specimen is then recorded. The thermo-stress is obtained by dividing the force by the specimen cross-sectional area. The specimen is released, the load is slowly reduced to zero, and the resulting shortening (ΔL) is measured. The thermo-elastic contraction is then calculated by dividing ΔL by the original specimen length.

The thermo-stress (σ) is then divided by the thermo-elastic strain ($\frac{\Delta L}{L}$) to produce the thermo-elastic modulus (E_T):

$$E_T = \frac{\text{Thermo-Stress}}{\text{Thermo-elastic Strain}} = \frac{(P/A)}{(\Delta L/_L)}$$

Tests reveal that the thermo-elastic strain, which is also the contraction springback under load, is not the same as the unloaded or free shrink rate. For this reason, the value ($\frac{\Delta L}{L}$) is plotted versus temperature to be used in analysis. At any given temperature the thermo-stress can be calculated from the plots of E_T versus temperature and ($\frac{\Delta L}{L}$) versus temperature.

This same test procedure has been accomplished with metals and it has been confirmed that Young's modulus and the standard free coefficient of thermal contraction will predict the stress accurately. Tests on various organic systems have revealed that the thermo-elastic modulus and thermo-elastic contraction must be used to predict analytically the stress in visco-elastic systems.

It also should be noted that test evaluations of organics such as foams indicate that they are considerably more critical in a biaxial stress field than in a uniaxial stress field. Discussion of the effect of biaxial stress fields on foam systems is contained in Paragraph 8.4.

8.3 HONEYCOMB BASE SYSTEMS

Once the appropriate material properties have been determined for the various materials which comprise the honeycomb base insulation system, conventional sandwich structural analysis methods may be employed to analyze these systems. Such analysis methods are given in the NR Structures Manual (Pub. 2546-J, October 1969). Analysis of edge closeouts can be made utilizing NR finite element program NARSAMS (NR report SD70-446) to determine edge loadings and stresses. Detail stress analysis of the honeycomb base insulation systems as used on the Saturn S-II stage is contained in NR report SID66-674.

In the case of the honeycomb core used for the S-II common bulkhead, a complex structural analysis method and computer program were developed for structural analysis of the bulkhead over a wide range of temperature gradients and pressures. Internal loadings and stresses are determined from the methods and equations presented in NR report SID STR 123 and 124.

Detail stress analysis of the S-II stage common bulkhead honeycomb core is contained in NR report SD69-337.

8.4 FOAM SYSTEMS

The thermal stress in the foam on a tank may be expressed by the equation:

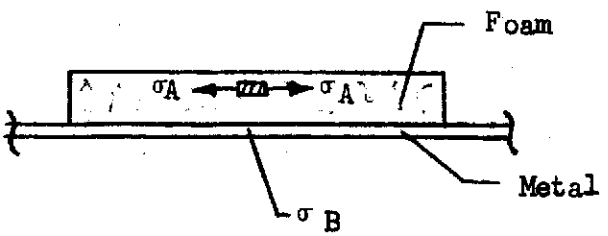

$$\sigma_A = \frac{E_A(\alpha_A \Delta T_A - \alpha_B \Delta T_B}{(1-M_A) + (1-M_B)\frac{E_A t_A}{E_B t_B}} \qquad (8\text{-}3)$$

where

σ_A = Thermal stress in foam (psi)

E_A = Thermo-elastic modulus of foam (psi)

α_A = Thermo-elastic contraction rate of foam (in/in °F)

ΔT_A = Differential temperature of foam (°F)

ΔT_B = Differential temperature of metal (°F)

μ_A = Poisson's ratio of foam

μ_β = Poisson's ratio of metal

t_A = Thickness of foam (inches)

t_B = Thickness of metal (inches)

E_B = Young's modulus of elasticity for metal (psi)

σ_B = Thermal stress in metal (psi)

For elastic materials such as metals, Equation 8-3 accurately predicts thermal stress if Young's modulus (E) and the conventional free contraction rate (α) are used. However, for visco-elastic materials such as foam, these constants will not accurately predict thermal stress. Therefore, new constants were conceived and determined by monostrain tests to allow more accurate predictions of thermal stress for visco-elastic materials.

Of significance in the analysis of foam systems is the effect of biaxial stress fields. Test evaluations of many foam systems have revealed that foams are considerably more critical in a biaxial stress field than in a uniaxial stress field. As an example, a fixed length monostrain test on spray-on foam caused a uniaxial stress of less than 50 percent of the foam's ultimate tensile strength at -300 F, while a biaxial thermal test caused severe rupture of the same foam at -240 F.

Conventional stress analysis equations predict the equivalent stress in a biaxial field for comparison to uniaxial tensile strength of the materials. This is accomplished by using Poisson's ratio as the dependent conversion factor as shown in Equation 8-3. As Poisson's ratio of the foam (μ_A) becomes large (approaches 1.0), the stress in foam (σ_A) becomes large. Current estimates of the value of Poisson's ratio for foam range as high as 0.8. Referring to Equation 8-3, this results in a biaxial stress level of five times that of a uniaxial stress field ($\mu_A = 0.0$).

To date efforts to determine Poisson's ratio by test have been unsuccessful. However, it appears that Poisson's ratio for spray-on foam should be in the range of 0.5 to 0.8 to satisfy Equation 8-3.

Structural analysis of foam systems such as those used on the Saturn S-II stage may be accomplished by utilizing NR finite element computer program NARSAMS.

9.0 DYNAMIC ANALYSIS

Analyses of the insulation protective panels have been performed during S-II derivative studies to determine their dynamic characteristics. The panels are generally designed of sandwich construction material which would be supported by posts attached to the main structure of the boost vehicle. The panels were interlocked with each other to produce shingle effect installation.

Dynamic analyses were performed to support Saturn S-II derivative vehicle design studies and included panel flutter analyses of the INT-21 mechanically attached polyimide erosion barrier design described in Paragraph 6.1.9 and the CIS meteoroid protection system panel design described in Paragraph 6.1.12. The panels were designed so that dynamic problems relating to force response and flutter were eliminated or minimized during the conceptual stage. The dynamic environment to which the panels would be exposed was determined from extrapolated S-II flight and static firing test data and from compiled wind tunnel test results.

Determination of the flutter characteristics are very complex and a flutter analyst must work closely with the designer to obtain the optimal panel design. In the Saturn S-II derivative studies, the panels were designed for flutter stability. Panel flutter could occur during ascent as the vehicle went through the transonic and maximum dynamic pressure regions. The panel design was accomplished by obtaining the appropriate guidelines defined by the performance of preliminary flutter analyses on the design conceptions. Parametric evaluations which included panel geometry, material, and support methods were investigated. The analyses were performed for the critical Mach numbers at altitudes determined for the specific mission trajectory.

9.1 DYNAMIC ENVIRONMENT

Acoustic and vibration environment for evaluation of some insulation material was obtained from S-II flight and static firing tests. The environment which was experienced by the insulation material was assumed to be that of the primary structure where spray foam and cork were bonded. This assumption was based on the very light weight of the insulation, which had negligible influence on the dynamic behavior of the primary structure.

Random vibration levels for the radial axis of the forward skirt from S-II flight data are presented in Figure 9.1-1. These data are typical to that used in determining the dynamic environment of the insulation system along the vehicle. The forward skirt energy levels began to build up at low frequencies and reached the peak value (2.6 g^2/Hz) at 90 Hz. The levels start to fall off as the frequency increases. The levels presented in this figure were obtained during liftoff and are the highest values obtained during S-II flight. The high intensity demonstrates the strength of the energy which was reflected from the ground and impinged on the vehicle during ignition and liftoff. Levels of similar magnitude have been observed at the aft skirt and the interstage. The frequencies for those cases have shifted to higher values. At transonic and mixiumum dynamic speeds, the vibration levels are lower than those observed at liftoff. From the overall standpoint, the forward skirt vibration levels are representative of the energy observed on S-II during flight.

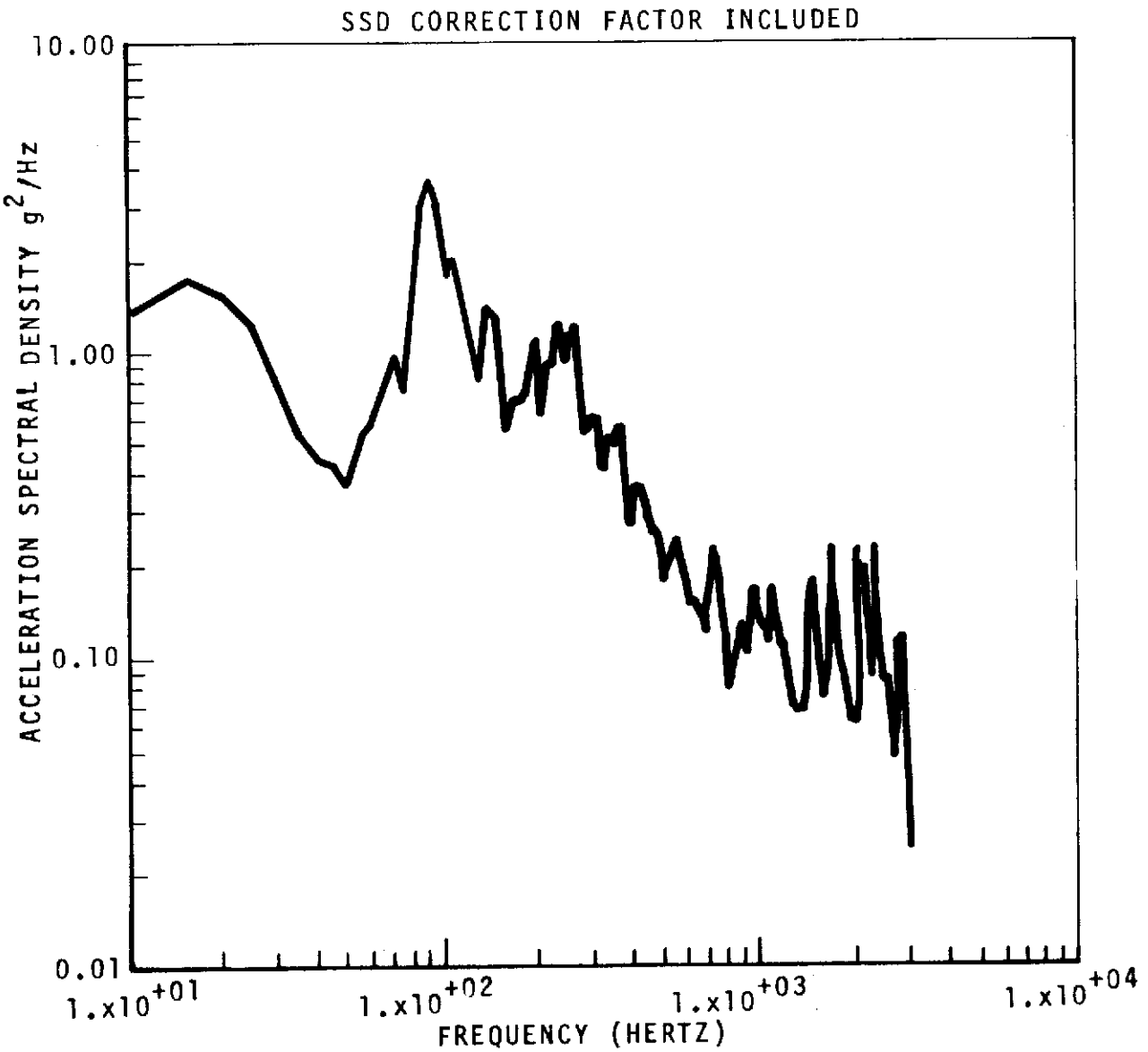

Figure 9.1-1. Forward Skirt Radial Axis Environment Random Vibration Environment

Figure 9.1-2 presents the Saturn S-II forward skirt point source acoustic environment. These data were recorded during liftoff, transonic, and max q phases of S-II flight. The peak sound pressure levels during transonic speeds reached 148 db at 20 Hz, 146 db at 80 Hz during liftoff, and 143 db at 100 Hz during max q. The data presented here were measured externally and is representative of the levels observed on the S-II.

S-II flight-derived dynamic environment data have been used in evaluation of insulation protective system design concepts. The expected vibration environment along with the calculated panel dynamic characteristics were used to determine the motion of the panels at resonance. Acoustic data were used to

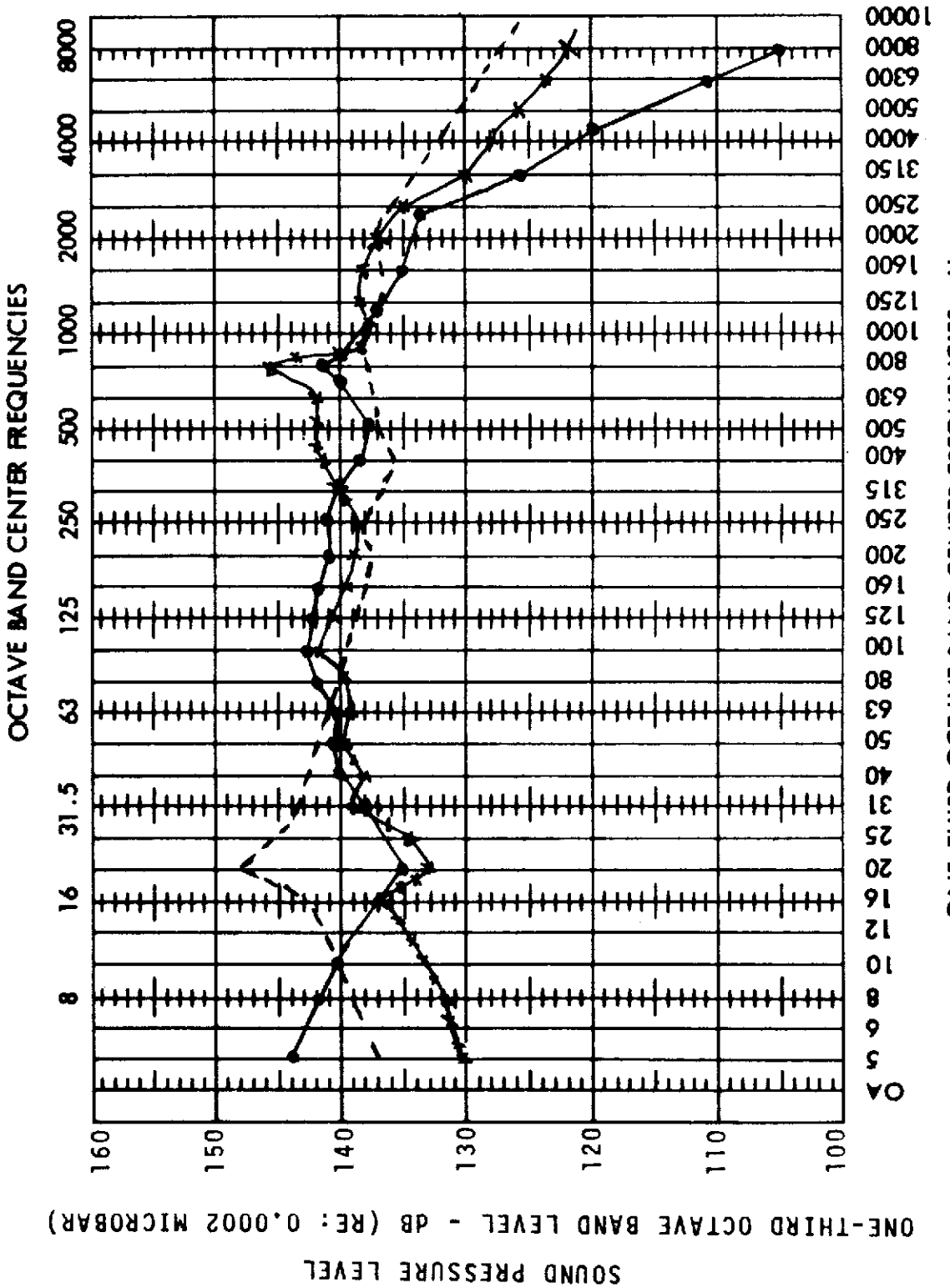

Figure 9.1-2. Forward Skirt External Acoustic Environment

to determine the motion of the panels at resonance. Acoustic data were used to determine the expected loading on the panel. The panel was designed to support the imposed dynamic loading adequately. The panel geometry and supporting methods were modified until the panel design was structurally sound and stable in flutter.

9.2 FLUTTER ANALYSIS

Preliminary flutter analyses of insulation and meteoroid protective panels have been performed at critical Mach numbers to assist the design group in obtaining an optimal panel design. Included in the analyses were recommendations for panel dimensions and support requirements which were used to obtain stable panels. The flutter criteria was applied and ground rules relating to the possibility of losing one support per panel were considered. A description of the panel flutter analysis and its application to the S-II derivative boost vehicle panels are presented herein.

9.2.1 Basic Data

The data required for performance of the panel flutter analysis have been defined in terms of structures, flight, and dynamic properties of the panels. The following descriptions of the data demonstrate their contribution to flutter analysis.

9.2.1.1 Structural Properties

The basic structural description incorporates the panel geometrical properties, mass, inertia, stiffness, and support points. The following sketch illustrates the typical panel geometric properties:

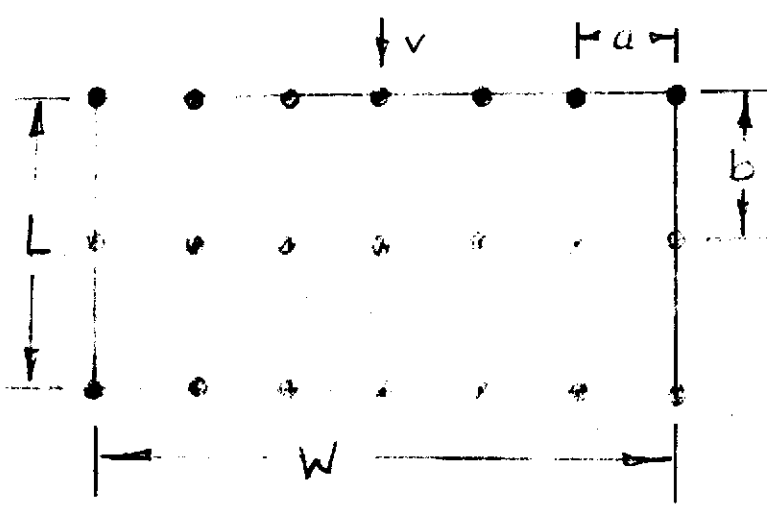

Basic support points on the panel describe rectangular patterns described as having the dimensions a inches wide and b inches long. The overall panel dimensions are identified by L and W where the length L is always in the direction of the airstream. The basic design concepts incorporate isotropic and sandwich construction. The materials considered in the panel design were aluminum, titanium, and polyimide.

The panel frequencies and mode shapes were calculated using existing NR programs which incorporate finite element modeling techniques. The basic structural properties are obtained using data as defined by the following sketch:

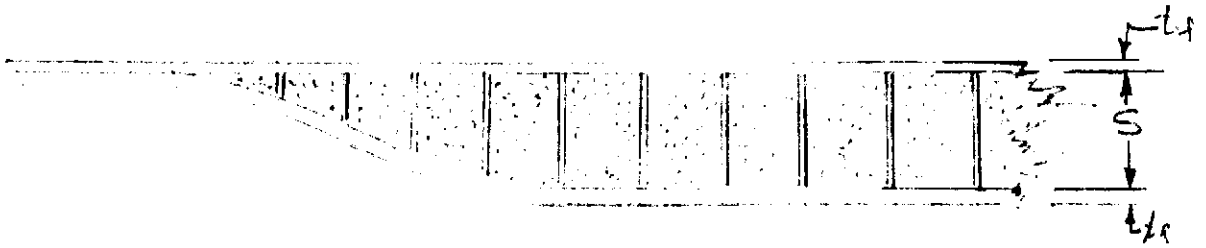

E = Young's modulus for material used, psi
Gfs = Facing sheet shear modulus, psi
S = Core height, inches
t_f = Facing sheet thickness, inches
ν = Poisson"s ratio
p = Mass density, snails/in^3
Gc = Core shear modulus in transverse and radial directions
μ = Running weight per unit width
t_{eff} = Effective flat plate thickness

The bending plate stiffness for a single isotropic plate is $D = Eh^2/12(1-\nu^2)$ where h is the plate thickness. The plate bending stiffness for facing sheets of equal thickness on honeycomb sandwich panels are derived from the following equation:

$$D = \frac{E\ t_f\ S^2}{2\ (1-\nu^2)}$$

The equivalent thickness of an isotropic plate is

$$t^3_{eq} = 6\ t_f\ S^2$$

It is easily seen that the most important structural properties are obtained by the geometric considerations. The most influential are the facing sheet thickness and core depth for sandwich material. The facing sheet thickness makes a significant weight contribution and the core depth contributes greatly to the stiffness values of the panel. The support points define the panel size.

The material properties are very significant. Young's modulus of elasticity varies from 2.6 x 10^6 psi for polyimide to 10.5 x 10^6 psi for aluminum and 16.5 x 10^6 psi for titanium. Thus for most purposes the metallic material could be preferred over synthetics; however, costs and fabrication problems present factors which influence material selection.

9.2.1.2 Flight Condition

The panel flutter calculations are made for the most critical regions encountered during flight. The trajectory determines the altitude, time, and Mach number where the maximum dynamic pressure occurs. The flutter calculations are made using these data. The NASA flutter criteria for determining the panel flutter boundaries are determined from the maximum dynamic pressure. For preliminary evaluations, the panel flutter calculations are made at the Mach number where max q occurred. This value is generally in the transonic speed range where the aerodynamic environment is very severe. The evaluations of panel structural design, support methods, and material properties have to be evaluated.

9.2.1.3 Panel Dynamic Properties

Natural frequencies and mode shapes of the protective panels are calculated for three boundary conditions: (1) using pinned supports with all edges free, (2) using pinned supports with two edges free and two edges simply supported, and (3) using pinned supports and all edges simply supported.

The geometry and finite element descriptions of a typical panel are presented in Figure 9.2.1.3-1. This panel is 62.75 inches wide and 66.47 inches long and has been divided by 14 rows and columns into 196 elements and nodal points. The basic structural properties of the panel have already been described.

Several subroutines were required to determine and plot the frequencies and mode shapes of the panel. The frequency variation for the first six modes of a polyimide panel as defined in Figure 9.2.1.3-1 are presented in Figure 9.2.1.3-2.

The panel with free-free edges, as expected, had the lowest frequencies. The first mode is 10.1 Hz and reaches 38.37 Hz at the sixth mode. The second one with two pinned edges is higher with a frequency value of 47.52 Hz for the first mode and 61.89 Hz for the sixth mode. The third case, with four pinned edges, has frequencies of 50.3 Hz for first mode and 9.12 Hz for the sixth mode.

Figures 9.2.1.3-3 through 9.2.1.3-8 present the frequencies and mode shapes of the six lower modes. The panel was supported at eight pinned points located within the panel. The edges were all free. It is seen that the motion is confined to the free areas located outside the boundaries of the support pattern.

Figures 9.2.1.3-9 through 9.2.1.3-14 present the frequencies and mode shapes for the panel supported at the eight pinned points and by the two pinned edges. Two edges on the panel are free. It is seen that the displacements are uniformly distributed along the panel outside the supports and depend on the mode of excitation.

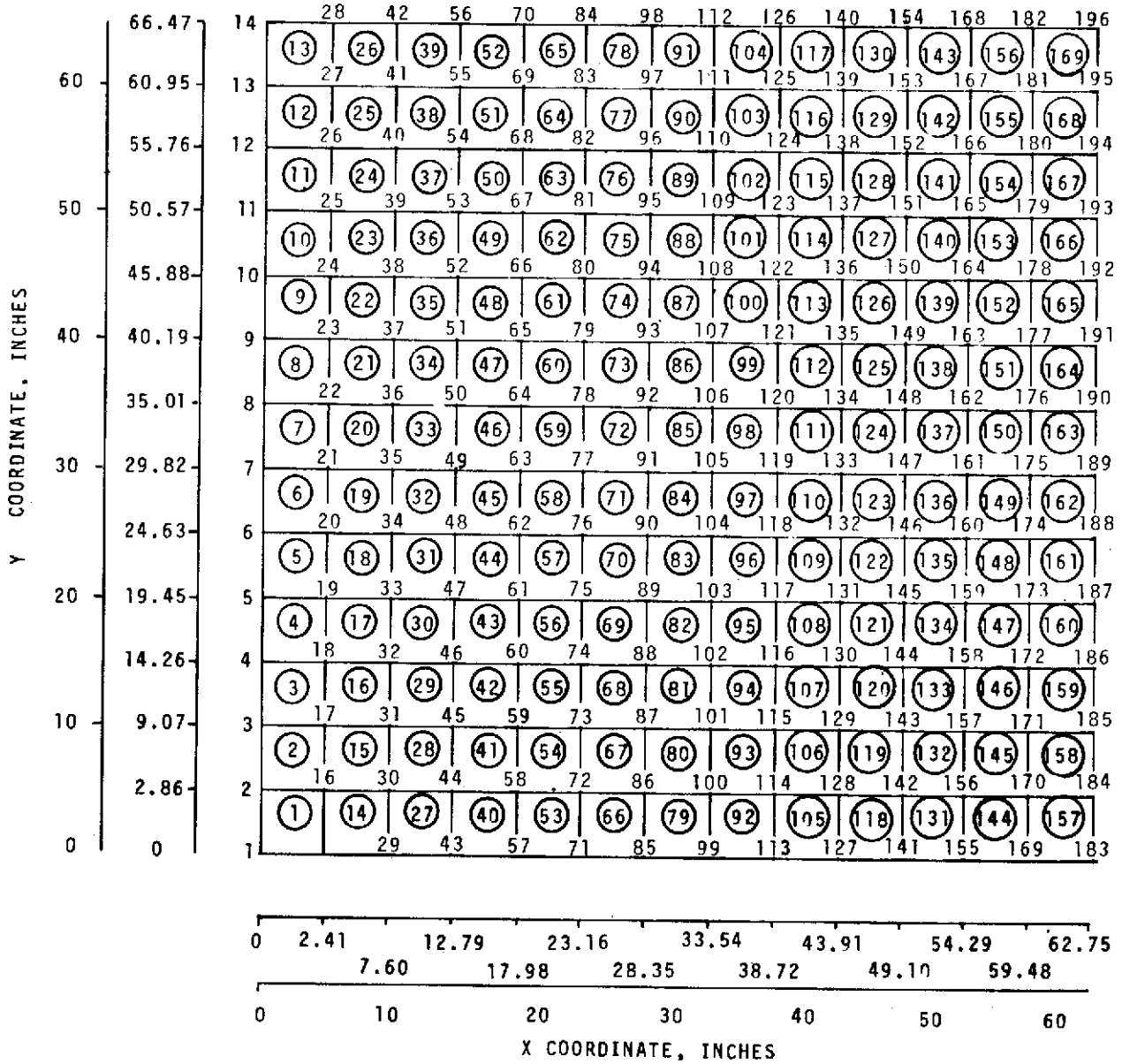

Figure 9.2.1.3-1. Aeroshear Erosion Carrier Panel Element and Node Point Matrix

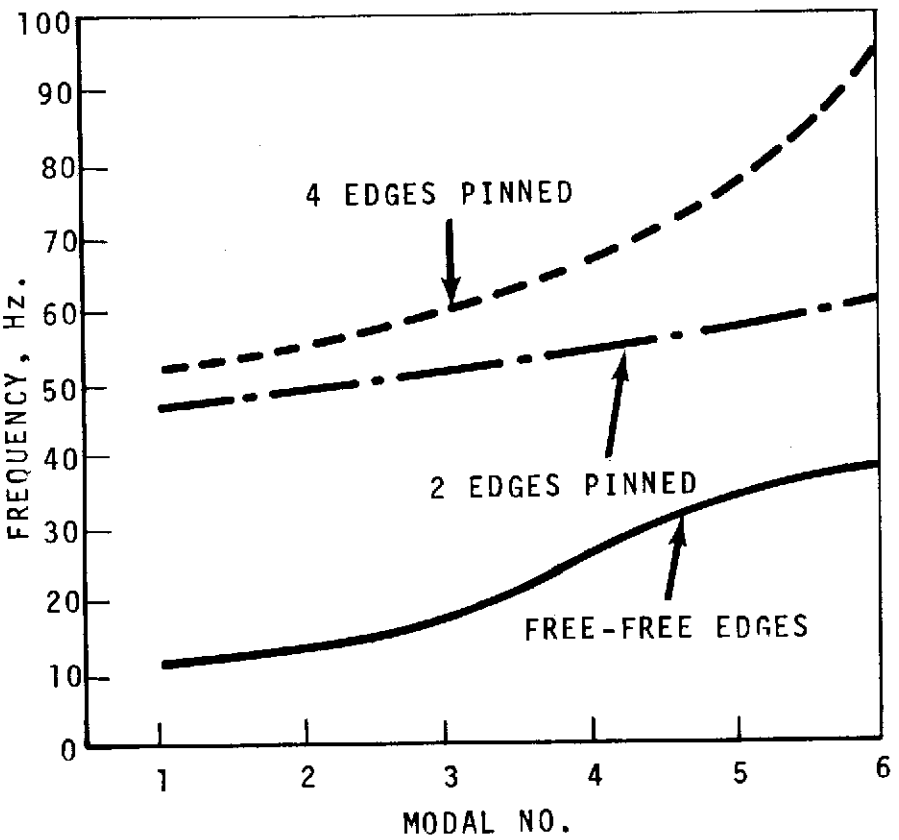

Figure 9.2.1.3-2. Frequency Variation of Three Different Boundary Conditions for Panel Simply Supported by Eight Pins

Figures 9.2.1.3-15 through 9.2.1.3-20 present the mode shapes and frequencies for the panel supported on all sides and at the eight internal pinned points. Again, it is seen that the panel displacements are uniquely defined by each mode. There are no displacements present at the panel supports; however, rotation of the elements about these supports is permitted.

Any change in the structural parameters of a panel has significant influence on the dynamics of the panel. The mode shapes are very sensitive to changes in the structure. In all the panel studies, the boundary conditions, number and location of support points, and structural parameters were obtained by performance of parametric studies to obtain the desirable panel design.

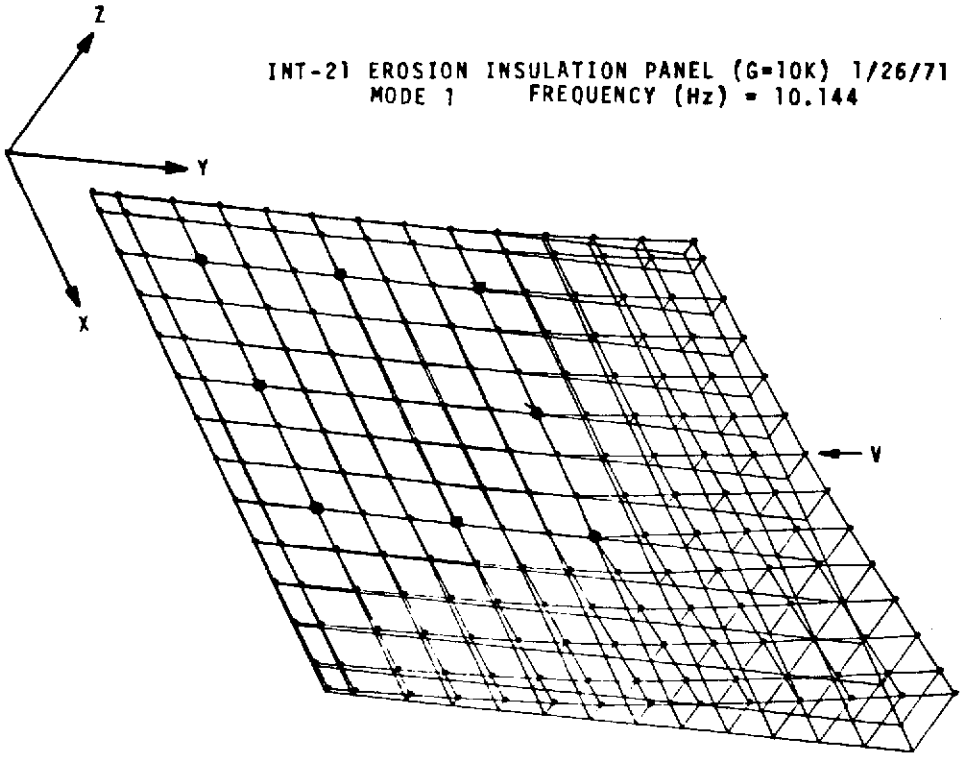

Figure 9.2.1.3-3. Panel With Eight Pinned Support Points and Free-Free Edges

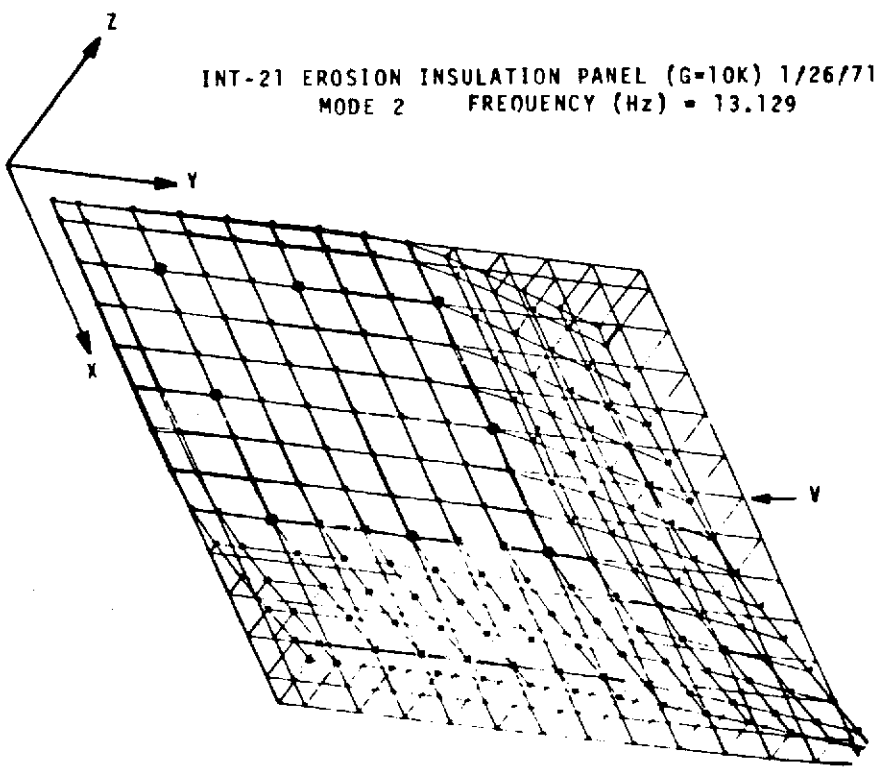

Figure 9.2.1.3-4. Panel With Eight Pinned Support Points and Free-Free Edges

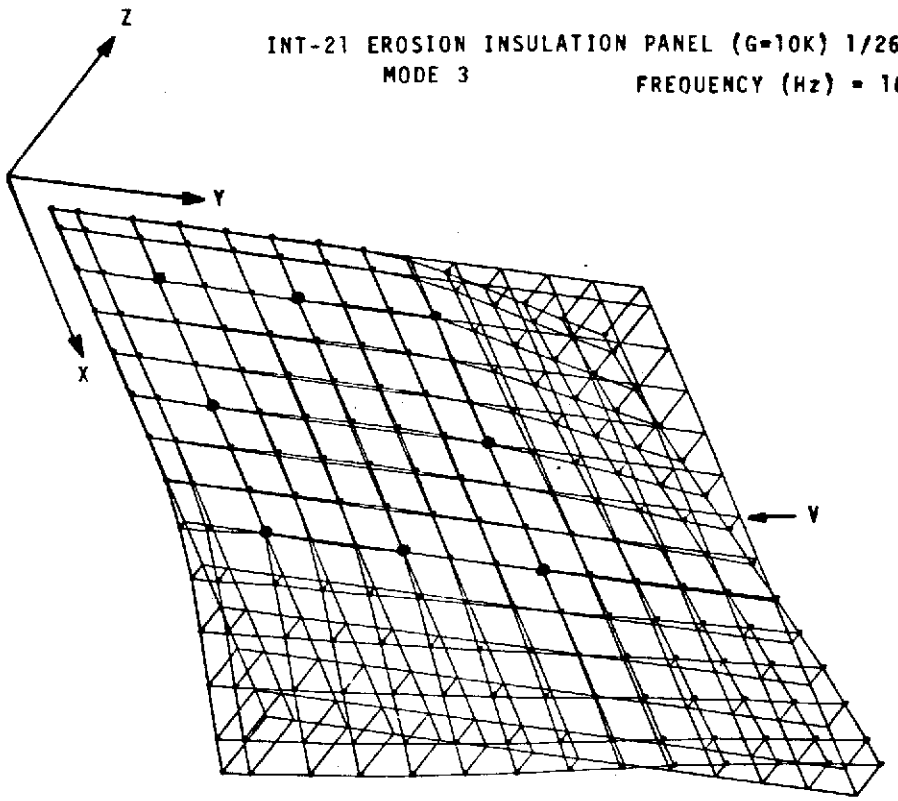

Figure 9.2.1.3-5. Panel With Eight Pinned Support Points and Free-Free Edges

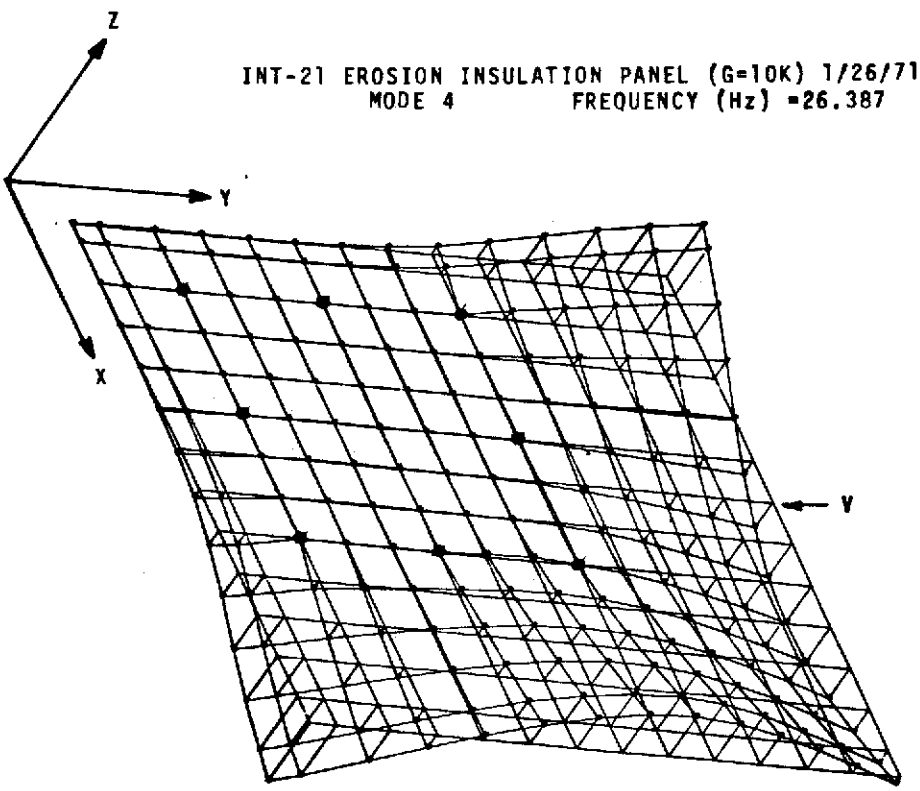

Figure 9.2.1.3-6. Panel With Eight Pinned Support Points and Free-Free Edges

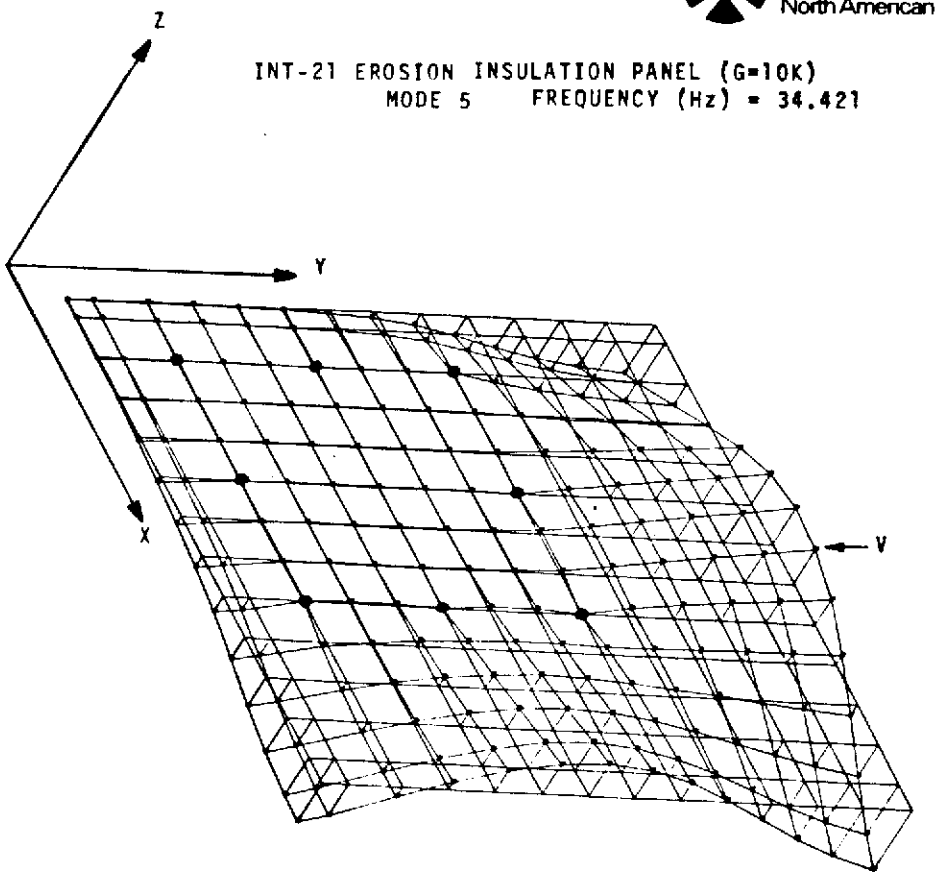

Figure 9.2.1.3-7. Panel With Eight Pinned Support Points and Free-Free Edges

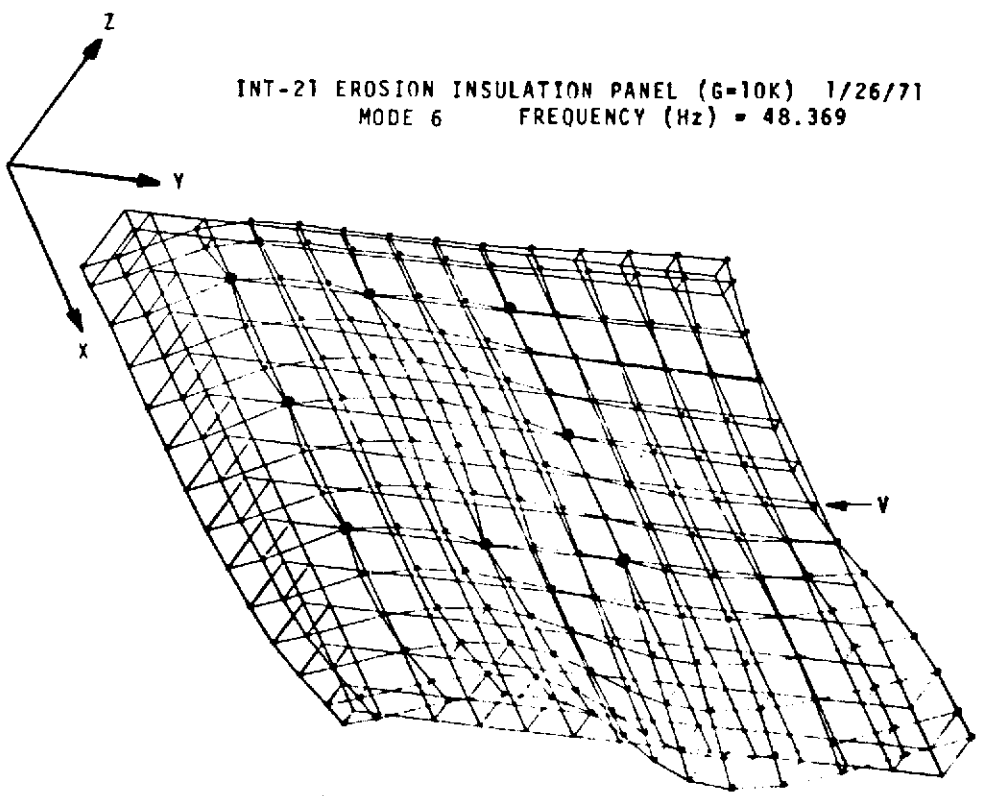

Figure 9.2.1.3-8. Panel With Eight Pinned Support Points and Free-Free Edges

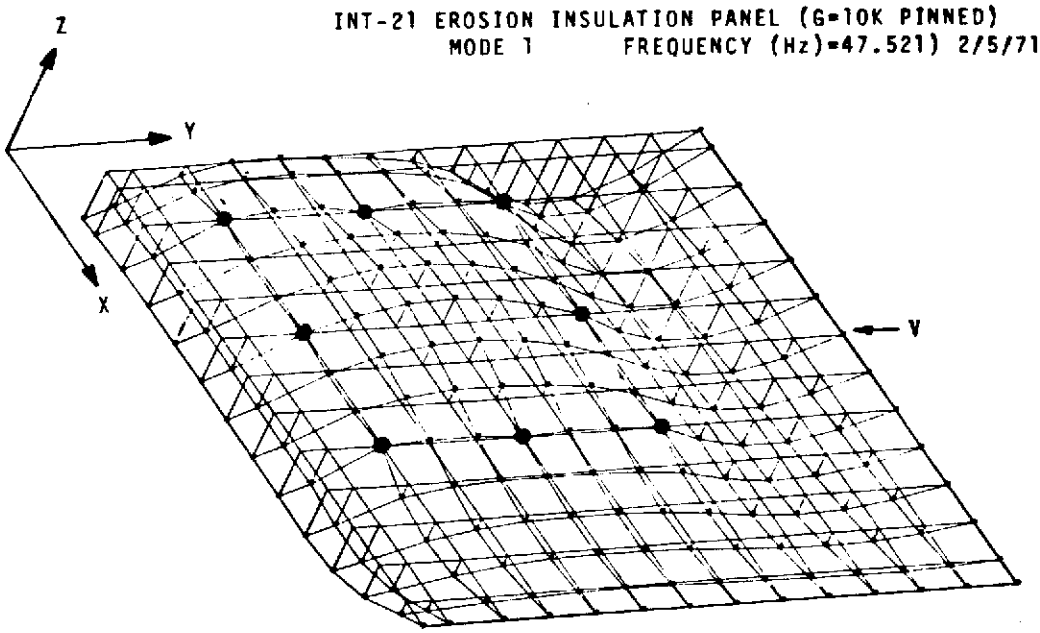

Figure 9.2.1.3-9. Panel With Eight Pinned Support Points and Two Pinned Edges

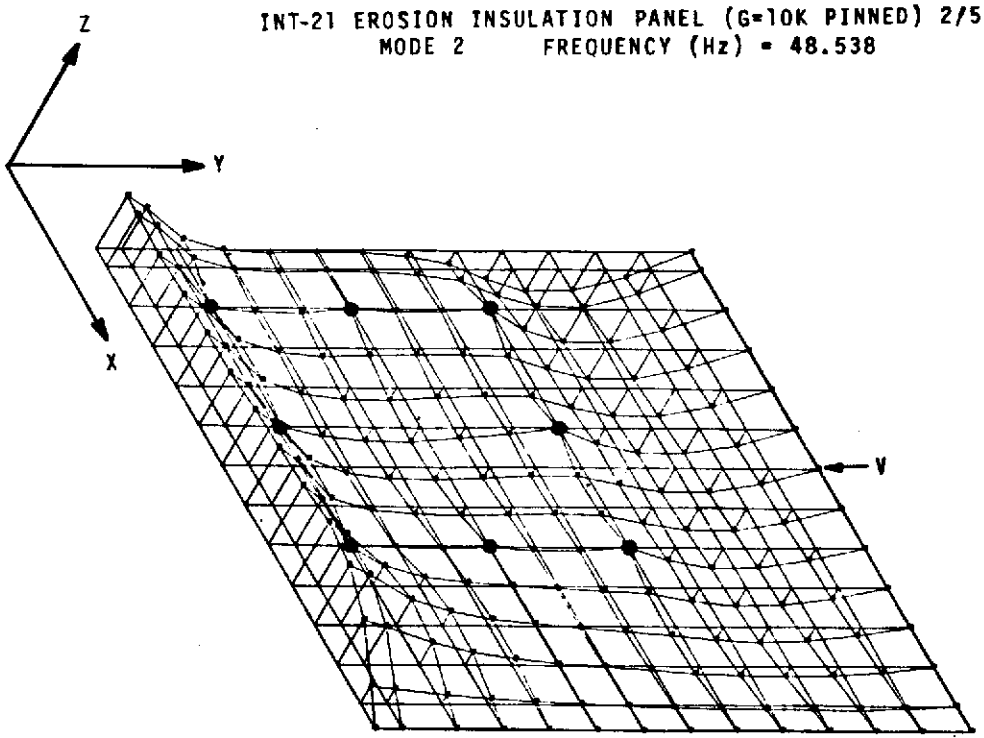

Figure 9.2.1.3-10. Panel With Eight Pinned Support Points and Two Pinned Edges

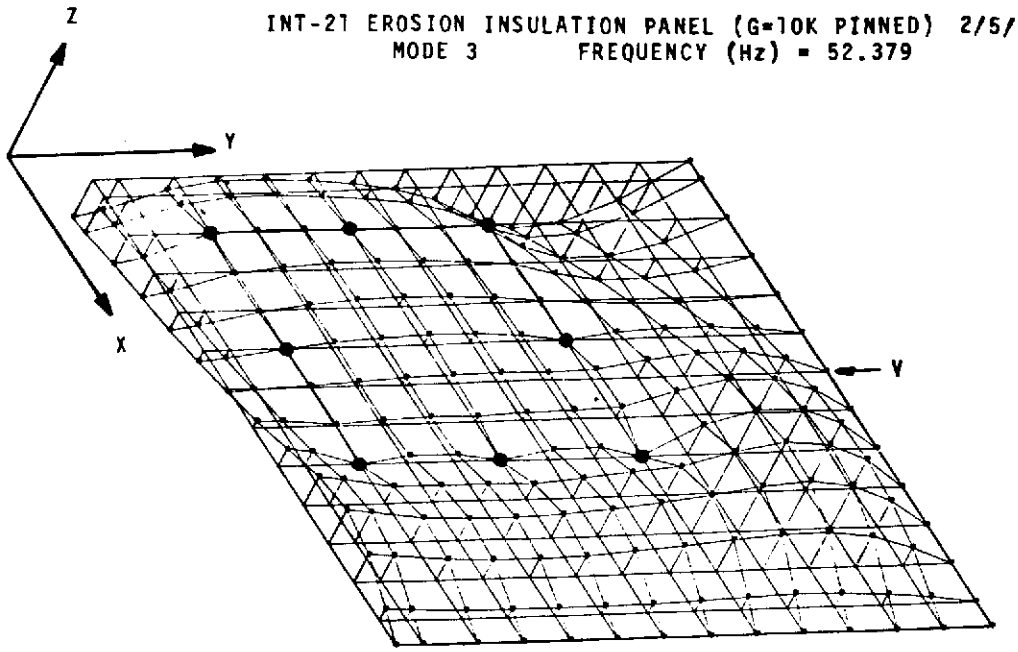

Figure 9.2.1.3-11. Panel With Eight Pinned Support Points and Two Pinned Edges

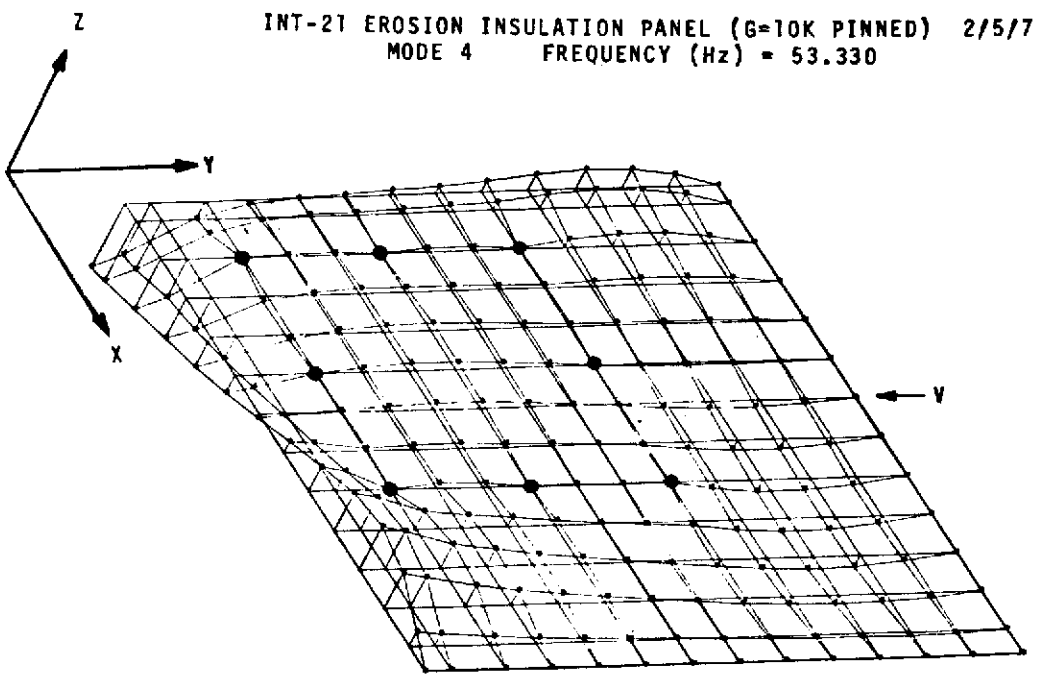

Figure 9.2.1.3-12. Panel With Eight Pinned Support Points and Two Pinned Edges

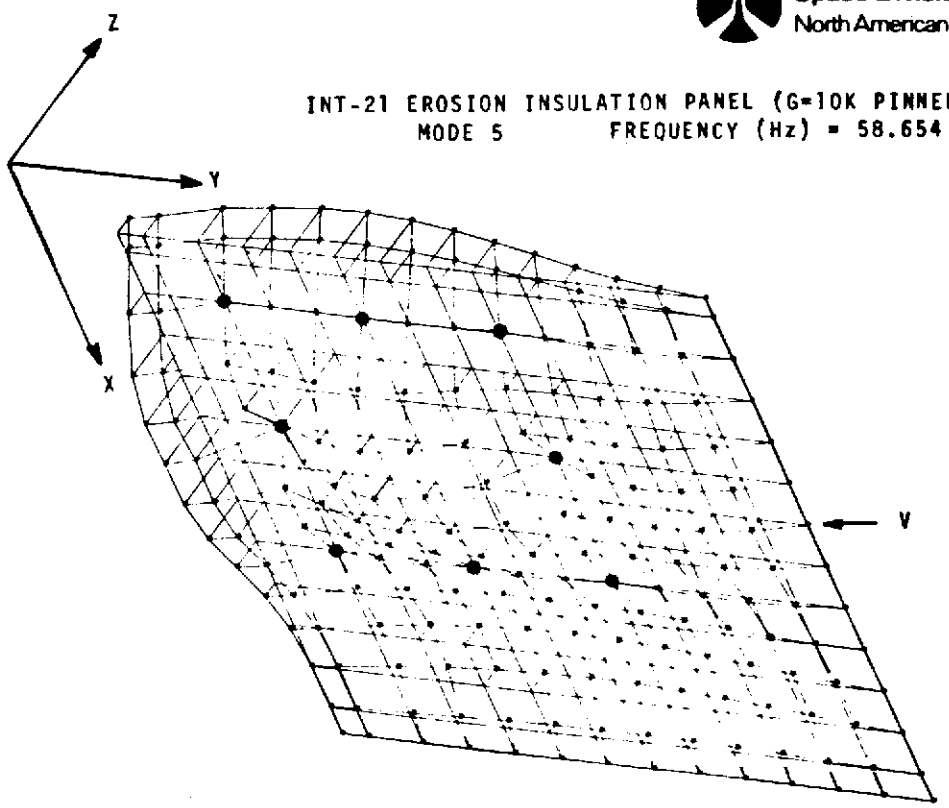

Figure 9.2.1.3-13. Panel With Eight Pinned Support Points and Two Pinned Edges

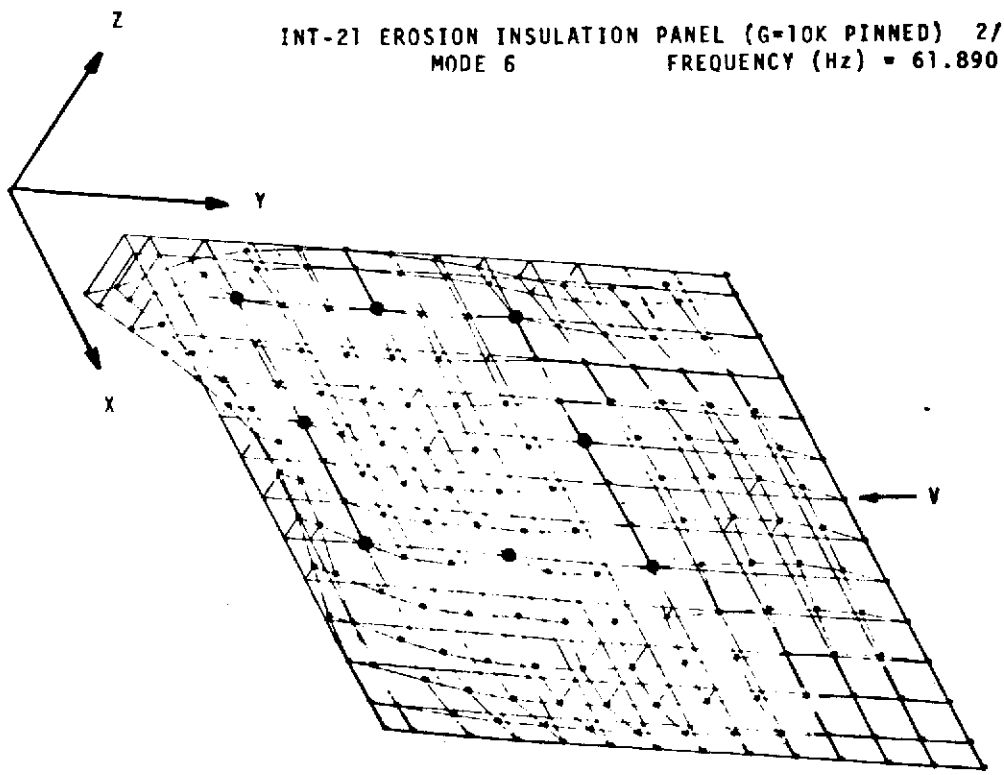

Figure 9.2.1.3-14. Panel With Eight Pinned Support Points and Two Pinned Edges

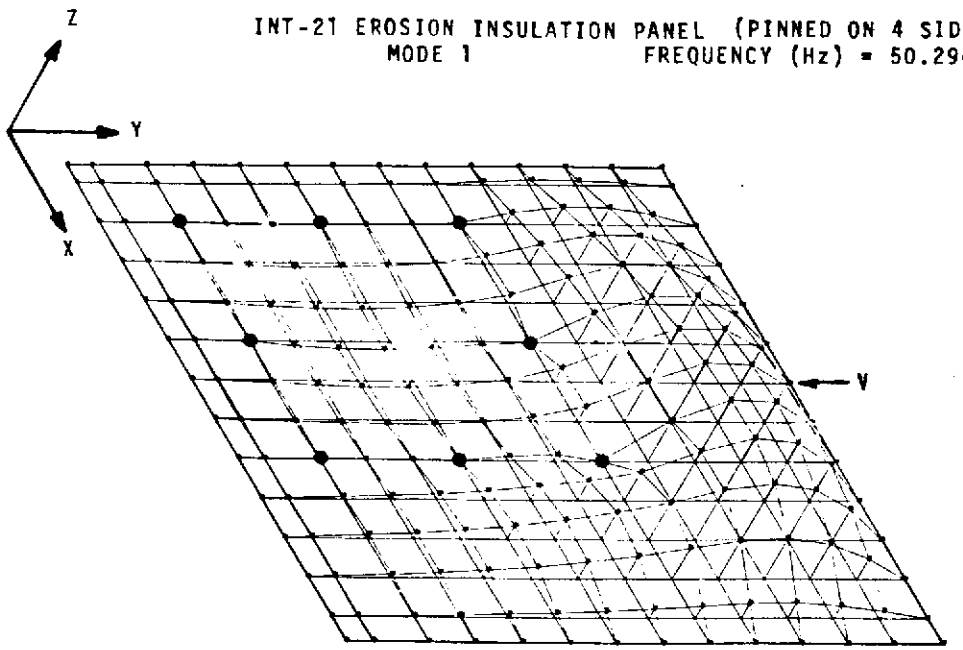

Figure 9.2.1.3-15. Panel With Eight Pinned Support Points and All Edges Pinned

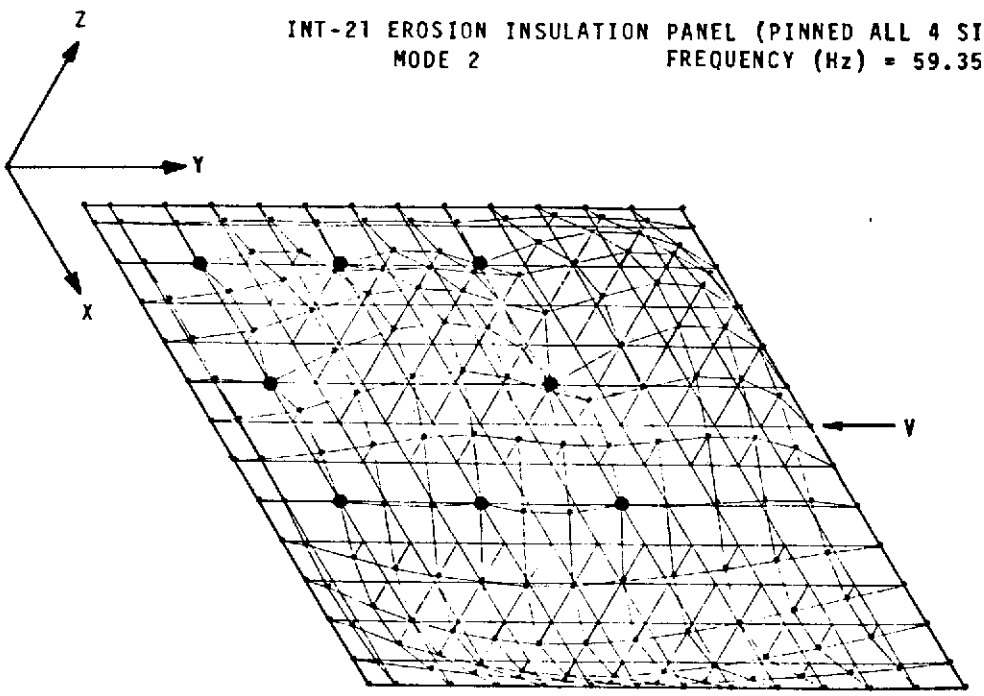

Figure 9.2.1.3-16. Panel With Eight Pinned Support Points and All Edges Pinned

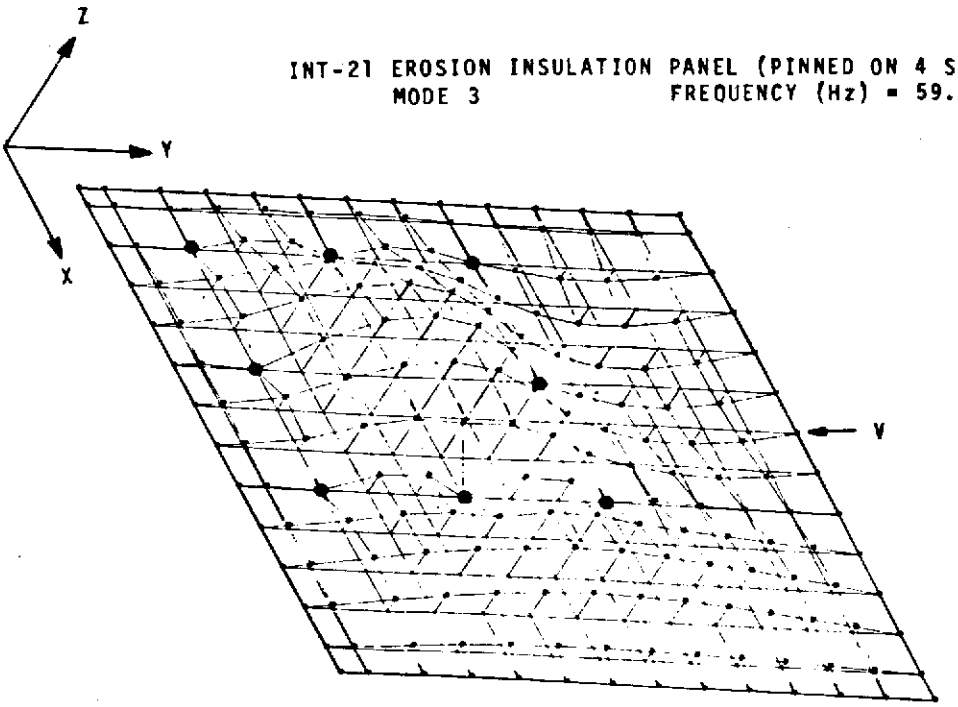

Figure 9.2.1.3-17. Panel With Eight Pinned Support Points and All Edges Pinned

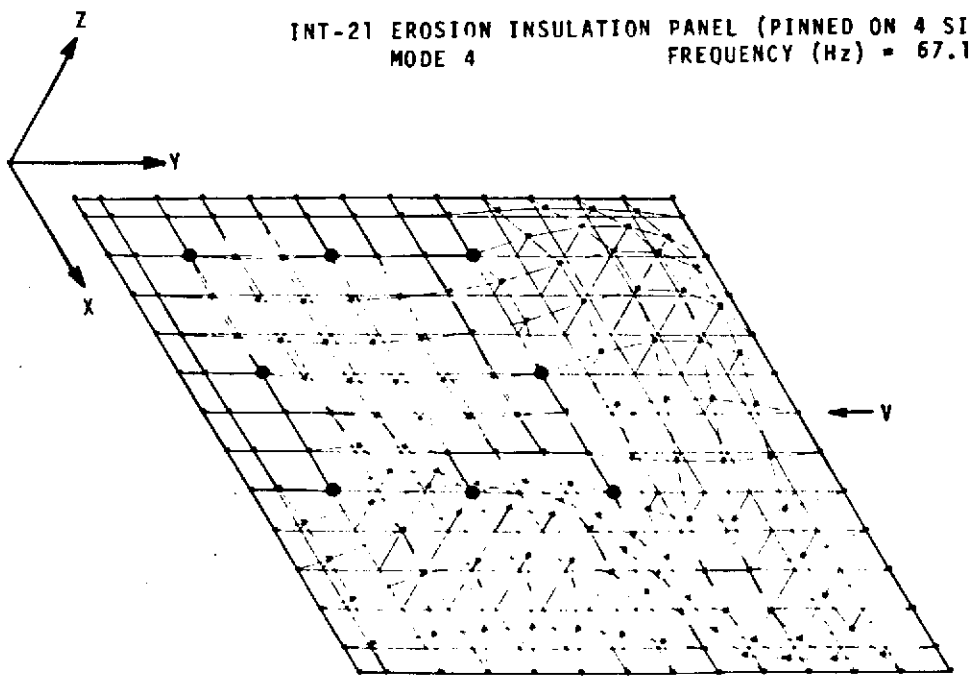

Figure 9.2.1.3-18. Panel With Eight Pinned Support Points and All Edges Pinned

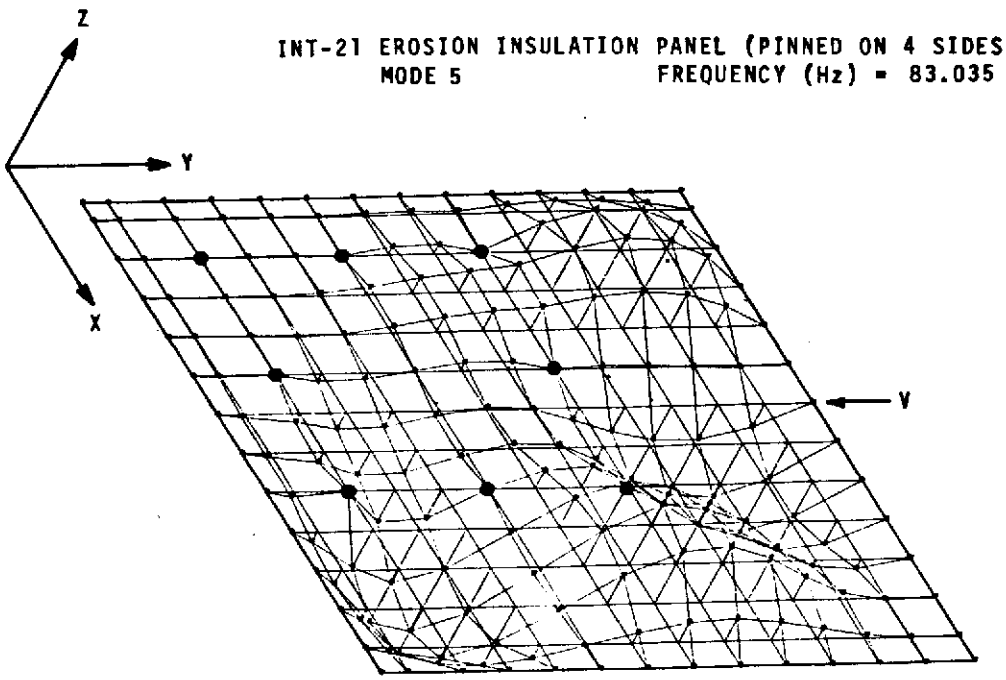

Figure 9.2.1.3-19. Panel With Eight Pinned Points and All Edges Pinned

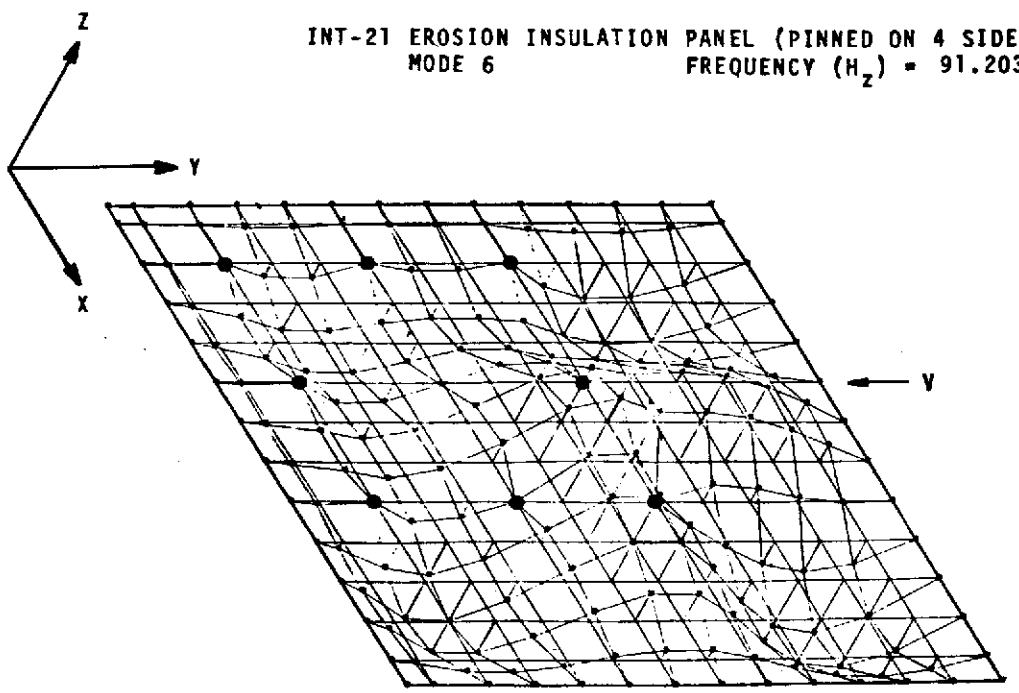

Figure 9.2.1.3-20. Panel With Eight Pinned Points and All Edges Pinned

9.2.2 Flutter Calculations

Preliminary flutter analyses have been performed on the high-performance insulation panels to assist in the basic design problems involving dimensional tradeoffs, basic support requirements, and geometrical considerations that might have some detrimental flutter influence. The flutter analysis is based on current analytical and empirical information available in the literature and the trajectory profiles defined for missions using these insulation systems.

9.2.2.1 Criteria

To satisfy the requirements for panel flutter stability, the NASA criteria have been used in all the panel flutter analyses. The criteris simply state that the panel should be designed so that the dynamic pressure where flutter occurs should be 50 percent higher than the maximum local dynamic pressures obtained in flight.

9.2.2.2 Flutter Equations

In derivation of the panel flutter equations, the basic differential equations assume small deflection thin plate theory which governs the equilibrium between the spring and the air loading.

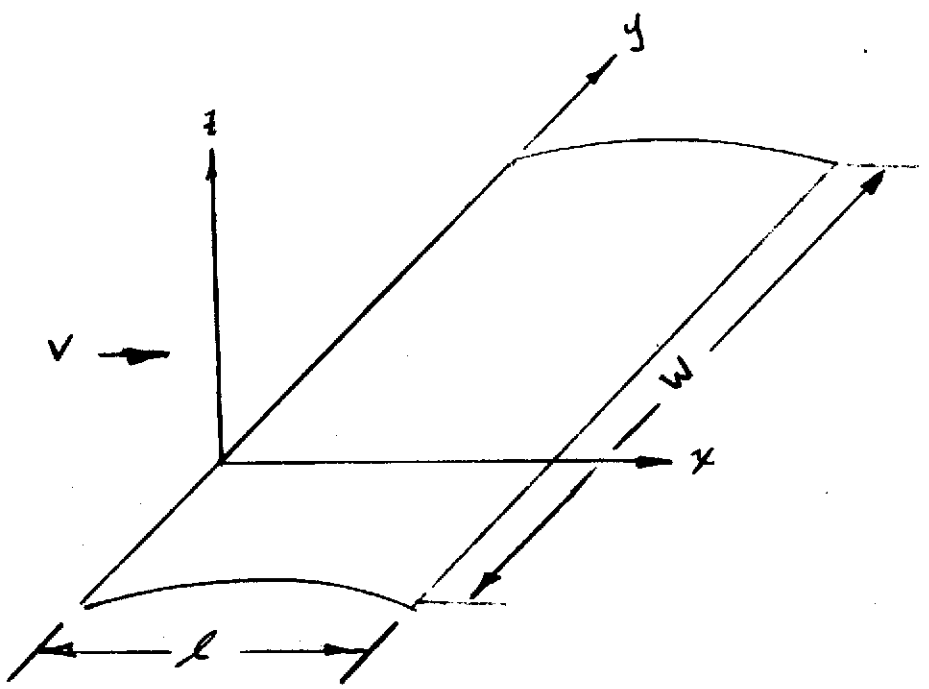

$$D\nabla^4 Z + Nx\, Zxx + Ny\, Zyy + MZtt = \frac{2}{\beta} q\, Zx$$

The air loading is shown on the right-hand side of the equation and is obtained by two dimensional static aerodynamics. The panel deflection shape is assumed to be in the following form:

$$\bar{Z}\ (x,y,t) = \bar{Z}_n\ (x)\ \sin\frac{nTl\ y}{w}\ i\ wt$$

and satisfies the simply supported boundary conditions at the edges.

After several transformations, the equation of motion is reduced to the following form:

$$\frac{\partial^4 \bar{Z}n}{\delta\xi^4} + A\frac{\partial^2 Zn}{\delta\xi^2} + \lambda\frac{\partial \bar{Z}n}{\delta\xi} - B\ \bar{Z}_n = 0$$

In characteristic form it is: $M^4 + AM^2 + \lambda N - B = 0$

and has two real roots, one positive and one negative and a pair of complex conjugates written as follows:

$$M_1 = -\alpha + \varepsilon \qquad M_3 = \alpha + i\ \delta$$

$$M_2 = -\alpha - \varepsilon \qquad M_4 = \alpha - i\ \delta$$

$$\delta = \sqrt{\frac{\lambda}{4\alpha} + \alpha^2 + \frac{A}{2}}$$

$$\varepsilon = \sqrt{\frac{\lambda}{4\alpha} - \alpha^2 - \frac{A}{2}} \qquad \beta = \sqrt{\frac{\lambda^2}{16\alpha^2} - 4\left(\alpha^2 + \frac{A}{4}\right)^2}$$

After the solution of the equation of motion is obtained in terms of the characteristic roots, the boundary conditions of the panel are substituted and the following transcendental equation is obtained:

$$\left[(\varepsilon^2 + \delta^2)^2 + 4\alpha^2\ (\delta^2 - \varepsilon^2)\right]\ \sin\delta\ \sinh\varepsilon = 8\ \alpha^2\varepsilon\delta\ (\cosh\varepsilon\ \cos\delta - \cosh 2\alpha)$$

To get a solution, A and λ and set and α is varied to satisfy the transcendental equation. The flutter point solutions of the transcendental equation is determined continusouly as λ is increased from 0. When λ reaches the point where the roots become complex, one root is unstable resulting in a flutter condition. It is at this value of where coalescence of the two lower modes take place.

Mach number and panel thickness correction factors have been incorporated in this flutter program to provide more exact solutions. The flutter frequencies and dynamic pressure are obtained from the solution of the transcendental equation.

9.2.2.3 Results

Flutter analyses were performed for numerous combinations of design conditions which included systematic variation of geometric, material, and support

parameters. For each of these studies, the frequencies and dynamic pressure where flutter occurred were determined. Structural and geometric parametric studies included varying individually the facing sheet thickness, core depth, plate bending stiffness, length, and width. Although several types of synthetic materials were considered, the flutter analyses were performed for titanium, aluminum, and polyimide panels.

Figures 9.2.2.3-1 and 9.2.2.3-2 present several typical methods of presenting the flutter results. Figure 9.2.2.3-1 presents the dynamic pressure where the panel flutters as a function of 1/w ratio for a panel with a fixed size and facing sheet thickness. A family of core sizes for these design conditions present the designer several alternative selections available. Figure 9.2.2.3-2 presents similar information with core depth and facing sheet thickness being held constant for varying values of 1/w. A family of panel lengths are shown here provide several alternative selections for defining the panel design.

Figure 9.2.2.3-3 presents an additional method of evaluating the analyses results. The panel stability (dynamic pressure at flutter) for panels of varying widths is plotted as a function of the panel length for fixed facing sheet thickness and core depth. These results provide the designer with adequate information necessary to detail the installation and functioning features required. The support spacing, panel dimensions, and material properties are defined so that an intelligent selection of a stable panel can be made.

9.3 DATA EVALUATION

The results of the flutter analysis are evaluated to provide for the establishment of adequate guidelines in obtaining a stable panel design. These results can be grouped into several categories which include geometric material and attachment effects. Each of these catagories makes significant contributions to the flutter stability of the panels.

9.3.1 Geometric Effects

Panel geometry changes are continuously being made. This is due to installation, operational, and functional requirements which require extensive redesign. The primary panel size is determined from these requirements. In general, the panel flutter analysis can be performed as these basic design requirements are being satisfied. The panel size (length and width) are selected so that installation requirements are satisfied. The panel thickness is also determined so that it satisfies the functional and operational requirements. The panels are analyzed for flutter and the geometry is evaluated for its influence on the flutter characteristics.

From the basic description (i.e., a panel of a given length and width ratio), the geometry of the panel can be systematically varied. When the panel length (1/w) increases, the dynamic pressure where panel flutter occurs is reduced and the panel becomes less stable. The panel length should be large enough to keep the dynamic pressure values above the flutter stability margins. When the length is reduced, the panel flutter dynamic pressure is increased, thereby making the panel more stable. These conditions can be obtained from numerous variations of panel lengths and widths in order to satisfy the basic design requirements.

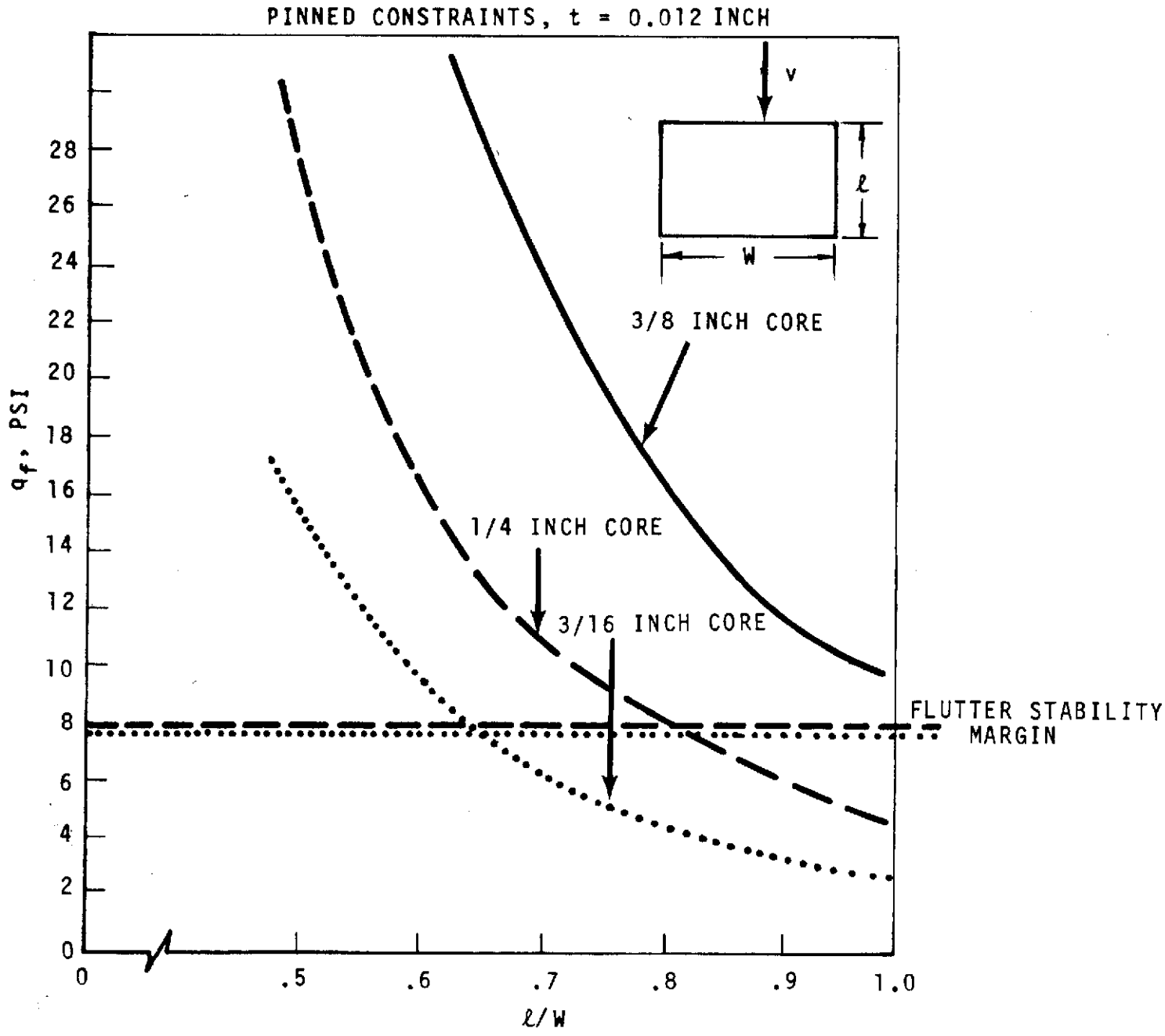

Figure 9.2.2.3-1. 30-Inch Wide Rectangular Panel Results for Varying L/W Ratios

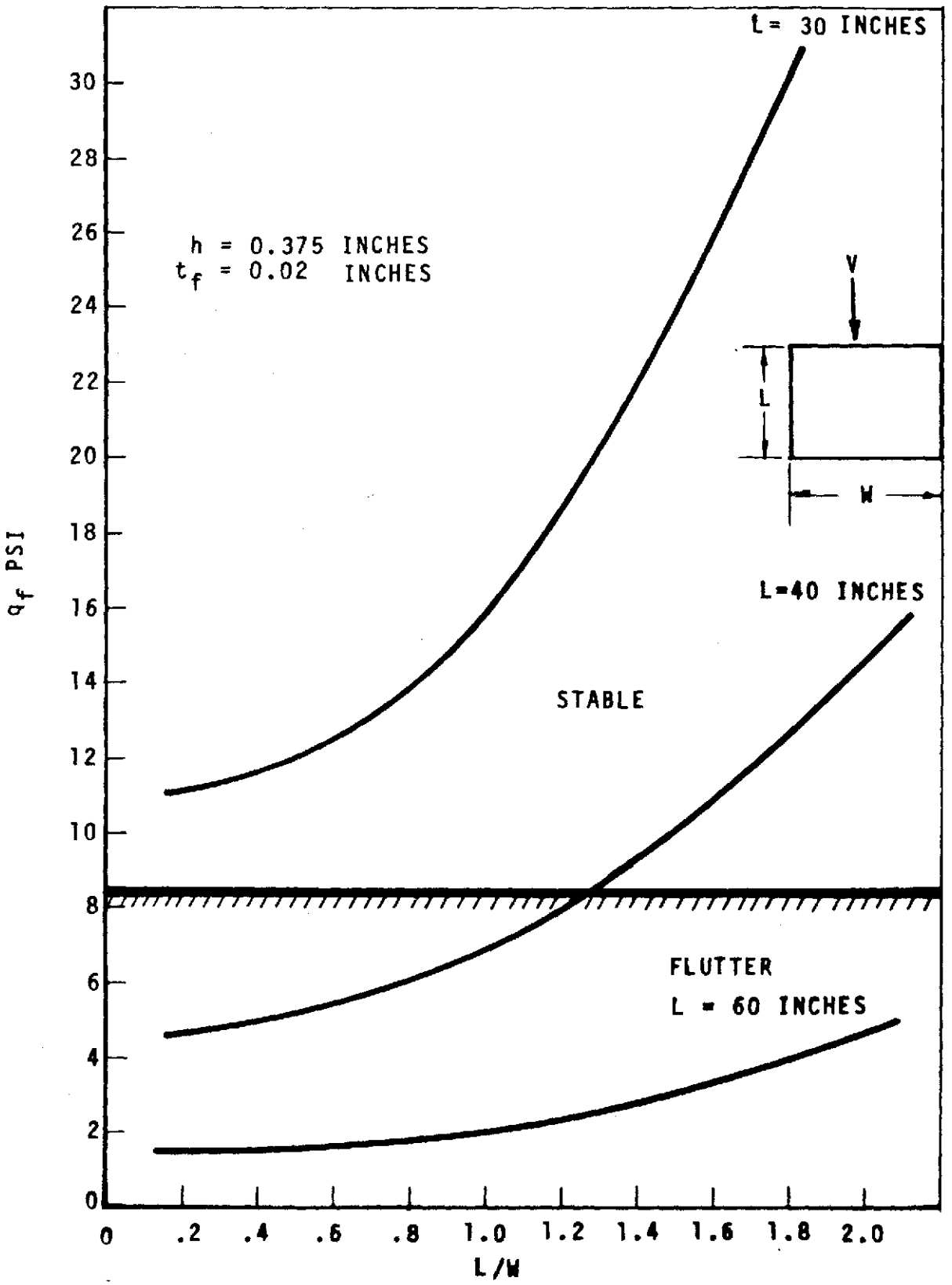

Figure 9.2.2.3-2. CIS Panel Flutter Studies

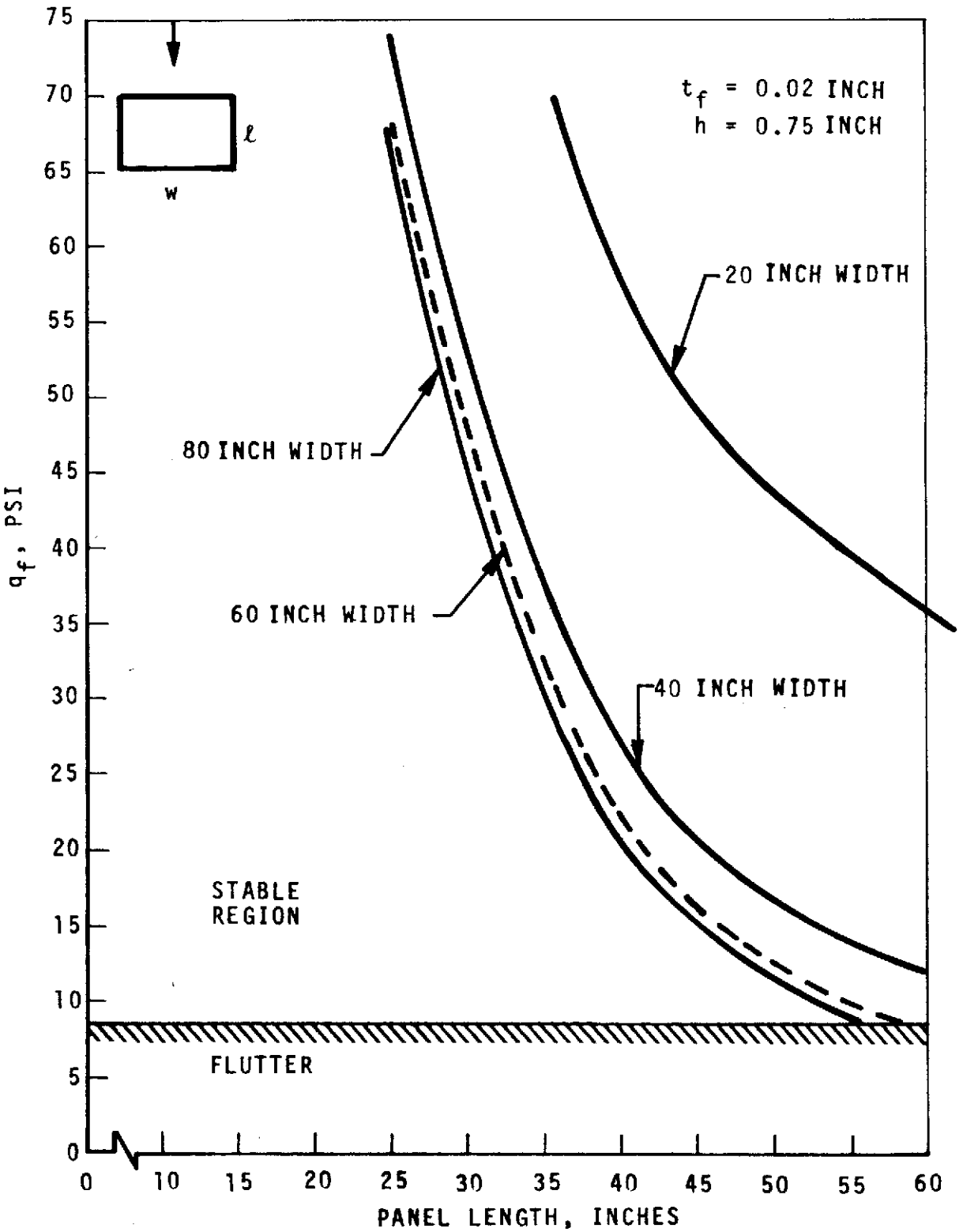

Figure 9.2.2.3-3. CIS Panel Flutter Analysis

Panel thickness variations are incorporated in several ways for sandwich panels. The panel thickness variations are performed by increasing the core depth, increasing the facing sheet thickness, or both. The variation in core depth is the most attractive in that the plate bending stiffness is substantially increased with a very small weight penalty. As the core depth is increase, the plate bending stiffness is increased by the square of the core depth. This large increase in stiffness causes the dynamic pressure where the panel flutters to increase very rapidly, thereby creating a stabilizing influence on the design. On the other hand, decrease in core depth has a destabilizing influence and causes the flutter dynamic pressure to decrease rapidly. The effectiveness of these two parameters, length and core depth, is illustrated in Figure 9.3.1-1. The example presented is for a 30-inch wide polyimide panel that was used in an S-II derivative study.

For a given panel thickness, if 1/w is held fixed, flutter stability decreases for the baseline panel as the width is increased. This condition simply states that smaller panels are less prone to flutter at a given critical dynamic pressure than larger panels. The major point is that to obtain the proper panel dimensions, the largest panel width possible should be obtained. Then the length and depth should be defined. To do this, several families of the appropriate parameters are required. One example of this procedure is presented in Figure 9.3.1-2. This illustration defines the variation of panel width and core depth for a defined S-II derivative vehicle panel. The designer has the option of selecting several sizes for a given configuration of established 1/w and thickness.

The facing sheet dimensions are also incorporated in the geometrical effects. Increasing facing sheet thickness contributes to flutter prevention by increasing plate bending stiffness. This variation also increases the weight of the panel and does little to improve the panel flutter characteristics. The initial approach to determining the desired facing sheet thickness is to obtain the initial value and perform parametric evaluations. For a typical design condition, the panel width and core height are held fixed. At a given value of t_f, the panel length, (1/w), is varied. As the length (1/w) increases, the panel becomes less stable. For a different value of t_f, the process is repeated and it is noted that the results improve slightly. Figure 9.3.1-3 illustrates the flutter results for a family of facing sheet thickness variations. At a given value of 1/w it is seen that the facing sheet thickness variations are not significant unless 1/w is low. These contributions to panel stability can provide large limitations to the panel design unless other geometric constraints are relaxed.

It has been demonstrated that geometric effects have a significant role in obtaining a stable panel. The panel size and dimensions should be optimized to insure that the panel design meets all the flutter requirements.

9.3.2 Material Effects

The question of what material to use in protective panels has to be examined continuously. The type of protection desired generally defines what material to use. If the panels are to be protected from flutter during ascent, the selection can be made from a large assortment of materials. If the requirements are for meteoroid protection, other types of material, depending on the

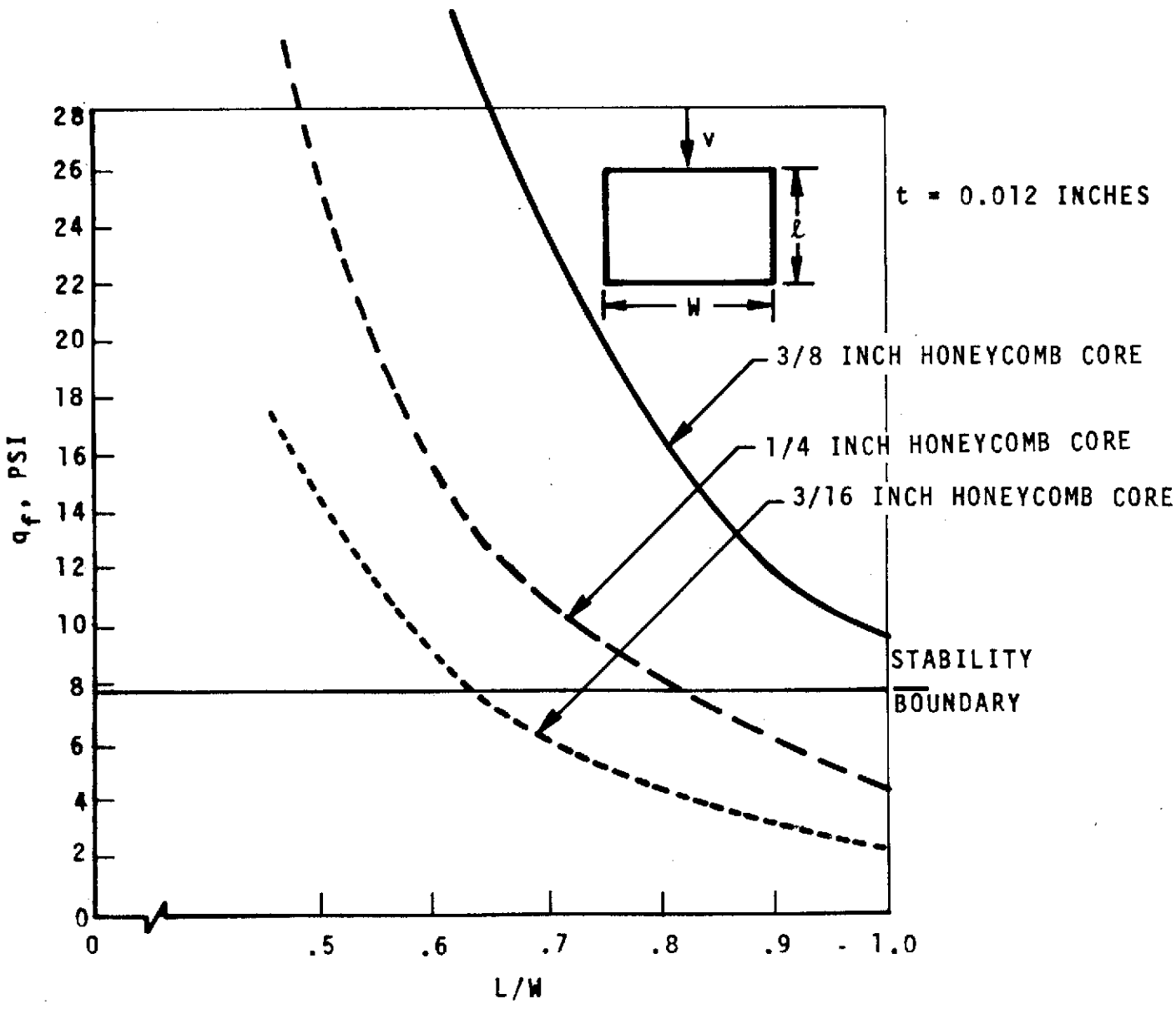

Figure 9.3.1-1. 30-Inch Rectangular Panel Stability Results for Varying L/W Ratios, Pinned Constraints

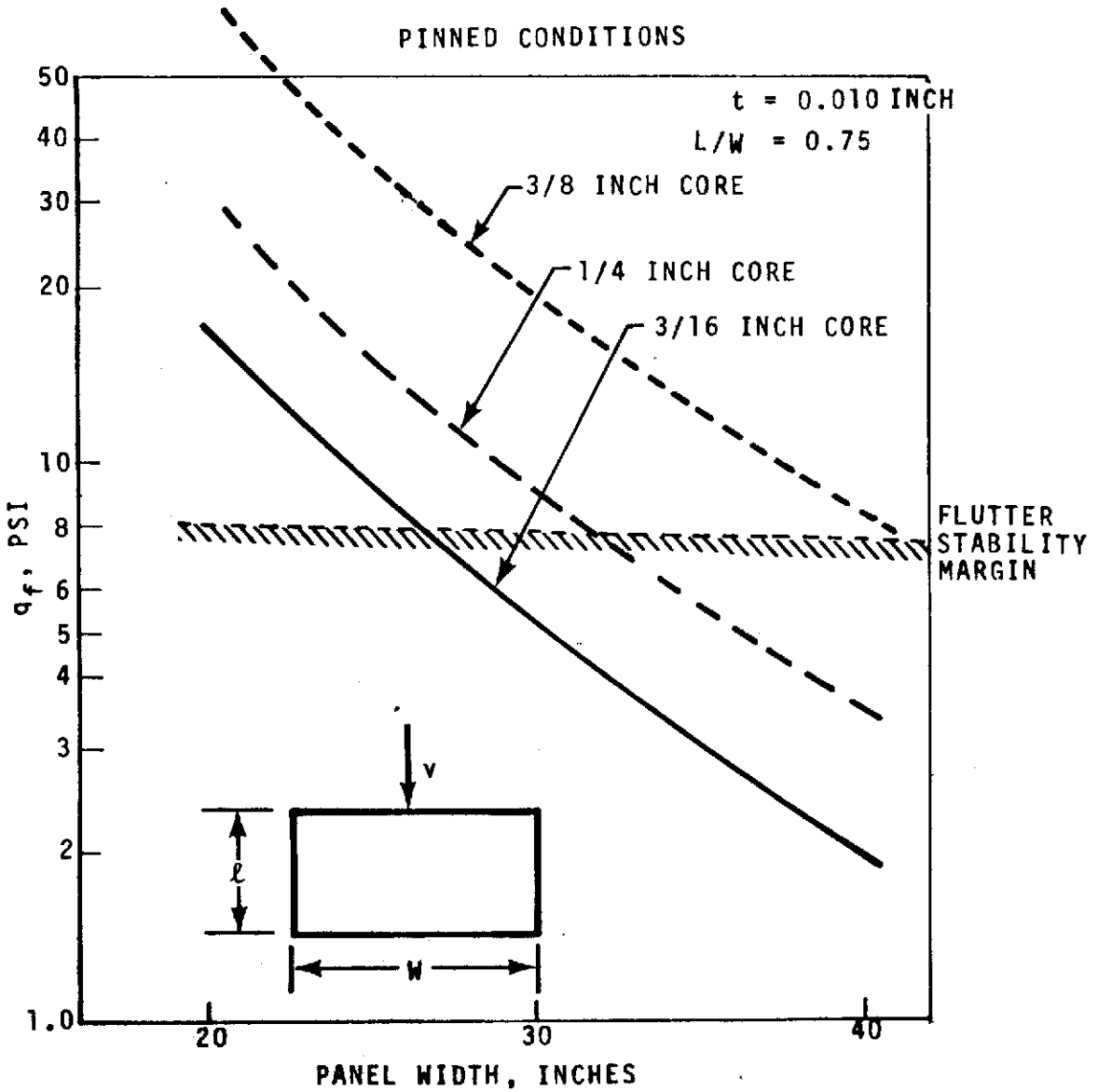

Figure 9.3.1-2. Rectangular Panel Stability Results

size, speed, and energy of the meteoroids, will have to be considered. For purposes of flutter stability, only three types of lightweight material have been studied. These included aluminum, titanium, and polyimide. The principal differences were their elastic properties. Young's modulus of elasticity for polyimide is 2.6 x 10^6 psi, for aluminum 10.5 x 10^6 psi, and for titanium 16.4 x 10^6 psi. The large differences in modulus of elasticity have a significant influence on the plate bending stiffness and flutter results. Titanium is the most desirable material and the most expensive. There are problems associated with bonding and processing of titanium into sandwich panels. Polyimide is inexpensive and easy to manufacture and has large appeal from the cost standpoint. The use of titanium panels allows the panel sizes to be larger than those of other materials. It also allows for ewer supports posts which contribute to heat flow into the fuel tank that is being insulated.

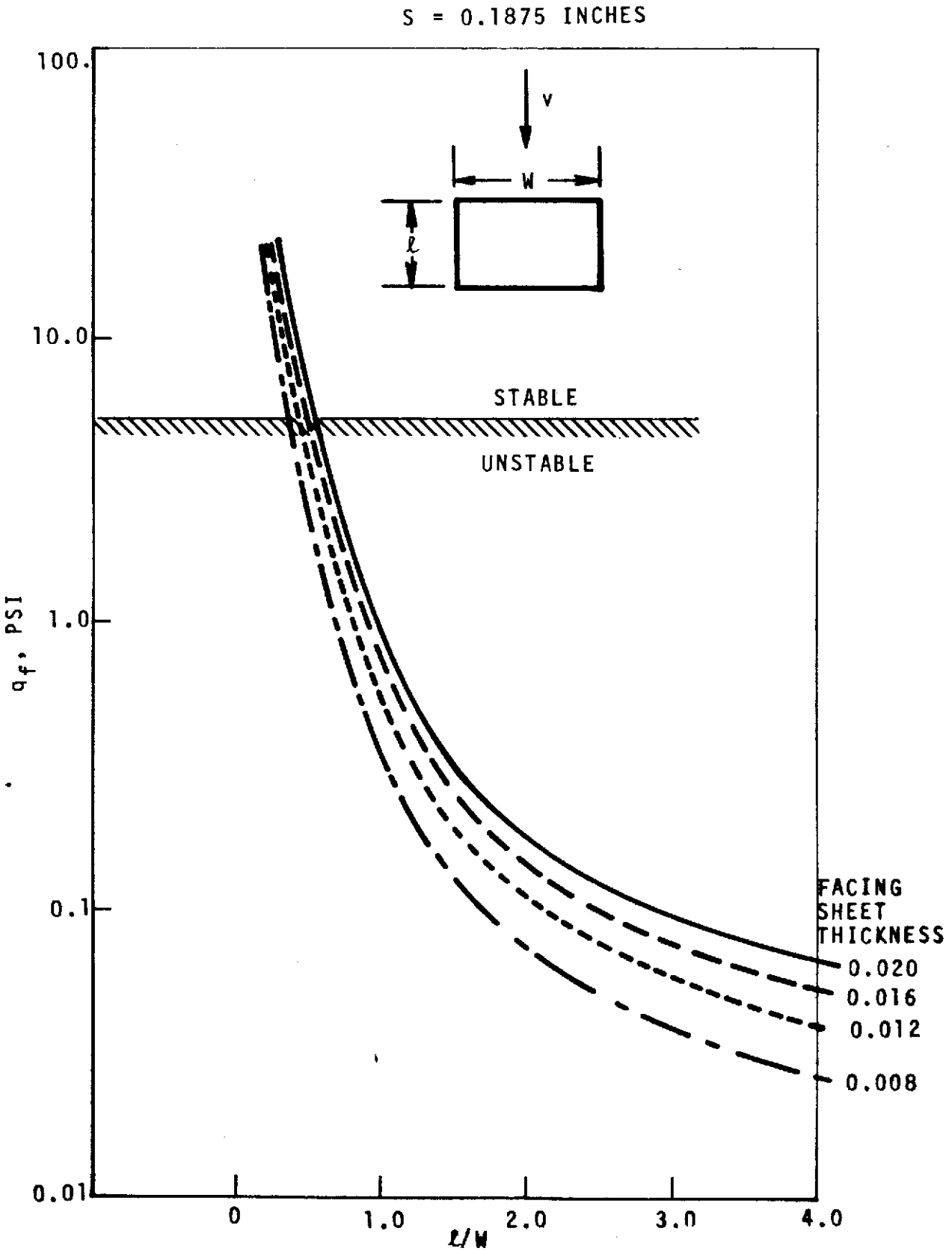

Figure 9.3.1-3. Panel Flutter Stability for 60-Inch Width, Core Height 0.1875 Inch

From a technical viewpoint, titanium has many advantages which make it a prime contender for use as insulation protective panel. Polyimide, on the other hand, requires more support points and has a lower plate stiffness but is less expensive. Aluminum is between the two materials in desirability. The designer can exercise an option on material. If the protective needs can be satisfied with geometric variations, polyimide should be considered. If other mission and design requirements are not satisfied with polyimide, then aluminum, titanium, or other materials will have to be considered.

9.3.3 Attachment Effects

The boundary conditions of the panels have a significant influence on the flutter stability of a panel. Generally, panel supports are described in terms of pinned or clamped conditions at the boundary.

Rows of bolts or rivets which support the panels at the inboard regions form sub-panels which are analyzed to define their stability properties. The support spacing is defined by the size of the sub-panels. It is important to keep the support spacing separated as far as possible to reduce the heat flow into the tank.

It is possible to overdesign a panel with numerous support points. This can be done simply by using several rows of supports closely spaced. However, the panel will be a heat source and all the high-performance insulation will not be used adequately and the mission requirements will not be met. On the other hand, insufficient support points will cause the panel to flutter, thereby destroying all the insulation and causing the mission to fail. The desirable design will hold the panels with enough supports to allow for redundancy. This type of panel support system requires flutter analysis evaluation from the inception of the design. Tests to evaluate the flutter characteristics of the panels should be performed on wind tunnels, acoustic chambers, or flight. These tests will insure the adequacy of the design.

9.4 SUMMARY

Specially designed insulation protective panels have been adequately analyzed for S-II derivative missions. These studies have provided the selection of optimal geometric, material, and support conditions by performance of parametric evaluations. The flutter analysis is preliminary and should be expanded to include angle of attack correction factors, curvature and cavity effects, and temperature differential considerations. Wind tunnel tests are required to evaluate and verify the analytical results.

Dynamic and acoustic data used in the insulation panel evaluation have been obtained from Saturn-Apollo flights and S-II static firing test data. The panel dynamic characteristics have been calculated using programs available in the Space Division. These results are in good agreement with exact solution calculations.

10.0 MATERIAL PROPERTIES

This section presents in graphic form the mechanical and physical properties of materials used in support of the Saturn S-II program. All data points graphically illustrated (indicated by symbols) were generated by tests in North American Rockwell laboratories. Only material properties with related test points could be graphically illustrated. Additional information may be obtained by use of a computer program (Section 15.0). The maximum and minimum values were plotted for each specific temperature tested, along with the average value of all specimens tested at that temperature. Because of insufficient data points, the curve between available data points is extrapolated based on previous experience with the characteristic of the material property being shown. Information pertaining to the thermal properties of the various materials may be found in Section 12.0

10.1 MATERIALS

The materials and their available test properties are given in Figures 10.1-1 through 10.1-38. The materials are:

a. Honeycomb composite for helium purge foam insulation system (Figures 10.1-1 and 10.1-2)

b. Lamination of phenolic glass/nylon (Figures 10.1-3 to 10.1-13)

c. Honeycomb core (Figures 10.1-14 to 10.1-18)

d. Adhesives (Figures 10.1-19 and 10.1-20)

e. Ablative (Figures 10.1-21 and 10.1-22)

f. Fabrics (Figures 10.1-23 and 10.1-24)

g. Foams (Figures 10.1-25 through 10.1-38)

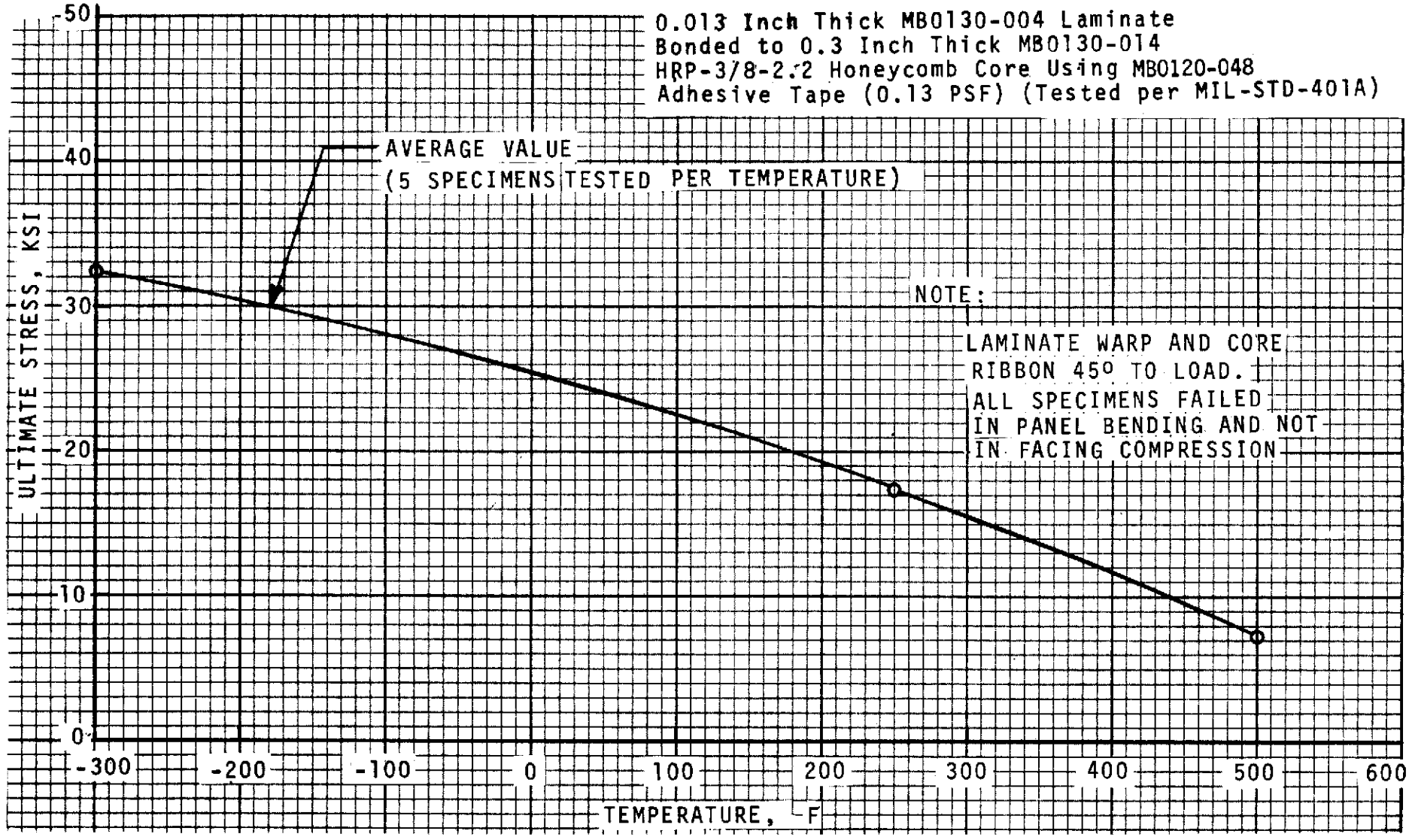

Figure 10.1-1. Edgewise Compressive Strength Versus Temperature

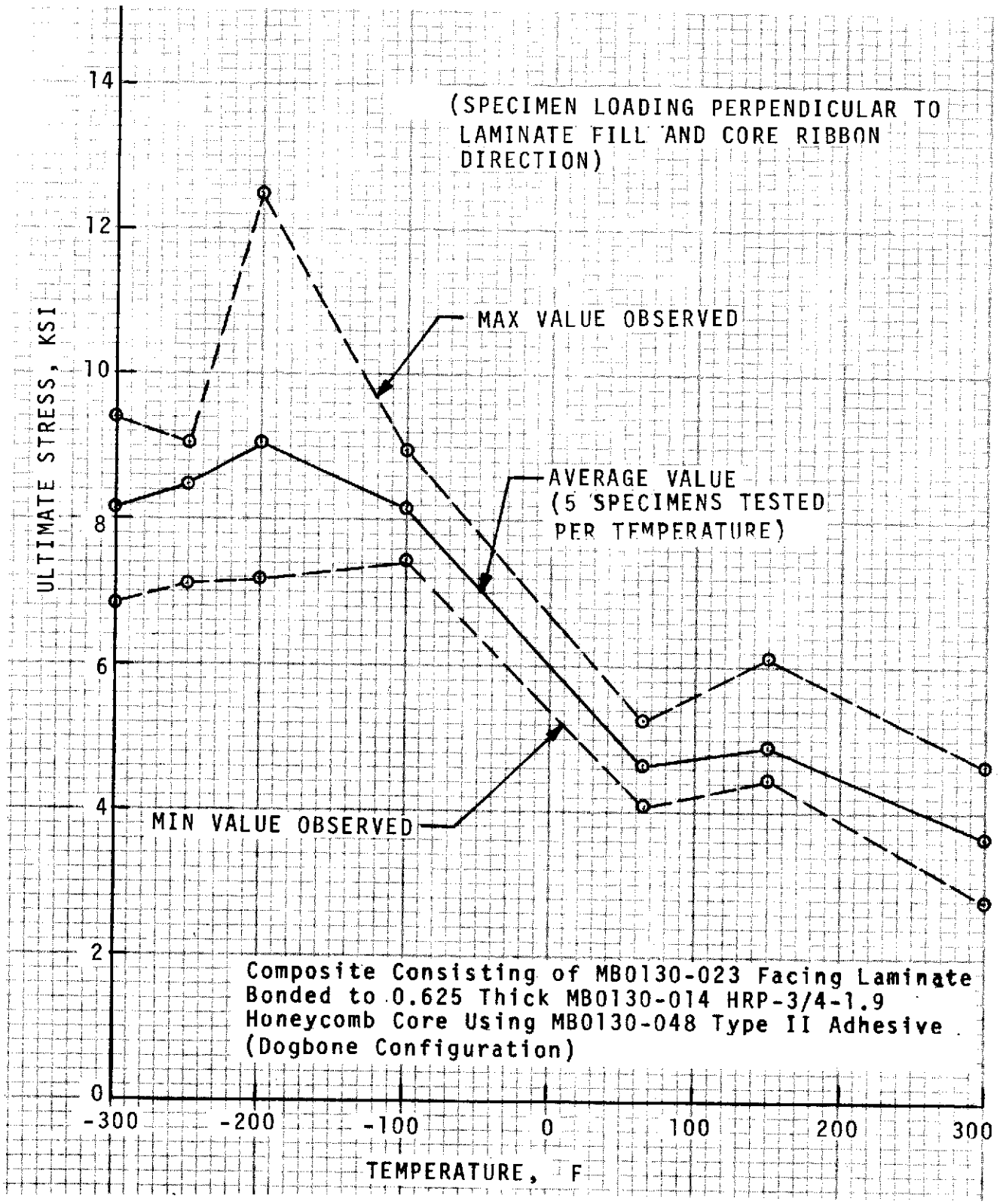

Figure 10-2. Ultimate Tensile Stress Versus Temperature

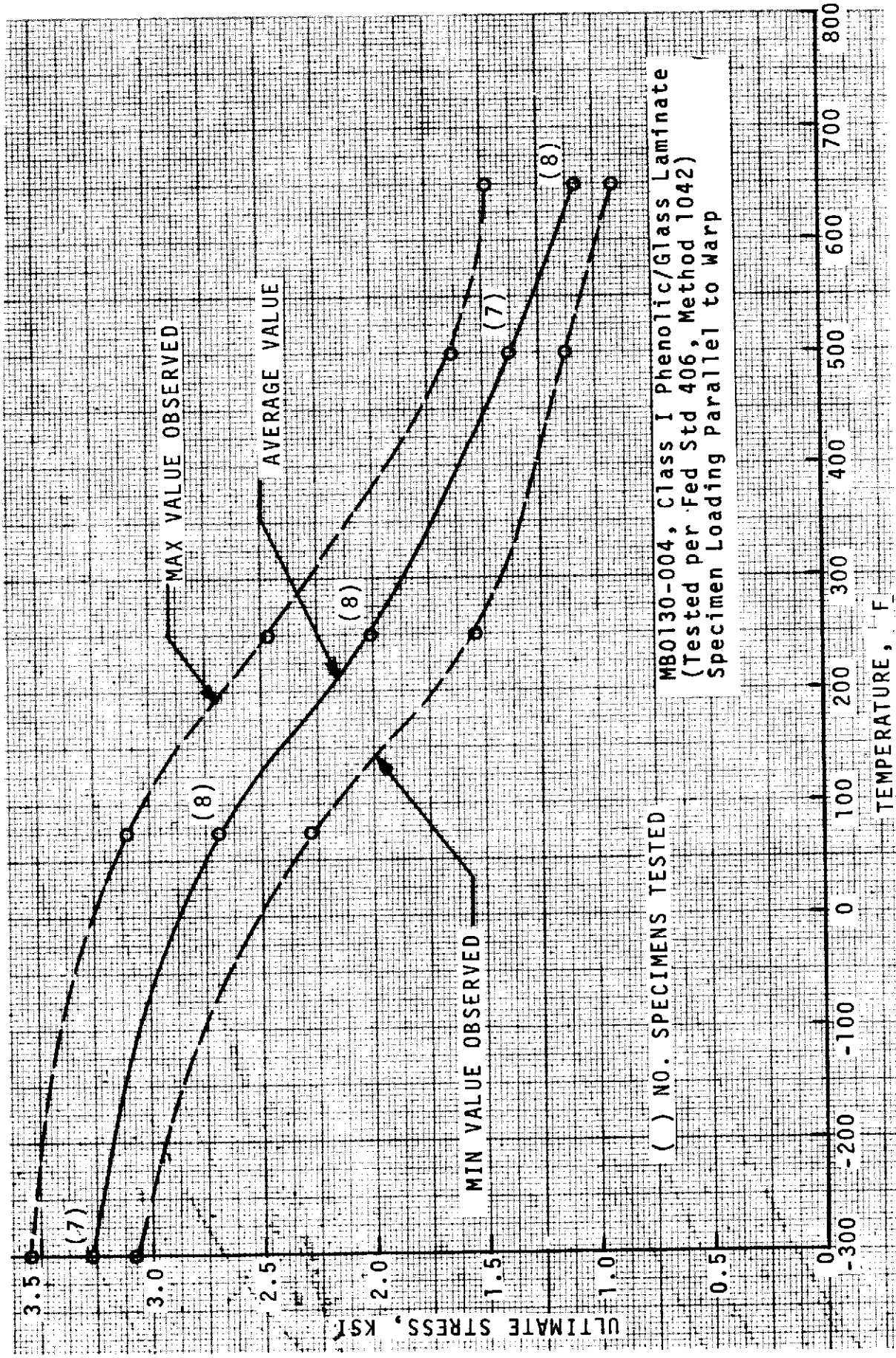

Figure 10.1-3. Interlaminar Shear Strength Versus Temperature

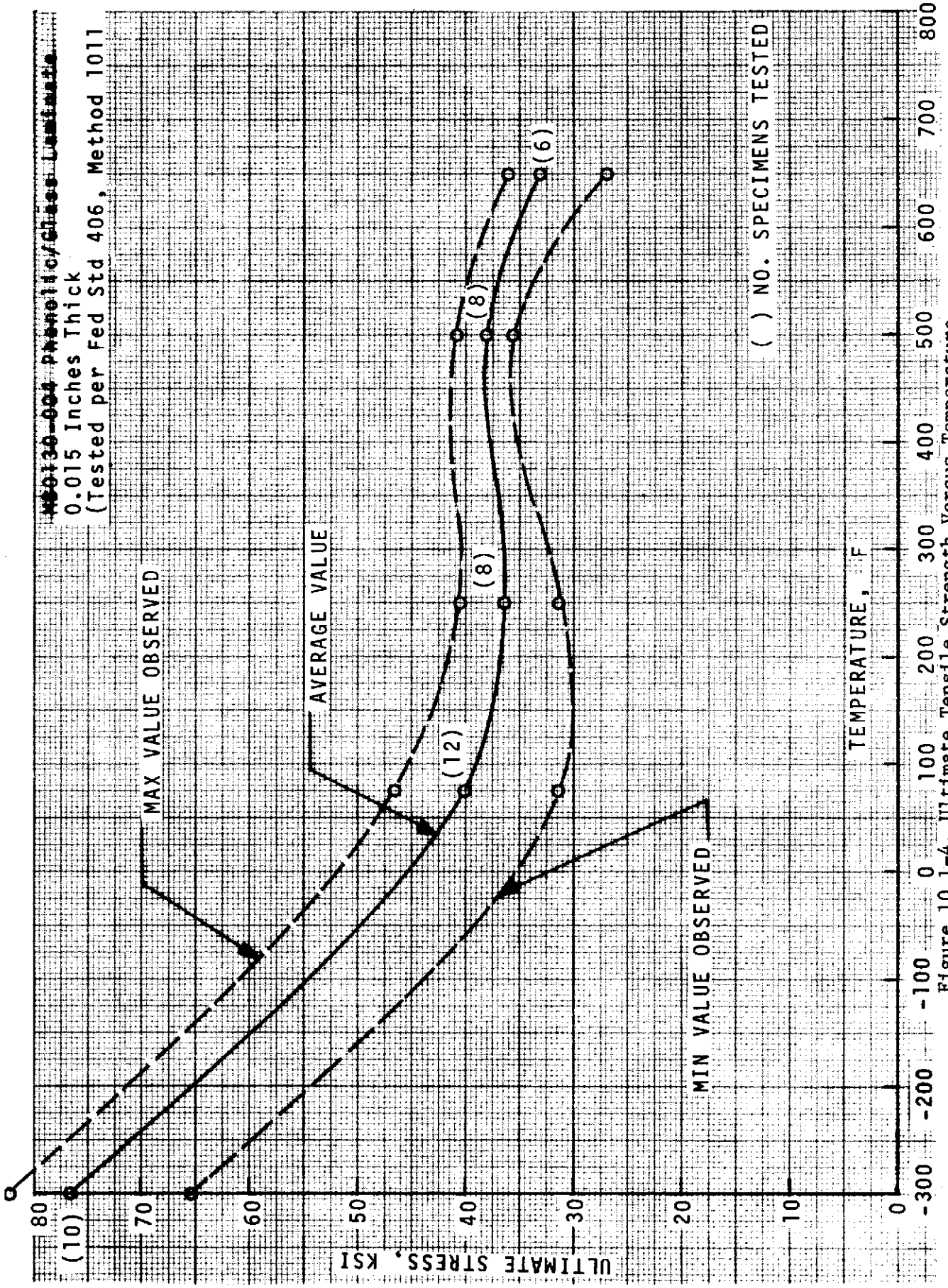

Figure 10.1-4. Ultimate Tensile Strength Versus Temperature - Specimen Loading Parallel to Warp

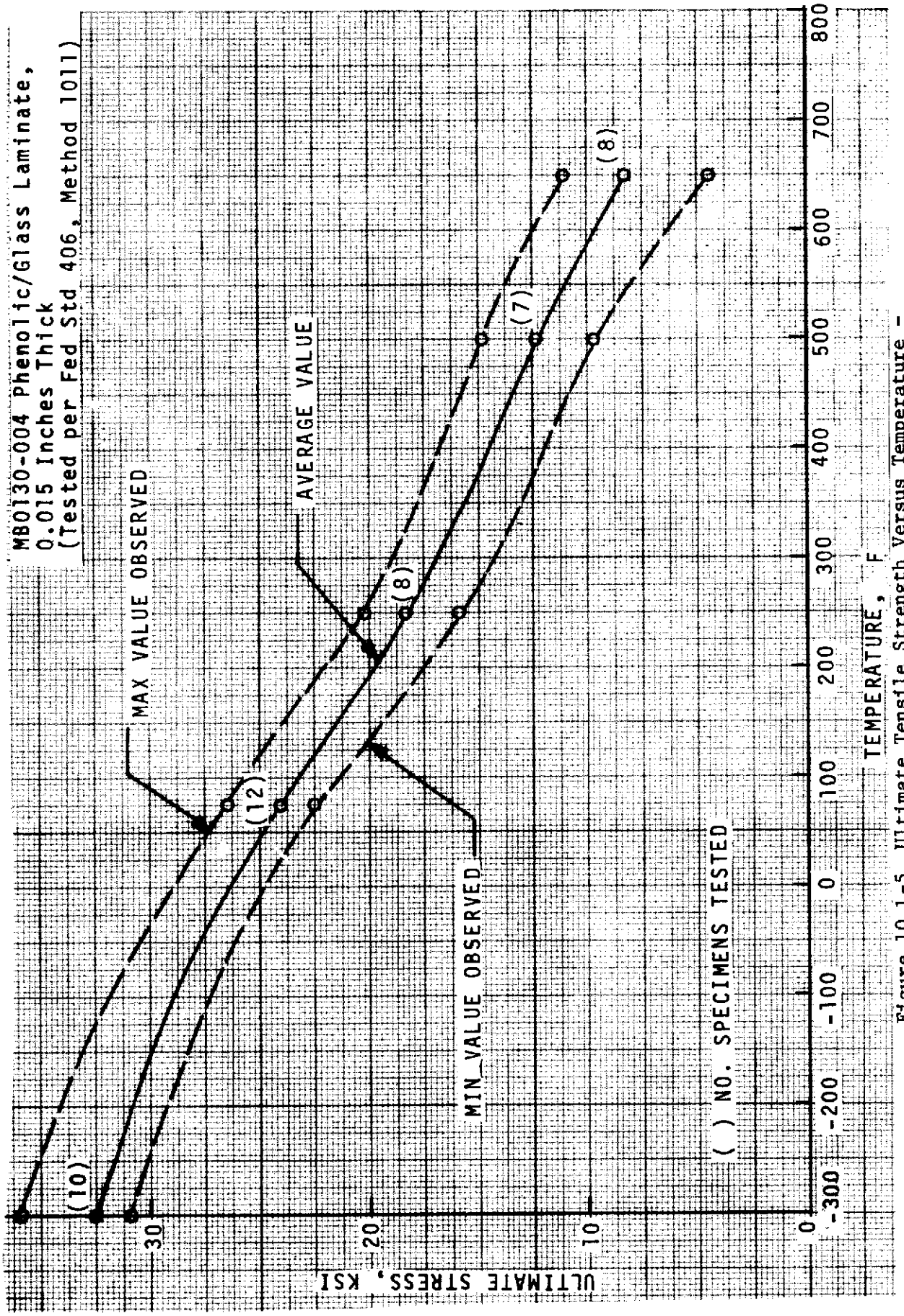

Figure 10.1-5. Ultimate Tensile Strength Versus Temperature - Specimen Loading 45° to Warp Direction

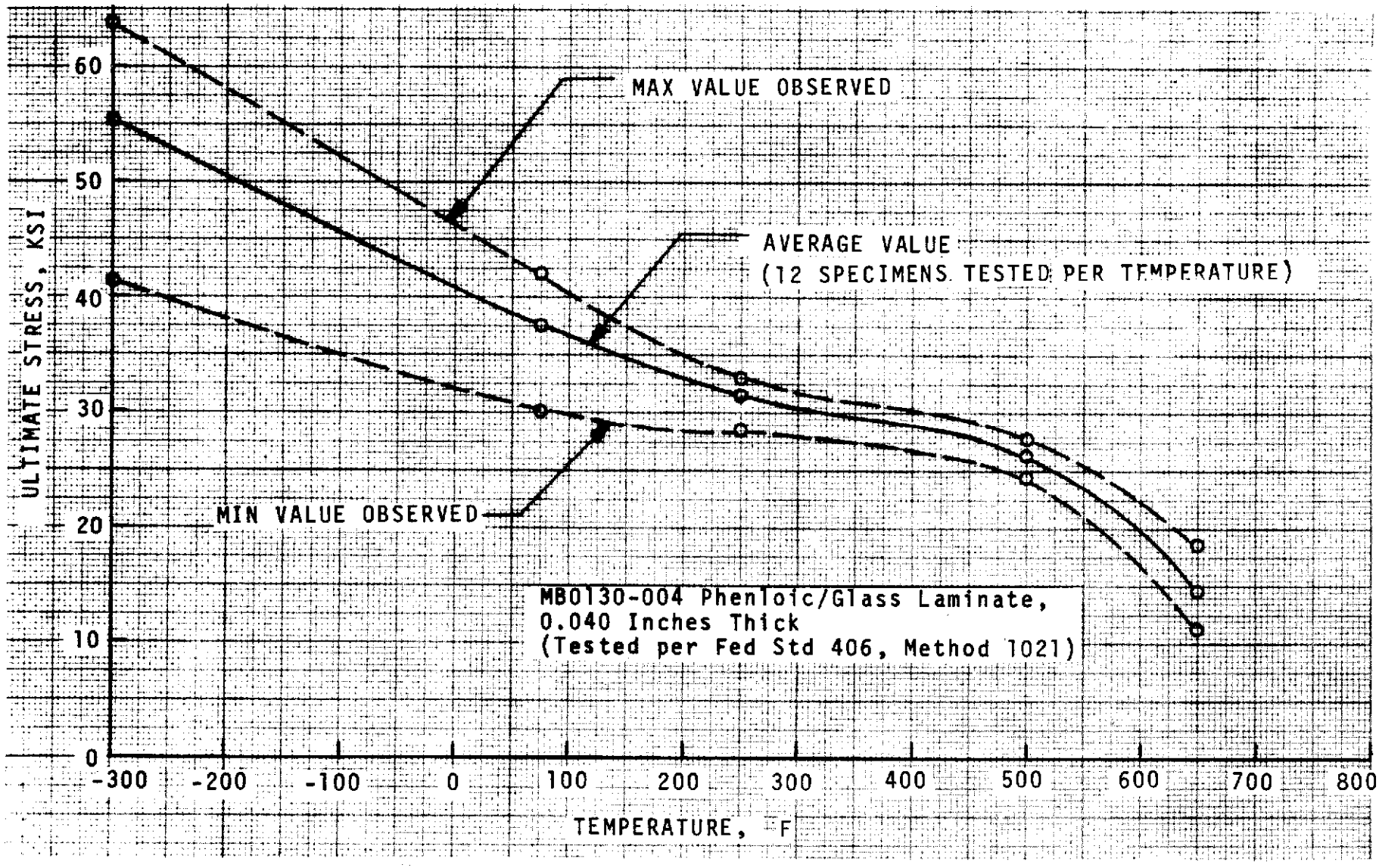

Figure 10.1-6. Edgewise Compressive Strength Versus Temperature - Specimen Loading Parallel to Warp

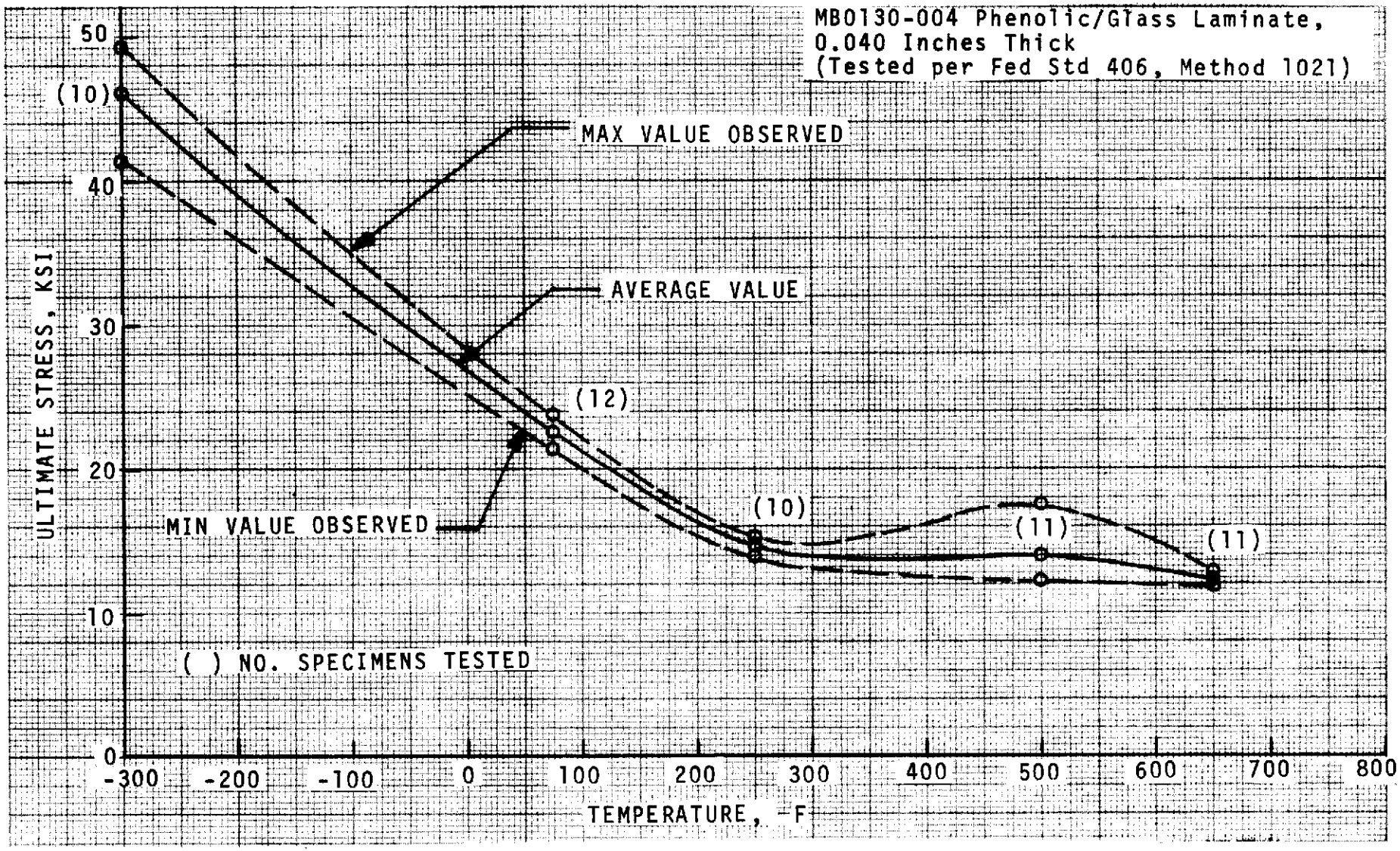

Figure 10.1-7. Edgewise Compressive Strength Versus Temperature - Specimen Loading 45° to Warp Direction

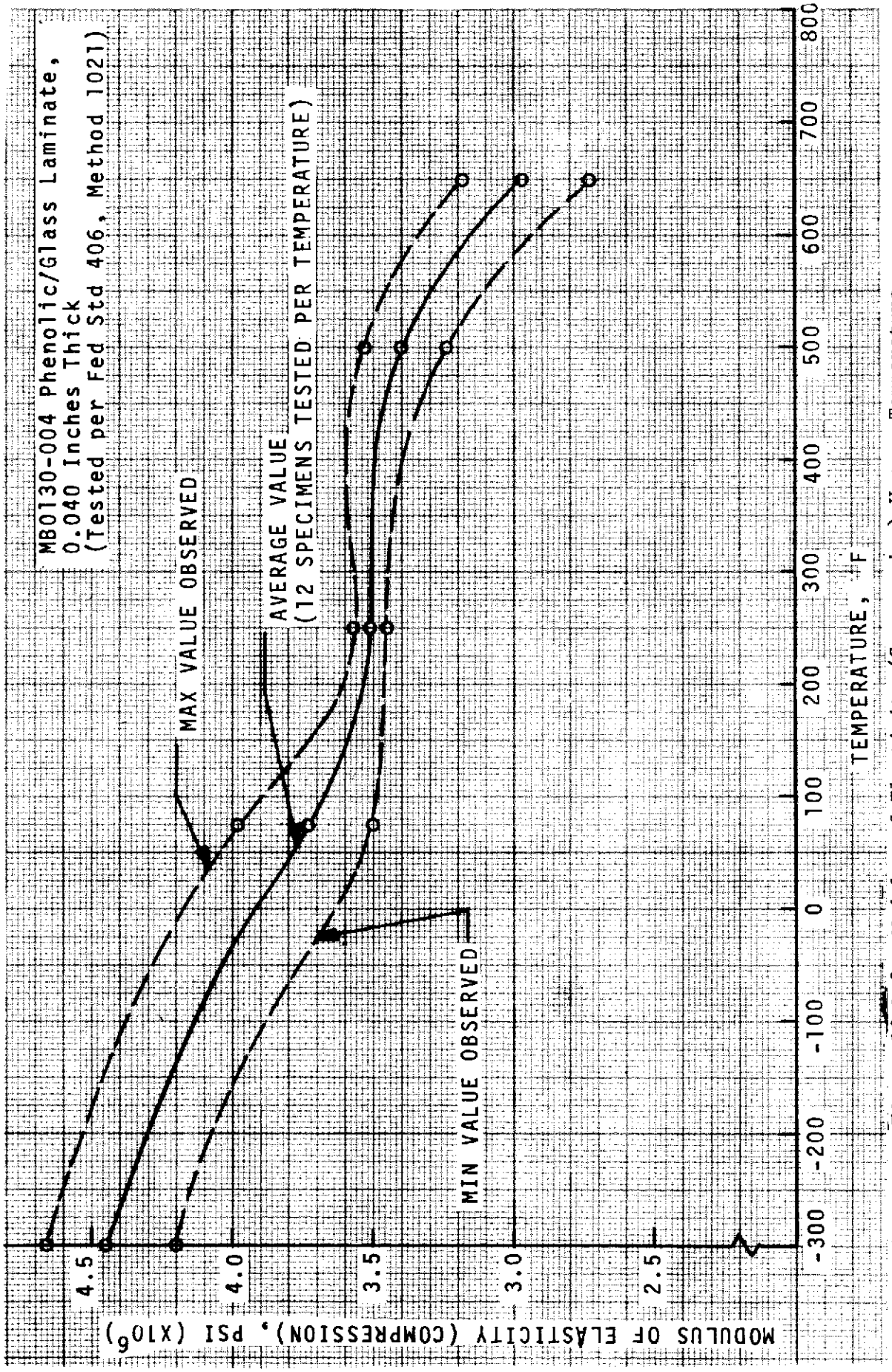

Figure 10.1-8. Modulus of Elasticity (Compression) Versus Temperature - Specimen Loading Parallel to Warp

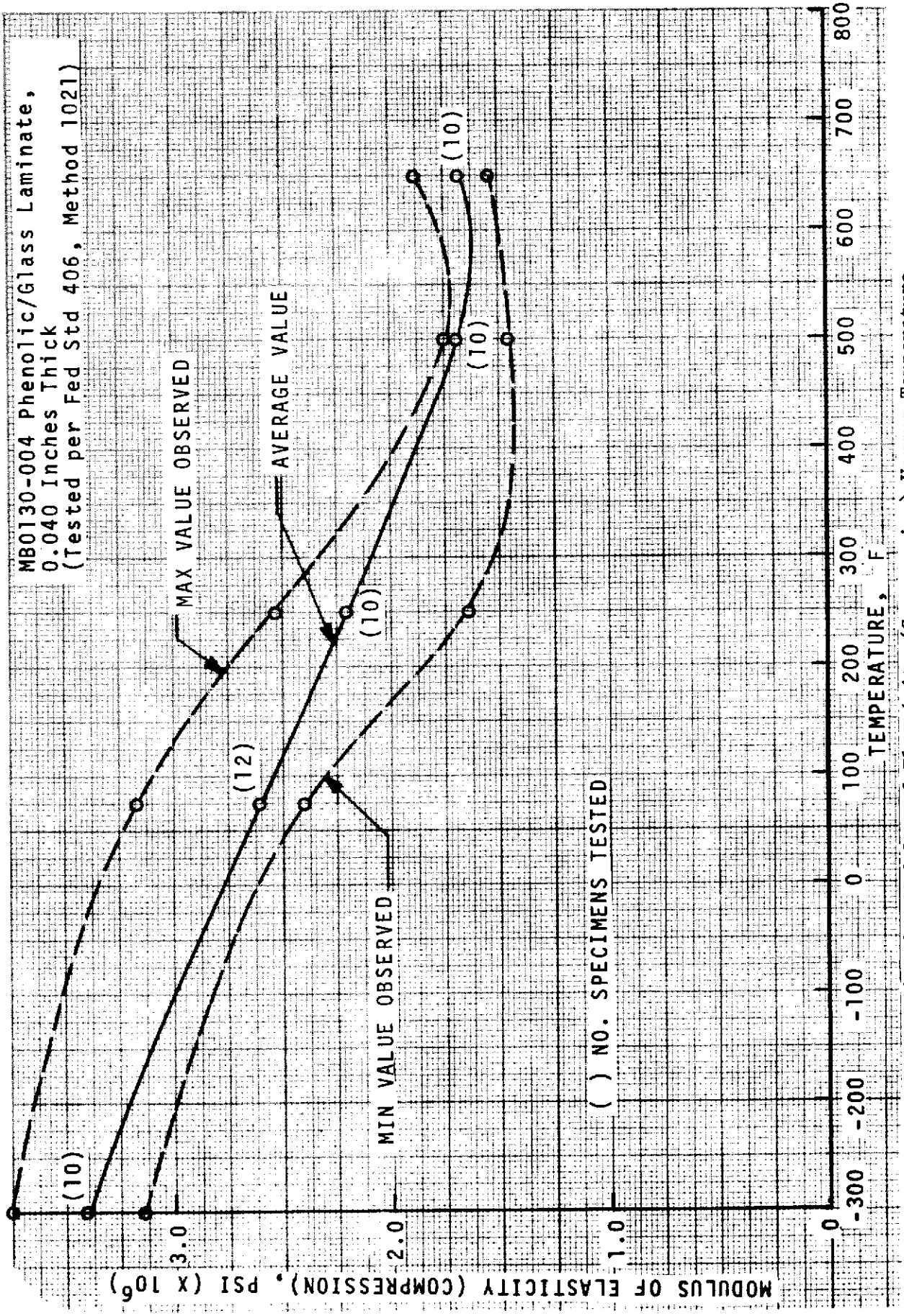

Figure 10.1-9. Modulus of Elasticity (Compression) Versus Temperature - Specimen Loading 45° to Warp Direction

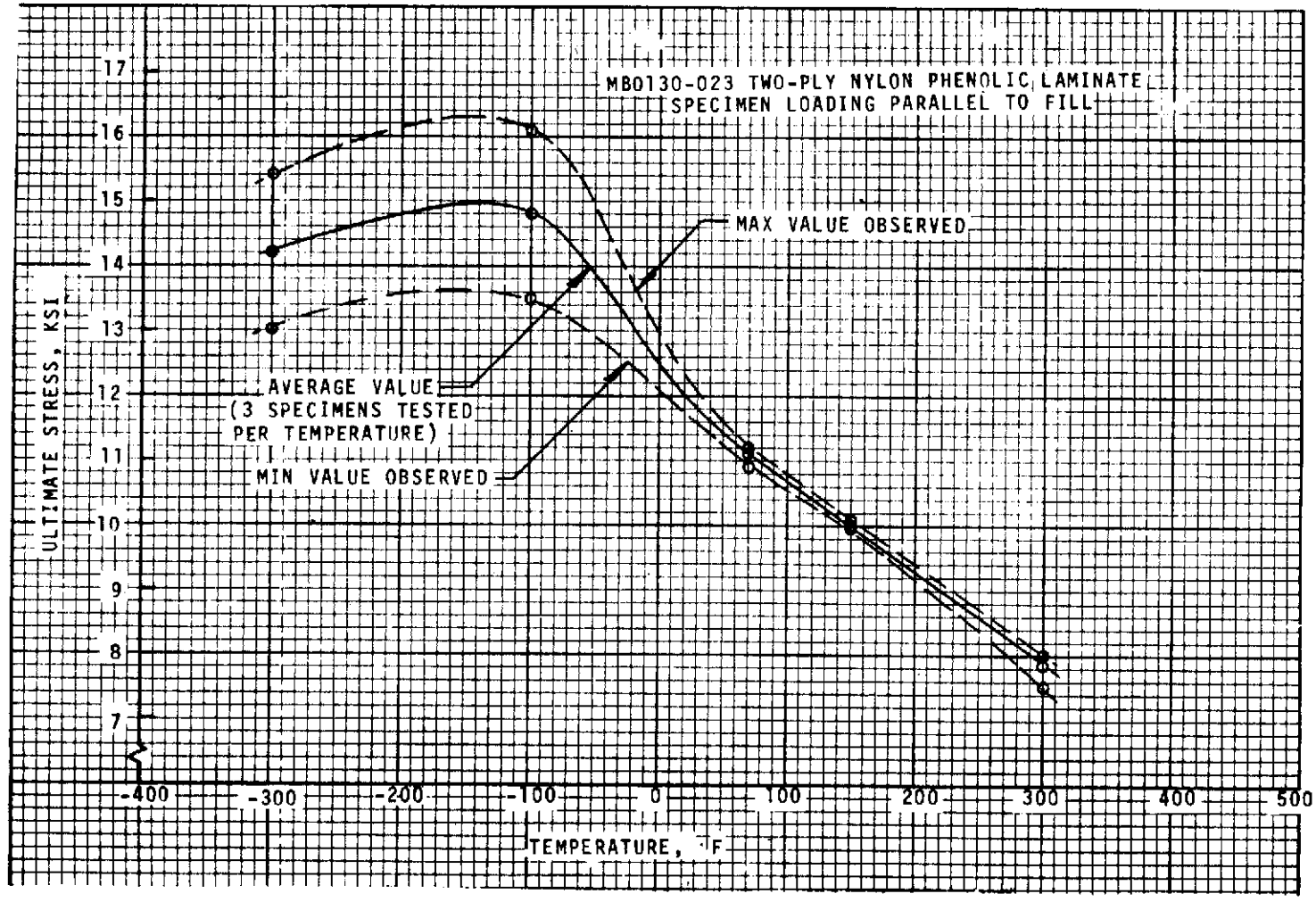

Figure 10.1-10. Ultimate Tensile Strength Versus Temperature

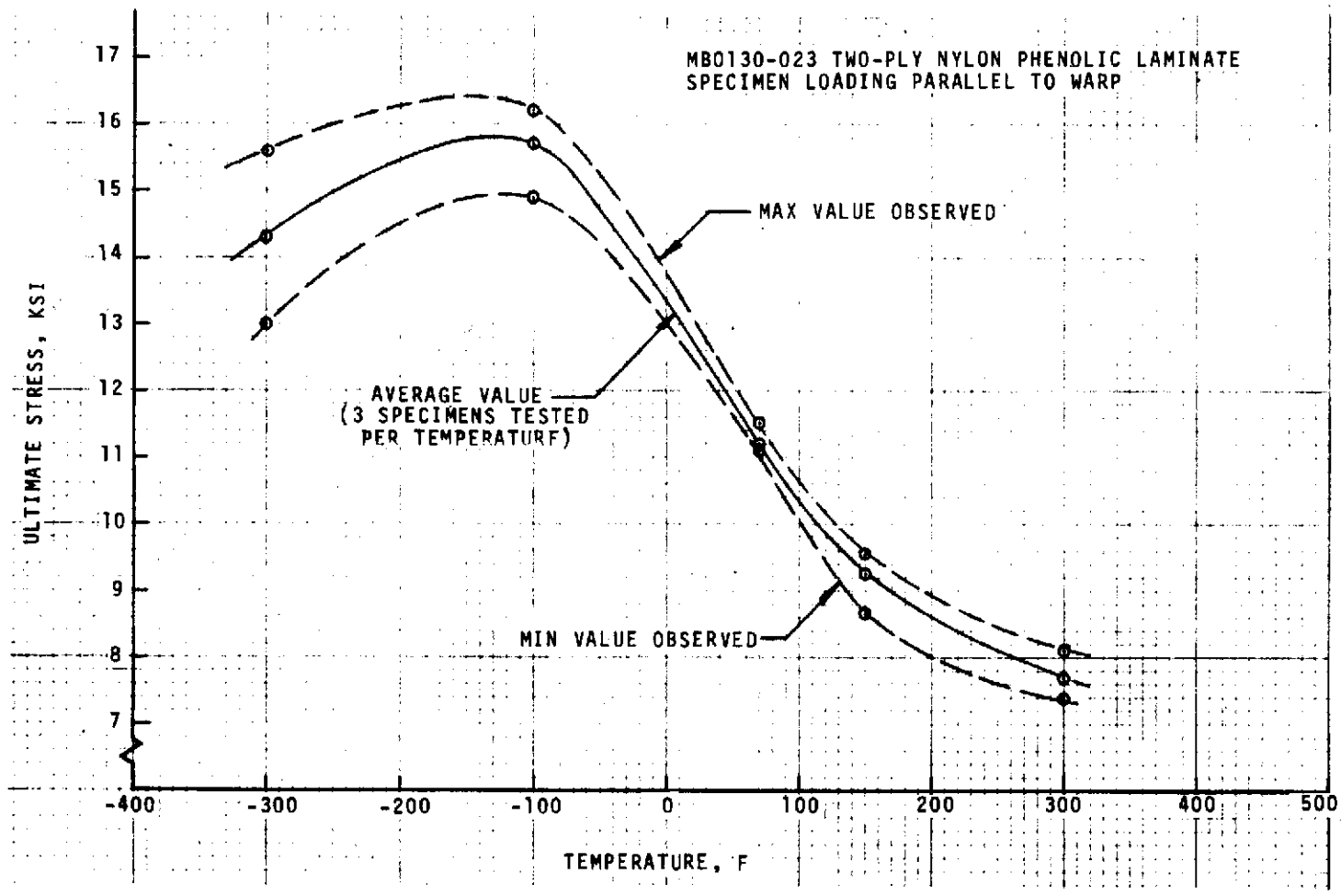

Figure 10.1-11. Ultimate Tensile Strength Versus Temperature

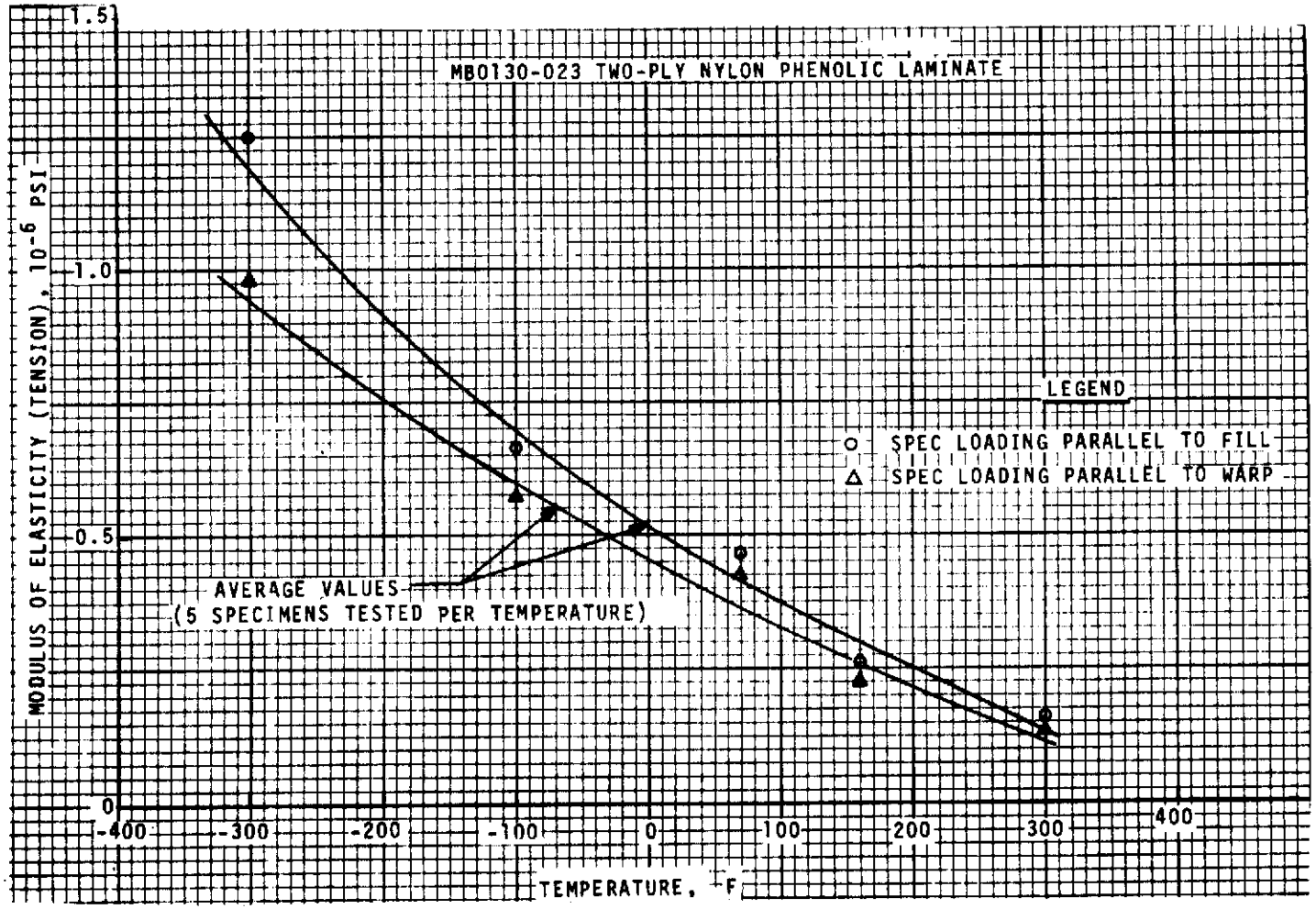

Figure 10.1-12. Modulus of Elasticity (Tensile) Versus Temperature

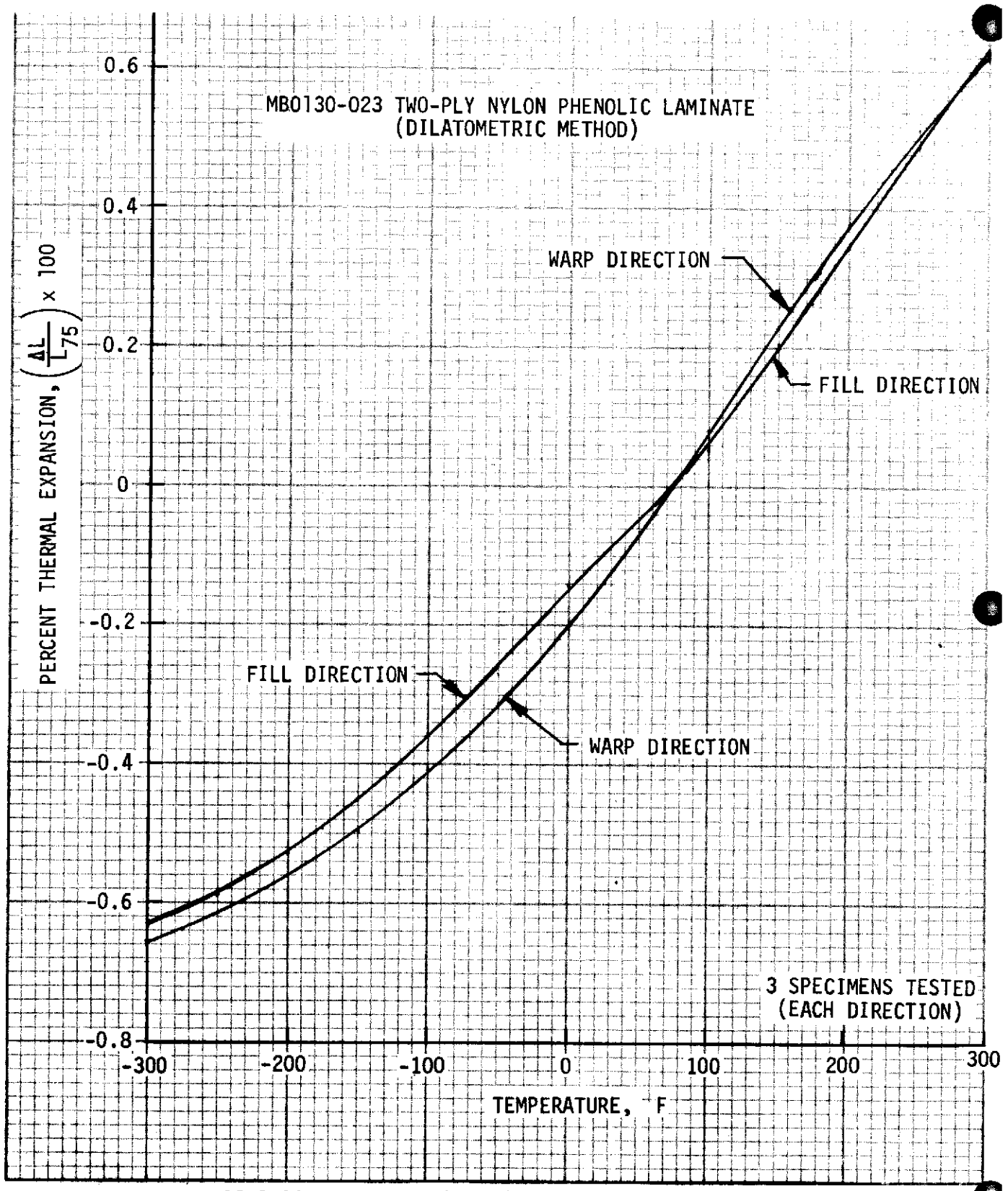

Figure 10.1-13. Average Thermal Expansion Characteristics

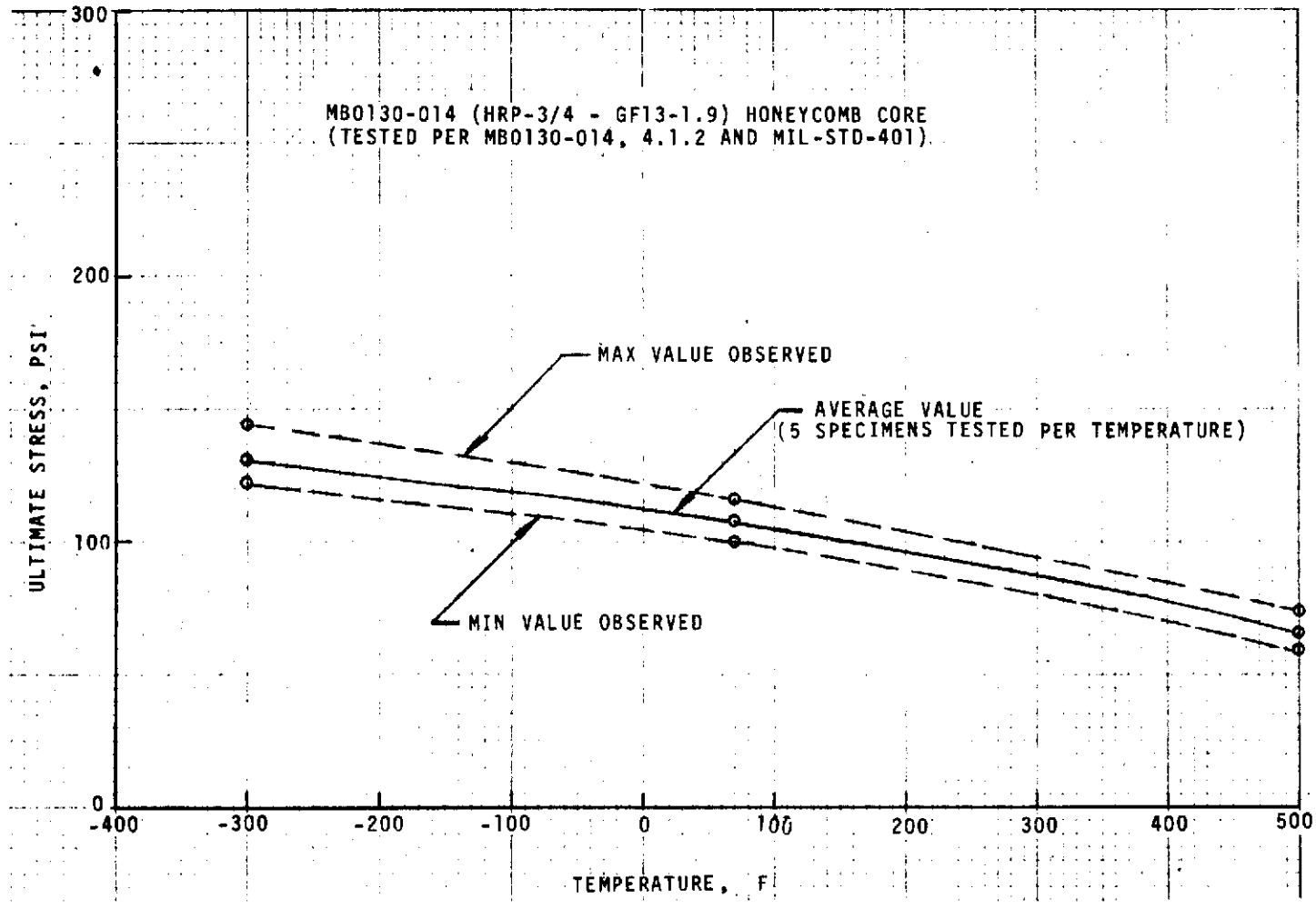

Figure 10.1-14. Flatwise Compressive Strength Versus Temperature

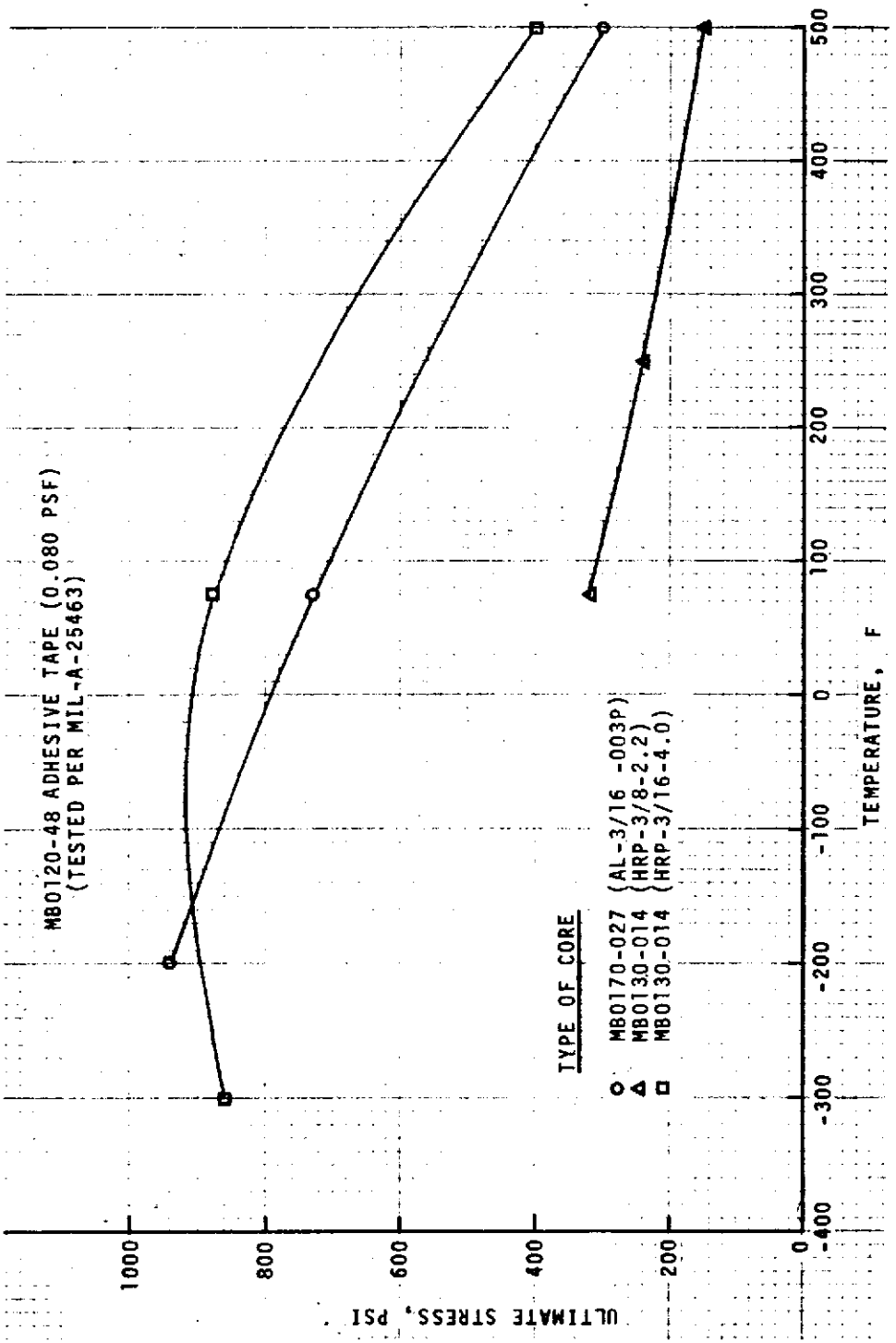

Figure 10.1-15. Ultimate Flatwise Tensile Strength Versus Temperature

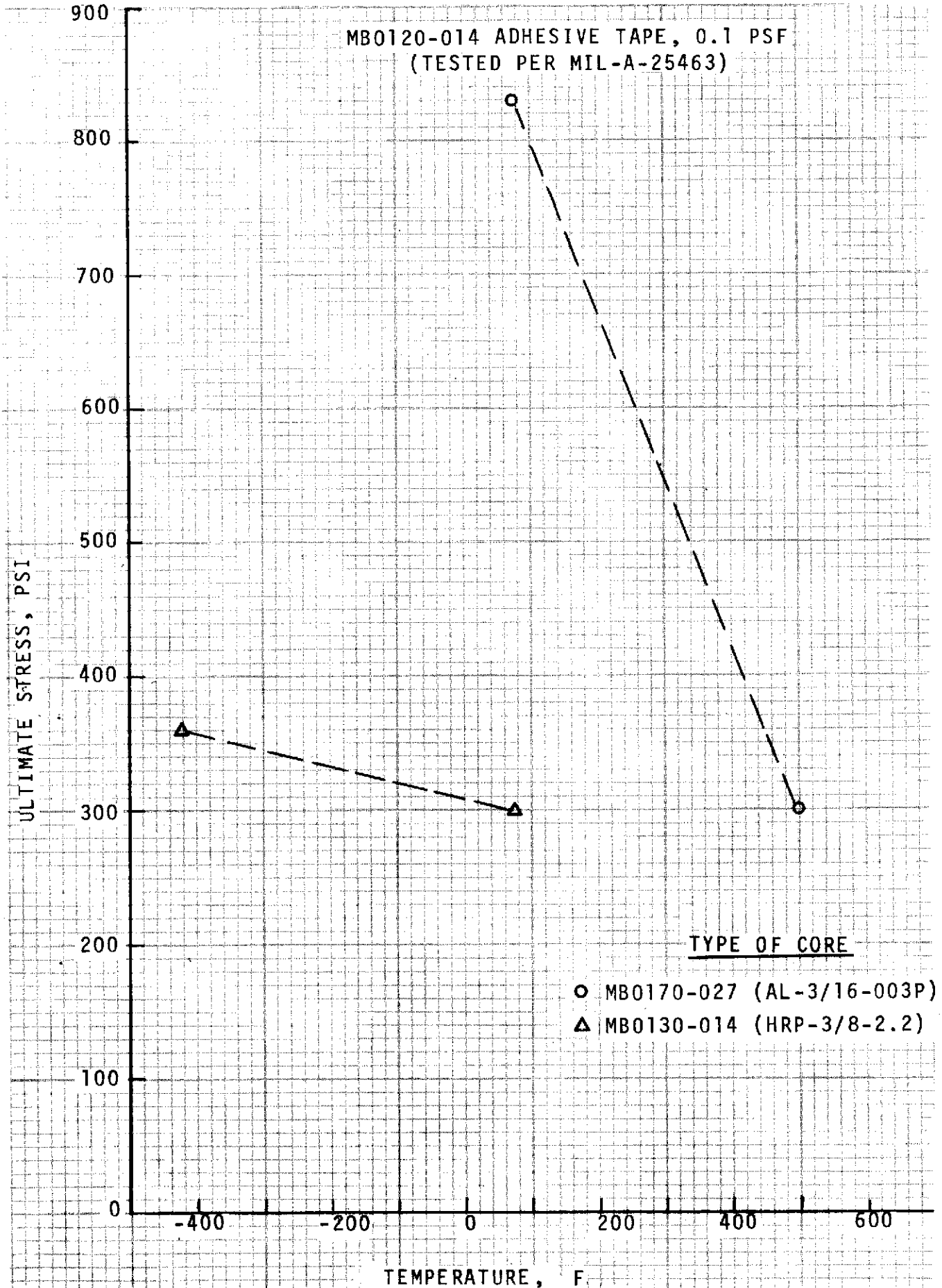

Figure 10.1-16. Ultimate Flatwise Tensile Strength Versus Temperature

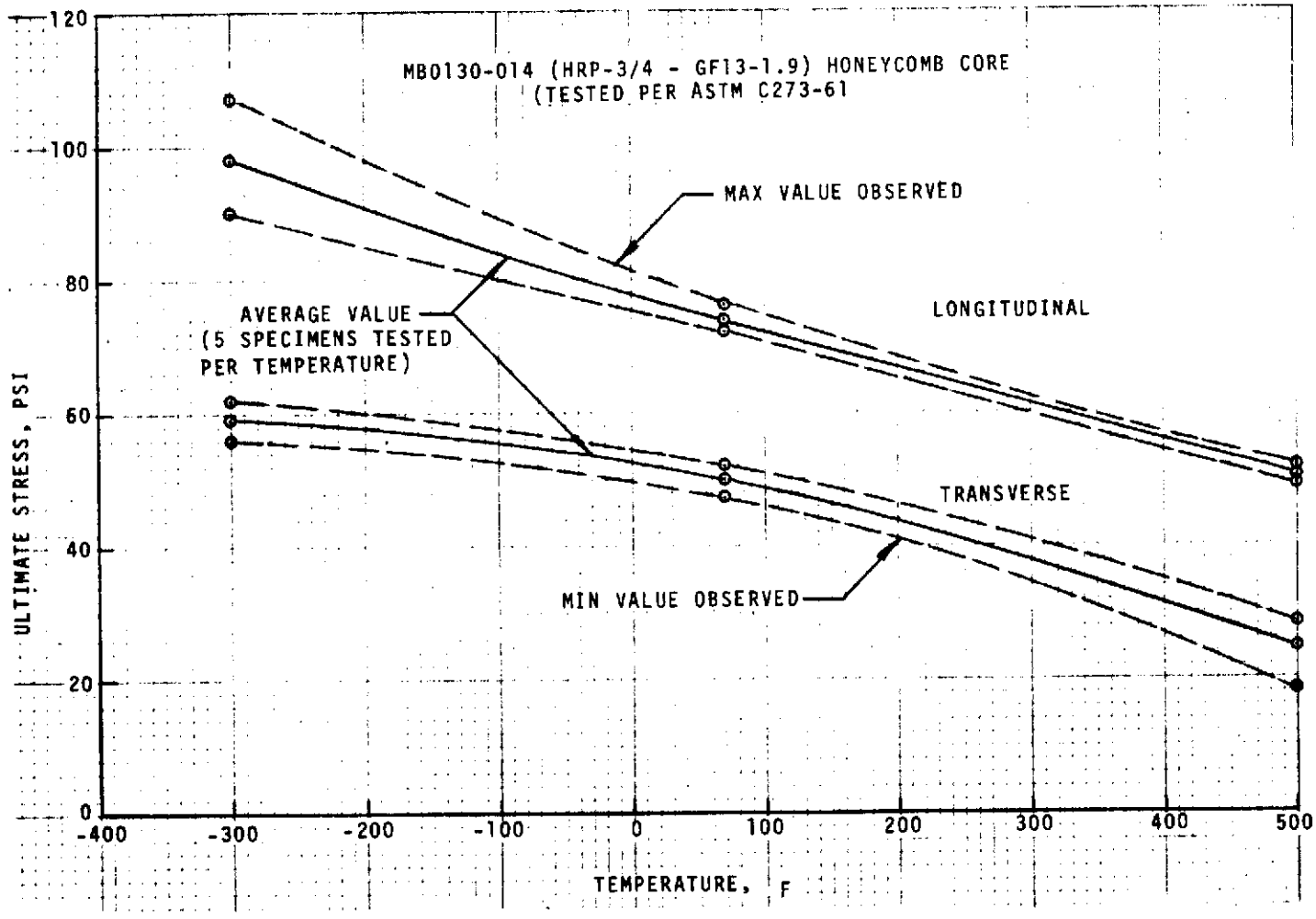

Figure 10.1-17. Ultimate Block Shear Strength Versus Temperature

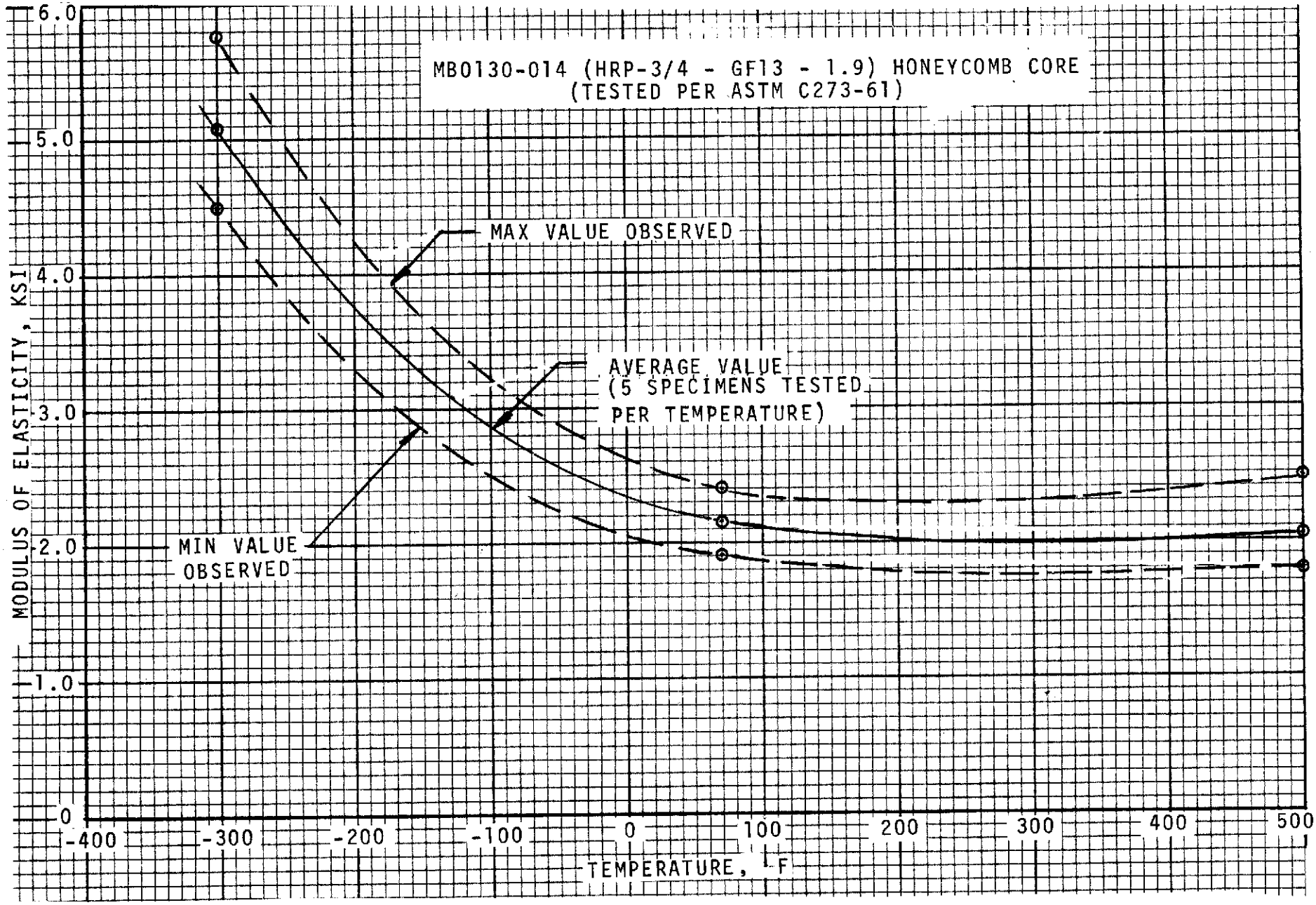

Figure 10.1-18. Transverse Block Shear Modulus Versus Temperature

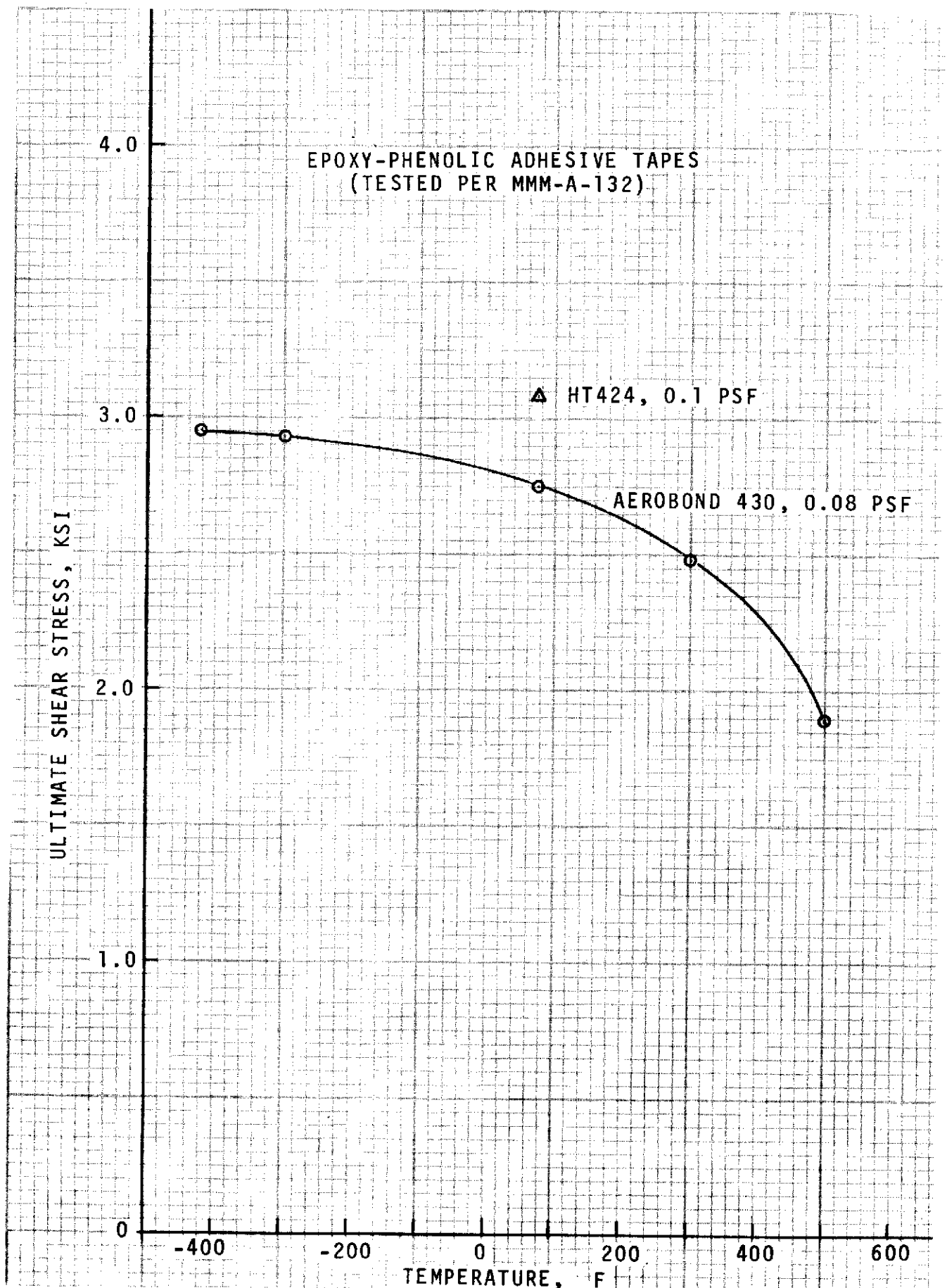

Figure 10.1-19. Ultimate Lap Shear Strength Versus Temperature

Figure 10.1-20. Thermal Contraction Versus Temperature

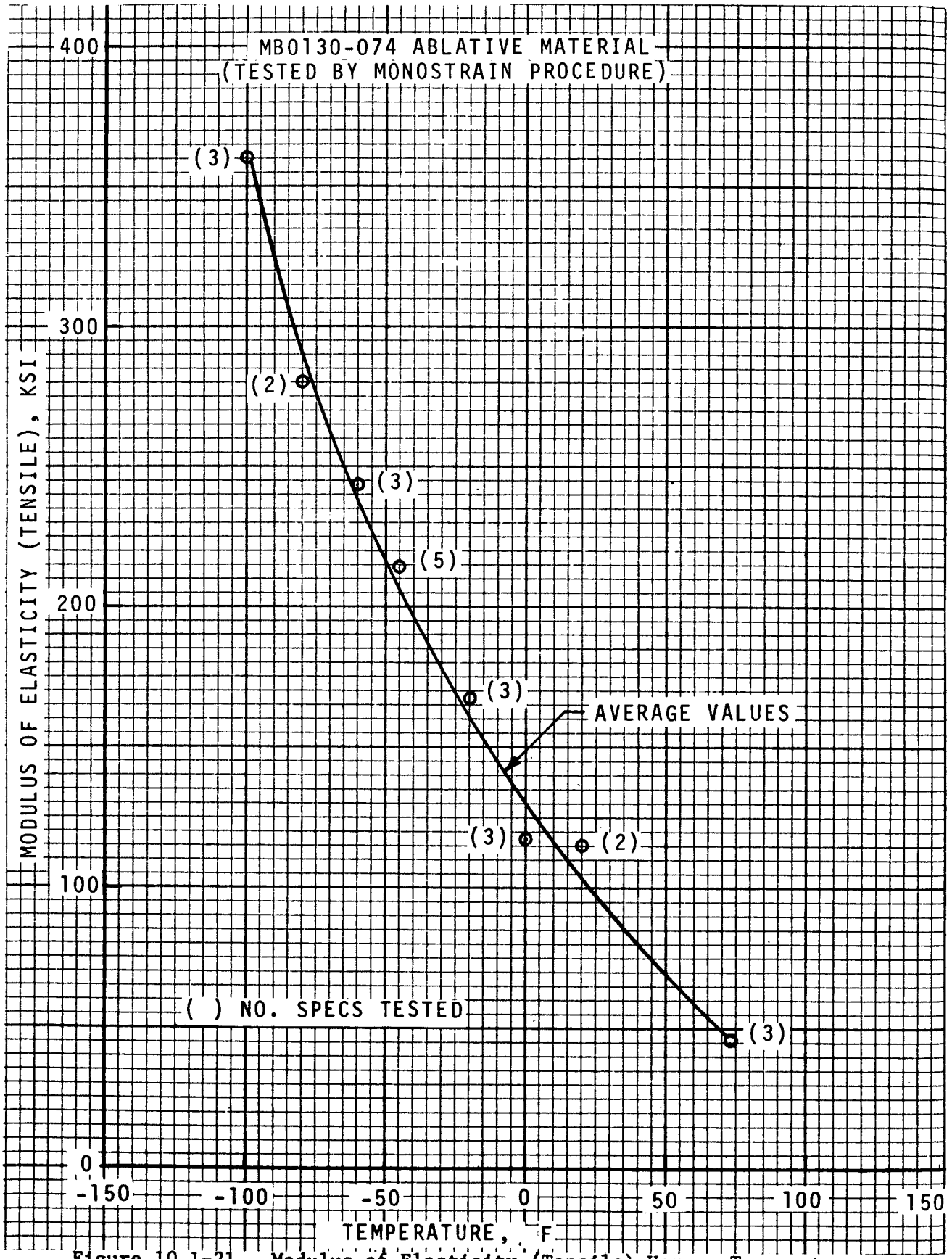

Figure 10.1-21. Modulus of Elasticity (Tensile) Versus Temperature

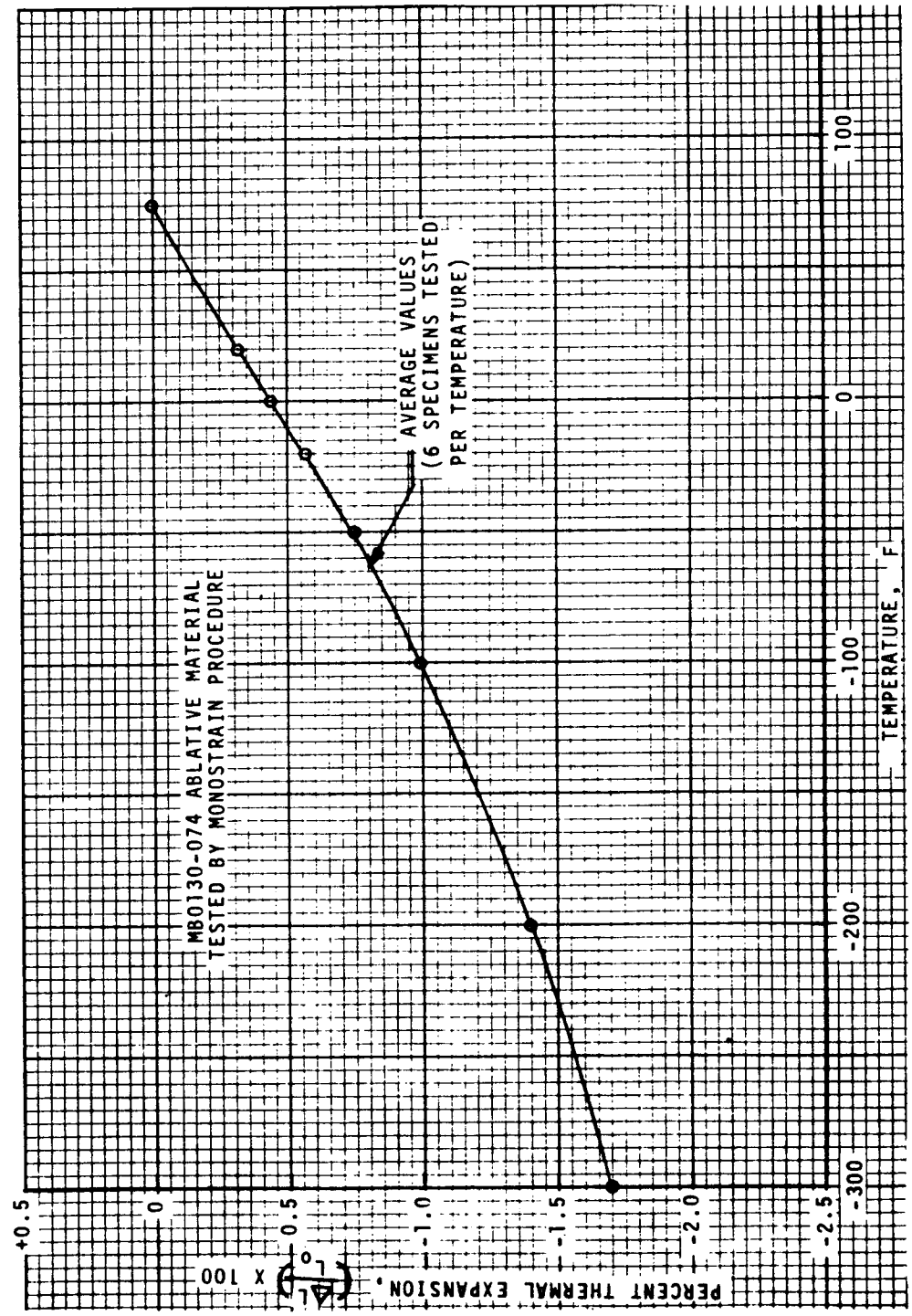

Figure 10.1-22. Thermal Contraction Versus Temperature

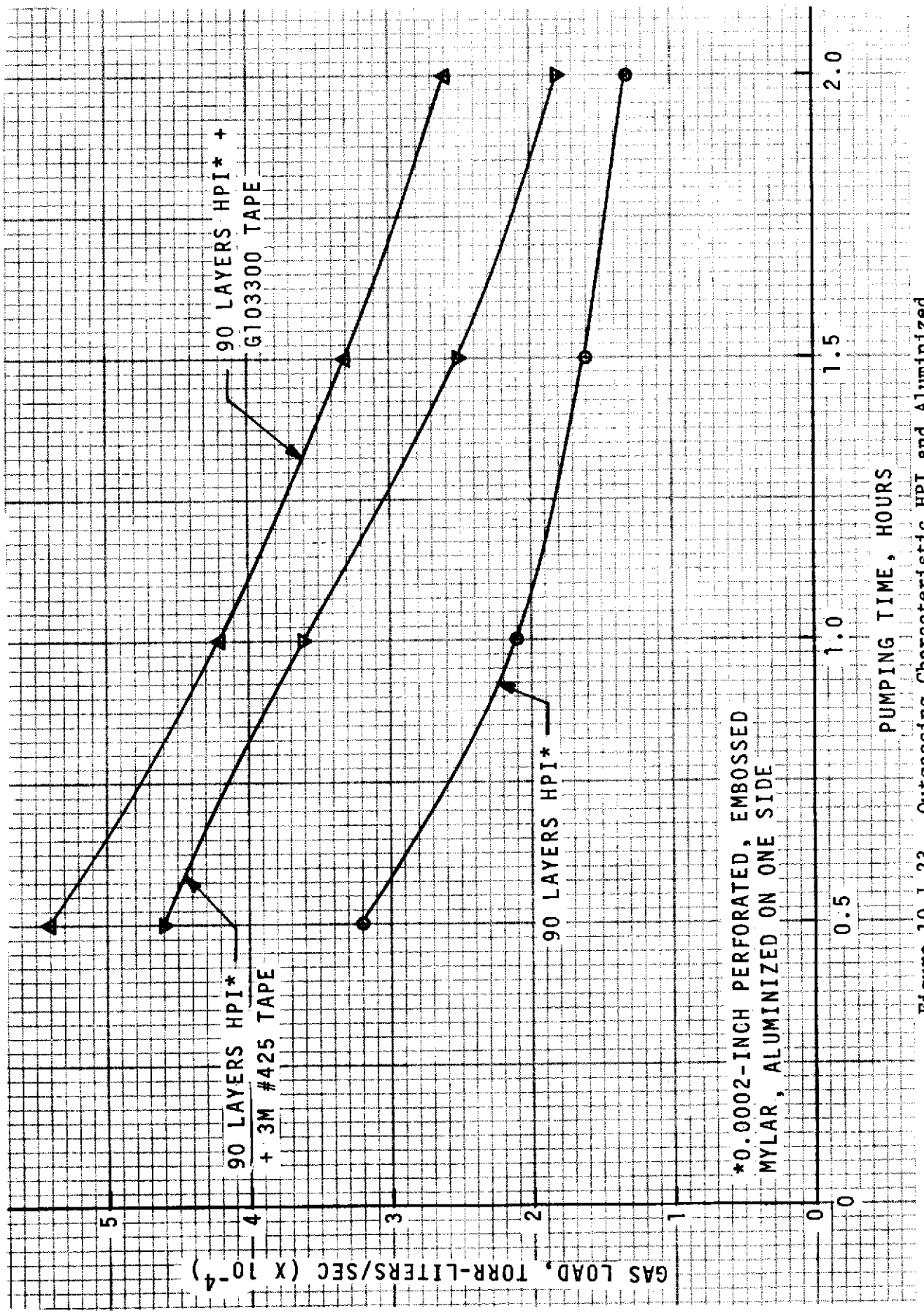

Figure 10.1-23. Outgassing Characteristic HPI and Aluminized Pressure-Sensitive Tape

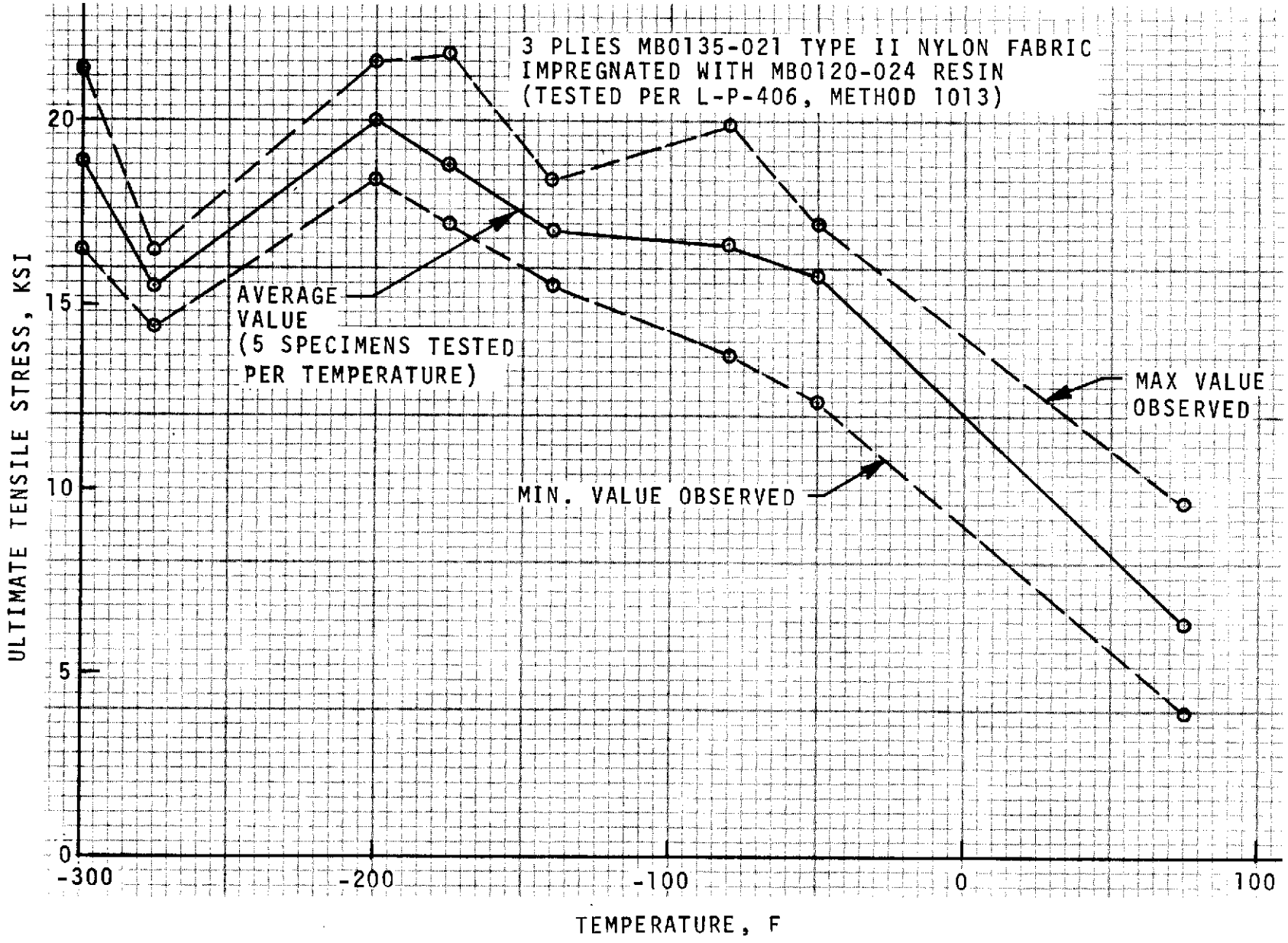

Figure 10.1-24. Ultimate Tensile Strength Versus Temperature

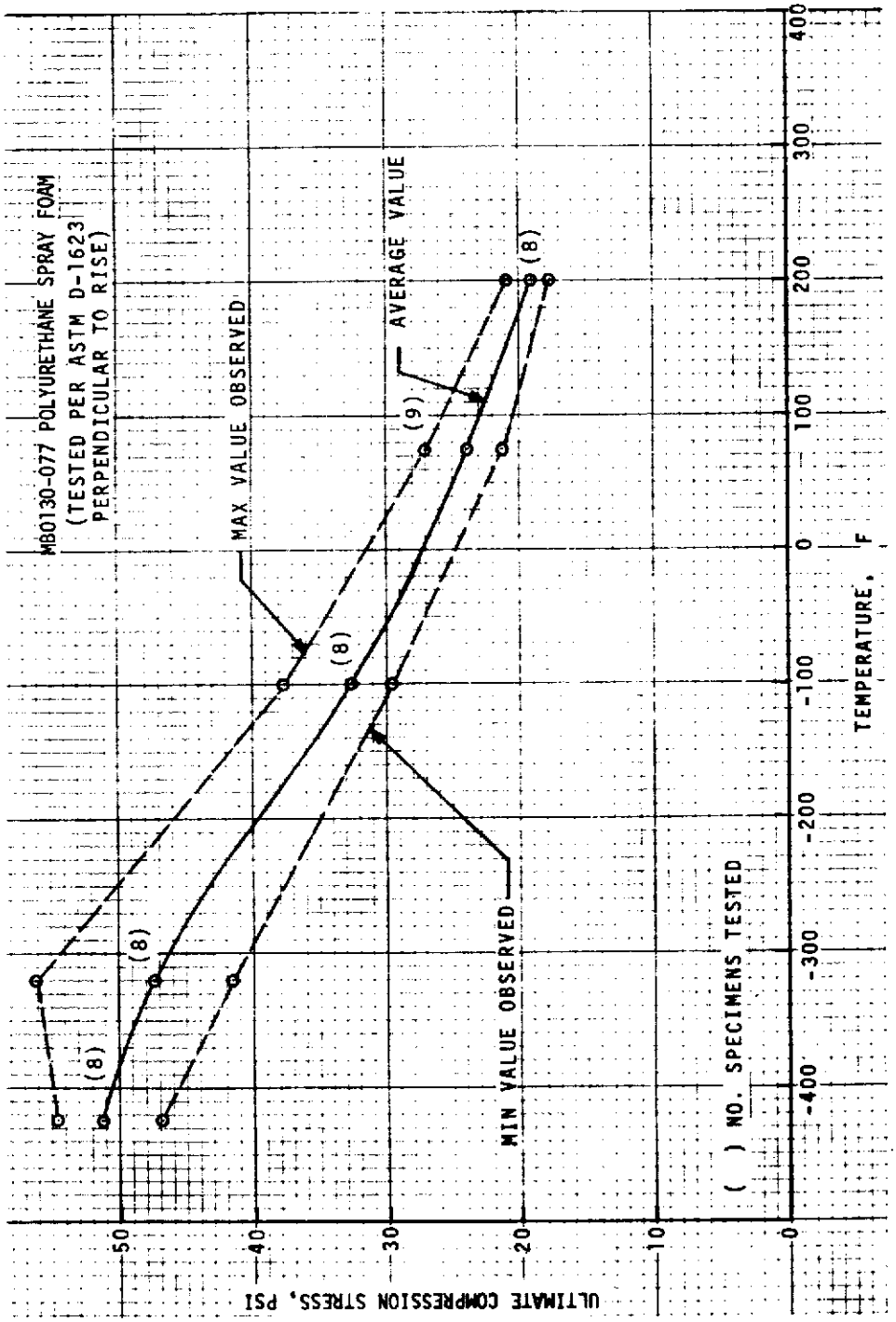

Figure 10.1-25. Ultimate Compressive Strength Versus Temperature

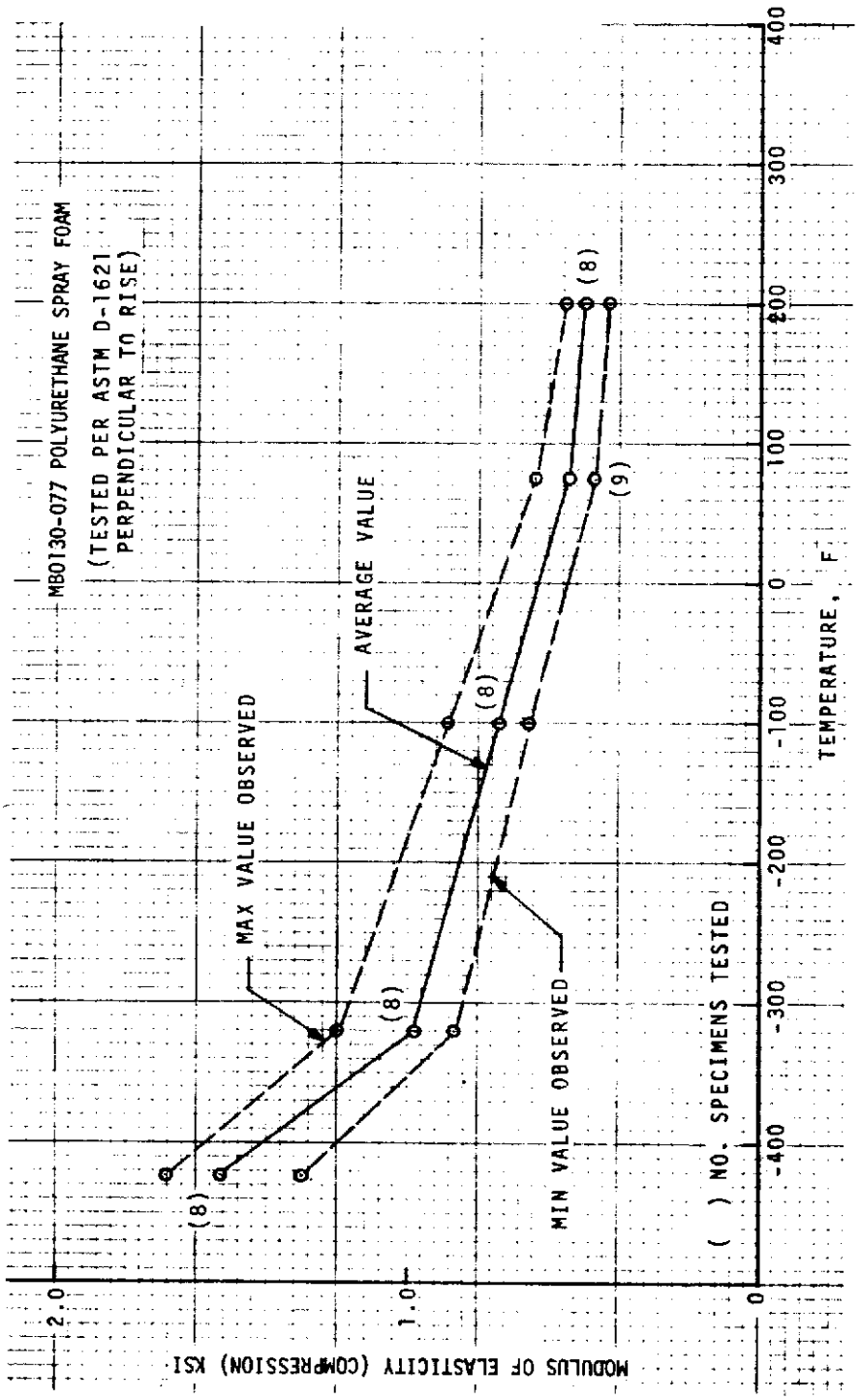

Figure 10.1-26. Modulus of Elasticity (Compression) Versus Temperature

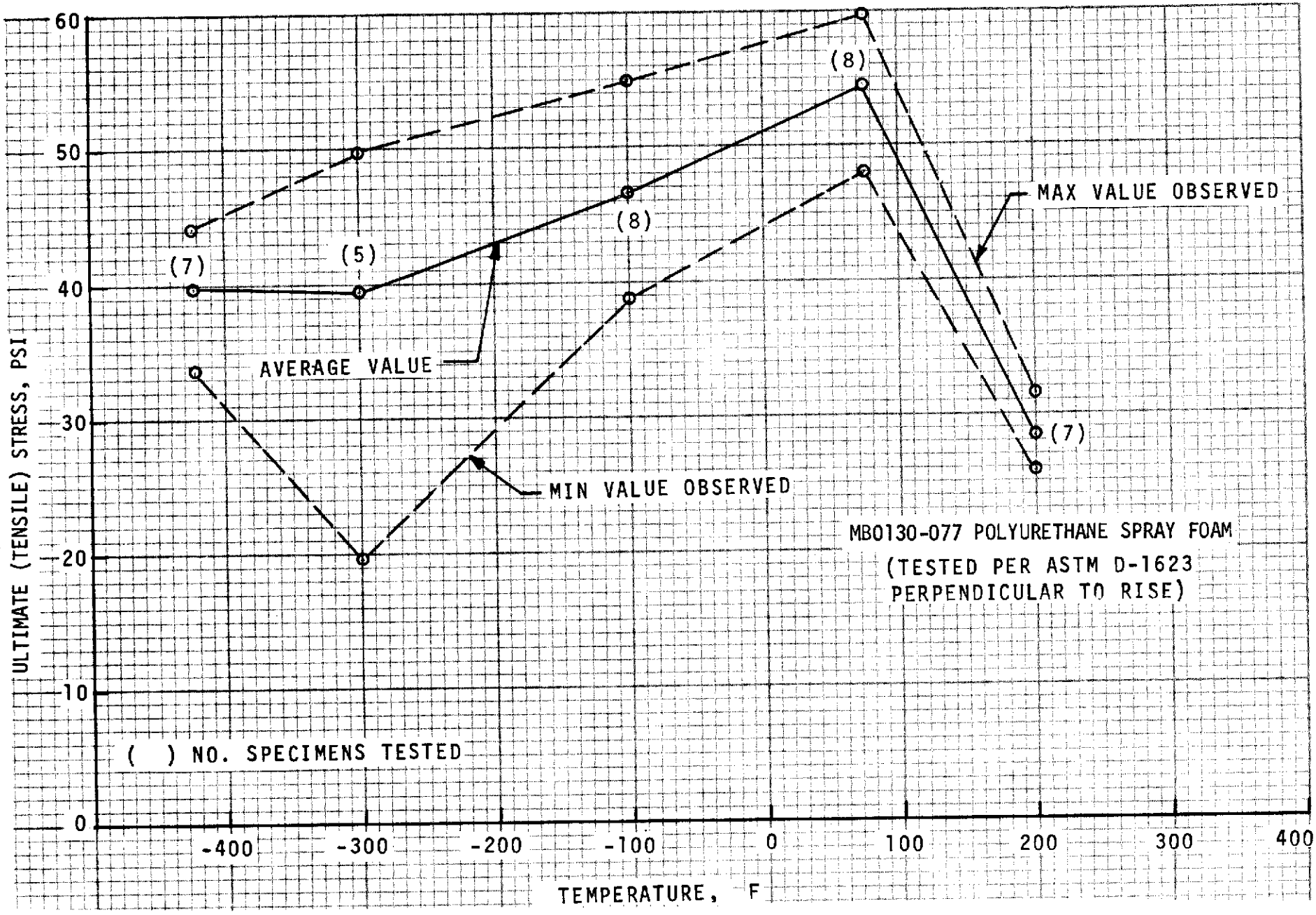

Figure 10.1-27. Ultimate Tensile Strength Versus Temperature

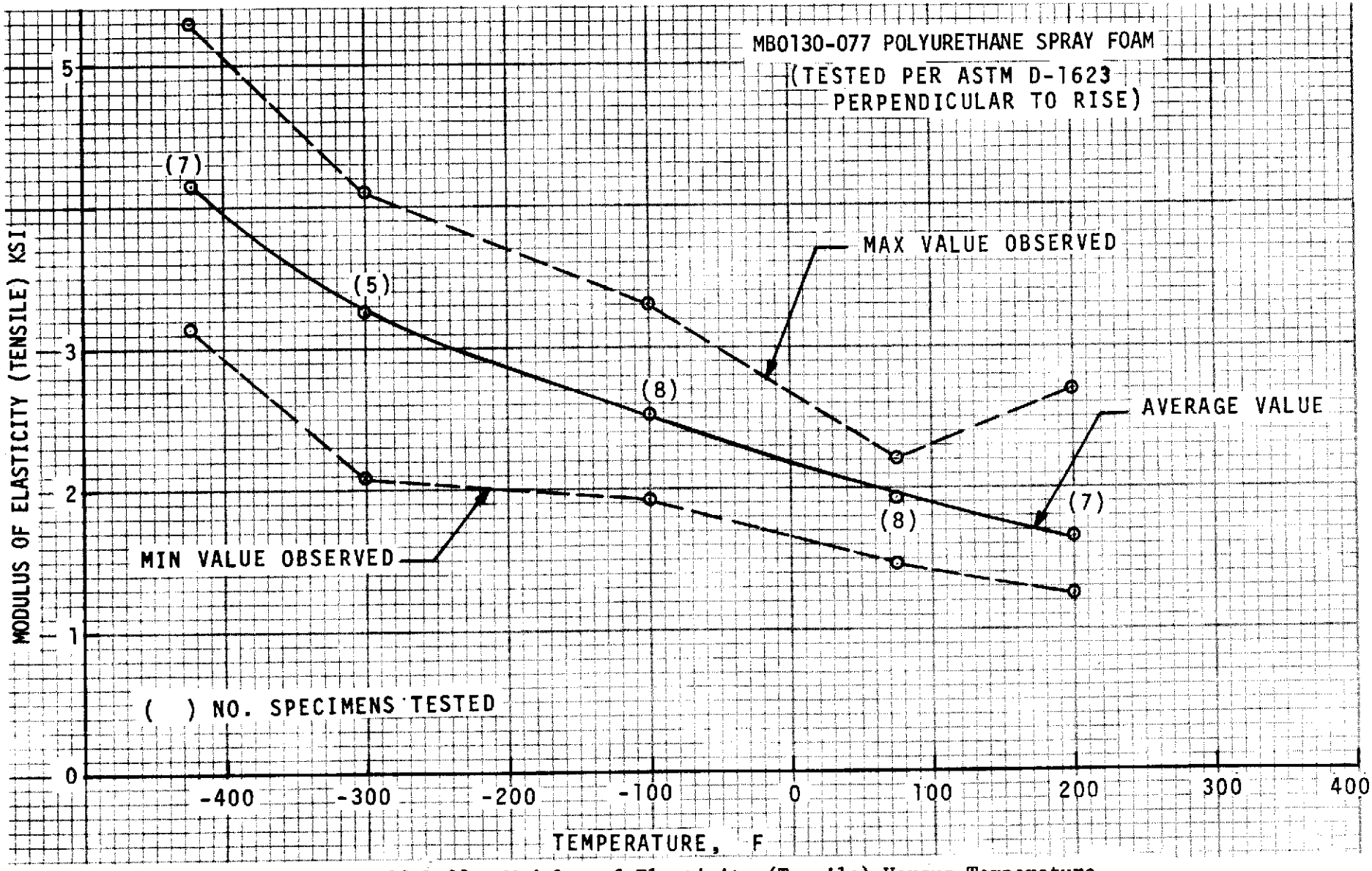

Figure 10.1-28. Modulus of Elasticity (Tensile) Versus Temperature

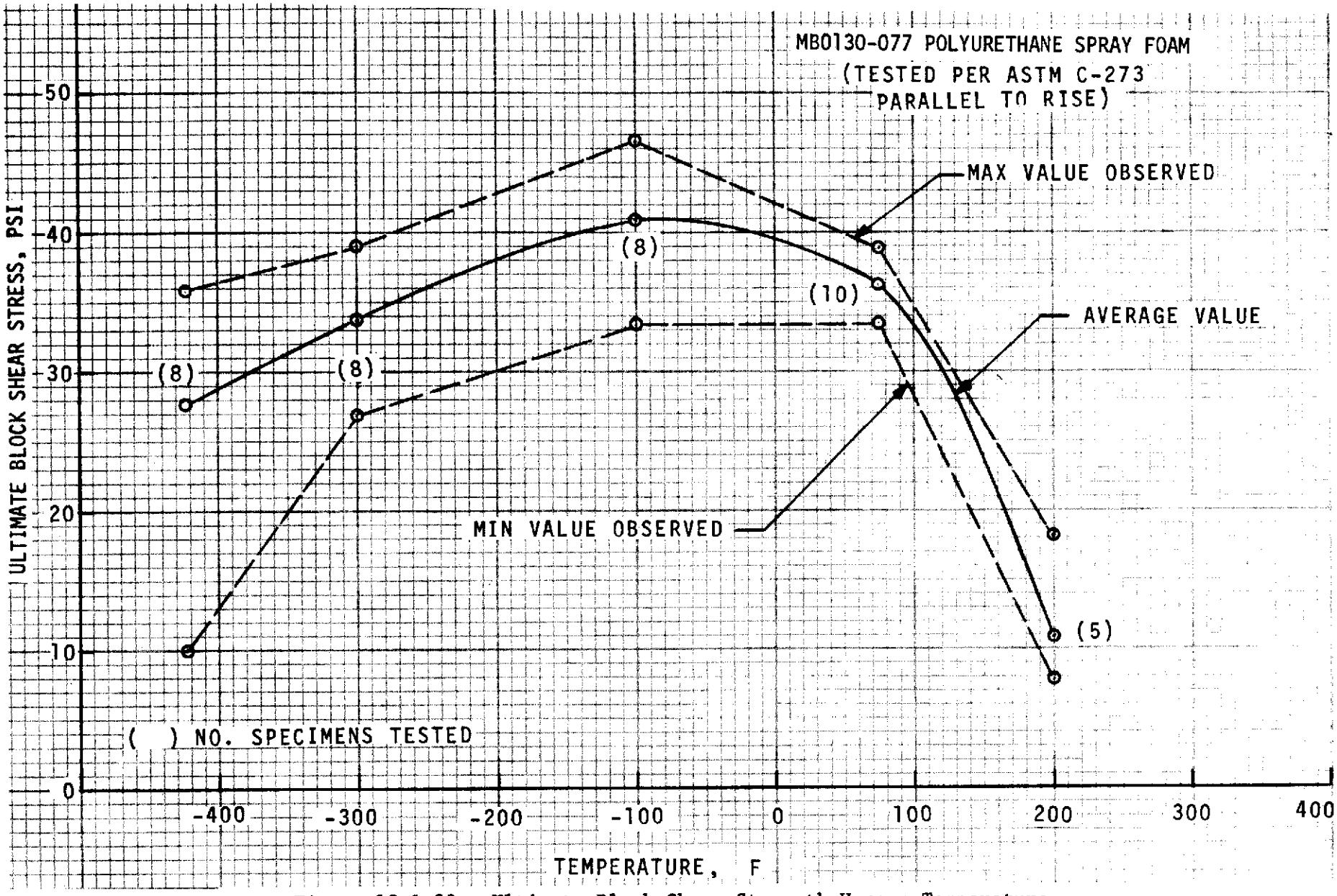

Figure 10.1-29. Ultimate Block Shear Strength Versus Temperature

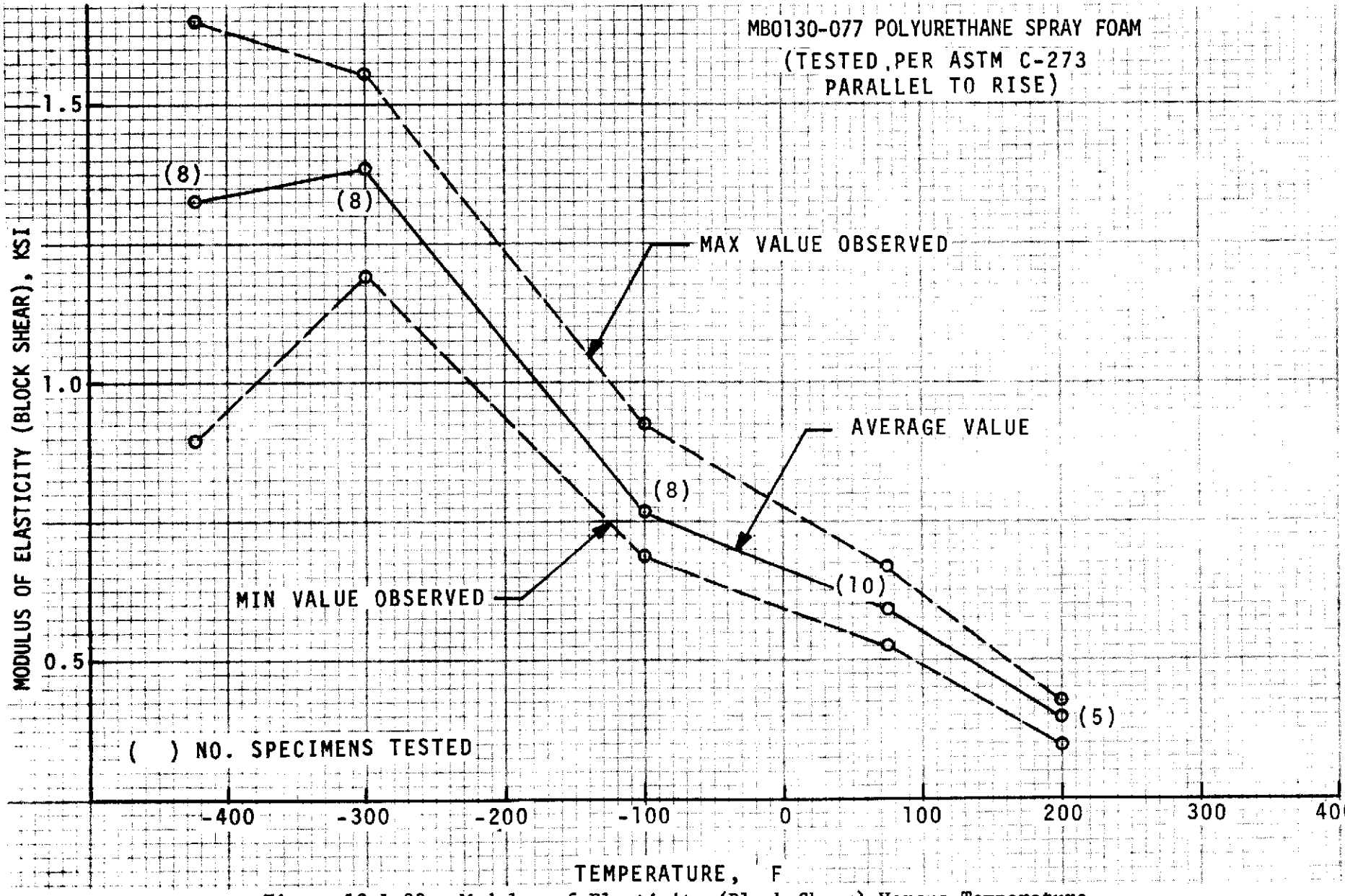

Figure 10.1-30. Modulus of Elasticity (Block Shear) Versus Temperature

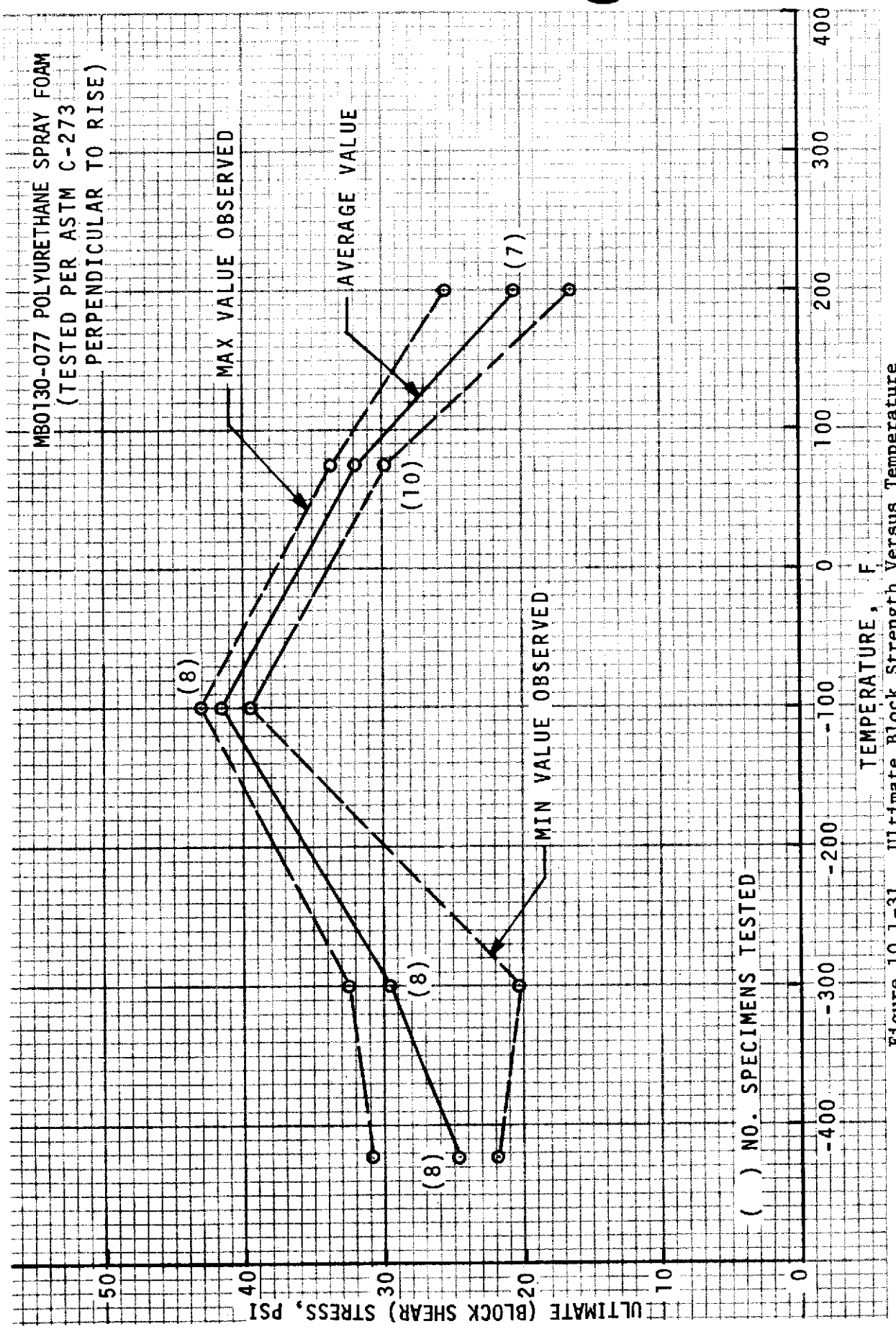

Figure 10.1-31. Ultimate Block Strength Versus Temperature

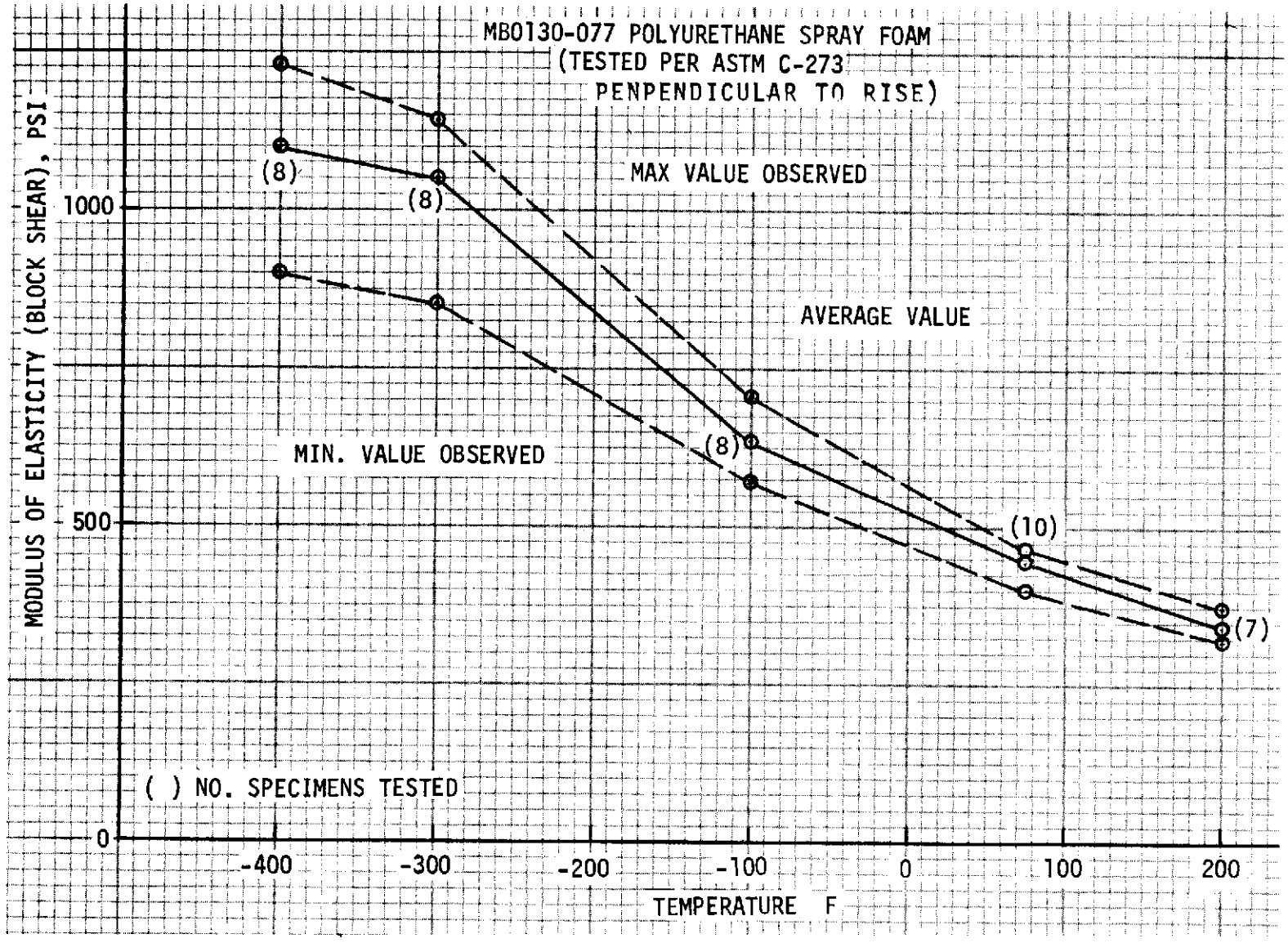

Figure 10.1-32. Modulus of Elasticity (Block Shear) Versus Temperature

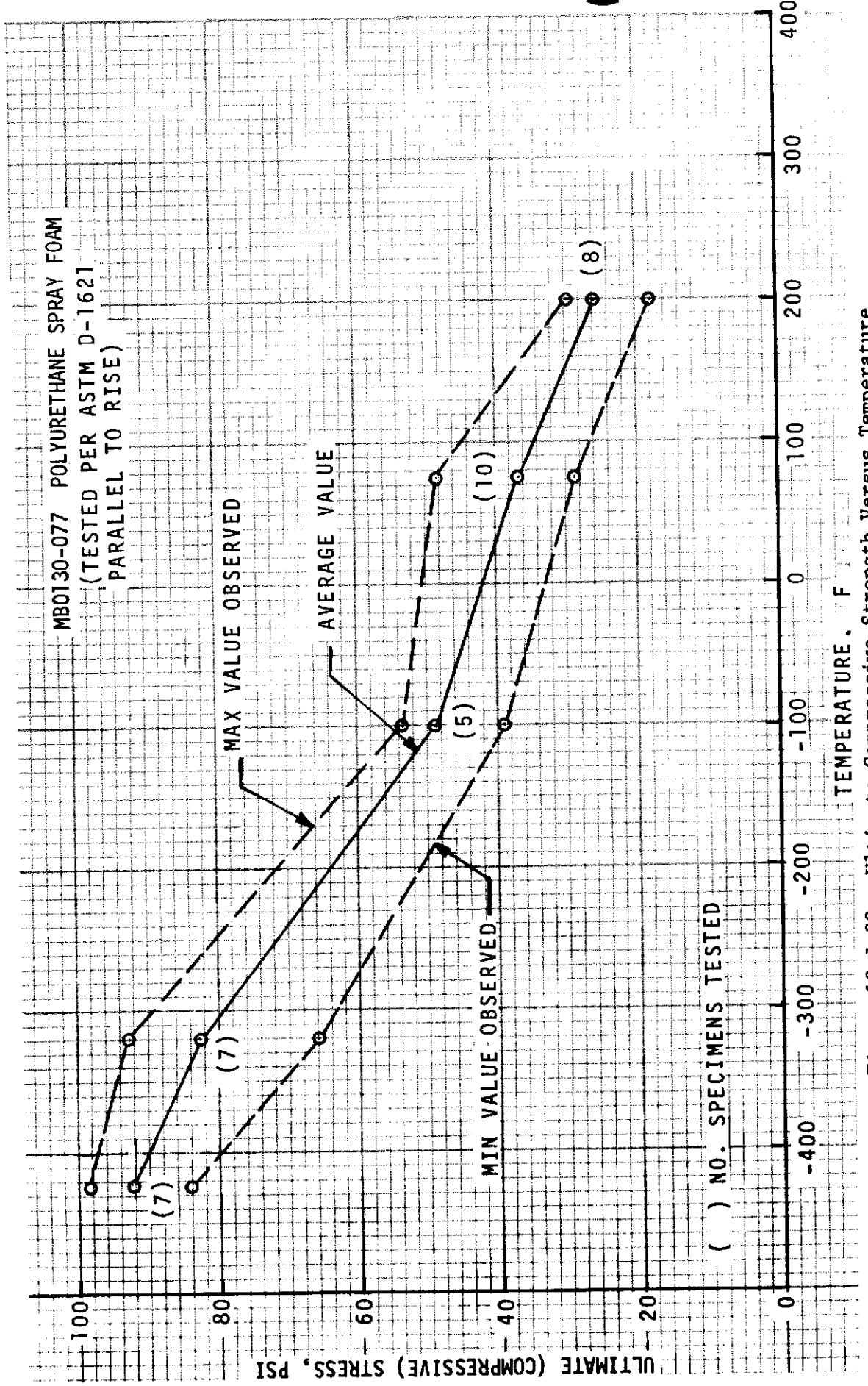

Figure 10.1-33. Ultimate Compressive Strength Versus Temperature

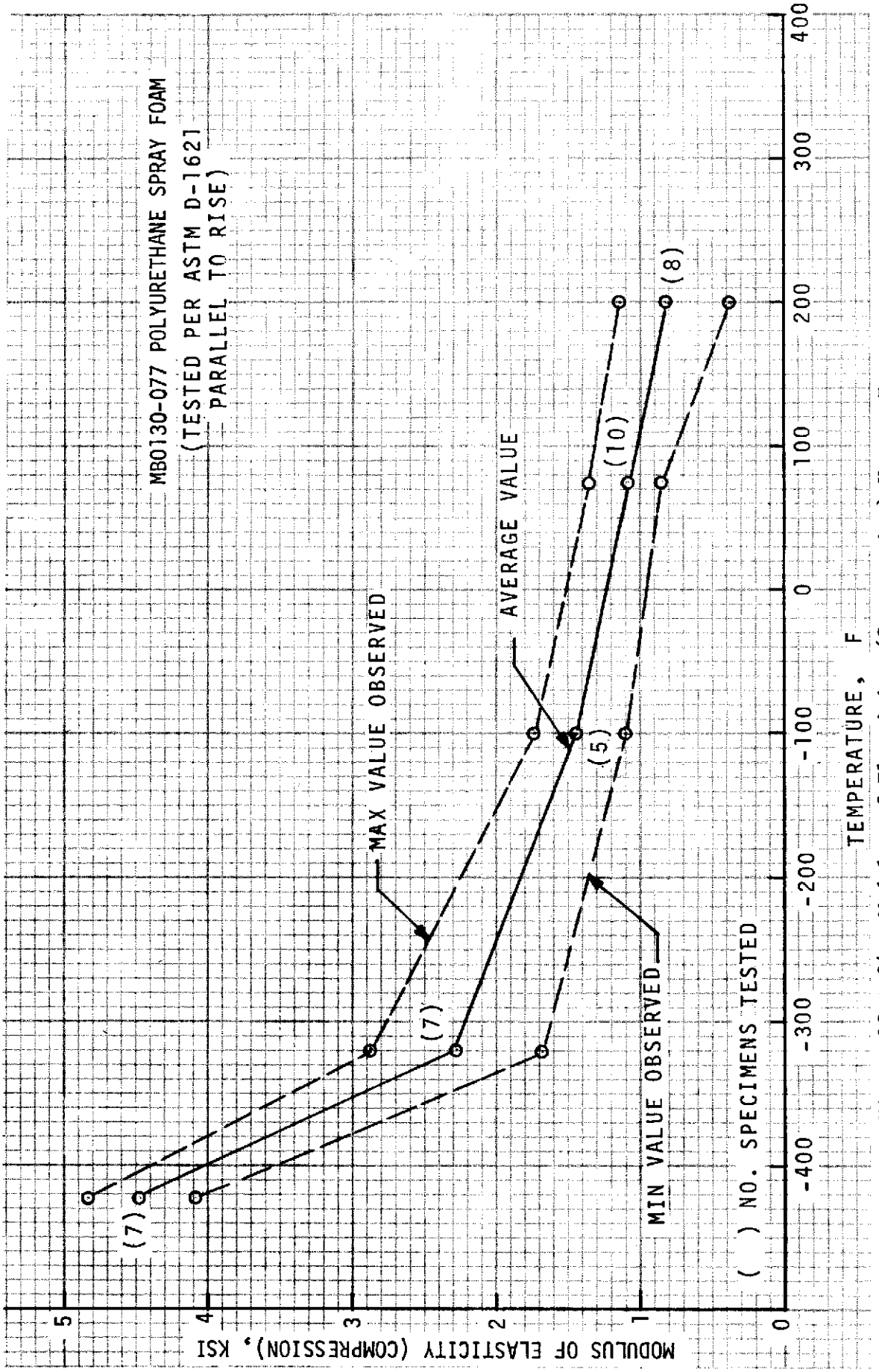

Figure 10.1-34. Modulus of Elasticity (Compression) Versus Temperature

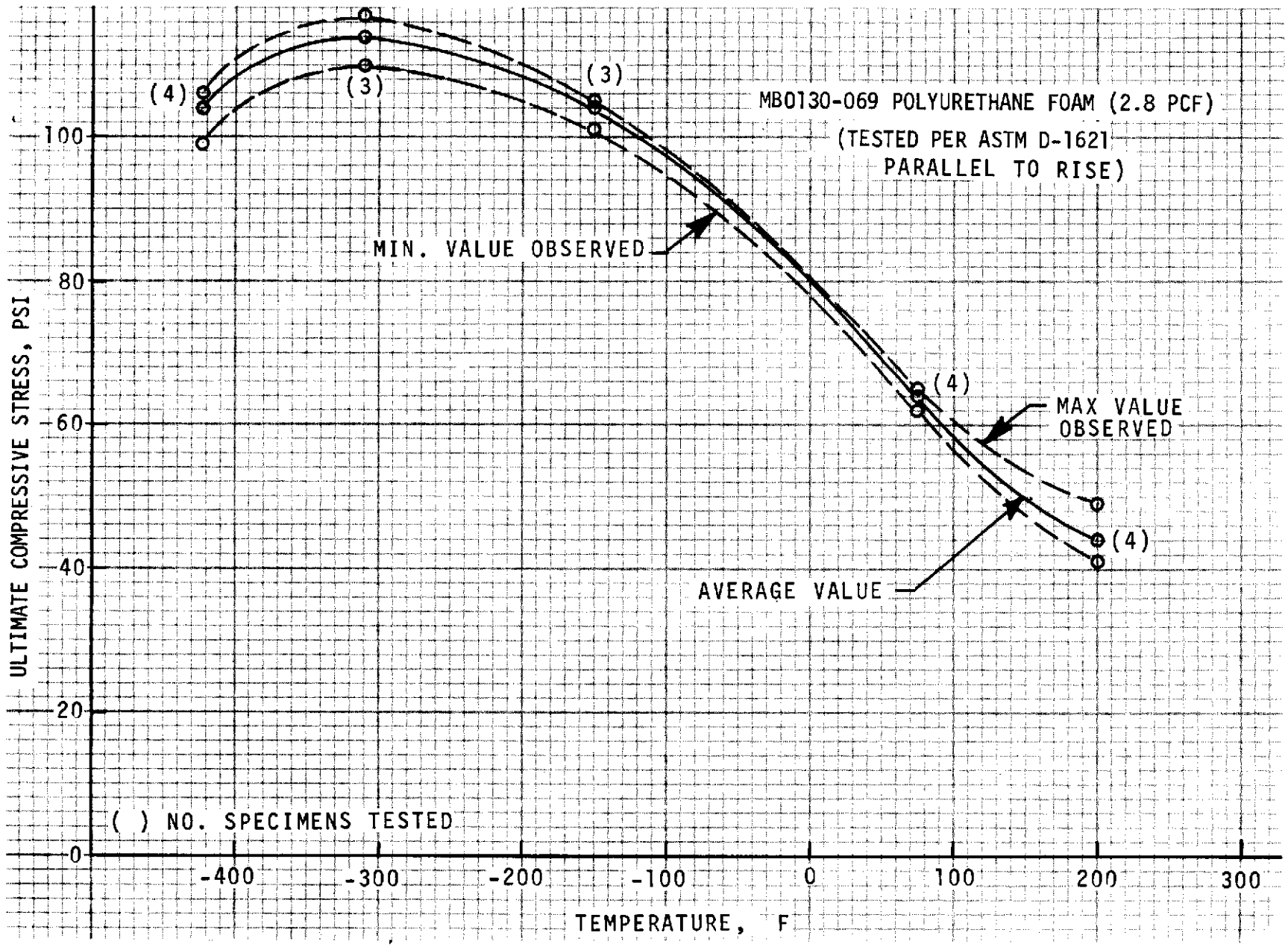

Figure 10.1-35. Ultimate Compressive Strength Versus Temperature

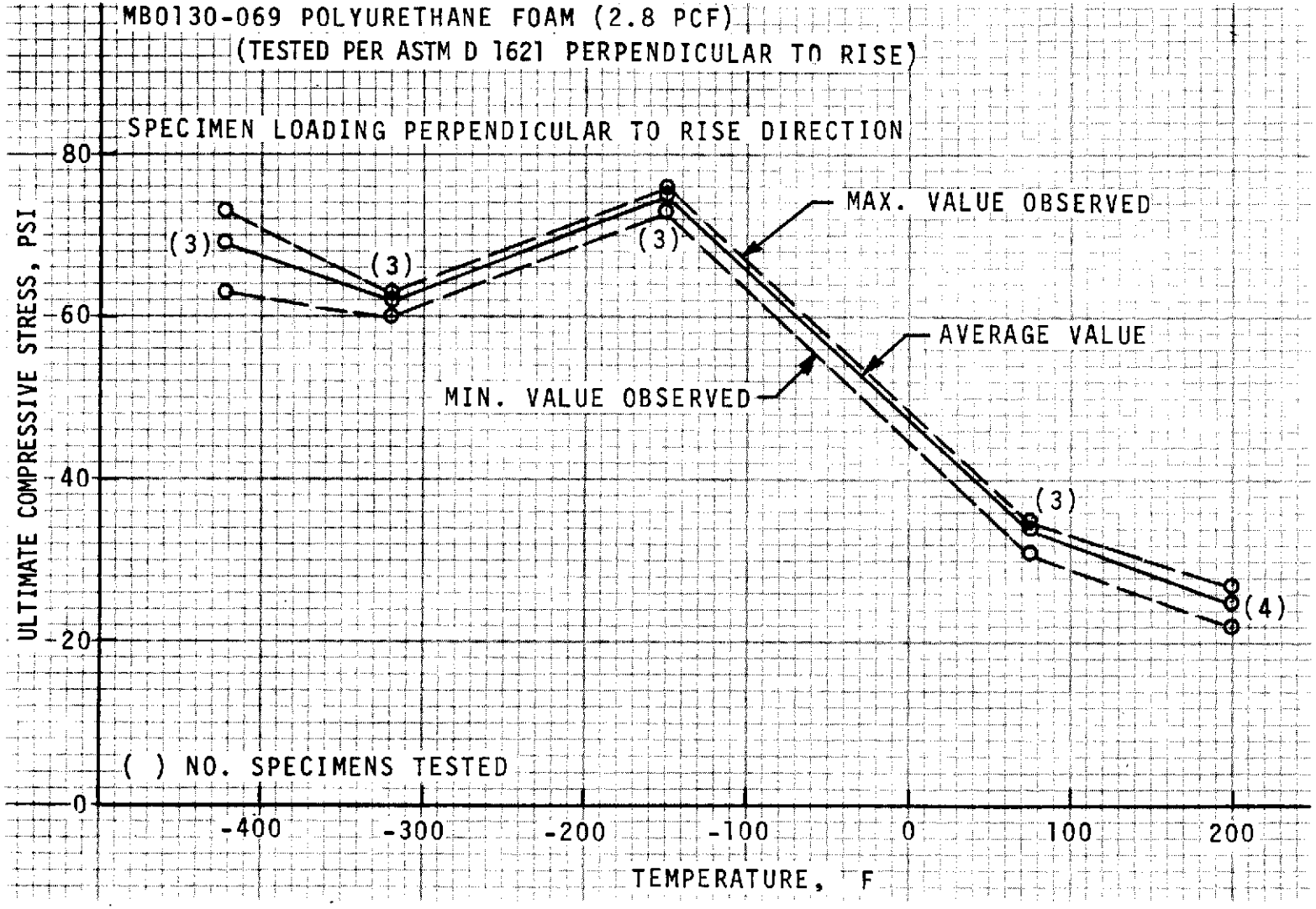

Figure 10.1-36. Ultimate Compressive Strength Versus Temperature

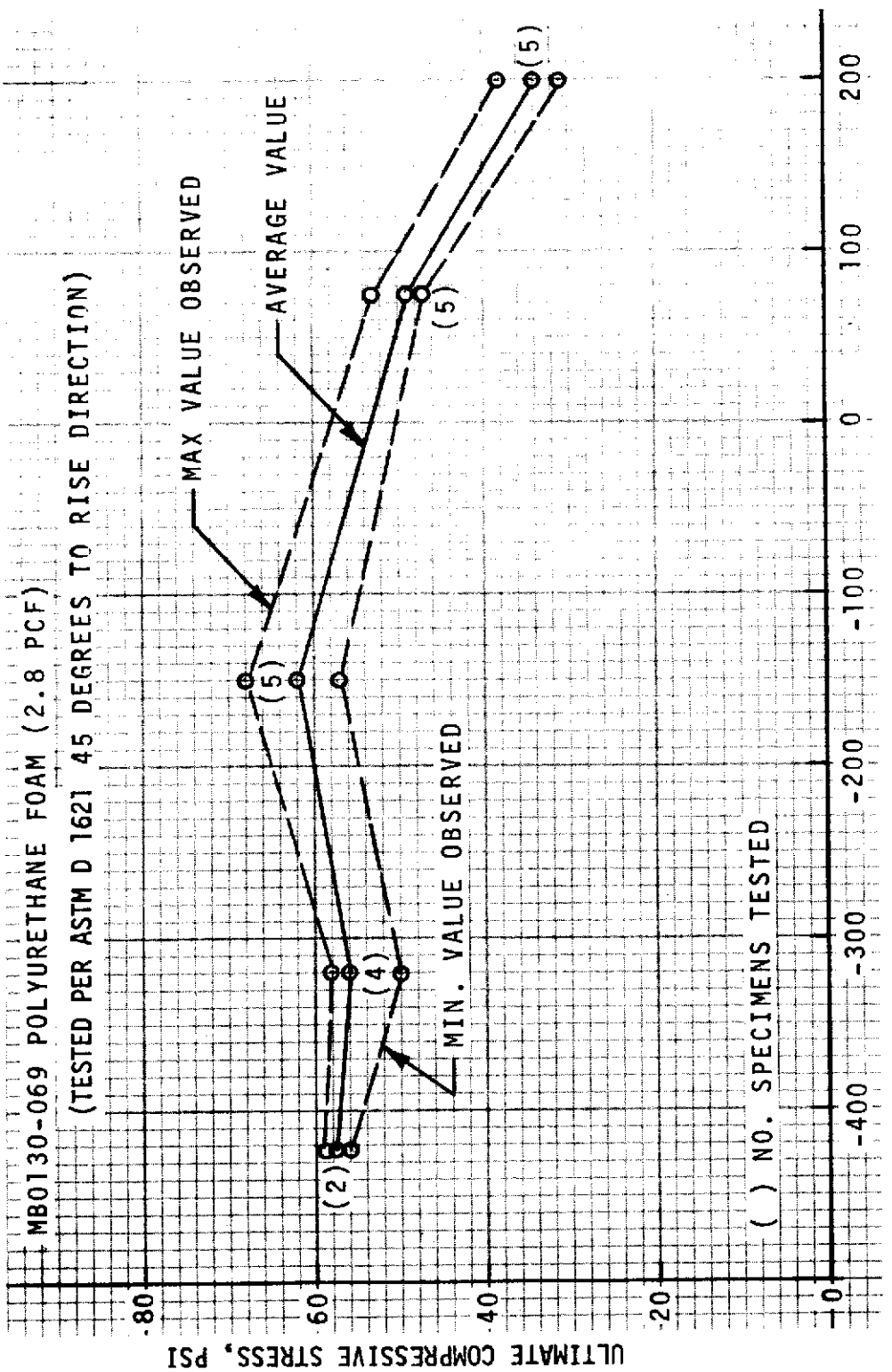

Figure 10.1-37. Ultimate Compressive Strength Versus Temperature

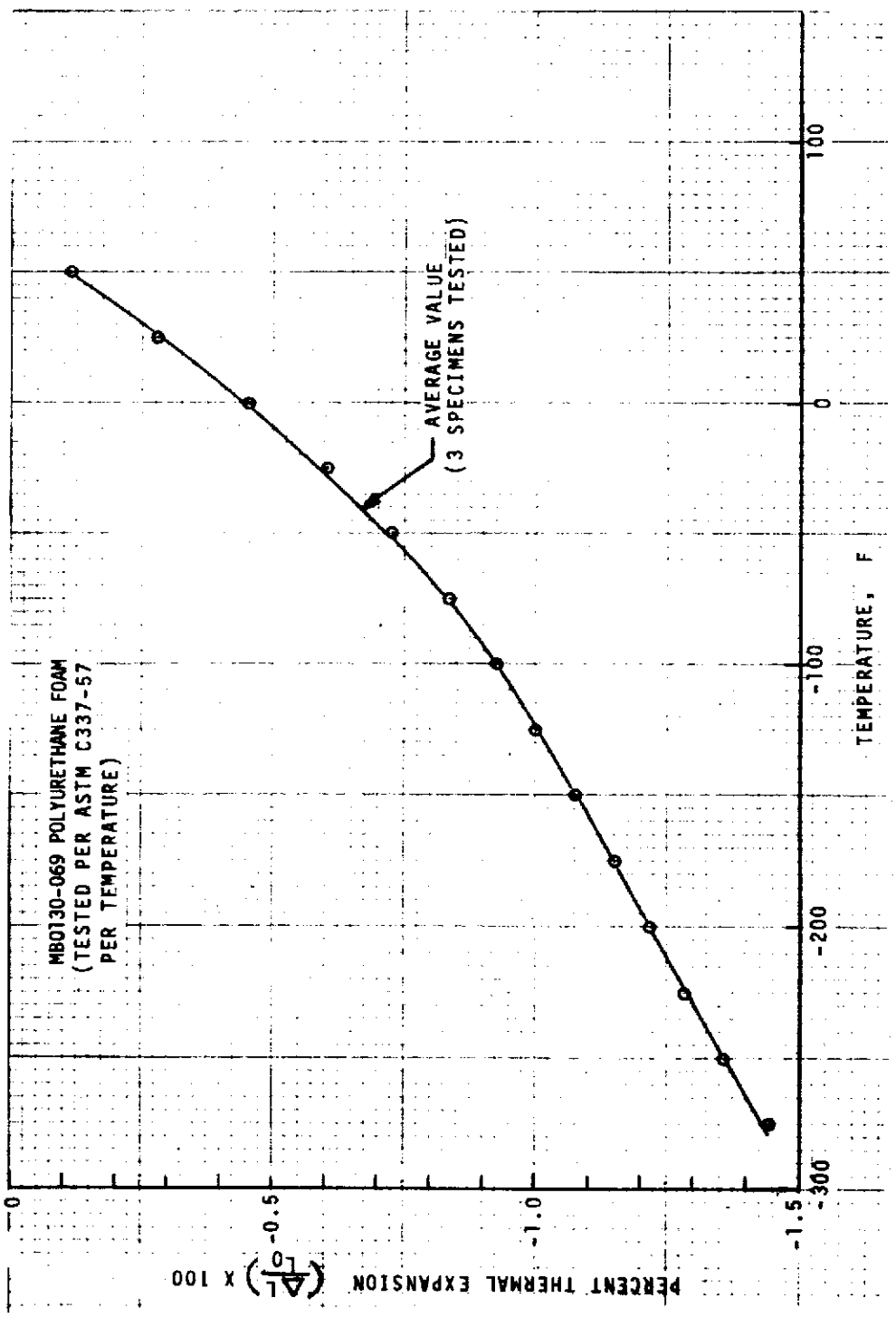

Figure 10.1-38. Thermal Contraction Versus Temperature

10.2 TESTING

Limited tests were conducted as part of the program to obtain fill-in data for foam systems that have possible application for internal insulation. This information was felt necessary to complement the S-II generated data which were obtained for externally applied insulations.

Although external and internal insulation must have the same thermal characteristics, the structural abilities are very different. For an external insulation the tank-foam interface is chilled to the cryogenic temperature. Foams in the 2-lb./ft.^{3} range have sufficient tensile and shear strength to meet the relative strain conditions. For this case the tank wall-foam bond also tends to reinforce the foam and allows it to move with the tank. An internally applied foam has the surface exposed directly to the cryogenic fluid while the foam-tank wall interface is near ambient or very warm compared to the surface exposed to the cryogenic fluid. The surface of the foams becomes highly loaded in this case and must be able to have higher load capability than for an external insulation. There is also no tank wall reinforcement in this case.

Tests were conducted to establish the structural characteristics of possible internal insulation candidates. The tests included ring-type tests to allow biaxial loading of foam specimens and structural properties tests to evaluate basic foam formulation effects.

10.2.1 Biaxial Ring Tests

The biaxial loading of the foam becomes very critical for an internal foam. Ring tests were devised to allow a uniform biaxial load to be applied to foam candidate materials. Figure 10.2.1-1 shows a typical specimen. Foam materials included General Plastics GP 3704 and Nopco BX 250A. Nopco BX 250A was used as a baseline for purposes of comparison.

Eight 36-inch-diameter ring specimens, four with Nopco BX 250A foam and four with GP 3704, were fabricated. The metal ring was 36 inches in inside diameter, 0.5 inch in wall thickness, and 3 inches in height. For three of the Nopco specimens the foam was bonded into the ring. The fourth specimen was sprayed into the ring. Foam was bonded into the ring for all of the GP 3704 specimens. The specimen configurations are summarized as follows:

a. Specimens 1 and 2

   Nopco BX 250 (0.942 A/B ratio) was bonded into the metal ring using 15 pbw (parts by weight) Zerotherm (polyurethane mixed with 15 pbw of milled glass fibers). After the adhesive had cured the center section of the foam was dished out as shown in Figure 10.2.1-1. The specimens were ready for cryoshock test.

b. Specimen 3

   Nopco BX 250 foam was sprayed into the interior of the metal ring (mix ratio 0.942 A/B ratio). After the foam was allowed to cure overnight, the foam was machined to the configuration shown in Figure 10.2.1-1.

c. Specimen 4

Nopco BX 250 foam (0.942 A/B ratio) was bonded to the metal ring using 35 pbw Zerotherm. After the adhesive had cured, the center section was dished out and uniaxial slits were placed in the foam 2.0 inches on center 1.0 inch.

d. Specimen 5

GP 3704 foam was bonded to the metal ring and bottom base plate (40 by 40 by 0.5 inches) using 35 pbw Zerotherm. A splice was placed in the center of the foam. The foam splice was made using 35 pbw Zerotherm. The center section of the foam was not dished out.

e. Specimen 6

GP 3704 foam was bonded to the metal ring and bottom base plate (40 by 40 by 0.5 inches) using 35 pbw Zerotherm. After the adhesive had cured, the center section of the foam was dished out as shown in Figure 10.2.1-1.

f. Specimen 7

Nine blocks of GP 3704 foam, 12 by 12 by 2 inches, were bonded to the metal ring and the bottom base plate (40 by 40 by 0.5 inches) using 35 pbw Zerotherm. The foam blocks were not bonded to each other. The foam blocks were joined by a "tendon joint" method as shown in Figure 10.2.1-2.

g. Specimen 8

GP 3704 foam was slitted and configured to the requirements specified in Figure 10.2.1-3. The foam was then bonded to the metal ring and base plate using 35 pbw Zerotherm as specified in the sketch. The sequence used for testing each of the foam specimens with gaseous and liquid nitrogen was varied. Generally, the tests required the chilling of the foam surface with gaseous nitrogen prior to "dumping" liquid nitrogen onto the foam surface. Test conditions and results for each specimen are summarized in Table 10.2.1-1.

10.2.2 Thermal Mechanical Analysis (TMA)

Foam material structural characteristics can be determined on the basis of TMA tests which show the contraction (expansion) behavior of foam with temperature. Comparative TMA data were obtained for varying fomulation and varying concentrations of the flame-retardant additive. Foams evaluated included General Plastics 3704 and an experimental CPR foam.

Data showing the expansion Δ L/L as a function of NCO/OH ratio are given in Tables 10.2.2-1 and 10.2.2-2. Data on Δ L/L for a varying flame-retardant additive (GP 3704 only) are given in Table 10.2.2-3.

Table 10.2.1-1. Results of Testing

SPECIMEN	TIME (MIN.)	FOAM TEMP (F)	METAL RING PLATE TEMP (F)	COOLING MEDIA	FOAM INSPECTION REMARKS
1	0	R.T.	R.T.	GN_2	START CHILLDOWN
	50	-260	50	GN_2	OK
	70	-320	45	LN_2	OK
	155	-320	45	NONE	LIQUID BOILED OFF SURFACE OF FOAM - NO CRACKS IN FOAM
	0	R.T.	R.T.	GN_2	DROPPED "BALL PEEN" HAMMER 2-1/2 FT 3 TIMES ONTO FOAM START CHILLDOWN
	30	-230	40	GN_2	OK
	32	-320	40	LN_2	OK
	115	-320	40	NONE	LIQUID BOILED OFF SURFACE OF FOAM - NO PROPAGATION OF INDENTATIONS CREATED BY DROPPING HAMMER ONTO FOAM
2	0	R.T.	R.T.	GN_2	START CHILLDOWN
	33	-300	40	GN_2	OK
	35	-320	25	LN_2	OK
	125	-320	25	LN_2	OK
	240	-320	25	NONE	LIQUID BOILED OFF SURFACE OF FOAM - NO CRACKS IN FOAM
	0	R.T.	R.T.	GN_2	THREE CRACKS INDUCED IN FOAM (1" x 1/4")
	32	-285	40	GN_2	CRACKS IN SURFACE OF FOAM HAD NOT PROPAGATED
	34	-320	40	LN_2	OK
	36	-320	40	LN_2	LARGE CRACK THRU STARTER CRACK "A" EXTENDING TO METAL RING
3	0	R.T.	R.T.	GN_2	START CHILLDOWN
	35	-300	50	GN_2	OK
	38	-310	50	GN_2 NO LN_2 ON SURFACE	FOAM BROKE 1/2" FROM METAL RING - ONE-HALF WAY AROUND THE PERIMETER OF THE RING

Table 10.2.1-1. Results of Testing (Continued)

SPECIMEN	TIME (MIN)	FOAM TEMP (F)	METAL RING PLATE TEMP (F)	COOLING MEDIA	FOAM INSPECTION REMARKS
4	0	R.T.	R.T.	GN_2	START CHILLDOWN
	20	-150	55	GN_2	
	25	-200	50	GN_2	CIRCUMFERENTIAL SLIT 1/3 AROUND PERIMETER IN FOAM
5	0	R.T.	R.T.	GN_2	START CHILLDOWN
	47	-270	60	GN_2	OK
	60	-310	55	GN_2	OK
	68	-320	55	LN_2	OK
	71	-320	50	LN_2	FOAM CRACK STARTED AT BONDLINE PROPAGATED TO FOAM RING
	78	-320	50	LN_2	PLACED CRACK IN FOAM (.25" x 1"). EDGE OF CRACK 4-1/2" FROM SPLICE (NORMAL) ON THE OPPOSITE SIDE OF ORIGINAL CRACK
	87	-320	50	LN_2	CRACK PURPOSELY ENLARGED TO .75" x 1"
	89	-320	50	LN_2	CRACK PURPOSELY ENLARGED TO 1.5" x 1". CRACK PAOPAGATED TO SECONDARY CRACK THRU JOINT AND AROUND PERIMETER.
6	0	R.T.	R.T.	GN_2	START CHILLDOWN
	45	-270	60	GN_2	OK
	48	-320	60	LN_2	OK
	50	-320	50	LN_2	3/4 INCH LN_2 ON SURFACE OF FOAM
	95	-320	50	LN_2	ADD LN_2 TO FOAM SURFACE
	100	-320	50	LN_2	FOAM CRACKED AROUND PERIMETER

Table 10.2.1-1. Results of Testing (Continued)

SPECIMEN	TIME (MIN)	FOAM TEMP (F)	METAL RING PLATE TEMP (F)	COOLING MEDIA	FOAM INSPECTION REMARKS
7	0	R.T.		GN_2	START CHILLDOWN
	20	-300	$\overline{65}$	GN_2	VISUAL - OK
	27	-320	--	LN_2	7/8 INCH LN_2 ON FOAM SURFACE
	30	-320	30	LN_2	
	50	-320	-10	LN_2	
	115	-320	-60	LN_2	
	125	--	--	--	LN_2 BOILED OFF
	140	R.T.	--	GN_2	START CHILLDOWN
	160	-320	-15	LN_2	
	200	-320	-40	LN_2	
	270	-320	-35	LN_2	
	280	-320	--	LN_2	ALLOW LN_2 BOIL OFF NORMALLY. NO VISIBLE DAMAGE TO FOAM
	0	R.T.	--	GN_2	START CHILLDOWN
	18	-310	55	GN_2	VISUAL - OK
	25	-320	40	GN_2	
	68	-320	-40	GN_2	
	198	-320	-70	GN_2	
	158	-320	-125	GN_2	
	218	-320	-150	GN_2	
	278	-320	-120	GN_2	REMOVED LIGHT FROST FROM OUTER METAL RING AND PLATE
	338	-320	-90	GN_2	
	398	-320	-45	GN_2	WARM BREEZE MELTED FROST
	458	-320	-30	GN_2	
	473	-320	--	GN_2	ALLOW LIQUID BOIL OFF. NO VISIBLE DAMAGE TO FOAM
	0	R.T.	--	GN_2	START CHILLDOWN
	35	-320	25	LN_2	LIQUID ON FOAM SURFACE
	95	-320	-40	LN_2	
	155	-320	-55	NONE	ALLOW LIQUID BOILOFF - NO VISIBLE DAMAGE IN FOAM

Table 10.2.1-1. Results of Testing (Continued)

SPECIMEN	TIME (MIN)	FOAM TEMP (F)	METAL RING PLATE TEMP (F)	COOLING MEDIA	FOAM INSPECTION REMARKS
7 (CONT.)	0	R.T.	--	GN_2	START CHILLDOWN
	15	-320	45	LN_2	LIQUID ON FOAM SURFACE
	75	-320	-15	LN_2	
	135	-320	-25	NONE	ALLOW LIQUID BOIL OFF - NO VISIBLE DAMAGE IN FOAM
	0	R.T.	--	GN_2	START CHILLDOWN
	30	-320	30	LN_2	LIQUID ON FOAM SURFACE
	90	-320	-25	LN_2	
	150	-320	-50	LN_2	ALLOW LIQUID BOIL OFF. NO CRACKS IN FOAM SURFACE
	0	R.T.	--	GN_2	START CHILLDOWN
	20	-320	20	LN_2	LIQUID ON SURFACE
	85	-320	-30	LN_2	ALLOW LIQUID BOIL OFF. NO CRACKS IN FOAM SURFACE
8	0	R.T.	R.T.	GN_2	START CHILLDOWN
	14	-14	55	GN_2	
	29	-280	--	GN_2	OK
	39	-320	45	LN_2	
	44	-320	40	LN_2	
	59	-320	30	LN_2	
	74	-320	--	NONE	ALL LN_2 BOILOFF - CRACKS NOTICED AT BOTTOM OF ALL GROOVES PROBABLY EXTEND TO TANK WALL

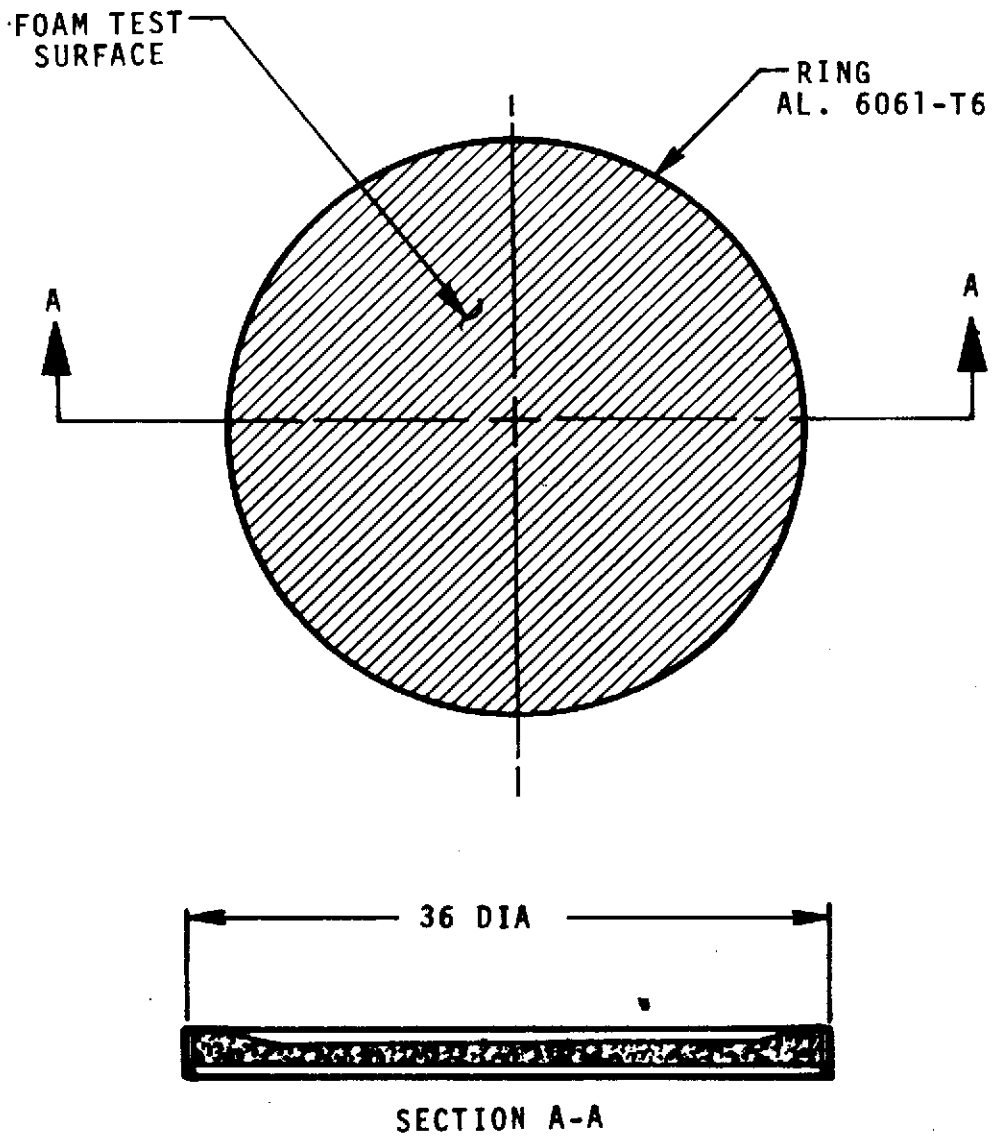

Figure 10.2.1-1. Configuration for Biaxial Ring Tests

Table 10.2.2-1. TMA Data on CPR Foams for Varying NCO/OH Ratio

NCO/OH Index Ratio	Density (lb./ft.^{3})	Δ L/L* (in/in x 10^{-3})	Type Foam
0.8	3.8	11.2	X-157-17-I
0.9	3.6	12.3	
1.0	3.5	12.6	
1.1	4.3	12.1	
1.2	3.8	11.6	
0.8	4.1	10.7	X-157-17-II
0.9	3.9	11.3	
1.0	3.9	10.3	
1.1	3.8	11.4	
1.2	3.7	12.9	
* -168 C to 25 C			

Table 10.2.2-2. TMA Data on GP 3704 for Varying NCO/OH Ratio

NCO/OH Index Ratio	Density (lb/ft^3)	Δ L/L* (in/in x 10^{-3})
0.9	3.9 - 4.2	11.6
1.0	3.7 - 4.3	11.2
1.05	4.0 - 4.4	9.6
1.1	3.9	12.4
1.15	3.7 - 4.0	11.3
* -168 C to 25 C		

Table 10.2.2-3. TMA Data on GP 3704 With Varying Percentage of Flame-Retardant Additive

Percent Flyrol Additive	Density (lb/ft^3)	L/L (in/in x 10^{-3})
4	4.1	9.0
6	4.2	10.5
8	4.3	9.1
10	4.6	9.9

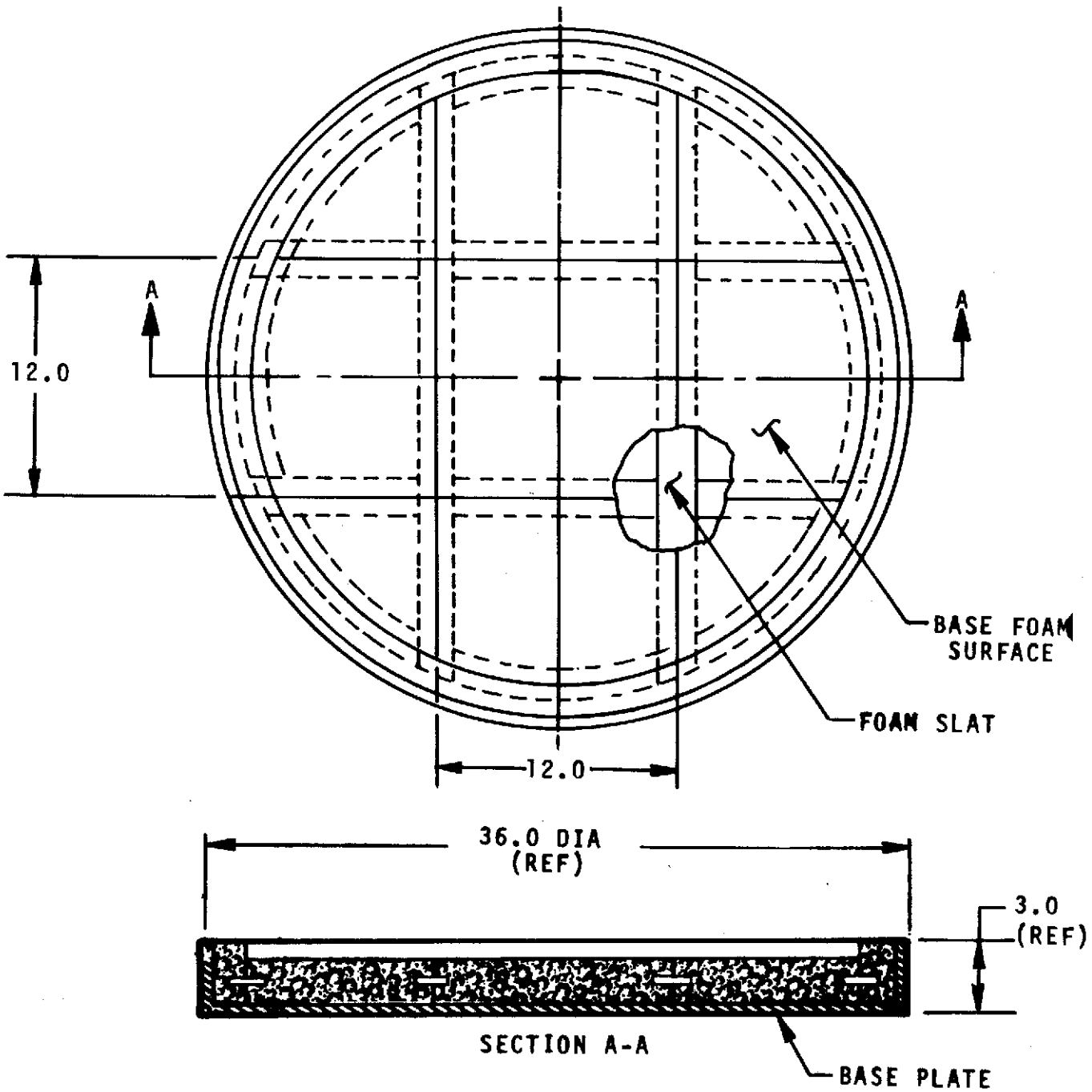

Figure 10.2.1-2. Configuration of Tendon Joint Specimen

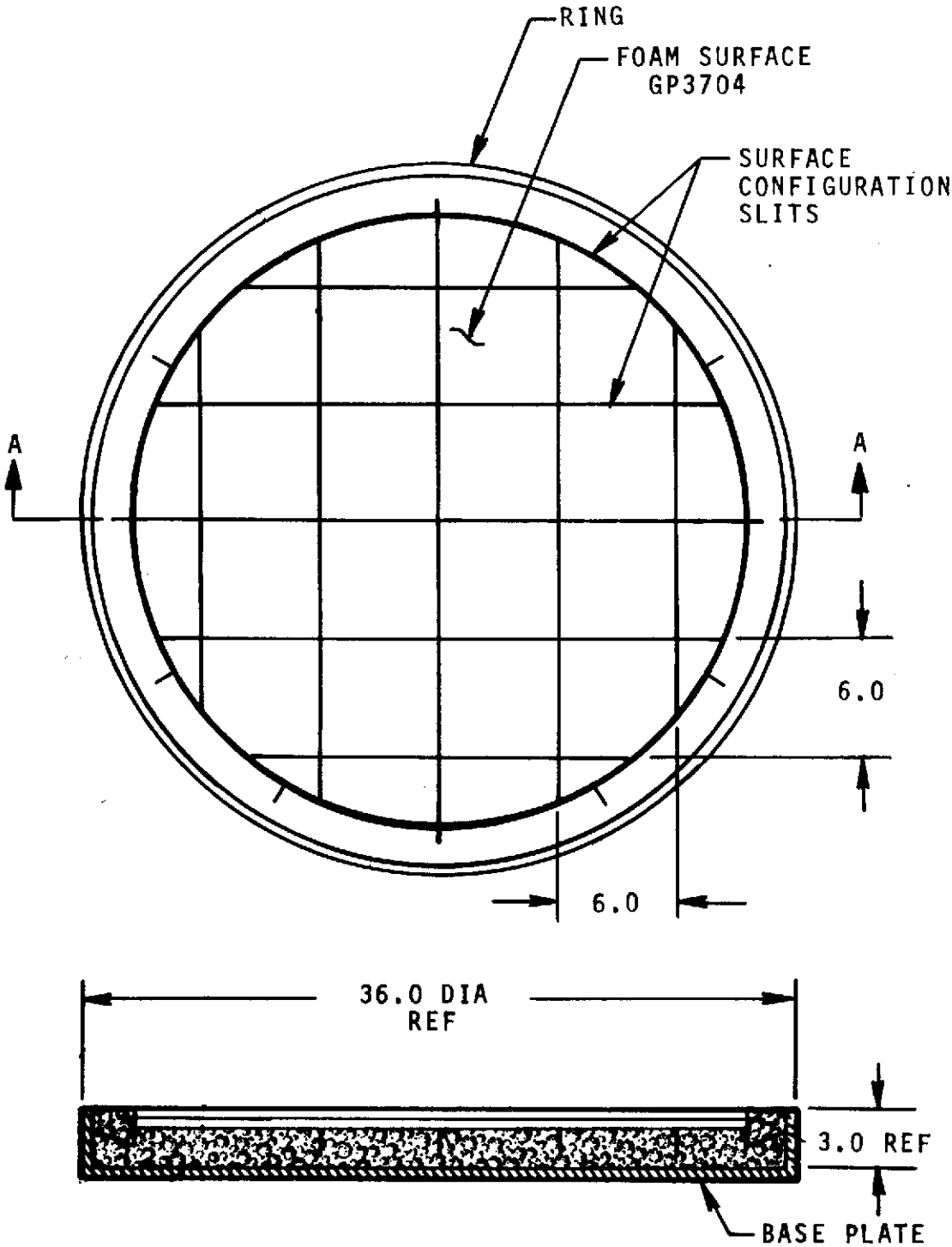

Figure 10.2.1-3. Configuration for Slitted Joint Specimen

11.0 MATERIAL PROCESSES

This section contains a brief discussion of surface finishes, primers, adhesives, coatings, and foam systems used in support of the Saturn S-II program. A general description of these materials is provided, including their chemical compound, storage life, mixing procedures, working life, cure requirements, and methods of application. Additional information may be obtained for these materials by use of the computer program (see Section 15.0).

11.1 SURFACE FINISH PROCESSES

11.1.1 General-Purpose Solvent Cleaning (MA0110-010)

This specification establishes materials and processes for general-purpose solvent cleaning, except vapor degreasing, and provides an index (Table 11.1.1-1) to general chemical processing specifications.

General-purpose solvent cleaning may be performed as a preliminary operation prior to additional cleaning or processing, or as a final general cleaning process when further cleaning or processing is not required.

11.1.2 Stripping Organic Finishes (MA0610-022)

This specification designates the materials and procedures to be used for stripping organic coatings from metals. It does not apply to the stripping of inorganic coatings nor to the stripping of coatings from nonmetals, nor does it authorize the use of liquid impact or centrifugal abrasive blasting equipment.

11.1.3 Surface Preparation of Metals/Nonmetals (MA0610-023)

This specification establishes the materials and procedures for preparing the surfaces of metals and nonmetals for adhesive bonding. It applies to parts and assemblies which can be processed by immersion or manual methods and only those materials indicated within the specification.

This specification does not apply to large parts or assemblies whose configuration or large surface area for bonding would require processing methods other than immersion or manual techniques.

11.2 PRIMERS

11.2.1 Adhesive Primer (MB0120-032)

This is a two-part epoxy resin base system requiring an elevated temperature cure and, in a fully cured condition, may be used continuously in a temperature range from -423 to 300 F. The material is intended to function in one or more of the following capacities:

a. A substrate for foam insulation.

Table 11.1.1-1. General Cleaning and Processing Specifications

Specification Title	Spec. No.
Cleaning Hydraulic System Components	MA0110-001
Cleaning of Aluminum and Aluminum Alloys	MA0110-011
Cleaning Ferrous Alloys	MA0110-012
Descaling and Passivation of Corrosion and Heat Resistant Alloys	MA0110-013
Cleaning and Protective Treatment of Magnesium Alloys	MA0110-014
Cleaning Titanium and Titanium Alloys	MA0110-015
Ultrasonic Cleaning	MA0110-017
Cleaning Parts of Propellant, Pressurizing and Circulating Systems	MA0110-018
Cleaning Copper and Copper Alloys	MA0110-019
Abrasive Cleaning	MA0110-020
Stripping Organic Finishes	MA0110-023
Surface Preparation of Metals and Nonmetals for Adhesive Bonding	MA0110-024
Cleaning and Conditioning of Metals for Brazing or Soldering Processes	MA0110-026
Cleaning Oxidizer System Parts and Assemblies Following Fluorescent Penetrant Inspection	MA0110-027
Steam Cleaning of Ferrous and Non-Ferrous Alloys	MA0110-028
Surface Treatment of Fluorocarbon Wire Insulation for Improved Adhesion	MA0110-029
Cleaning Plastic, Glass and Elastomeric Materials	MA0110-030

b. A substrate for adhesive bonding.

c. A corrosion barrier for the metal substrate.

11.2.1.1 Storage Life

The unmixed adhesive primer has a minimum shelf life of six months at a temperature of 80 F or less. The mixed adhesive primer may be stored up to six days at a maximum temperature of 120 F. The container must be covered in a manner that will prevent contamination or solvent loss by evaporation.

11.2.1.2 Mixing

Mixing of the primer system requires that Components I and II be thoroughly agitated to provide a homogeneous blend prior to combining them to form the primer solution. The fillers in Component I have a tendency to settle in the container. Therefore, following agitation a stirring or mixing stick should be used to dig to the bottom of the container to determine if complete dispersion of the filler materials has been achieved.

After assuring that the individual components are properly blended, five parts by weight of Component I are added to four parts by weight of Component II and thoroughly mixed. The nine parts of mixed primer are then diluted with methyl ethyl ketone (MEK). The maximum amount of solvent allowed is 40 parts by weight. For all spray applications, it is desirable to add the maximum allowable amount of solvent (MEK) to avoid "cobwebbing" of the primer during spraying. Cobwebbing is the formation of thread-like deposits of primer which accumulate on or adjacent to the priming surface, causing discontinuities on the cured coating.

11.2.1.3 Application

Conventional spray equipment is used to apply the primer to the substrate. During spray application, the mixed primer must be kept under constant agitation to assure that components do not separate. When a large volume of primer is being sprayed, mechanical agitation devices should be used. Spray application of the primer to the surface requires practice and patience. The first coat of primer should be very light and subsequent coats should be applied with moderation to avoid runs or sagging of the coating.

Preliminary thickness measurements of the uncured primer are made prior to elevated temperature cure of the material. This measurement should be made at least two hours after the latest application of the primer. If measurements are made before two hours, the material is too soft and will give an erroneous reading. If the results of the thickness measurement show that the primer is too thin, additional material is

applied to provide the required thickness. If the uncured primer is too thick, it should be removed from the metal with MEK in the thick areas and re-applied to meet the specification thickness requirements.

Additional coats of primer may be applied at any time prior to the elevated temperature cure but care must be exercised to avoid runs or sags. All primed parts must be air-dried for a minimum of 30 minutes after the final coat to permit partial evaporation of the solvent in the primer. During the time between primer application and placement in the oven for cure, care must be taken to protect the part from contamination. If paint or other particles are trapped on the primer prior to cure, they may ignite or char during the high-temperature cure and burn holes in the primer.

11.2.1.4 Cure

The cure requires the primed part be heated (in a certified circulating air oven) to 240±10 F and held for 30±5 minutes, then the temperature raised to 290±10 F for 180±10 minutes, or 340±10 F for 60±10 minutes.

11.2.1.5 Problems

a. Application: When bare aluminum and Freon-blown foam insulation are in contact and subjected to environmental exposure, active and aggressive surface corrosion of the aluminum results. The active nature of the corrosion has been attributed to the Freon in the foam acting with moisture from the atmosphere and providing a solution chemically hostile to aluminum. Therefore, the MB0120-032 adhesive primer must completely cover the aluminum for corrosion protection. The primer acts only as a barrier to moisture or other active chemicals in the system; small pinholes in the primer therefore provide a site for active corrosion initiation.

b. Cure: During the cure cycle of a part or assembly thermal strain can be induced, causing buckling, unless the temperature variation over the curing part or assembly is kept to a minimum.

11.2.1.6 Commercial Similarity

Pittsburgh Plate Glass Co. primer M602 or equivalent commercial products will qualify to this specification.

11.2.2 Type II Primer (MB0120-042)

This is a two-part modified polyester/isocyanate system which consists of a polyester resin, Component B, and a polyphenyl polyisocyanate (PAPI) curing agent, Component C. It is used as a primer on metal details, polyvinylfluoride, and polyethylene terephthalate (polyester) materials. The Type II primer is specifically designed for continuous use at -423 to 120 F in high strength applications.

11.2.2.1 Storage Life

Components B and C have minimum shelf lives of three and six months, respectively, when stored in their unopened original containers at 60 to 90 F. The material may gel when stored below 60 F, but heating will restore it to its fluid state.

Pot life of one quart of the mixed primer at 75±15 F is eight hours. This applies to both thinned or unthinned primer.

11.2.2.2 Mixing

The material specification requires that mixing instructions be stated by the manufacturer on the container label. The primer, following mixing in accordance with the manufacturer's instructions, is thinned to a brushing or spraying consistency by adding solvent consisting of 30-percent MEK and 70-percent toluene by weight. A brushing consistency is obtained by combining 100 parts by weight of the mixed primer with 100 parts by weight of the thinner mixture. A spraying consistency is obtained by combining 100 parts by weight of the mixed primer with 180 parts by weight of the thinner mixture.

11.2.2.3 Working Life

The working life of one quart of mixed primer, thinned or unthinned, is eight hours minimum at 75±15 F. The working life is the length of time after which the material no longer exhibits the desired brushing or spraying consistency.

11.2.2.4 Application

The mixed MB0120-042 Type II primer is applied to the cleaned faying surfaces by brushing or spraying to a continuous dried film thickness of 0.0005 inch maximum. For most applications, the primer is applied by brushing because of the hazards involved with spraying volatile materials. One box-coat of primer is sufficient to obtain the primer requirements.

Surfaces requiring MB0120-042 Type II primer, in areas where spray-foam will later be applied, are to be cleaned by wiping with MEK solvent using Masslinn towels until no evidence of soil is visible on the clean wiper. The solvent is not permitted to air-dry on the surfaces because contaminants diluted by the solvent will remain on the surface when the solvent evaporates.

Environmental control during the application of the MB0120-042 Type II material is generally established at 60 to 90 F and 70-percent relative humidity maximum. These requirements may differ slightly among the various controlling process specifications and the appropriate specification always should be consulted.

11.2.2.5 Cure

The primer requires a minimum cure of 4 hours at 75±15 F prior to any bonding or foam insulation application.

11.2.2.6 Comments

The application of the MB0120-042 Type II primer requires a continuous dried film thickness of 0.0005 inch maximum. Since the primer is opaque, assurance of a continuous film cannot be determined visually after the primer is cured. Therefore, it is necessary that the actual application of primer be monitored to assure complete coverage. One box-coat of the primer is sufficient for adequate mechanical properties and will not exceed the 0.0005-inch maximum thickness requirement.

When MB0120-042 Type II primer is applied over bare aluminum and foam insulation is subsequently applied, severe and aggressive corrosion will result when the materials are climatically exposed. This incompatibility, however, appears to be accelerated in the presence of MB0120-042 Type II primer. Therefore, in no case is MB0120-042 Type II primer to be applied over bare aluminum that will later be foam insulated. This restriction includes application over scratched or defective MB0120-032 primer.

Details primed with the MB0120-042 Type II material may be stored a maximum of 45 days after priming prior to subsequent foaming or bonding operations. If the storage life is exceeded, the surface can be solvent-wiped with MEK and reprimed in accordance with the procedures previously described. The solvent will not remove completely the existing MB0120-042 Type II primer and therefore removal of the primer should not be expected.

11.2.2.7 Commercial Similarity

Primer M manufactured by Furane Plastics, Inc., or an equivalent commercial product will qualify to this specification.

11.2.3 Adhesive Primer (MB0120-047)

This is a thermosetting material-type solvent-carried liquid primer. It is used primarily to coat prepared surfaces of metal, most thermosetting plastics, and metal honeycomb cores as a prerequisite to structural bonding with epoxy-phenolic tape adhesive. The primer may be furnished in two types to be used in the following environments:

Type I - For continuous use between -423 and 180 F.
Type II - For continuous use between -300 and 300 F, and short times between 300 and 500 F.

Two separate materials meet the requirements of this specification: two-component P-413 and single-component HT-424B.

11.2.3.1 Storage Life

Both types of the primer have minimum storage life of six months when Type I is stored at 40 F or less and Type II is stored at 0 F or less. Mixed P-413 primer, when stored at 40 F, has a recommended storage life of 30 days.

11.2.3.2 Mixing

HT-424B primer is a single-component material and requires no mixing. After it is removed from storage refrigeration and prior to its application it should be allowed to sit for two hours at room temperature. This primer also should be thoroughly agitated or stirred before use to insure a homogeneous mixture of the primer's constituents.

P-413 primer is a two-component system and both components should be allowed to stand at least two hours at room temperature after removal from refrigeration and before mixing. Before using it the two components should be thoroughly mixed in an equal-volume ratio.

11.2.3.3 Application

Both primer systems may be applied by conventional brush or spray techniques. The HT-424B must be thinned before spraying in a volume ratio of 1 part primer to 1.5 parts HT-424B primer thinner. The P-413 primer needs no additional preparation. No matter which technique is used, both primers should be applied in single coats 0.0005 to 0.001 inch thick and each coat should be allowed to air-dry for 30 minutes before the application of another coat. Both primer systems should be applied when the ambient temperature is 75F$\pm$10 F and the relative humidity is 70 percent or less. Care must be exercised when applying the primers so as to avoid any runs or sags. The primer coats also must be protected from contamination during air drying. Foreign particles on the surface of the primer could damage the finish of the primer during the elevated temperature cure.

11.2.3.4 Cure

The primer may be fully cured upon heating to 330 to 350 F for 45 minutes or 12 hours at 250 to 270 F. Provided that a thermosetting adhesive is to be used over this primer, the primer may be partially cured at 150$\pm$10 F for 50-60 minutes. The thermosetting adhesive also must have a cure of sufficient temperature and time to fully cure the primer and itself.

11.2.3.5 Comments

Before the application of any adhesive the parts or details should be solvent-wiped and dried. The solvent should not be allowed to air-dry but should be wiped off with a cotton rag or cellulose tissue, thus avoiding possible contamination of the primer surface because of dissolved particles in the solvent.

The thickness of the primer should be measured after a semi-cure and not after the air drying. The primer is not hard enough after a 30-minute air dry.

Any excess primer or runs in the primer may be removed with MEK before oven curing and the part re-primed to meet the thickness requirements.

11.2.3.6 Commercial Similarity

Prime HT-424B manufactured by American Cyanamid Co. or equivalent commercial product will qualify to this specification.

11.2.4 Epoxy Primer (MB0125-047)

This material is a pigmented two-part primer. Component I consists of an epoxy ester polymer, pigmented with titanium dioxide, zinc chromate, and lead chromate in a solvent mixture of n-butyl acetate and MEK. Component II is an amine curing agent in a solvent carrier consisting of MEK and a mixture of low boiling hydrocarbons with methanol. This primer is used primarily on etched aluminum surfaces to provide a corrosion-preventive coating having a surface that is receptive to polyurethane foam. This material is acceptable for use at cryogenic temperatures.

11.2.4.1 Storage Life

The primer (both components) has a maximum storage life of 12 months when stored at 75±15 F. Material that surpasses this age requirement may, in some cases, be requalified and used within 30 days of the requalification. Mixed primer must be discarded if not used within eight hours after its initial mixing.

11.2.4.2 Mixing

Since Component I of the primer system contains a large volume of inorganic solids, it must be thoroughly stirred or shaken to achieve a smooth, uniform consistency prior to mixing. To mix the two components, one volume of Component II is added slowly to one volume of Component I, stirring constantly.

11.2.4.3 Application

The primer should be applied to the cleaned substrate by spraying to achieve a continuous dried film thickness. This thickness may vary from 0.0006 to 0.003 inch depending on the surface to which it is applied. The surfaces primed should be observed under magnification (8 to 10 power) to insure a continuous coating and in no case should more than three coats of primer be applied. When additional coats of primer are used they should not be applied until the previous coat has cured a minimum of 75 minutes at 65 to 90 F. This is the tack-free time (see Figure 11.2.4.3-1).

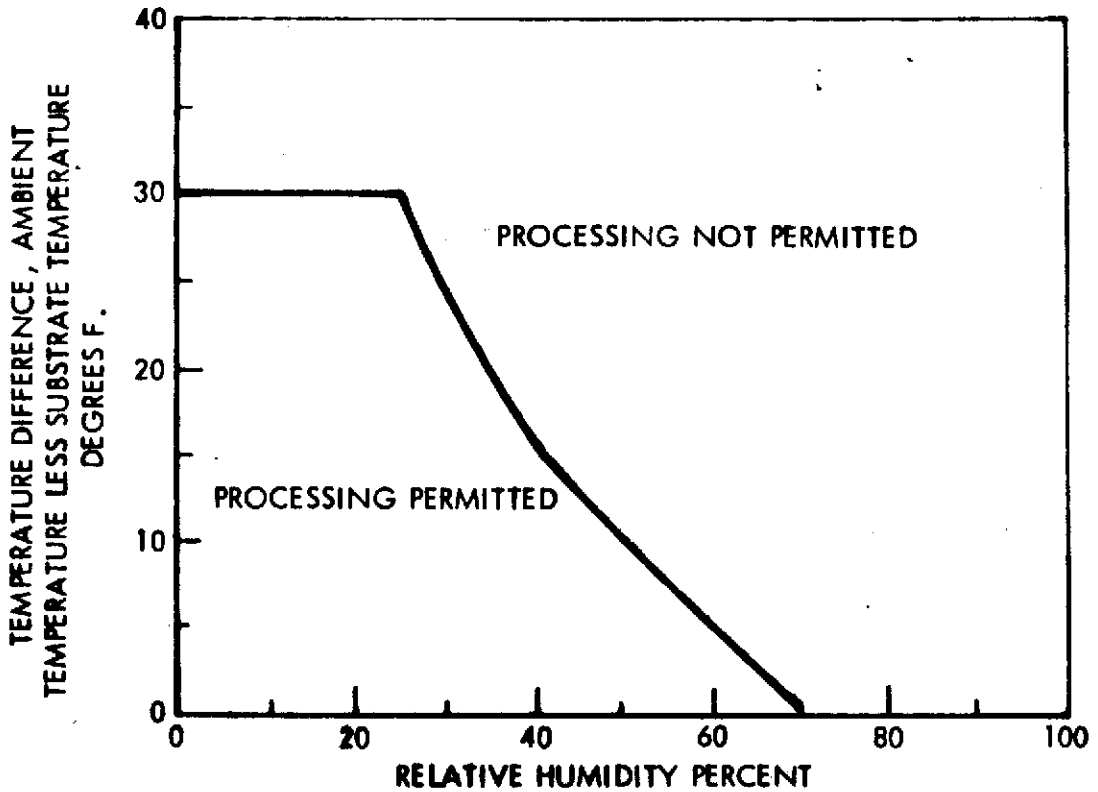

NOTES: (1) PROCESSING IS PERMITTED WHEN THE SUBSTRATE IS WARMER THAN THE AMBIENT TEMPERATURE.
(2) THE MINIMUM SUBSTRATE TEMPERATURE DURING PRIMER APPLICATION SHALL BE 65 F.
(3) SUBSTRATE TEMPERATURE CONTROL IS NOT REQUIRED WHEN NONE OF THE SUBSTRATES INVOLVED ARE METALLIC OR PRIMED METALLIC SURFACES.

Figure 11.2.4.3-1. Substrate Temperature Control During Application of MB0125-047 Primer

11.2.4.4 Cure

The primer requires a minimum cure of 12 hours at 65 F minimum. The time specified for the room-temperature cure may be accumulated at or above the minimum cure temperature provided that both the substrate and the immediate environment are at 65 F minimum for the first three hours following application.

11.2.4.5 Comments

The use of Freon-pressurized aerosol spray equipment is not prohibited; however, use of such a device should be limited to small areas where optimum inspection can be achieved. These devices have a tendency to spurt the primer onto the surfaces being primed, causing an irregular coating. In most cases conventional spray equipment is sufficient to achieve a good coating. This primer's adhesion characteristics are very sensitive to surface contamination. Therefore, great care must be taken when cleaning and maintaining the surfaces to which this primer is to be applied.

11.2.4.6 Commercial Similarity

Koropon 515-701 primer manufactured by Desoto, Inc., or equivalent, will qualify to the requirements of this specification.

11.3 ADHESIVE SYSTEMS

11.3.1 Epoxy Resin Adhesive (MB0120-008)

This is a mineral-filled epoxy resin base (Part A) and a liquid amine curing agent (Part B). The adhesive is supplied in separately packaged ingredients (Class 1) or a single pre-mixed package (Class 2) in a frozen condition. The adhesive system is room-temperature cured for bonding metallic and non-metallic materials for continuous usage at temperatures of -250 to 300 F and short-term usage from 300 to 500 F.

11.3.1.1 Storage Life

Storage life for the separately packaged ingredients (Class 1) is 12 months for the base resin (Part A) at maximum temperature of 40 F or 45 days at 85 F or below. The hardener (Part B) may be stored for 24 months at a maximum temperature of 85 F. The storage life of single-package (Class 2) ingredients is 60 days at -40 F or below.

11.3.1.2 Mixing

The separated ingredients are supplied in kit form and should be allowed to warm to room temperature in the sealed containers prior to mixing. When mixing in quantities of less than a full kit, the proportions are as specified on the kit. To facilitate mixing, the components may be warmed to 130 F maximum prior to mixing. This procedure shortens the working life by 15 minutes, regardless of the ambient temperature.

In using the single package, the adhesive is allowed to thaw to working consistency prior to exposing to the atmosphere.

11.3.1.3 Working Life

The working life of a 200+15 gram batch is as specified in Table 11.3.1.3-1.

Table 11.3.1.3-1. Adhesive Working Life

Ambient Temperature (°F)	Class 1* (min.)	Class 2** (min.)
60 to 70	60	90
71 to 80	45	60
81 to 90	30	30
91 to 100	15	15

*From time mixing is complete
**From time of thawing to working consistency

11.3.1.4 Application

The adhesive must be capable of being readily applied to aluminum surfaces at temperatures between 60 and 90 F at a relative humidity of 30 to 90 percent.

11.3.1.5 Cure

The adhesive must meet all requirements after being cured to one of the following cycles:

a. Seven days at 65 F minimum.

b. Six hours at 115 to 180 F.

c. Two hours at 200 to 250 F.

11.3.1.6 Comments

It is recommended for control of adhesive thickness that MB0135-008 scrim cloth be used.

11.3.1.7 Commercial Similarity

Hysol 934 manufactured by Hysol Division, Dexter Corporation, Pittsburg, Calif., or an equivalent commercial product will qualify to this specification.

11.3.2 Foaming Tape Adhesive System (MB0120-014)

This is a foaming-tape adhesive system for use at temperatures from -423 to 500 F. The bare material is an epoxy-phenolic which is capable of meeting the requirements of MIL-A-5090, Type III.

11.3.2.1 Storage Life

The adhesive tape must have the capability of meeting density requirements after being stored up to two months at 0 F or less.

11.3.2.2 Application

The adhesive tape is capable of being applied to aluminum and glass fabric honeycomb core edges at temperatures between 65 and 85 F and a relative humidity of 30 to 95 percent.

11.3.2.3 Cure

The lap shear strength of the foaming tape must meet the requirements of the specification after 60 minutes at 340±10 F and an applied vacuum 10 to 15 inches of mercury.

11.3.2.4 Comments

The foaming tape adhesive system is used for splicing honeycomb core materials, for core edge bonding to inserts, and in areas where no bonding pressure can be obtained, in addition to structural bonding.

11.3.2.5 Commercial Similarity

The adhesive tape is manufactured by Adhesive Engineering Co., San Carlos, Calif., and identified as 2015 Part A. Any equivalent commercial product will qualify to this specification.

11.3.3 Modified Epoxy Adhesive (MB0120-023)

This is a modified epoxy adhesive paste and primer system suitable for continuous use in temperature range of -423 to +120 F. It is available in two types: for usage when curing temperature is above 60 F and when curing temperature is below 60 F. The first type is for bonding in a controlled environment, the second type is intended for field environment.

11.3.3.1 Storage Life

The base resin, hardener, and unmixed primer may be stored for six months in unopened containers at a temperature of 80 F or below.

11.3.3.2 Mixing

The adhesive is supplied in a two-part system consisting of a base resin and a hardener. The two components are supplied in kit form, separately proportioned and ready for mixing. For mixing quantities of less than a full kit, mixing proportions are supplied by the manufacturer on the kit.

11.3.3.3 Working Life

The working life of 400 grams of the mixed adhesive is as follows:

a. Type 1 - 60 minutes minimum at 60 to 80 F.

b. Type 2 - 30 minutes minimum at 45±5 F.

11.3.3.4 Application

The adhesive is worked onto the faying surface to afford maximum wetting of the substrate. A continuous, uniform layer of adhesive is applied to an approximate thickness of 0.005 inch to each faying surface. Where necessary because of mismatch, or when thickness is critical to design, adhesive-impregnated glass scrim is used for control of the adhesive thickness. The application of the primer is done within an environment of 70-percent humidity or less and a temperature between 60 and 90 F.

11.3.3.5 Cure

Type I adhesive system may be cured to any of the following conditions:

a. Forty-eight hours at 75±15 F.

b. Eight hours at 125±5 F.

c. One hour at 150±5 F.

Type II adhesive system is cured for seven days with a minimum temperature of 40 F.

11.3.3.6 Comments

The faying surface is prepared for bonding in accordance with requirements of Specification MA0610-023. The maximum time allowed between surface preparation and adhesive application is 12 hours.

11.3.3.7 Commercial Similarity

Lefkoweld 109, Leffingwell Chemical Co., Whittier, Calif., or equivalent commercial product will qualify to this specification.

11.3.4 Polyurethane Resin (MB0120-024)

This system is suitable for continuous use in the temperature range of -423 to ±120 F. This material is suitable for adhesive bonding or sealing metals, non-metals, and gas barrier plastic-type films such as polyvinyl-fluoride and polyethylene terephthalate. This material is non-corrosive to metals.

11.3.4.1 Storage Life

The resin has a storage life of six months when stored in the original unopened container at a temperature of 50 to 80 F.

11.3.4.2 Mixing

The resin is mixed using 100 parts by weight of resin and 12.5 parts by weight of curing agent. The curing agent is melted at 250±20 F prior to mixing with the resin.

11.3.4.3 Working Life

The working life of one quart of the mixed resin is a minimum of two hours at a temperature of 75±5 F.

11.3.4.4 Application

The adhesive is applied to both faying surfaces with a suitable applicator, such as a putty knife or spatula, in such a manner to minimize air entrapment within the adhesive. A continuous layer of adhesive should be maintained between the assembled parts of 25±5 grams per square foot. The working area environment must be maintained at a temperature between 60 and 90 F and a relative humidity of 70 percent or less.

11.3.4.5 Cure

Two time cycles are available for cure of the adhesive system:

a. Seven days at a temperature of 70 F minimum.

b. Twelve hours at 75±5 F followed by four at 160±5 F.

11.3.4.6 Comments

Surface preparation for application of the adhesive system is processed per Specification MA0610-023 and the adhesive should be applied within 12 hours after cleaning.

11.3.4.7 Commercial Similarity

Crest 7343 manufactured by Crest Products Co., Santa Ana, Calif., or an equivalent commercial product will qualify to this specification.

11.3.5 Thixotropic Paste (MB0120-026)

This is a trixotropic paste adhesive system with a base of epoxy-phenolic for use in splicing honeycomb core materials, for core edge filler, and reinforcing filler in areas of localized stress. This material is suitable for continuous service at temperatures from -423 to 300 F and for a short period up to a temperature of 500 F.

11.3.5.1 Storage Life

The unmixed components have a maximum storage life of six months when stored in closed container at a temperature of 40 F or below or eight days when stored at room temperature (85 F maximum).

11.3.5.2 Mixing

The thixotropic paste adhesive is supplied in kit form, with each component separately proportioned and ready for mixing.

11.3.5.3 Application

The mixed adhesive paste must be capable of being readily applied to aluminum and glass fabric honeycomb core edges and faces at temperatures between 60 to 90 F and a relative humidity of 30 to 95 percent.

11.3.5.4 Cure

The cure of the paste usually requires step cure cycles to prevent warpage of the assembly during application of temperature. The following cure cycle is recommended:

a. Raise temperature from ambient to 100 F in 60 minutes.

b. Raise temperature from 100 to 330 F in 30 to 120 minutes.

c. Hold at 340±10 F for a minimum of 45 minutes.

d. Cool under pressure to 200 F or less.

11.3.5.5 Comments

All bonded surfaces are to be cleaned per appropriate cleaning specification.

11.3.5.6 Commercial Similarity

HT-424 thixotropic paste manufactured by American Cyanamid Co., Torrance, Calif., or equivalent commercial product will qualify to this specification.

11.3.6 Foaming Epoxy-Phenolic (MB0120-030)

This is a foaming, epoxy-phenolic, paste adhesive system used in splicing honeycomb core materials, for core edge bonding to inserts, and in areas where no bonding pressure can be obtained. This material is suitable for continuous service at temperatures up to 300 F and for short time service from 300 to 500 F.

11.3.6.1 Storage Life

The paste has a minimum storage life of three months when stored in the original unopened containers at a temperature of 0 F or below.

11.3.6.2 Mixing

The adhesive is supplied as a one-component system consisting essentially of of epoxy-phenolic materials. It will be a smooth homogeneous mixture when received.

11.3.6.3 Application

The adhesive is capable of being readily applied to aluminum and glass fabric honeycomb core edges and faces at temperatures between 65 and 85 F and relative humidity of 30 to 95 percent.

11.3.6.4 Cure

The cure cycles are shown in Table 11.3.6.4-1. Cure Cycle A has a reduced temperature requirements and cure Cycle B has an increase in temperature requirements but a reduction in the time required at temperature.

Table 11.3.6.4-1. Adhesive Cure Cycles

Operation	Cure A	Cure B
Heat rise	Ambient to 100 F in 60 minutes (maximum)	Ambient to 100 F in 60 minutes (maximum)
Heat rise	100 to 230 F with maximum temperature variation of 70 F in 30 to 90 minutes	100 to 230 F with maximum temperature variation of 70 F in 30 to 90 minutes
Maintain temperature	240±10 F until maximum temperature variation reaches 20 F	240±10 F until maximum temperature variation reaches 20 F
Heat rise	240 to 280 F in 30 to 90 minutes	240 to 330 F in 30 to 90 minutes
Maintain temperature	290±10 F for 180 minutes minimum	340±10 F for 60 minutes minimum
Cool under pressure	150 F or less	150 F or less
Note: Thermocouple readings must be monitored continuously by automatic temperature recorders.		

11.3.6.5 Comments

The adhesive expands from 250 to 450 percent of its initial thickness and has an extrusion rate of 35 grams per minute minimum.

11.3.6.6 Commercial Similarity

HT424D material manufactured by American Cyanamid Corp., Torrance, Calif., or equivalent commercial product will qualify to this specification.

11.3.7 Modified Epoxy Paste (MB0120-034)

This modified epoxy adhesive paste is for continuous use in the temperature range of -423 to 425F. This material is suitable for adhesive bonding of metals and non-metals, except that it is not to be used for honeycomb sandwich face-to-face bond.

11.3.7.1 Storage Life

The adhesive paste has a shelf life of nine months when stored in the original unopened container at temperatures of 50 to 90 F.

11.3.7.2 Mixing

The adhesive is supplied as a three-part system consisting of a base resin and two hardeners. The three components are supplied in kit form, separately proportioned and ready for mixing. The quantity contained in each container is recorded on the label. For mixing less than kit quantities, mixing is in the same weight proportions as supplied in the kit. Part B must be blended thoroughly with the base resin prior to mixing Part A with the base resin.

11.3.7.3 Working Life

The working life of a mixed 150-gram batch of adhesive is a minimum of 30 minutes at temperatures up to 90 F.

11.3.7.4 Application

Apply the adhesive to both faying surfaces with a suitable applicator, such as a spatula or putty knife. The working area is maintained at a temperature of 60 to 90 F and a relative humidity of 70 percent or less.

11.3.7.5 Cure

The mixed adhesive paste is cured for 24 hours at a minimum temperature of 65 F.

11.3.7.6 Comments

The faying surfaces are cleaned per the applicable cleaning specification.

11.3.7.7 Commercial Similarity

Lefkoweld 211, manufactured by Leffingwell Chemical Co., Whittier, Calif., or equivalent commercial product will qualify to this specification.

11.4 COATINGS

11.4.1 Polyurethane Coating (MB0125-045)

This is an elastomeric polyurethane base coating material which serves as protection for foam insulation by preventing water absorption and by imparting flame retardance and fungus resistance. This coating is intended for use over rigid polyurethane foam insulation (with the "natural skin" removed). The coating consists of two parts: an isocyanate base (Part A) and a modified curing agent (Part B). The modified curing agent consists of components in the following ratio:

Component	Parts by Weight (±1%)
Curing Agent (duPont MOCA)	1.0
TiO_2 paste	1.0
Fyrol FR-2 (fire retardant)	1.4
Solvent 66-C-28 (R-66)	0.6

11.4.1.1 Storage Life

The material has a minimum storage life of three months at 60 to 80 F. Its minimum working life is two hours.

11.4.1.2 Mixing

Parts A and B of the system should be combined in a one-to-one ratio by weight until a homogeneous mixture is attained. It is desirable to use a paint shaker for mixing to minimize exposure of the material to moisture in the atmosphere. Since the coating is a catalyzed system, the maximum amount of material to be mixed at one time is one gallon. Also, the material should never be thinned because it will not cover the substrate sufficiently when thinned. dd.

11.4.1.3 Application

The material should be applied to the insulation by means of a short-nap roller. Since the coating material is heavy and viscous, long-nap rollers tend to give the coating a poor irregular surface. Short-nap rollers of nylon, mohair, and lambskin have proven satisfactory.

A nylon brush should be used to apply the coating where roller application is not practical.

For best results it is recommended that three coats of the material be applied, with a significant drying time between coats. Certain environmental controls should be exercised during the processing and application of this coating: the ambient temperature should lie between 60 and 90 F and the relative humidity is recommended at 70 percent maximum.

11.4.1.4 Cure

The required cure cycles of single and multiple coats of this material are given in Table 11.4.1.4-1.

Table 11.4.1.4-1. Cure Cycles for MB0125-045 Polyurethane Coating

	Temperature (°F)			
Cure	60 - 85	85 - 90	90 - 110	110 - 120
A*	24 hours	16 hours	12 hours	8 hours
B**	120 hours	72 hours	48 hours	16 hours

*Cure A is the minimum time at the designated temperature between coats of MB0125-045 material.
**Cure B is the minimum cure at the designated temperature of the third coat of MB0125-045 material prior to application of the color coat.

11.4.1.5 Comments

The surface to which the coating is to be applied should be kept as clean as possible so most processing should be done in an enclosed area. The extent of enclosure should be determined based on the size of the area being coated and the prevailing environmental conditions.

11.4.1.6 Commercial Similarity

CS-3333 coating, manufactured by Chem Seal Corp. of America, or an equivalent product will qualify to this specification.

11.4.2 Synthetic Elastomer Base Coating (MB0125-036)

This coating consists of a chlorosulfonated polyethylene base, solvents, pigments, and other additives. This material is used primarily for protection of external insulation by preventing excessive water absorption and fungi growth. The performance characteristics of this material are listed in Table 11.4.2-1.

Table 11.4.2-1. Synthetic Elastomer Base Coating Performance

Function	Acceptable Results
Sprayability	Produce no cobwebbing. Produce a uniformly smooth coating.
Fungi resistance	Generate no growth
Maintain film continuity	Develop no breaks or cracks in coating
Drying time	Be tack-free 40 minutes after being applied to external insulation

11.4.2.1 Storage Life

The coating can be stored in the original unopened containers at 60 to 80 F for six months minimum from date of manufacture.

11.4.2.2 Mixing

The material must be thoroughly mixed prior to application using a paint shaker or similar device. If the coating is to be thinned, four parts of the paint can be mixed with one part of toluene.

11.4.2.3 Application

The material is preferably applied with conventional spray equipment. Caution must be exercised when spraying to avoid a too dry or too wet spray. Dilution of the coating can be used to regulate the wetness of the spray. Brush application, using a nylon brush, also may be employed. Two or three coats should be applied to form a film thickness of three to five mils.

11.4.2.4 Curing

As stated earlier, the tack-free time is about 40 minutes. In most environmental conditions 30 minutes should be allowed between coats and 12 hours of air-drying before handling.

11.4.2.5 Comments

Where necessary all details to be primed may be cleaned with MB0210-005 solvent. This coating is usually used to coat cork and cork details where fungi resistance is necessary. In other areas where the same protection is necessary, consideration should also be given to MB0125-046.

11.4.2.6 Commercial Similarity

Any material equivalent to EC2241 manufactured by the Minnesota Mining and Manufacturing Co. will satisfy this specification.

11.4.3 Vinyl Coating (MB0125-046)

This material is a vinyl polymer, one-component, air-drying paint system. It is used primarily as a color top-coat over other coatings or foams. The material is pigmented to provide a low-gloss nominal white finish which will not discolor with age or climatic exposure.

11.4.3.1 Storage Life

The unmixed coating has a storage life of 120 days from the date of manufacture when stored in the original unopened container at 70±10 F.

11.4.3.2 Mixing

This material must be thoroughly blended to achieve a homogeneous consistency. If thinning is required, 5 percent maximum by weight of Dyna-Therm V-400 reducer may be used.

11.4.3.3 Application

This material can be applied by paint roller or brush in the temperature range of 60 to 90 F and a relative humidity of 70 percent or less. Its application is very similar to MB0125-045 using a short-nap roller and nylon brush. The number of coats applied depends on how many are required to provide a continuous and distinct white surface. This material is most often used over coatings such as MB0125-045; however, it can also be used directly over foam systems. Extensive usage over large areas of foam not previously treated with a coating should be avoided.

11.4.3.4 Curing

The material must be allowed to air-dry a minimum of four hours at 60 to 90 F before handling or applying additional coats. The final cure is 48 hours at 60 to 90 F and this air-drying time, at the appropriate temperature, may be cumulative.

11.4.3.5 Comments

When not in use, the mixed material must be stored in tightly closed containers to prevent contamination and solvent loss.

Environmental control requirements for the application of this vinyl color coat are identical to those used for the MB0125-045 polyurethane coating. This material, however, is less susceptible to moisture absorption.

11.4.3.6 Commercial Similarity

The V-455 white vinyl coating manufactured by Dyna-Therm or an equivalent commercial product will meet the requirements of this specification.

11.5 FOAM SYSTEM

11.5.1 Low-Density Polyurethane Foam (MB0130-069)

This is a two-component, room-temperature curing, low-density polyurethane foam in-place material. It is supplied as two liquid components, Part A being isocyanate and Part B the polyol component. The material is suitable for continuous service in the temperature range of -423 to 250 F in applications requiring moderate structural strength and excellent thermal insulation properties.

11.5.1.1 Storage Life

The storage life of the components, when stored at 60 to 74 F in the original package, is 150 days.

11.5.1.2 Mixing

Mixing is accomplished using automatic proportioning and mixing devices or by propeller-type mixers. The material must be completely mixed within 25 seconds when being mixed with a propeller-type mixer, but this time may be extended when using an automatic mixing device. The mixed material must be free of visible entrapped air bubbles exceeding 1/16 inch in diameter. Mixing extends to the edges of the container so that no unmixed component material remains along the sides or bottom. The use of a spatula is recommended to blend unmixed components into the main body of the mix.

11.5.1.3 Application

The mixed material is poured into a mold prior to the initiation of foaming. An effort is made to apply the major portion of the mixed material directly to the bottom of the cavity. Multiple pours may be made to fill the mold cavity completely. The foam-in-place material must have cured until it is nondeformable to the touch and the temperature at the surface is less than 120 F. The working area is maintained at a temperature of 65 to 90 F and a relative humidity of 70 percent or less.

11.5.1.4 Cure

The mixed material is cured for a minimum of 24 hours at a temperature of 70±10 F. The material is not to be disturbed or moved for at least four hours after the initiation of foaming.

11.5.1.5 Comments

If the material is to be foamed to the apparent density requirement of the applicable material specification, all mold surfaces are heated to 110±10 F prior to pouring.

11.5.1.6 Commercial Similarity

CPR348-3 foam manufactured by CPR Division of Upjohn Co., Torrance, Calif., or equivalent commercial product will qualify to this specification.

11.5.2 Flame Retardant, Polyurethane Foam (MB0130-077)

This flame retardant is a two-component, room-temperature-curing, two-pound density foam for spray application. The material is supplied as two liquid components: a polyphenyl methane poly-isocyanate and a polyether polyol. The isocyanate component is labeled as Component A and the polyol base component labeled as Component B. Component B contains an F-11 fluorocarbon blowing agent, a silicone surfactant, amine catalyst, organic-metallic

catalyst, dehydroxy phosphonate flame-retardant, and polyol. The materials are suitable for continuous service in the temperature range of -423 to 120 F or short-time exposure to temperatures up to 550 F.

11.5.2.1 Storage Life

The shelf life of the components when stored at 60 to 74 F in the original sealed container, with free air circulation on all exposed exterior surfaces of the container, is 90 days.

11.5.2.2 Mixing

Polyurethane foam conforming to MB0130-077 is applied by equipment with internal mixing systems. The equipment employed must have demonstrated capability of applying the foam to meet the density, tensile strength, and cryogenic strain compatibility requirements of the specification. The equipment is adjusted to provide the component ratio specified on the container. Prior to spray application the foam component ratio is taken at the spray gun and calculated as follows:

$$\frac{\text{Weight Component A}}{\text{Weight Component B}} = y \pm 0.02$$

where y is the component ratio specified on the container.

11.5.2.3 Application

Surfaces being foamed are cleaned per applicable cleaning specification and primed. The temperature of the metallic surface will meet the requirements shown in Figure 11.5.2.3-1. Each foaming operation is immediately preceded by a density check. If the spray operation is interrupted for more than 30 minutes the density check is repeated. Prior to application of the foam to the metallic surface, sufficient foam is sprayed onto a disposable surface to assure all solvent has been flushed from the spray gun. Each application of foam is accomplished by moving the impingement area from the disposable surface to the detail part without interrupting spray dispensation.

11.5.2.4 Cure

The spray foam must remain undisturbed for 16 hours minimum at a controlled temperature and relative humidity (Figure 11.5.2.3-1) prior to initiating machining that extends to the metal surface. Prefabricated foam details and spray foam-filled honeycomb core may be machined or trimmed after four hours of cure. The foam is then cured an additional 40 hours minimum at a temperature of 60 to 90 F and a relative humidity of 70 percent maximum, prior to application of the finish coatings. Untrimmed or uncoated foam is maintained in an environment of 70-percent relative humidity maximum, regardless of temperature. The foam is cured an additional 72 hours minimum prior to cryogenic (-423 F) exposure of the aluminum substrate. Only the first 16 hours are required to be continuous within the controlled environment (Figure 11.5.2.3-1). The remaining cure may be continuous or cumulative at temperatures between 60 and 90 F and a maximum relative humidity of 70 percent.

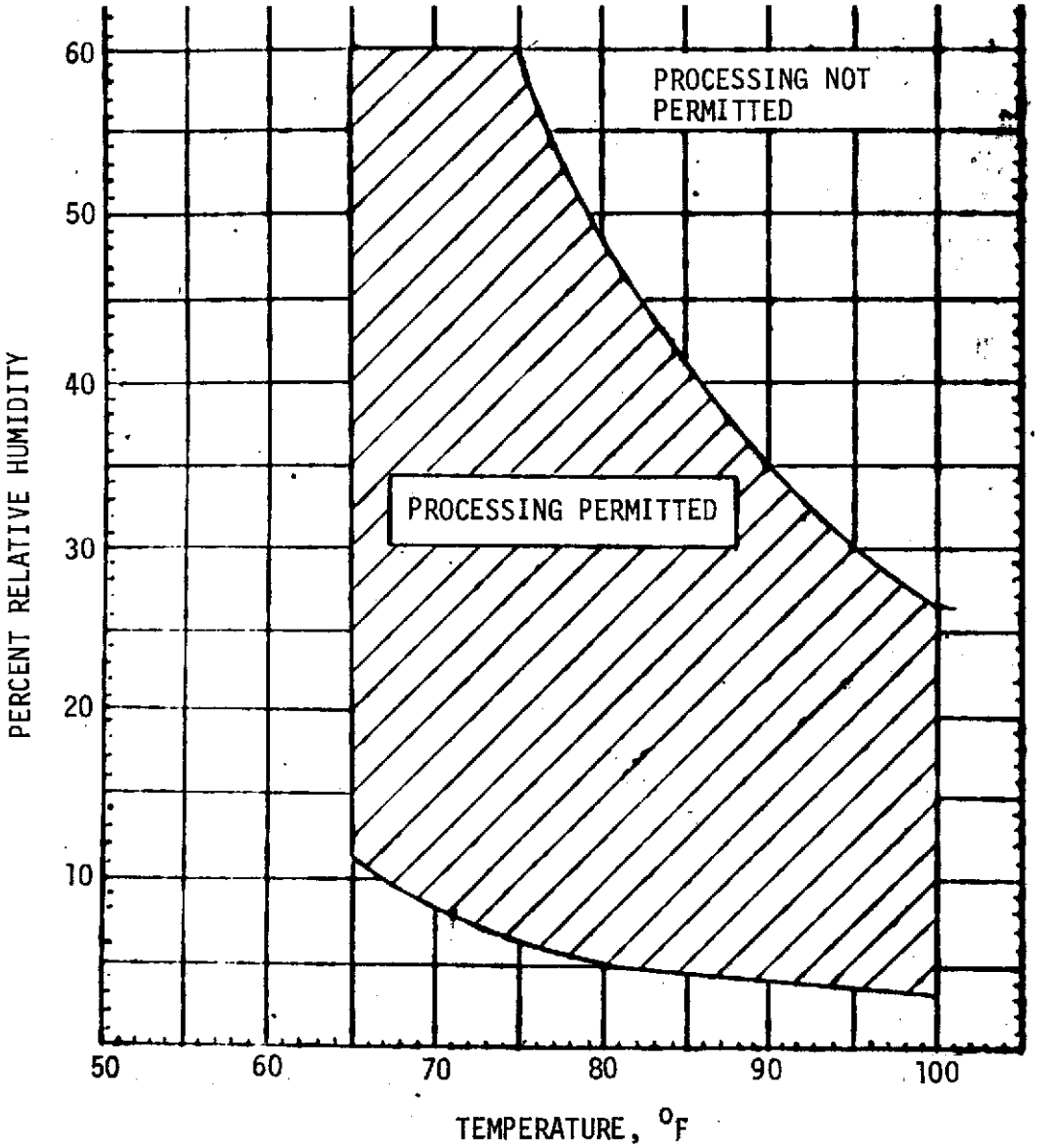

Figure 11.5.2.3-1. Temperature Versus Relative Humidity Requirements

11.5.2.5 Comments

When spray foam operations are performed at field sites, the work area environmental conditions specified are to be observed during application of the spray foam. In addition, the environmental temperature surrounding the entire stage must be 80 F minimum at the time of spraying and the lowest environmental temperature surrounding the entire stage during the preceding three hours must be a minimum of 77 F. The substrate must be at a stable temperature of 80 F minimum during the spray foam application.

11.5.2.6 Commercial Similarity

Nopco BX-250 manufactured by Nopco Chemical Division, Los Angeles, Calif., or equivalent commercial product will qualify to this specification.

12.0 MATERIAL PROPERTIES (THERMAL)

The following sections present the results of laboratory, field, and flight tests conducted to determine the thermal properties of insulation materials which were either utilized on the Saturn S-II program or considered for use on S-II derivatives. Knowledge or estimate of thermal properties (e.g., thermal conductivity, specific heat, and emittance) of insulation materials used or considered for use on S-II basic or derivative vehicles was required in support of thermal analyses efforts. Where the necessary data were not available from handbooks, tests were planned and conducted to obtain the information required. In many cases estimates of material thermal properties were employed in the analyses with the intention of recalculating if subsequent test data showed that the original thermal properties estimates were unconservative.

12.1 ADHESIVES

No tests were run to determine thermal properties of adhesives. The adhesive layers employed in S-II insulation systems were always very thin, so that the error in such factors as computed temperatures and heat leaks due to using handbook values or estimates for adhesive thermal properties was believed inconsequential.

12.2 PRIMERS

No tests were run to determine thermal properties of primers. As in the case of adhesives, it is believed that the error in such factors as computed temperatures and heat leaks due to using assumed or handbook values for the thermal properties of the very thin primer substrate layer employed in S-II insulation systems is inconsequential.

12.3 SEALANTS

While no thermal properties tests were run on sealants alone, tests of foam and composite insulation samples which employed the sealants (Dynatherm and Chemseal) were performed. Thus the contribution of these sealants to the thermal properties of the insulation system in question are included in the appropriate section.

12.4 HONEYCOMBS

No thermal properties tests were conducted on honeycomb structure alone. Tests were conducted on composites employing honeycomb structure. The results of these tests are presented in Subsection 12.9.

12.5 FOAMS

The thermal properties of the spray-on-foam insulation (SOFI) utilized on the S-II program as honeycomb fill in the composite S-II tank sidewall insulation and as a 0.75-inch layer on tank sidewalls were evaluated. Thermal properties of honeycomb fill are based on NR laboratory test data. Thermal properties of the 0.75-inch foam sidewall insulation is

based on LH_2 boiloff data obtained from tests of Thor tanks conducted by MDAC at their Sacramento Field Test Facility. These data were originally reported in SID 68-394. SOFI sidewall insulation erosion rates due to aerodynamic heating and shear stress during Saturn V launch were estimated based on test data obtained utilizing the NASA X-15 aircraft. These results were originally reported in NR-SD letter 69MA5502.

12.5.1 NR Laboratory Tests of Foam

Tests were conducted in the Space Division laboratory to determine the thermal conductivity of CO_2 - blown CPR 1021-2 polyurethane foam. This is the foam used as honeycomb fill in the basic S-II cryogenic tank sidewall insulation on S-II-1 through -3. The data obtained in these tests are shown in Figure 12.5.1-1 (data applicable to Paragraph 6.1.1). Foam thermal conductivities in air for mean temperatures from 100 to 300 F were determined utilizing a guarded hot plate. Foam thermal conductivities in a vacuum for mean temperatures from ≈ -250 to 0 F were determined with a thermal comparator.

The apparent thermal conductivity versus temperature of the NOPCO BX-250A (ρ = 2 lb/ft^3) spray foam was determined per ASTM method C177-63. This type foam was used directly as sidewall insulation on the propellant tanks of the S-II-8 and subsequent vehicles. The testing was conducted by the NR laboratory over a range in mean sample temperatures from -300 to 200 F. Foam batches with densities of 1.91, 2.04, and 2.34 lb/ft^3 were tested. The resulting thermal conductivity data, applicable to Paragraph 6.1.4, is presented in Figure 12.5.1-2. As shown, the apparent thermal conductivity (parallel to the foam rise direction) varied from 0.08 Btu-in./hr.-ft.^{2} at a mean temperature of -300 F to 0.2 Btu-in./hr.-ft.^{2}-F at a mean temperature of 200 F.

12.5.2 Thermal Characteristics Based on LH_2 Tank Boiloff Testing

Test tanks insulated with SOFI by NR were employed in hydrogen boiloff tests conducted at the MDAC Sacramento facility. The thermal characteristics of the foam were determined based on temperature data from imbedded thermocouples together with tank heat leak data. The tank heat leak was calculated based on (1) liquid level sensor data, and (2) data from a Venturi flow meter used to measure the effluent H_2 boiloff.

The foam conductivity based on test data is compared with analytically determined values in Figure 12.5.2-1 (data applicable to Paragraph 6.1.4). As shown, at mean temperatures less than 350 R, the calculated foam conductivity agrees well with analytical estimates. The discrepancy between test data and analytical values at mean temperatures greater than 350 R is believed due to the diffusion of air into the foam cells at these temperatures. It is theorized that at lower temperatures the Freon gas encapsulated within the foam cells will solidify and produce a vacuum in the foam voids.

The temperature gradient within the foam was determined based on data from the imbedded thermocouples together with calculations based on the

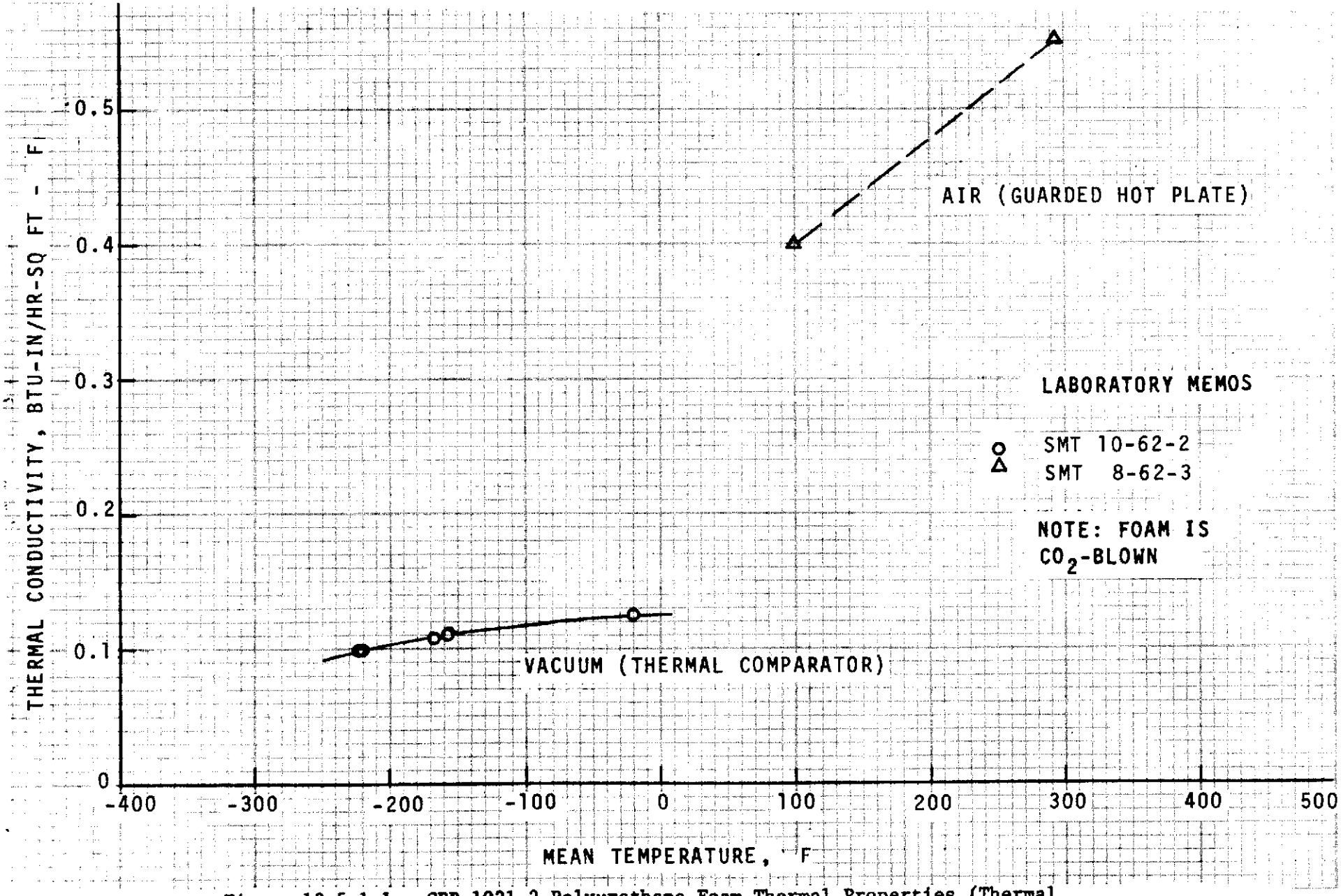

Figure 12.5.1-1. CPR 1021-2 Polyurethane Foam Thermal Properties (Thermal Conductivity in Air and Vacuum vs Temperature)

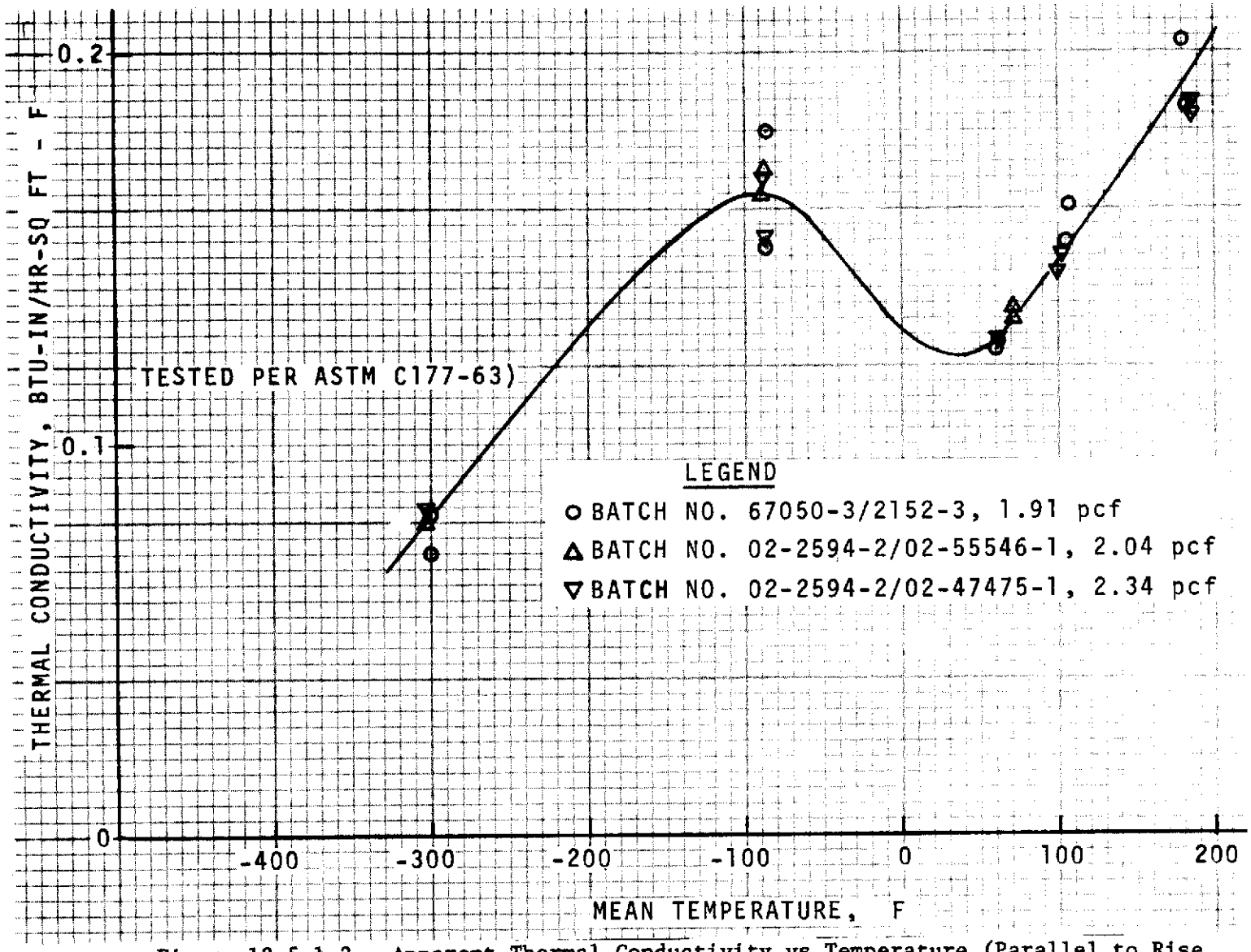

Figure 12.5.1-2. Apparent Thermal Conductivity vs Temperature (Parallel to Rise Direction) Nopcofoam BX-250A Spray Foam (MB0130-077)

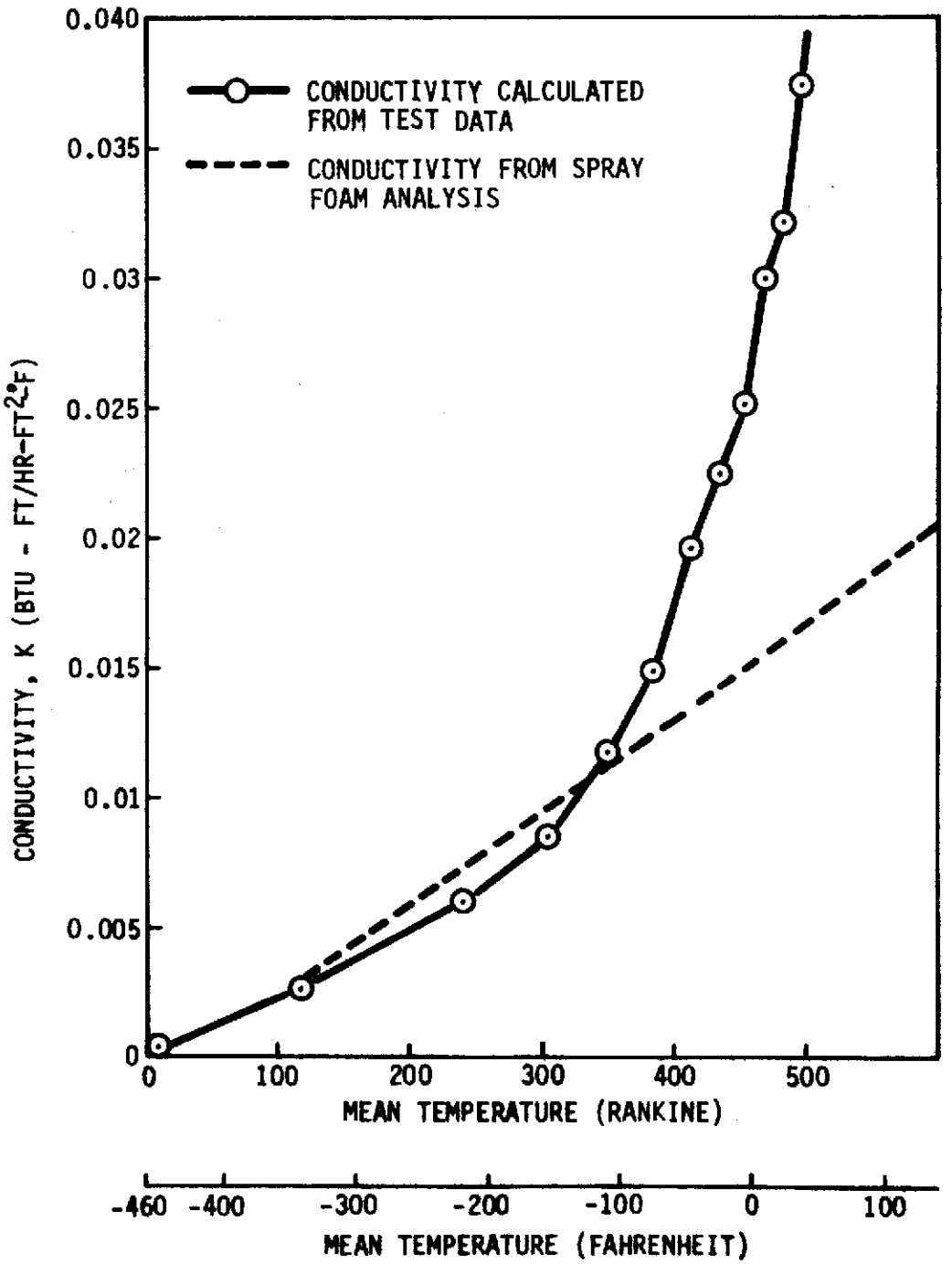

Figure 12.5.2-1. Spray Foam Insulation Thermal Conductivity Curves

measured heat leak and the calculated foam conductivity values shown in Figure 12.5.2-1. The temperature profile thus determined is shown in Figure 12.5.2-2 (data applicable to Paragraph 6.1.4). Also shown in the figure for comparison are temperature profiles calculated on the basis of analytically determined foam conductivity for foam thicknesses of 0.5 and 1.2 inches. As shown the temperature profile based on conductivity calculated from test data agrees well with the previously determined profiles based on analytical foam conductivity values.

The anticipated heat leak through SOFI when applied to an LH_2 tank sidewall, based on test data, is shown in Figure 12.5.2-3 (data applicable to Paragraph 6.1.4). Also shown is the expected heat leak, based on analytically estimated foam conductivity. As shown, the test data indicate that the heat leak through SOFI can be about 20 percent greater than analytically predicted based on theoretical conductivity values.

12.5.3 X-15 Erosion Test of Foam

To determine the effects of Saturn V aerodynamic heating and shear on the erosion of S-II foam, a test program utilizing NASA's X-15 was conducted. During this program instrumented panels fabricated from SOFI were attached to the X-15 speed brakes and flown through a range of flight conditions designed to simulate S-II tank sidewall boundary layer conditions during Saturn V launch. Data from thermocouples imbedded within the panels were used to determine the foam erosion rates under simulated nominal Saturn V launch conditions. The results of these tests are shown in Table 12.5.3-1 and Figures 12.5.3-1 and 12.5.3-2.

Table 12.5.3-1. Summary of Spray Foam Erosion on S-II Stage Based on X-15 Flight Test Specimen Results

Affected Region	Time When Noted Erosion Starts From Saturn V Liftoff (sec)	Average Erosion Rate Up to J-2 Engine Start (mils/sec)
Basic Sidewall	110	3 - 4
Single Protuberance Influenced Region	108	4 - 5
Multiple Protuberance Influenced Region	105	25
Estimated 1° Ramp	107	10

Notes
1. Engine start on S-II stage occurs at approximately 160 sec after Saturn V liftoff.
2. No allowance for intersecting shocks resulting from the presence of protuberances.

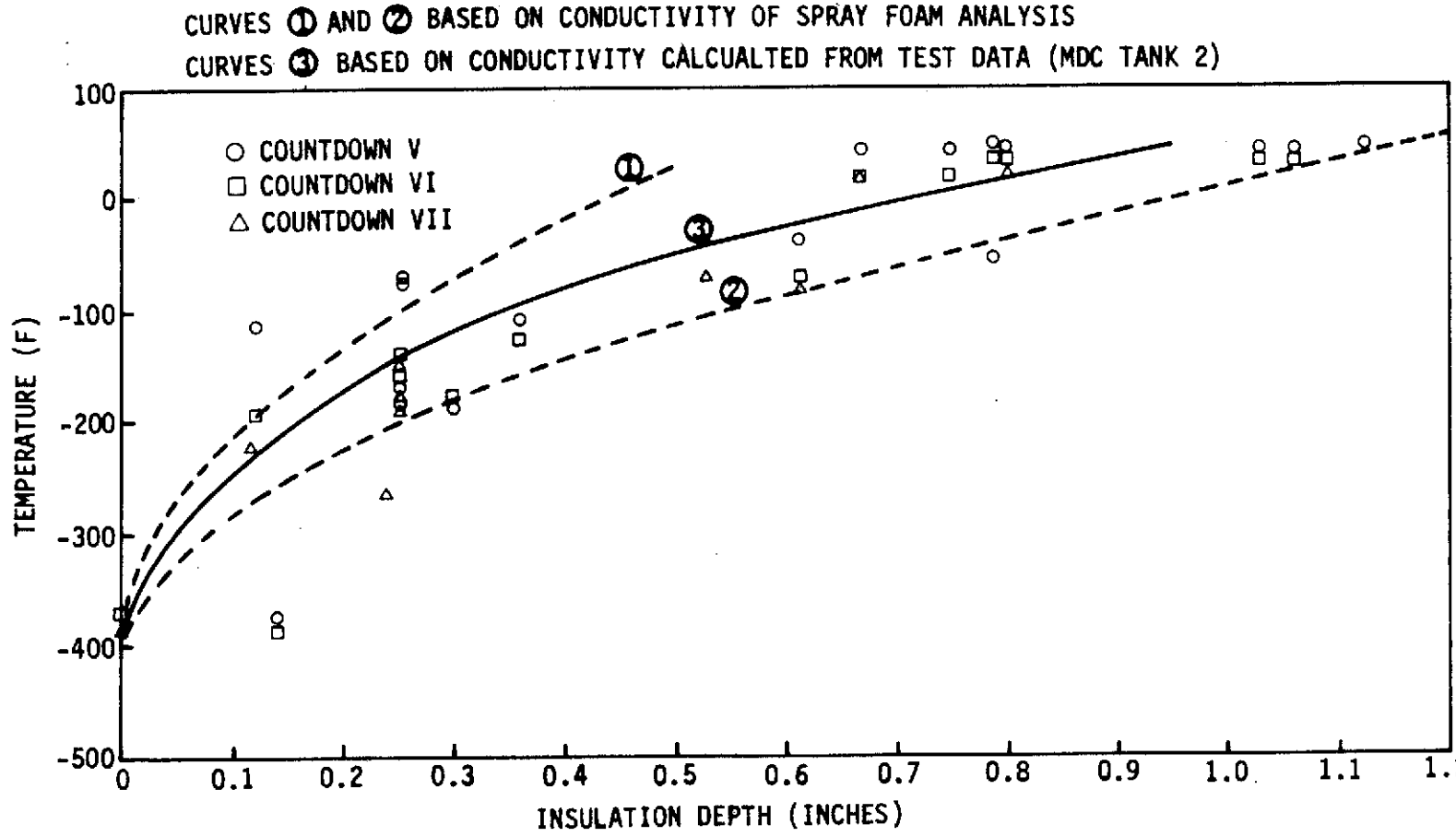

Figure 12.5.2-2. Insulation Temperature Profile

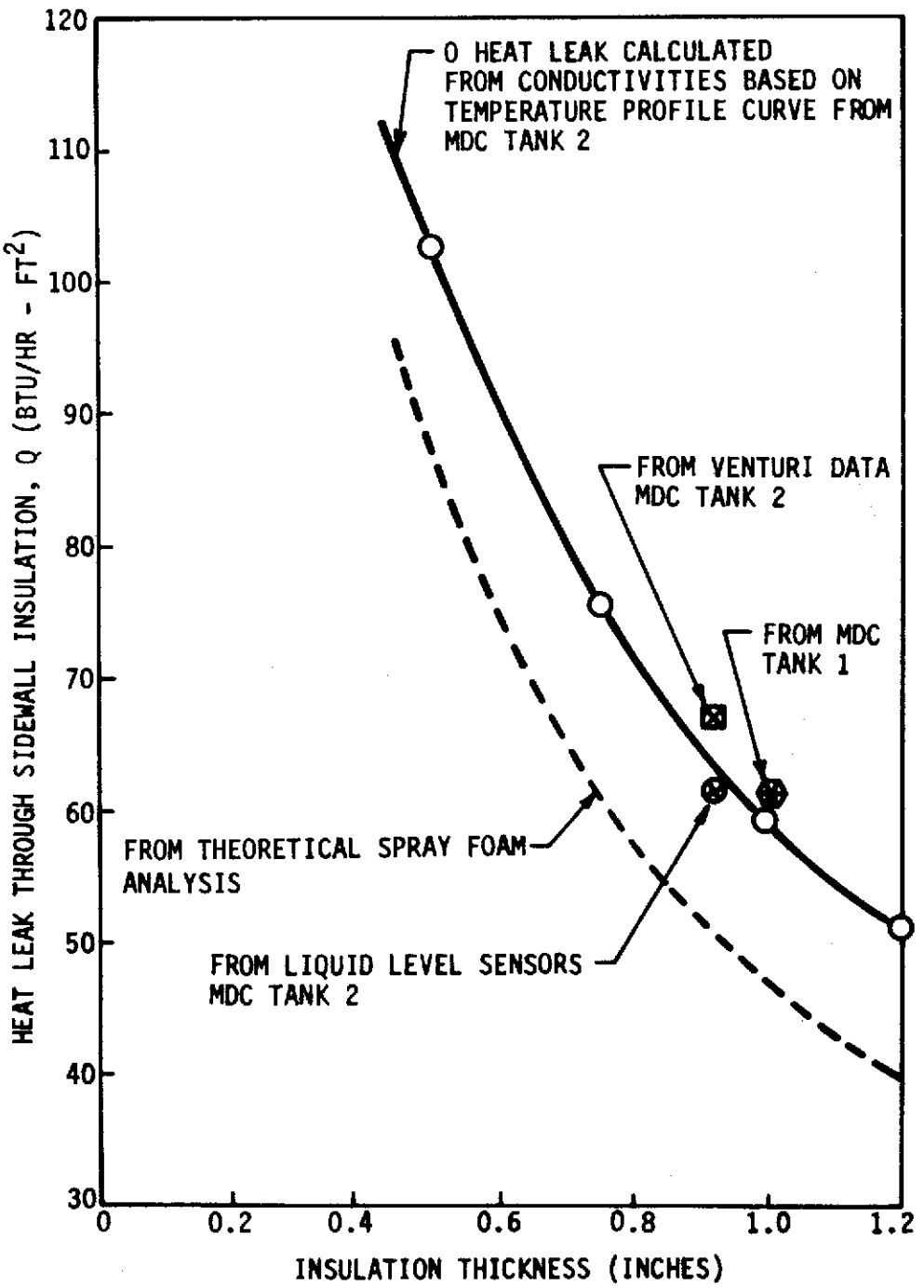

Figure 12.5.2-3. Heat Leak Rates as a Function of Spray Foam Insulation Thickness

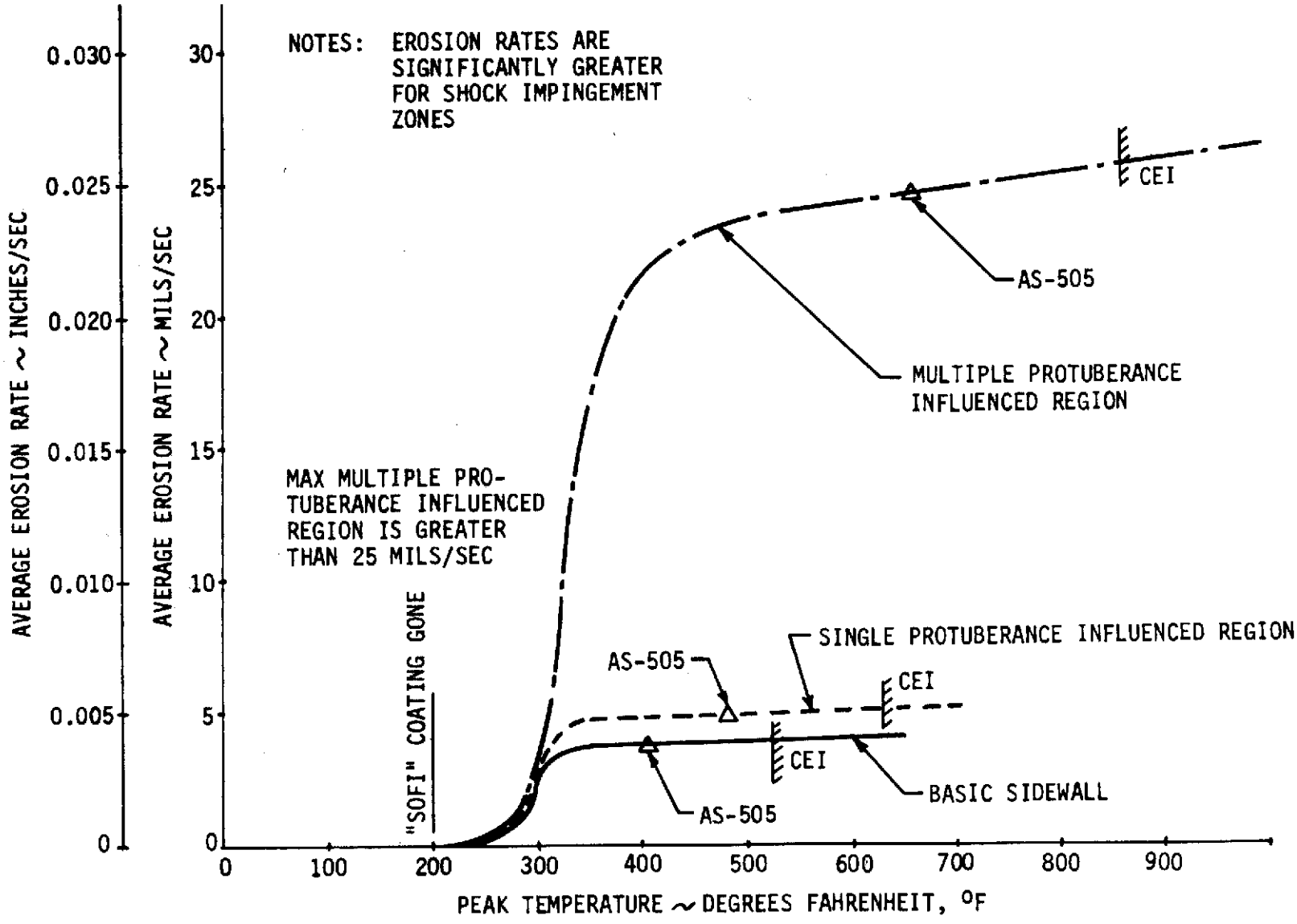

Figure 12.5.3-1. Average Erosion Rate vs Peak SOFI Peak Temperature

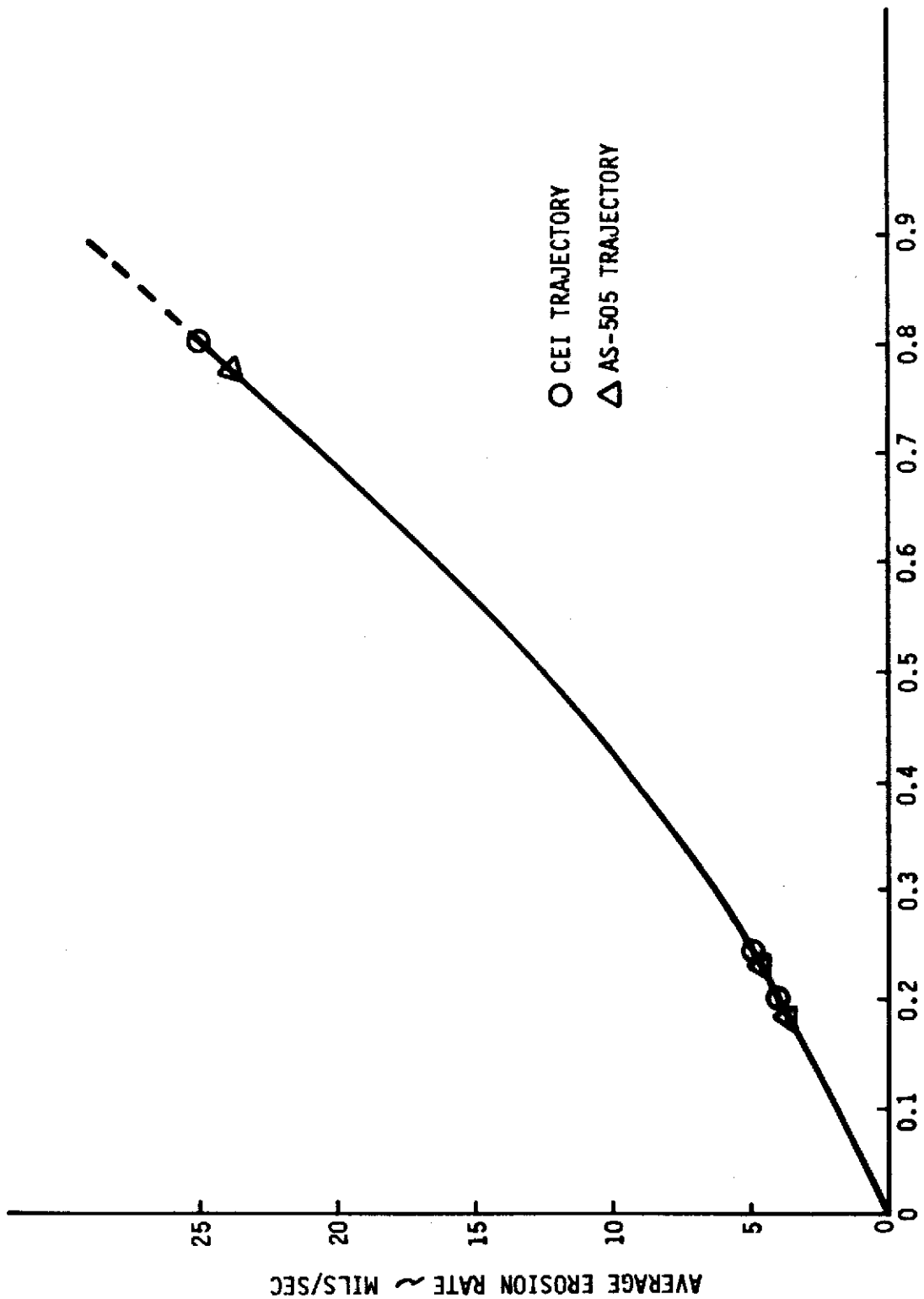

Figure 12.5.3-2. Average Erosion Rate vs Aero Shear During S-IC Boost Phase Prior to S-II Ignition

12.6 FABRIC

Fabric insulation materials were employed in the heat shield flexible curtain composite used on the Saturn S-II and were considered for use on S-II derivatives. NR subcontracted laboratory tests, per ASTM C177-63, were conducted to determine the apparent thermal conductivity of HITCO Irish refrasil fabric (Type C1154-48, 60 lb./ft.^{3}) and HITCO refrasil batt (Type B-1570, 16.1 lb./ft.^{3}) (used on S-II-13 and -15). These data are presented for a mean temperature range of 1000 F to 2100 F in Figures 12.6-1 and 12.6-2 for the apparent thermal conductivity at 1.2 Torr nitrogen of the 60.5 lb./ft.^{3} and 16.1 lb./ft.^{3} materials, respectively. As shown in Figure 12.6-1, the apparent thermal conductivity at 1.2 Torr nitrogen of the 60.5 lb./ft.^{3} HITCO Irish refrasil fabric (Type C1554-48) varied from 0.175 Btu-in./hr.-ft.^{2}-F at a mean temperature of 1000 F to 0.505 Btu-in./hr.-ft^2-F at a mean temperature of 2100 F. Figure 12.6.2 presents similarly the apparent thermal conductivity at 1.2 Torr nitrogen of 16.1 lb./ft^3 HITCO Irish refrasil batt (Type B-1570) versus mean temperature. As shown in Figure 12.6-2, the apparent thermal conductivity of this 16.1 lb./ft.^{3} batt material varied from 0.275 Btu-in./hr.-ft.^{2} at a mean temperature of 930 F to 1.24 Btu-in./hr.-ft.^{2}-F at a mean temperature of 2100 F.

12.7 FIBERGLASS

12.7.1 Fiberglass Batting

Tests were performed in the Space Division laboratory on samples of Johns-Manville Micro-Fibers. This material is used in the form of fiberglass batting which is employed on the S-II stage as propellant feed line insulation. Small sample tests of the 4 lb./ft.^{3} Micro-Fibers were conducted in a 10^{-2} Torr vacuum: (1) in the mean temperature range from 100 to 750 F with a thermal comparator, and (2) in the mean temperature range from -300 to -100 F with a guarded hot-plate per ASTM C177-45. The results of these tests are plotted in Figure 12.7.1-1 (data applicable to Paragraph 6.2.4). As shown, the apparent thermal conductivity of the 4 lb./ft.^{3} Micro-Fibers varied from $\approx$ 0.005 Btu-in./hr.-ft.^{2}-F at a mean temperature of -250 F to $\approx$0.15 Btu-in./hr.-ft.^{2}-F at a mean temperature of 770 F.

Similar small samples of the 4 lb./ft.^{3} Micro-Fibers were tested in air at 760 Torr per ASTM-C177-45 to determine the apparent thermal conductivity in air. The tests were made over a mean temperature range of 150 to 515 F. The results of these tests, plotted in Figure 12.7.1-2 (data applicable to Paragraph 6.2.4), show that the apparent thermal conductivity in air at 760 Torr of the 4 lb./ft.^{3} Micro-Fibers varied from 0.275 Btu-in./hr.-ft.^{2}-F at a mean temperature of 155 F to 0.480 Btu-in./hr-ft.^{2}-F at a mean temperature of 515 F.

The enthalpy relative to a 75 F datum plane of the 4 lb./ft.^{3} Micro-Fibers was determined by small sample tests per ASTM C351-54T. These tests were conducted over a temperature range of 150 to 350 F. The

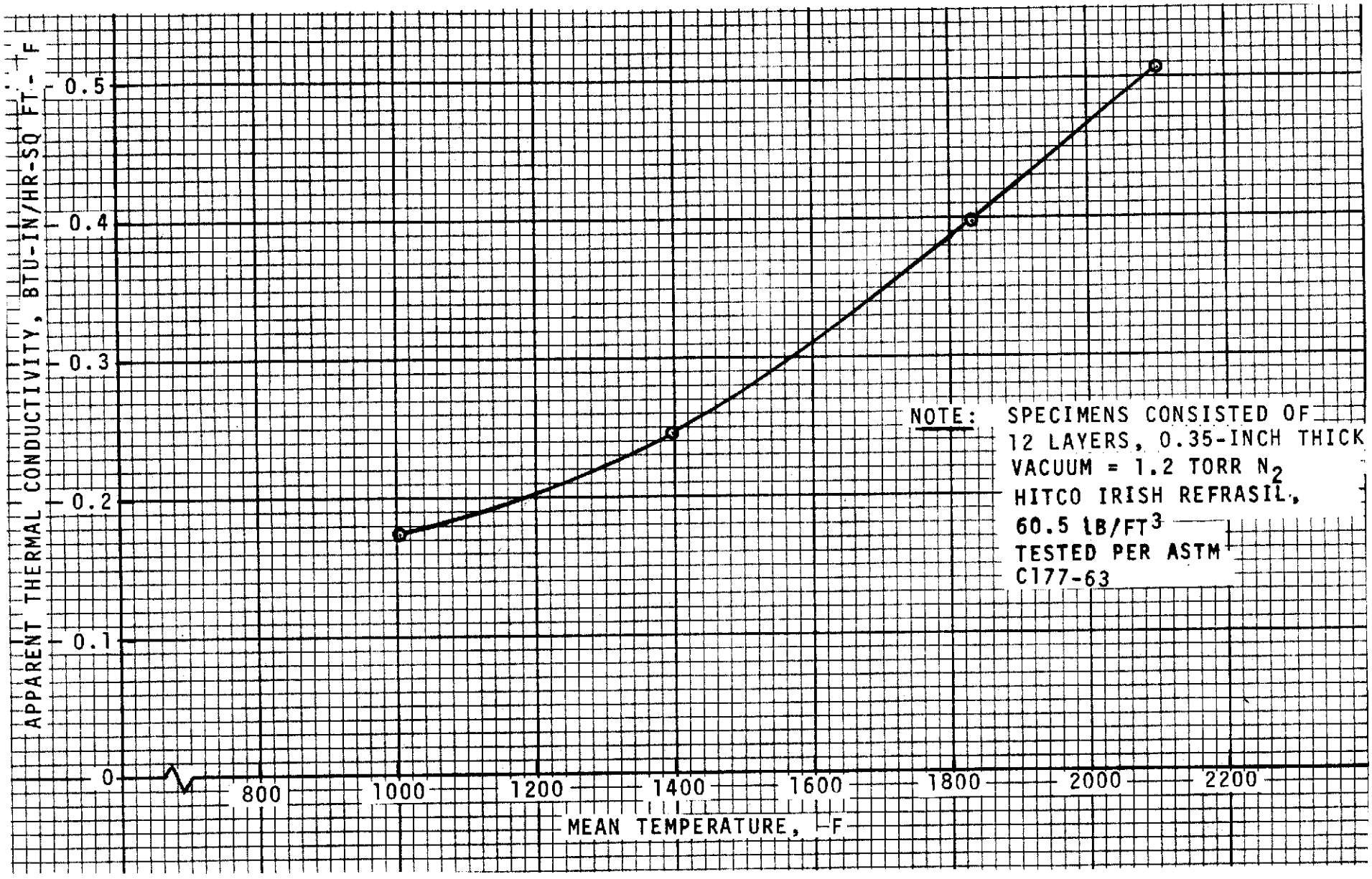

Figure 12.6-1. Heat Shield Flexible Curtain Material Thermal Properties
(Thermal Conductivity of Irish Refrasil Fabric
Type C1554-48 in Vacuum vs Temperature)

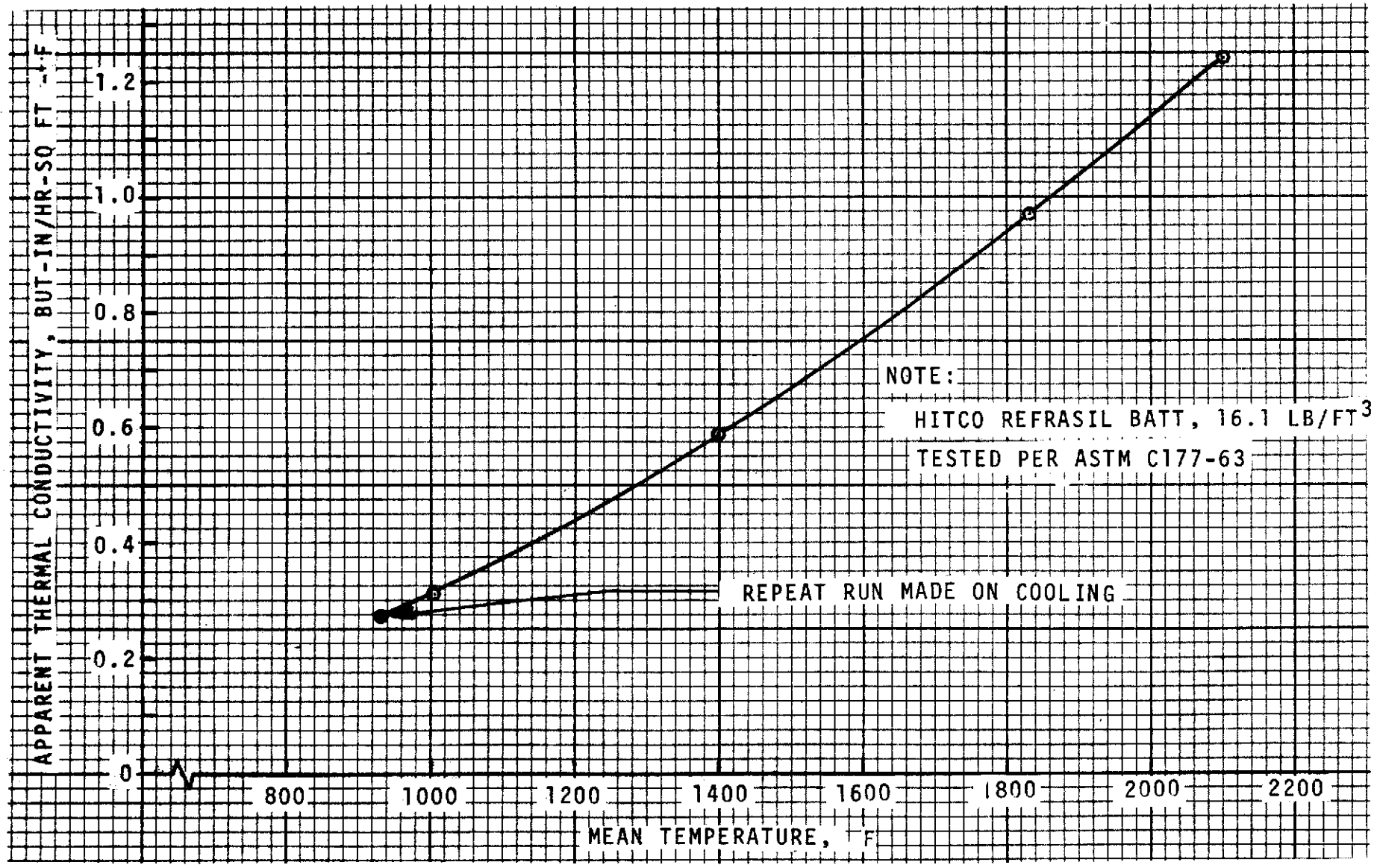

Figure 12.6-2. Heat Shield Flexible Curtain Material Thermal Properties (Thermal Conductivity of Refrasil Batt, Type B-1570, vs Temperature)

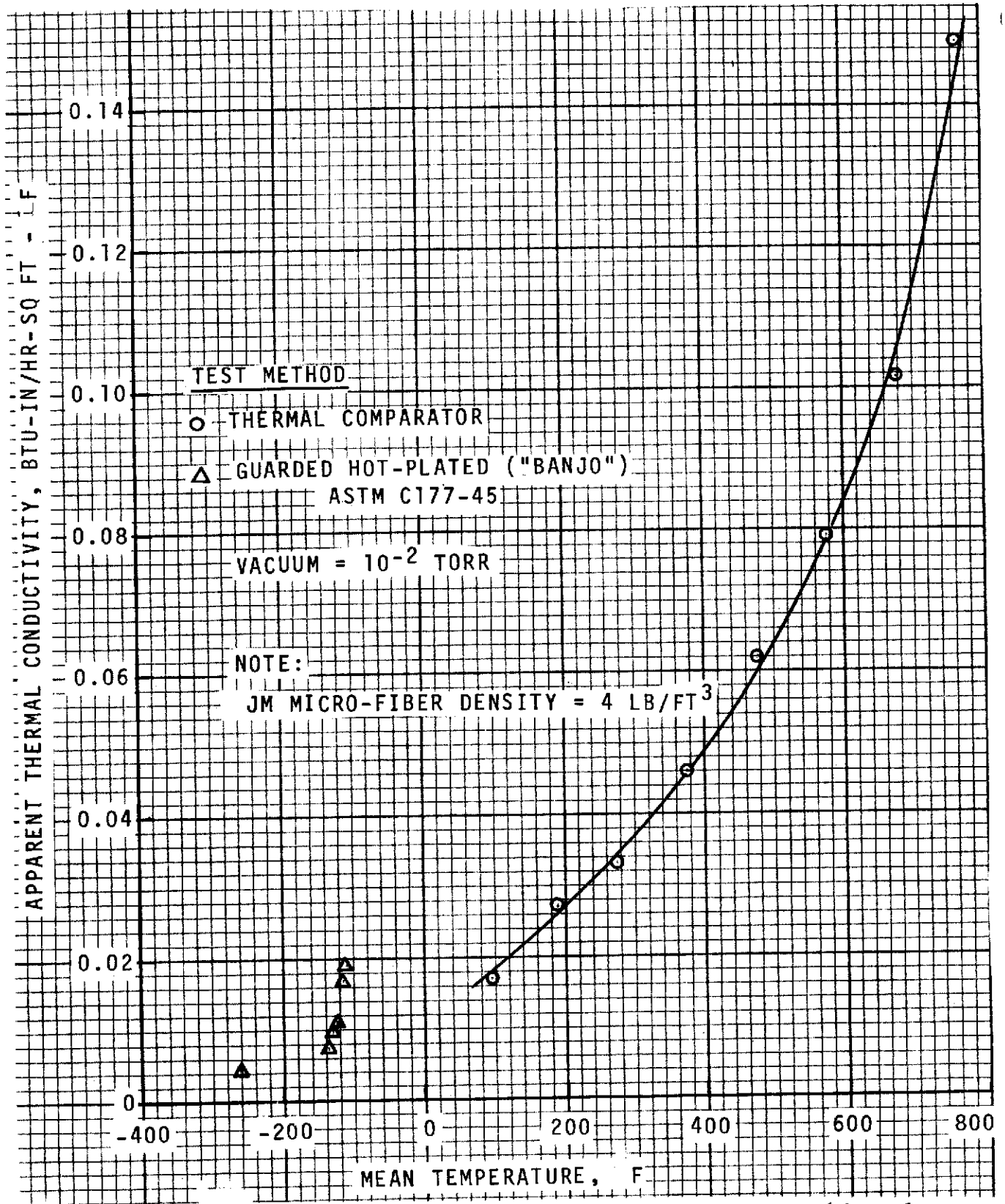

Figure 12.7.1-1. Johns-Manville Micro-Fibers Thermal Properties (Thermal Conductivity in Vacuum vs Temperature)

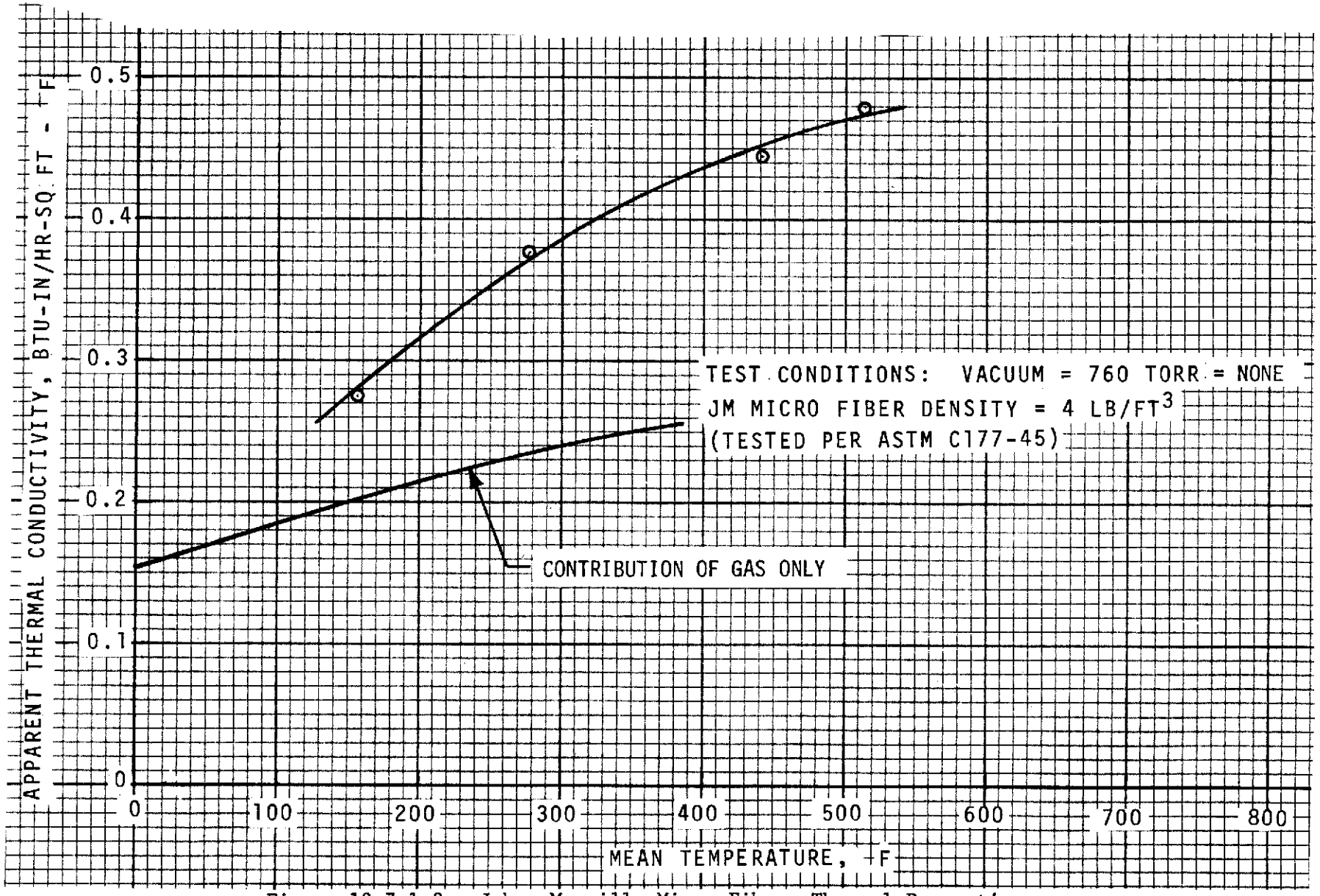

Figure 12.7.1-2. Johns-Manville Micro-Fibers Thermal Properties
(Thermal Conductivity in Air vs Temperature)

results, plotted in Figure 12.7.1-3 (data applicable to Paragraph 6.2.4), show that the enthalpy of 4 lb./ft.^{3} Micro-Fibers varies from 13.5 Btu/lb. at 150 F to 71.5 Btu/lb. at 350 F.

12.7.2 Fiberglass/Phenolic Facing Sheet

Tests to determine the thermal conductivity of fiberglass phenolic sheet laminate materials (MB0130-004, Class I), used as facing sheet in the S-II rigid heat shield composite, were conducted in the SD laboratory. Results of tests of two materials conducted per ASTM C177-45 over a range of mean temperatures from 100 F to 350 F, are shown in Figure 12.7.2-1 (data applicable to Paragraph 6.3.1). These data were originally reported in Laboratory Memo SMT 8-62-1. Both of the materials tested meet the MB0130-004, Class I requirements, hence, the data shown in Figure 12.7.2-1 are indicative of the variance which must be considered in assuming a value for thermal conductivity of the S-II heat shield facing sheet.

12.8 METALS

No thermal properties tests were performed on metals as the necessary data are available from many handbook sources (e.g., References 33 and 34).

In general, the heat transfer properties of metals are well known as compared to values for organics and thus no special testing was initiated.

12.9 COMPOSITES

Composites utilized for thermal control purposes on the S-II stage or studied under an S-II funded technology study are:

a. Honeycomb-filled tank sidewall insulation.

b. Honeycomb insulation (unfilled) as employed on the S-II common bulkhead.

c. Base heat shield - rigid portion.*

d. Base heat shield - flexible curtains.

*The composite insulation system employed in the rigid portion of the heat shield was tested to determine its structural integrity when subjected to the thermal, pressure, and vibrational environments anticipated during both a nominal S-II stage mission and during various S-II failure modes. It was not believed necessary to determine the thermal characteristics of this composite system, as reasonable variations in the assumed characteristics would only cause inconsequential changes in the temperature profile through the composite.

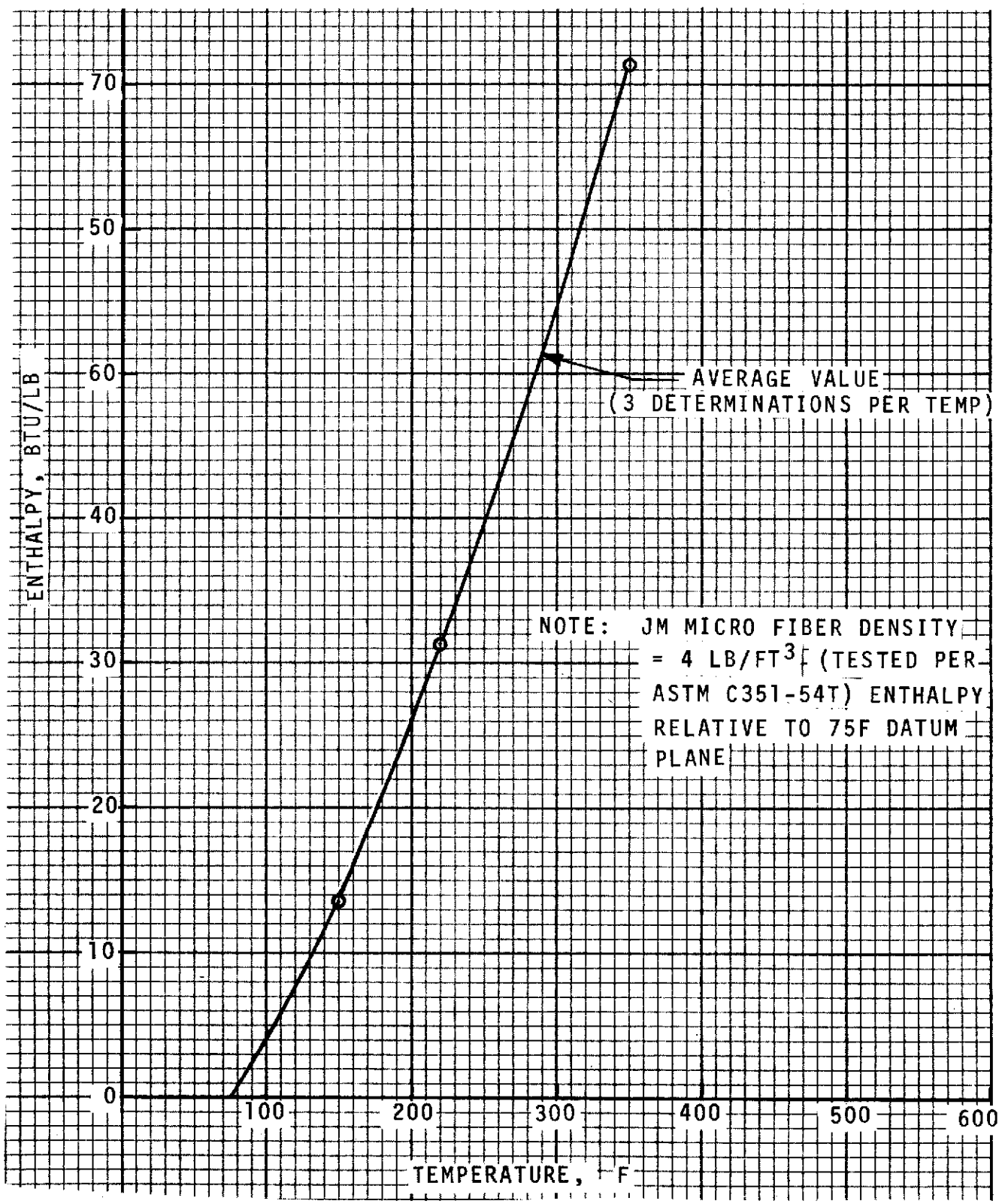

Figure 12.7.1-3. Johns-Manville Micro-Fibers Thermal Properties (Enthalpy vs Temperature)

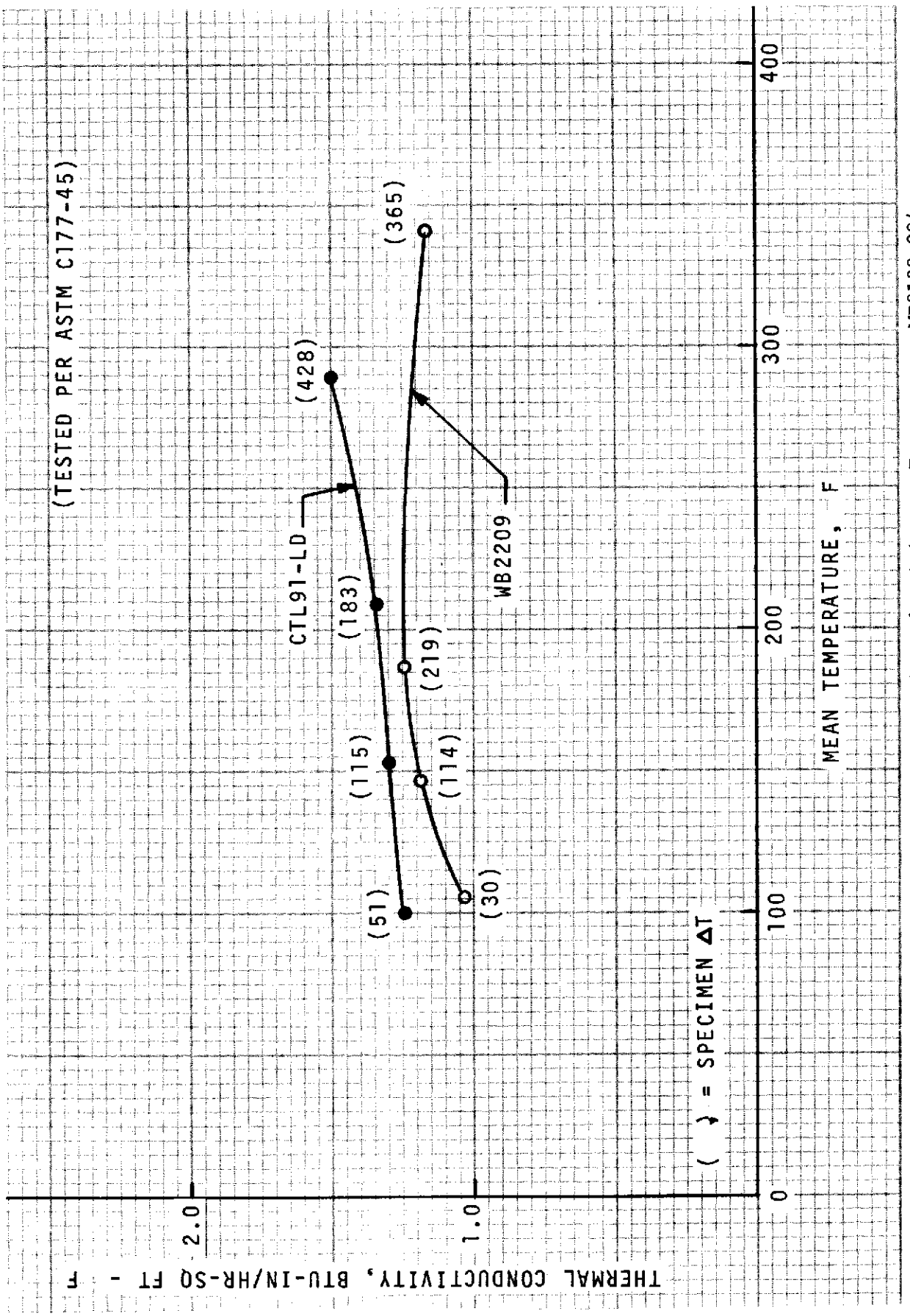

Figure 12.7.2-1. Apparent Thermal Conductivity vs Temperature MB0130-004, Class I, Phenolic/Glass Laminates

e. Multi-layer insulation, considered for use on a reusable S-II stage.

f. Cork bonded, over foam tank sidewall insulation

g. Cork for equipment container insulation.

In the following paragraphs the available thermal properties of the above composites are presented and discussed.

12.9.1 Honeycomb Filled Sidewall Insulation

Space Division laboratory tests were conducted to determine the thermal conductance of samples of ≈1.5-inch-thick foam-filled, helium-purged honeycomb, the system employed as tank sidewall insulation on the S-II vehicle. The makeup of these samples is shown in Figure 12.9.1-1 (data applicable to Paragraph 6.1.1). The samples employed facing sheets top and bottom to facilitate helium purge; otherwise the makeup is the same as the S-II sidewall insulation. The thermal comparator method was employed with a cold face temperature of -320 F and a hot face temperature of from -25 F to 125 F. The results of these tests are plotted in Figure 12.9.1-2 (data applicable to Paragraph 6.1.1). The data shown indicate a slight variation in thermal conductance with hot face temperature and a more significant variation with sample thickness.

12.9.2 Common Bulkhead Insulation

Based on small (2-square-inch) sample tests, conducted by the Martin Co. for NR, the thermal conductivity of helium-purged honeycomb insulation as employed on the S-II common bulkhead is as shown in Figure 12.9.2-1 (data applicable to Paragraph 6.1.2). This information was obtained from Reference 32.

12.9.3 Cork - Erosion Protection

Cork was employed on the S-II vehicle as erosion protection over foam and as thermal protection for electrical equipment containers. Tests were conducted by the Space Division Laboratory to determine the thermal characteristics of MB0130-020 cork sheet, 30.5 lb./ft.^{3}. This cork sheet is suitable for use in either of the above applications. Tests were conducted per ASTM C177 to determine the thermal conductivity and per ASTM C177 to determine the thermal conductivity and per ASTM C351 to determine the mean specific heat. The results of these tests are summarized in Table 12.9.3-1 (data applicable to Paragraph 6.1.8).

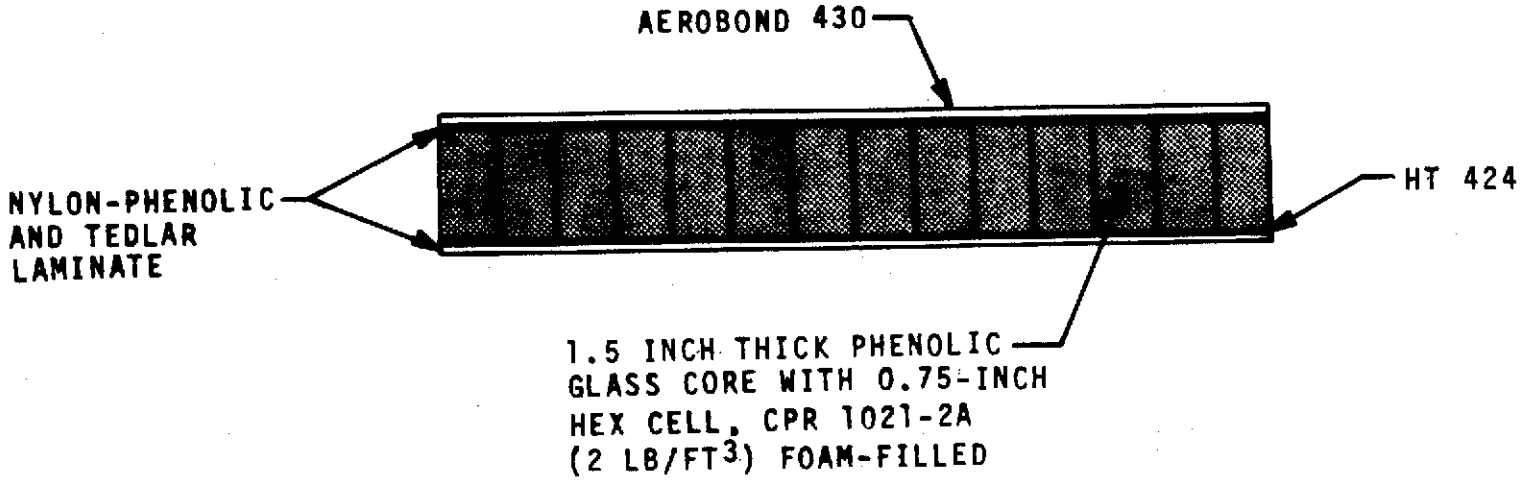

Figure 12.9.1-1. 1.5-Inch Foam-Filled Honeycomb Core Specimen

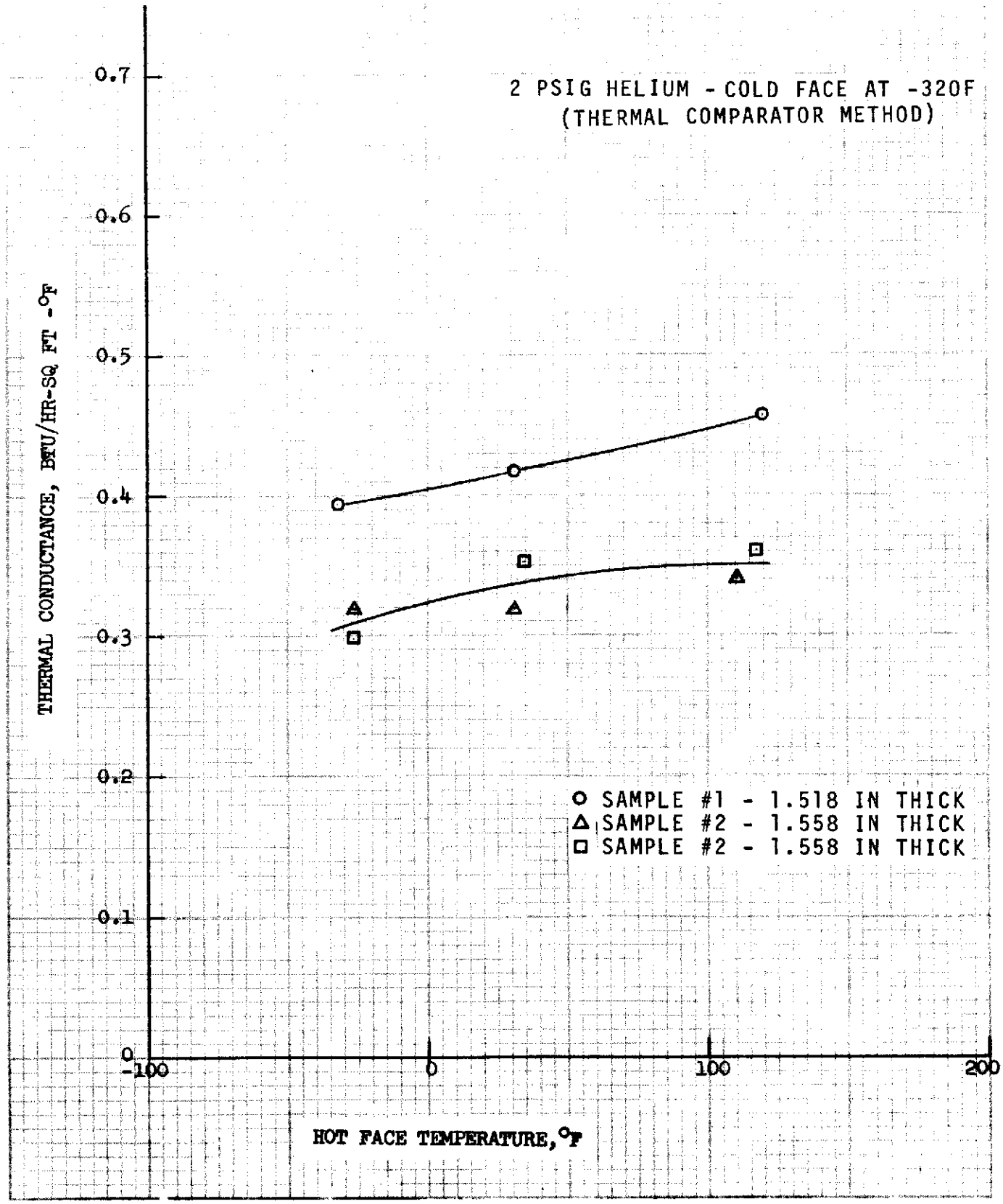

Figure 12.9.1-2. Thermal Conductance vs Temperature 1.5-inch Foam Filled Honeycomb Core

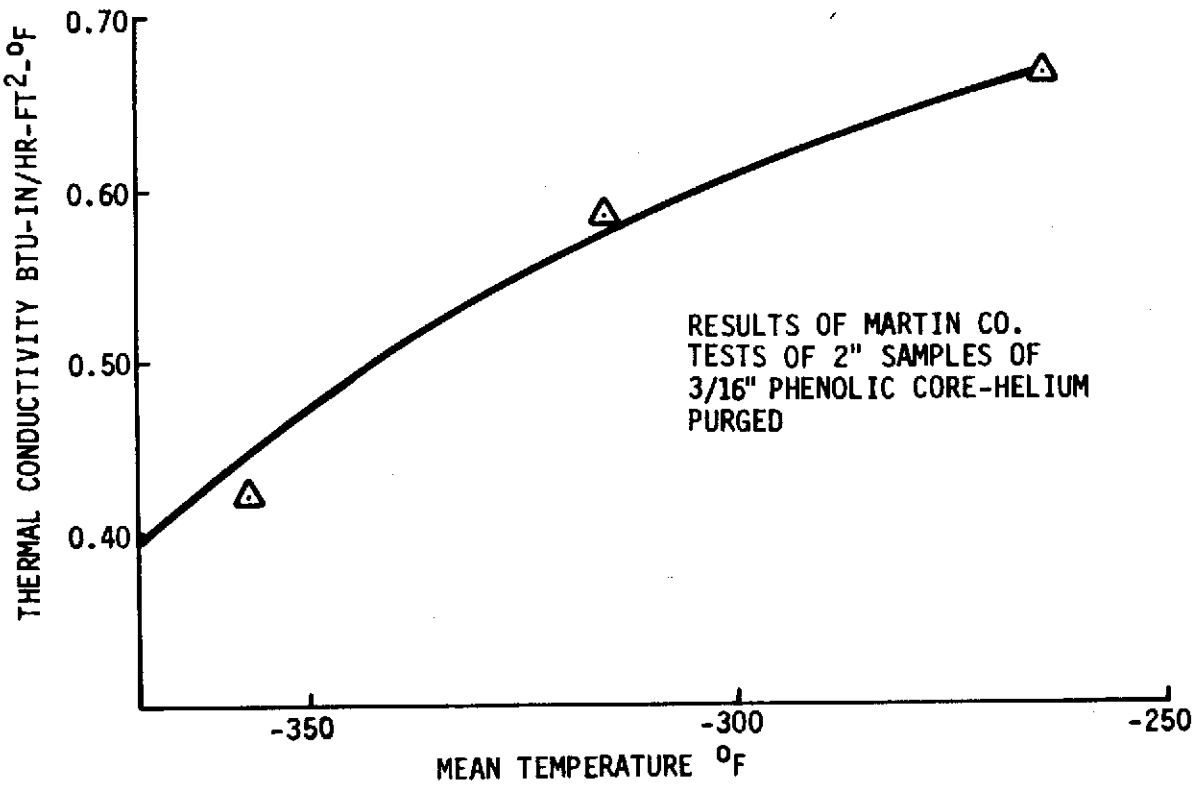

Figure 12.9.2-1. Thermal Conductivity of Common Bulkhead Insulation vs Mean Temperature

Table 12.9.3-1. Thermal Characteristics of Cork Sheet (30.5 lb./ft.^{3}, Ambient Environment, MB0130-020)

Property (Units)	Test Method	Test Temp (F)	No. of Specs	Avg	Max.	Min
Thermal Conductivity (Btu-in./hr./ft.^{2}F)	ASTM C177	83.2 93.0		0.54 0.57	0.55	0.54
Mean Specific Heat (Btu/lb.-F)	ASTM C351	70 - 220	2	0.55	0.55	0.54
Category: A-III-8; Source: SMT 1-66-5						

12.9.4 Multi-Layer Insulation

Multi-layer insulation (MLI) systems utilizing embossed aluminized Mylar (NARSAM-2, North American Rockwell singly aluminized Mylar) were studied as part of an S-II technology program to develop a reusable insulation system for cryogenic tanks. Thermal properties of aluminized Mylar, MLI systems, and MLI support posts were determined as was the emittance degradation of NARSAM-2 due to wear (SD 71-263, Final Report Saturn S-II Advanced Technology Studies; Study 3-Cryo Storage Thermal Improvement, Feb. 15, 1972).

12.9.4.1 MLI Emittance

Total hemispherical emittance tests of many samples of NARSAM-2, produced by a number of different manufacturers, were performed by A.D. Little, Inc. for NR. Tests were performed on NARSAM-2 samples both before and after embossment and perforation.

In some instances, the MLI had been embossed more than once to improve stack height. Aluminum thickness varied depending on the number of aluminizing passes and aluminum thickness per pass.

It was found that coatings built up in successive exposures (e.g., on a rotating drum) had the best pre-embossed surface emittance even though the opacity of the MLI was not as complete when the vacuum was broken between passes as that produced in a continuous process in two passes. No correlation was obtained for the relationship between aluminum thickness and degradation in emittance due to embossing the aluminized surface. Metallized thickness of 250 to 300 Å appeared to yield the most consistent results (target value $\epsilon_{AL} = 0.045$); however, other process variables such as vacuum level, surface temperature, and roll speed (coating thickness per pass) appear to be critical.

The Mylar utilized for much of the multi-layer insulation has a thermal memory. The embossing or formation of dimples in the material is done at an elevated temperature on flat sheets. When these sheets are heated above 140 F and are under strain the embossing relaxes, which in turn can change the spacing between sheets and the total heat leak.

An attempt to correlate MLI aluminum thickness, resistivity, and emittance was only moderately successful. Surface variations produce a wide range of resistivities, and as is the case with opacity, the resistivity of the MLI provides only an indication of expected emittance. Again, the MLI resistivity-capacity-emittance relationship varies with metallizing process, probably because of resulting differences in coating grain structure.

Figure 12.9.4.1-1 (data applicable to Paragraph 6.1.10) is a plot of all significant emittance tests. The variations discussed are exemplified by the ranges of thickness associated with single emittance samples in

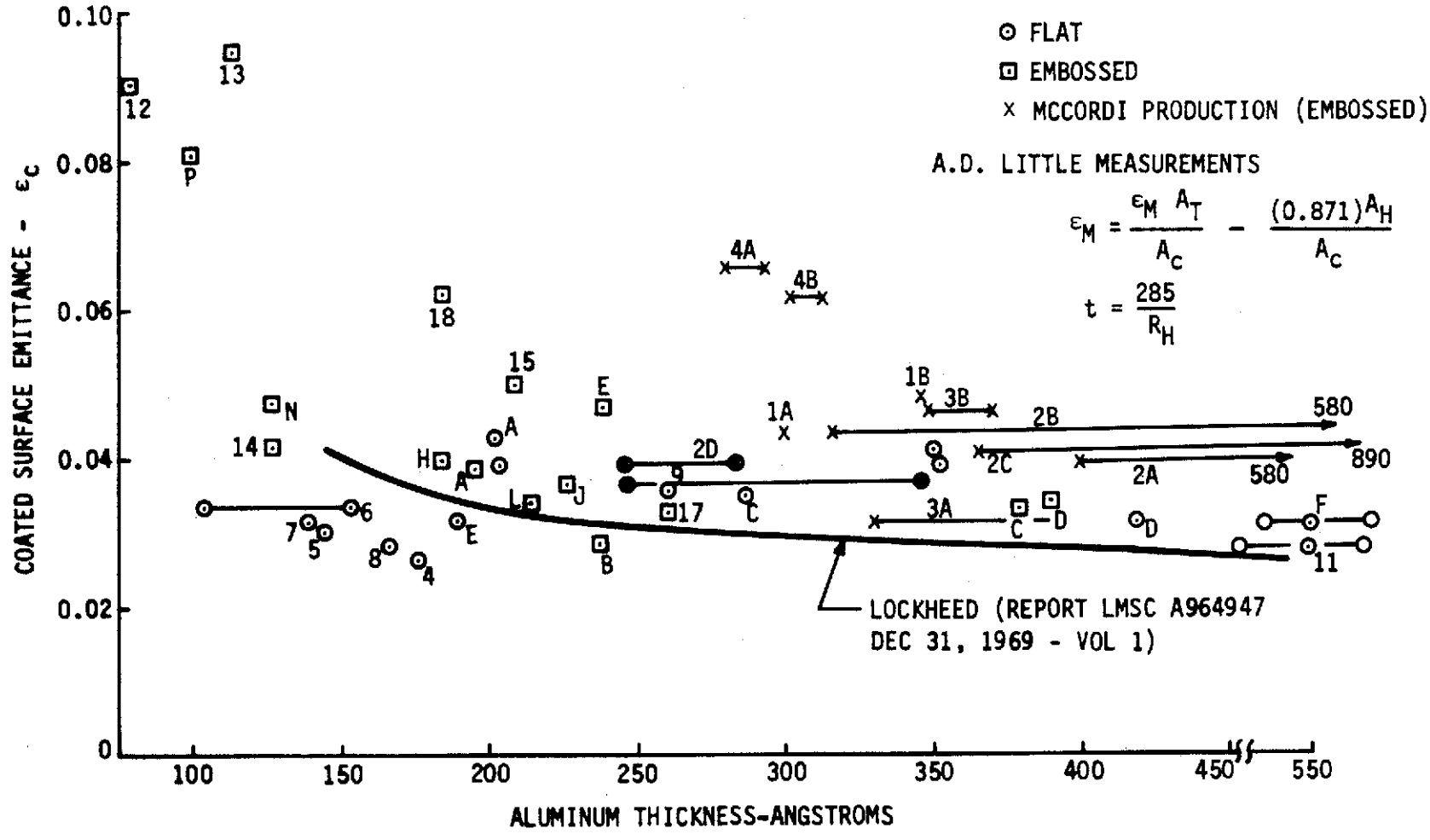

Figure 12.9.4.1-1. Total Hemispherical Emittance of Aluminized Mylar

many cases. Identification data for the pre-production tests are provided in Table 12.9.4.1-1 and for production material in Table 12.9.4.1-2. Data from both tables are applicable to Paragraph 6.1.10.

The McCordi production NARSAM-2 material was produced in four lots and tested as three shipments of material, lots 503 and 504 comprising the second shipment. With the exception of two samples having an emittance $\epsilon_{AL} = 0.047$, all others from the first two shipments were within the 0.045 specification. The third shipment, Lot 505, was significantly above specification. Later tests on Lots 504 and 505 samples (designated by *** and * in Table 12.9.4.1-1) provided values betwen $\epsilon_{AL} = 0.036$ and 0.051, emphasizing the variation in measured values.

12.9.4.2 NARSAM-2 MLI Thermal Conductivity

Flat plate calorimeter tests were performed by A.D. Little, Inc. on three samples as follows:

a. In specification MLI ($\epsilon_{AL} \leq 0.045$), 2-percent area perforations, Roll 110, Lot 504.

b. Out of specification MLI ($\epsilon_{AL} > 0.045$), 2-percent area perforations, Roll 116, Lot 505.

c. Out of specification MLI ($\epsilon_{AL} > 0.045$), 0-percent area perforations, Lot 505.

The tests were performed by stacking twelve 11.5-inch-diameter MLI sheets between two surfaces with temperatures fixed at approximately

$$T_{hot} = +80 \text{ F and } T_{cold} = -320 \text{ F}$$

Tests were conducted by first establishing the uncompressed stack height and compressing in intervals to establish the thermal conductivity (K_{MLI}) as a function of layer density. After completing the series, tests were repeated for discrete points by first repeating the previous layer density that had registered the lowest K_{MLI}. A plot of K_{MLI} versus layer density for all test points is provided by Figure 12.9.4.2-1 (data applicable to Paragraph 6.1.10). The pertinent test measurements are provided in Tables 12.9.4.2-1 through 12.9.4.2-3 (data applicable to Paragraph 6.1.10).

12.9.4.3 Emittance Degradation of NARSAM-2 Due to Wear

Tests were conducted by A.D. Little, Inc. to determine the effects of wear on emittance on both the aluminum and Mylar sides of NARSAM-2 MLI. Two samples of the aluminum side rubbed against Mylar, and one with Mylar rubbed against an aluminum side were measured.

The rubbing surface was the resulting ridges of the embossment peaks. The opposite side of the MLI was the surface rubbed against.

Table 12.9.4.1-1. Pre-Production Material Properties Summary

* Number of Embossment Passes

A. D. LITTLE TEST I.D.	SUPPLIER	SPECIAL PROCESSING	EMBOSS	HOLES PER 2¼ INCH DIAMETER	RESISTIVITY	THICKNESS	ϵ_M MEASUREMENT EMITTANCE	ϵ_{AL} COATED SURFACE	I.D.
2-D	COBURN	REEMBOSSED 9 GA B/U	2*	29.5	3.621	78.7	.1035	.090	12
3-F	COBURN	REEMBOSSED 20 GA B/U	2	30.	2.489	114.	.1085	.095	13
1-C	COBURN	REEMBOSSED NO B/U	2	29	2.229	127.	.0556	.042	14
4-B	COBURN	REEMBOSSED NO B/U	1	31	1.257	226.	.0523	.037	J
G-B	COBURN	REEMBOSSED 12 GA B/U	1	25.3	1.368	208.	.0618	.050	15
5-A	COBURN		0	0	1.402	203	.0387	.039	16
7-G	McCORDI	NR/SD CALORIMETER	1	26	1.087	262.	.0461	.033	17
8-H	COBURN		0	30.5	1.509	189.	.0467	.032	E
GF-01	COBURN	REEMBOSSED/McCORDI	1	30.5	1.190	239.	.0618	.047	E
GF-02	McCORDI		0	0	0.801	356.	.0389	.039	H
GF-03	McCORDI		1	0	1.555	183.	.0402	.040	H
GF-04	NAT. MET.		0	0	1.389	205.	.0427	.043	A
GF-05		EMBOSSED/McCORDI	1	0	1.463	195.	.0393	.039	A
GF-06			0	0	0.811	351.	.0411	.041	B
GF-07		EMBOSSED/McCORDI	1	0	1.194	238.	.0291	.029	B
GF-08			0	0	0.998	285.	.0352	.035	C
GF-09		EMBOSSED/McCORDI	1	0	0.750	380.	.0332	.033	C
GF-10			0	0	0.680	419.	.0305	.031	D
GF-11		EMBOSSED/McCORDI	1	0	0.737	387.	.0336	.034	D
NORRIS 01	COBURN	BACK-UP - 9 GA ON MYLAR SIDE	2	32	2.853	99.	.0955	.081	P
NORRIS 02		BACK-UP - 9 GA ON ALUM SIDE	2	25	1.542	185.	.0780	.062	18
NORRIS 03		BACK-UP - 4 GA ON MYLAR SIDE	2	24	1.320	216.	.0453	.034	L
NORRIS 04		BACK-UP - 4 GA ON ALUM SIDE	2	31.5	2.240	127.	.0615	.047	N

Table 12.9.4.1-1. Pre-Production Material Properties Summary (Cont)

A. D. LITTLE TEST I.D.	SUPPLIER	SPECIAL PROCESSING	EMBOSS	HOLES PER 24 INCH DIAMETER	RESISTIVITY	THICKNESS	ϵ_M MEASUREMENT EMITTANCE	ϵ_{AL} COATED SURFACE	I.D.
NORRIS 4	SCHJELDAHL	REPEATED METALLIZING	0	0	1.593	185.	.0265	.027	4
					1.600	178.			
		PASSES ON A DRUM	0	0	1.607	177.			
					1.694	168.			
NORRIS 5		BACKING	0	0	1.876	152.	.0303	.030	5
					1.900	150			
NORRIS 6			0	0	1.864	153.	.0341	.034	6
					1.834	155.			
					2.779	103.			
					2.696	106.			
NORRIS 7			0	0	2.013	142.	.0316	.032	7
					2.118	134.			
NORRIS 8			0	0	1.727	165.	.0289	.029	8
					1.707	167.			
NRA 1	McCORDI	TWO METALLIZING PASSES	0	0		540.		.027	11
NRA 2			0	0		564.		.031	F
NRA 3			0	0				.036	9

Table 12.9.4.1-2. NARSAM-2 MLI Production Material Emittance Test Results Summary

LOT NUMBER	ROLL NUMBER	NUMBER OF 0.060 IN. HOLES	MEAS. EMITTANCE ϵ_M	AL SURFACE EMITTANCE ϵ_{AL}	Ω/□	THICKNESS Å	REMARKS	I.D. NUMBER
C-30250	107	39.	0.0619	0.043	0.985	289.	LEADING EDGE **	1A
	107	39.	0.0658	0.047	0.839	340.	TRAILING EDGE	1B
	101 *	37.5	0.0927	0.075	29.67 CENTER	9.8	DARKEST BROWN COLOR	
					9.54 LEFT TOP	29.9		
					22.11 RIGHT TOP	12.9		
503	109	40	0.0568	0.039	0.710	400.	LIGHT BROWN	2A
					0.490	580.	COLOR, TRAILING	
					0.508	560.	EDGE	
	109	38.5	0.0604	0.042	0.923	310.	NO DISCOLORATION,	2B
					0.614	465.	TRAILING EDGE	
					0.490	580.		
	109	37	0.0574	0.040	0.770	370.	DARK BROWN COLOR,	2C
					0.779	366.	TRAILING EDGE	
					0.320	890.		
504	110, 111, 112	37	0.0570	0.039	1.014	281	LIGHT BROWN COLOR	2D
					1.010	282		
					1.180	241		
		40.5	0.0505	0.031	0.870	327	NO DISCOLORATION	3A
					0.837	390		
					0.795	358		
		39	0.0655	0.047	0.825	345	DARK BROWN COLOR	3B
					0.789	361		
					0.780	365		

Table 12.9.4.1-2. NARSAM-2 MLI Production Material Emittance Test Results Summary (Cont)

LOT NUMBER	ROLL NUMBER	NUMBER OF .060 IN. HOLES	MEAS. EMITTANCE ϵ_M	AL SURFACE EMITTANCE ϵ_{AL}	$\Omega/\square$	THICKNESS • A	REMARKS	I.D. NUMBER
505	114	37	0.0839	0.067	0.980 1.030	291 277	LEADING EDGE	4A
	117	38	0.0805	0.063	0.920 0.948	310 301	TRAILING EDGE	4B
504 ***	110	37	0.0668	0.049	1.470	193		3C
504 ≠	110	36	0.0528	0.036	1.118	255		
504 ≠	110	37	0.0604	0.043	0.970	293		
505 ***	116	40.5	0.697	0.051	0.900 2.070	256 137		4C

* THIS ROLL NOT SHIPPED TO NR-SD

** LEADING AND TRAILING EDGE PERTAINS TO METALLIZING RUN

*** DATA TAKEN FROM CALORIMETER SAMPLES

≠ DATA TAKEN FROM WEAR TEST SAMPLES AT ZERO CYCLES

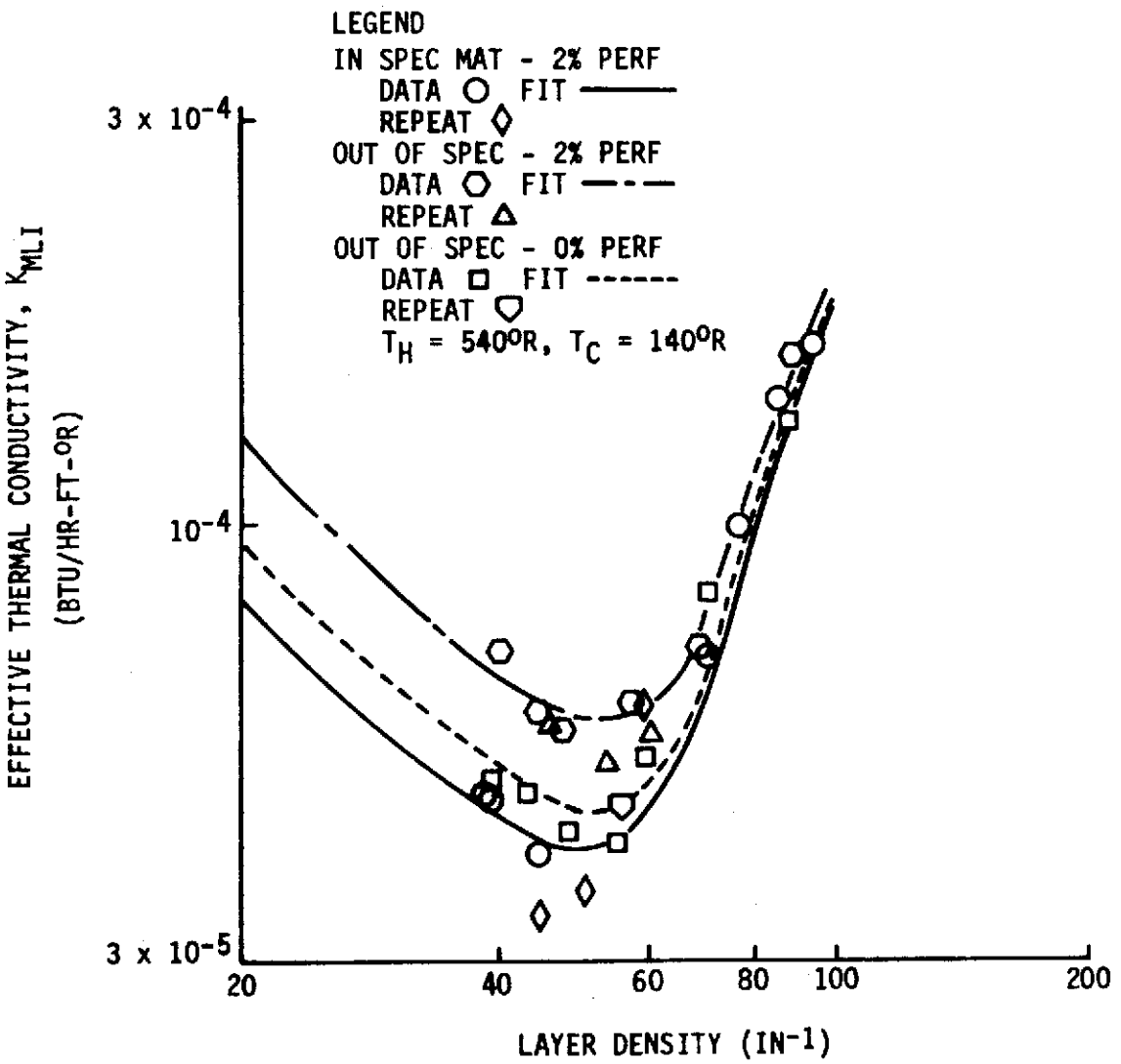

Figure 12.9.4.2-1. NARSAM-2 Flat Plate Calorimeter Data

Table 12.9.4.2-1. Performance of NARSAM-2 Material That Met Emittance Specification (AL 0.045); 2% Area Perforation

Load (psi)	q/A (Btu/hr-ft^2)	T_h (°F)	Stack Height (in.)	Layer Density (shields/in.)	Conductance (Btu/hr-ft^2-°F)	K_{MLI} (Btu/hr-ft-°F)
0.72 to 1.44×10^{-4}	1.127	85	0.248	48.4	0.00279	5.76×10^{-5}
"	1.083	84	0.265	45.3	0.00269	5.94
"	1.150	80	0.294	40.8	0.00288	7.04
"	1.085	79.8	0.229	52.4	0.00272	5.22
"	1.41	79	0.196	61.2	0.00353	5.76
0.008	1.975	79	0.172	69.8	0.00495	7.10
0.0052	5.647	78	0.132	90.9	0.01419	15.6
			Repeat Points			
0.72 to 1.44×10^{-4}	1.092	80.6	0.226	53.1	0.0273	5.14
"	1.044	77.6	0.265	45.3	0.0263	5.80
"	1.392	80.5	0.196	61.2	0.003477	5.68

Identification and Physical Data:
- Lot 504
- Roll 116
- 12 Layers - 11.5 in. diameter
- Weight - 6.7 grams
- Cold Side Temperature, T_c = -320°F

Table 12.9.4.2-2. Performance of NARSAM-2 Material That Met Emittance Specification (Al 0.045); 2% Area Perforation

Load (Psi)	q/A (Btu/hr-ft^2)	T_h (°F)	Stack Height (In)	Layer Density (Shields/in)	Conductance (Btu/hr-ft^2°F)	K_{MLI} (Btu/hr-ft°F)
0.72 to 1.44×10^{-4}	0.724	81.5	0.310	38.7	1.80×10^{-3}	4.66×10^{-5}
"	0.728	82.6	0.267	44.9	1.80	4.02
"	0.736	81.9	0.307	39.1	1.83	4.67
0.01	2.08	84.2	0.169	71.0	5.16	7.29
0.028	3.08	80.5	0.153	78.4	7.20	9.86
0.055	4.44	76.7	0.139	86.3	11.2	12.7
0.10	6.09	77.3	0.125	96.0	15.3	15.9
			Repeat Points			
0.72 to 1.44×10^{-4}	0.615	79.5	0.269	44.6	1.54	3.44
"	0.740	78.2	0.239	50.2	1.86	3.67
"	1.48	82.8	0.199	60.3	3.67	6.09

Identification & Physical Data:

Lot 504
Roll 110
12 Layers - 11.5 in. diameter
Weight = 6.7 grams
Cold Side Temperature, T_c = -320°F

Table 12.9.4.2-3. Performance of NARSAM-2 Material With Greater than Specification Emittance (AL 0.045,) Unperforated)

Load (psi)	q/A (Btu/hr-ft^2)	T_h ($^\circ$F)	Stack Height (in)	Layer Density (Shields/in)	Conductance (Btu/hr-ft^2-$^\circ$F)	K_{MLI} (Btu/hr-ft-$^\circ$F)
0.74 to 1.48 x 10^{-4}	0.827	85.5	0.277	43.3	0.00204	4.71 x 10^{-5}
↕	0.769	80.2	0.303	39.6	0.00192	4.86
	0.814	80.2	0.249	48.2	0.00203	4.22
	0.932	79.6	0.216	55.6	0.00233	4.20
	1.29	79.9	0.197	60.9	0.00313	5.3
0.01	2.37	79.5	0.168	71.4	0.00593	8.31
0.07	4.59	80.5	0.138	86.9	0.0115	13.2
			REPEAT POINT			
0.74 to 1.48 x 10^{-4}	1.04	82.0	0.214	56.1	0.00258	4.6

Identification and Physical Data
Lot 505
Roll - No Identification
12 Layers - 11.5 in Diameter
Weight = 6.9 gm
Cold Side Temperature, T_c = -320°F

A device was fabricated which cycled the sample through 1/4-inch strokes with MLI loading of ≈0.01 psi. Emittance measurements were taken on the aluminum side after 0, 250, 500, 750, and 1000 cycles. The Mylar side was measured after 0, 500, and 1000 cycles. The results are shown in Table 12.9.4.3-1 (data applicable to Paragraph 6.1.10) and indicate very little emittance degradation with wear.

Table 12.9.4.3-1. Wear Effects on NARSAM-2 Emittance

1/4-Inch Cycles	1 meas	1 AL	2 meas	2 AL	3 meas	3 MY
0	0.053	0.036	0.061	0.043	0.352	0.340
250	0.054	0.036	0.062	0.044	-	-
500	0.056	0.038	0.062	0.044	0.351	0.340
750	0.056	0.039	0.063	0.045	-	-
1000	0.058	0.041	0.064	0.046	0.360	0.348

Sample 1 - Lot 504, Roll 110, 36 holes.
Sample 2 - Lot 504, Roll 110, 37 holes.
Sample 3 - Lot 504, Roll 110, 38.5 holes.

12.9.4.4 Thermal Conductance of MLI Support Posts

Tests were performed in the NR test laboratory to determine the thermal conductance of MLI support posts. The support posts were fabricated of a fiberglass-reinforced epoxy resin material. The tests utilized an axial heat flow comparator approach for direct measurement of post conductance. Test data were obtained over the mean temperature range -152 to -243 F. MLI support post conductance as a function of mean temperature for posts having a 12.9-mil wall thickness is presented in Figure 12.9.4.4-1 (data applicable to Paragraph 6.1.10).

12.9.4.5 Overall MLI System Properties

Based on the test results presented coupled with analysis--the predicted effective thermal conductivity and density of NARSAM-2 MLI installed as described in SD 71-263, using molded MLI support posts, are: (1) K_{EFF} = 5.01 x 10^{-5} Btu/hr.-ft.-F, and (2) ρ = 1.75 lb.ft.^{3}.

12.9.4.6 MLI Outgassing Characteristics

The outgassing characteristics of MLI both with and without the presence of pressure-sensitive tape (used in MLI layup and repair) was determined by NR laboratory tests. The results of these tests are presented in Figure 12.9.4.6-1 (data applicable to Paragraph 6.1.10).

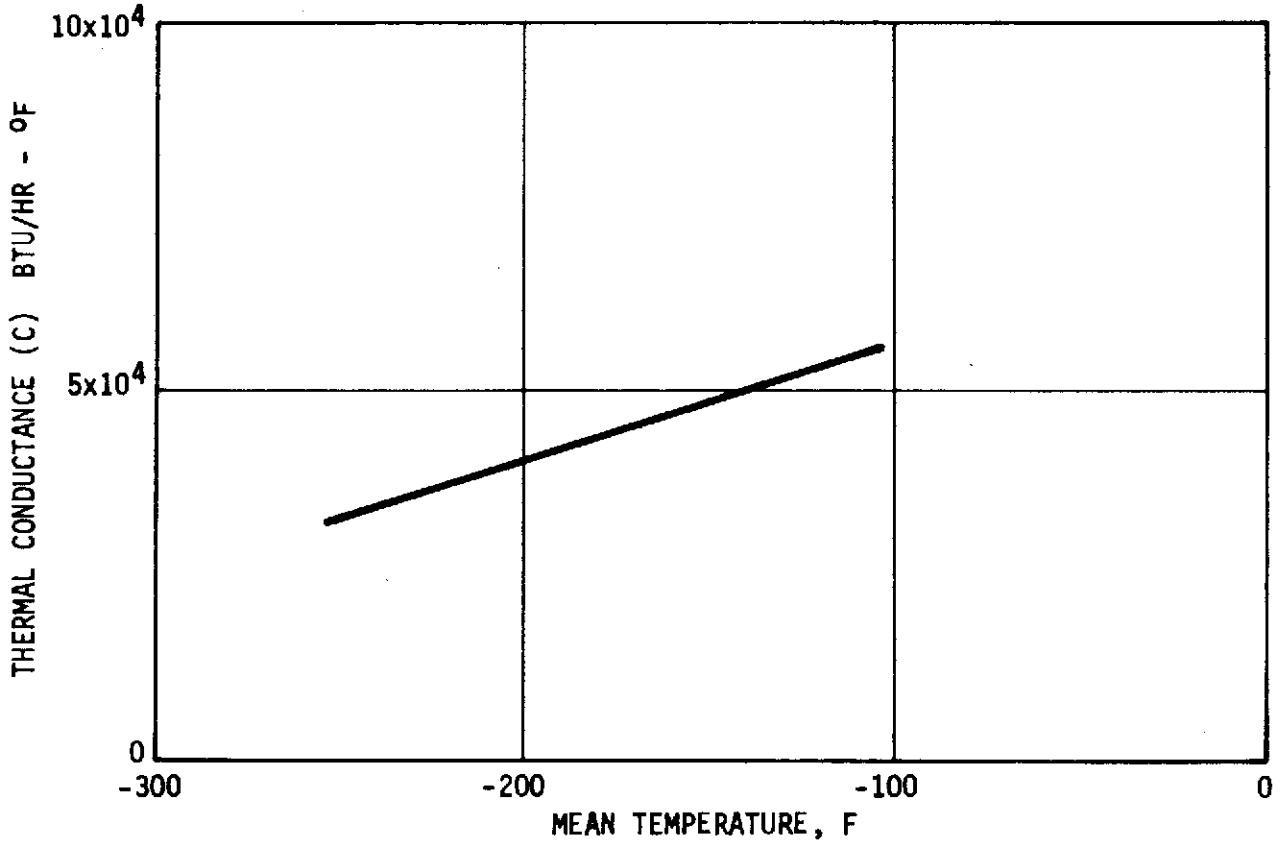

Figure 12.9.4.4-1. Thermal Conductance (C) Versus Mean Temperature of 1-Inch Long MLI Support Post

12.9.5 Base Heat Shield - Flexible Curtains (S-II-13 and S-II-15 only)

The Space Division Laboratory conducted tests of samples of flexible curtain composite consisting of 0.2-inch B1570 batt sandwiched between two layers of C1554-48 fabric. Tests were conducted per ASTM C177-63 to determine the thermal conductance versus mean temperature at 1.2 Torr (nitrogen). Tests were run at mean temperatures from 930 to 2100 F. The results of these tests are plotted in Figure 12.9.5-1 (data applicable to Paragraph 6.3.5). As shown, the thermal conductance was found to vary from 1.55 Btu/hr.-ft.^{2}-F at a mean temperature of 930 F to 6.10 Btu/hr.-ft.^{2}-F at a mean temperature of 2120 F. Tests of similar samples were conducted at 6 x 10^{-2} Torr (argon) to determine the total normal emittance versus temperature. Tests were made both by the reflectance method (0.35 - 15.0 microns) and by the sliding specimen technique at temperatures from 1000 to 2200 F. The results of these tests are plotted in Figure 12.9.5-2 (data applicable to Paragraph 6.3.5). The reflectance method indicated higher emittance values than the sliding specimen technique except at 1000 F. The total normal emittance was found to decrease with increasing temperature regardless of test method. The low and high value of total normal emittance regardless of the method of determination were found to vary from 69.5 percent at 1000 F to 54.0 percent at 2200 F.

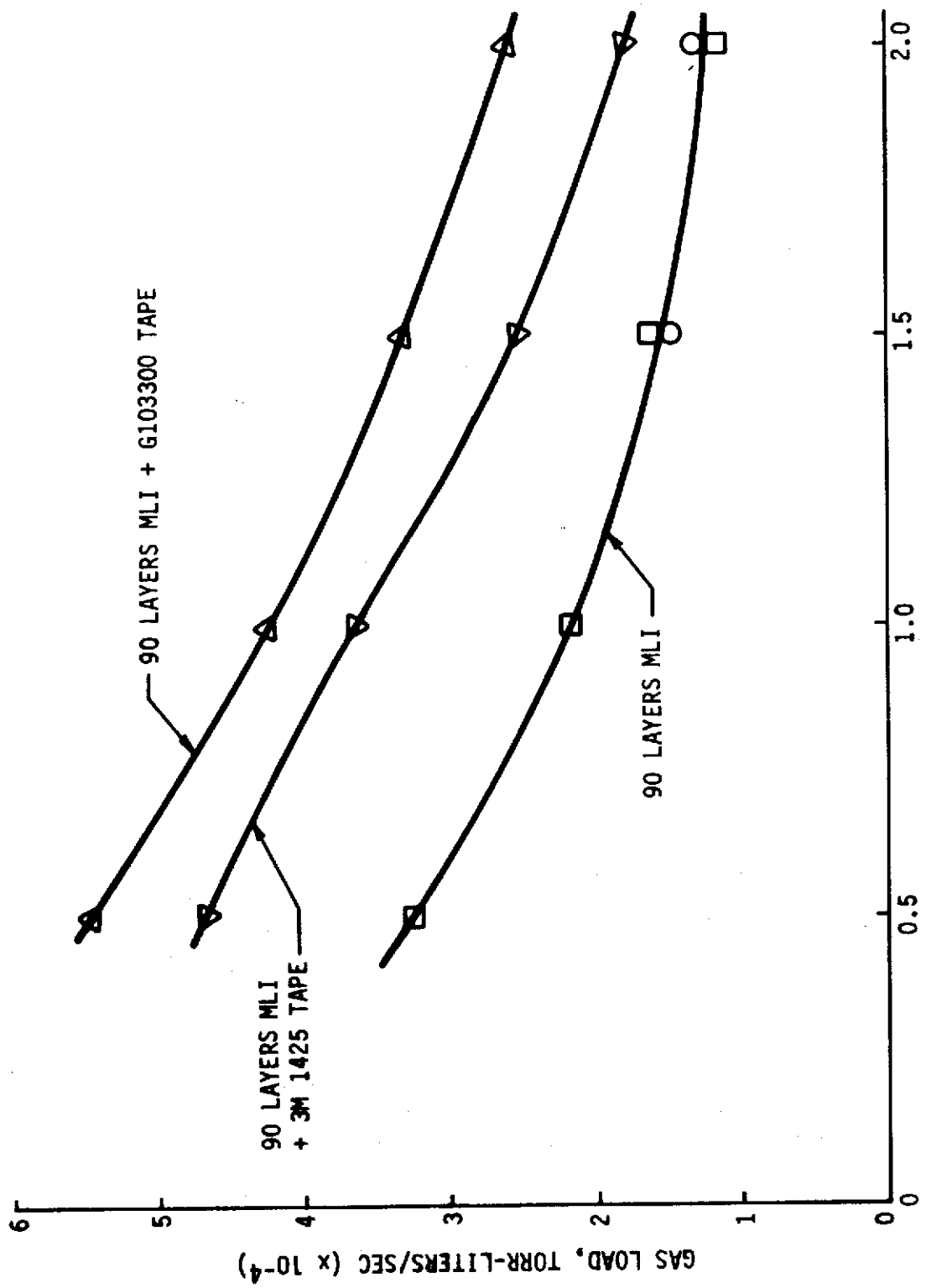

Figure 12.9.4.6-1. Outgassing Characteristics, MLI and Aluminized Pressure-Sensitive Tape

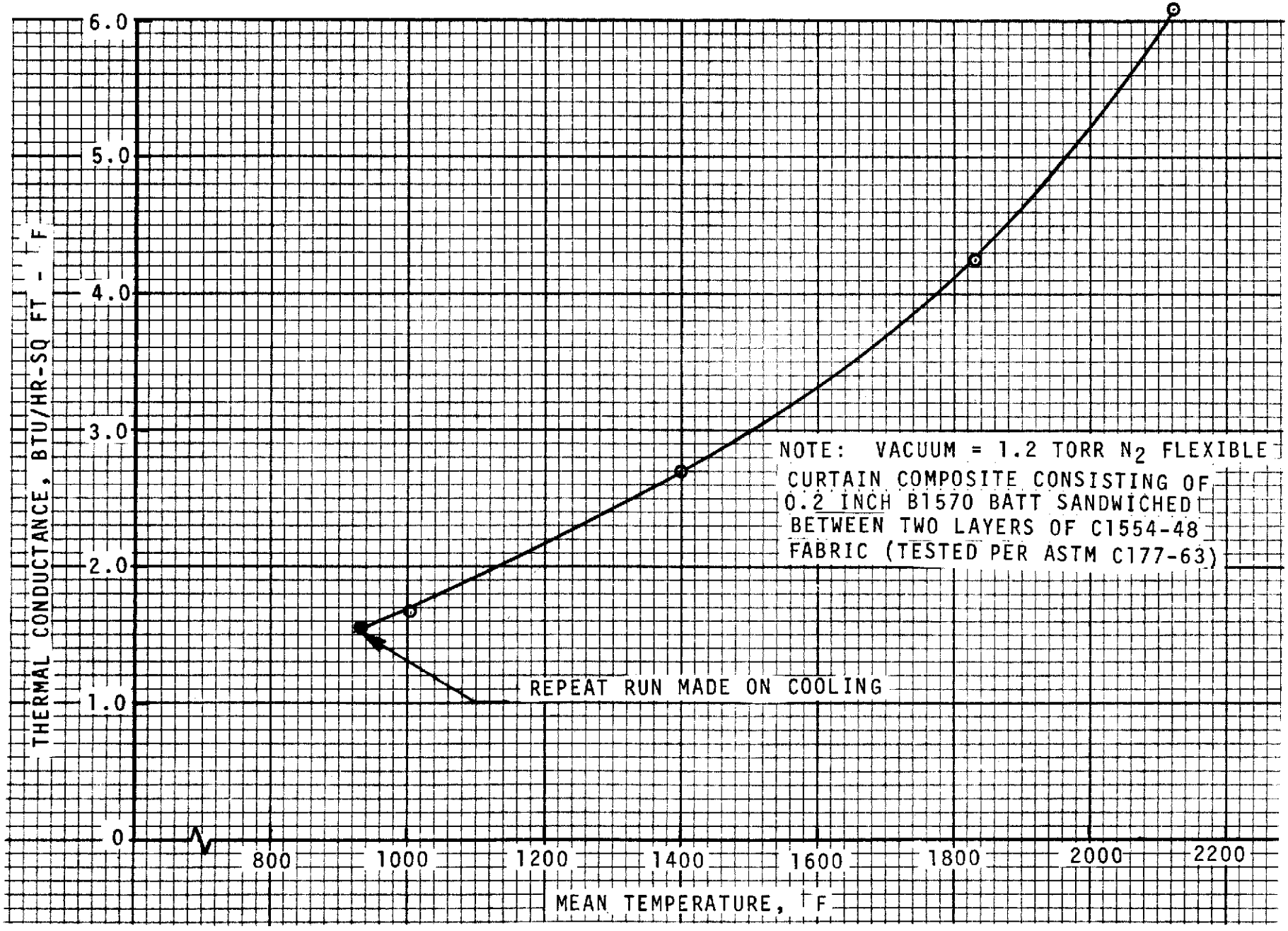

Figure 12.9.5-1. Heat Shield Flexible Curtain Composite Thermal Properties (Thermal Conductance in Vacuum vs Temperature)

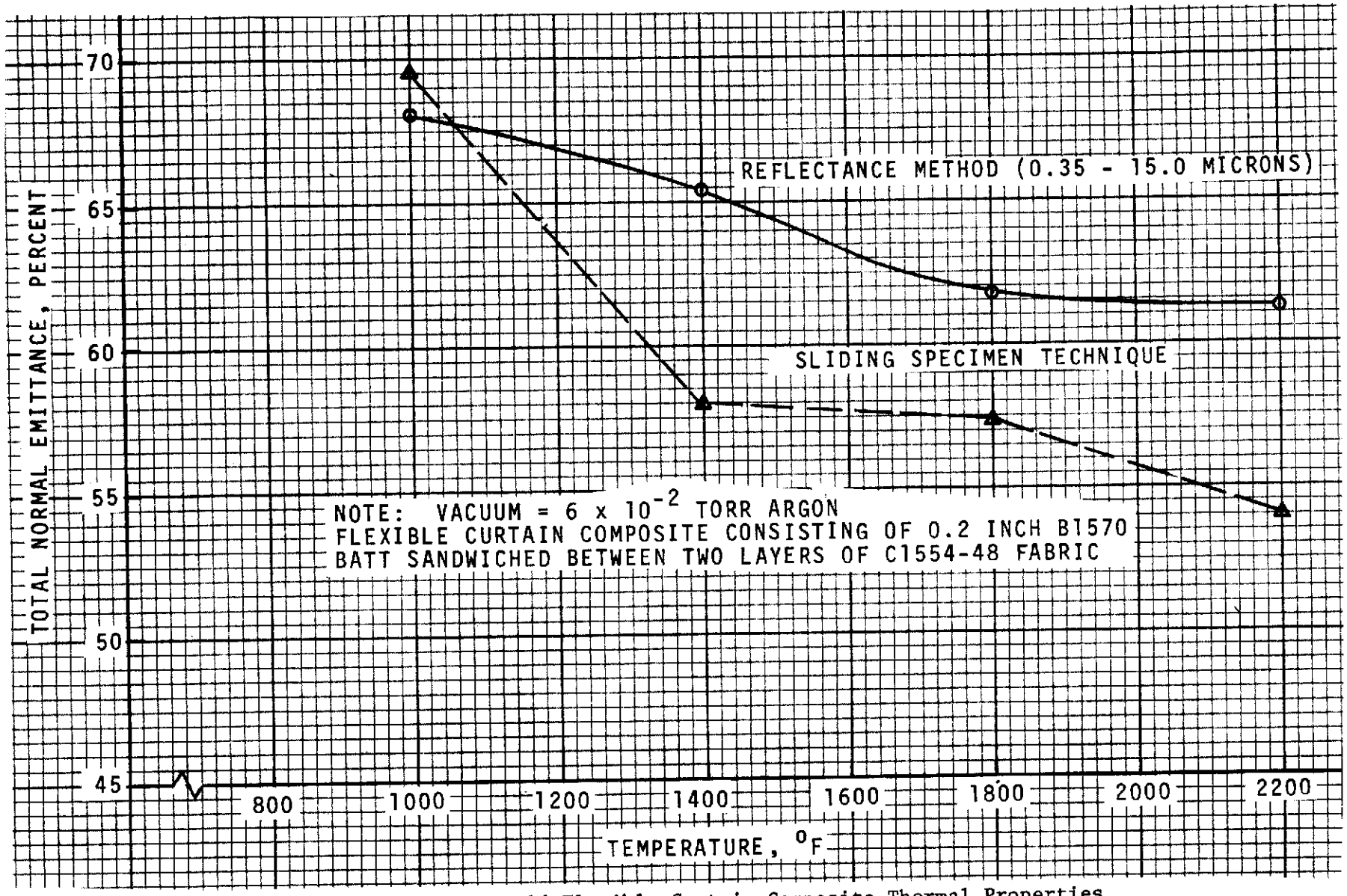

Figure 12.9.5-2. Heat Shield Flexible Curtain Composite Thermal Properties
(Total Normal Emittance in Vacuum vs Temperature)

12.9.6 Cork - Thermal Protection For Electrical Containers

Cork of ≈7 lb./ft.^{3} density was employed on the S-II stage as thermal insulation within the covers and sides of the forward and aft equipment containers. Tests per ASTM C351-54 of samples of Armstrong 7326 Insulcork with a density of 6.7 lb./ft.^{3} were conducted to determine the specific heat, thermal conductivity, and enthalpy of this material. The specific heats determined in these tests are presented in Table 12.9.6-1. The apparent thermal conductivity in air at 760 Torr versus mean temperature of Armstrong 7326 Insulcork, ρ = 6.7 lb./ft.^{3}, was determined per ASTM C177-45 method. The results of these tests are presented in Figure 12.9.6-1 (data applicable to Paragraph 6.4.1). The apparent thermal conductivity in air at 760 Torr of this material varied from 0.265 Btu-in./hr.-ft.^{2}-F at a mean temperature of 100 F to 0.348 Btu-in./hr.-ft.^{2}-F at a mean temperature of 287 F.

The enthalpy relative to a 75 F datum plane of Armstrong 7326 Insulcork, ρ = 6.7 lb./ft.^{3}, was determined per ASTM C351-54T for a temperature range from 150 to 450 F. The results of these tests are plotted in Figure 12.9.6-2 (data applicable to Paragraph 6.4.1). The enthalpy of this material relative to a 75 F datum varied from 35 Btu/lb. at 150 F to 218 Btu/lb. at 450 F.

Table 12.9.6-1. Thermal Characteristics of Armstrong 7326 Insulcork, 6.7 pcf

Property (units)	Test Methods	Test Temp (°F)	No. of Specs	Test Results		
				Avg	Max.	Min
Mean Specific Heat	ASTM C351-54T	80 - 150	2	0.465	0.47	0.46
		84 - 220	2	0.465	0.47	0.46
		88 - 350	2	0.57	0.57	0.57
		98 - 450	2	0.585	0.59	0.58
Category: D-1; Source: LM No. SMT 3-64-9						

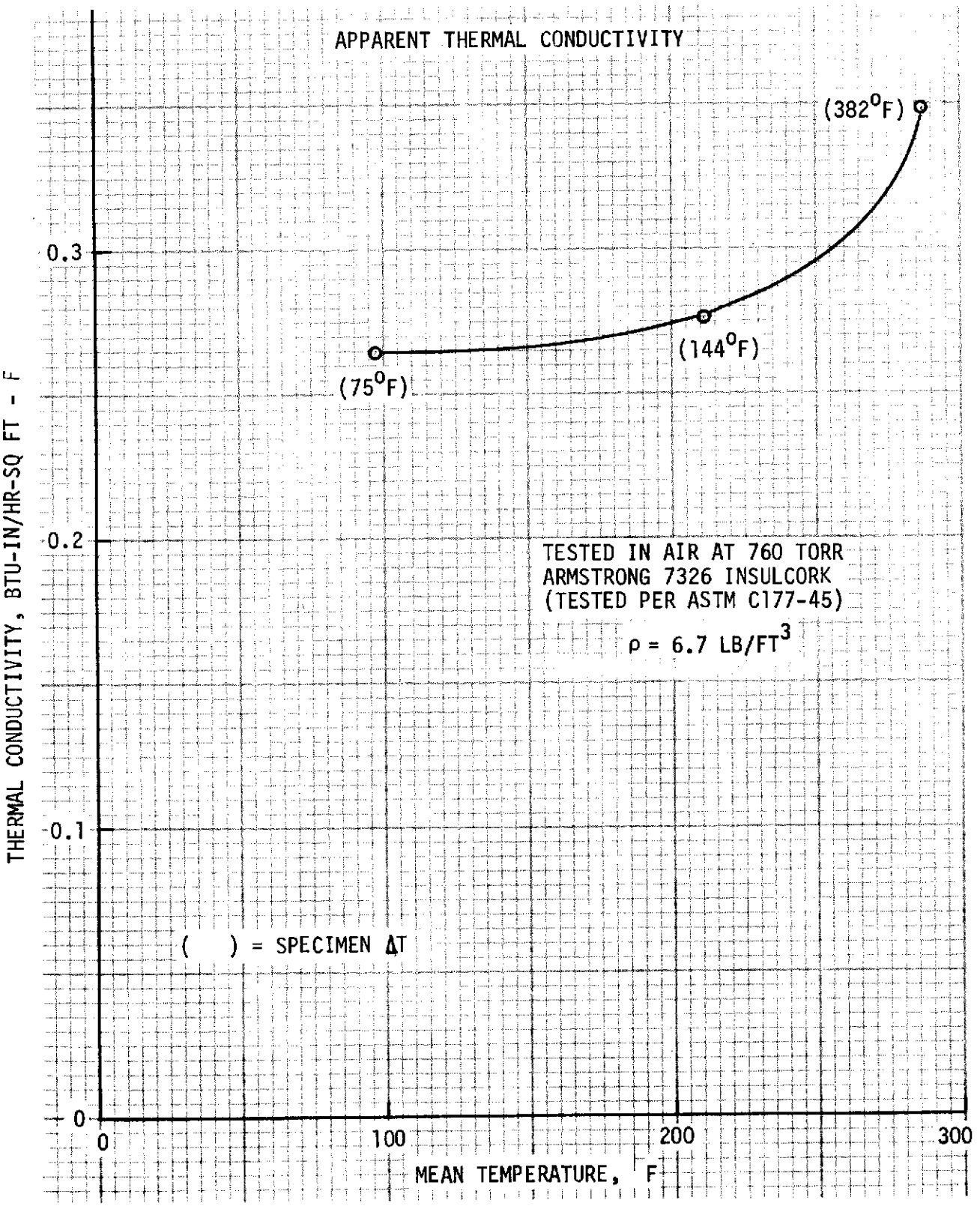

Figure 12.9.6-1. Thermal Conductivity of Armstrong 7326 Insulcork in Air Versus Mean Temperature

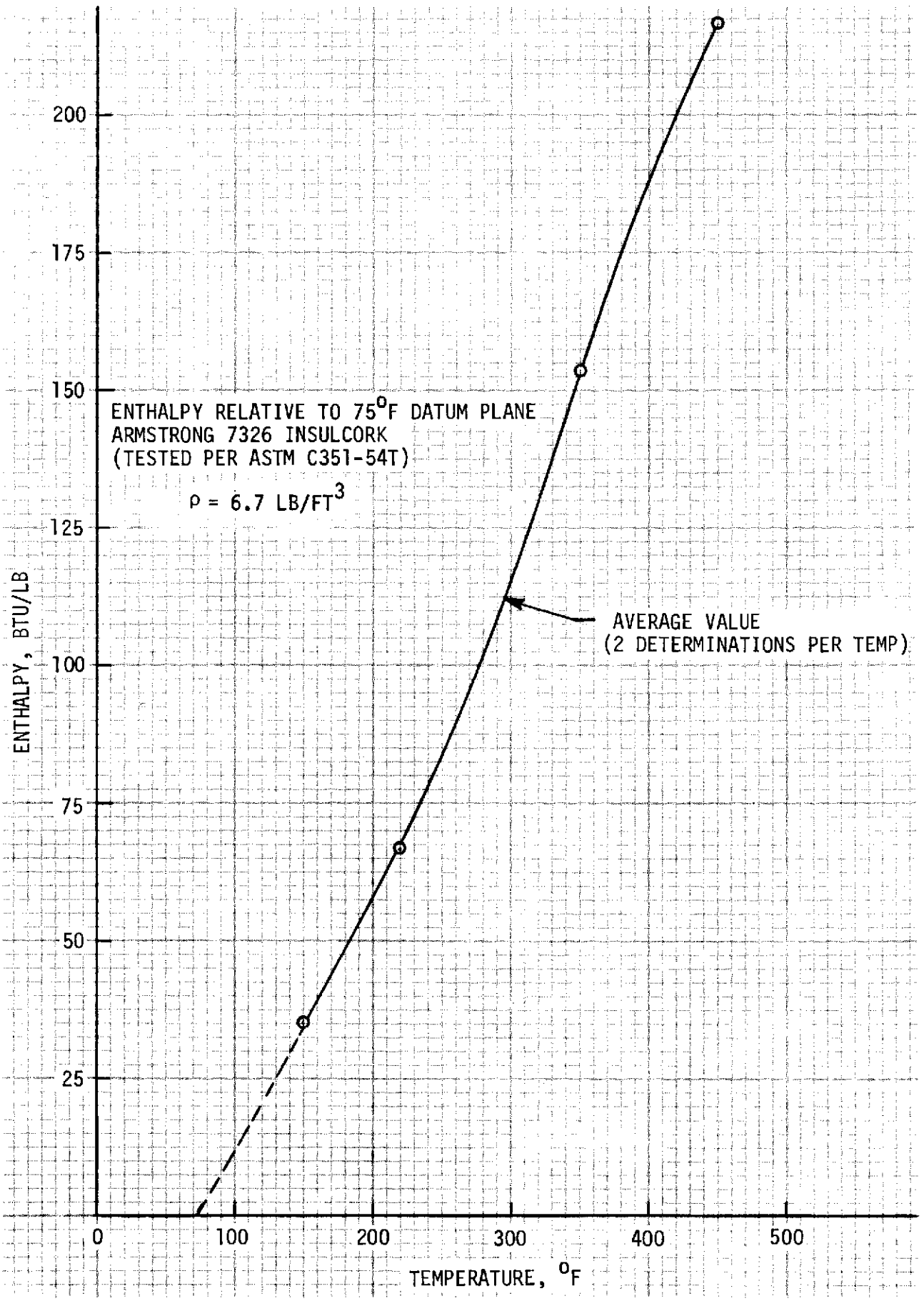

Figure 12.9.6-2. Enthalpy of Armstrong 7326 Insulcork Versus Temperature

13.0 RELIABILITY

13.1 INTRODUCTION

A reliability rating can be used in two ways. The first and most useful is a trade table comparison figure with a competing design. The second is as a probability of success number. The second usage should be considered as only an indication because differences in individual data and methodology can produce different numerical values. Thus the design tool of reliability will optimize hardware and provide confidence in fulfillment of requirements. The application of the reliability discipline and its tools to structural design problems such as insulation is difficult and requires a great deal of expertise. The reliability failure rate (λ) for passive components based on random failures is extremely low (for practical purposes, negligible), and therefore evaluations must utilize factor of safety, ultimate strength, expected loads, and design methodology to achieve a meaningful design reliability rating (number).

The various procedures used by reliability are phase-oriented. In the design phase the design reviews, failure mode effects analysis (FMEA), failure mode cause analysis (FMCA), and apportionment/prediction methods are applied to assure a high probability of success. In the manufacturing phase failure reporting and problem solution, acceptance test, and sampling statistics are used in conjunction with the Quality Control department to assure delivery of a reliable product and to eliminate any unforeseen design problems. In the operational phase field failure reporting and analysis with appropriate corrective action and statistical failure trend analysis assure the maintenance of the apportioned reliability and provide an accurate assessment of the product.

Application of reliability methodology to the preliminary insulation design begins with examination of the concept and separation into components. Historical data on these components are gathered. The proposed environment for the design is formulated and historical data, if any, are composed and adjusted for usefulness. An FMEA is performed in conjunction with the establishment of a reliability model. An apportionment to individual components or subsystems is made. The design is then evaluated by a tradeoff exercise and the final design is modeled (success logic diagram). The FMEA is updated and a prediction is made. At two or more significant milestones in the design development, a formal review is held to provide visibility and direction to the design process. Upon completion of the final design review, the reliability process is completed for the design phase.

13.2 DEFINITION OF TERMS AND PARAMETERS

Definitions of reliability terminology may be found in the North American Rockwell Space Systems publication 541-R 9-62, Definition of Reliability Terms. The more significant terms are as follows.

a. Apportionment - Assignment of a reliability requirement to subsystems and components in accordance with their complexity and other factors so that system reliability requirements will be achieved if each subsystem or component meets its requirement.

b. Assessment - The evaluation of a system from operational data to determine how well it meets the reliability goal.

c. Critical Part - A part whose failure to meet specified requirements would result in the product failing to serve the purpose for which it is intended.

d. Environment - The aggregate of all the conditions and influences which affect the operation of equipment and components (e.g., physical location and operating characteristics of surrounding equipment and components; temperature, humidity, and contamination of surrounding air; operational procedures; acceleration; shock and vibration; radiation; and method of utilization).

e. Failure - Inability of an item to meet its minimum specified performance.

f. Failure Mode - The physical description of the manner in which a failure occurs. Also, in an analysis of design reliability (FMEA), a description of the manner in which an equipment function may be affected by a failure.

g. Failure-Random - Failures whose occurrences in any given interval of time is unpredictable.

h. Failure Rate (λ) - The average number of failures occurring per unit time in a set time interval.

i. Mean Time Between Failure (MTBF) - The mean operating time of the equipment between independent (random) failures, the reciprocal of the failure rate for exponentially distributed times to failure.

j. Reliability - The probability of attaining a specified performance under specified considerations for a specified period of time.

13.3 INFORMATION SOURCES

Information sources can be divided into two categories: data and methodology. An excellent total coverage for reliability methodology is Reliability Engineering, ARINC Research Corporation, Prentice Hall 1965 - Second Edition. The designer will be more concerned with failure data sources. The primary failure data sources are:

a. Hughes - Hughes Aircraft has published failure rate data gathered from the SatCom Satellites built by Hughes. These data are available from the Reliability group and are the most up-to-date and accurate information available. These are usage data. The primary drawback is correlation with the usage component and the fact that the data are primarily electronic. This is the first preferred data source.

b. FARADA (Failure Rate Data Handbook), published by U.S. Naval Fleet Missile Systems Analysis and Evaluation Group, Corona, Calif. - This is a tri-service and NASA failure rate data program participated in by industry. Failure rates are determined from in-service usage and number of failures, operating hours, and sources are given. Both electronic and mechanical parts are covered. This source is excellent. The main problems are correlating the used component with one listed in FARADA and the age of the data. This is second in preferred data sources.

c. MIL Handbook 217A (Reliability Stress and Failure Rate Data), published by the Department of Defense, 1965 - This source provides both failure rate data and methodology. It is primarily an electronic parts failure rate source. This is the third source in preference for failure rate data.

d. NAVWEPS 00-65-502 (Handbook of Reliability Engineering), published by Bureau of Naval Weapons, 1964 - This document is primarily a methodology text and a very good one from an elementary viewpoint.

e. AVCO Martin Failure Rate Manual - This manual presents generic failure rates for all types of components. It also presents modifiers (k factors) and their application for various environmental influences. This is an excellent manual, its main drawback being that it was published in 1962 and has not been updated. This is the fourth preferred failure rate list.

Other sources of failure rates and reliability methodology exist and are available from Reliability group engineers. The sources listed are the most readily available and cover the field thoroughly.

13.4 PHYSICS OF FAILURE

As discussed in the introductory paragraph, the primary reliability approach for consideration of passive components is to examine the design safety factors of parameter and load distributions. A second and more detailed approach is the failure mode cause analysis (FMCA) which is discussed in Paragraph 13.6. The FMCA requires extensive knowledge and analysis of the physics of failure of the material in question and its detail design application.

The physics of failure knowledge of materials encompasses a wide range of phenomena, some examples of which are: (1) mode of failure under different types of stress (e.g., crack formation under tension, bond peel strength under transverse load, crush resistance under compression, all of the above under temperature, moisture, and all other applicable environmental conditions), (2) fastener techniques (bonding, inserts), susceptibility to sharp angles (internal), and (4) finishing and surface treatment.

All these areas require extensive knowledge by the designer of the material properties and application environment. His knowledge will be applied to the FMCA in conjunction with the reliability engineer and constitutes the physics of failure concept in the reliability design analysis.

13.5 STATISTICS AND PROBABILITY

Statistics and probability as applied to insulation design will involve almost exclusively the determination of the spread of the mechanical and thermal parameters of the concerned material and its expected environmental and use loads. The designer's problem is to formulate the use and application methodology of the material so that an adequate safety margin exists between the lower limit of the material parameters and the upper limit of the environmental and usage loading (Figure 13.5-1).

Upper and lower limits are defined by the 2- or 3-sigma (σ) points of the variable distribution curve. Sigma denotes the standard deviation of the variable value distribution. The standard deviation is, in turn, a measure of the spread, scatter, or dispersion of the distribution. Thus a 2σ limit will include 95.44 percent of the values and a 3σ limit will include 99.72 percent of the values (Figure 13.5-2). Sigma is calculated as the square root of the variance, thus:

$$\sigma = \left[\frac{1}{n} \sum_{i=1}^{n} \left(x_i - \bar{x}\right)^2\right]^{\frac{1}{2}}$$

where x_i is a measurement, $\bar{x}$ is the measurement mean, and n is the total number of measurements. This applies only for normally distributed data. Other types of data distribution can be handled by Reliability engineers.

13.6 FMEA'S AND FMCA'S

The FMEA and FMCA are two of the primary and most useful tools of reliability engineering. They both serve to enforce a detailed examination of the design and the interactions and interdependence of the component parts and the external and internal environments applicable to their use. FMEA and FMCA flow charts are presented in Figures 13.6-1 and 13.6-2. The FMEA task definitions and instructions are as follows:

a. Task 1. Item Identification - Items are identified to functional subsystem and identifiable assemblies within (e.g., valves, regulators, electrical modules, connecting tubes, wire harness, and motor mechanism). Part number and title are included. Note: A brief description of function within the system should be given. In this task, the subsystems and identifiable assemblies contained in each subsystem are listed as described in appropriate engineering documents. Entries are to be numbered 1.1, 1.2, 1.3, etc., consecutively.

b. Task 2. Failure Modes - Possible failure modes (e.g., short or open circuit, no output, out of tolerance, valve open or closed, external or internal leakage, regulator, or tank over or under pressure) are listed. Human events or functions which create hazardous conditions are included. The failure modes which are characteristic of the assembly under study for the subject phase should be listed. The detail ways in which the failure could occur should not be included because they are the concern of a lower-level failure cause analysis. Thus, the characteristic failure modes of a valve are: fail open, fail closed, rupture, external leakage, and internal leakage. The causes, such as external leakage due

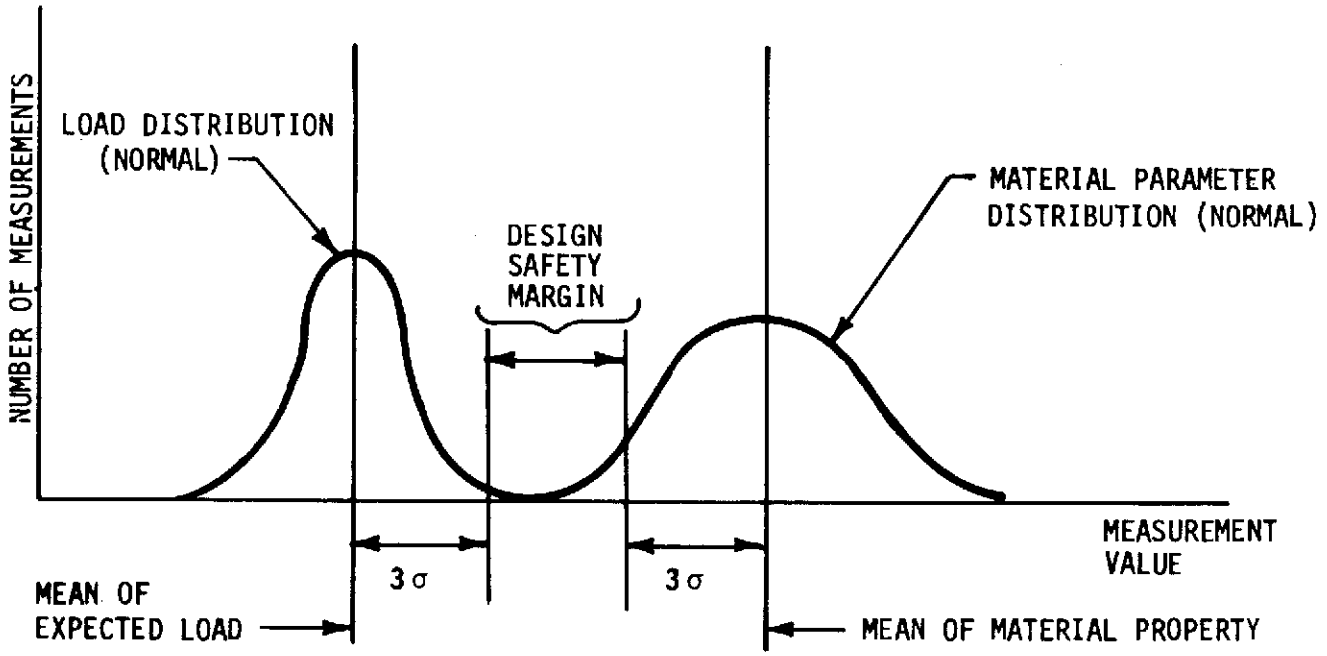

Figure 13.5-1. Design Safety Margin

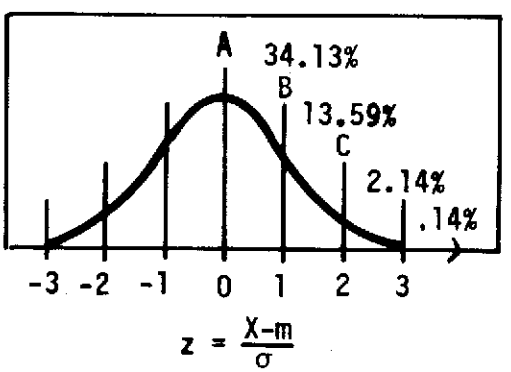

Figure 13.5-2. Percentage of the Population in Various Intervals of a Normal Distribution

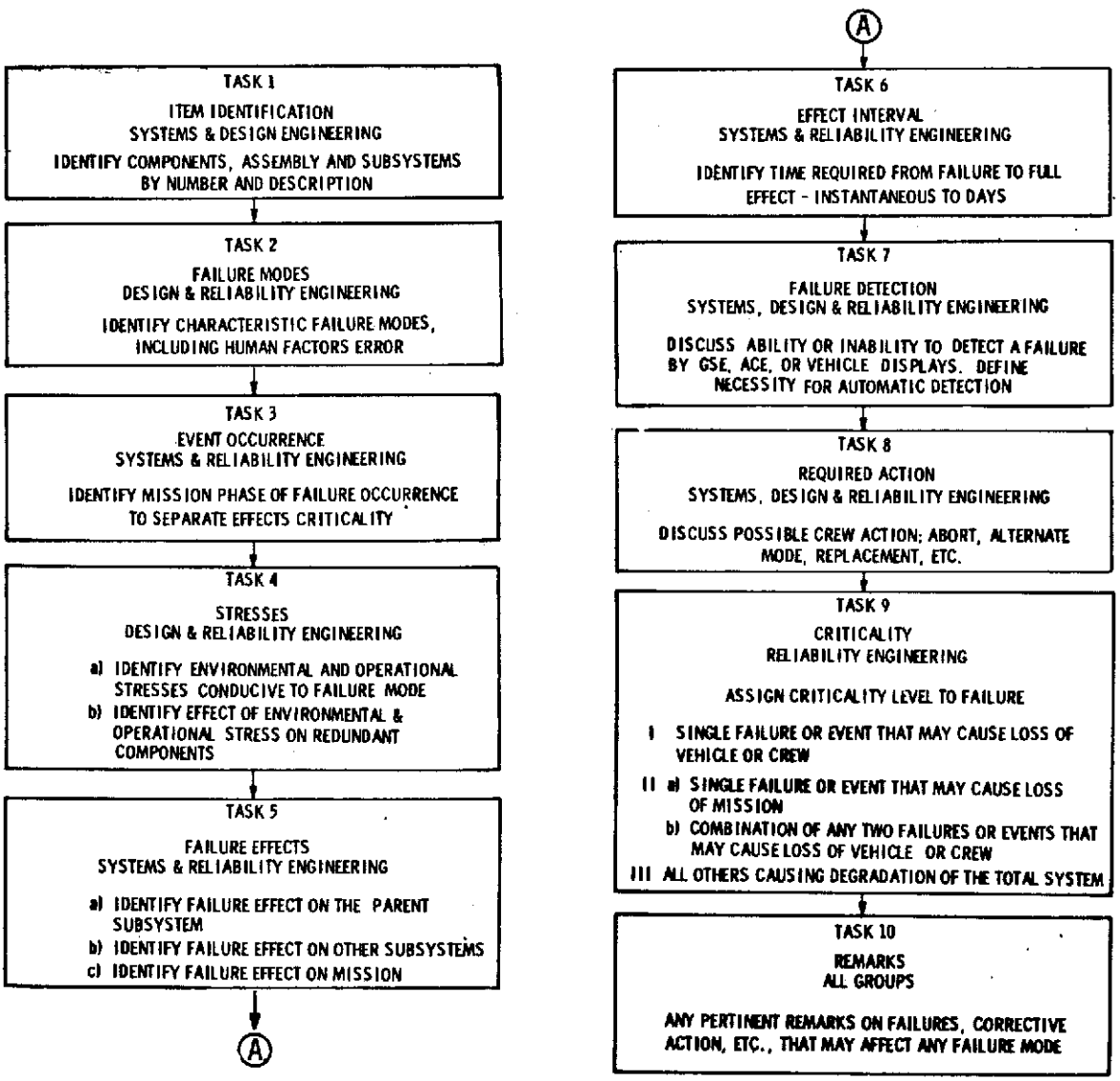

Figure 13.6-1. FMEA Task Flow Chart

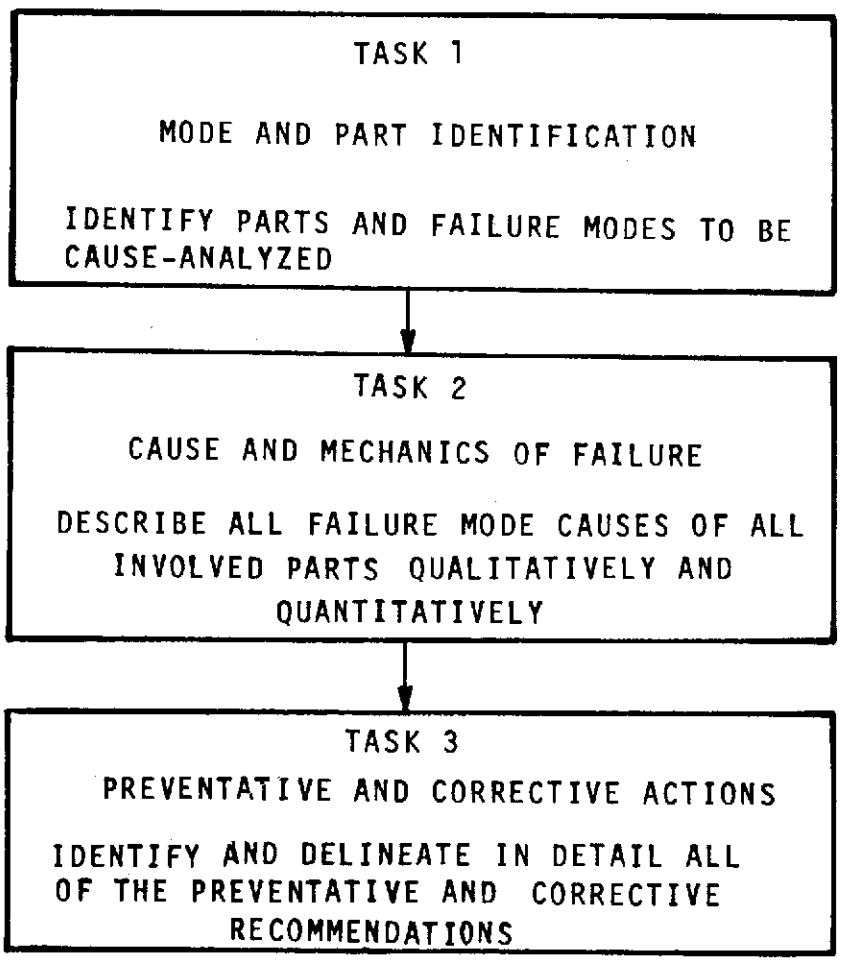

Figure 13.6-2. FMCA Task Flow Chart

to broken seal, cracked housing, porous casting, and scored stem, will be studied in cause analysis and are not to be listed here. Failure modes are to be numbered 2.1.1, 2.1.2, 2.2.1, etc., to coordinate with its item number from Task 1.

c. Task 3. Event Occurrence (Mission or Checkout Phase) - This task identifies the mission phase or phases during which the task failure mode can occur and have a pertinent effect in this or subsequent phases. The purpose in identifying phases is to separate the conditions under which a given failure mode could have different effects. Thus, the same failure during checkout and during the mission may in the former phase merely delay the launch and in the latter phase cause loss of the crew or mission (abort). A short description of the mission phases appears in this column. Reference to the engineering system documentation should be made. State the probability of the failure mode occurring in this phase. There should be an entry for each failure mode, numbered 3.1.1, 3.1.2, 3.2.1, etc.

d. Task 4. Stresses - Conducive to Failure (inherent weakness of the assembly): Some equipment items are more likely to fail under one stress condition than others. For example, a relay contact chatter failure mode is most likely to result from vibration or shock, while a bearing in a piece of rotating hardware is more likely to fail as a result of temperature. The conditions which are the most likely to cause the failure modes listed to occur are placed in this column. Reference to environmental criteria specification should be made. There should be an entry for each failure mode. Numbers are from 4A.1.1 to 4A.1.n.

Effect on Redundancy Within the System: In this task special attention should be given to the possibility that if the piece of equipment is susceptible to failure in a given environmental condition, the same environmental stress could cause both units of a redundant pair to fail simultaneously, negating any beneficial objectives of the redundancy. Include any notes and comments regarding the benefits or liabilities of redundancy in the circumstances involved. There should be an entry for each item number (4B.1.1 to 4B.1.n).

e. Task 5. Effects - Failure effects are listed for (a) system, (b) other systems, and (c) mission (describing in detail the ramifications and alternatives). Note: a, b, and c are listed separately. The effect of a failure on the system, other systems, and mission is described here. For example, a check valve can fail open, fail closed, leak externally, and leak internally (major failure modes). The effect of failing closed can be loss of some redundancy within a subsystem, and the effect of failing open or internal leak can be explosion and loss of the entire system. The effects of each item failure mode are numbered by task (5), item (1), failure mode (1), and effect on a, b, and c (i.e., 5.1.1a, 5.1.1b, 5.1.2a, etc.).

f. Task 6. Effect Interval - This task contains a notation of the time from failure occurrence to full effect in estimated time units. The information to be included should range from milliseconds for those failures having instantaneous effects to days for such items as slow leakage of expendables. The units to be employed are therefore milliseconds, minutes, hours, or days. Numbering is from 6.1.1.

g. Task 7. Failure Detection - The ability to detect the failure with ground support equipment or crew display (automatically or manually) is discussed. Included is the capability of checking redundant and nonoperating units during ground checkout. When a failure occurs, the total effect may take place in microseconds or develop over a comparatively long period. Providing that the crew, ground personnel, or automatic sensors can detect and identify the failure, corrective action may be possible to minimize, defer, or prevent the failure effects. Some failures may require an abort action resulting in loss of mission objectives but protecting the crew. Other failures may allow alternate modes of operation which allow achievement of primary mission objectives. It is important that the analysis identify the failure modes on which corrective action can be taken, indicate whether the failures are detectable and identifiable, and determine if sufficient time for human reaction is available or if automatic reaction is required. Primary required instrumentation also should be listed.

h. Task 8. Action (e.g., switch to alternate mode or abort - automatic or manual, etc.) - This task contains a notation of the possible crew action such as abort or switch to alternate modes to circumvent specific equipment failure modes. When human reaction times would be too slow for corrective action, an indication of the need for or presence of automatic reaction capability is noted. Numbering is 8.1.1 a, b, c, etc.

i. Task 9. Criticality (Example) - Criticality categories are:

I. A single failure or event which may cause loss of personnel or vehicle.

II. a. A single failure or event which may cause loss of mission.
b. A combination of any two failures or events which may cause loss of personnel or vehicle.

Note: Abort is mandatory after first unit failure.

III. All others.

This task defines the effect of the failure on the stated mission for the system being analyzed. The criticality categories are noted here in accordance with the definitions noted in the heading. Where appropriate, descriptive words such as "scrub," "hold," "none," may be listed in addition to the notation of Category III. There should be an entry for each item failure mode (9.1.1). Detailed criticality definition may differ from program to program.

j. Task 10. Remarks - Included here is action recommended to appropriate organizations with respect to each failure mode (e.g., design changes, inspection techniques, maintenance provisions, checkout capabilities, operational procedures, and quality control methods). Probability of occurrence of the failure modes is indicated as "low" for very remote failures and "high" for failures which are possible. A brief statement of justification for the probability of occurrence classification also should be included. This task is provided for brief narrative explanation of any additional information or clarification of former entries. Comments regarding the probability of the failure occurring are to be included in all cases. The reasons why the probability of occurrence is very remote or reasonably possible should be indicated. Among the information items which should be considered for inclusion in this task are the following:

1. Responsibilities of various functional groups pertinent to the prevention or evaluation of failure mode, such as quality control action, test program planning, maintainability or spares effects in logistics or procurement problems for purchasing action.

2. Recommendations where single-point failure mode elimination is impractical. An example is the pressure capsule of a submersible, the single failure of which could be catastrophic. A redundant capsule is impractical, so design efforts must take all steps to maximize the reliability of the capsule.

3. Recommendations for minor design changes such as the addition of redundant components or simplification of design by elimination of unnecessary complexity.

4. Discussion of the failure mode relative to its occurrence when the system is operating or non-operating. The capability of checking non-operating equipment during checkout is important.

5. Comments regarding the capability of independently checking the operation of redundant components during countdown and the mission. For redundancy to be effective, the knowledge that both units of a a redundant pair are functional is necessary.

6. Information regarding the interaction of failure modes among systems and interfaces or interrelationships among operational phases.

7. Comments pertinent to changes in operational procedures for more effective and reliable equipment operation.

FMCA task definitions and instructions are as follows:

a. Task 1. Mode and Part Identification - This task lists the failure mode (or modes) to be cause-analyzed. They are listed in the same manner as s they were identified in the referenced effects analysis. Hardware and software designations, part numbers, and specification numbers involved are also to be listed.

b. Task 2. Cause and Mechanics of Failure - All of the conceivable reasons for the possible occurrence of the subject failure mode are listed in this task. A particular failure mode may have one or several possible causes (e.g., failure of a valve to open might be due to a broken spring, open solenoid, dirt particles, differential thermal expansion, etc.). Most of these causes pertain to lower equipment level items. Causes will be pursued down to the lowest equipment level or process necessary. This section will be both quantitative and qualitative by listing both general conditions and specific values involved in the failure cause.

c. Task 3. Preventive and Corrective Action - Existing and recommended precautions established to preclude the failure mode from occurring or reduce the probability, reduce effect, etc., will be identified. Included are design features, manufacturing and inspection techniques, maintenance plans and acceptance test plans, quality assurance provisions, prelaunch check provisions, etc. Associated with each cause listed, at the effective equipment level, are the reasons why the cause should not occur, or action to be taken to prevent or eliminate the possibility. In general, the preventive action will be aimed at eliminating the failure mode, making it fail-safe, minimizing the effect, or minimizing the probability of occurrence. The corrective action will follow the program objectives. In addition, all other pertinent information should be included in this task. In all cases, the probability of the cause of failure occurrence should be indicated by discussing the reasons why it is considered possible or remote. Specific assignments should be indicated, such as special inspections or extra process controls to be imposed by the Quality Control department, special testing necessary, or preventive maintenance provisions by Logistics.

13.7 SUCCESS LOGIC

Success logic is the third primary tool of reliability engineering analysis. A complete success logic analysis results in a mathematical model for the reliability of the system, allows prediction and assessment values to be calculated, and provides the basis for redundancy and redesign recommendations. The analysis consists of defining all system functions required for mission success. The system is then broken down to a component part level; the more detailed the level, the more accurate will be the system model. All components required to operate for a particular function to succeed are then blocked out in series. Alternate success paths are defined (e.g., active parallel and standby redundancy or degraded mode operations). This step is performed for all functions and all mission phases. Operational time and failure rates assigned to individual components will define reliability.

Any hardware area that does not meet its reliability apportionment as defined by the success logic may then be redesigned or backed by an alternate path to achieve its goal. Success logic analysis is performed by the reliability engineer in close conjunction with the design engineer.

13.8 PROCEDURES (Figure 13.8-1)

Upon receiving design requirements and specifications, the designer should contact the responsible reliability engineer. The reliability engineer will establish failure criteria and criticality definitions for the program and provide a reliability goal (number) where appropriate. Redundancy requirements such as fail operational--fail safe (FO/FS) also will be established.

A preliminary system (design) model will be established by the reliability engineer in conjunction with the designer.

An apportionment based on this preliminary model will be made by the reliability engineer and furnished as a guide to the design engineer.

A preliminary success logic diagram will be constructed by the reliability engineer as the design is developed. This will provide suggestions as to redundancy requirements and component improvement.

The reliability engineer will perform an FMEA in conjunction with the designer. A criticality list and single-point failure list will result. Evaluation of FMEA results may lead to requirements for one or more FMCA's. These will be performed by the designer in conjunction with the reliability engineer and any consultants deemed necessary.

A test program will be formulated by reliability, design, and quality control to assure that the design fulfills its operational and environmental requirements. Acceptance and production test procedures and sample sizes will be stated.

Depending upon the extent of the program, reliability will establish a production and field operational failure reporting system (Figure 13.8-2). The designer will assist reliability in the solutions and corrective actions associated with production and field failures.

13.9 NUMBERS, CONFIDENCE, TESTS

The reliability number, goal, or prediction is an estimate of the success probability of the design. There are a number of basic assumptions involved in the calculation of the reliability number that must be examined for validity in each application. The primary assumption is that the components being described are beyond the infant mortality point and have not yet reached the wearout stage (i.e., the failure rate is constant). A second major assumption is that only random or chance failures are involved. All components are operated within their (internal and external) stress levels. There is no time-dependent component degradation in the operational period under consideration.

Other cases may be treated but are highly theoretical and quite uncommon.

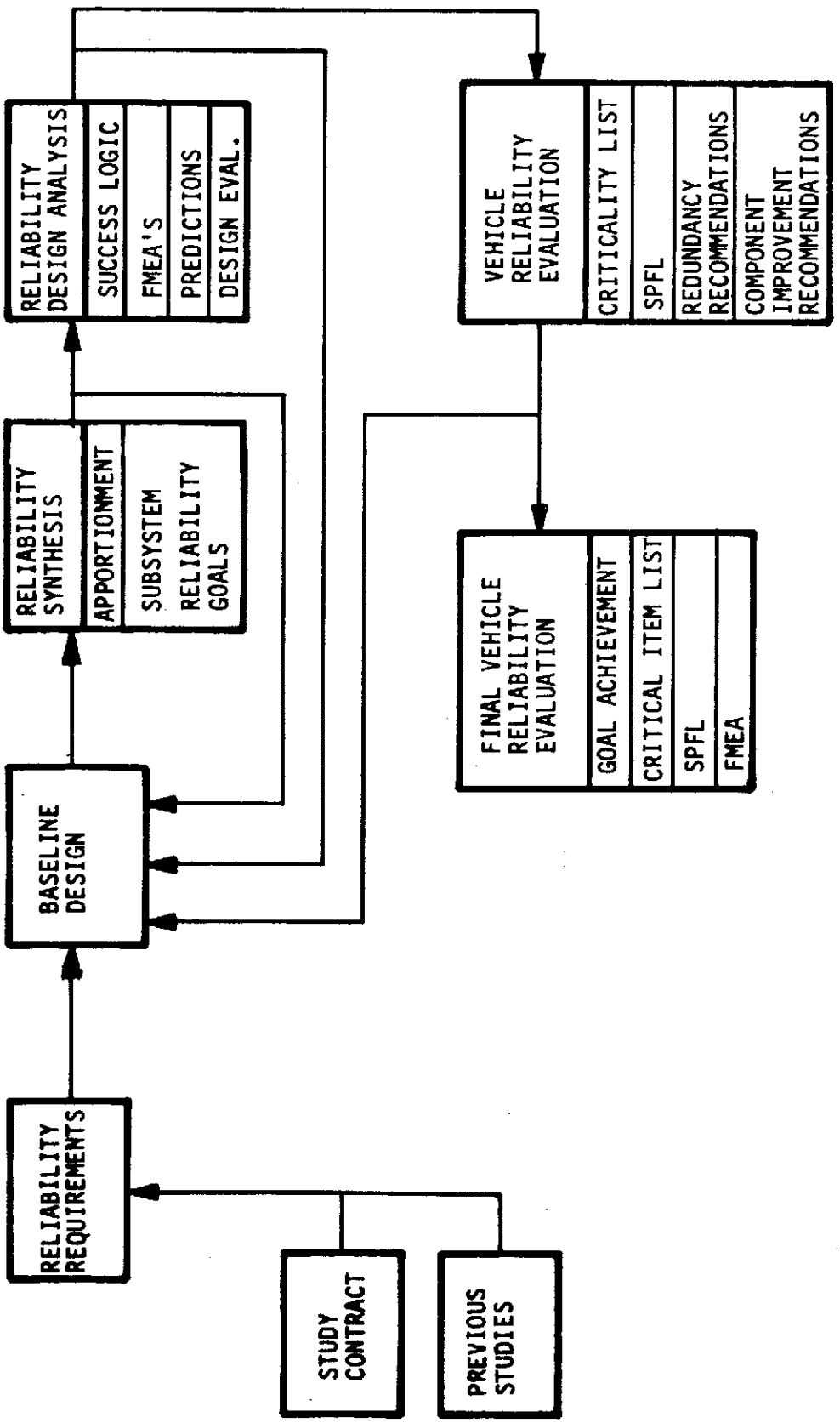

Figure 13.8-1. Reliability Development Study

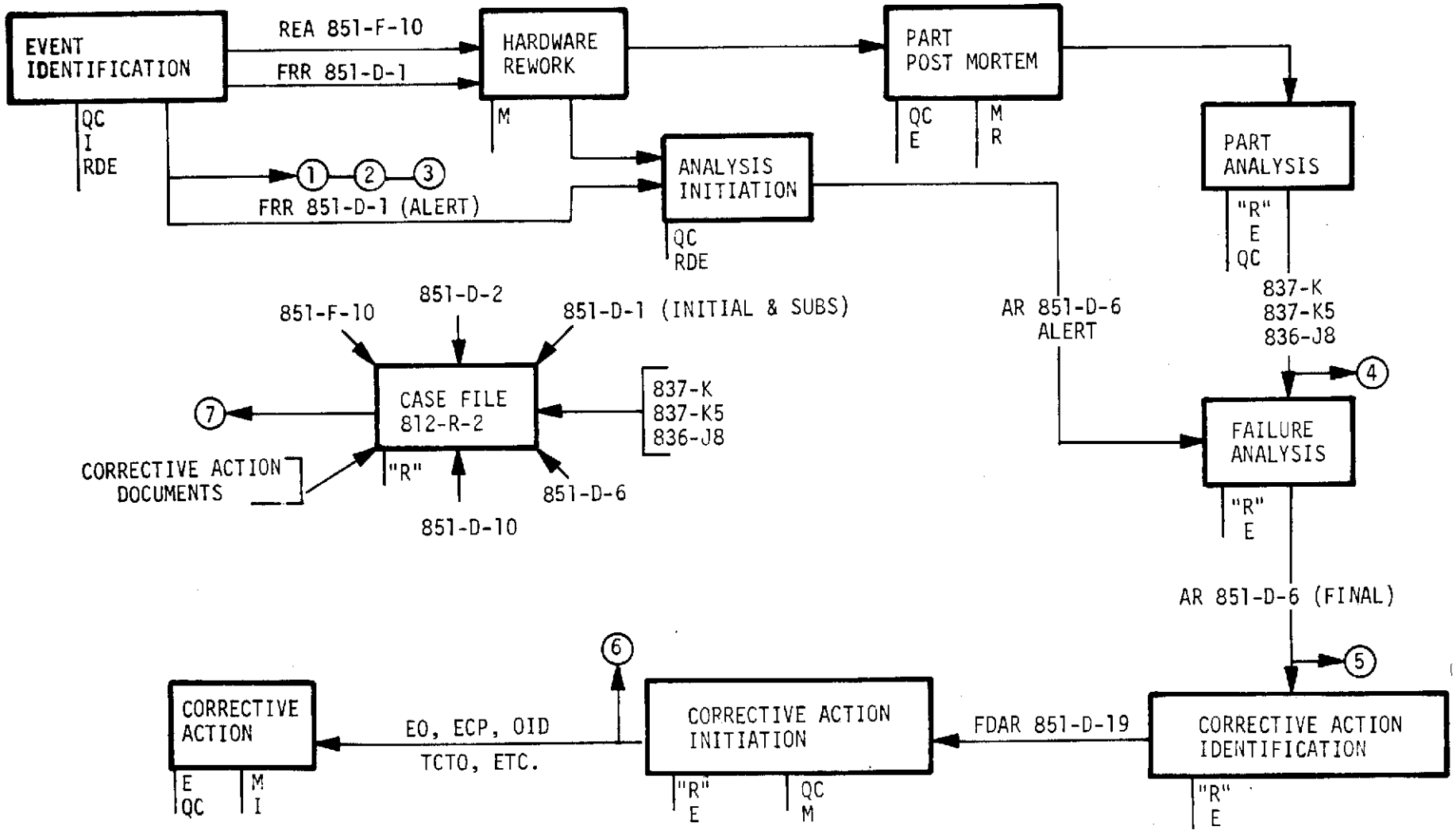

1 INPUT TO THE CONFIGURATION ACCOUNTING SYSTEM
2 INPUT TO THE OPERATIONAL REPORTING SYSTEM
3 INPUT TO THE REMOVAL RATE MEASUREMENT SYSTEM
4 INPUT TO THE PARTS MANAGEMENT SYSTEM
5 INPUT TO THE FAILURE RATE MEASUREMENT SYSTEM
6 INPUT TO THE FAILURE RECURRENCE MONITORING SYSTEM
7 INPUT TO THE "R" DATA AUDITING SYSTEM

R = RELIABILITY
RDE = RELIABILITY DISPOSITION ENGINEER
E = ENGINEERING
QC = QUALITY CONTROL
I = INSPECTION
M = MANUFACTURING

Figure 13.8-2. Reliability - Quality Control Problem Surveillance and Correction

The confidence levels imposed upon a reliability number are a measure of its usefulness, a type of numerical tolerance. As an example, a one-sided 90 percent confidence level on a 0.95 reliability number implies that 90 percent of the time the reliability will be 0.95 or better. Statistically, confidence is a relative measure of the correctness of an estimated number. The confidence may be increased by increasing test time and/or sample size.

Reliability testing (life, overstress, environmental, etc.) is performed to provide detailed knowledge of the properties and physical limits of the component under consideration. In addition, all accumulated test and use time, when adjusted for the particular situation, may be used to increase confidence values.

Hardware testing is divided into various purposes and phases (i.e., development, acceptance, production, etc., and component, black box, system, etc.). Each type of test must be designed by the design engineer, reliability engineer, quality engineer, and production engineer to produce specific knowledge about specific parameters under specific conditions. Thus, coordination between the designer and reliability engineer is mandatory for maximum use of test time and results.

13.10 APPORTIONMENT, PREDICTION, ASSESSMENT

The three techniques of apportionment, prediction, and assessment are used to assign a quantitative value to system reliability. The apportionment technique requires knowledge of the overall mission and system success requirements (reliability responsibility) and the system design concept (design engineer responsibility) to as detailed a level as possible. The reliability and design engineers then divide the design into its major subsystems. Various weighting factors (numerical value) can then be assigned to each subsystem. Weighting factors include complexity, function importance, and checkout complexity. The weighting factor, mission time, and success goal are then manipulated to provide a realistic reliability goal for each subsystem so that the mission success probability will be achieved if each subsystem goal is met. This goal then becomes part of the designer's requirements specification.

The reliability prediction is based upon the success logic diagram and is essentially a reliability mathematical model of the system. The success logic is based upon the actual system design and the correctness of the model is the responsibility of both the reliability and design engineers. Primary responsibility is with reliability. The completed model will show all subsystem components in their correct relationship to provide a success path for the subsystem functions. Assignment of operating time/cycles and failure rates to the components in the model, and the mathematical relationships of the model representing series, parallel, standby, and degraded operation will produce an overall reliability number. This number's relation to the subsystem goal (over, equal, under) will indicate the requirement for more redundancy, component improvement, redesign, satisfactory design, or possible reduction in complexity if the prediction exceeds the goal. Thus, the prediction is also a design tool and provides insight as well as quantitative value.

The assessment of the design is based upon actual field operational time and field failure data. Failure reporting provides visibility as to what components and subsystems are failing and the failure modes. The comparison of field data and the model prediction provides quantitative evaluation as to the correctness of the model and the field performance of the system.

13.11 MISCELLANEOUS

The reliability engineer is available to the designer at all times to provide consultation as to selection of components, design approaches, vendor selection, redundancy, and redundancy type recommendations. The unique background and data available to reliability provides a wide visibility in practically all engineering disciplines and the designer should be aggressive in availing himself of the design knowledge of the reliability group.

14.0 SYSTEM SAFETY

System safety considerations include the prevention of injury to employees or loss or damage to the insulation during the fabrication, installation, and use of insulation systems. Safety standards used during the S-II program are detailed in the four-volume set, Space Division Safety Standards, Publication 543-G-35, -36, -37, and -38. Additional details on hazards associated with solvents and chemicals are contained in Specification MA0117-001, Handling of Dangerous and Flammable Liquids and Chemicals.

Items that should be emphasized have been extracted from these documents and are presented in this section.

14.1 FABRICATION

Good industrial practice will minimize the chance of injury to personnel while fabricating the component parts of these insulation systems. The tools and equipment used can be rendered safe by designing the facility in accordance with Industrial Safety Design Standards (Publication 543-G-35). Equipment should be operated in accordance with Industrial Safety Operations Standards (Publication 543-G-36).

14.1.1 Ventilation

Flammable solvents (e.g., methyl ethyl ketone) and toxic chemicals (e.g., isocyanate) are used in the fabrication of insulation systems. A ventilation system should be designed and used to reduce the concentration of flammable materials below the explosive limit or the concentration of toxic chemicals below the maximum allowable concentration, whichever requires the greater volume of ventilating air.

Spray-foam dust, although considered physiologically inert, may cause difficulty if inhaled in concentrations greater than 50 million particles per cubic foot. This factor may be the key factor in design of the ventilation air.

Polyurethane dust is explosive at concentrations of 0.025 ounce per cubic foot or greater. This factor may size the capacity of the ventilation system if it is governing in those areas where foam is machined or sanded.

Dust collecting systems, or any spark or ignition source that may be exposed to concentrations of dust exceeding 0.015 ounce per cubic foot, must comply with the National Electric Code for Class II, Division I, environments.

14.1.2 Training and Certification

Most, if not all, of the components of these insulation systems require manual operations and the personnel who perform them must be properly trained.

Training should include the use of the actual equipment and supplies to be used in producing the final part. It should include a thorough orientation in the hazards involved with the chemicals and tools and the protective equipment that must be used to counter these hazards. When the employee has demonstrated his ability to perform these operations satisfactorily he should be given a certification of this fact. This certification should be presented before performing these operations on a deliverable article. The employee should be re-certified periodically, or when a change is made in the processes.

14.1.3 Protective Clothing and Equipment

Personal protective equipment will be regarded as secondary protection to be used only when personnel hazards cannot be designed out of the system. For example, it is more desirable to provide an adequate dust collection system than to require that individuals wear breathing masks. In some cases, however, the hazard cannot be designed away. An example would be the requirement to wear clean nylon gloves while performing most of these insulation processes. Not only is the skin protected from caustic or toxic materials, but insulation components are also protected from contamination by fingerprints.

Airline masks are required when spraying polyurethane foams. Primer systems that contain amines also require airline masks. Coverall, gloves, and shoe covers are recommended to prevent skin exposure when applying primers, foam, or strippers. Eye protection is required when working with liquid chemicals.

14.1.4 Parts Protection During Handling and Storage

Completed or partially completed insulation details must be protected from contamination and damage during handling, transportation, and storage.

14.1.5 Compressed Air-Driven Tools

Air-drive tools should be used in preference to electrically powered motors to eliminate sparking and arcing in the fabrication of insulation components.

The compressed air source should be maintained at a pressure of less than 150 psig. The air supply should be free of oil, water, or other contaminants.

If quick-disconnects are used on air hoses they should be of the self-sealing type to prevent whipping of the hose when it is disconnected. If quick-disconnects are not used the pressure should be vented from the hose before disconnecting.

Air hoses and fittings should be examined daily and replaced when damaged or worn.

14.1.6 Housekeeping

The dust and debris generated in the fabrication of insulation components must be continuously removed from the work area. The dust will be vacuumed from in-process components and work surfaces. Excess foam and honeycomb that result from fabrication will be bagged as they are generated and periodically removed from the work area.

14.1.7 Hazard Analysis

All supervisors involved in fabricating insulation components should conduct a hazard analysis of the operations for which they are responsible. This analysis should be conducted before the start of fabrication or when changes are made in techniques or materials. A detailed analysis should be conducted of each step in the fabrication process to verify that the risk of injury to personnel or damage to hardware has been minimized.

14.1.8 Fire Protection

If supervision or Protective Services judge the risk of fire to be high during any operation, a fireman must be present during that operation.

14.1.9 Electrical Equipment

All electrical equipment used in fabricating insulation systems must comply with California Electrical Code for Class II, Division I, environments.

14.2 INSTALLATION

The safety considerations listed in the previous section also apply to the installation of insulation. Because of the nature of the installation process, however, some points should be emphasized.

14.2.1 Training and Certification

Generally speaking, the mechanics who install insulation components will be required to process a greater variety of components, using a greater variety of techniques, than the mechanics who fabricate these components. Installation mechanics, then, should receive different training than fabrication mechanics. The requirements for certification of the required skills still apply, however.

14.2.2 In-Process Inspection

Each step in a sequence of installation operations should be verified to be completed in accordance with the applicable drawings and specifications before proceeding to the next step.

14.2.3 Damage to Insulation

Because insulation is more fragile than other structural components, extra care must be taken while installing insulation components.

14.3 OPERATION

Many of the hazards associated with insulation systems cannot be eliminated in the design phase. The continued successful operation of insulation systems is dependent on the manner in which it is operated.

14.3.1 Proof-Testing

Purged insulation systems should be proof-tested with a compatible gas after installation to 125 percent of the maximum pressure it will see in service.

14.3.2 Contamination of Interior Surfaces

Before the introduction of purge gases into insulation systems it should be verified that no contamination will be introduced with the gas. Contaminating solids or gases in the helium purge gas used in honeycomb systems could block the flow passages and other gases will condense and solidify at LH_2 temperatures. The solidified gases would gas off when the insulation warmed up and provide a local, unplanned pressurization source which could damage the insulation.

Moisture or other corrosion initiators introduced into vacuum-jacketed lines could lead to loss of vacuum. Once corrosion is initiated within the annulus it is difficult or impossible to verify the condition of the line.

Contamination of the purge gase with a minimum of 2 percent oxygen could combine with leaking hydrogen and lead to a combustible reaction when an initiation source was present.

14.3.3 Purge Gas Pressure

The gas pressure of purged systems should have relief valves or other protective devices installed to insure that the maximum allowable pressure is not exceeded.

Critical areas of pressurization control are tank surfaces that could be damaged by negative pressure (e.g., the forward bulkhead of the LH_2 tank with honeycomb installation). If the outer facing sheet on the forward bulkhead is pressure-tight but the tank wall bond has failed the

tank will be subject to the applied gas pressure. If this pressure is 0.5 psi greater than the tank pressure, the forward bulkhead could be buckled by the difference. Before pressurizing the forward bulkhead the tank wall bond must be verified to be sound or the tank pressure verified to be greater than that to be applied in the insulation. The purge gas should then be introduced into the tank. The insulation should have a positive pressure that will prevent the backflow of air and condensable gases through minute cracks or openings that are otherwise acceptable. The flow rate of the purge gas must be of such a quantity that it will not contract and develop negative pressure in the insulation when the purge is chilled to cryogenic temperature.

14.3.4 Chilldown

The chilldown rate and propellant fill rate of the tank should be controlled carefully to prevent the contraction of the tank wall from introducing stresses at the insulation bond line that will separate the insulation from the tank wall.

14.3.5 Inspection After Cryogenic Exposure

After each cryogenic exposure the insulation should be inspected for damage. Damaged areas should be repaired and tested before another cryogenic exposure.

14.3.6 Damage to Insulation

The applied insulation is relatively fragile and easily damaged by impact. Care should be exercised when working in the vicinity of insulation. When the surface is penetrated insulation efficiency is reduced and weathering is accelerated. If the penetration is deep enough to approach the tank wall on foam system, cryopumping will lift "divots" of the foam on cryogenic exposure. When the exterior of honeycomb insulation is struck by heavy objects the facing sheet can be delaminated. When the honeycomb is pressurized by purge gas further delamination could occur by the "zipper" effect and lead to loss of large areas of the facing sheet.

Positive protection must be given to the insulation when work is going on in adjacent areas. Tools or other heavy objects that could be dropped or kicked from above and strike the insulation should be restrained to prevent their impact on insulation surfaces.

14.3.7 Restraint of Bellows

The bellows of vacuum-jacketed lines can be damaged by over-extension if the ends of the line are not restrained when the line is pressurized. Care should be exercised to prevent external damage from objects falling on or striking against them.

14.4 DESIGN CHECKLIST

A safety design checklist is used to assure that potential hazards are uncovered and that proper safety procedures are taken. Typical checklist questions are:

1. Have the requirements for the insulation system been precisely defined?
2. Has a study been conducted to determine all the different systems that will satisfy the requirements?
3. Was a trade study conducted on the candidate systems?
4. Did the trade study include safety considerations?
5. Did the trade study include producibility considerations?
6. Did the trade study include overall cost considerations?
7. Was adequate experimental data available for all candidate systems?
8. Has the chosen system been adequately developed to begin production?
9. Has a hazard analysis been conducted on the chosen system?
10. Has each hazard identified been designed out of the system to the maximum extent possible?
11. Has each step in the fabrication process been specified?
12. Is each step in the production process verifiable?
13. Are special skills or equipment required in the production process?
14. Are these skills available?
15. Has a method been established to keep special skills current?

16. Does a method exist to verify that the mechanic has the required, current, skills?

17. Has Industrial Safety reviewed the facility plans where the system will be produced?

18. Have periodic safety inspections of the facility been scheduled?

19. Will the facility ventilation system reduce toxic byproducts below the maximum allowable concentration?

20. Will the facility ventilation system reduce explosive vapors below the lower explosive limit?

21. Will the facility ventilation system reduce flammable dust below the lower explosive limit?

22. Can explosive dust or vapors accumulate to hazardous concentrations within the ventilation system?

23. Has all electrical equipment been specified in accordance with California Safety Orders or National Electrical Code?

24. Have adequate safeguards been taken to reduce the risk of contamination of insulation surfaces?

25. Will any part of the insulation system corrode the substrate throughout its life cycle?

26. Is the necessary protective clothing and equipment available to protect operating personnel?

27. Does a means exist to insure that personnel wear protective clothing when needed?

28. Have individual parts-protection containers been provided for transport and handling of high value parts?

29. Do means exist to insure that all other parts of insulation systems will not be damaged while handling or transporting?

30. Has the moisture and oil content of shop air for air tools been specified at an acceptable level?

31. Do means exist to insure that oil and water content of shop air remain at an acceptable level?

32. Have operating personnel been trained to avoid the hazards of using compressed air?

33. Does a means exist to insure that dust and debris will not accumulate in the work area to contaminate the insulation surfaces?

34. Has the insulation system been designed so that damage to adjacent surfaces will be minimized during installation or repair?

35. Has a proof-pressure test been specified for the installed, purged insulation systems?

36. Have repair techniques been specified for all areas of the insulation system?

37. Has the allowable contamination level of purge gases been specified?

38. Do adequate means exist to insure that interior surfaces of insulation systems do not become contaminated?

39. Is it possible to inspect the interior of insulation systems for degradation?

40. Have suitable pressure relief valves been designed into purge gas systems to prevent overpressurization?

41. Has the chilldown rate or time been specified?

42. Has the possibility of negative pressure in purged insulation systems been eliminated?

43. Have tests and checkout procedures been reviewed by Engineering to verify that systems are properly utilized?

44. Are bellows restrained when pressurized?

15.0 TEST METHODS

All laboratory test reports pertaining to the insulation designs identified in Section 6.0 were identified and retrieved from the laboratory files. The various test methods used were identified and data in support of Sections 10.0, 12.0, and 15.0 were extracted from the lab reports. Since there were more data available than could be included in this report a computer program was set up to enable efficient retrieval of test data. Lab report numbers may be retrieved from the computer by any of the following parameters:

a. Application class/chemical class (e.g., foam, pour/polyurethane); see Table 15.0-1.

b. NR material specification number (e.g., MB0130-069); see Table 15.0-2.

c. Commercial Designation (e.g., CPR-348); see Table 15.0-3.

After the computer identifies the lab report number, the report may be obtained from the laboratory files. The computer also will identify all ASTM or other standard tests which were reported in each lab memo.

15.1 DEFINITIONS

15.1.1 Engineering Tests

15.1.1.1 Development Tests

Engineering development tests are conducted on initial preprototype materials, components, partial subsystems, and subsystems to determine if the selected designs are capable of satisfying engineering requirements and environmental conditions. These tests should verify all requirements necessary to produce a complete set of engineering drawings describing this insulation system.

15.1.1.2 Verification Tests

Verification tests are conducted on prototype insulation components and systems that are in a finalized design and pre-production configuration to determine if they will satisfy design requirements and environmental conditions.

15.1.1.3 Qualification Tests

Qualification tests are conducted to demonstrate the ability of engineering test parts and materials to perform specified functions within specified limits, under operating conditions of maximum adversity as established in applicable procurement, material, and process specifications.

Table 15.0-1. Sample Computer Print Out Lab Memo Index by Application Class and Chemical Class

INSULATION COMMONALITY ASSESSMENT STUDY

APPLICATION CLASS FOAM, POUR TA-48
CHEMICAL CLASS POLYURETHANE

NO AMER SPEC NUMBER	COMMERCIAL DESIGNATION # / COMMERCIAL COMP. NAME	TEST TYPE / TEST NO	LAB REPORT NUMBER	DATA BANK I.D.
MB0130-069	CPR-348 CPR UPJOHN CO.		431-6025	
MB0130-069	CPR-348 CPR UPJOHN	FLAMMABILITY ASTM D-1692	SPA-7-65-9	
MB0130-069	CPR-348 CPR UPJOHN	ABSORPTION H2O ASTM D-2127	SPA-7-65-9	
MB0130-069	CPR-348 CPR UPJOHN	TGA	4896-9025	
MB0130-069	CPR-348 CPR UPJOHN	SHEAR STRESS ASTM C-273	SPA-7-65-9	
MB0130-069	CPR-348 CPR UPJOHN	DENSITY ASTM D-1622	SPA-7-65-9	
MB0130-069	CPR-348 CPR UPJOHN	TENSILE STRESS ASTM D-1623	SPA-7-65-9	
MB0130-069	CPR-348 CPR UPJOHN	COMP. STRESS ASTM D-1621	SPA-7-65-9	
MB0130-069	CPR-348 CPR UPJOHN	NITROGEN CONTENT	4896-9025	
MB0130-069	CPR-348 CPR UPJOHN CO.		SPA-10-65-9	

Table 15.0-2. Sample Computer Print Out Lab Memo Index by North American Rockwell Specification Number

INSULATION COMMONALITY ASSESSMENT STUDY
TA-48

NR SPEC. NO. MB0130-069

APPLICATION CLASS / CHEMICAL CLASS	COMMERCIAL DESIGNATION & COMMERCIAL COMP. NAME	TEST TYPE / TEST NO	LAB REPORT NUMBER	DATA BANK LOC.
FOAM, POUR POLYURETHANE	CPR-348		411-0324	
FOAM, POUR POLYURETHANE	CPR-348		411-0003	
FOAM, POUR POLYURETHANE	CPR-348		SPA-10-65-9	
FOAM, POUR POLYURETHANE	CPR-348	DENSITY ASTM D-1622	SPA-7-65-9	
FOAM, POUR POLYURETHANE	CPR-348	THERMAL COND. ASTM C-177	SPA-7-65-9	
FOAM, POUR POLYURETHANE	CPR-348	SHEAR STRESS ASTM C-273	SPA-7-65-9	
FOAM, POUR POLYURETHANE	CPR-348	TENSILE STRESS ASTM D-1623	SPA-7-65-9	
FOAM, POUR POLYURETHANE	CPR-348	COMP. STRESS ASTM D-1621	SPA-7-65-9	
FOAM, POUR POLYURETHANE	CPR-348	COEF. THERM. EXPA. ASTM C-337	SPA-7-65-9	
FOAM, POUR POLYURETHANE	CPR-348	FLAMMABILITY ASTM D-1692	SPA-7-65-9	

Table 15.0-3. Sample Computer Print Out Lab Memo Index by Commercial Designation

INSULATION COMMUNALITY
ASSESSMENT STUDY
TA-48

COMMERCIAL DESIG. # CPR-348

APPLICATION CLASS CHEMICAL CLASS COMMERCIAL NAME	TEST TYPE TEST NO	LAB REPORT NUMBER	DATA BANK I.D.
FOAM, POUR POLYURETHANE CPR UPJOHN	COEF. THERM. EXPA. ASTM C-337	SPA-7-65-9	
FOAM, POUR POLYURETHANE CPR UPJOHN	COMP. STRESS ASTM D-1621	SPA-7-65-9	
FOAM, POUR POLYURETHANE CPR UPJOHN	DENSITY ASTM D-1622	SPA-7-65-9	
FOAM, POUR POLYURETHANE CPR UPJOHN	TENSILE STRESS ASTM D-1623	SPA-7-65-9	
FOAM, POUR POLYURETHANE CPR UPJOHN	SHEAR STRESS ASTM C-273	SPA-7-65-9	
FOAM, POUR POLYURETHANE CPR UPJOHN	NCO/OH RATIO	4896-9025	
FOAM, POUR POLYURETHANE CPR UPJOHN	NITROGEN CONTENT	4896-9025	

15.1.1.4 Material Property Tests

Material property tests are conducted to determine specific material characteristics and suitability of materials for standard use on spacecraft.

15.1.2 Quality Assurance Tests

15.1.2.1 Process Verification Tests

These tests are performed on test coupons fabricated by production personnel simultaneously with the production hardware the coupons represent. The correlation of the test coupon to the production hardware will vary from one application to the next, relative to design complexity. For example, a set of lap shear test coupons, when successfully tested, will provide confidence in surface preparation, adhesive mix, and the cure parameters of time, temperature, and pressure. However, if the lap shear coupons (metal) represent a non-metallic bond, the correlation to surface preparation is lacking. It must be accepted that process verification test coupons provide only partial assurance in the quality of the end product. Other aspects of quality assurance are established in Section 15.3.

15.1.2.2 Quality Verification Tests

These tests are performed on the completed production hardware and are intended to verify hardware conformance to design requirements. The test may be a complete system test, as in the case of the basic insulation proof pressure test. More often the application of this testing technique involves random sampling based on statistical analysis such as PQV testing of spray-on foam.

15.2 TEST DESCRIPTIONS

15.2.1 Test/Usage Matrix

Table 15.2.1-1 is a matrix which identifies the predominate usage of the various types of tests.

15.2.2 Test Methods

This subsection presents detailed descriptions of each of the tests identified in Table 15.2.1-1.

Table 15.2.1-1. Test/Usage Matrix

15.2.2.X Paragraph Number	ASTM No.	Title	Engineering Tests				QA Tests	
			A	B	C	D	E	F
1.	C177	Thermal Conductivity		x		x		
2.	C271	Density of Core Material				x		
3.	C273	Block Shear				x		
4.	C297	Flatwise Tension				x	x	
5.	C351	Specific Heat				x		
6.	C363	Delamination of Honeycomb				x		
7.	C364	Edgewise Compression				x		
8.	C365	Flatwise Compression				x		
9.	C393	Flexure/Sandwich				x		
10.	C480	Flexure/Sandwich/Creep				x		
11		Permeability Testing of Insulation Systems				x		
12.	D732	Shear/Laminate				x		
13.	D790	Flexure/Laminate				x		
14.	D897	Tensile/Adhesive				x		
15.	D903	180° Peel/Adhesive				x		
16.	D952	Bond Strength				x	x	
17.	D953	Bearing Shear/Laminate				x		
18.	D1002	Lap Shear/Adhesive				x	x	
19.	D1433	Flammability				x		
20.	D1622	Apparent Density				x	x	
21	D1638	Water Content of Urethane Foam Raw Materials				x		
22.	D1638	Amine Equivalent and Hydroxyl Number				x	x	
23.	D1653	Moisture Vapor Permeability				x		
24.	D1692	Flammability				x	x	
25.	D1781	Honeycomb Peel				x	x	
26.	D1876	T Peel/Adhesive				x	x	
27.	D1940	Porosity of Rigid Cellular Plastics				x	x	
28.	D2127	Water Absorption				x		
29.	D2344	Horizontal Shear				x		
30.	D2345	Inner Laminar Shear				x		
31.		Tensile Monostrain Torsional Shear (M&P 3330-001)				x		

Legend
A = Development B = Verification C = Qualification D = Material Property E = Process Verification F = Quality Verification

Table 15.2.1-1. Test/Usage Matrix (Cont)

15.2.2.X Paragraph Number	ASTM No.	Title	Engineering Tests A	B	C	D	QA Tests E	F
32.		Accelerated Weathering (FED #141)				x		
33.		30x30 Cryogenic Tank and Environment	x	x	x			
34.		Percent Freon in Foam (MB0130-077)				x		
35.		Conductivity by Round Guarded Tank at LH_2 Temperature	x	x				
36.		Infrared Spectrophotometry	x			x		
37.		Differential Scanning Calorimetry (DSC)	x			x		
		Differential Thermal Analysis (DTA)	x			x		
38.		Thermal Mechanical Analysis (TMA)	x			x		
39.		Thermo Gravimetric Analysis (TGA)	x			x		
40.		Humidity Exposure (MIL STD 810 #507)				x		
41.		Salt Fog Exposure (MIL STD 810 #509)				x		
42.		Compressive Properties of Rigid Plastics (ARTC-11)				x		
43.		Moisture Absorption of Cellular Plastics, Tech. Bulletin No. 5, Hygrodynamics				x		
44.		PQV	x	x				
45.		Vacuum Plate	x					x
46.		Cryogenic Strain Compatibility (MB0606-050)	x	x	x		x	x
47.	E-288	Linear Thermal Expansion, SMT (Method 1)	x			x		
48.	E-288	Linear Thermal Expansion, SMT (Method 2)	x			x		
49.		Total Normal Emittance (Method 1)	x			x		x
50.		Total Normal Emittance (Method 2)	x			x		x

Legend
A = Development B = Verification C = Qualification D = Material Property E = Process Verification F = Quality Verification

Table 15.2.1-1. Test/Usage Matrix (Cont)

15.2.2.X Paragraph Number	ASTM No.	Title	Engineering Tests				QA Tests	
			A	B	C	D	E	F
51.		Air Permeation Rate						
52.		Aerothermal Test	x	x				
53.		Aeroshear Test	x	x				
54.		Low-Pressure Thermal Effects	x					
55.		High-Termperature Thermal Effects	x					
56.		Torsional Shear Modulus Foam Materials				x		
57.		Thermal Conductance, Insulation Support Posts	x					
58.		Outgassing Rate	x			x		
59.		Carbon, Nitrogen, and Hydrogen Analysis of Plastic Materials	x			x		
60.		Evaluation Test of Tension Membranes for Multilayer Insulation	x					
61.		Guarded Calorimeter Evaluation of Insulation System	x	x		x		
62.		Multilayer Insulation Molecular Flow Test	x			x		
63.		Cryogenic and Combined Environment Testing of S-II Cylinder No. 1 Insulation	x	x	x			
64.		Cryogenic Test Tank 8 ft. x 8 ft.	x	x				
65.		Cryogenic Test Tank	x		x			
66.		Flow and Thrust Testing of Polyimide Panels	x					
67.		Cryogenic Testing of S-II Feedline Elbow	x	x				

Legend
A = Development
B = Verification
C = Qualification
D = Material Property
E = Process Verification
F = Quality Verification

15.2.2.1 Heat Transport Measurements

a. Overall Objective: Determination of the heat transmission characteristics of insulation materials and composites in their usage environments.

b. Description:

1. Test Article: The methods used in support of the S-II program for measurement of the heat transport properties have all involved steady-state conditions and have utilized, with one exception, flat slab specimens (high ratio of area to path length) commensurate with measurements of poorly conducting materials. The exception is the axial heat flow method used for relatively high conductivity materials.

   For measurements on good insulators, two principal approaches were used. One, an absolute method called the guarded hot plate technique, is comprehensively described in ASTM Standard C177. The heat flux is determined by direct measurement of heater power, assuming half this power is dissipated equally through each of two identical specimens between which the guarded heater is sandwiched. Several different test systems utilizing this approach were instrumental in generating S-II insulation system design and performance data.

   The second approach, called the thermal comparator technique, involves the use of a reference material of known thermal conductivity, which is placed in series with the unknown specimen between a heat source and sink. The temperature drop through the reference material is the basis for determining the heat flux through the specimen. This method is inherently less accurate than the guarded hot plate technique.

   A third approach, used in some subcontracted testing, involves a calorimetric method of measuring heat flux at cryogenic temperatures. The specimen is placed between a heater and guarded cold plate. Fluid boiloff from the center cold plate, termed the calorimeter, is a measure of the heat flux through the specimen. This is similar in principle to the guarded hot plate technique.

2. Test Conditions: Temperature and atmosphere surrounding and within the specimen were varied, from -423 F to above ambient temperature and from 10^{-4} Torr to slightly positive pressures. Gaseous atmospheres included air, nitrogen, and helium.

3. Type of Data: Data are usually presented as apparent mean thermal conductivity, k, of insulation materials or mean thermal conductance, $\bar{C}$, of insulation composites. These quantities are defined by the following equations.

$$\overline{k}_{app} = \frac{(q/A)\,\Delta X}{\Delta T}$$

$$\overline{C}_{app} = \frac{(q/A)}{\Delta T}$$

where

(q/A) = Heat flux
X = Path length
T - Difference between temperatures at hot and cold faces of the slab

The terms thermal conductivity or conductance refer to heat transport by conduction only. For low-density insulation (always mixed-phase systems) the terms apparent or effective thermal conductivity are preferred, taking into account heat transfer by radiation and gaseous conduction and convection as well as by solid conduction. Typical units for conductivity are (Btu/hr.-ft.^{2}-^{o}F/in.) and conductance (Btu/hr.-ft.^{2}-^{o}F.).

4. Test Equipment:

   (a) Guarded hot-plate apparatus (air only) (Figure 15.2.2.1-1).

   (b) Thermal comparator apparatus (Figures 15.2.2.1-2, -3, and -4)

   (c) "Banjo" envelope-type cold plate apparatus (Figures 15.2.2.1-5 and -6).

   (d) LH_2 "banjo" modification (Figure 15.2.2.1-7).

c. Materials Tested: These techniques have been applied to the measurement of heat transport properties of insulation materials and composites, multilayer insulation, and standoff and structural materials for a host of S-II applications (e.g., tankage, equipment containers, heat shield, and transfer lines).

d. References:

1. ASTM C177, Standard Method of Test for Thermal Conductivity of Materials by means of Guarded Hot Plate.

2. NR/SD Material and Process Procedure 3340-001, Elevated Temperature Thermal Conductivity (Air-Cooled Guarded Hot Plate).

3. Milnes, M. V., Low-Temperature Thermal Conductivity Apparatus. NAA/S&ID, SDL 408 (Sept. 9, 1963).

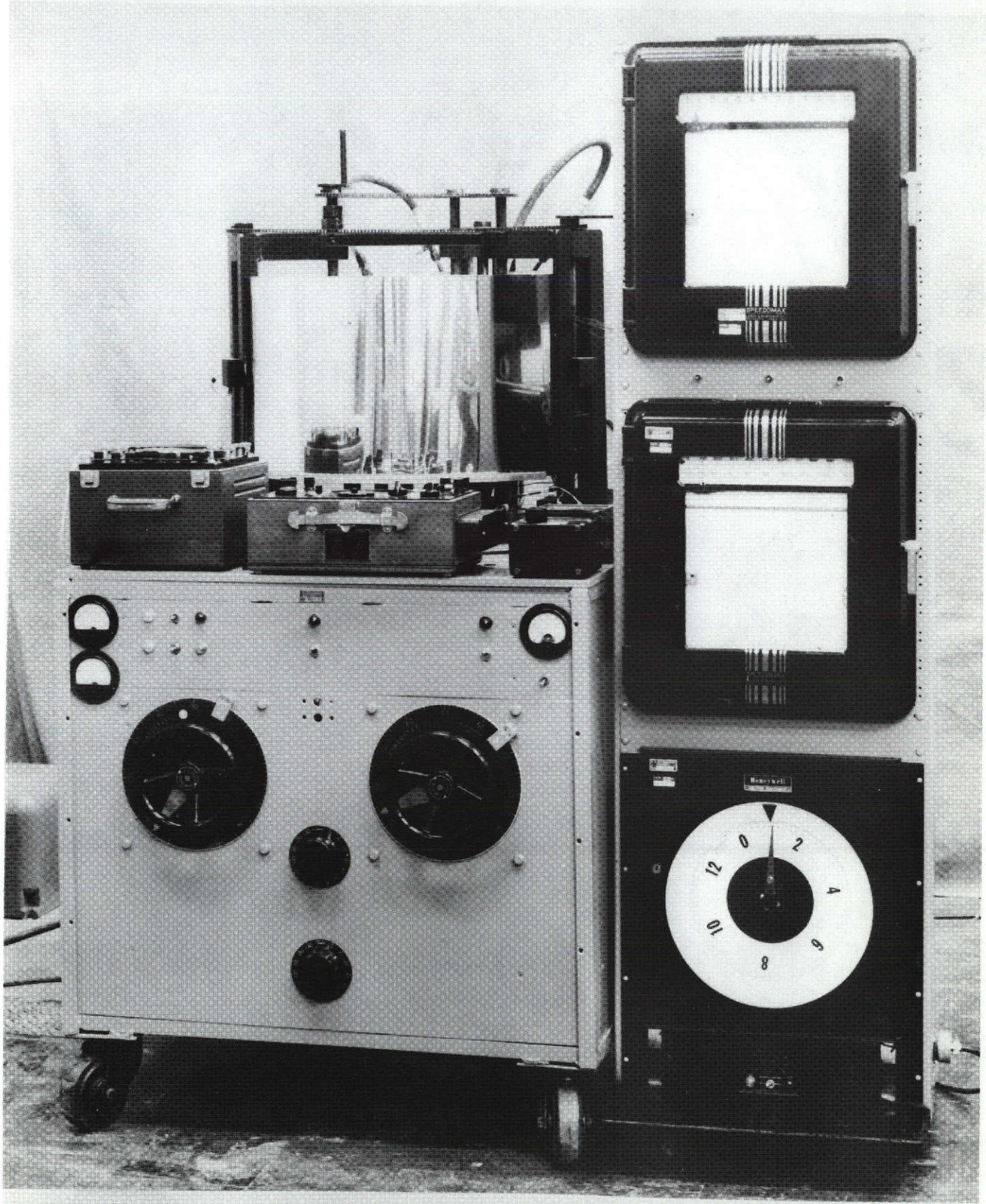

Figure 15.2.2.1-1. Heat Transport Measurements Equipment Guarded Hot Plate Apparatus (Air Only)

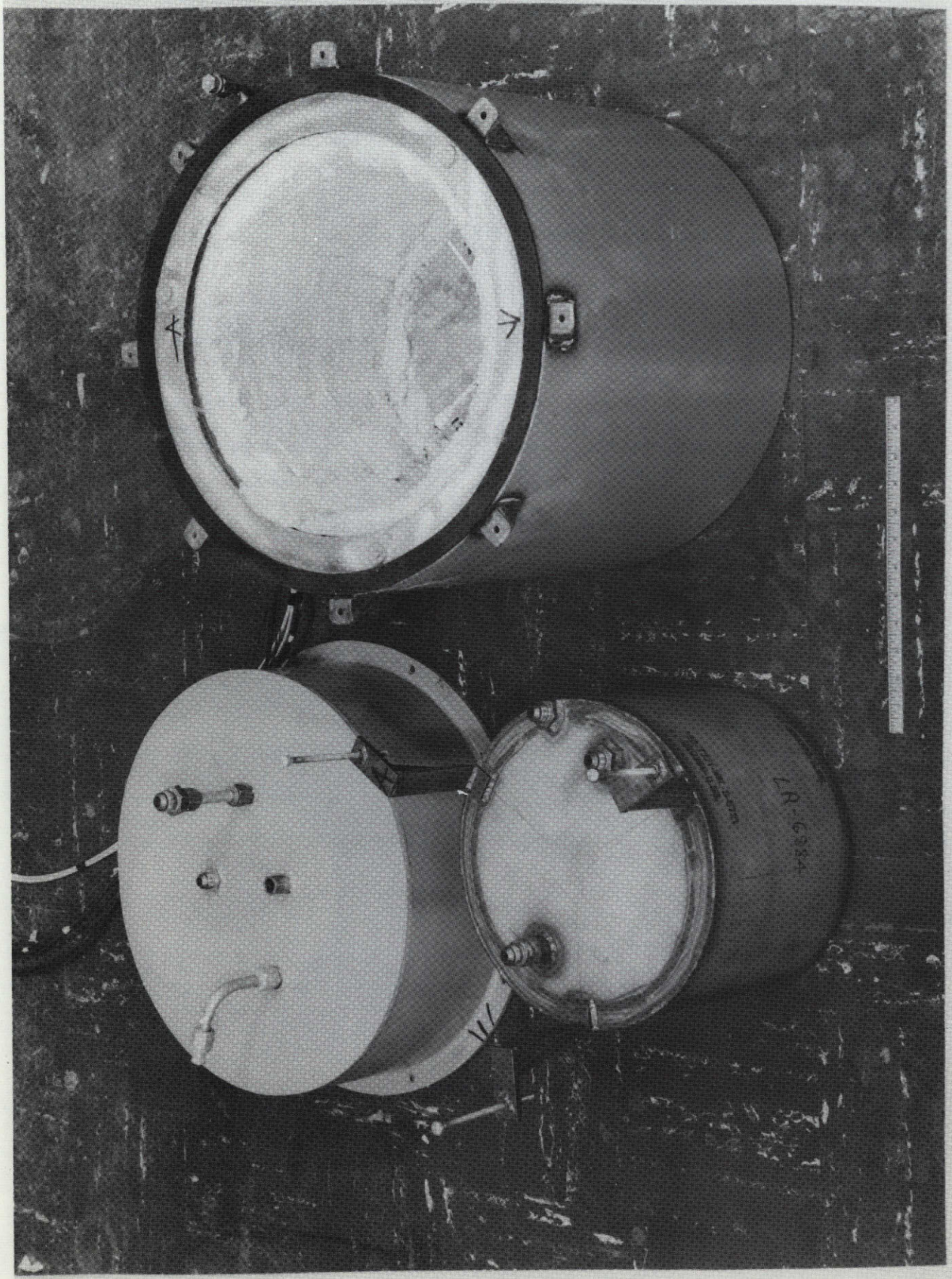

Figure 15.2.2.1-2. Heat Transport Measurements Equipment Thermal Comparator Apparatus

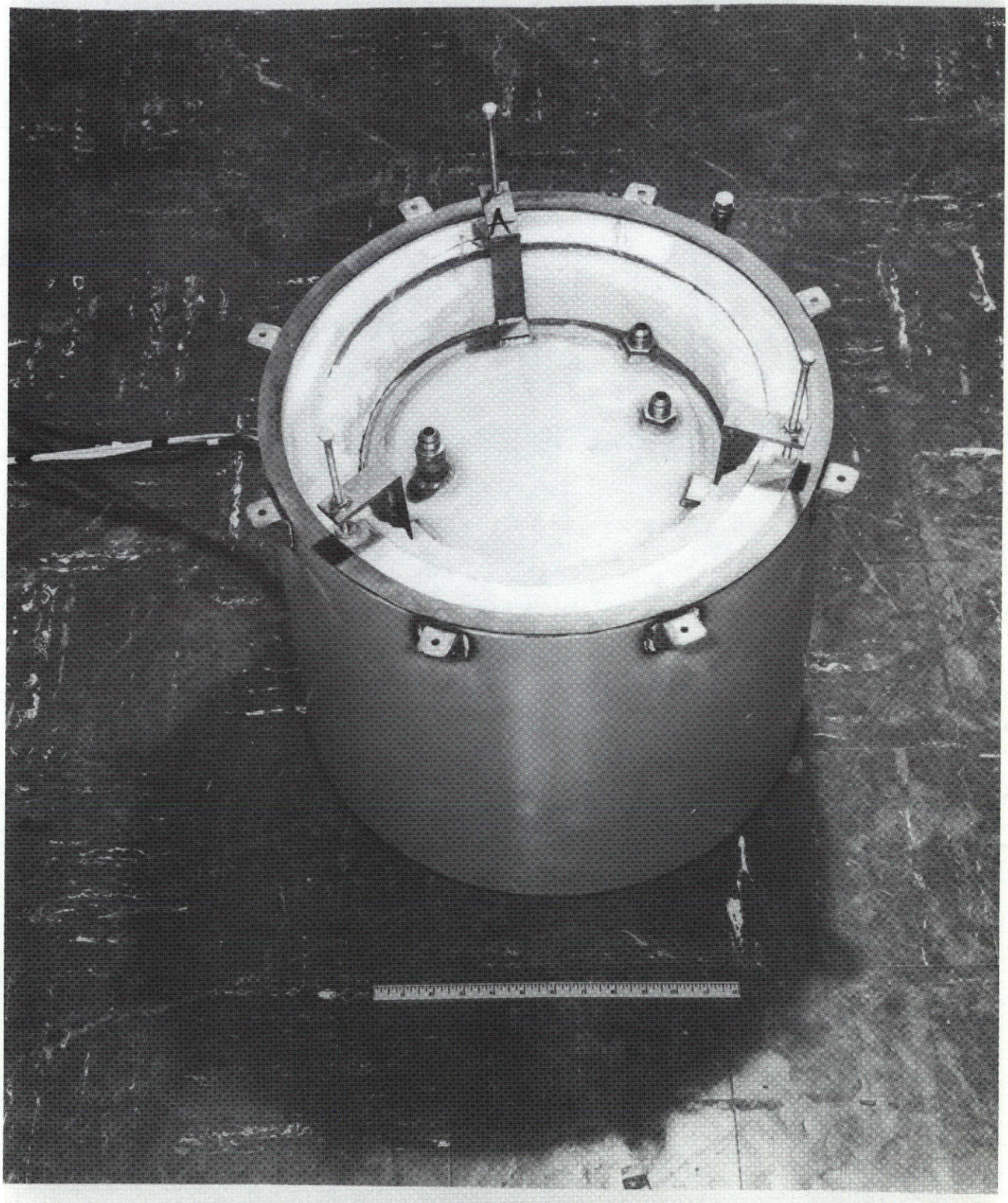

Figure 15.2.2.1-3. Heat Transport Measurements Equipment Thermal Comparator Apparatus

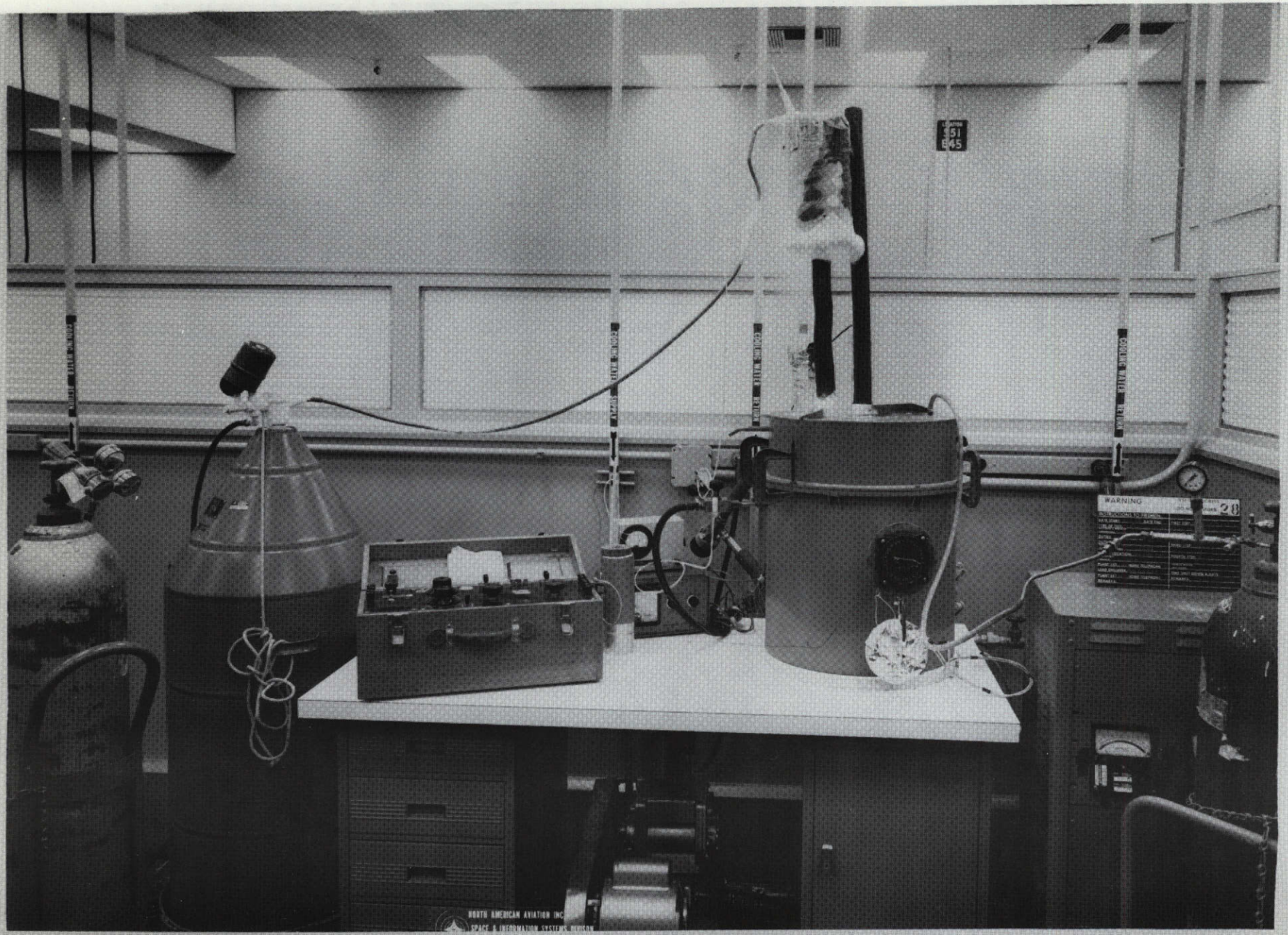

Figure 15.2.2.1-4. Heat Transport Measurements Equipment Thermal Comparator Apparatus

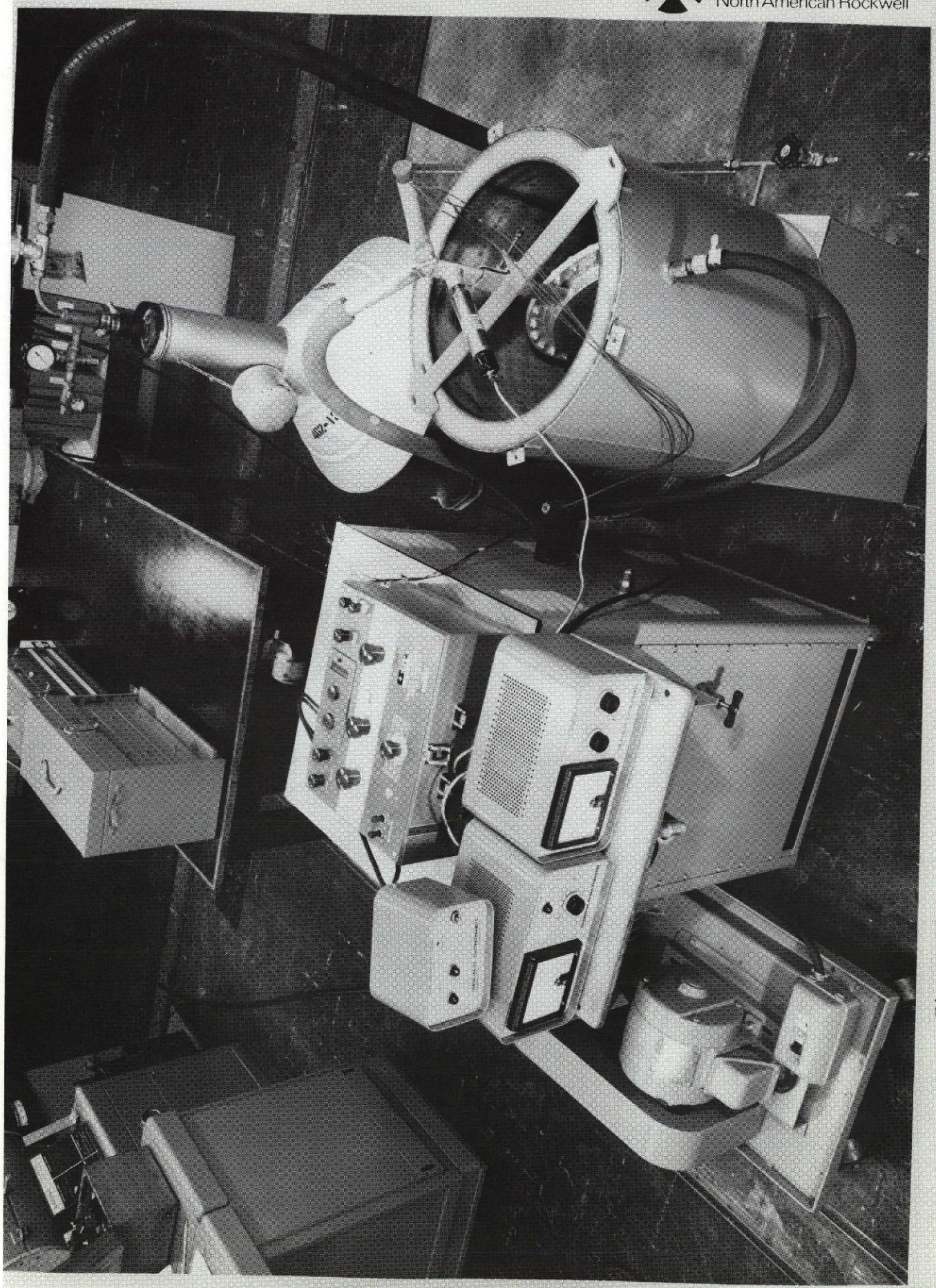

Figure 15.2.2.1-5. Heat Transport Measurements Equipment Banjo, Envelope Type Apparatus

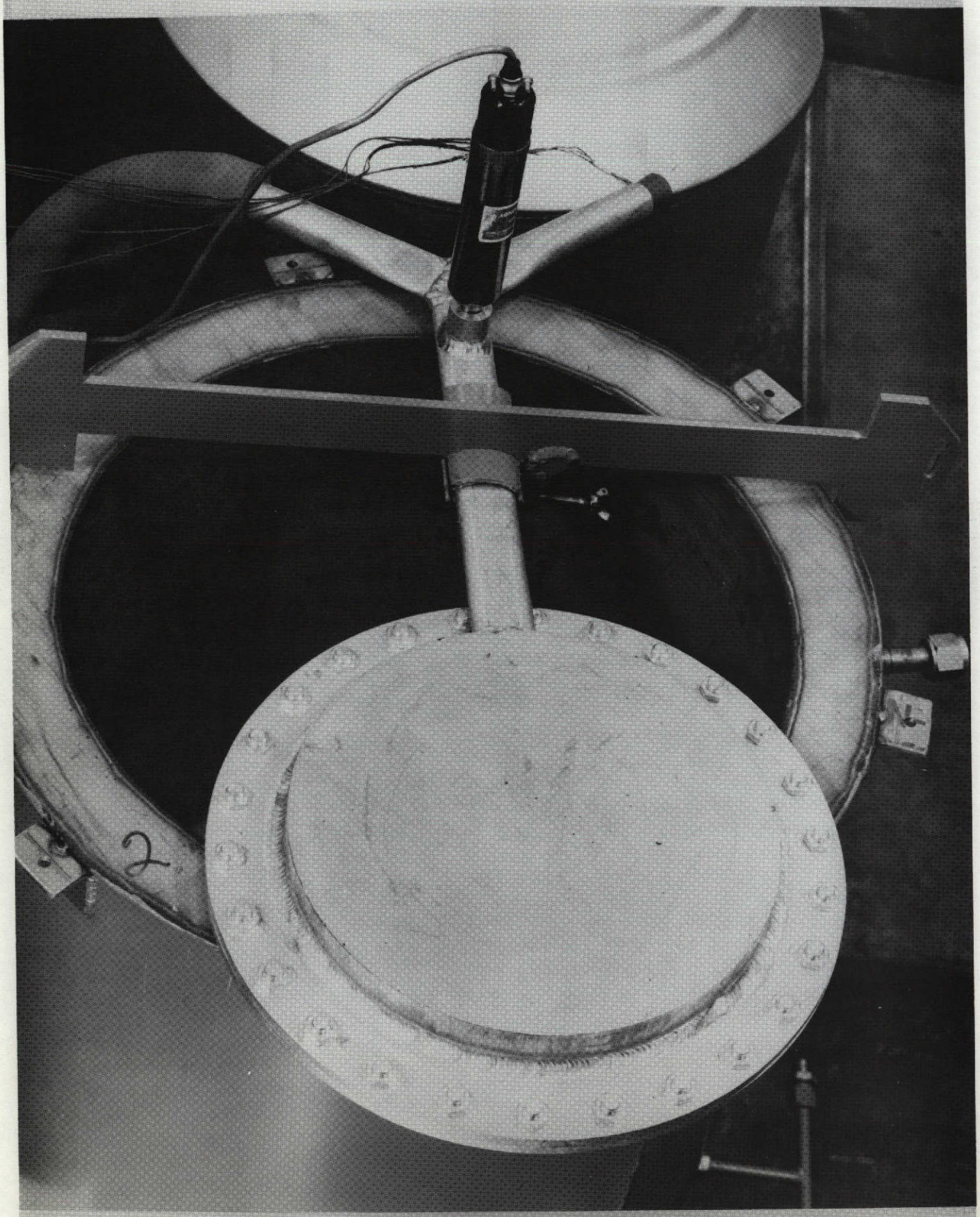

Figure 15.2.2.1-6. Heat Transport Measurements Equipment Banjo, Envelope Type Apparatus

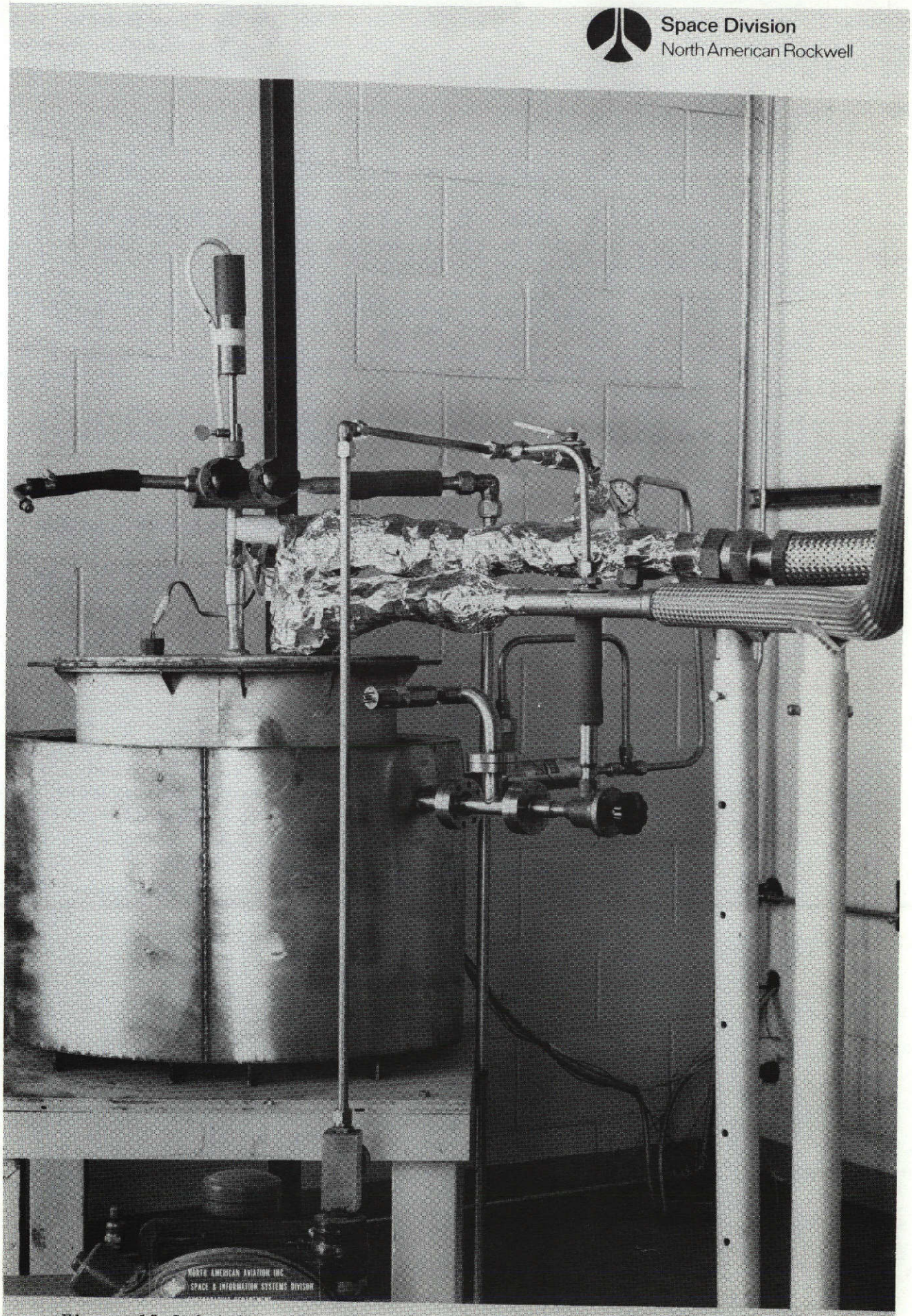

Figure 15.2.2.1-7. Heat Transport Measurements Equipment LH_2 "Banjo" Modification

4. Green, W. W., and Zanella, F. M., Thermal Measurements on Saturn S-II Insulation. NAA/S&ID, SDL 454 (April 1964).

5. Milnes, M. V., et al, Thermal Conductivity of Cryopumped Layer of S-II Double Seal Insulation. NAA/S&ID, SID 65-681 (July 12, 1965).

6. Engineering Laboratory Report Saturn S-II Insulation Specimens. Beech Aircraft Crop. Lab Report 13585 (Nov. 13, 1962).

15.2.2.2 Density of Core Materials for Structural Sandwich Constructions

a. Overall Objective: This method covers the determination of the density of core materials of structural sandwich constructions.

b. Description:

1. Test Article: The specimen consists of a 3-inch (7.62-cm) length by 3-inch (7.62-cm) width of sandwich core material. At least three specimens are tested for quality acceptance use. Design data requirements should make use of at least 12 samples to furnish average values and standard deviation to indicate variability and reliability of data for selecting appropriate design values.

2. Test Conditions: The specimen is subjected to conditioning of such duration that the specimen will have attained constant weight. This may be achieved by subjecting specimens to Standard ASTM atmospheric conditions of 73.4 $\pm$ 2 F (23 $\pm$ 1 C), and 50 $\pm$ 2 percent relative humidity or by placing the specimens in an oven to a temperature of 122 $\pm$ 2 F (40 $\pm$ 1 C). After conditioning the specimens are weighted to an accuracy of $\pm$ 0.5 percent and measured to an accuracy of $\pm$ 0.5 percent.

3. Type of Data: The core density in pounds per cubic foot is calculated as follows:

$$\text{Density} = \frac{FX1728}{LXWXT}$$

where

F = Final weight after conditioning, in pounds
L = Length of specimen after conditioning, in inches
T = Thickness of specimen after conditioning, in inches
W = Width of specimen after conditioning, in inches

Note: If all measurements are more conveniently made in the metric system the density is calculated and converted to English units as follows:

$$\text{Density, lb. per cu.ft.} = \frac{A}{B} \times 62.4$$

where

A = Weight of specimen, in grams
B = Volume of specimen, in cubic centimeters
62.4 = Factor for conversion from grams per cubic centimeter to pounds per cubic foot

4. Test Equipment: Drying oven, analytical balance, desiccator, and micrometer, gauge or caliper capable of measuring accurately to 0.001 inch.

c. Materials Tested: Any core materials used in sandwich construction.

d. Reference: ASTM C271-61 and MIL-STD-401 B.

15.2.2.3 Shear Test in Flatwise Plane of Flat Sandwich Construction of Sandwich Cores

a. Overall Objective: This method covers the determination of shear properties of sandwich construction associated with shear distortion of planes parallel to the edge plane of the sandwich. It covers the determination of shear strength parallel to the plane of the honeycomb sandwich and the shearings modulus associated with strains in a plane normal to the facings. The test may be conducted on bare core materials.

b. Description:

1. Test Article: Test specimens have a thickness equal to the thickness of the sandwich, a width not less than twice the thickness, and a length not less than 12 times the thickness except as otherwise specified.

2. Test Conditions: Testing is accomplished in the environmental and temperature of the most rigid intended use of the end item. Test temperatures will range from -252 C (-423 F) to 537 C (1000 F).

3. Type of Data: Data include load at failure, the dimensions of the core or sandwich tested, and the shear strength (psi).

4. Type Equipment: Test machine is a 60,000-pound capacity Riehle. Figure 15.2.2.3-1 shows the test setup.

c. Materials Tested: Materials includes honeycomb sandwich and foam.

d. Reference: ASTM C-273.

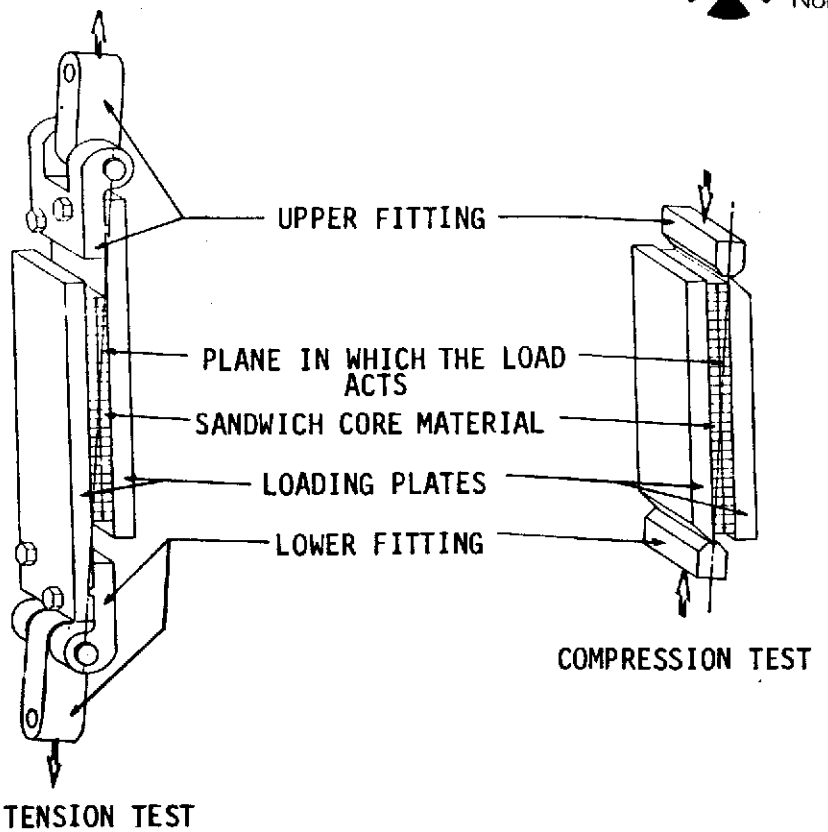

Figure 15.2.2.3-1. Arrangement of Apparatus and Test Specimen for Shear Tests in Tension and in Compression

15.2.2.4 Tension Testing of Flat Sandwich Constructions in Flatwise Plane

a. Overall Objective: This method covers the procedure for determining the strength in tension, flatwise, of the core, or of the bond between core and facings, of an assembled sandwich panel. The test consists of subjecting a sandwich construction to a tensile load normal to the plane of the sandwich, such loads being transmitted to the sandwich through thick loading blocks bonded to the sandwich facings.

b. Description:

1. Test Article: Test specimens must be square or round and equal in thickness to the thickness of the structural sandwich panel. A minimum of 4 square inches of core or sandwich is used for evaluation and at least one complete cell.

2. Test Conditions: Testing is accomplished in the environment and temperature of the most rigid intended use of the end item. Test temperatures will range from -252 C (-423 F) to 537 C (1000 F).

3. Type of Data: Data include load at failure, the dimensions of the core or sandwich tested, and the ultimate tension strength.

4. Test Equipment: Test machine is a 10,000-pound capacity Riehle. Figure 15.2.2.4-1 shows the test setup.

TENSION TEST FOR SANDWICH CONSTRUCTIONS (C 297)

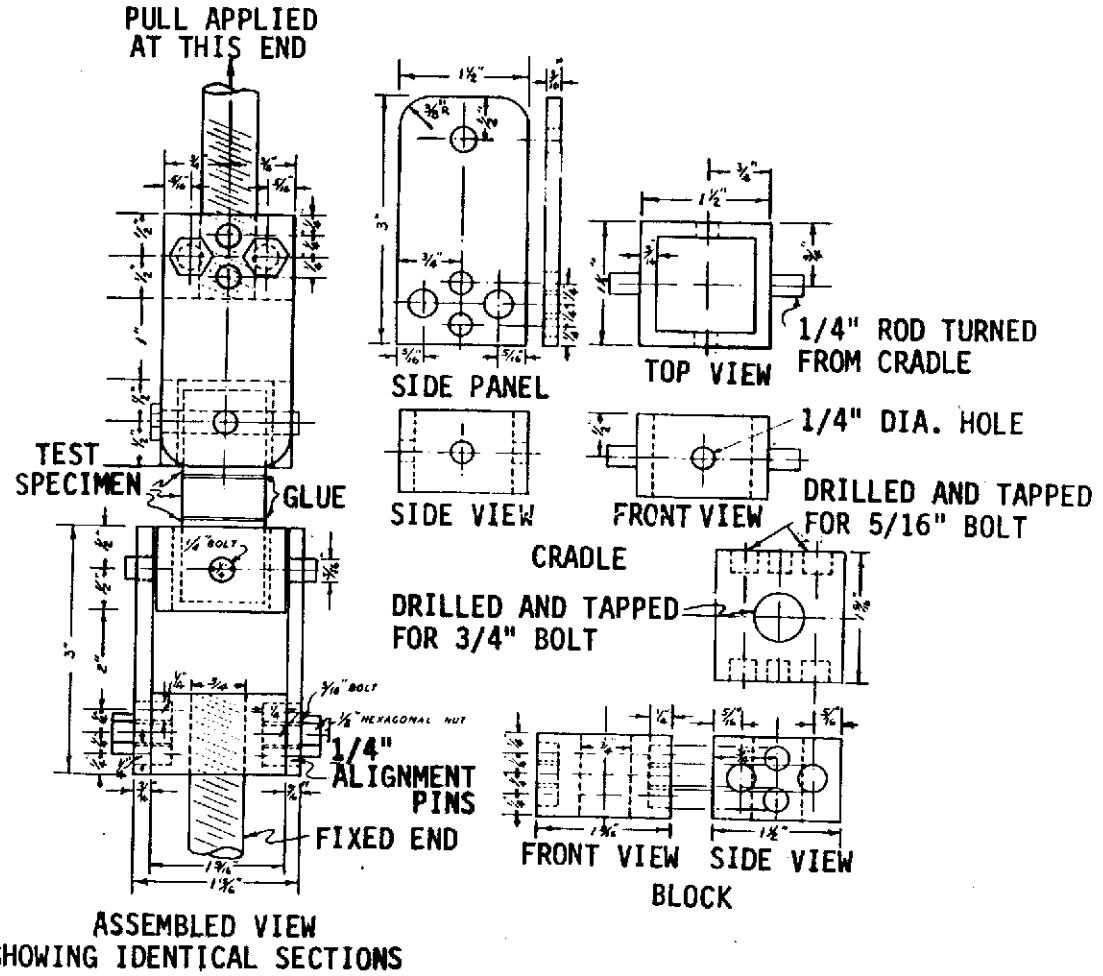

Figure 15.2.2.4-1. Loading Fixture for 1-in. Square Test Specimen for Tension Flatwise Test

c. Materials Tested: Materials tested include honeycomb sandwich and foams.

d. Reference: ASTM C-297.

15.2.2.5 Heat Capacity Measurements

a. Objective: Determination of the heat storage capacity of insulation materials.

b. Description:

1. Test Article: Specimens are selected at random as required to provide test material representative of the lot sampled. A dried specimen of as large a mass as practical is used.

2. Test Conditions: The method used was the classical method of mixtures, the basis of the technique of drop calorimetry. In this method, described in detail in ASTM C351, the specimen is heated to an elevated temperature, where it is permitted to equilibrate. It is then dropped into a thermally isolated mass of liquid. The enthalpy increase of the liquid and calorimeter is equated to the enthalpy decrease of the specimen.

3. Type of Data: The test results are usually expressed as the mean heat capacity Cp, where the subscript p implies the heat capacity at constant pressure. This quantity is defined as follows:

$$\overline{C_p} = \frac{H}{T}$$

where

ΔH = Change in enthalpy of specimen, Btu/lbn
ΔT = Temperature change of specimen, ^{o}F

Mean heat capacity data are commonly presented as a function of mean temperature, a practice which is to be avoided. Since the true or point heat capacity, defined as

$$Cp = \left(\frac{\partial H}{\partial T}\right)$$

is not necessarily a linear function of ΔT, it follows that two different values of Cp can be obtained for the same mean temperature, for different ΔT's. A preferred method is to tabularize the mean specific heat data, giving the temperature interval to which each value applies.

4. Test Equipment: The test setup is shown in Figure 15.2.2.5-1.

c. Materials Tested: Heat capacity measurements are usually performed for material systems whose dynamic thermal behavior is of principal concern (e.g., ablators and heat shield materials). They may also be of interest for liquid storage tank insulations, where cooldown time will be a function of insulation heat capacity, among other factors.

d. References:

1. ASTM C351, Standard Method of Test for Mean Specific Heat of Thermal Insulation.

2. NR/SD Material and Process Procedure 3340-003, Mean Specific Heat (Drop Calorimeter).

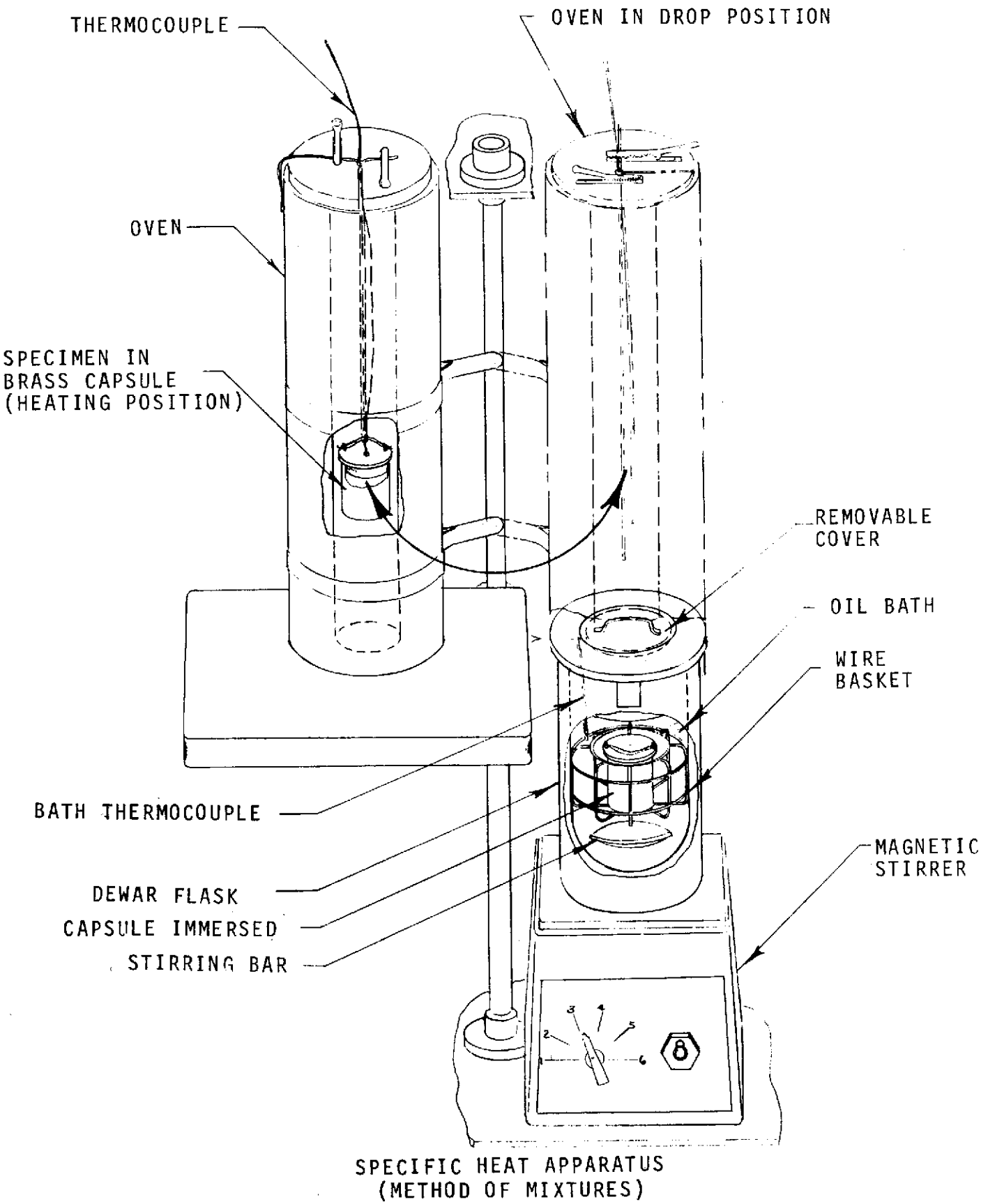

Figure 15.2.2.5-1. Test Set-Up, Heat Capacity Measurements

15.2.2.6 Standard Method of Test for Delamination Strength of Honeycomb Type Core Material

a. Overall Objective: This method covers the procedure for determining the delamination strength (the node-to-node bond) of honeycomb core materials.

b. Description:

1. Test Article: The test specimens are 5 inches wide by 10 inches long with a test section 8 inches between the load pins.

2. Test Condition: Air, ambient relative humidity, and test temperatures from -252 C (-423 F) to 537 C (1000 F).

3. Type of Data: The delamination strength calculated by the formula:

$$F = \frac{P}{LT}$$

where

F = Delamination strength, lb./in.^{2}
P = Ultimate tensile force, lb.
L = Width of specimen, n
T = Thickness of specimen, n

4. Test Equipment: Universal-type tensile test machine. The test setup and specimen are shown in Figure 15.2.2.6-1.

c. Materials Tested: Honeycomb core materials.

d. Reference: ASTM C363.

15.2.2.7 Method of Test for Edgewise Compressive Strength of Flat Sandwich Constructions

a. Overall Objective: This method of test is for determination of compressive properties of flat structural sandwich constructions in a direction parallel to the plane of the sheet of the sandwich.

b. Description:

1. Test Article: The test specimen is rectangular in cross-section, measuring at least 2 inches wide but not less than twice the total thickness. The unsupported length (dimension parallel to applied load) is not greater than 12 times the thickness. The ends of the specimen are cast in plastic or Cerrobend metal to prevent early buckling failure of facings due to separation of facings from core at the point of contact with the loading plates. Cast ends are machined flat and parallel prior to test. Five specimens are tested per material, test condition, or test temperature.

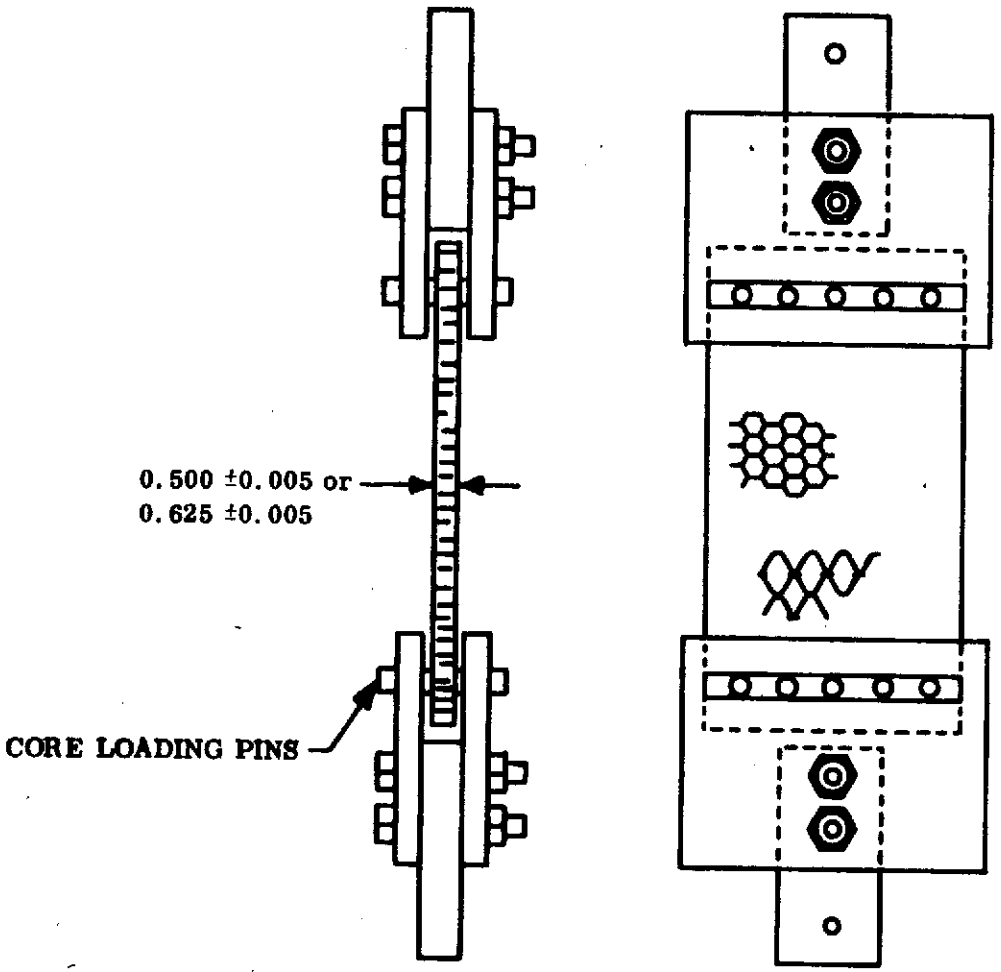

Figure 15.2.2.6-1. Apparatus for Node Strength Tests

Loading is accomplished in a universal-type testing machine, and an autographic recording of loading versus specimen deformation is provided.

2. Test Conditions: Special conditioning may apply, in which case it is defined. Edgewise compression testing is performed at test temperatures from -184 C (-300 F) to 537 C (1000 F).

3. Type of Data: The test report includes specimen description, specimen measurements, conditioning or preparation procedures, type of failure, failing load, and the maximum stress obtained in facings.

4. Test Equipment: A 100,000-pound Riehle test machine or equivalent.

c. Materials or Systems Tested: This method of test is for use in evaluation of adhesives and materials in flat sandwich-type constructions.

d. Reference: ASTM C-364.

15.2.2.8 Flatwise Compressive Strength of Sandwich Cores

a. Overall Objective: This test method covers procedures for determining compressive properties of sandwich cores. These properties are usually determined for design purposes in a direction normal to the plane of facings as the core would be placed in a structural sandwich construction. The test procedures pertain to compression in this direction in particular, but also can be applied with possible minor variations to determine compressive properties in other directions.

b. Description:

1. Test Article: Test specimens are of core or sandwich construction and are of square or circular cross-section having areas not exceeding 16 square inches, but not less than one square inch or less than one complete cell.

2. Test Conditions: Testing is accomplished in the environment and temperature of the most rigid intended use of the end item. Test temperatures will range from -252 C (-423 F) to 537 C (1000 F).

3. Type of Data: Includes load at failure and the dimensions of the core or sandwich tested and the ultimate compressive strength (psi).

4. Test Equipment: Test machine 10,000-pound capability and deflectometer. The test setup is shown in Figure 15.2.2.8-1.

c. Materials Tested: Materials tested includes honeycomb sandwich and foam.

d. Reference: ASTM C-365.

15.2.2.9 Method for Flexure Test of Flat Sandwich Constructions

a. Overall Objective: This method is for determining properties of flat sandwich constructions subjected to flatwise flexure in such a manner that the applied moments produce a curvature of the plane of the facing sheets of the sandwich.

b. Description:

1. Test Article: The test specimen is rectangular in cross-section. The width and length of the specimen varies depending on sandwich construction and the properties to be determined.

Loading is applied at quarter span points with use of a universal-type test machine. Loading versus deflection at midspan is autographically recorded.

Five specimens per type or condition are tested per test temperature.

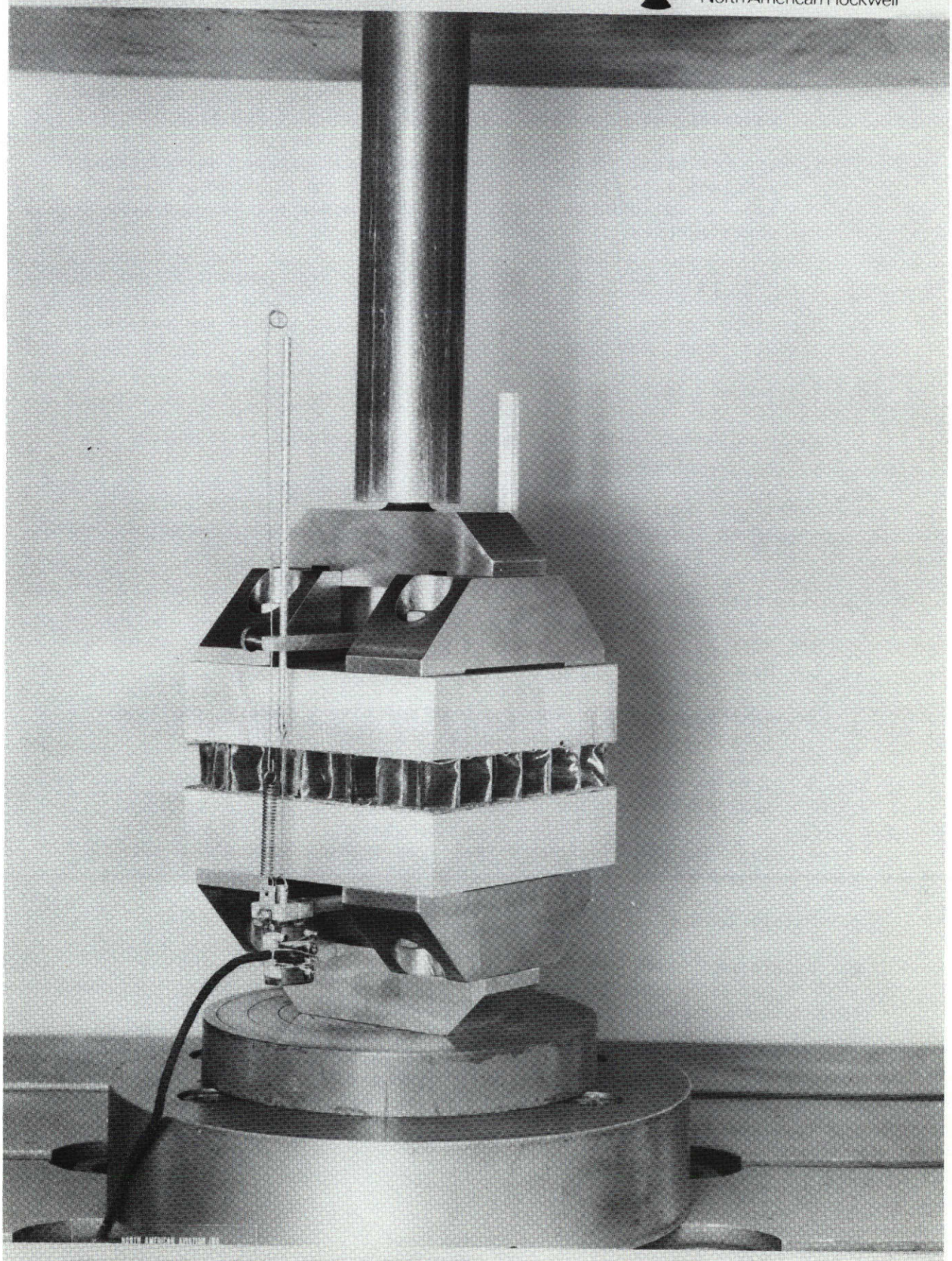

Figure 15.2.2.8-1. Test Set-Up Flatwise Compressive Strength of Sandwich Cores

2. Test Conditions: Flexure properties may be determined at test temperatures from -184 C (-300 F) to 537 C (1000 F).

3. Type of Data: The test report includes specimen description, specimen measurements, conditioning or preparation procedures, type of failure, the calculated core shear stress, and core shear modulus.

4. Test Equipment: A 60,000-pound Riehle test machine or equivalent.

c. Materials Tested: This method of test is for use in the evaluation of sandwich core materials.

d. Reference: ASTM C393.

15.2.2.10 Standard Method of Test for Flexure-Creep of Sandwich Constructions

a. Overall Objective: This method covers a procedure for determing the creep characteristics and creep rate of sandwich constructions loaded in flexure.

b. Description:

1. Test Article: The specimen must measure 3 inches in width by 12 inches long.

2. Test Conditions: Air, ambient relative humidity, and test temperatures from -184 C (-300 F) to 537 C (1000 F).

3. Type of Data: The creep rate deflection rate in inches per hour for an applied stress.

4. Test Equipment: A universal-type tensile test machine (Figure 15.2.2.10-1).

c. Materials Tested: Sandwich constructions.

d. Reference: ASTM C480.

15.2.2.11 Permeability Testing of Insulation Systems

a. Overall Objective: This method defines the procedure for determining the permeation rate of helium or hydrogen through foam and evacuated insulation systems. The test consists of exposing the insulation to gaseous pressurant and determining the rate at which gas permeates the insulation.

b. Description:

1. Test Article: The insulation test specimen must be of representative thickness and 4-inch diameter bonded to the test chamber (Figure 15.2.2.11-1).

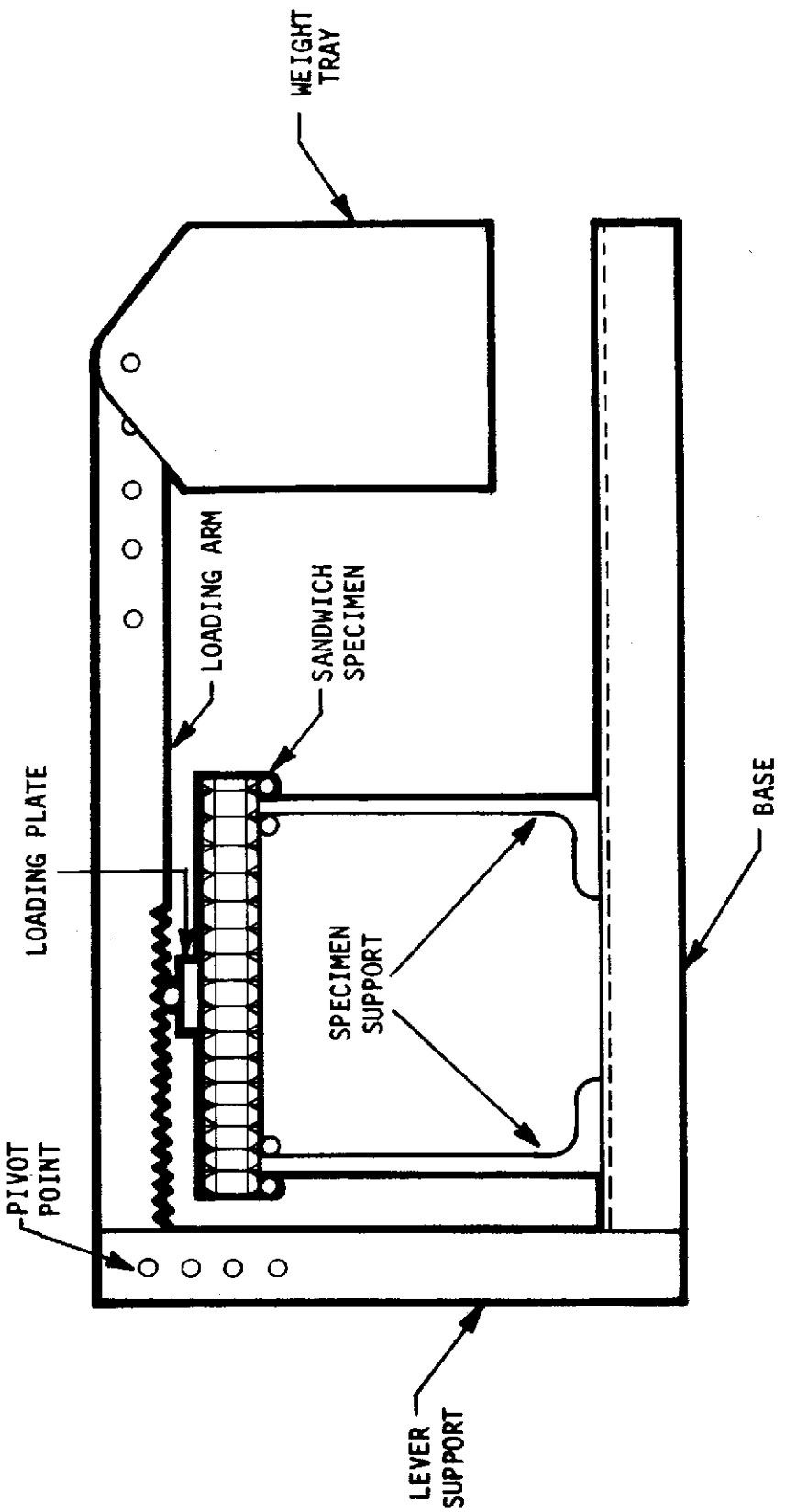

Figure 15.2.2.10-1. Creep Test Apparatus and Loading System

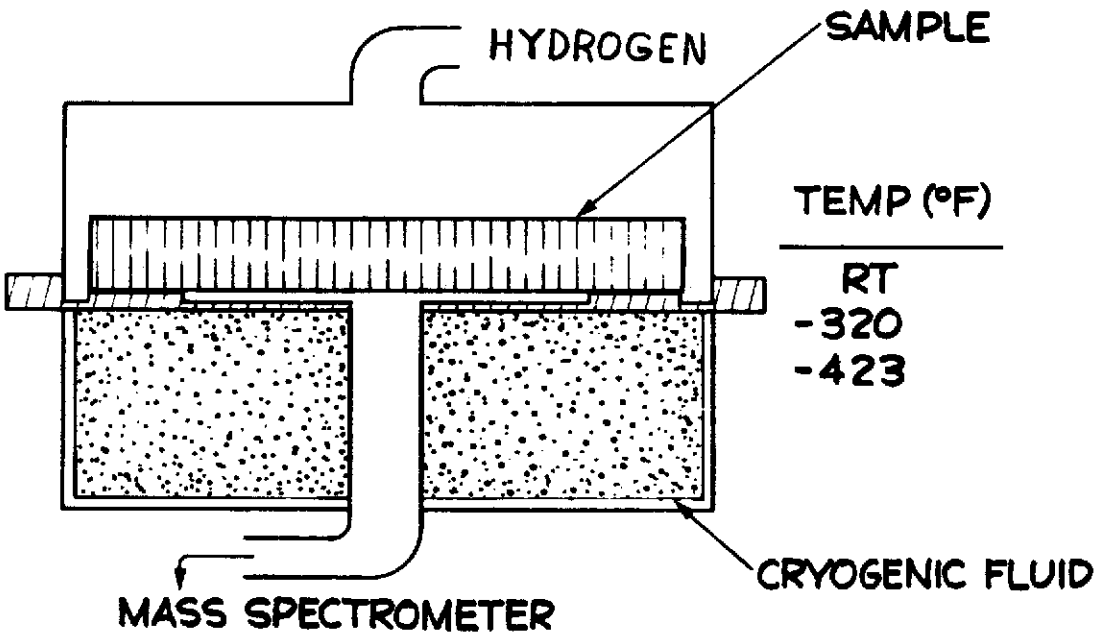

Figure 15.2.2.11-1. Permeability Test

2. Test Conditions: Testing is accomplished in the environment and temperature of the most rigid intended use of the insulation. Test temperature will range from ambient to -423 F with pressure in the range of ambient to 5 psig.

3. Test Data: Data include temperature, pressure, and leakage of pressurant through the insulation.

4. Test Equipment: Test chamber and mass spectrometer.

c. Material Tested: Primary materials tested are foam insulation systems.

15.2.2.12 Method of Test for Shear Strength of Plastics

a. Overall Objective: This method covers thepunch type of shear test and is intended for use in determining the shear strength of test specimens in the form of organic plastic sheets.

b. Description:

1. Test Article: The test specimen configuration is 2 inches square or 2 inches in diameter and may be of a thickness from 0.005 to 0.500 inch. The upper and lower surfaces of the test specimen are flat and parallel. Five specimens are tested per material or test condition.

2. Test Condition: Shear properties may be determined in the temperature range of -184 C (-300 F) to 537 C (1000 F). Conditioning of plastics is in accordance with the methods of conditioning of plastics per ASTM D618.

3. Type of Data: The test data include complete materials identification, specimen dimensions, test conditions, conditioning procedures, and the calculated shear strength in pounds per square inch for each specimen.

4. Test Equipment: A 30,000-pound capacity Riehle test machine or equivalent is used. The punch-type shear tool is shown in Figure 15.2.2.12-1.

c. Materials Tested: This method of test is intended for use in providing shear strength data on all organic plastic sheet materials.

d. Reference: ASTM D732 and FED STD 406.

15.2.2.13 Standard Method of Test for Flexural Properties of Plastics

a. Overall Objective: This method covers procedures for determination of the flexural properties of plastics.

b. Description:

1. Test Article: The specimen width must be 1/2 inch or 1 inch and the length must be 16 times the thickness plus 2 inches.

2. Test Conditions: Conditions are ambient air and relative humidity and temperatures from -252 C (-423 F) to 537 C (1000 F).

3. Type of Data: Flexural strength, flexural modulus, and loading versus deflection characteristics.

4. Test Equipment: Universal-type tensile test machine, deflectometer, and a strain recorder. Figure 15.2.2.13-1 shows a typical test setup.

c. Materials Tested: Laminated or molded, sheet or plate plastic materials.

d. Reference: ASTM D790.

15.2.2.14 Method of Test for Tensile Properties of Adhesives

a. Overall Objective: This method of test is for comparative tensile properties of adhesives when tested at various temperatures and under defined conditions of pretreatment.

b. Description:

1. Test Article: The test specimen consists of two identical metal blocks which are aligned and bonded together. The metal blocks are of a square or a round configuration and are designed for attachment of self-aligning grips which will permit loading to be applied axially through the centroid of the test specimen. Five specimens are tested for each type of adhesive or test temperature.

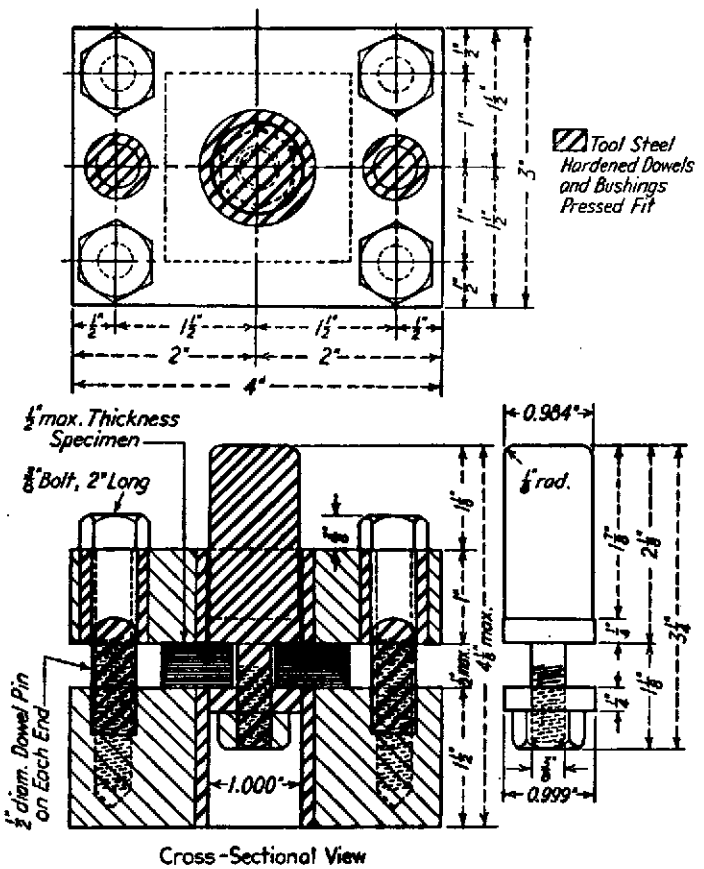

Figure 15.2.2.12-1. Punch-Type Shear Tool for Testing Specimens 0.005 to 0.500 Inches in Thickness

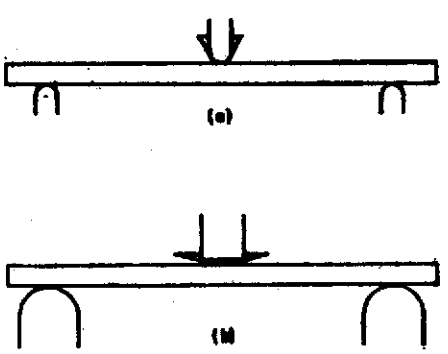

(a) Minimum radius = 3.2 mm (⅛ in.).
(b) Maximum radius supports = 1⅛ times specimen depth, maximum radius loading nose = 4 times specimen depth (minimum length of chord defining arc in contact with the specimen = 2 times specimen depth).

Figure 15.2.2.13-1. Allowable Range of Loading Nose and Support Radii for Specimen 6.4 mm (1/4 in.) Thick

2. Test Conditions: Conditioning is not required for metal-to-metal bonds. The tensile properties of adhesives are determined at test temperatures from -252 C (-423 F) to 537 D (1000 F).

3. Type of Data: The test report includes identification of the adhesive and adherends, method of specimen preparation, loading rate, type of failure (adhesive or cohesive) individual failing loads, and averages calculated in pounds per square inch.

4. Test Equipment: A 20,000-pound Riehle test machine or equivalent; a test fixture is shown in Figure 15.2.2.14-1, and a test specimen in Figure 15.2.2.14-2.

c. Materials or Systems Tested: This method of test is intended for use in providing tensile properties of paste and adhesive type systems.

d. Reference: ASTM D-897.

15.2.2.15 Standard Method of Test for Peel or Stripping Strength of Adhesives

a. Overall Objective: This method of test is intended for determination of the comparative peel or stripping characteristics of adhesives when tested under defined conditions.

b. Description:

1. Test Article: The test specimen consists of one piece of flexible material, 1 by 12 inches, bonded for 6 inches at one end to one piece of rigid material, 1 by 8 inches, with the unbonded portions of each piece face to face.

2. Test Conditions: Ambient air and relative humidity and test temperatures from -252 C (-423 F) to 537 C (1000 F).

3. Type of Data: The actual peel or stripping strength in pounds per inch of width.

4. Test Equipment: A universal-type tensile test machine (Figure 15.2.2.15-1).

c. Materials Tested: Adhesives.

d. Reference: ASTM D903.

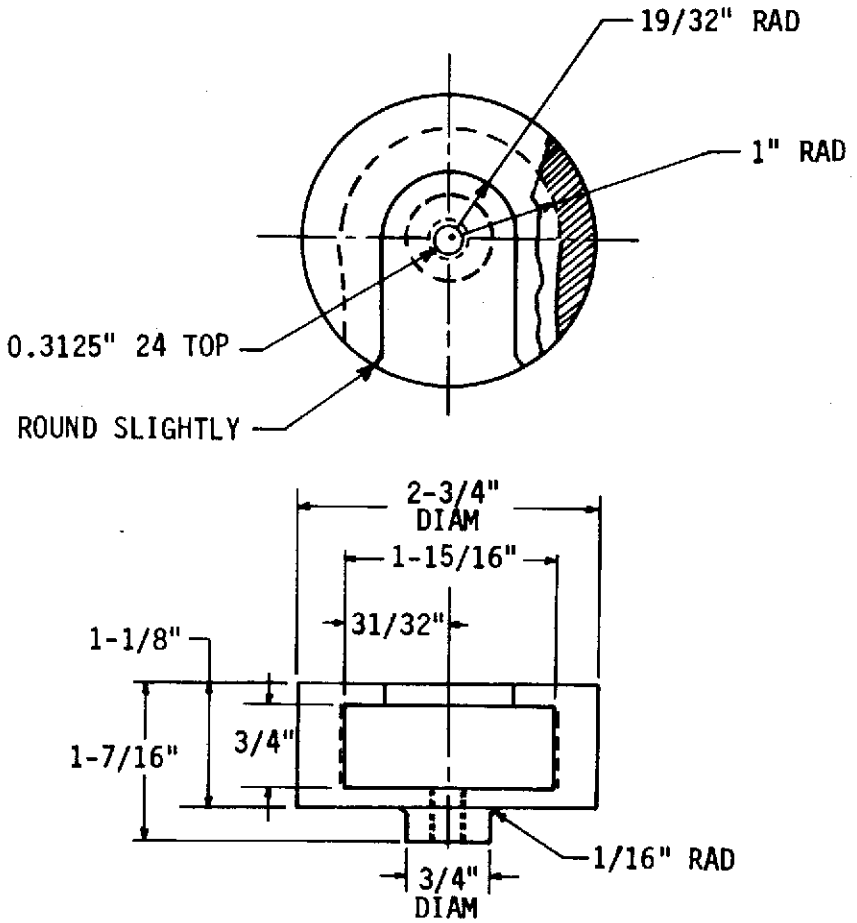

Figure 15.2.2.14-1. Corrosion Preventive Finish Test Grips (Cold-Rolled Steel)

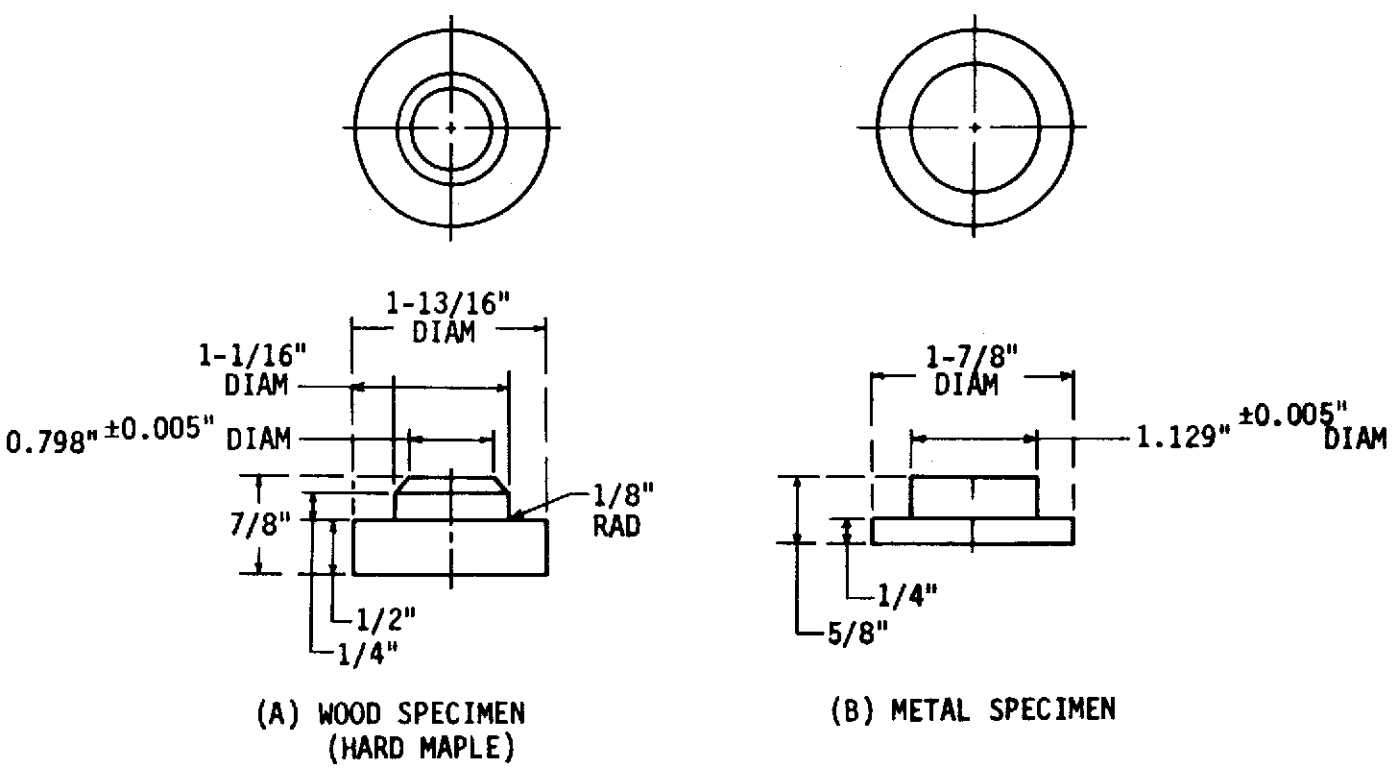

Figure 15.2.2.14-2. Tensile Test Specimens

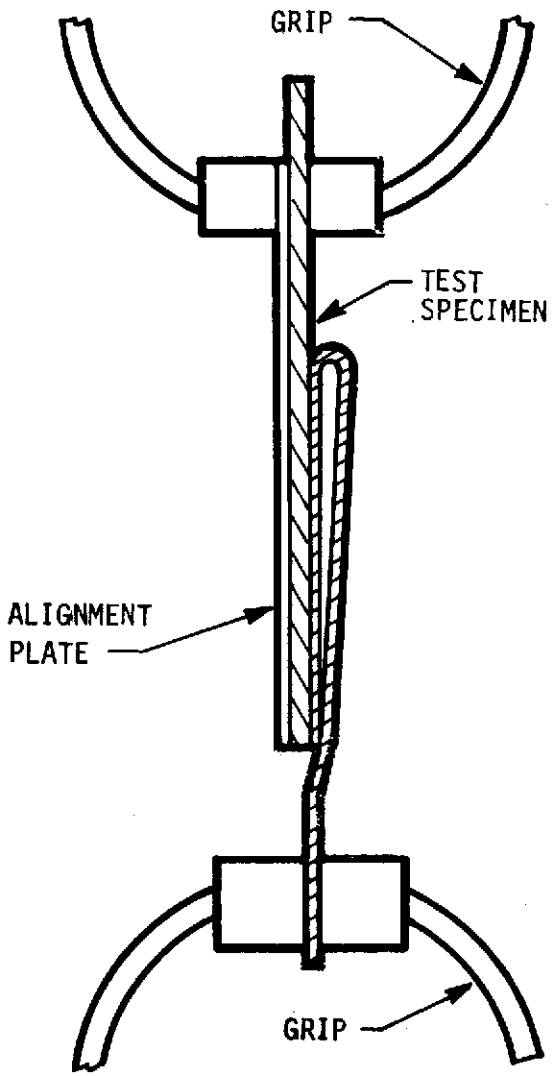

Figure 15.2.2.15-1. Specimen Under Test

15.2.2.16 Standard Method of Test for Bond Strength of Plastics

a. Overall Objective: This method of test covers determination of the bond strength or ply adhesion strength of sheet plastic.

b. Description:

1. Test Article: The specimen must consist of sheet material and be 2 inches square.

2. Test Conditions: Ambient air and relative humidity and test temperatures from -252 C (-423 F) to 537 C (1000 F).

3. Type of Data: Tensile strength in pounds per square inch. When applied to laminated plastics it is a measure of interlaminar or intralaminar strength. When applied to nonlaminated plastics the test is a measure of the cohesive strength of the material.

4. Test Equipment: Universal-type tensile test machine. Figure 15.2.2.16-1 shows a typical test assembly.

c. Materials Tested: Laminated and nonlaminated plastics.

d. Reference: ASTM D952.

15.2.2.17 Standard Method of Test for Bearing Strength of Plastics

a. Overall Objective: This method is intended for use in the determination of the bearing strength of rigid plastics in sheet or molded form.

b. Description:

1. Test Article: The specimen measures 1/8 or 1/4 inch in thickness by 2 inches wide and 5 inches in length. The distance from the center of the bearing hole to the edge of the specimen divided by the diameter of the hole is the edge distance ratio. (Figure 15.2.2.17-1).

2. Test Conditions: Ambient air and relative humidity, and test temperatures from -252 C (-423 F) to 537 C (+1000 F).

3. Type of Data: Bearing strength in pounds per square inch at 4 percent deformation of the hole diameter.

4. Test Equipment: Universal-type tensile test machine with strain recorder and a bearing-type extensometer.

c. Materials Tested: Laminated or molded, sheet or plate plastic materials.

d. Reference: ASTM D953.

15.2.2.18 Metal-to-Metal Lap Shear

a. Overall Objectives: This method is intended for determining the comparative shear strength of adhesives for bonding metals when tested on a standard specimen and under specified conditions of preparation and testing.

b. Description:

1. Test Article: Test specimens are usually overlapping 1-inch wide 4-inch long strips and 0.064 inch in thickness. The overlap is usually 1/2 inch.

2. Test Conditions: Testing is accomplished in the environment and temperature of the most rigid intended use of the end item. Test temperatures will range from -252 C (-423 F) to 537 C (1000 F).

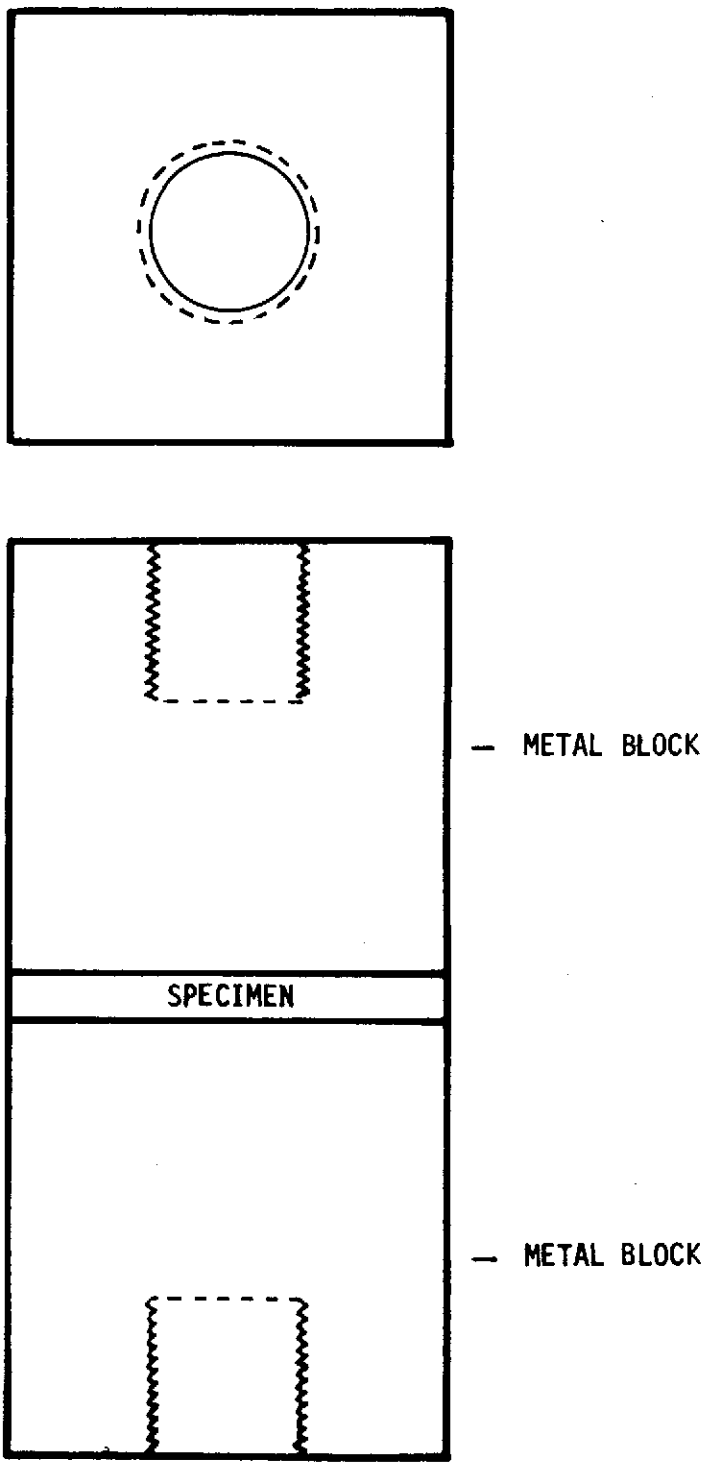

Figure 15.2.2.16-1. Test Assembly for Bond Strength Test

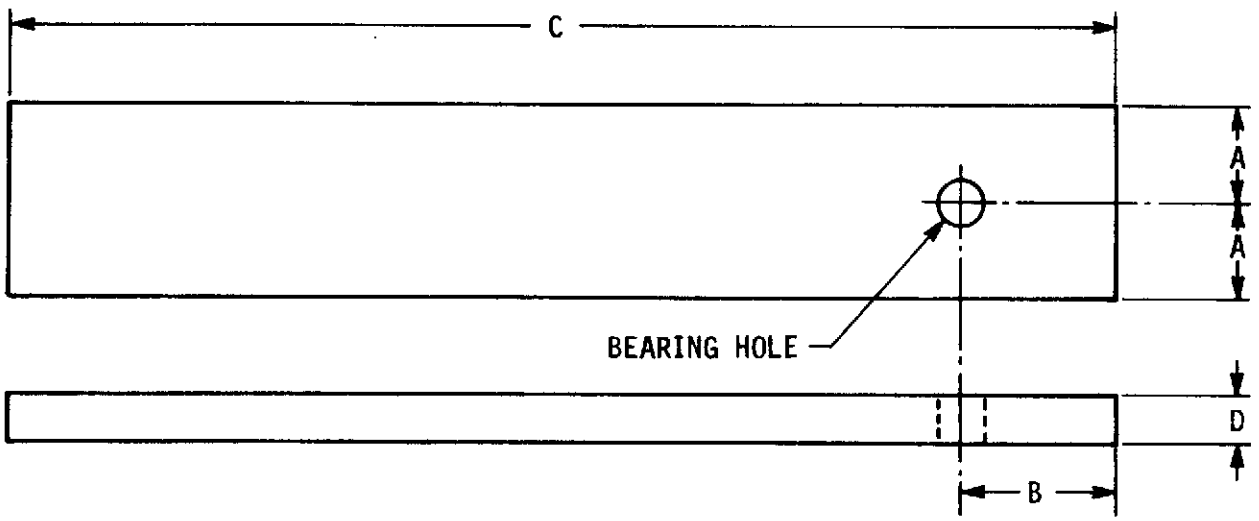

TYPE	DIMENSIONS, IN [α]				
	A	B	C	D	REAM HOLE TO
I.....	0.469 ± 0.005	0.750 ± 0.005	4-3/4	1/8	0.126 ± 0.001
II.....	0.469 ± 0.005	0.750 ± 0.005	4-3/4	1/4	0.251 ± 0.001

[α] ALL FRACTIONAL DIMENSIONS SHALL BE HELD TO PLUS OR MINUS 1/64 IN TOLERANCE

$$\text{EDGE DISTANCE RATIO} = \frac{B}{\text{HOLE DIAMETER}}$$

Figure 15.2.2.17-1. Dimensions of Bearing Strength Test Specimens

3. Type of Data: Includes load at failure, the nature and type of failure (cohesion in adhesive or metal, or adhesion) for each specimen, and the ultimate shear strength (psi).

4. Test Equipment: Test machine of 10,000-pound capacity; test setup is shown in Figure 15.2.2.18-1.

c. Materials Tested: Include all tape and paste adhesive systems (i.e., Lefkoweld 109, HT424, EP934).

d. Reference: ASTM D-1002.

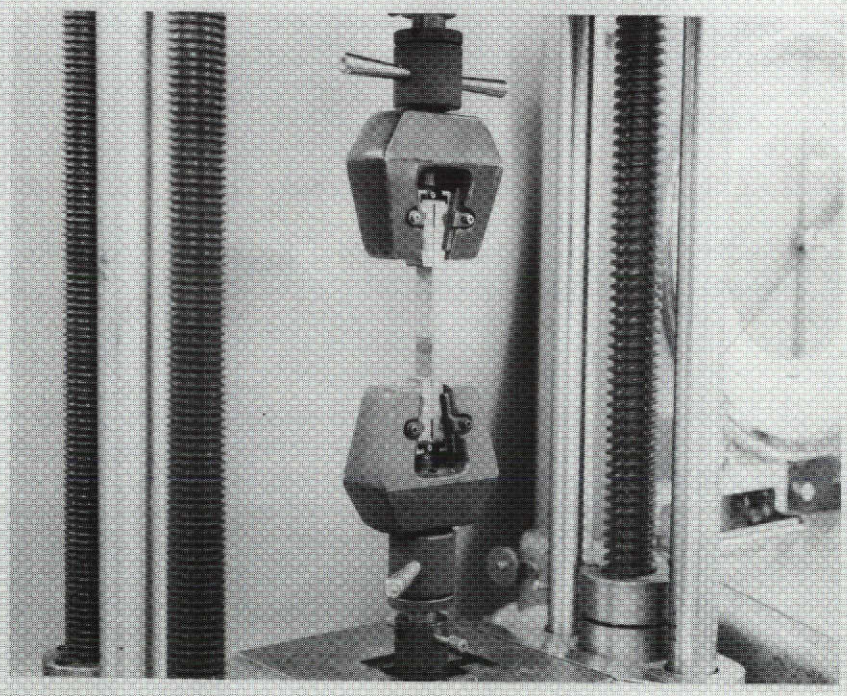

Figure 15.2.2.18-1. Lap Shear Test Set-Up

15.2.2.19 Flammability

a. Overall Objective: To determine the relative flammability of flexible plastic films or thin sheets relative to burning rate and self-extinguishing characteristics.

b. Description

1. Test Article: Free films of various coatings with dimensions of 3 inches by 9 inches.

2. Test Condition: Test at ambient conditions. Butane gas to be used as fuel and the igniter flame produced at tip of a No. 22 hypodermic needle jet 1/2 inch from film specimen held at 45 F.

3. Type of Data: Average burning rate in inches per second. Self-extinguishing or nonburning results.

4. Test Equipment: None.

c. Materials Tested: Polyurethane, vinyl, and hypalon.

d. Reference: ASTM D-1433.

15.2.2.20 Determination of Apparent Density of Rigid Cellular Plastics

a. Overall Objective: This method covers a procedure for determining the apparent density of cellular materials.

b. Description:

1. Test Article: The test specimen must be of a shape whose volume can be calculated and not less than 1 cubic inch in volume. The test specimen must be free from surface skin wherever possible.

2. Test Conditions: Test specimens must be conditioned per Procedure A of Methods of Conditioning Plastics and Electrical Insulating Materials for Testing, ASTM D618. Five specimens per sample are to be tested.

3. Type of Data: Apparent density, average value.

4. Test Equipment: Analytical balance and micrometer dial gauge.

c. Materials Tested: Rigid cellular plastics including urethane foams.

d. Reference: ASTM D1622.

15.2.2.21 Water Content of Urethane Foam Raw Materials

a. Overall Objective: This method covers a procedure for determining the percentage of water contained in the urethane foam components (polyols).

b. Description:

1. Test Article: A maximum of five grams of raw polyol.

2. Test Conditions: Gaseous nitrogen (20 to 50 cc per minute) ambient temperature.

3. Type of Data: Percentage of water by weight.

4. Test Equipment: Beckman KF-3 Aquameter

c. Materials Tested: Urethane foam raw materials (polyols).

d. Reference: ASTM D-1638.

15.2.2.22 Determination of Amine Equivalents and Hydroxyl Numbers of Urethane Foam Raw Materials

a. Overall Objective: These methods cover procedures for determining the amine equivalents and hydroxy numbers of urethane foam raw materials.

b. Description:

1. Test Article: Samples of the raw materials, isocyanate and polyol, taken from sealed containers as received from the vendor.

2. Test Conditions:

(a) Amine Equivalent - The isocyanate component is reacted with dibutylamine to form a urea. The excess amine is determined by back titration with hydrochloric acid.

(b) Hydroxy Number - The hydroxyl groups of the polymeric glycol or ester are acetylated with a solution of acetic anhydride in pyridine. The excess reagent is decomposed with water and the acetic acid formed is titrated with standard sodium hydroxide solution.

3. Type of Date: Average values for hydroxyl number and amine equipment.

c. Materials Tested: Urethane foam raw materials.

d. Reference: ASTM D1638.

15.2.2.23 Moisture Vapor Permeability

a. Overall Objective: To determine the rate at which moisture will pass through coating films.

b. Description:

1. Test Article: Free films of various coatings. Specimen to be circular disc approximately 3-1/4-inch diameter and thickness of film to be specified.

2. Test Condition: At 25 $\pm$ 1 C. Inside the permeability cup R.H. to be 100 percent. Outside of cup to be phosphorous pentoxide dessicant atmosphere.

3. Type of Data: Specific permeability (gm. - mm/day - sq.m.).

4. Test Equipment: Permeability cut, low-humidity chamber.

c. Materials or Systems Tested: Hypalon, vinyl, polyurethane, butyl, acrylic, and Saran.

d. Reference: ASTM D-1653.

15.2.2.24 Flammability of Plastic Foams and Sheeting

a. Overall Objective: This method covers a procedure for comparing the relative flammability of plastic foams and sheeting materials.

b. Description:

1. Test Article: One specimen, 0.5 by 2 by 6 inches.

2. Test Conditions: Ambient air relative humidity, and temperature.

3. Type of Data: Classification of the material as "non-burning by this test," "self-extinguishing by this test," or "burning by this test." Extent of burning when a material is reported as "self-extinguishing by this test," and also the apparent cause such as melting, dripping, or smothering. The burning rate of the material (inches per minute) when it is reported "burning by this test." Density (pounds/cubic feet) of material.

4. Test Equipment: None; test setup is shown in Figure 15.2.2.24-1.

c. Materials Tested: Urethane foam.

d. Reference: ASTM D-1692.

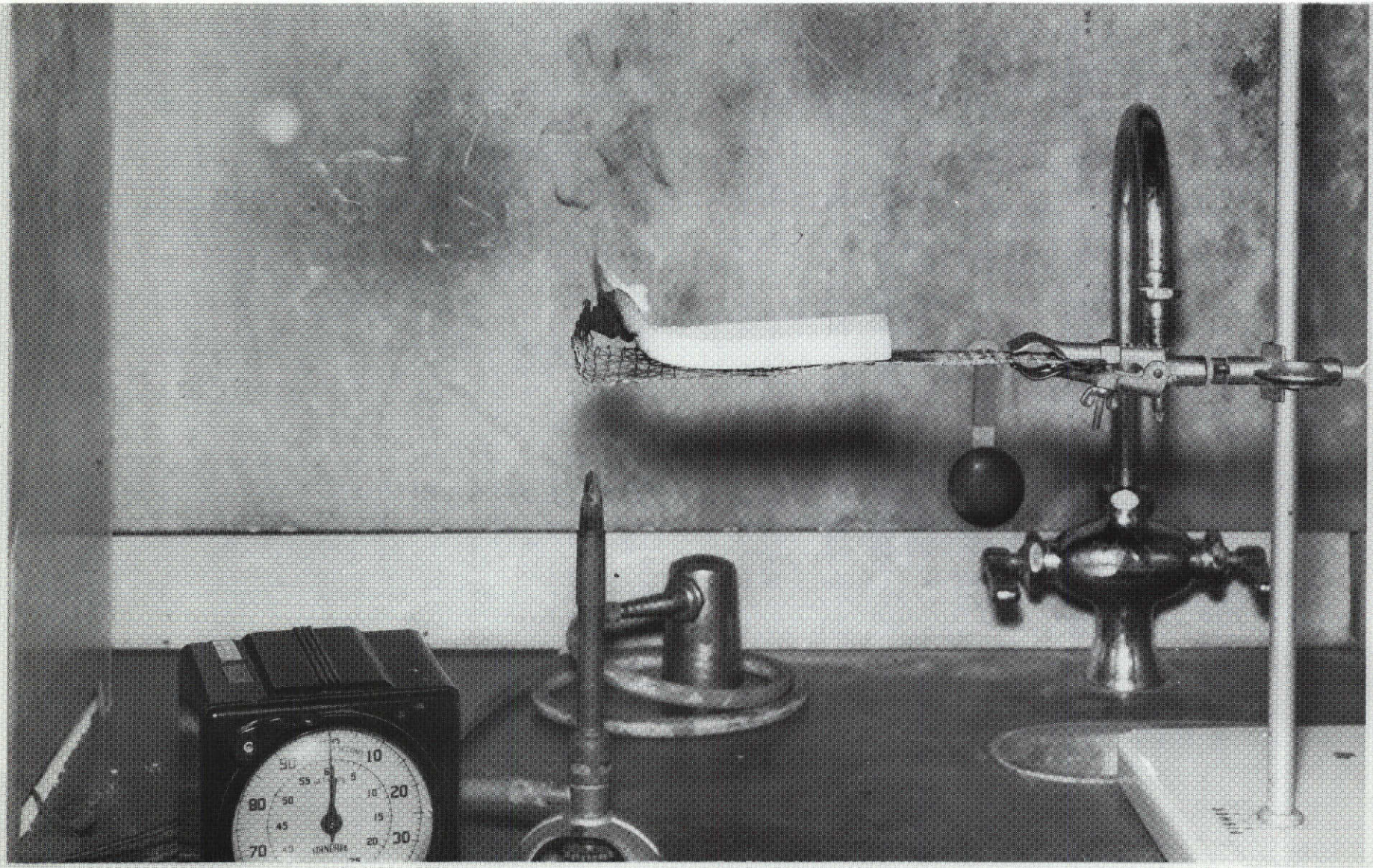

Figure 15.2.2.24-1. Test Set-Up and Flammability Test Apparatus

15.2.2.25 Peel Testing of Adhesives With the Climbing Drum Method

a. Overall Objective: This method is used for determination of the relative peel resistance of adhesive bonds between a relatively flexible adherend and a rigid adherend.

b. Description:

1. Test Article: The test specimen is 3 inches wide by 12 inches long, including a 1-inch overhang of the flexible adherend at one end. The rigid adherend may consist of metal plate or a sandwich construction. Five specimens are tested for each adhesive, type of preconditioning, or special preparation, and for each test temperature. An autographic recording of peeling load versus peeling distance is obtained.

2. Test Conditions: Conditioning is not required for laminated assemblies containing only metal adherends. Special conditioning may apply, in which case it is defined. Peel testing may be performed at test temperatures from -252 C (-423 F) to 260 C (500 F).

3. Type of Data: The test report includes adhesive identification, specimen dimensions, type of failure (adhesive or cohesive), and the average peel torque in inch-pounds per inch of width for each specimen.

4. Test Equipment: Test machine is a 10,000-pound capacity Riehle; the test setup is shown in Figure 15.2.2.25-1.

c. Materials Tested: This method of test is intended for use in providing peel strength properties of paste and adhesive tape systems when a flexible adherend is bonded to a rigid metal or sandwich type structure.

d. References: ASTM D-1781.

15.2.2.26 Method of Test for Peel Resistance of Adhesives (T-Peel Test)

a. Overall Objective: This method is used in determination of the relative peel resistance of adhesive bonds between flexible adherends.

b. Description:

1. Test Article: The test specimen consists of two flexible adherends 1 inch wide and 12 inches long. Approximately 9 inches of the length is prepared and bonded per test requirements. The 3-inch unbonded end is bent apart for clamping in grips of a test machine. Five specimens are tested for each type of adhesive or test temperature.

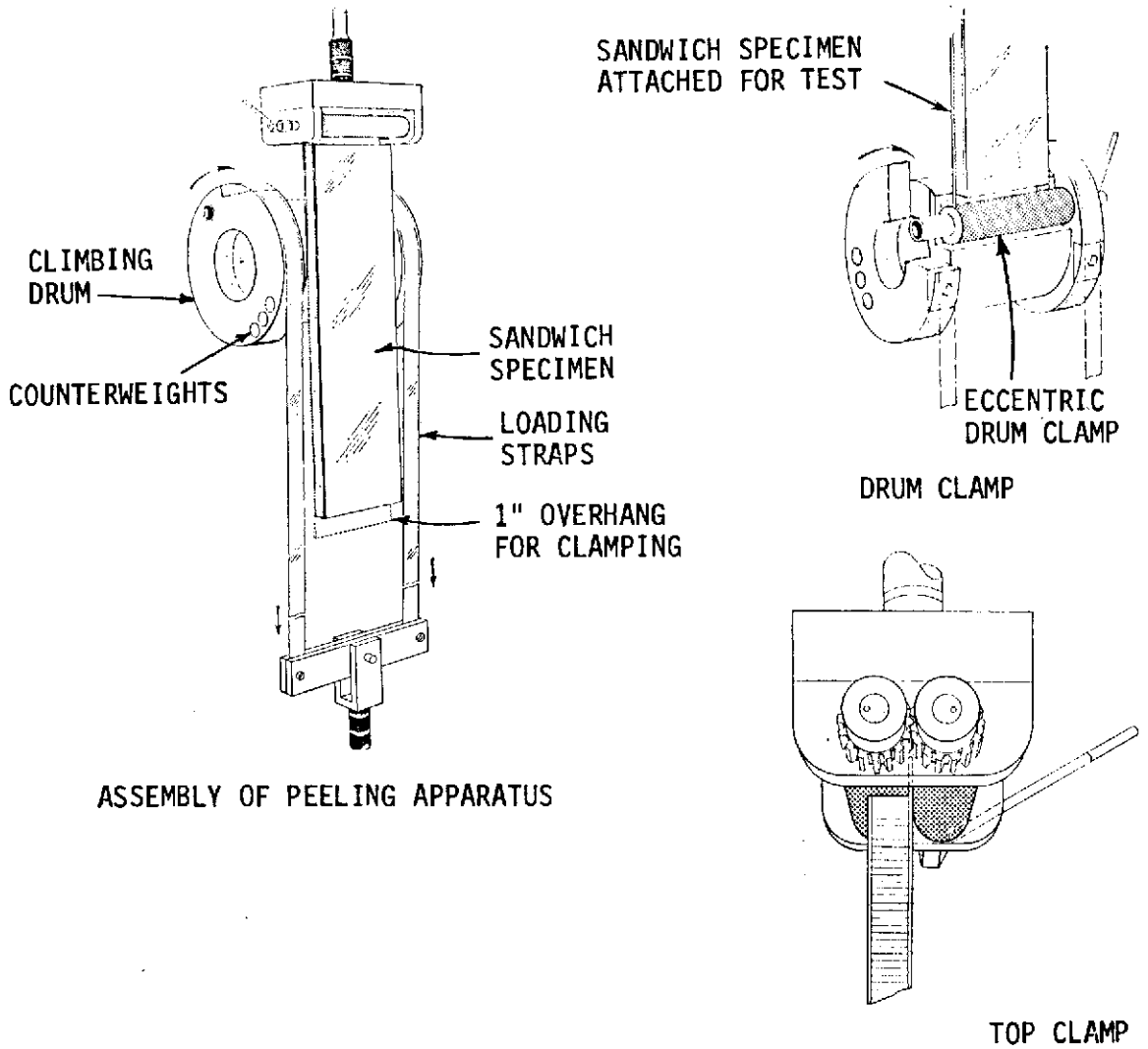

Figure 15.2.2.25-1. Test Set-Up, Peel Testing of Adhesives with the Climbing Drum Method

2. Test Conditions: Conditioning is not required for laminated assemblies consisting of metal adherends only. Pell strength may be determined in the temperature range of -252 C (-423 F) to 537 C (1000 F). An autographic recording of peeling load versus peeling distance is provided.

3. Type of Data: The test report includes identification of the adhesive and adherends specimen dimensions, conditioning, type of failure (adhesive or cohesive), and the average T-peel strength in pounds per inch of width for each specimen.

4. Test Equipment: A 10,000-pound Riehle test machine or equivalent; a test specimen is shown in Figure 15.2.2.26-1.

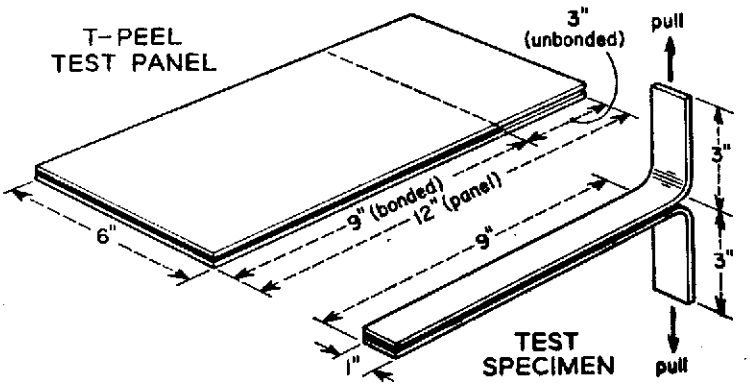

Figure 15.2.2.26-1. Test Panel and Test Specimen

c. Materials or Systems Tested: This method of test is intended for use in providing peel strength data on paste and tape adhesive systems.

d. References: ASTM D-1876.

15.2.2.27 Porosity of Rigid Cellular Plastics

a. Overall Objective: This method covers a procedure for determining a numerical value for the percentage of volume occupied by closed cell, open cell, and cell walls of cellular urethane foam insulation.

b. Description:

1. Test Article: One specimen, 0.8 by 3 inches.

2. Test Conditions: Ambient air, relative humidity, and temperature.

3. Type of Data: Percentage of closed cells and apparent density (pounds/cubic feet) values.

4. Test Equipment: None, laboratory test setup

c. Materials Tested: Urethane foam and flexible foam.

d. Reference: ASTM-D-1940.

15.2.2.28 Water Absorption of Rigid Cellular Plastics

a. Overall Objective: This method covers a procedure for determining the absorption of water of cellular urethane foam insulation when immersed under a 2-inch head of water.

b. Description:

1. Test Article: One specimen, 1 by 4 by 4 inches.

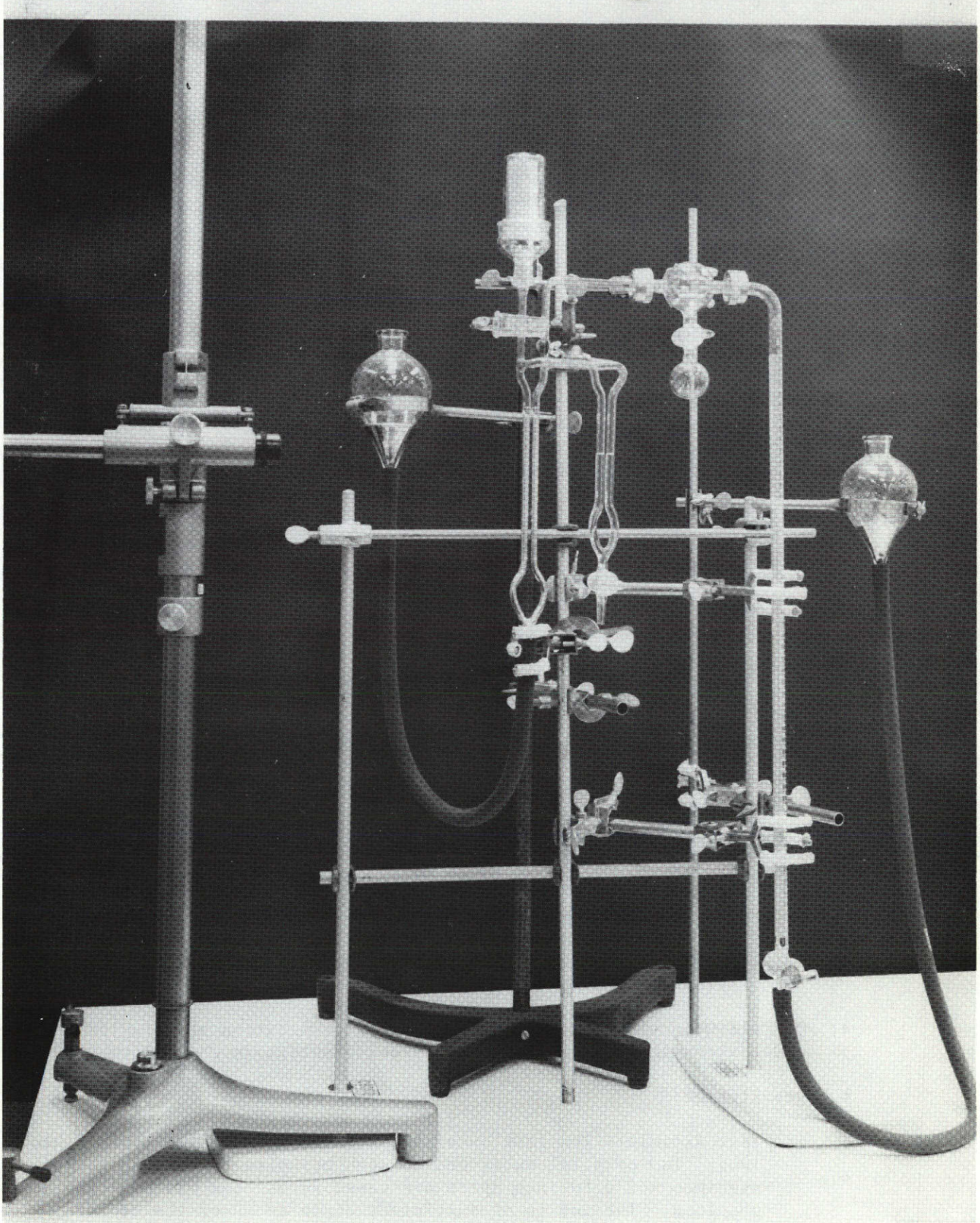

Figure 15.2.2.27-1. Test Set-Up, Porosity of Rigid Cellular Plastics

2. Test Conditions: Immersed under a 2-inch head of water for a period of 24 hours. Water at ambient temperature.

3. Type of Data: The amount of water absorbed by the specimen during the immersion per unit area (gram/1000 square centimeter and pounds/ square feet), also, per unit volume (gram/1000 cubic centimeter).

4. Test Equipment: The test setup is shown in Figure 15.2.2.28-1.

c. Materials Tested: Urethane foam.

d. Reference: ASTM D-2127.

15.2.2.29 Standard Method of Test for Apparent Horizontal Shear Strength of Reinforced Plastics by Short Beam Method

a. Overall Objective: This method covers the determination of the apparent horizontal shear strength of parallel fiber-reinforced plastics.

b. Description:

1. Test Article: The specimen is 0.250 inch wide by 6.35 inches long and 0.125 inch thick.

2. Test Conditions: Ambient air, relative humidity, and test temperature from -252 C (-423 F) to 537 C (1000 F).

3. Type of Data: The apparent shear strength in pounds per square inch.

4. Test Equipment: Universal-type tensile test machine and shear test fixture (Figure 15.2.2.29-1).

c. Materials Tested: Reinforced plastics.

d. Reference: ASTM D2344.

15.2.2.30 Method of Test for Interlaminar Shear Strength of Reinforced Plastic Structures

a. Overall Objective: This method is for determination of interlaminar shear strength of structural reinforced plastics in sheet form.

b. Description:

1. Test Article: The test specimen measures 1 inch wide by 8 inches long. Two parallel cuts, one on each opposite face of the specimen and 0.50 inch apart are sawed across the width of the specimen. The cut is of sufficient depth to sever the center lamina located midway between the two faces of the laminate. Side supporting plates are attached over the center of the specimen to prevent peeling effect on loading (Figure 15.2.2.30-1).

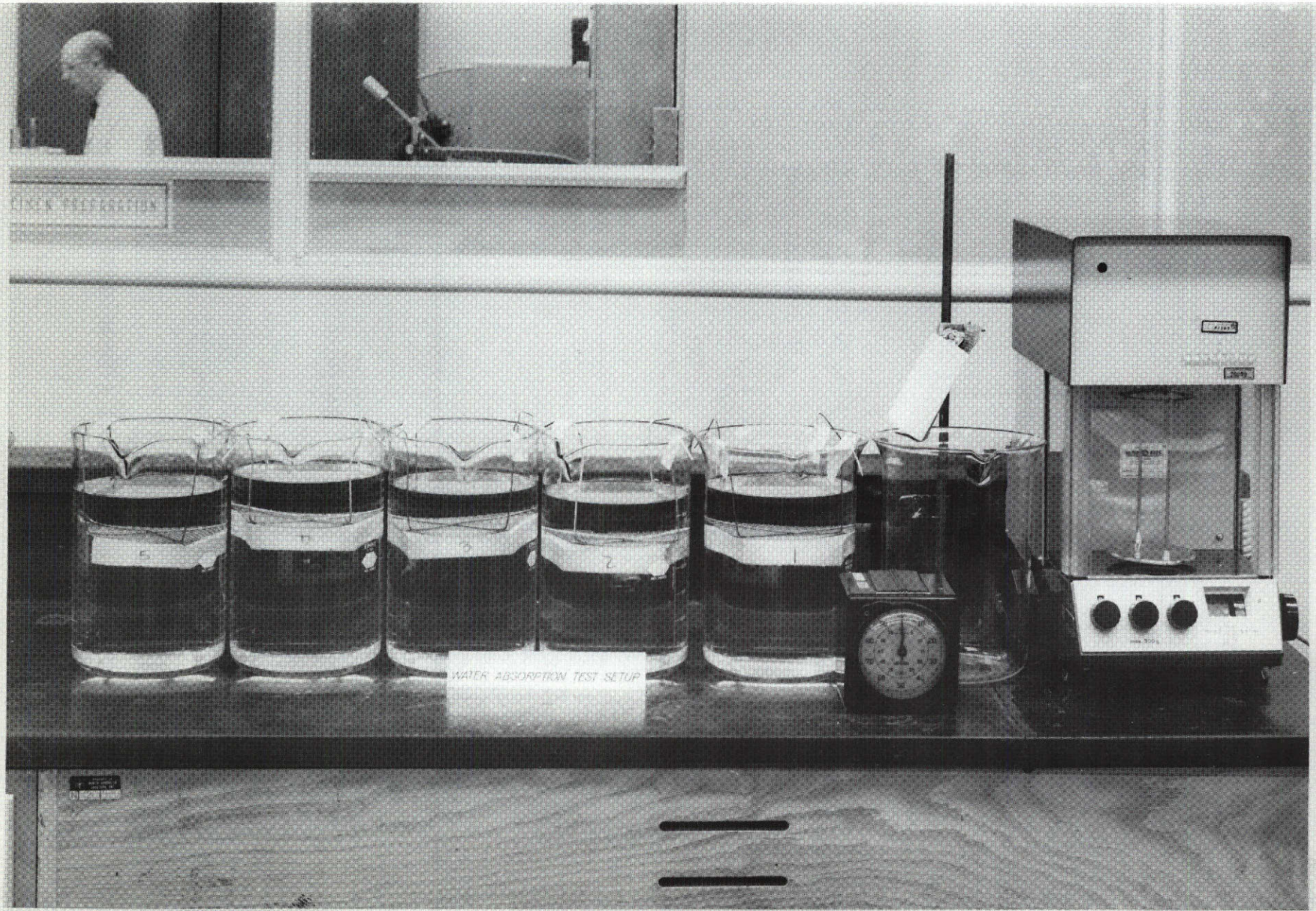

Figure 15.2.2.28-1. Test Set-Up, Water Absorption of Rigid Cellular Plastics

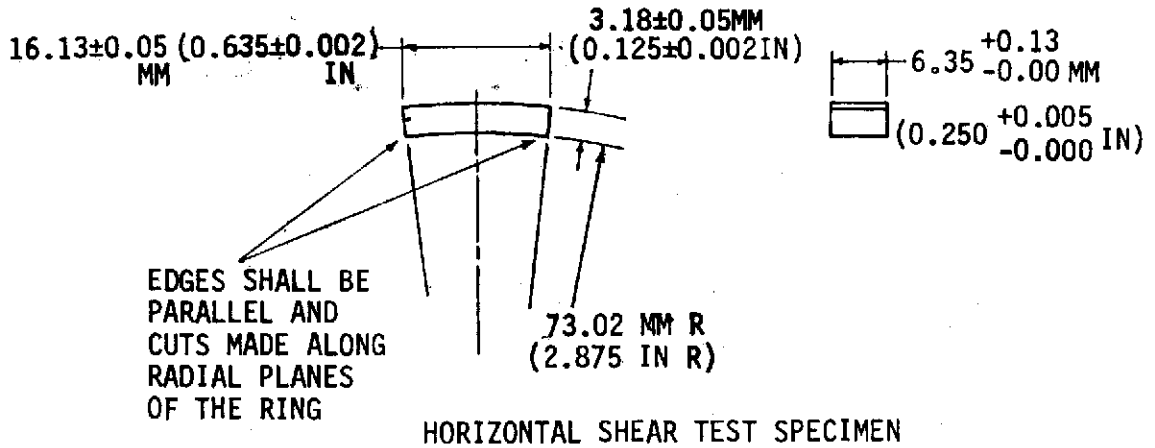

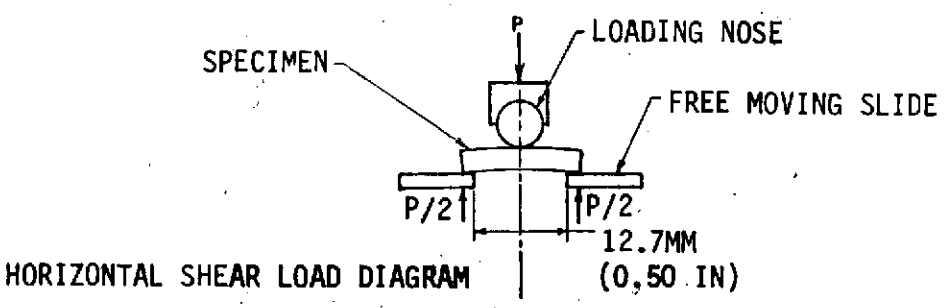

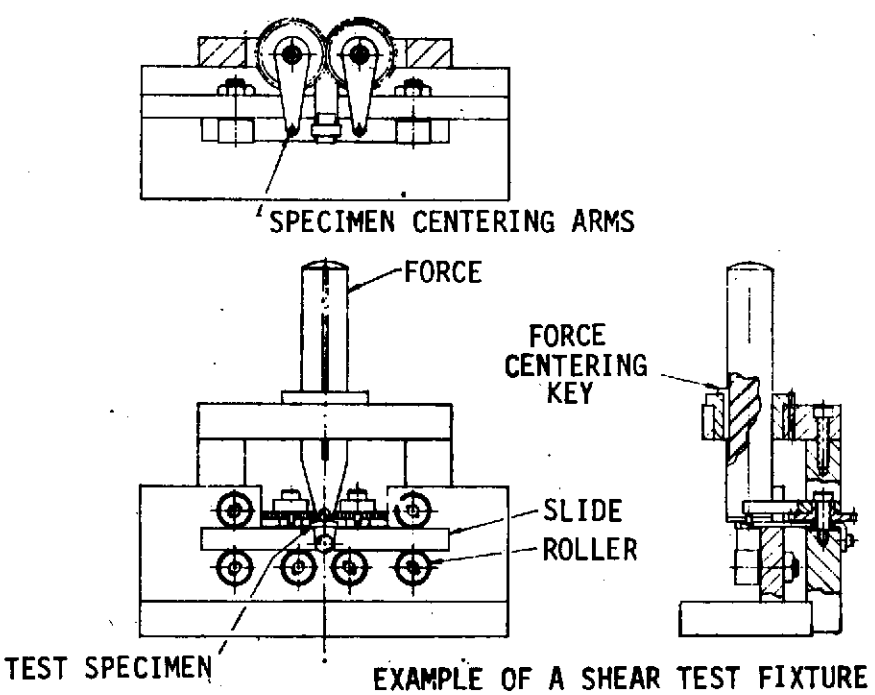

Figure 15.2.2.29-1. Sheat Test Fixtures

The specimens are inserted in grips and loaded in a universal-type testing machine. Five specimens are tested per material or test condition.

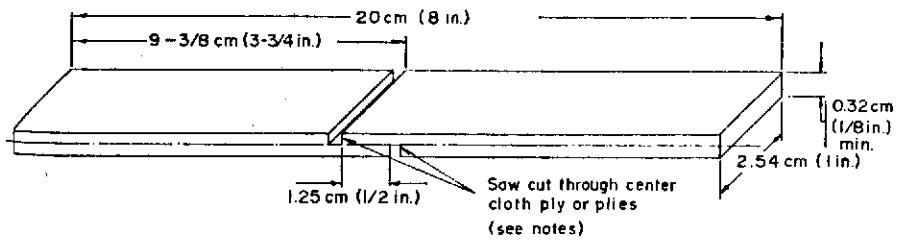

NOTE 1—Saw cuts must be parallel within 0.08 cm (0.030 in.).
NOTE 2—Depth of saw cut shall be as follows:
(a) ½ laminate thickness plus thickness of 1 ply, or
(b) ½ laminate thickness plus 0.01 cm (0.005 in.) or minus 0, if thickness per ply or number of plies unknown.

Figure 15.2.2.30-1. Test Specimen

2. Test Conditions: Interlaminar shear properties may be determined at test temperatures from -184 C (-300 F) to +537 C (1000 F). Test specimens are preconditioned if required per Procedure B of ASTM D618.

3. Type of Data: The test report includes identification of test materials, preparation and conditioning procedures, specimen dimensions, and the calculated interlaminar shear strength in pounds per square inch of area.

4. Test Equipment: A 10,000-pound capacity Riehle test machine or equivalent.

c. Materials Tested: This method of test is used on structural reinforced plastics in sheet form with a minimum thickness of 0.125 inch.

d. Reference: ASTM D2345.

15.2.2.31 Monostrain Testing of Plastics, Adhesives, and Foam Materials

a. Overall Objective: The object of this type of testing was to provide the physical properties in tension of organic materials. The specific organic material was tested excluding foreign metallic attachment details.

b. Description:

1. Test Article; One specimen 27 inches long and 1 inch wide. The actual configuration is shown in Figure 15.2.2.31-2.

2. Test Conditions: -184 C (-300 F) to 427 C (800 F).

3. Type of Data: Thermolelastic modulus, Young's modulus, thermolelastic contraction, free contraction, ultimate tension strength, percent of elongation, and coefficient of thermal expansion. Thermolelastic modulus and contraction measurements

are determined on those materials that exhibit viscoelastic effect (relaxation of load in a test specimen with no change in strain).

4. Test Equipment: A test machine of 10,000-pound capacity Riehle, load cell of 20-pound capacity; a cold chamber of -300 F capability, a dial gauge (0.0001), and an extensometer system for recording load versus deflection. The test setup is shown in Figure 15.2.2.31-1.

c. Materials Tested: Laminates, honeycomb composites, foam, adhesive, adhesive primers, and aluminized Mylar.

d. Reference: M&P Procedure 3330-001.

15.2.2.32 Accelerated Weathering

a. Overall Objective: To determine the resistance of coatings to the effect of weather elements under accelerated condition of light and water spray cycles.

b. Description:

1. Test Article: Various coatings on metallic and nonmetallic substrates for exterior use. Dimensions to be specified.

2. Test Condition: Total number of exposure cycles or hours to be specified. Each cycle is two hours, consisting of 102 minutes of light without water and 18 minutes of light with water spray.

3. Type of Data: Chalking, blistering, crazing, chipping discoloration, adhesion failure.

4. Test Equipment: Weathering machine (Atlas Model XW-R Weatherometer)

c. Materials or Systems Tested: Polyurethane, acrylic, vinyl, Hypalon.

d. Reference: Federal Test Method STD No. 141, Method 6152.

15.2.2.33 Structural Verification Testing of Insulation System With Combined Environments (30 by 30 Test Tank)

a. Overall Objective: This method covers the procedure for verifying the structural integrity of liquid hydrogen tankage sidewall insulation system and closeout configurations during simulated ground hold and flight conditions. The test consists of exposing the insulation system to repetitive fill and drain cycles with liquid hydrogen and exposure to aerodynamic heat and pressure profiles while vibrating the insulation system at liquid hydrogen temperatures.

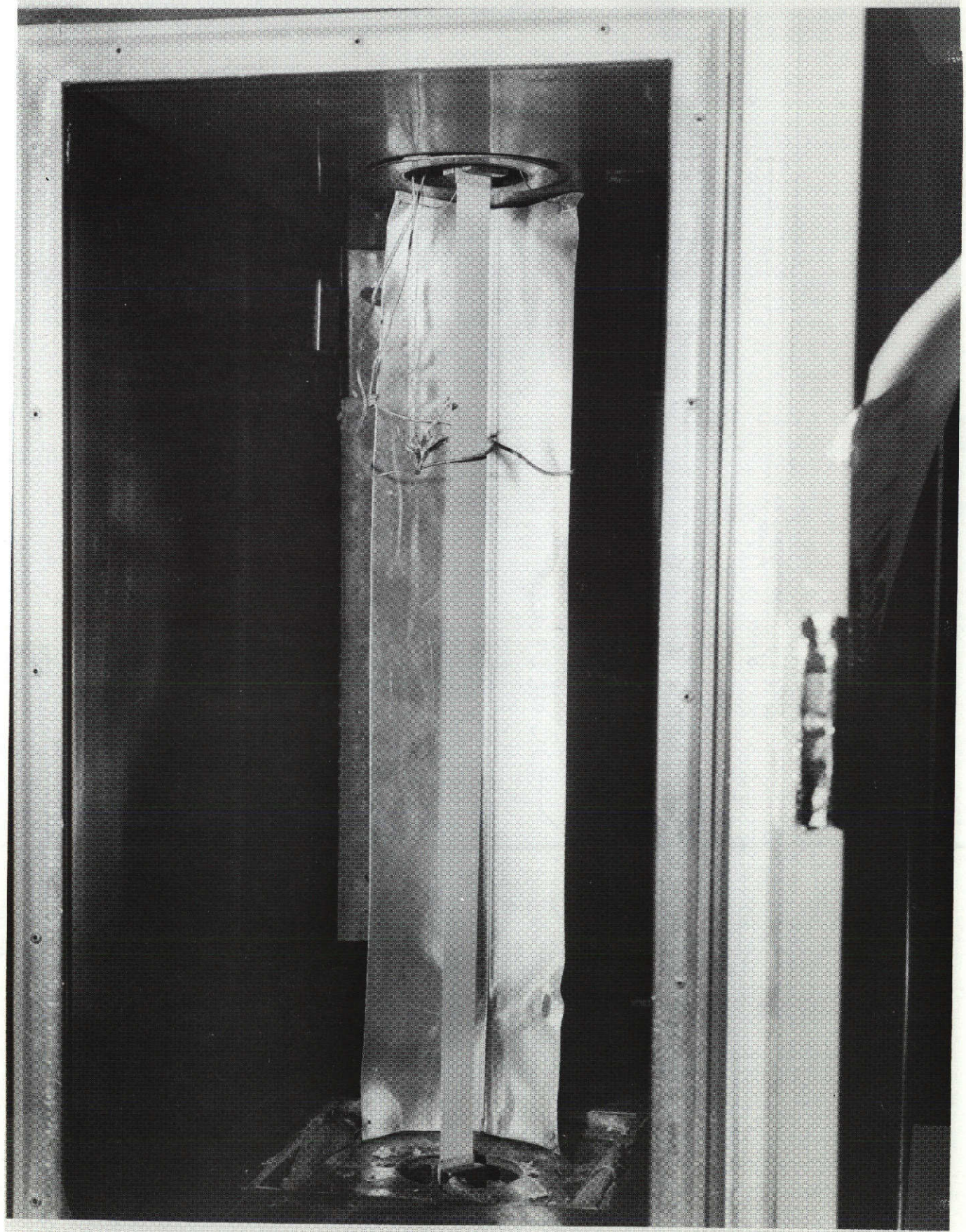

Figure 15.2.2.31-1. Test Set-Up, Monostrain Testing of Plastics, Adhesives and Foam Materials

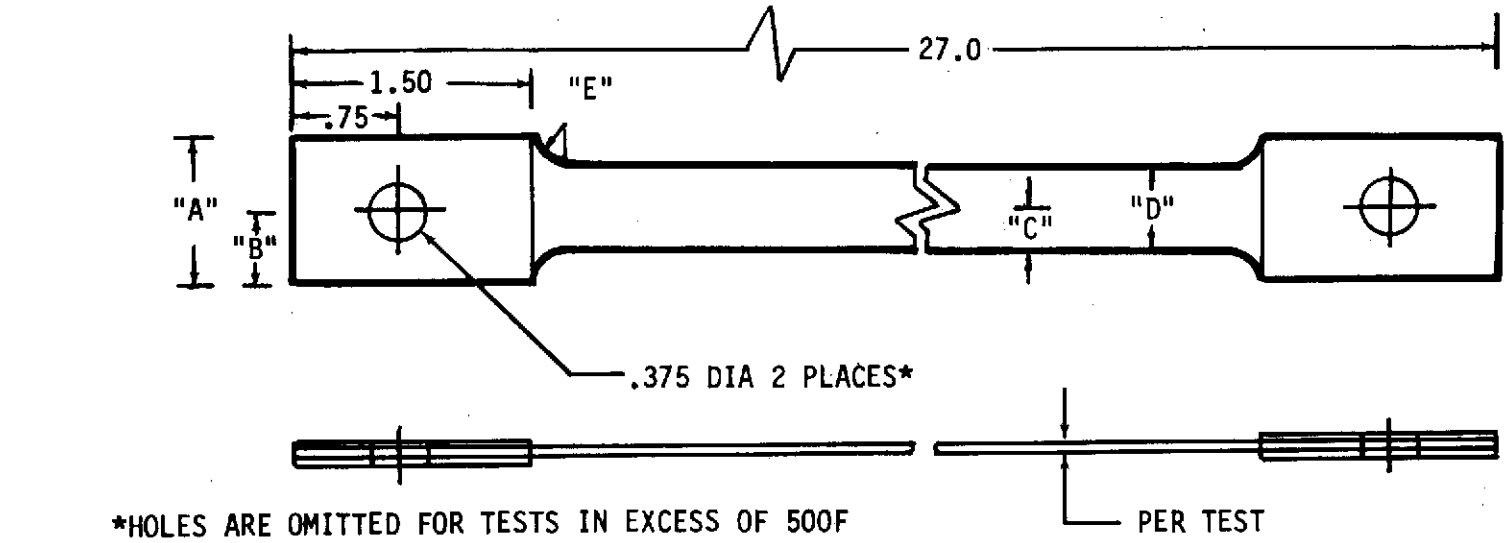

TYPE 3 SPECIMENS ONLY

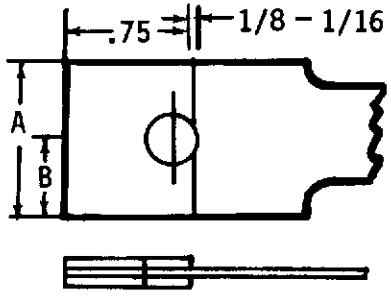

	"A"	"B"	"C"	"D"	"E"
TYPE 1	1.00	.50	.50	1.00	0
TYPE 2	1.00	.50	.37	.75	.25
TYPE 3	1.50	.75	.50	1.00	

Figure 15.2.2.31-2. Configuration of Monostrain Specimen

b. Description:

1. Test Article: The insulation system test specimen shall be 24 by 24 inches bonded to the 198 inch radius face of the 30 by 30-inch test tank. (Figure 15.2.2.33-1).

2. Test Conditions: Testing is accomplished in the environment and temperature of the most rigid intended use of the insulation system. Test temperatures will range from -423 to 550 F, pressure from ambient to 8 psig and vibration levels to 0.61 g^2/cp.

3. Type of Data: Data include insulation system temperature during all test phases and time-based profile of pressures and temperatures during simulated flight. During vibration, response characteristics of tank-mounted accelerometers are recorded.

4. Test Equipment: Shaker system, radiant heat equipment, and tankage with necessary controls and equipment (Figure 15.2.2.33-2).

c. Materials Tested: Honeycomb, purged and evacuated insulation, and foam insulation system.

d. Reference: SID 66-361.

15.2.2.34 Freon Content of Freon-Blown Urethane Foams

a. Overall Objective: This method covers a procedure for determining the weight percent Freon present in Freon-blown urethane foams.

b. Description:

1. Test Article: Test samples are taken randomly from production runs. Sheets 1 to 3-mils thick are cut from the samples using a microtome. Analysis specimens are disks approximately 0.5 inch in diameter. Three runs are made per foam sample.

2. Test Conditions: The specimens are weighed to within 0.1 milligram and then crushed at high pressure in a purge stream of helium. The gas is led into a gas chromotograph for analysis. Weight percentage is calculated using the perfect gas law and the peak area of the chromotogram. Instrument calibration is carried out using a Freon in helium gas standard.

3. Type of Data: Weight percentage of Freon.

4. Test Equipment: NR-designed and built gas chromotograph and sampling system.

c. Materials Tested: Freon-blown urethane foams.

d. Reference: NR Specification MB0130-077.

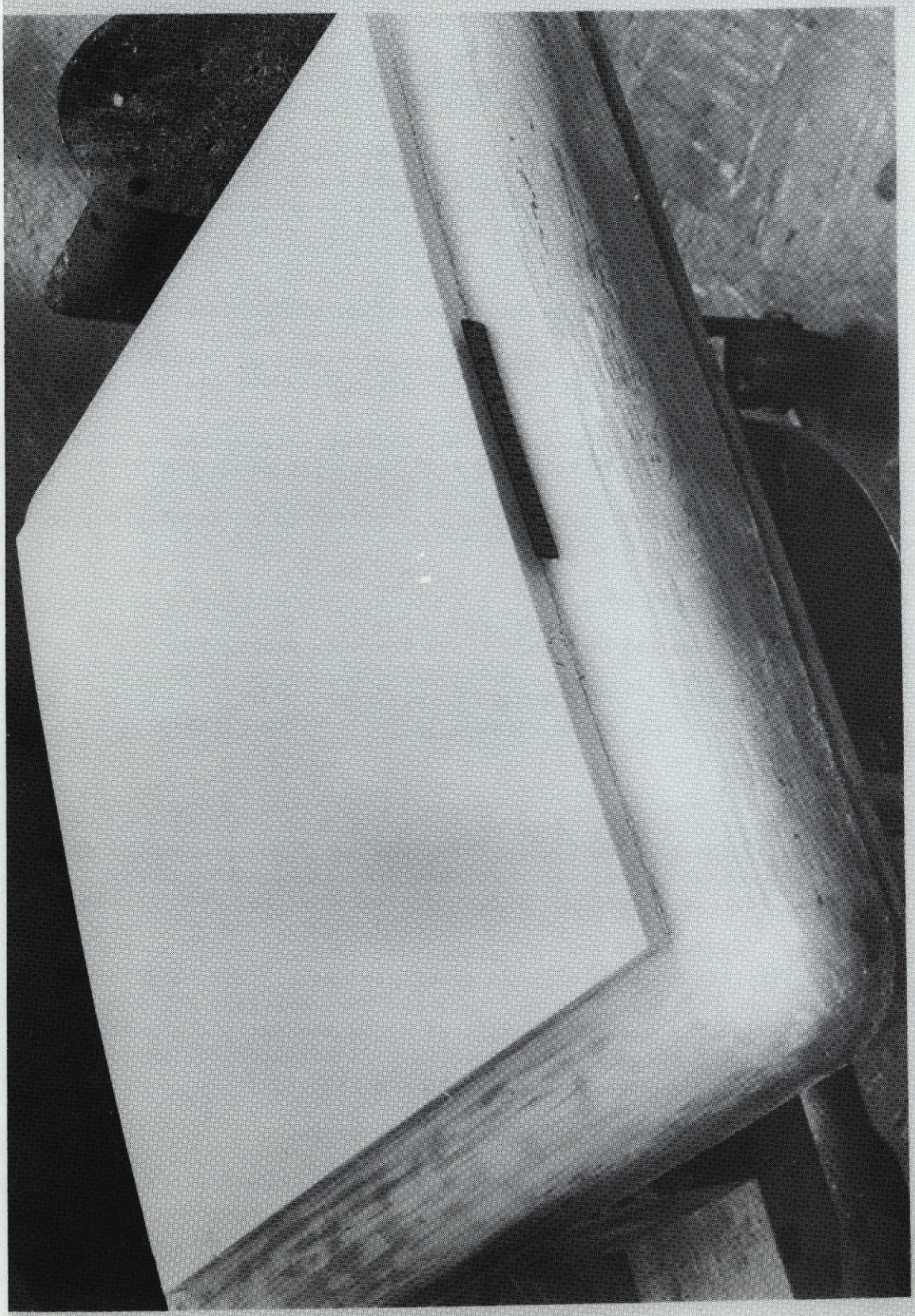

Figure 15.2.2.33-1. Typical Test Specimen Test Tank With Foam Installed After Sanding to 1/2 Inch Thickness

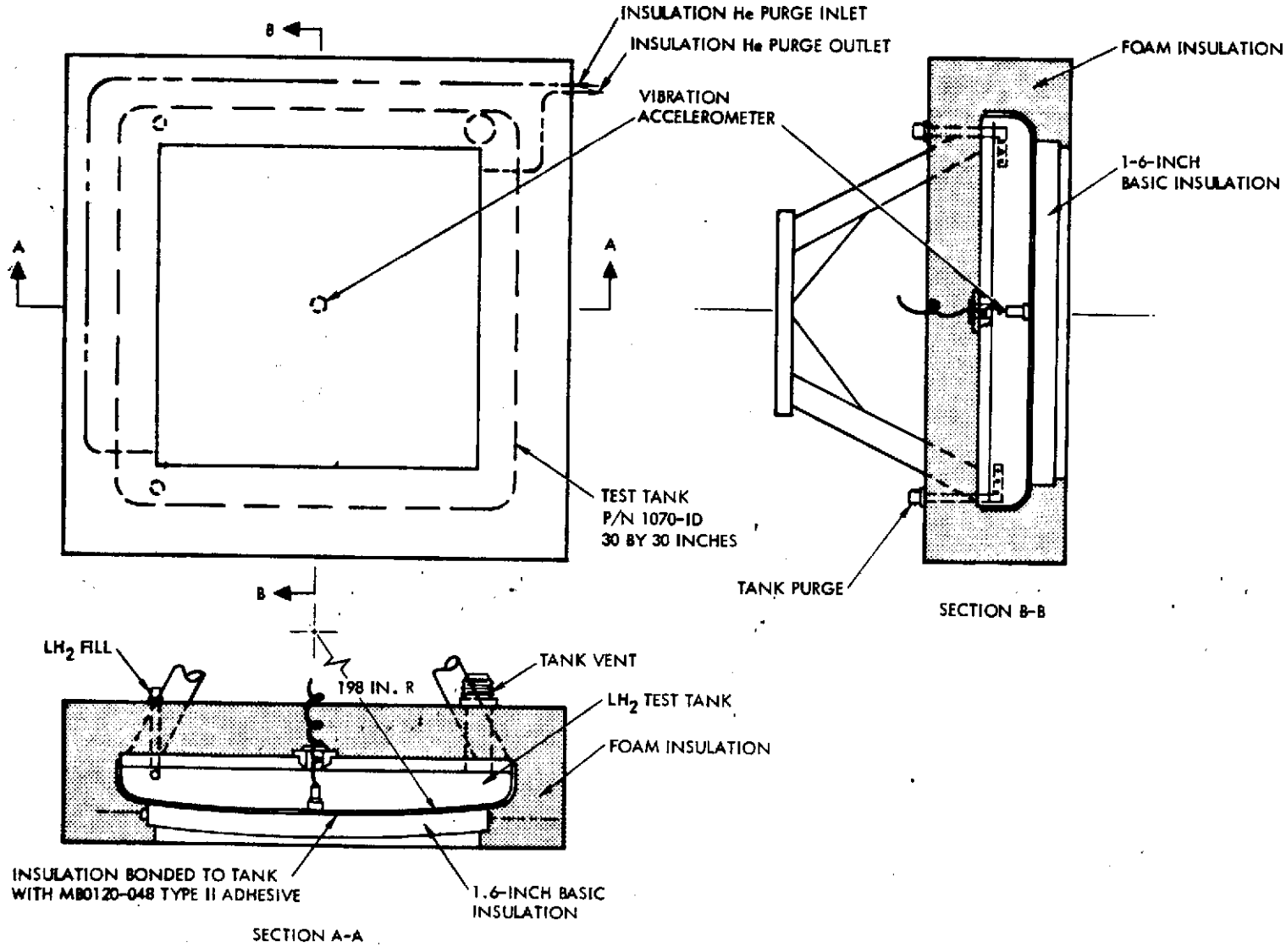

Figure 15.2.2.33-2. Schematic of Test Set-Up for Panel 237

15.2.2.35 Thermal Properties Evaluation of Insulation System for Liquid Hydrogen Tank Sidewall (Round Guarded Tank)

a. Overall Objective: This method covers the procedure for determining the thermal conductivity, K, of insulation systems designed for liquid hydrogen sidewall application. The test consists of exposing the tank side of the insulation to liquid hydrogen and measuring the loss of hydrogen due to heat flux through the insulation.

b. Description:

1. Test Article: The insulation system test specimen is 17 inches in diameter bonded to the common face of a 4-gallon tank shrouded by a 20-gallon test tank (Figures No. 15.2.2.35-1 through -4).

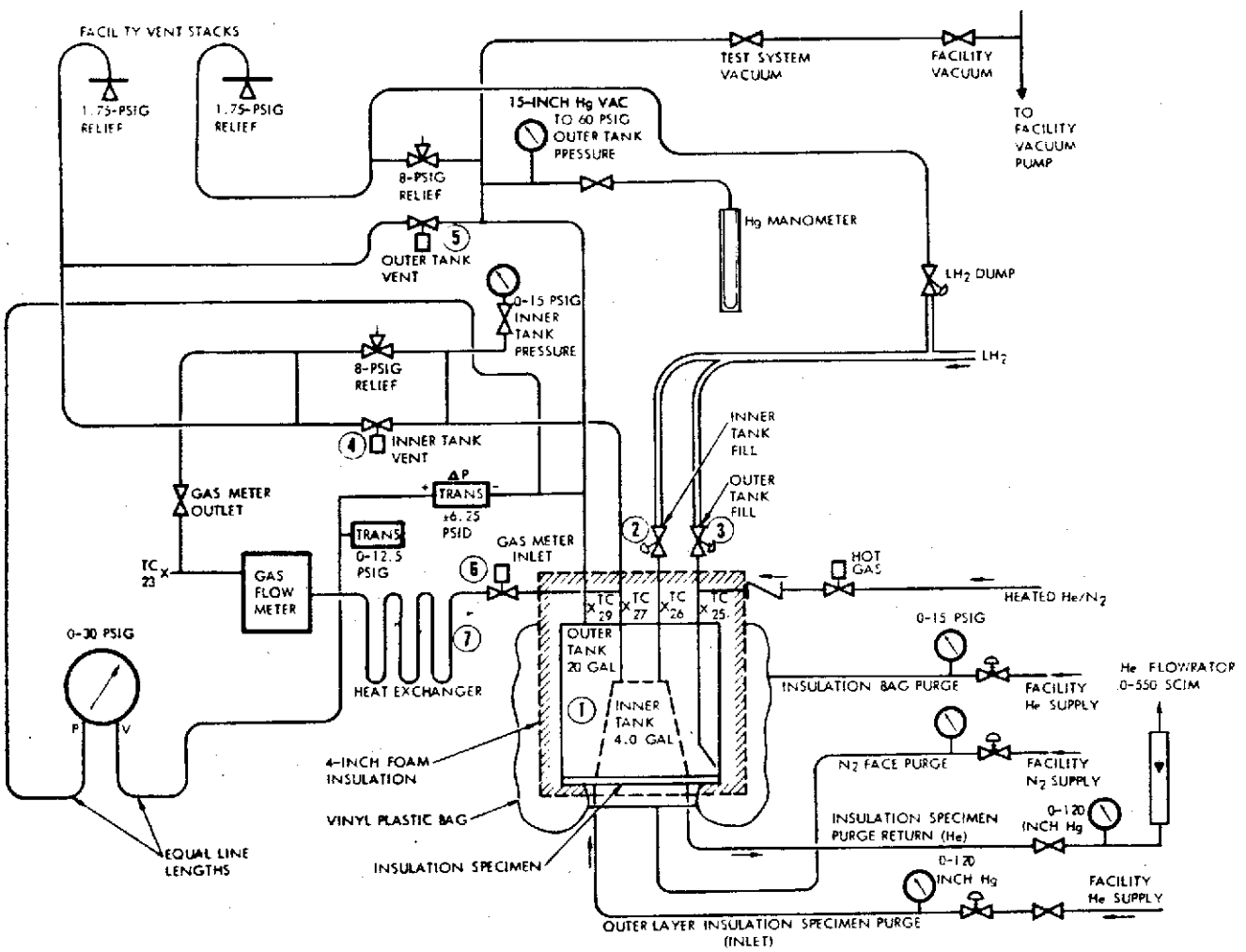

Figure 15.2.2.35-1. Test Systems Schematic

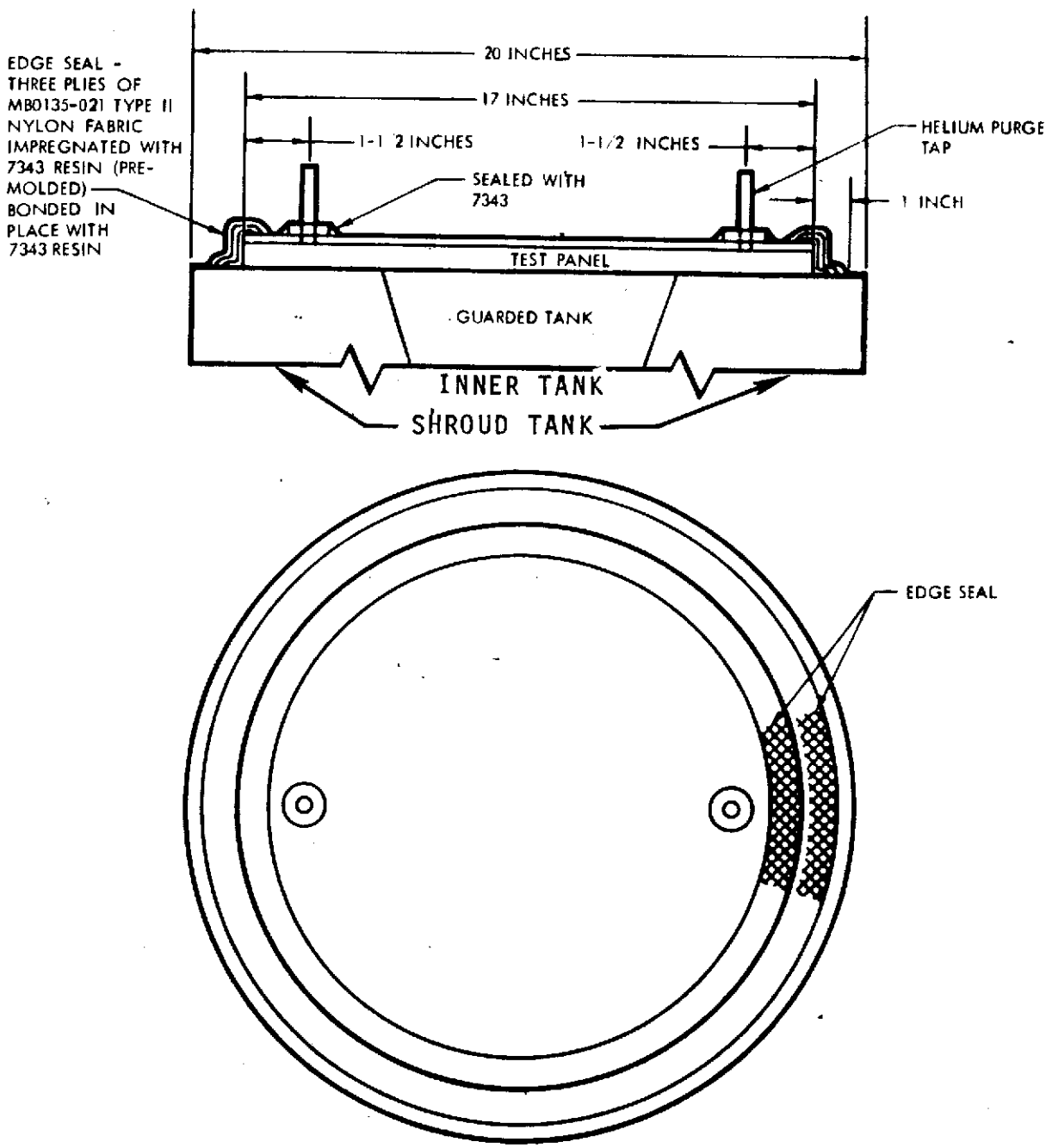

Figure 15.2.2.35-2. Insulation Panels Bonded to Test Tank for Cryogenic (LH_2) Thermal Conductance Tests

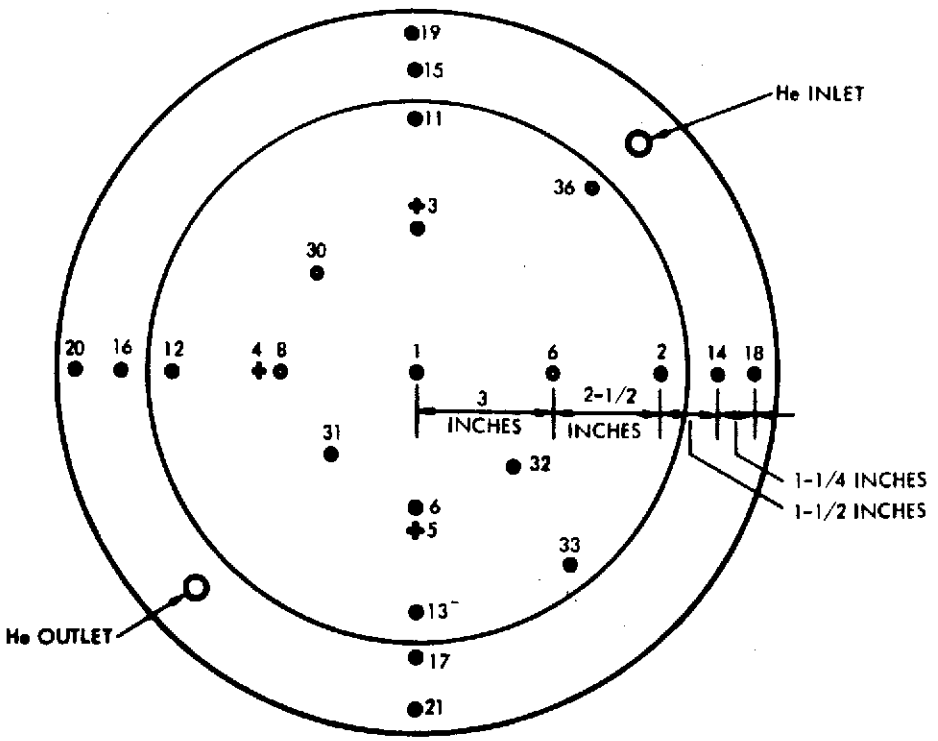

SYM	TC NO.	LOCATION
●	1	INSULATION EXTERNAL SURFACE
✚	2-5	INSULATION INTERMEDIATE SURFACE
●	6-21	INSULATION EXTERNAL SURFACE
	22	AMBIENT
	23	ICE BATH
	24	CO_2 BATH (DRY ICE AND ACETONE)
	25-28	TANK WALL
●	29-36	INSULATION EXTERNAL SURFACE
	37	OUTER TANK FILL LINE
	38	INNER TANK FILL LINE
	39	OUTER TANK VENT
	40	INNER TANK VENT
	41	GAS FLOW METER
	42	He PURGE INLET LINE
	43	He PURGE OUTLET FLOWRATER
	44	He PURGE INLET O INSULATION FACE
	45	He PURGE OUTLET O INSULATION FACE
	46	He PURGE INSULATION FACE
	47	ICE BATH
	48	CO_2 BATH (DRY ICE AND ACETONE)

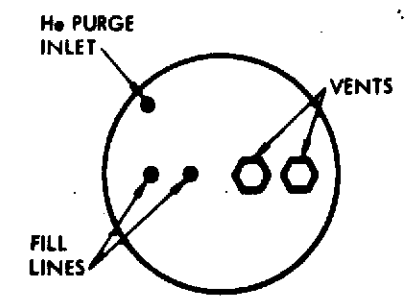

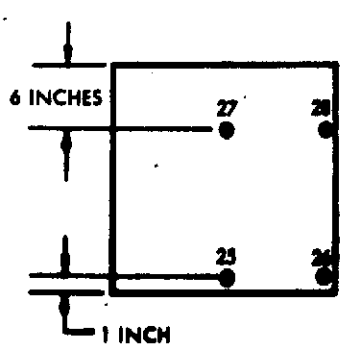

Figure 15.2.2.35-3. Thermocouple Locations for Thermal Conductance Testing

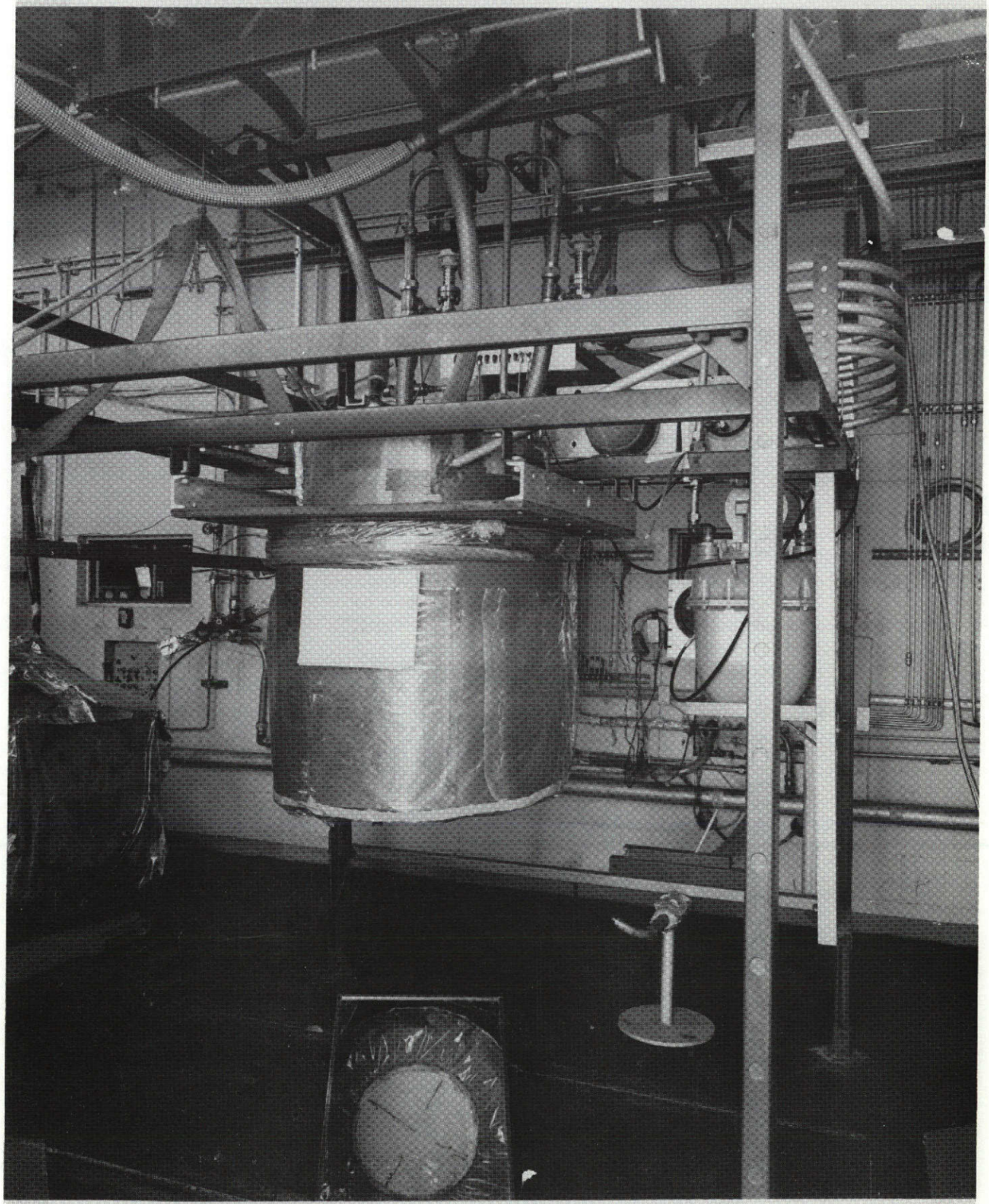

Figure 15.2.2.35-4. Test Set-Up Round Guarded Tank

2. Test Conditions: Testing is accomplished in the environment and temperature of the most rigid intended use of the insulation system. Test temperatures range from -423 F on the tank side of the insulation and from -320 F to + 350 F ambient side. Internal insulation pressures range from 0 to 25 psia.

3. Type of Data: Data include insulation system pressures and temperatures, tankage liquid level, and boiloff of hydrogen from guarded tank. Thermal conductivity values are calculated.

4. Test Equipment: Round guarded tankage with necessary controls and equipment, flow and temperature equipment.

c. Materials Tested: Honeycomb insulation (evacuated and purged) and foam insulation systems.

d. Reference: SID 66-362.

15.2.2.36 Infrared Analysis of Urethane Foam Raw Materials

a. Overall Objective: This method covers a procedure for determining the infrared spectra of urethane foam raw materials over the 2.5- to 15-micron weavelength region.

b. Description:

1. Test Article: Samples of the raw materials, isocyanate and polyol, taken from sealed containers as received from the vendor.

2. Test Conditions: Thin films of the raw materials on infrared sodium chloride plates. Percent transmission measured over the wavelength 2.5 to 15 microns.

3. Type of Data: Infrared spectra over the 2.5- to 15-micron wavelength range. Generic identification of polymer types.

4. Test Equipment: Sodium chloride plates or disks free from surface irregularities or hazing and spectrophotometer.

c. Materials Tested: Urethane foam raw materials.

d. Reference; Operating manual for the infrared spectrophotometer being used for test.

15.2.2.37 Differential Thermal Analysis (DTA) and Differential Scanning Calorimetry (DSC)

a. Overall Objective: Determination of first, second, and higher-order phase transitions, decomposition temperatures, solvent retention, purity, transition enthalpies, specific heat, heat of reaction, identification of materials, and degree of crystallinity.

b. Description:

1. Test Article: Sample size and nature are test-dependent. Samples can be solids, powders, crystals, or liquid. Maximum sample size (100 milligram) is used for specific heat measurement by DSC.

2. Test Conditions: Temperature range is 120 C (-184 F) to 1600 C (2912 F); choice of atmosphere including vacuum to 1 mm; temperature program rates are 0.5 C to 100 C per minute; constant temperature as a function of time.

3. Type of Data: Phase transitions, temperatures of decomposition, material solvent retention, specific heat, enthalpy of transition, purity and identification of materials, and degree of crystallinity of non-metallics.

4. Test Equipment: Dupont 900 and 990 Thermal Analyzers with DTA and DSC modules covering temperature changes to 1600 C (2912 F).

c. Materials Tested: Non-metallic and metallic, minerals, and inorganic salts.

d. References: Operating manuals for the Dupont 900 and 990 thermal analyzers.

15.2.2.38 Thermal Mechanical Analysis (TMA)

a. Overall Objective: This method covers a procedure for determining the thermal expansion, compression, tension, and penetration properties of a meterial as a function of temperature and load.

b. Description:

1. Test Article: One specimen, 0.25 cubic inch nominal.

2. Test Conditions: The analysis is normally run in an air atmosphere but inert and reactive gases may be used. Temperature range is -190 C (-310 F) to 500 C (932 F) for foam materials. The maximum heating capacity of the instrument is 1000 C.

3. Type of Data: Thermal expansion [Δ L/L (inch/inch)] and thermal expansion coefficient, α, may be measured. In addition, behavior of a foam system may be studied under the conditions of compressive and tensile loads. Softening points and first, second, and higher-order transitions may also be obtained.

4. Test Equipment: DuPont 900 and 941 Thermal Analyzer (Figure 15.2.2.38-1).

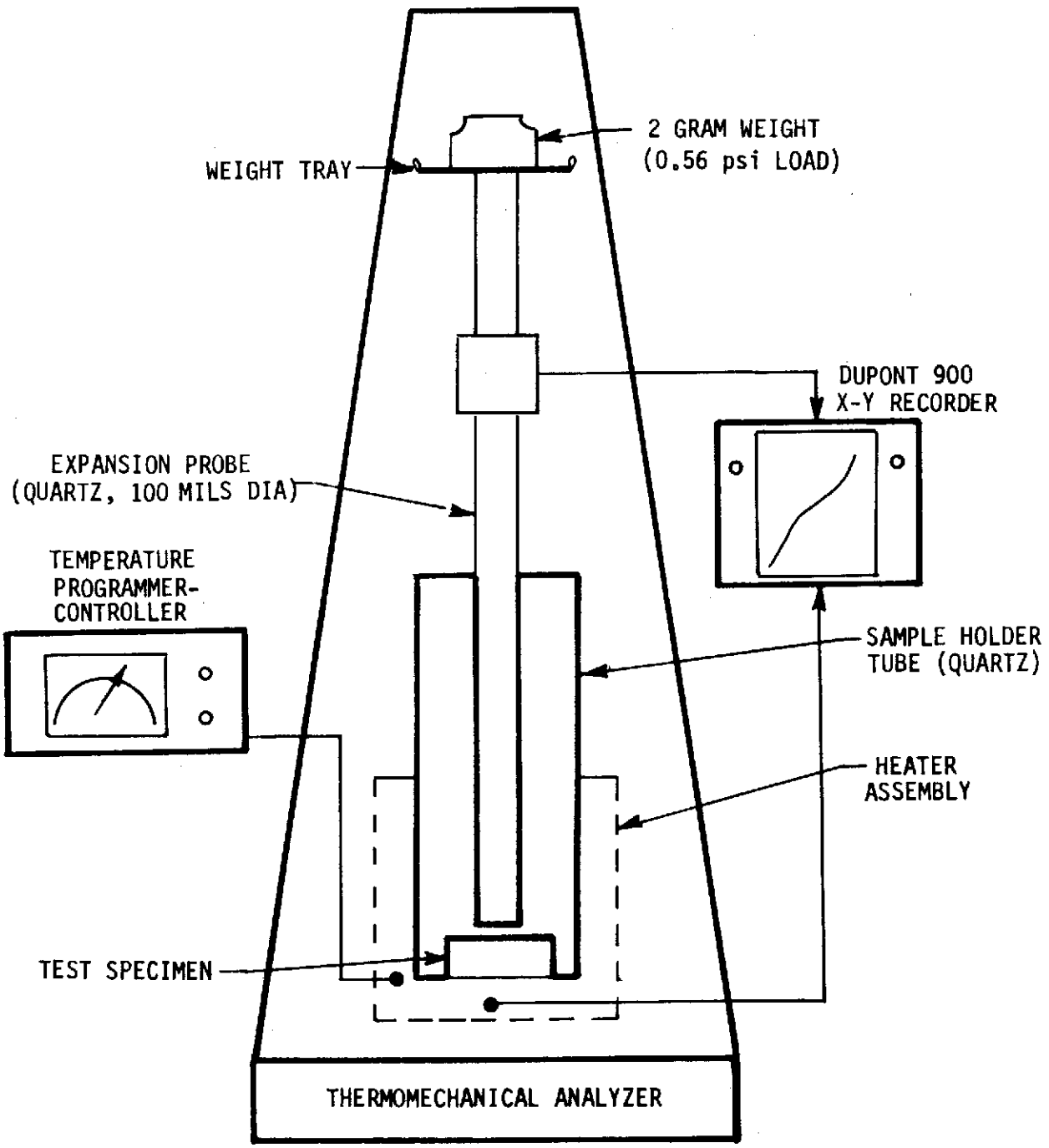

Figure 15.2.2.38-1. Test Set-Up, DuPont 941 Thermochemical Analyzer

c. Materials Tested: Urethane foam, plastics, laminates, adhesives, miscellaneous polymeric materials, and metallics.

d. Reference: DuPont Instrument Manual 900 Thermal Analyzer and Modulus.

15.2.2.39 Thermogravimetric Analysis (TGA)

a. Overall Objective: To measure weight loss of a material as a function of temperature in selected gaseous environments or in vacuum.

b. Description:

1. Test Article: Small pieces of the test sample ranging in weight from 1 to 100 milligram. Initial sample size depends on density and analytical objective.

2. Test Conditions: Environment is air, inert gasses, some corrosive gases, vacuum to 1 micron; temperature range is 21 C (70 F) to 1177 C (2150 F); temperature program rates are 0.5 to 100 C per minute; isothermal hold as a function of time at any temperature to 1177 C (2150 F).

3. Type of Data: Weight loss as a function of temperature and weight loss as a function of time at constant temperature.

4. Test Equipment: DuPont 990 Thermal Analyzer and 951 TGA module. Cahn RG 2000 Electrobalance with Micro TGA kit.

c. Materials Tested: Non-metallic and metallic materials, minerals, and inorganic salts.

d. References: Operating manuals for the DuPont 990 thermal analysis unit and 951 TGA module. Operating manual for the Cahn RG2000 electrobalance.

15.2.2.40 Humidity Exposure

a. Overall Objective: To determine the resistance of coatings to the effect of a warm, highly humid atmosphere.

b. Description:

1. Test Article: Various coatings in metallic and non-metallic substrates. Dimensions to be specified.

2. Test Conditions: Duration of test to be specified; 240 hours (10 cycles) are normally suggested as a minimum. Each temperature/humidity cycle consists of 8 hours at 160 F and 95 percent relative humidity, plus 16 hours at 68 to 100 F and 95 percent relative humidity.

3. Type of Data: Film failure such as blistering, peeling, and crazing. On metal substrates, extent of corrosion.

4. Test Equipment: Humidity chamber capable of temperature and humidity control.

c. Materials or Systems Tested: Epoxy-phenolic, epoxy, polyurethane, hypalon, silicone, acrylic, and vinyl.

d. Reference: MIL-STD-810, Method 507.

15.2.2.41 Salt Fog Exposure

a. Overall Objective: To determine the resistance of coatings to the effect of salt atmosphere and their ability to protect the metal substrates from corrosion.

b. Description:

1. Test Article: Various coatings on metallic and non-metallic substrates. Dimensions to be specified.

2. Test Condition: Duration of test to be specified. Unless otherwise specified, salt solution to be 5-percent sodium chloride, chamber temperature to be 92 to 97 F, atomizing nozzle pressure to be 12 to 18 psi.

3. Type of Data: Film failure such as blistering, peeling, crazing, and flaking. Extent of metal corrosion and corrosion creep.

4. Test Equipment: Salt fog chamber with necessary support racks.

c. Materials or Systems Tested: Epoxy-phenolic, epoxy, polyurethane, hypalon, silicone, acrylic, and vinyl.

d. Reference: MIL-STD-810, Method 509.

15.2.2.42 Standard Method of Test for Compressive Properties of Rigid Plastics

a. Overall Objective: This method is designed for use in determining the compressive properties of rigid organic plastics.

b. Description:

1. Test Article: The test specimen measures 1 inch wide by 3 inches long. The thickness of the specimen may be 1/16 inch up to 1/4 inch.

2. Test Conditions: Ambient air and relative humidity and test temperatures from -252 C (-423 F) to 537 C (1000 F).

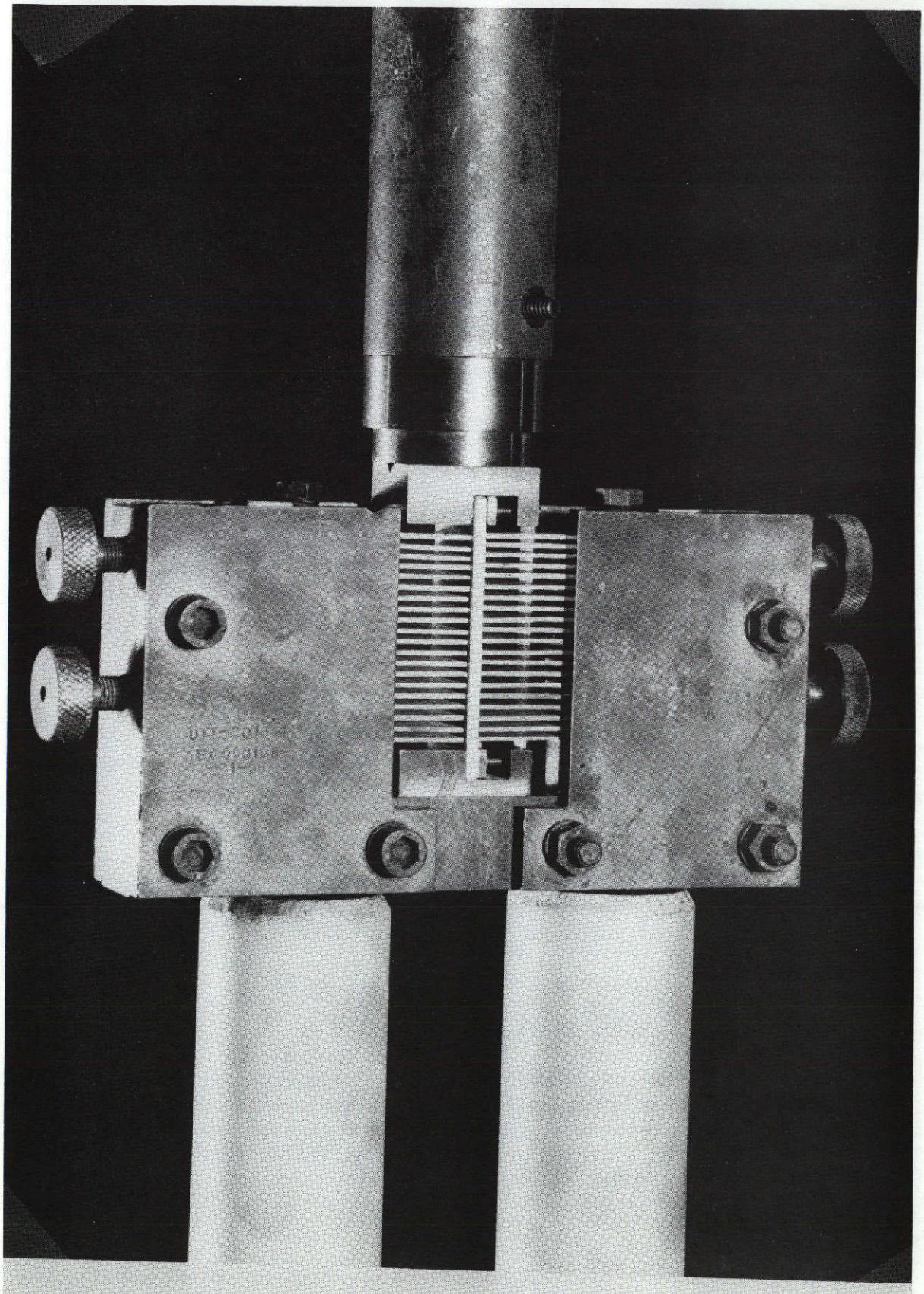

Figure 15.2.2.42-1. Compression Test Setup

3. Type of Data: Ultimate stress and compressive modulus of elasticity.

4. Test Equipment: Universal-type tensile test machine with strain recorder and a compression test fixture with extensometer.

c. Materials Tested: Rigid organic plaster sheets, solid or laminated.

d. Reference: ARTC-11.

15.2.2.43 Moisture Adsorption of Cellular Plastics

a. Overall Objective: This method covers a procedure for determining the adsorption of water vapor at a given relative humidity and temperature over a specified period by cellular plastic materials.

b. Description:

1. Test Article: Test specimens must be approximately 4 inches wide by 4 inches long by 1 inch thick. Test specimens must be machined or sawed from the sample so as to have a smooth edge. The six surfaces will be made smooth by sanding with No. 0, or finer, sandpaper.

2. Test Conditions: Selected relative humidities over the range from 10 to 97 percent. Temperature range 20 to 30 C. Time period as required. Five specimens per sample.

3. Type of Data: Weight percent water vapor adsorbed, average value and weight per unit area of surface available for adsorption.

4. Test Equipment: Humidity chambers, and thermostatically controlled oven of suitable compartment size.

c. Materials Tested: Urethane, polystyrene, and silicon foams, certain composites, porous potting, and adhesive systems.

d. Reference: Hygrodynamics, Technical Bulletin No. 5.

15.2.2.44 Product Quality Verification (PQV)

a. Overall Objective: This method covers a procedure for determining the flatwise tensile strength of foam insulation as applied to the production flight hardware. The equipment is also used to measure the deflection of a facing sheet of a laminated structure in order to verify areas of debond.

b. Description:

1. Test Article: External surface of the production hardware to be tested. Test area varies up to a maximum test plug of 2.75 inches in diameter (5.94 square inches).

2. Test Conditions: The test is performed at ambient conditions on the production hardware. The PQV test device is capable of load applications up to 700 pounds. Ultimate loading is determined by the variable test area.

3. Type of Data: In the case of foam insulation, tensile strength is determined. If the failure occurs at the foam-structure interface, the bond strength to the structure is determined. When used to measure facing sheet deflection of a laminated structure, the existence of a debond area is verified. If standards or known debond areas are utilized, actual areas of hardware debond may be estimated.

4. Test Equipment: The PQV test device (Figure 14.2.2.44-1) was developed and fabricated by NR.

5. Special Considerations: When the PQV test is performed on foam insulated structures, the test is destructive. Provisions must be made for repair of the test zone. When measuring facing sheet deflection, a test plug is bonded to the laminate for loading. Provisions must be made for plug removal and surface renovation of the temporary bond area.

c. Material Tested: Urethane foam, metallic or non-metallic laminate facing sheets.

d. Reference: NR Quality Control Specification MQ0501-034.

15.2.2.45 Vacuum Plate

a. Overall Objective: This method covers a procedure for locating debonded cork insulation when located on relatively flat cork areas.

b. Description:

1. Test Article: External cork insulated areas of the S-II stage Test area is a function of vacuum plate dimensions.

2. Test Conditions: The test is performed at ambient conditions.

3. Type of Data: Debonded areas in excess of 2 inches in diameter are detectable. Repeated testing will locate the periphery of the debond area.

4. Test Equipment: The vacuum plate test equipment was developed and fabricated by NR. The device consisted of a 1-inch thick plastic plate with standoff legs on one surface to create a vacuum chamber. A dial deflection indicator was located in the center of and normal to the plate. As vacuum was drawn, the unbonded cork moved into the vacuum chamber and was recorded on the dial indicator as a function of deflection.

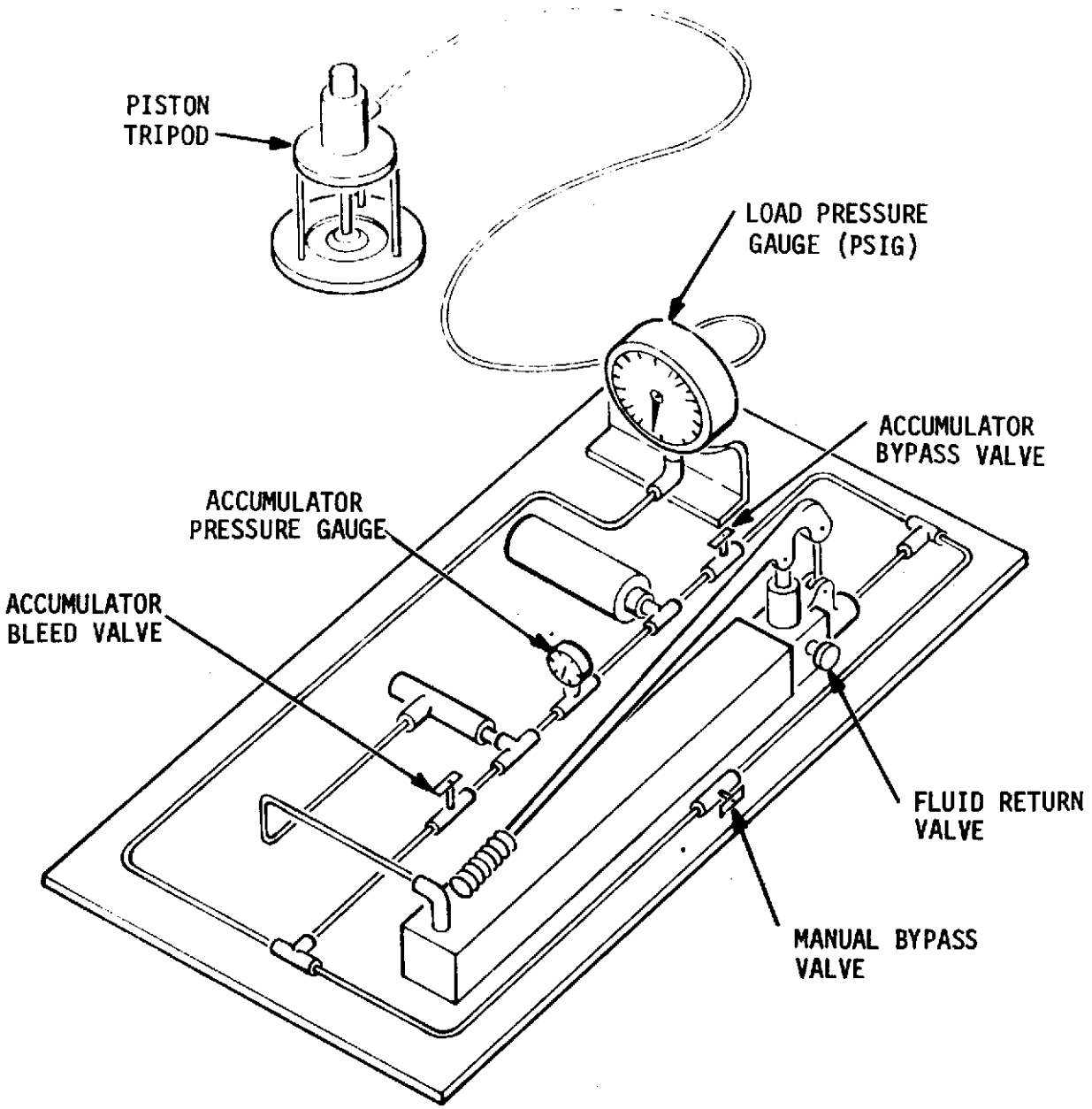

Figure 15.2.2.44-1. Product Quality Verification (PQV) Device 1376

c. Material Tested: Installed cork insulation 1/4-inch thick.

d. References: NR Launch Operations Test Preparation Sheet STD-696 and Laboratories and Test Report LR 6491-4568, Development of Inspection Method for Bonded Cork-Foam Structure, Saturn S-II, (Sept. 3, 1970).

15.2.2.46 Cryogenic Strain Compatibility Testing on Aluminum/Spray Foam-Bonded Specimens

a. Overall Objective: This procedure defines the testing methods and test equipment utilized in the performance of cryogenic strain compatibility testing of aluminum/spray foam-bonded specimens. The procedure is compatible with the testing requirements specified in NR Specifications MA0606-050 and MB0130-077. Data obtained are useful in development, control, and preparation of adhesive and spray foam material specifications.

b. Description:

1. Test Article: The test specimen generally consists of a 2014 aluminum test coupon, 0.125 inch thick, 2 inches wide, and approximately 19 inches long in the constant area section. The test foam is sprayed on one side of the coupon, 0.75 inch thick, 3 inches wide, and approximately 20 inches long (Figures 15.2.2.46-1, -2, and -3).

2. Test Conditions: The metal specimen is brought to a temperature of -247.2 C (-413 F) to -252 C (-423 F) in 30 minutes minimum, while maintaining 40 to 100 F on the upper surface of the foam. Time is recorded from start of liquid hydrogen flow. A tension stress of 72,000 ± 1000 psi is applied to the metallic test specimen. The stress is applied and released at a maximum rate of 50,000 psi per minute. Applied stress is removed at the same rate and the specimen warmed to at least -129 C (-200 F) using warm helium gas prior to inspection.

3. Type of Data: The specimen is thoroughly inspected for signs of bond or foam failure.

4. Test Equipment: Temperature recorders, loading system capable of applying a 30,000-pound force to the specimen. The specimen is shown in Figure 15.2.2.46-1. A cross-section view shows specimen setup, thermocouple, insulating cap and heating plate. System test set up is shown in Figures 15.2.2.46-4, -5, -6, and -7.

c. Materials or Systems Tested: The specimen used is typical of the S-II liquid hydrogen tank construction and the test evaluates the compatibility of the aluminum and the polyurethane spray foam insulation.

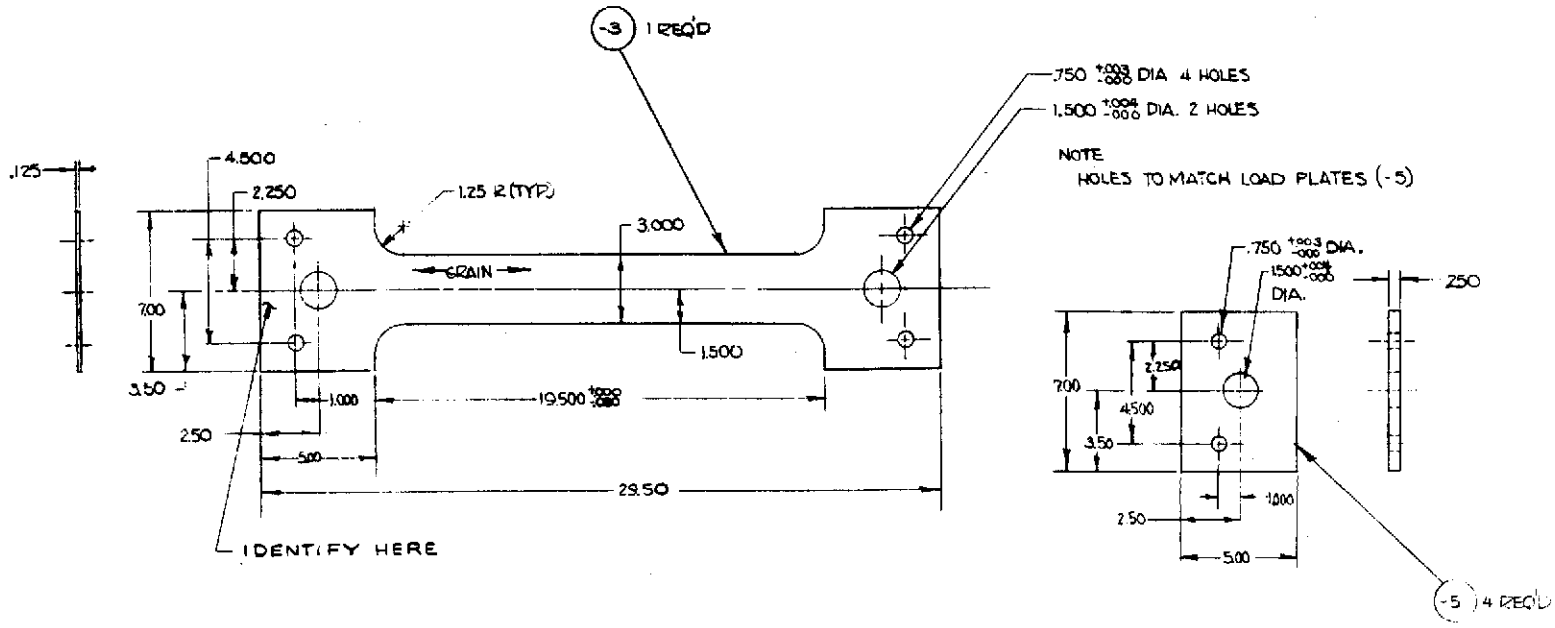

QTY REQD	QTY REQD	QTY REQD	QTY REQD	QTY REQD	QTY REQD	PART OR IDENTIFYING NO.	NOMENCLATURE OR DESCRIPTION	CODE IDENT	MATERIAL	DATA: SPECIFICATION SIZES, NOTES, SUPPLIERS	LINE NO.
											005
											004
					4	-5	PLATE		URES SHEET	QQ-S-[illegible] 321 347 .250 X 5.00 X 7.00	003
					1	-3	SPECIMEN		ALUM. ALLOY	MIL-A-[illegible] 7014 T6 .125 x 7.00 x 29.50	002
						LET STD-0008					001

LIST OF MATERIAL OR PARTS LIST

3. DRWG SIMILAR TO 6954-50
2. MACHINE AS PER AL-45
1. IDENTIFY AS PER AL-45
NOTES: UNLESS OTHERWISE SPECIFIED:

ITEM	QTY	MODEL	NEXT USING DRAWING	END ITEM NO.	THRU
-5		PER TEST			
-3		PER TEST	TEST		
REQD PER END ITEM				EFFECTIVE ON	

APPLICATION (USAGE) DATA

HEAT TREAT

FINISH

UNLESS OTHERWISE SPECIFIED: DIMENSIONS ARE IN INCHES. TOLERANCES ON:
DECIMALS XX = ± .03, .XXX = ± .010; ANGLES ±30'
HOLES NOTED "DRILL"
.013 THRU .040 : +.001 -.001
.041 THRU .130 : +.002 -.001
.131 THRU .229 : +.003 -.001
.230 THRU .500 : +.004 -.001
.501 THRU .750 : +.005 -.001
.751 THRU 1.000 : +.007 -.001
1.001 THRU 2.000 : +.010 -.001
DO NOT SCALE PRINT

DR BY W.J. COOK 4-7-67
CHK BY [illegible]
APPROVED BY
E.J. FINEL 4-10-67

NORTH AMERICAN AVIATION, INC.
SPACE and INFORMATION SYSTEMS DIVISION
12214 LAKEWOOD BLVD., DOWNEY, CALIFORNIA

TENSILE SPECIMEN - FOAM STRAIN COMPATIBILITY TEST

CODE IDENT NO.	SIZE	
03953	C	LET STD-0003

SCALE QUARTER SIZE SHEET

Figure 5.2.2.46-1. Metal Detail for Cryogenic Strain Compatibility Test Specimen

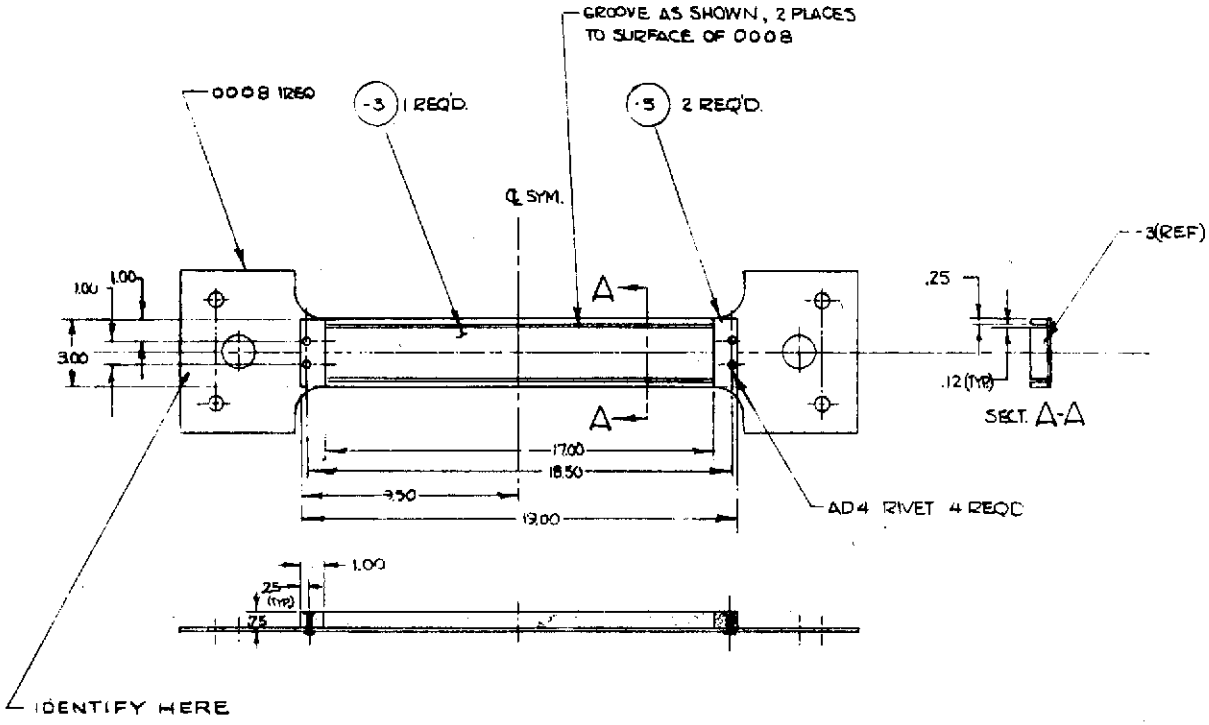

3. DRWG SIMILAR TO 6954-51
2. MACHINE AS PER AL-45
1. IDENTIFY AS PER AL-45
NOTES: UNLESS OTHERWISE SPECIFIED:

QTY REQD	QTY REQD	QTY REQD	QTY REQD	QTY REQD	QTY REQD	PART OR IDENTIFYING NO.	NOMENCLATURE OR DESCRIPTION	CODE IDENT	MATERIAL	DATA: SPECIFICATION SIZES, NOTES, SUPPLIERS	LINE NO.
											005
											004
					2	-5	BLOCK		NYLON SHT	PER TEST .75 x 1.00 x 3.00	003
					1	-3	BLOCK		FOAM	PER TEST .75 x 3.00 - 17.00	002
						LET STD-0009	SPECIMEN ASSY				001

LIST OF MATERIAL OR PARTS LIST

ITEM	QTY	MODEL	NEXT USING DRAWING	END ITEM NO.	THRU
		TEST	TEST		
REQD PER END ITEM				EFFECTIVE ON	

APPLICATION (USAGE) DATA

HEAT TREAT

FINISH

UNLESS OTHERWISE SPECIFIED:
DIMENSIONS ARE IN INCHES.
TOLERANCES ON:
DECIMALS ANGLES
.XX= ± .03
.XXX= ± .010 ±30'
HOLES NOTED "DRILL"
.013 THRU .040 : +.001 -.001
.041 THRU .130 : +.002 -.001
.131 THRU .229 : +.003 -.001
.230 THRU .500 : +.004 -.001
.501 THRU .750 : +.005 -.001
.751 THRU 1.000 : +.007 -.001
1.001 THRU 2.000 : +.010 -.001

DO NOT SCALE PRINT

DR BY	WESLEY COOK	4-20-67
CHK BY	[illegible]	4-21-67
APPROVED BY		
		4-21-67

NORTH AMERICAN AVIATION, INC.
SPACE and INFORMATION SYSTEMS DIVISION
12214 LAKEWOOD BLVD., DOWNEY, CALIFORNIA

SPECIMEN ASSY - FOAM
STEAM (TENSILE) COMPATIBILITY
TEST

CODE IDENT NO.	SIZE	
03953	C	LET STD-0009
SCALE ¼ SIZE		SHEET

Space Division
North American Rockwell

Figure 15.2.2.46-2. Specimen With Foam Attached, no Center Line Slit

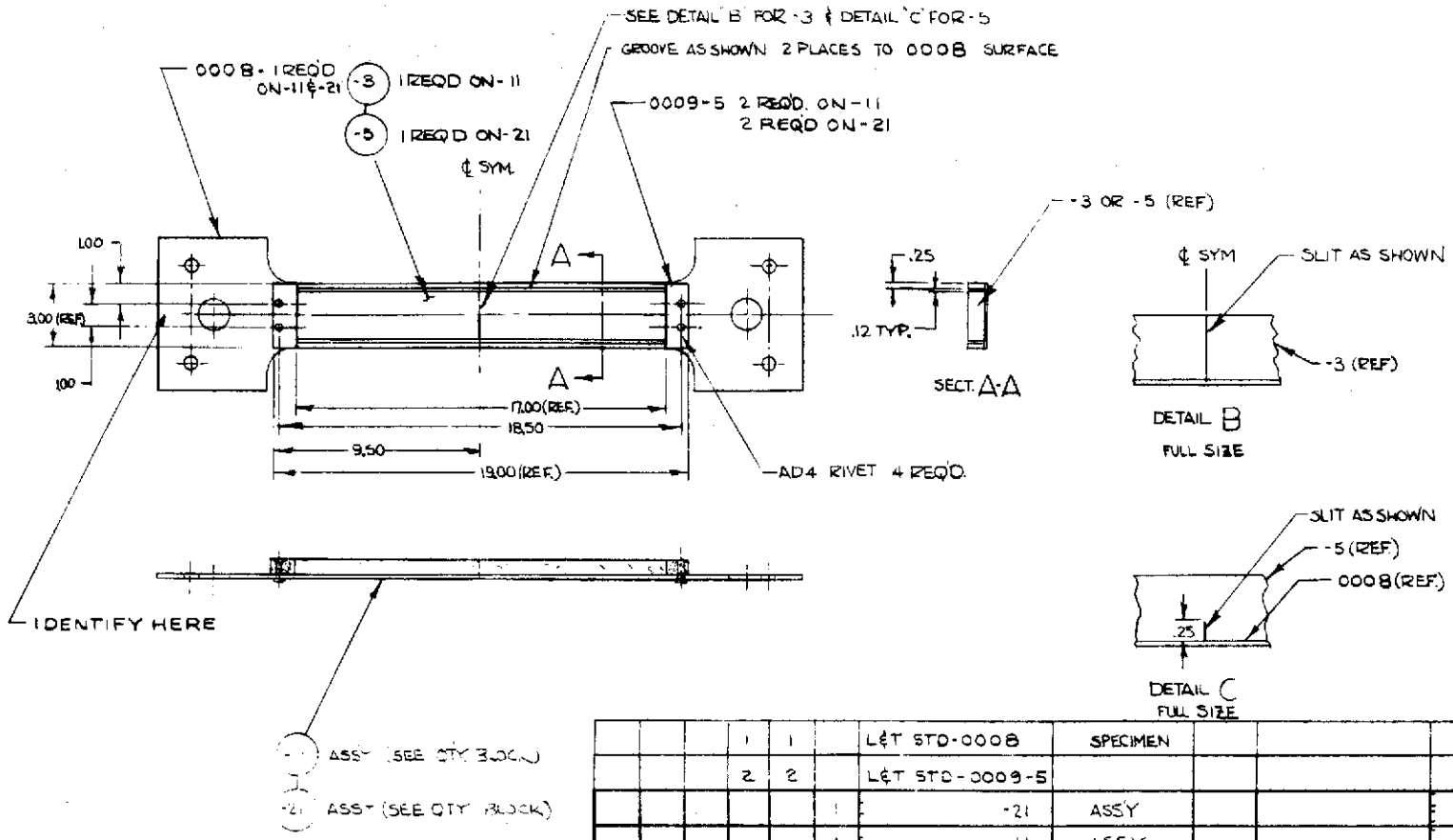

QTY REQD	QTY REQD	QTY REQD	QTY REQD	QTY REQD	QTY REQD	PART OR IDENTIFYING NO.	NOMENCLATURE OR DESCRIPTION	CODE IDENT	MATERIAL	DATA: SPECIFICATION SIZES, NOTES, SUPPLIERS	LINE NO.
			1	1		LET STD-0008	SPECIMEN				007
			2	2		LET STD-0009-5					006
					1	-21	ASSY				005
					1	-11	ASSY				004
			1			-5	BLOCK		FOAM	PER TEST .75 x 5.00 x 17.00	003
				1		-3	BLOCK		FOAM	PER TEST .75 X 3.00 X 17.00	002
						LET STD 0010	SPECIMEN ASSY				001

LIST OF MATERIAL OR PARTS LIST

NOTES: UNLESS OTHERWISE SPECIFIED:
1. IDENTIFY AS PER AL-45
2. MACHINE AS PER AL-45
3. DRWG SIMILAR TO 6954-52

ITEM	QTY	MODEL	NEXT USING DRAWING	END ITEM NO.	THRU
-21		TEST	TEST		
-11		TEST	TEST		

REQD PER END ITEM — EFFECTIVE ON

APPLICATION (USAGE) DATA

HEAT TREAT

FINISH

UNLESS OTHERWISE SPECIFIED:
DIMENSIONS ARE IN INCHES.
TOLERANCES ON:

DECIMALS	ANGLES
.XX = ± .03	
.XXX = ± .010	±30'

HOLES NOTED "DRILL"

.013	THRU .040	+.001 -.001
.041	THRU .130	+.002 -.001
.131	THRU .229	+.003 -.001
.230	THRU .500	+.004 -.001
.501	THRU .750	+.005 -.001
.751	THRU 1.000	+.007 -.001
1.001	THRU 2.000	+.010 -.001

DO NOT SCALE PRINT

DR BY WESLEY COOK 4-20-67
CHK BY [illegible] 4-24-67
APPROVED BY [illegible] 4-24-67

NORTH AMERICAN AVIATION, INC.
SPACE and INFORMATION SYSTEMS DIVISION
12214 LAKEWOOD BLVD., DOWNEY, CALIFORNIA

SPECIMEN ASSY.- FOAM STRAIN (TENSILE) COMPATIBILITY TEST (SLITTED)

CODE IDENT NO. 03953 | SIZE C | LET STD-0010

SCALE 1/4 | SIZE | SHEET

Figure 15.2.2.46-3. Specimen With Foam Attached, Center Line Slit

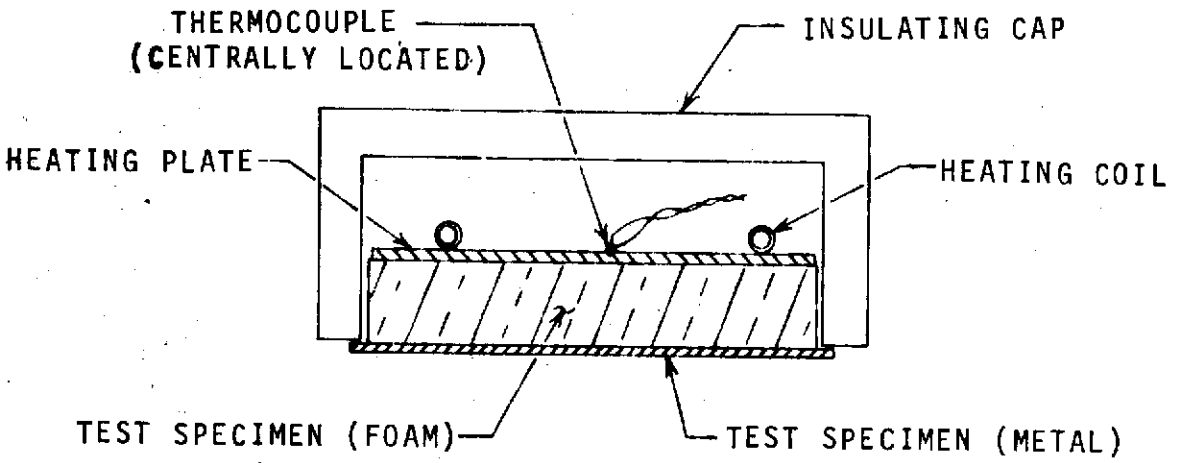

Figure 15.2.2.46-4. End Section of Test Specimen, Insulating Cap and Heating Plate

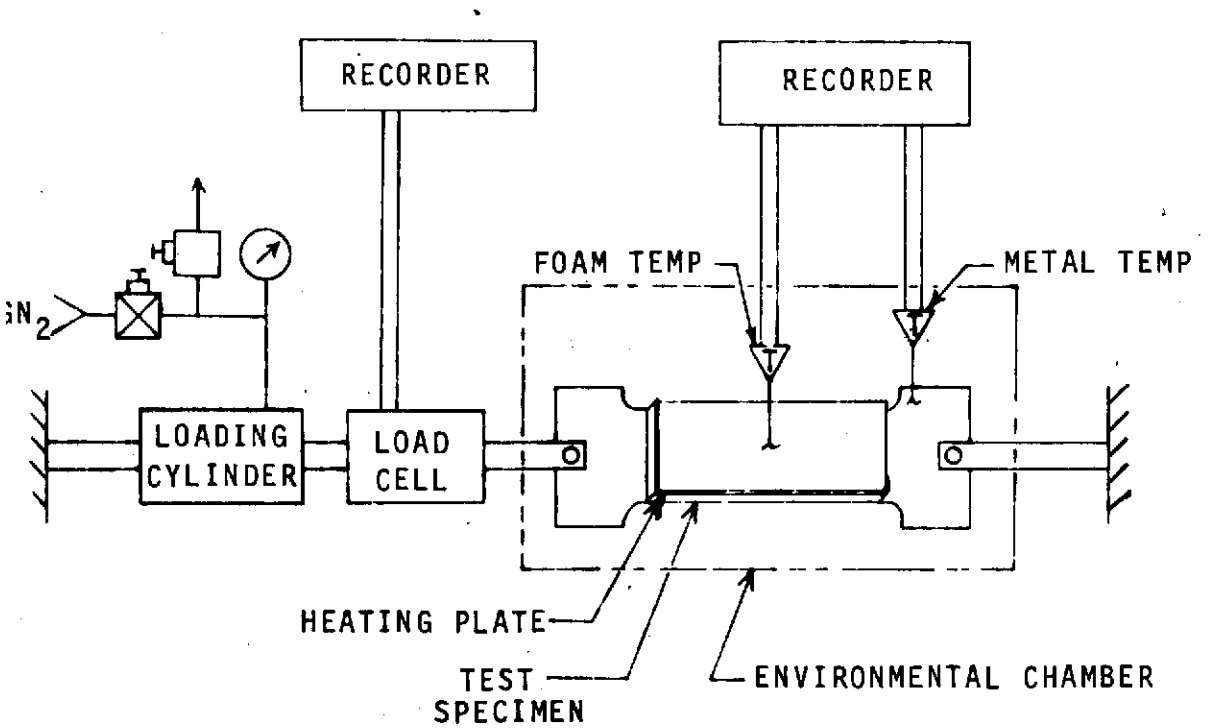

Figure 15.2.2.46-5. Instrumentation Block Diagram

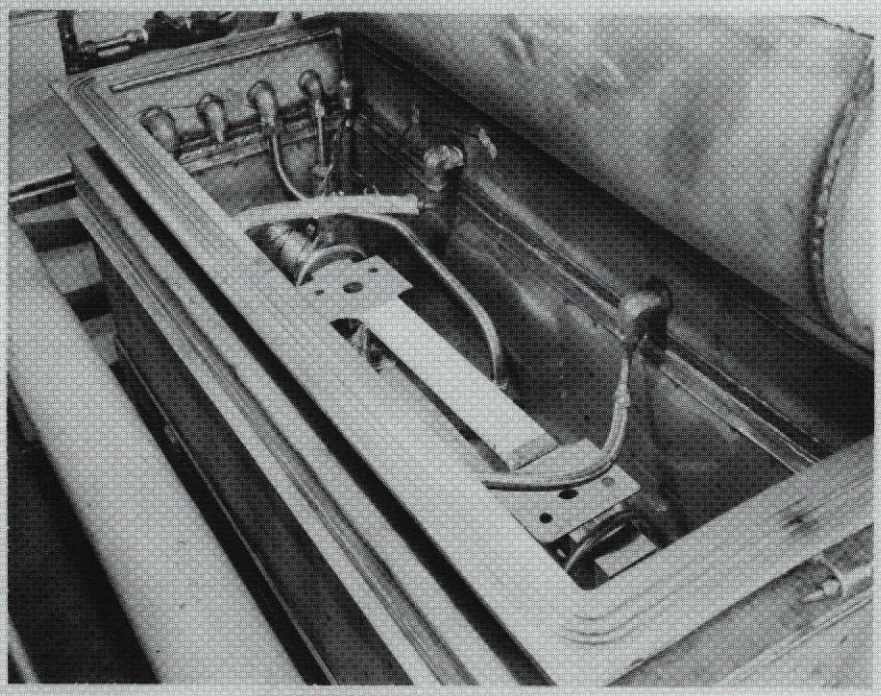

Figure 15.2.2.46-6. Cryogenic Strain Compatibility Test Set-Up

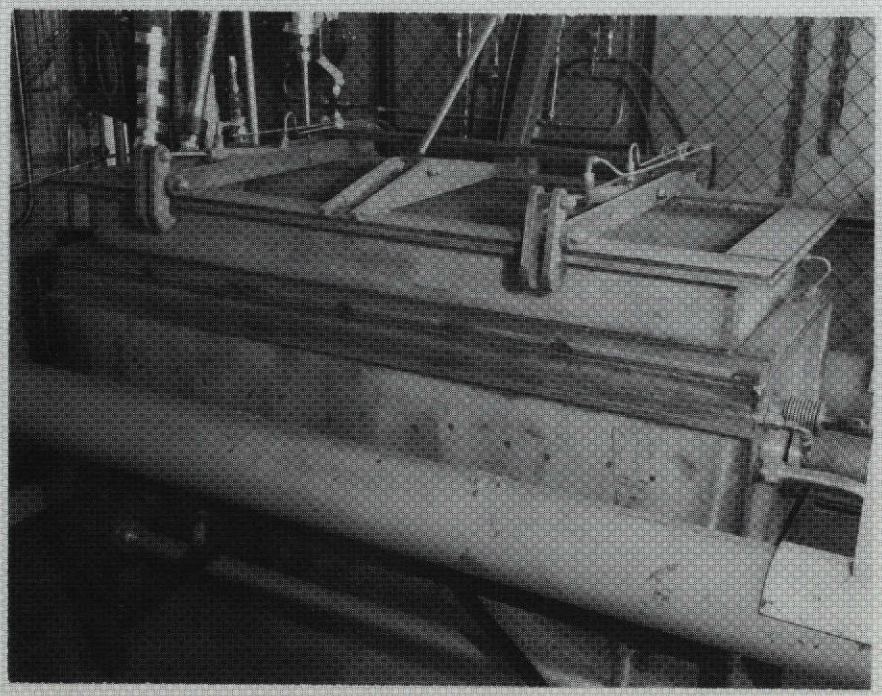

Figure 15.2.2.46-7. Cryogenic Strain Compatibility Test Set-Up

d. References:

1. MA 0606-050, Spray Application for Two-Pound Density Polyurethane Foam Material.

2. MB 0130-077, Flame Retardant Polyurethane Foam, Two-Pound Density, for Spray Applications.

15.2.2.47 Linear Thermal Expansion (Method 1)

a. Overall Objective: To determine the free expansion and contraction of specimens of S-II insulation facing laminate and facing laminate bonded to HRP core.

b. Description:

1. Test Article: Specimens used consisted of typical sections of the laminate and HRP core assembly. The length was approximately 40 inches, the thickness 1/2 inch, and the width 3 to 4 inches.

2. Test Conditions: The specimens were tested by a modification of the ASTM E228 dilatometric method. A stainless steel chamber with heating and cooling provisions was used instead of a quartz dilatometer tube.

3. Type of Data: The free expansion or contraction of the specimen was measured with a dial gage, the readings were subsequently corrected for the expansion of the 321 stainless steel.

4. Test Equipment: Laboratory thermal expansion test apparatus.

c. Materials Tested: Includes any solid material where linear thermal expansion is considered significant.

d. Reference: Laboratory report SMT 2-66-11.

15.2.2.48 Linear Thermal Expansion (Method 2)

a. Overall Objective: To determine the free expansion and contraction of specimens of S-II insulation facing laminate and facing laminate bonded to HRP core.

b. Description:

1. Test Article: The test specimen used was approximately 40 inches long. The original method was modified since the laminate specimens were not rigid enough to support their own weight without deflecting. The top end of the specimen was fastened securely and the bottom end left hanging freely.

2. Test Conditions: The specimens were tested by a modification of the ASTM E 228 dilatometric method. A stainless steel chamber with heating and cooling provisions was used instead of a quartz dilatometer tube.

3. Type of Data: The change in length was determined with the use of a cathetometer, focusing on a reference target, attached to the specimen and projecting from the bottom of the chamber.

4. Test Equipment: Laboratory thermal expansion test apparatus.

c. Materials Tested: Includes any solid material where linear thermal expansion is considered significant.

d. Reference: Laboratory report SMT 2-66-1.

15.2.2.49 Total Normal Emittance (Method 1)

a. Overall Objective: To determine the relative emissive power of non-blackbody surfaces.

b. Description (Method 1):

1. Test Article: The specimen is approximately 1 inch in diameter and whatever thickness the end use item is intended to be.

2. Test Conditions: The total normal emittance is determined as ratio of total emissive power of the specimen, measured at a given temperature, to that of a blackbody cavity at the same temperature. Temperature ranged to 1800 F.

3. Type of Data: The emissive power is a direct function of measured EMF, therefore, the emittance

$$EN = \frac{EMF_{NB}}{EMF_{BB}}$$

NB - Non-black body
BB - Black body

For partially transmitting materials, a series of metal backings behind the specimen permit determination of the average emittance through solution of a set of simultaneous equations.

4. Test Equipment: A Honeywell Radiamatic pyrometer with calcium fluoride lens was used as a detector, for the wave length interval 0.3 to 10 microns. Detector EMF output was measured with a Wenner potentiometer and reflecting galvanometer. A three-zone tubular furnace with 2000 F (1093.3 C) capability housed the blackbody cavity or specimen assembly. Figure 15.2.2.49-1 shows a typical test setup and apparatus.

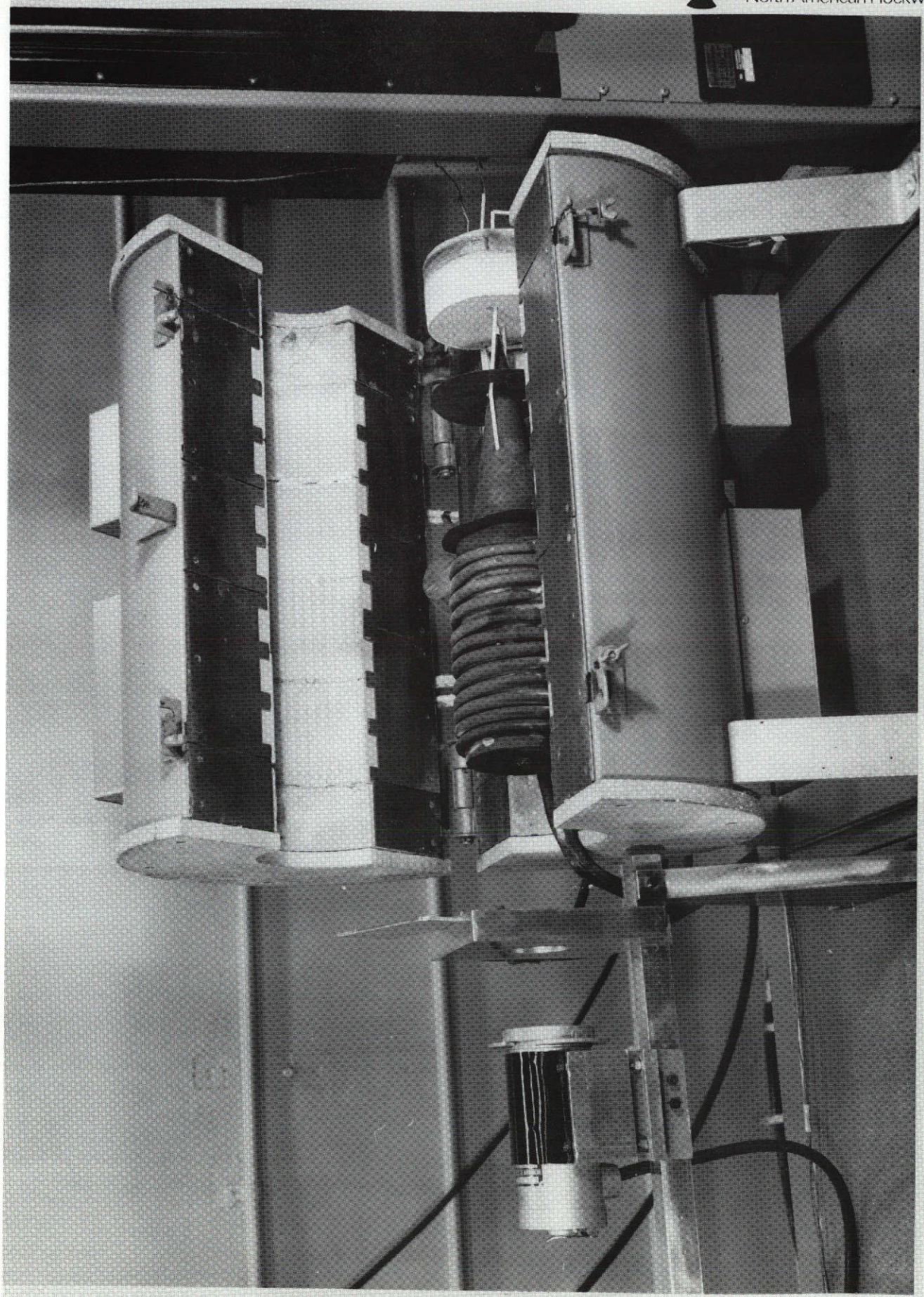

Figure 15.2.2.49-1. Typical Test Set-Up and Apparatus

c. Materials Tested: The obsolete Space Division apparatus was used to measure the Sil-Temp #84 material.

d. Reference: Lab Memo SMT 7-63-8.

15.2.2.50 Total Normal Emittance (Method 2)

a. Overall Objective: To determine the relative emissive power of non-blackbody surfaces.

b. Description (Method 2):

1. Test Article: The specimen is approximately 1 inch in diameter and whatever thickness the end use is intended to be.

2. Test Conditions: The sliding specimen technique, shown in Figures 15.2.2.50-1 and -2, makes use of a cylindrical black cavity radiator heated isothermally to the desired test temperature. A water-cooled aperture is placed in the front of the cavity and the test specimen is positioned in the rear of the cavity (Position A of Figure 15.2.2.50-2) on a suitable pushrod. There it is heated by radiation until it reaches equilibrium with the cavity walls. Temperature ranged to 3000 F.

3. Type of Data: The 100-percent blackbody emissive power is obtained by sampling the radiation through the aperture with a Barnes R4F2 radiometer. Focusing on the cavity was at a small angle to the plane of the aperture. A level of zero percent is obtained by blocking the aperture with an opaque screen. The specimen is then moved rapidly forward, diminishing the radiation through the aperture as it moves (Curve B). Held against the aperture, it cools slowly, resulting in a decrease in the time rate of change of measured radiation. The knee of the curve (Position C of Figure 15.2.2.50-2) is taken as the emittance of the specimen at the test temperature, expressed as percent. Typical energy trace is shown in Figure 15.2.2.50-2.

4. Test Equipment: The sliding specimen emittance apparatus is shown in Figure 15.2.2.50-1.

c. Materials Tested: The NR apparatus shown in Figure 15.2.2.50-1 was used to measure the flexible curtain material.

d. Reference: TFD 71-1185 NR/LAD.

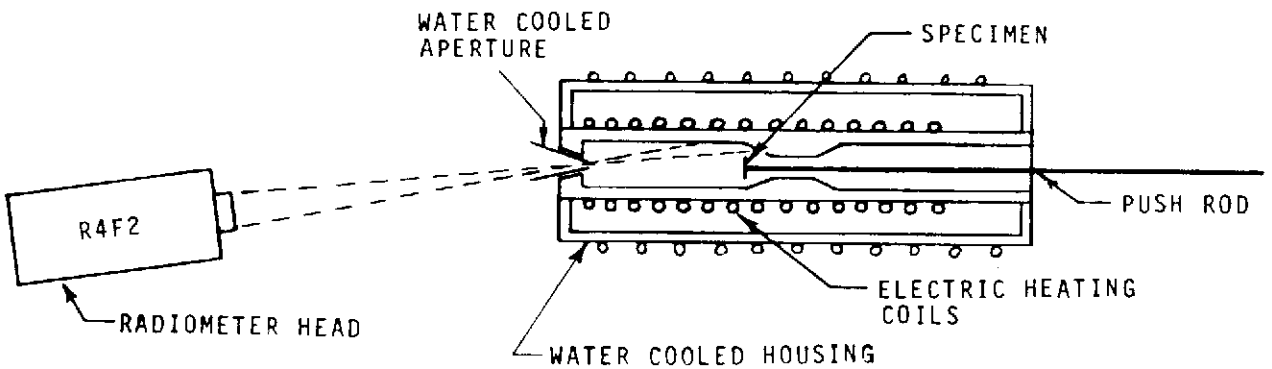

Figure 15.2.2.50-1. Sliding Specimen Emissivity Test Apparatus

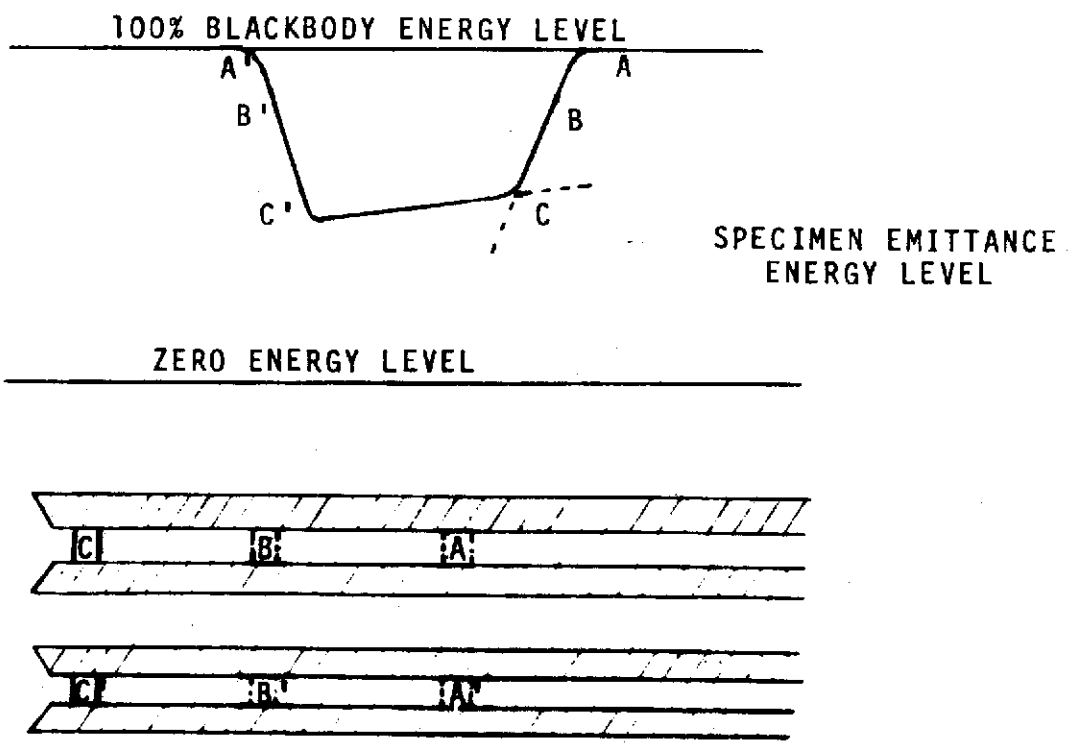

Figure 15.2.2.50-2. Typical Energy Trace for the Sliding Specimen Emissivity Test

15.2.2.51 Air Permeation Rate

a. Overall Objective: To determine the rate at which air permeates through solid film materials and composites under the influence of a constant partial pressure differential.

b. Description:

1. Test Article: The test specimen used is approximately 1-1/2 inches in diameter and 1/4 inch in thickness.

2. Test Conditions: A vacuum-decay technique was developed in which the specimen separates two chambers, one pressurized with the test gas or open to atmosphere and the other evacuated. The pressure increases (or the vacuum is said to decay), which indicates the air permeation rate through the specimen.

3. Type of Data: The rate of pressure increase is measured and is related to the permeation rate by the following expression:

$$G = (3.59 \times 10^{-4}) \left(\frac{dp}{de}\right) \left(\frac{V}{AT}\right)$$

where

G = Permeation rate, cc at STP/hr-sq. cm

V = Cell volume, cc

A = Area of permeation, sq. cm.

T = Temperature, K

$\frac{dp}{de}$ = Rate of pressure rise, microns/hr.

The test apparatus is limited by its design to operation at or near room temperature.

4. Test Equipment: Vacuum decay test cell setup (Figure 15.2.2.51-1).

c. Materials or Systems Tested: This apparatus was used to evaluate the Tedlar vapor barrier, the facing laminated composite, and coatings for application over the external insulation.

d. References: Lab Report No. SDL 354.

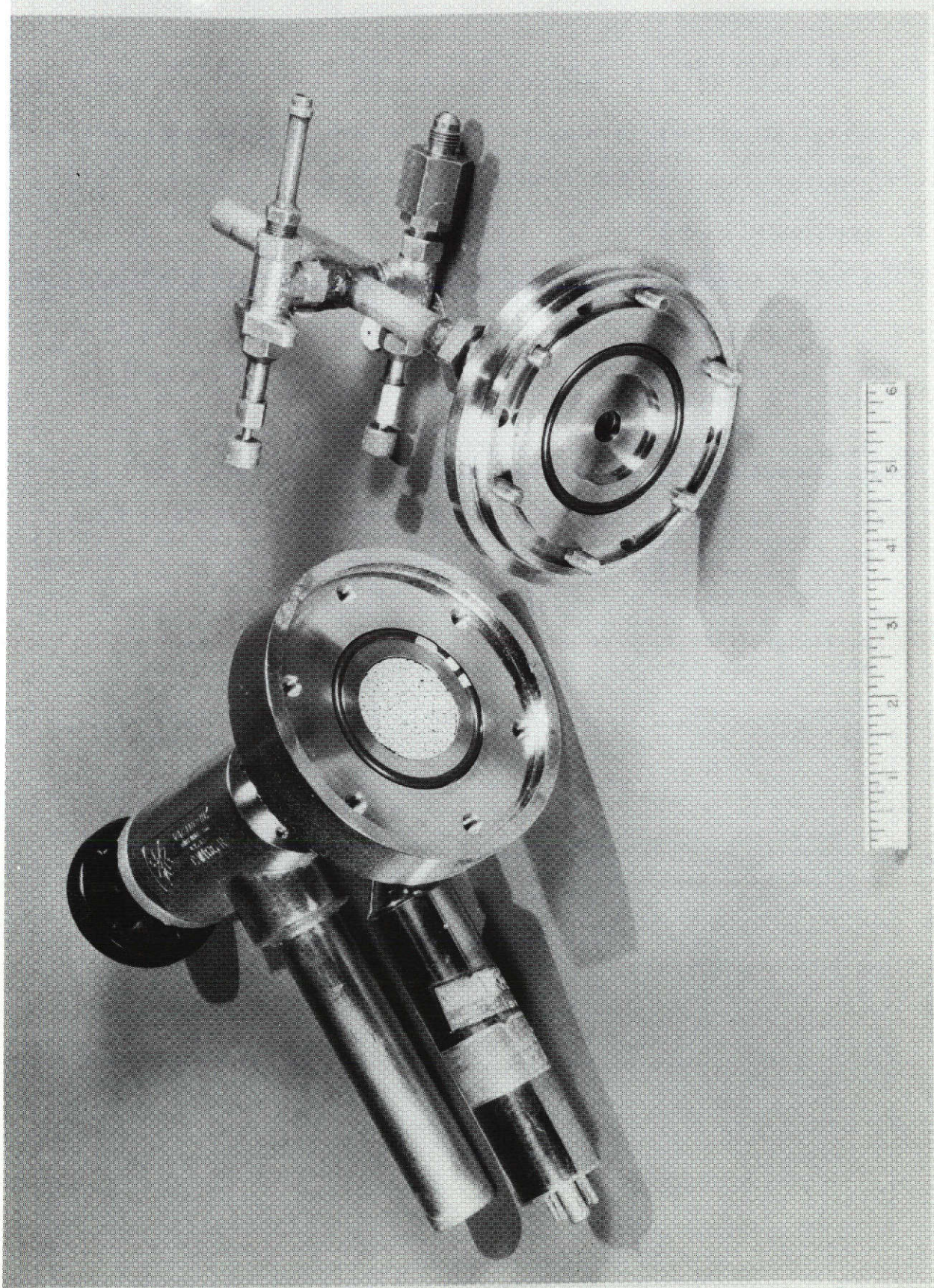

Figure 15.2.2.51-1. Air Permeation Rate Test Equipment

15.2.2.52 Method of Test for Effects of Thermal and Aerodynamic Environmental Parameters

a. Overall Objective: This method simulates thermal and aerodynamic environmental parameters which occur during launch and entry and permits determination of the effect on materials.

b. Description:

1. Test Article: The specimen size is 1-1/4 inches in diameter for a stagnation model and 2 inches wide by 5 inches long for the laminar flow models.

2. Test Conditions: A continuous supersonic flow of a simulated air mixture of nitrogen and oxygen (Figure 15.2.2.52-1).

3. Type of Data: Temperature profile, weight loss, surface temperature, recession rate.

4. Test Equipment: Three plasma arc heaters with electrical input capacities from 120 to 1000 kw, two vacuum chambers, and 12 triple voltage saturable core reactor-type rectifiers supplying power of 500 kw continuously and 100 kw intermittently.

c. Materials Tested: Foam insulation, ablatives, coating, and heat shield flight instrumentation.

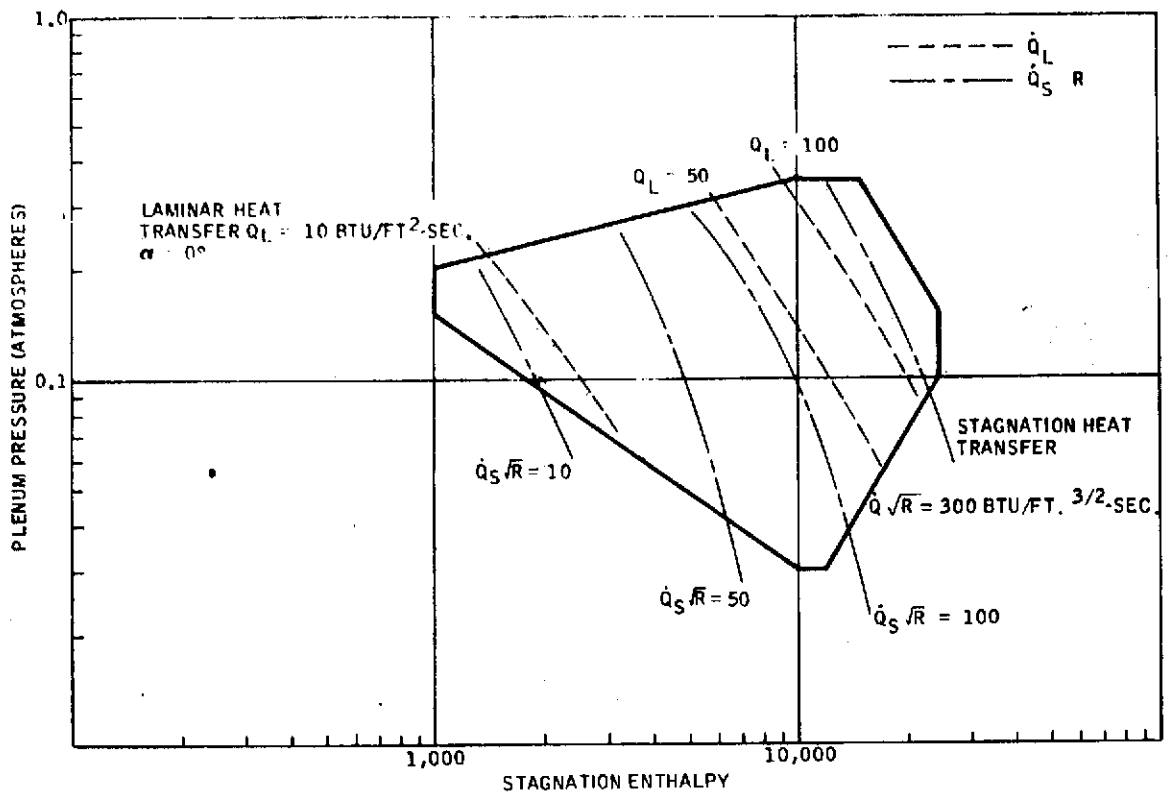

Figure 15.2.2.52-1. Plasma Tunnel Typical Performance

d. Reference: Lab Memo LR 8298-3201, "Operational Procedure of L&T 144 KW Low-Pressure Plasma Arc Tunnel."

15.2.2.53 Method of Test for Effects of Aerodynamic Shear Forces During Flight

a. Overall Objective: This method of test simulates the aerodynamic shear forces which act on surfaces of high-speed vehicles and permits determination of the effect upon materials and coatings.

b. Description:

1. Test Article: The specimen size is 4 by 7.7 inches and forms one side of the gas flow duct on the facility.

2. Test Conditions: Air or nitrogen gas. Radiant heat with programmed heat flux levels to 200 Btu/lb-ft^2/sec. Typical operating conditions are shown in Figure 15.2.2.53-1.

3. Type of Data: Temperature profile, recession rate, surface temperature, weight loss.

4. Test Equipment: Graphite slab heater and test setup are shown in Figure 15.2.2.53-2.

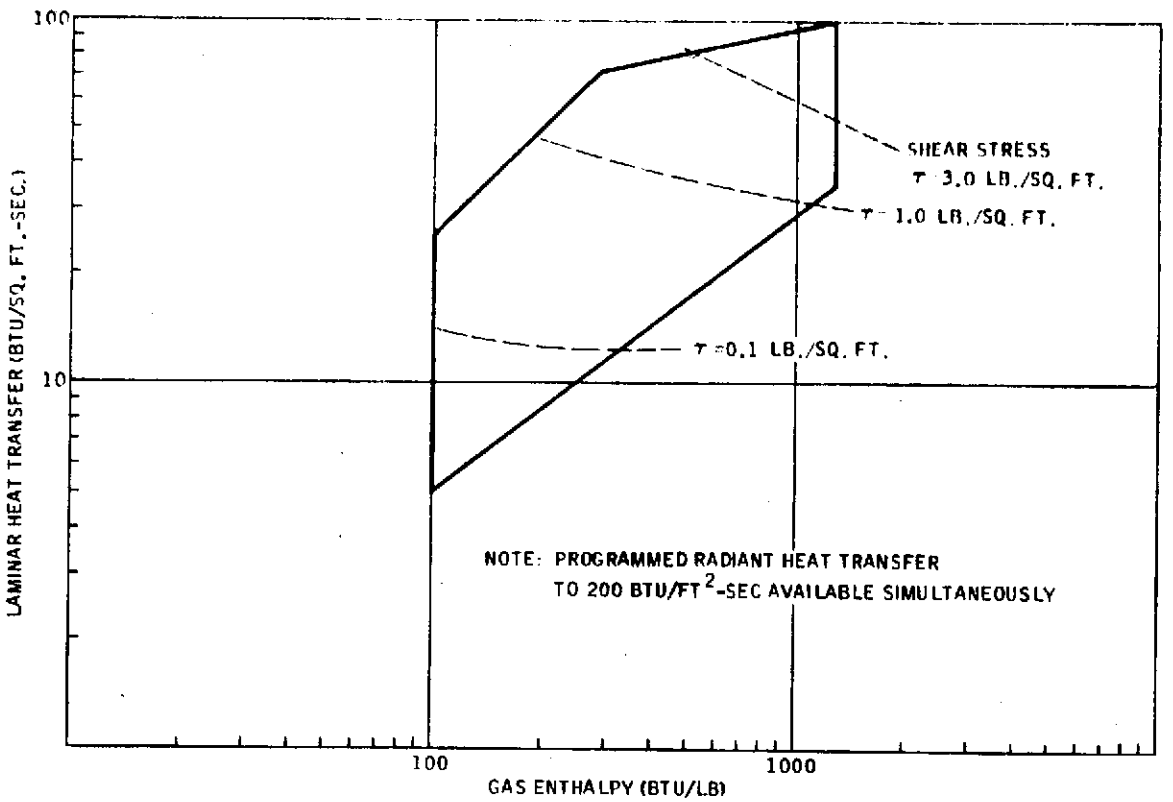

Figure 15.2.2.53-1. Aeroshear Tunnel Typical Performance

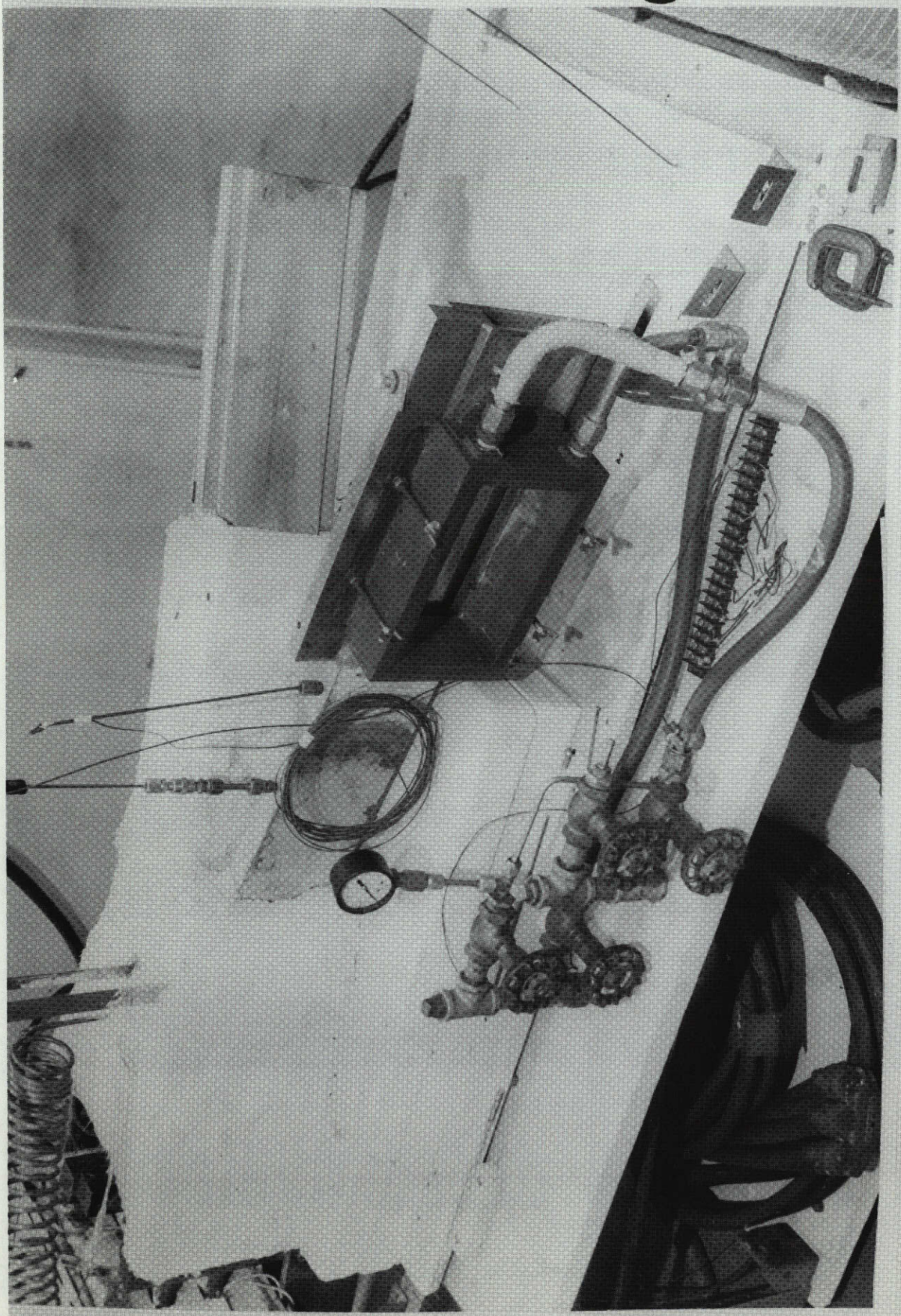

Figure 15.2.2.53-2. Aerodynamic Shear Force Simulation Test Set-Up

c. Materials Tested: Foam insulation, ablatives, and flight instrumentation for heat shields.

d. References: Lab Test Report LR 6810-3202, "Aeroshear Testing of Polyimids, Sandwich Over Spray Foam."

15.2.2.54 Method of Test for Simulation of Thermal Effects Occurring on Vehicles During Low Ambient Pressure Conditions

a. Overall Objective: This method used in the thermal altitude test facility provides simulation of thermal effects during low ambient pressure conditions.

b. Description:

1. Test Article: The specimen size is flexible but is usually limited to one square foot.

2. Test Conditions: Vacuum to 1 x 10^{-6} TORR, test temperature to 2760 C (5000 F), heat flux to 40 Btu-ft^2/sec.

3. Type of Data: Temperature profile.

4. Test Equipment: 6-foot long by 30-inch diameter vacuum chamber with 1500 cfm mechanical and a 20,000 cfm oil diffusion pump. A radiant heating apparatus as shown in Figure 15.2.2.54-1.

c. Materials Tested: Foam insulation, ablatives, and flight instrumentation for heat shield applications.

d. Reference: Lab Memo C179-9008, "Saturn S-II Aerodynamic Heat Resistant Test Results for Cook 402 Pour Foam."

15.2.2.55 Method of Test for Effects of High Temperature Thermal Environmental Conditions on Materials

a. Overall Objective: This test method with the test facility permits determination of effects on materials, structures, and systems resulting from aerodynamic heating or other thermal environments.

b. Description:

1. Test Article: Specimens may be up to approximately 400 square feet.

2. Test Conditions: Temperature to 3000 F, heat flux to 100 Btu-ft^2/sec., pressure to 1 x 10^6 TORR.

3. Type of Data: Temperature profile.

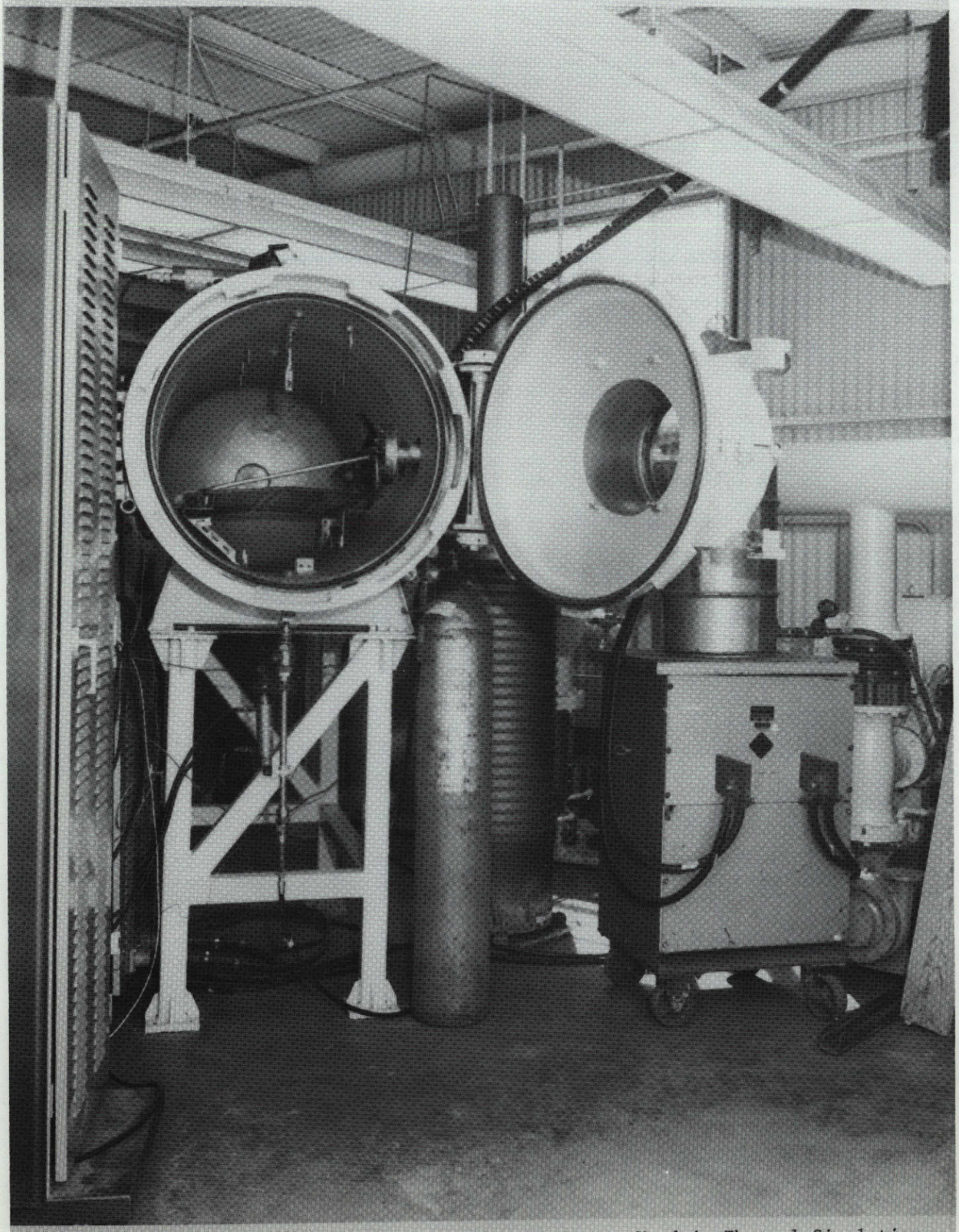

Figure 15.2.2.54-1. Radiant Heating Apparatus Used in Thermal Simulation Effects Study

4. Test Equipment: Thirty-six channels of closed logs radiant heating control computers and Ignitron power controllers, a transformer vault rated at 7500 kva continuous and approximately 15000 kva for 5 minutes, a 36-channel remote control console, 100 channels of continuous recording oscillographs, three 12-channel radiant heating control computers (analog), and tubular quartz infrared lamp ovens with a power density of 100 kw per square foot per Figure 15.2.2.55-1.

c. Materials Tested: Ablatives, refractories, and metallic structures.

d. References: NR Report SID 66-691 Apollo Spacecraft 004A Structural Thermal Tests.

15.2.2.56 Torsional Shear Modulus of Foam-Type Materials

a. Overall Objective: The test method covers procedures for determining the torsion shear modulus value of foam-type materials. Using this shear modulus in conjunction with the elastic modulus, Poisson's ratio may be obtained analytically which is useful in design purposes. Test materials are limited to those which can be cast, machined, or otherwise fabricated into a tubular configuration. Ultimate torsional shear strength may also be determined with this test; however, it is not the prime objective.

b. Description:

1. Test Article: Test specimens are tubes approximately 14 inches in length with an outside diameter of from 3/4 to 1-5/8 inch depending on the material being tested. Wall thickness will also vary from 1/8 to 1/2 inch.

2. Test Conditions: Testing is carried out from room temperature to -300 F (-148.9 C).

3. Type of Data: Includes graph of torsion load versus angle of twist with specimen dimensions for calculation of torsional shear modulus.

4. Test Equipment: Torsion load cell 50 inch-pound capacity, torsion loading device, two rotary potentiometers to measure angular twist, cryogenic chamber. Figures 15.2.2.56-1 and -2 show the test setup.

c. Materials Tested: Materials tested include pour foam and spray foam materials.

d. Reference: Lab Memo LR9420-4025, "Determination of Torsional Shear Modulus in Foam Materials."

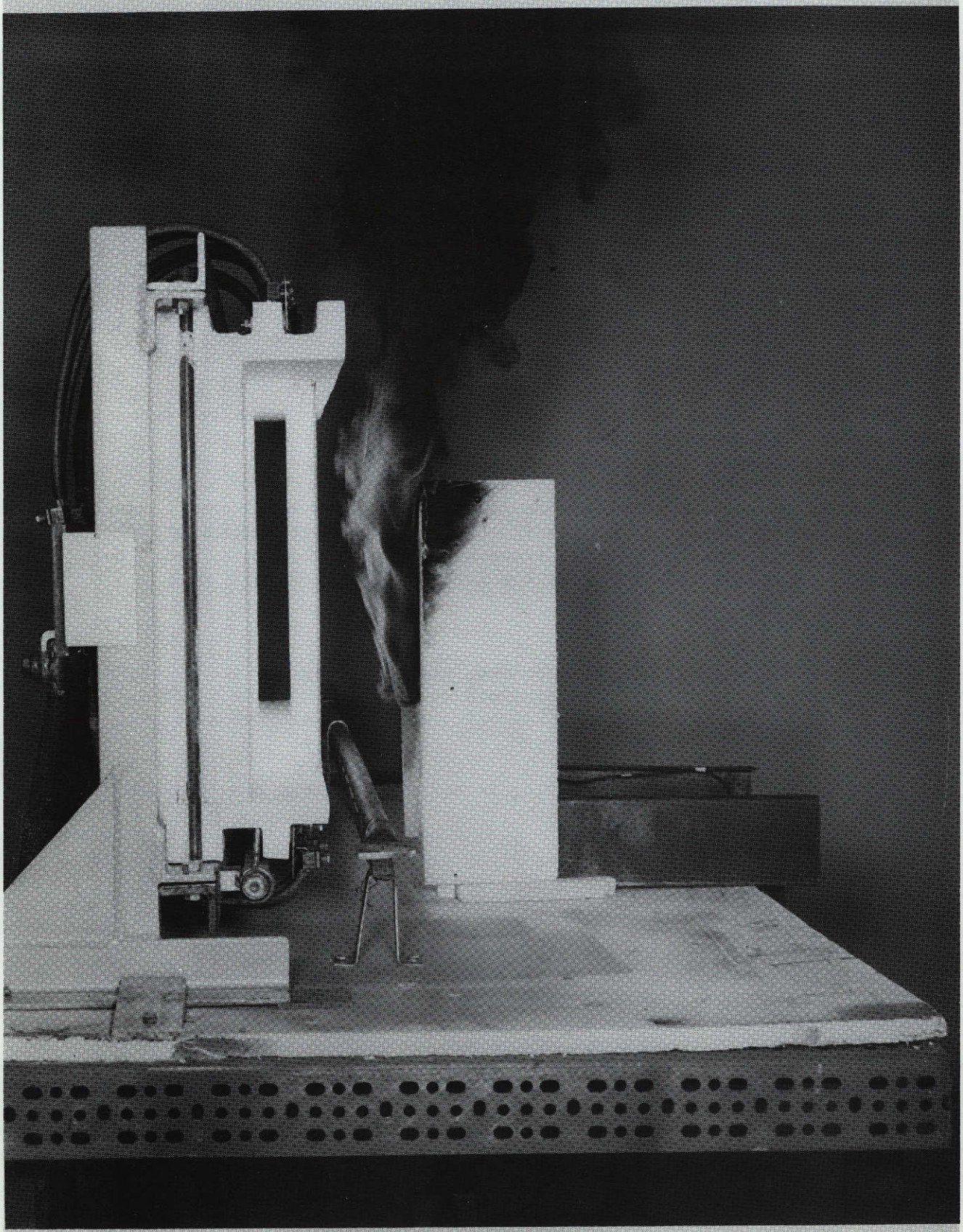

Figure 15.2.2.55-1. Aerodynamic Heating or Thermal Environmental Test Set-Up

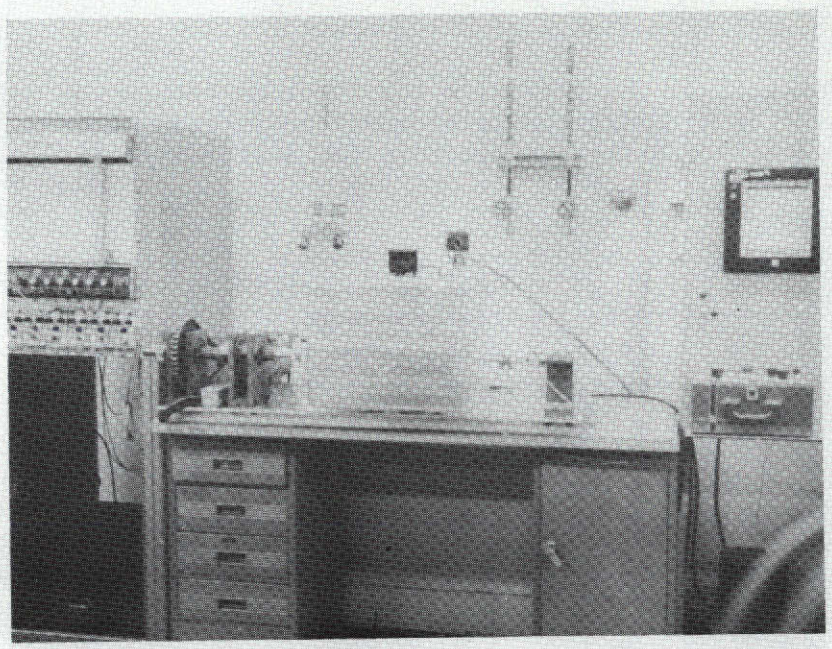

Figure 15.2.2.56-1. Overall View of Torsion Test Set-Up Showing Cold Chamber and Instrumentation

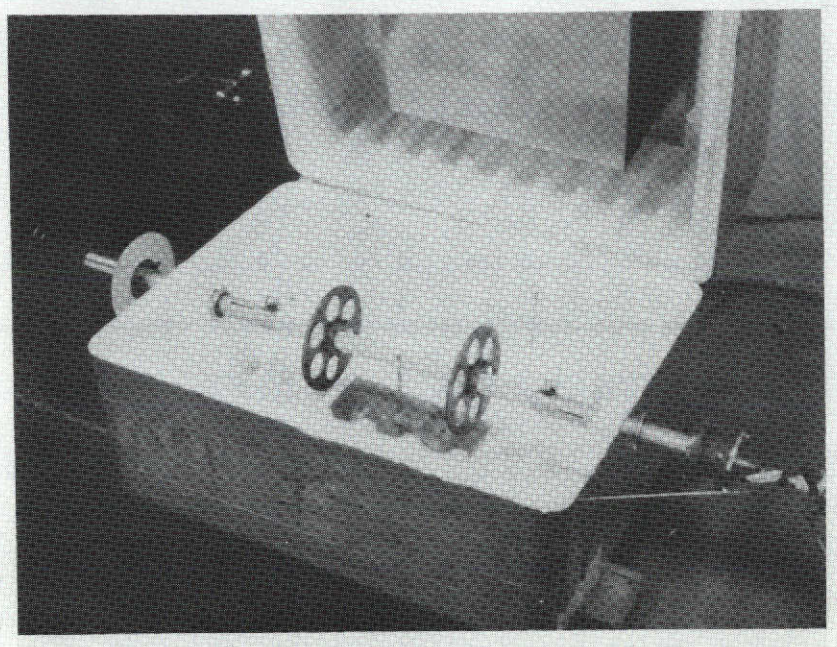

Figure 15.2.2.56-2. View Showing Torsion Load Cell and Chamber Interior With Test Specimen and Potentiometer Drive Wheels

15.2.2.57 Thermal Conductance of MLI Support Posts

a. Overall Objective: To determine the low-temperature thermal conductance of a fiberglass-reinforced epoxy resin material configured as a tubular support post for multi-layer insulation.

b. Description:

1. Test Article: An axial heat flow comparator approach was used. A tubular reference material was bonded to the MLI post specimen and an overall temperature difference impressed across the series thermal resistances of the assembly.

2. Test Conditions: Low-temperature thermal conductance -537 C (-423 F) to -53.9 C (-65 F) can be determined with the use of thermocouples situated along the exterior surface of the tube assembly at measured intervals, permitting measurement of the axial temperature gradient in both the unknown and reference specimens. Stray heat paths were minimized by foaming around the assembly.

3. Test of Data: From the steady-state temperature data, the dimensions of the specimens, and literature data for the standard material, the conductance of the post can be calculated as follows:

$$C = A,\ K_s \left(\frac{\Delta T_1}{\Delta X_1}\right)\left(\frac{\Delta T_2}{\Delta X_2}\right)^{-1}$$

where

C = Thermal conductance for 1-inch post, Btu/hr.-^{o}F

A_1 = Area of reference specimen, sq. ft.

K_s = Thermal conductivity of reference material, Btu-in./hr.-sq. ft. -^{o}F

$\frac{\Delta T_1}{\Delta X_1}$ = Temperature gradient in reference specimen ^{o}F/in.

$\frac{\Delta T_2}{\Delta X_2}$ = Temperature gradient in test specimen, ^{o}F/in.

4. Test Equipment: Heater, cold plate, Honeywell Controller (Figure 15.2.2.57-1).

c. Materials Tested: MLI support posts.

d. Reference: LR 9133-4464.

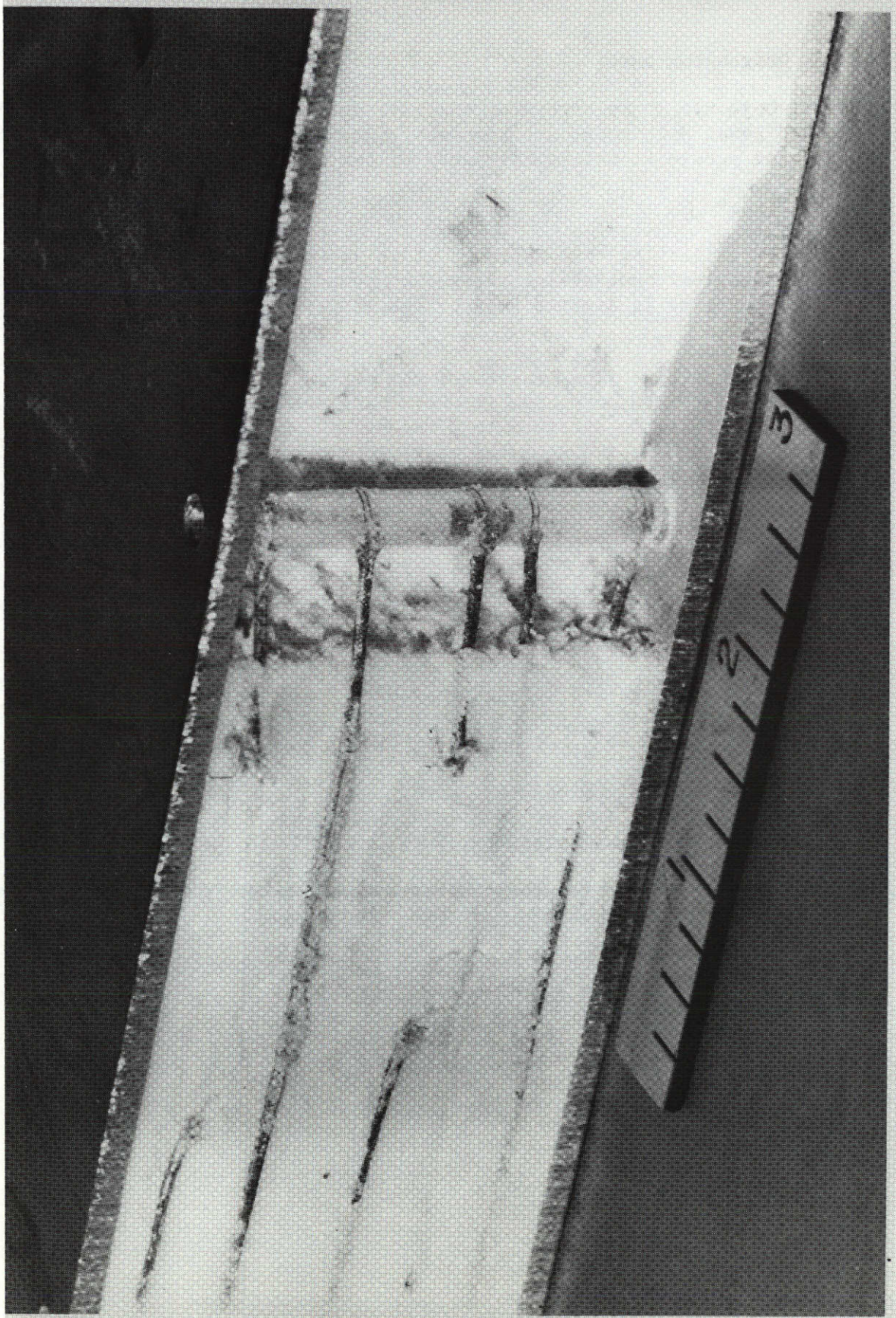

Figure 15.2.2.57-1. Specimen Assembly

15.2.2.58 Outgassing Rate

a. Overall Objective: To determine the rate at which adsorbed and absorbed gases and vapors are removed from solid surfaces exposed to reduced pressure, utilizing vacuum system pumpdown curves.

b. Description:

1. Test Article: By this approach it is possible to estimate quantitatively outgassing rates from pumpdown curves. The specimen size is limited only by the size of the bell jar available.

2. Test Conditions: The essence of the method consists in interposing between a chamber containing the specimen and the pumping system an aperture in a thin plate. Measurements of pressure on both sides of the aperture are noted as functions of pumping time.

3. Type of Data: When the chamber pressure is $<10^{-4}$ Torr the gas throughout is given by

$$Q = C\ (P-P^1)$$

where

Q = Throughput, Torr-liters/sec.

C = Conductance of aperture, liters/sec.

P = Upstream pressure, Torr.

P^1 = Downstream pressure, Torr.

The data are corrected for chamber outgassing and leakage by subtracting values obtained for the empty chamber.

4. Test Equipment: Four-inch CVC diffusion pumping system and 15-inch bell jar (Figure 15.2.2.58-1).

c. Materials Tested: Multi-layer insulation and various tapes used in MLI layup.

d. Reference: LR 9133-4432.

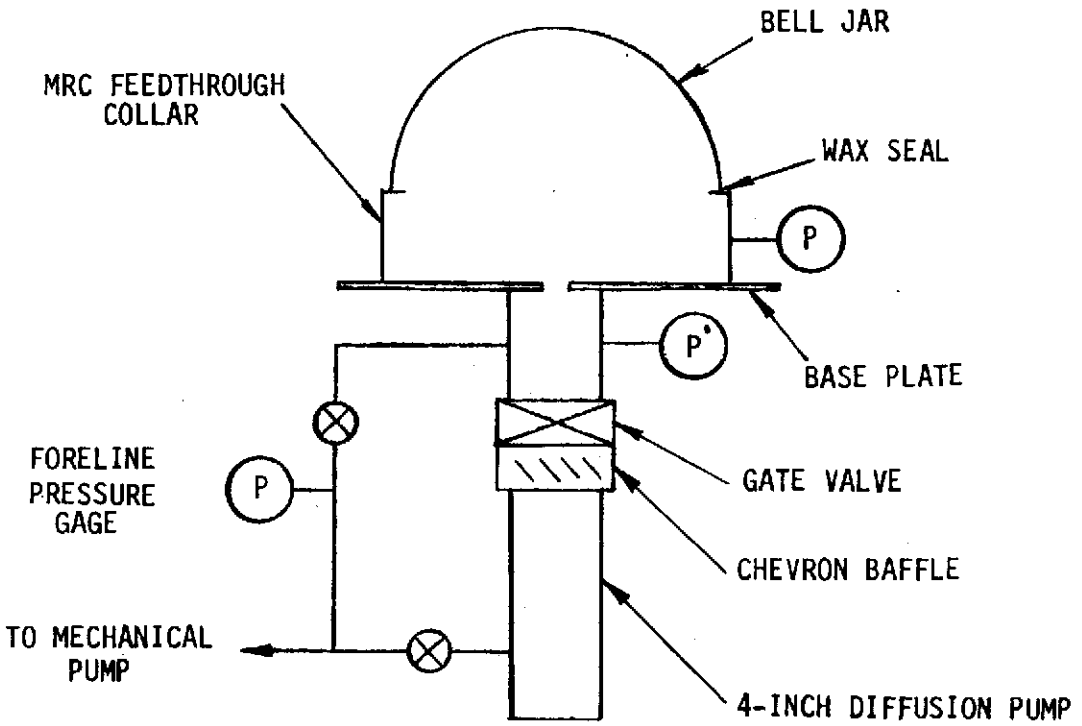

Figure 15.2.2.58-1. Vacuum System Schematic

15.2.2.59 Carbon, Hydrogen, Nitrogen Analysis of Plastic Materials

a. Overall Objective: This method covers a procedure for analyzing plastic materials for percent by weight elemental carbon, hydrogen, and nitrogen present.

b. Description:

1. Test Article: Size of sample is dependent on estimated percentage of elements present. Nominal sample size is approximately 1 milligram. Solids are powdered prior to analysis; liquids are used directly.

2. Test Conditions: Samples are mixed with manganese dioxide catalyst and subsequently introduced into a heater maintained at 700 C (1292 F). The volatile products of the oxidative decomposition, CO_2, H_2, N_2, are purged with He into a gas chromatographic system. The percent elements present are calculated from peak areas of the chromatogram. NBS organic standards are used for instrument calibration.

3. Types of Data: Percent by weight carbon, hydrogen, nitrogen.

4. Test Equipment: F&M Scientific 185 carbon, hydrogen, nitrogen analyzer.

c. Materials Tested: Non-metallic materials, organic compounds.

d. Reference: Operating manual for the F&M Scientific 185 C, H, N, Analyzer.

15.2.2.60 Evaluation Test of Tension Membrane and MLI used on 105-Inch Diameter Tank

a. Overall Objective: The objective of this test was to determine the effectiveness of the tension membrane in conjunction with the insulation system and supporting posts when subjected to purge gas pressure at various temperatures, to determine flow rate at various pressures and temperatures, and to determine at what temperature a permanent set takes place in the MLI. Varied test panel configurations, simulating the MLI installed on the tank sidewall, were subjected to room temperature and high temperature gas purges.

b. Description:

1. Test Article: A 52-inch by 52-inch test fixture was utilized for conducting these tests. The fixture was designed so that when a 50-inch by 50-inch panel of MLI was installed, there would be a 48-inch by 48-inch flow area exposed to a purge gas source. One side of the MLI was exposed to the gas source, while the other side of the MLI was exposed to the atmosphere. The perimeter of the MLI was sealed so that all purge gas had to flow through the MLI.

2. Test Conditions: Seven MLI configurations were tested. With a given MLI configuration installed in the test fixture, the elevation of the center of MLI was measured. The purge gas flow rate to the MLI was then increased until the static pressure under the MLI was 0,1, 0.2, and 0.3 inch of water. For each purge gas temperature, parameters for the following static pressures were measured and recorded: 0.1, 0.2, 0.3, 0.2, and 0.1 inch of water. The purge gas temperature for each configuration was regulated at ambient, +125 F, and +140 F. Each MLI configuration was tested with the tension membrane at ambient, +125 F, and +140 F, and without the tension membrane at +140 F only. Gaseous nitrogen was used as the test fluid. One test specimen was tested at 0.3 inch of water at the following purge gas temperatures: +140 F, +175 F, +200 F.

3. Type of Data: Purge gas flow and temperature, center elevation of the MLI, MLI internal temperatures; and MLI static pressures.

4. Test Equipment: Flow meters, pressure gauges, temperature recorders. Test setup and specimen are shown in Figure 15.2.2.60-1.

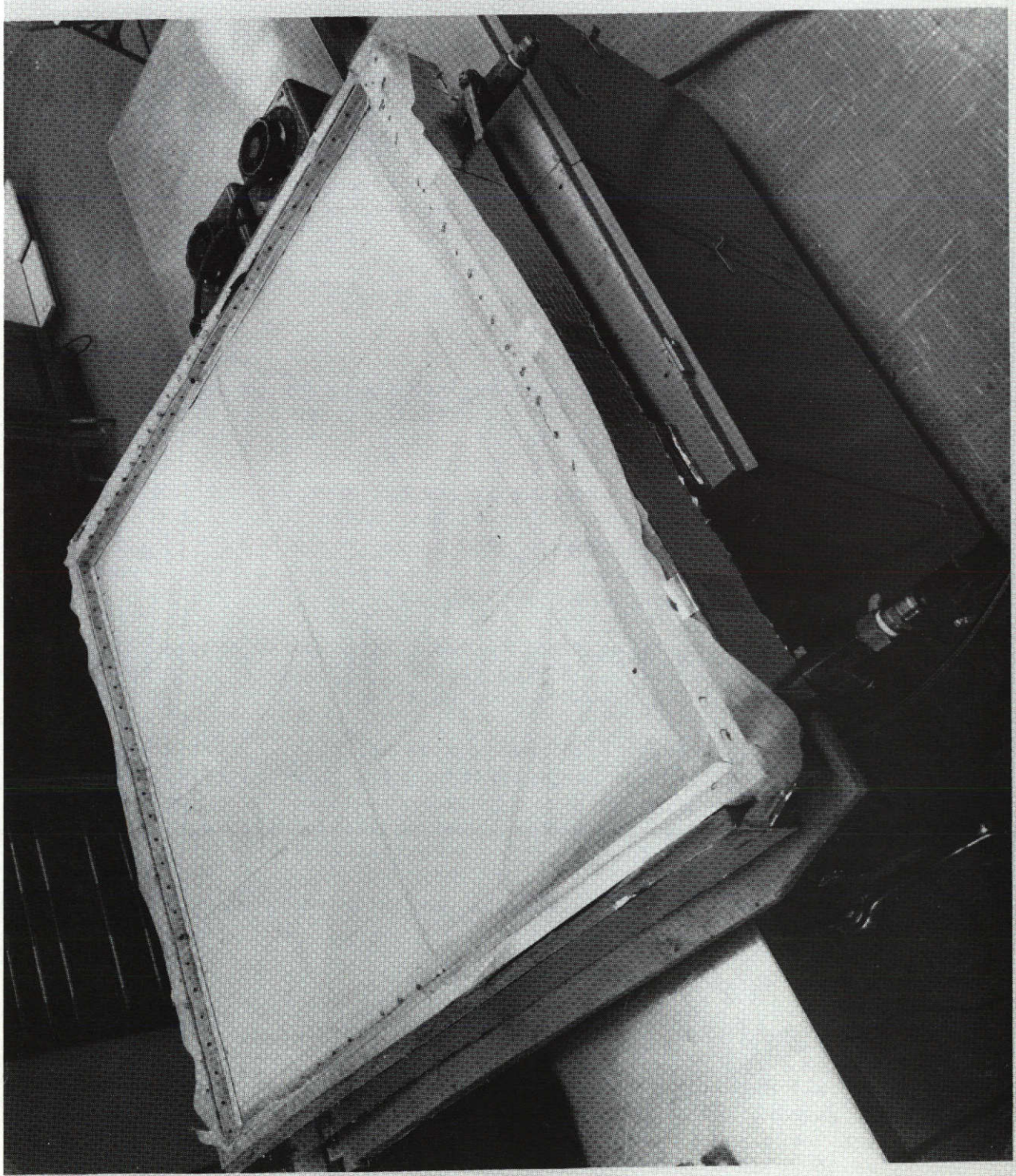

Figure 15.2.2.60-1. Test Set-Up and Test Specimen Tension Membrane

c. Materials Tested: Multi-layer insulation (with and without perforations) with and without a tension membrane.

d. Reference: LR 9133-3101.

15.2.2.61 Guarded Calorimeter Evaluation of High-Performance Insulation (HPI) System

a. Overall Objective: This method covers the procedure to evaluate and determine the effectiveness of a composite insulation system (foam, meteoroid protection, and multi-layer insulation) designed for LH_2 storage in a space environment. The test consists of measuring the loss of hydrogen from a guarded calorimeter in a vacuum of 10^{-5} Torr.

b. Description:

1. Test Article: The composite insulation system is applied to the 3-foot by 7-foot guarded calorimeter (Figure 15.2.2.61-1). The geometry of the calorimeter is shown in Figure 15.2.2.61-2.

2. Test Conditions: Testing is accomplished with the calorimeter installed in a vacuum chamber maintained at a minimum of 10^{-5} Torr. Test temperatures range from ambient to -423 F; pressures range from 10^{-6} Torr to 4 psig, and flow of gaseous hydrogen ranges from 0 to 4000 scfh.

3. Type of Data: Data include insulation system and vacuum chamber pressures and temperature. Calorimeter temperatures, pressures, and flow are also recorded.

4. Test Equipment: A chamber system 4 feet by 8 feet with associated vacuum pumps and controls, calorimeter with valves and controls, flow measuring system, liquid hydrogen delivery system, and a 250-channel data acquisition system. Figure 15.2.2.61-3 is a conceptual schematic of the test system.

c. Material Tests: Materials tested are high-performance composite insulation systems.

d. References: SD 70-441 and SD 851-137.

15.2.2.62 Multi-Layer Insulation Molecular Flow Test

a. Overall Objective: The following method was used to determine the outgassing and venting characteristics of aluminized Mylar (embossed and perforated) insulation, installed in a vacuum chamber, as shown in Figure 15.2.2.62-1, and subjected to conditioning/ evacuation tests.

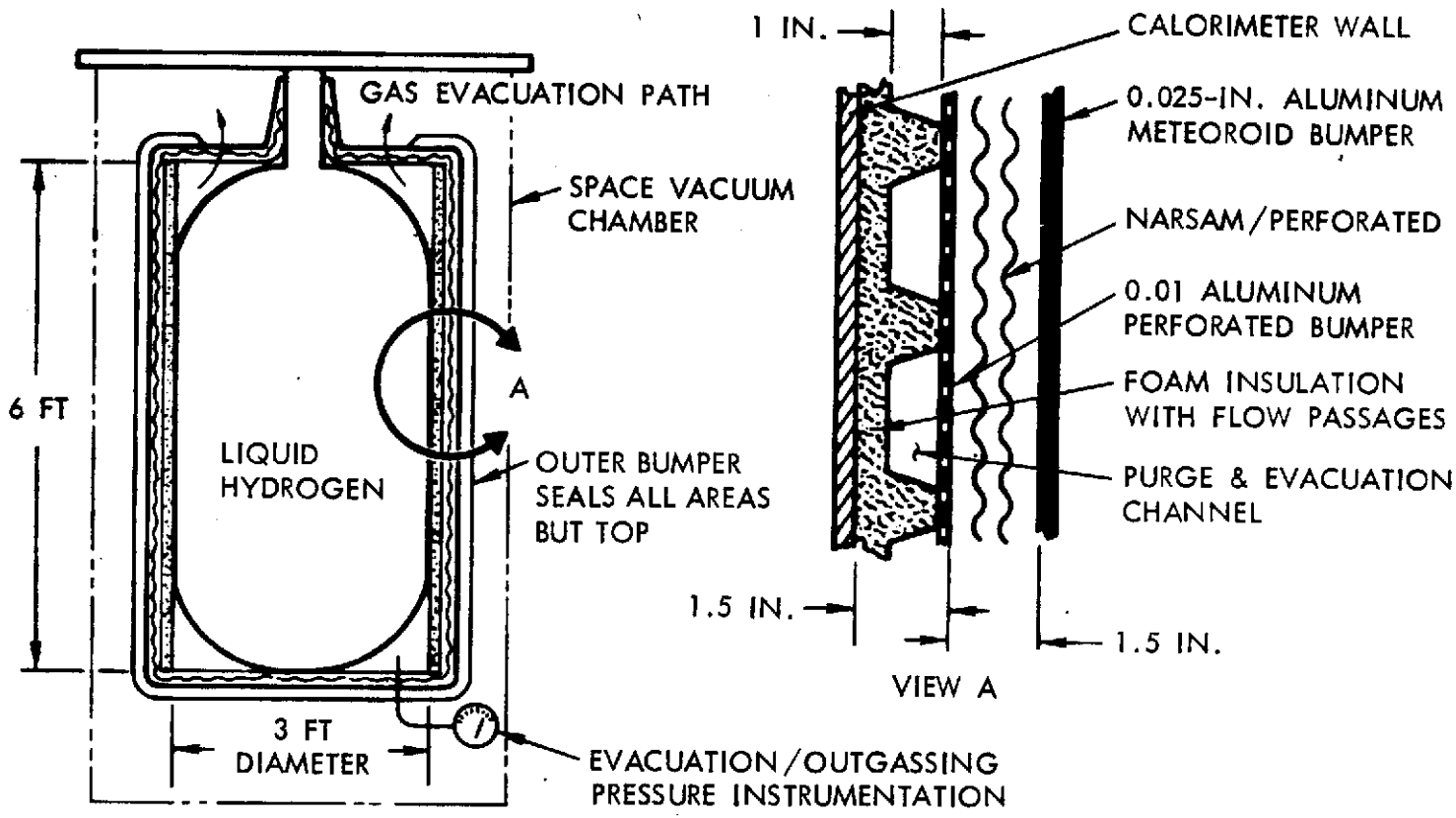

Figure 15.2.2.61-1. HPI Composite/Calorimeter Assembly

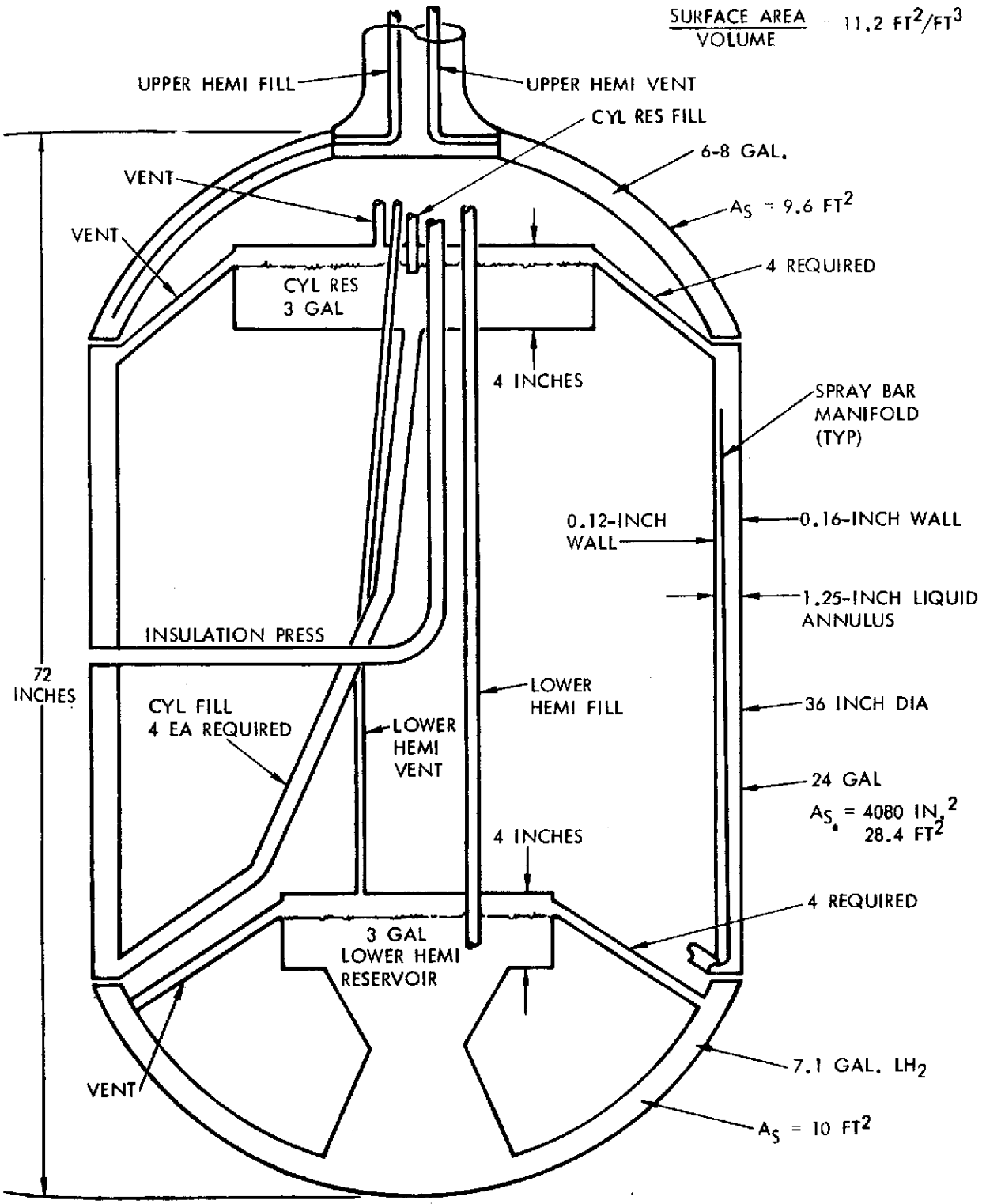

Figure 15.2.2.61-2. Volumetric Geometry of Calorimeter

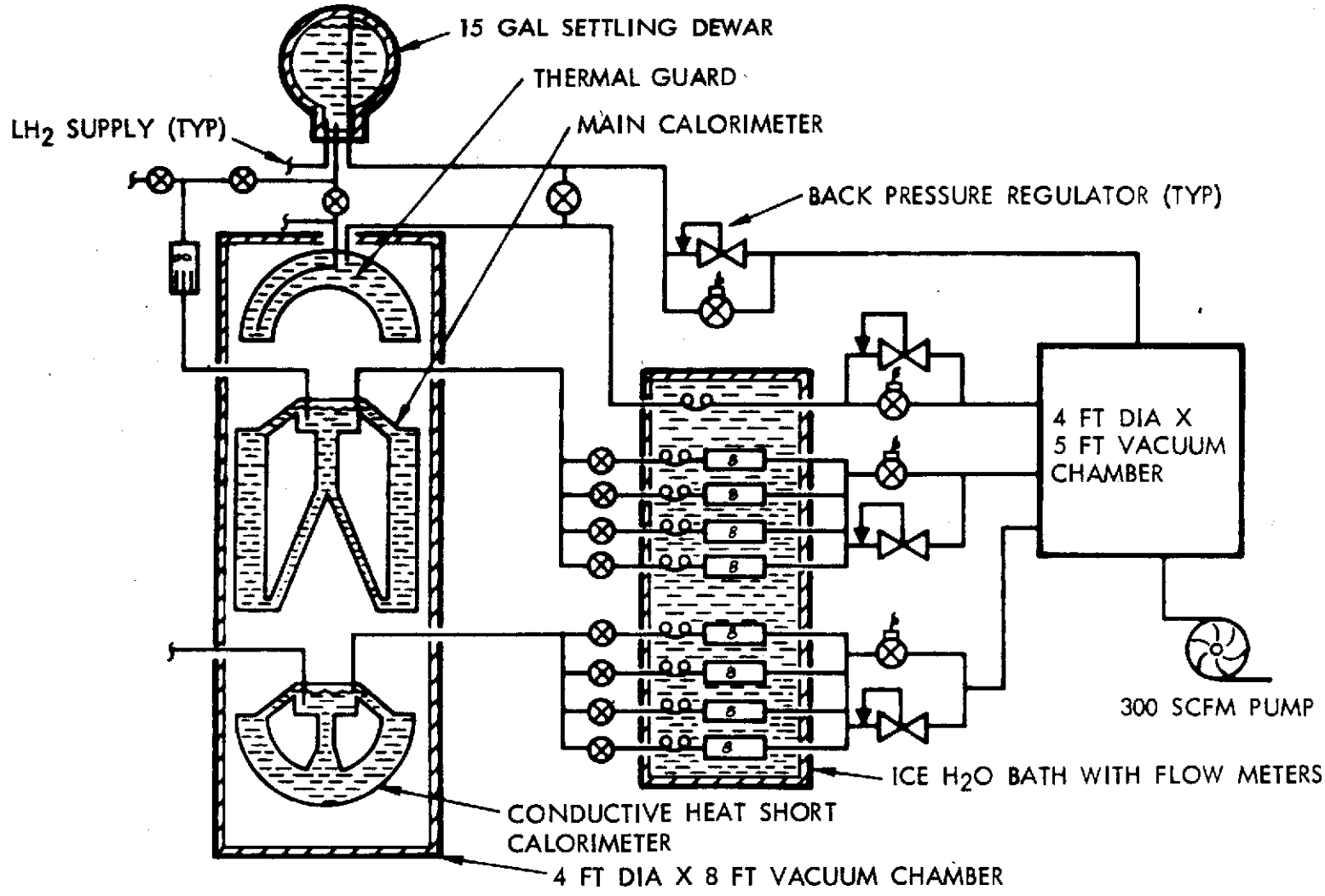

Figure 15.2.2.61-3. Cryogenic Calorimeter Conceptual Schematic

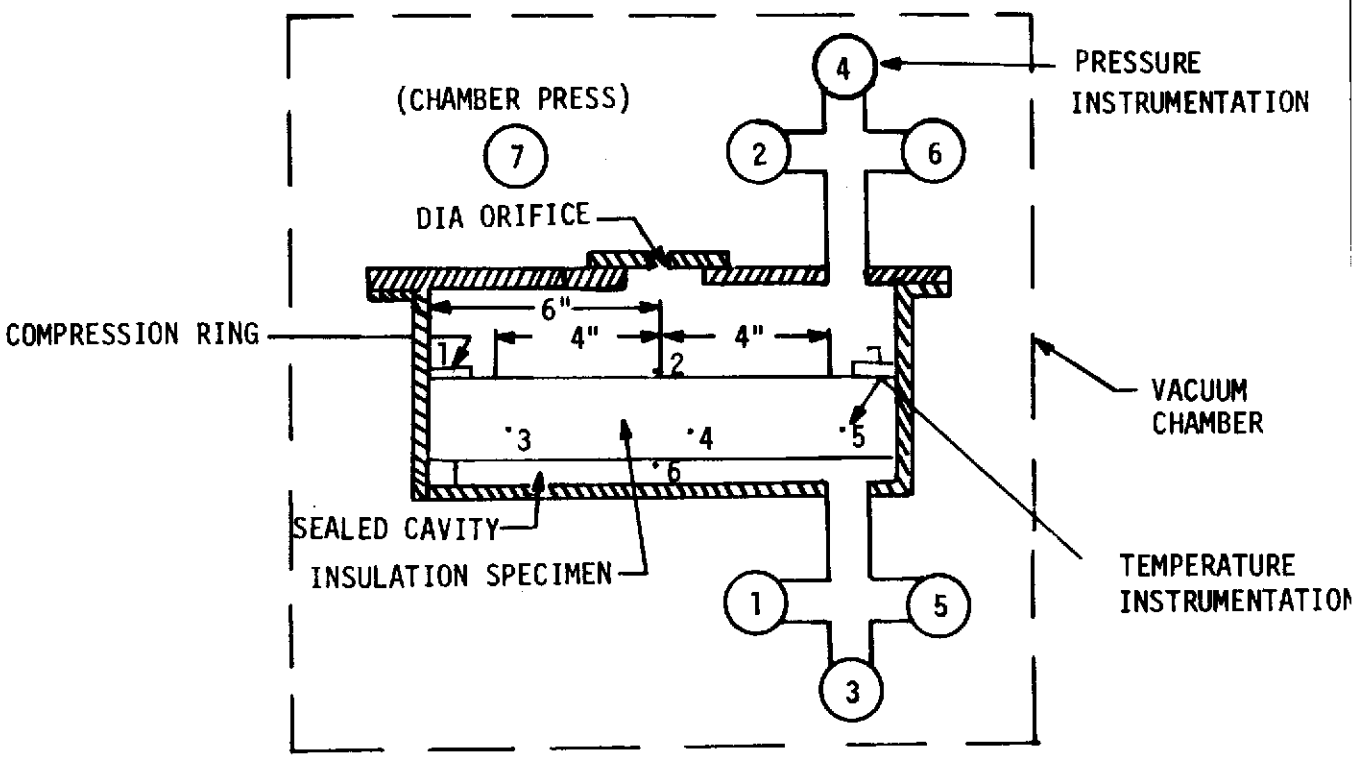

PRESSURE INSTRUMENTATION

NO.	TYPE	RANGE (TORR)
1	ION GAGE	1×10^{-3} to 1×10^{-8}
2	ION GAGE	1×10^{-3} to 1×10^{-8}
3	BARATRON	1×10^{-1} to 1×10^{-8}
4	BARATRON	1×10^{-1} to 1×10^{-2}
5	MAGNEVAC	760 to 1×10^{-2}
6	MAGNEVAC	760 to 1×10^{-3}
7	ION GAGE	1×10^{-3} to 1×10^{-8}

TEMPERATURE INSTRUMENTATION (ALL LOCATED ON SAME DIAMETER)

NO.	TYPE	RANGE (^{o}F)
1	THERMOCOUPLE	M100 to 100
2	↕	↕
3	↕	↕
4	↕	↕
5	↕	↕
6	THERMOCOUPLE	M100 to 100

Figure 15.2.2.62-1. Schematic-MLI Molecular Flow Test

b. Description:

1. Test Article: The test article consisted of 90 layers of 12-inch diameter MB0135-034 aluminized Mylar. Uniform compression around the periphery of the specimen resulted in a seal forcing evacuation of the trapped gasses through the vent holes in the Mylar.

2. Test Conditions: A pre-conditioning exposure was conducted on the test specimen prior to each of the nine evacuation tests to determine the effects of storage, vacuum drying, moisture contamination, and hot gas drying on the evacuation rate. Differential pressure across the specimen was measured using thermocouple gauges, absolute pressure transducers, and ion gauges, to obtain data in the range from ambient pressure to 1×10^{-5} Torr. Specimen temperatures ranged from 135 F to -100 F.

3. Type of Data: Data obtained included dew point, absolute pressures, specimen and fixture temperature, and gas flow rates.

4. Test Equipment: Test equipment consisted of a 6-foot diameter, 14-foot long vacuum chamber with oil diffusion and mechanical vacuum pumps. Instrumentation consisted of ionization vacuum gauges, absolute pressure transducers, pressure recorders, millivolt recorders, and temperature recorders.

c. Material Tested: MB0135-034 Type II aluminized Mylar.

d. References: NR/SD Specification MB0135-034, Laboratory Test Report LR 19133-3201.

15.2.2.63 Cryogenic and Combined Environment Testing of Insulation System for Bolting Ring and No. 1 Cylinder For S-II (24-Square Inch Test Tank)

a. Overall Objective: This method covers the procedure for determining the structural and thermal characteristics of insulation for bolting ring and No. 1 cylinder, as applicable to liquid hydrogen tankage. The test consists of subjecting the insulation system, installed on the test tankage, to repeated fill and drain cycles with liquid hydrogen and simulation of flight profiles: pressure, temperature, and vibration.

b. Description:

1. Test Article: The test insulation system is fabricated and installed on the 24-square-inch test tank, in accordance with NR process specifications. Configuration of the test tankage is shown in Figure 15.2.2.63-1.

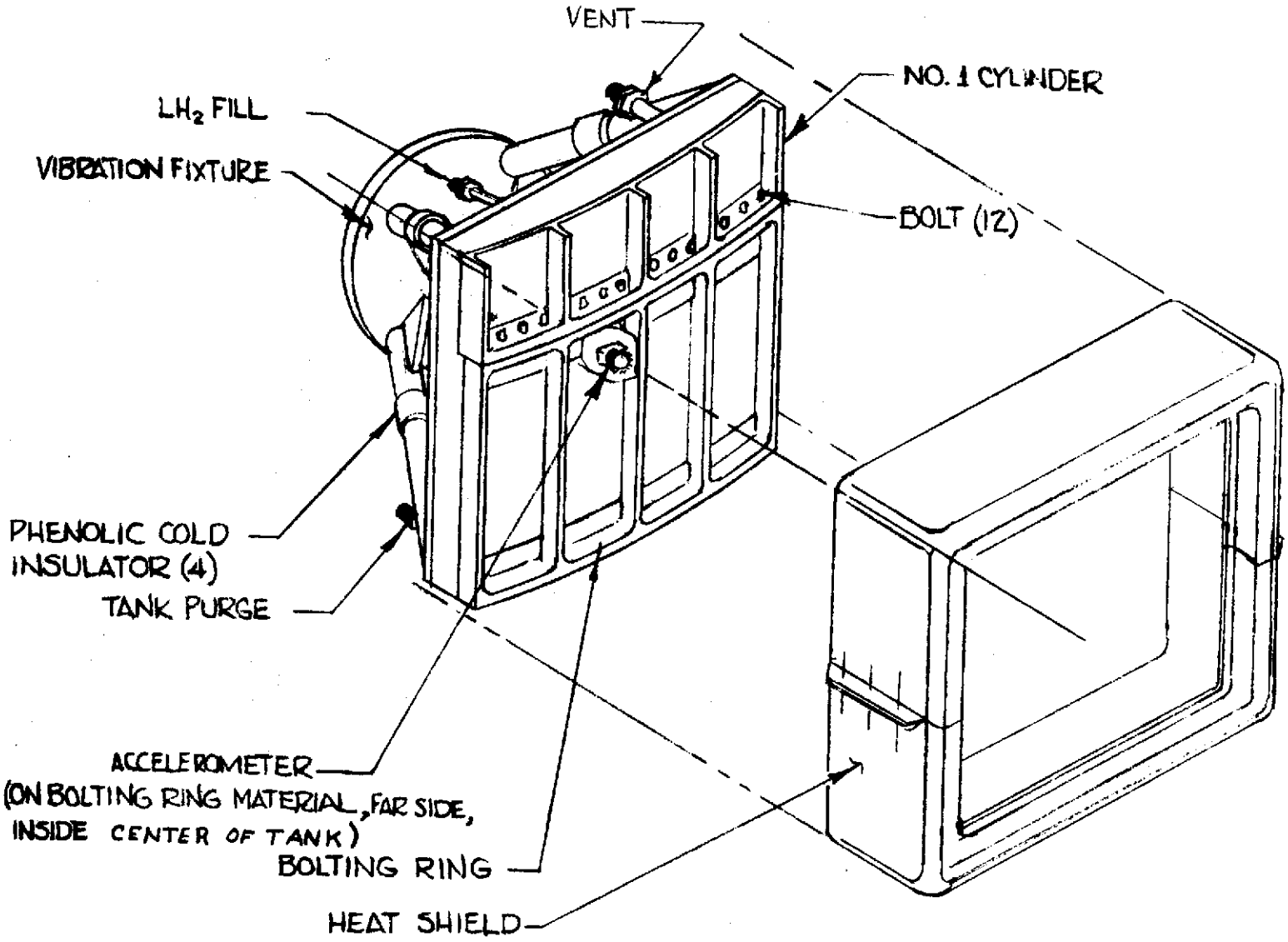

Figure 15.2.2.63-1. Saturn S-II 24" x 24" Bolting Ring and No. 1 Cylinder Combined Environments Test Tank

2. Test Conditions: Testing is accomplished in the environment and temperature of the most rigid intended use of the insulation system. Test temperatures will range from -423 to 450 F, and test pressure from ambient to 8.0 psig. Maximum vibration levels are 14.5 g RMS.

3. Type of Data: Data include insulation system temperatures during all test phases and time-based profiles of pressure and temperature during simulated flight. During vibration, response characteristics of tank-mounted accelerometers are recorded.

4. Test Equipment: Shaker system, hot gas equipment, and tankage with associated valves and controls.

c. Materials Tested: The primary materials tested are foam insulation systems.

d. Reference: LM 311-7002.

15.2.2.64 Cryogenic Test of Insulation System on 8-Foot by 8-Foot by 1-Foot Tankage

a. Overall Objectives: This method convers the procedure for evaluating the fabrication techniques and design characteristics of large scale insulation system samples installed on an 8-foot by 8-foot by 1-foot tank. The test consists of repetitive fills of the tankage, temperature holds to 24-hour duration, and drainage of the liquid hydrogen.

b. Description:

1. Test Article: Test specimen is in the range of 5 square feet to 8 square feet, fabricated and installed per applicable NR process specification on the test tank. Figure 15.2.2.64-1 shows a 7-foot by 7-foot insulation system installed on the tankage.

2. Test Conditions: Testing is accomplished with an ambient external environment while the tank is maintained filled with liquid hydrogen. Internal insulation pressure ranges from 0.1 mm Hg to 2200 mm Hg.

3. Type of Data: Data include time-temperature and pressure history, insulation pressure, leakage rates, and flow rates.

4. Test Equipment: Test tankage with associated control and valving. Figure 15.22.64-2 shows the test schematic and Figure 15.2.2.64-3 gives detail of the purge control and gas sampling station.

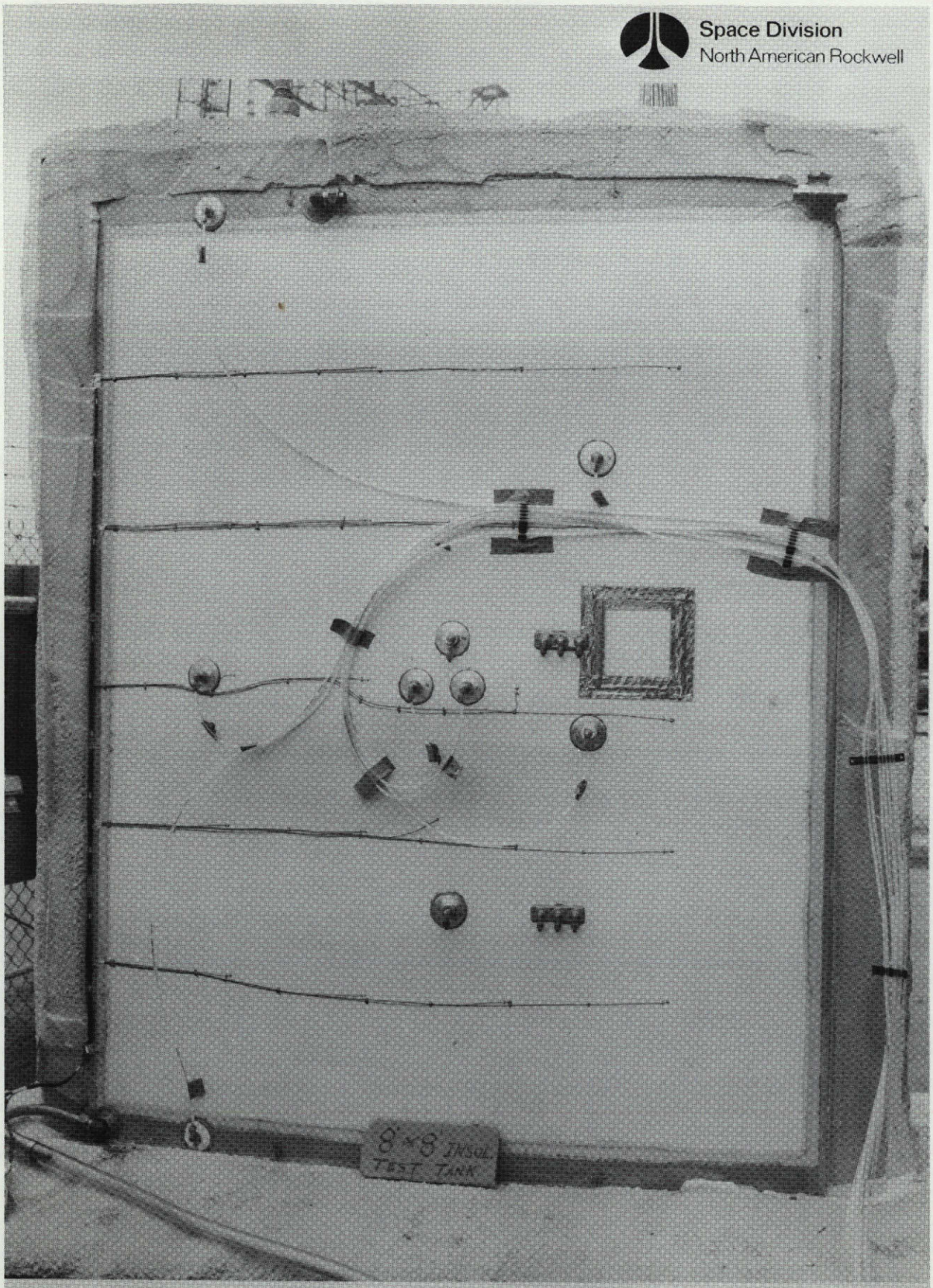

Figure 15.2.2.64-1. Cryogenic Test Tank Prepared for Test

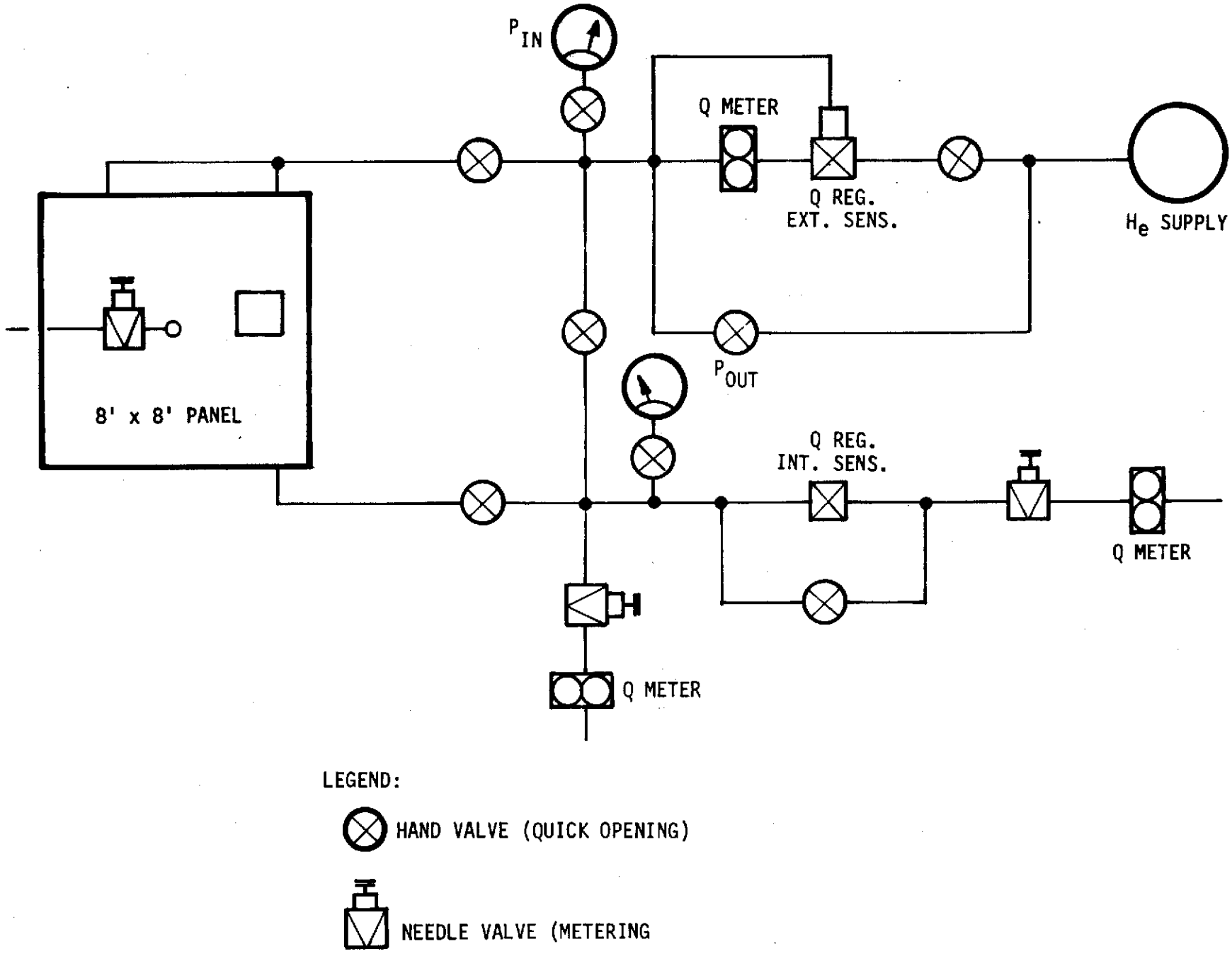

Figure 15.2.2.64-2. Schematic 8' x 8' Cryogenic Test Tank

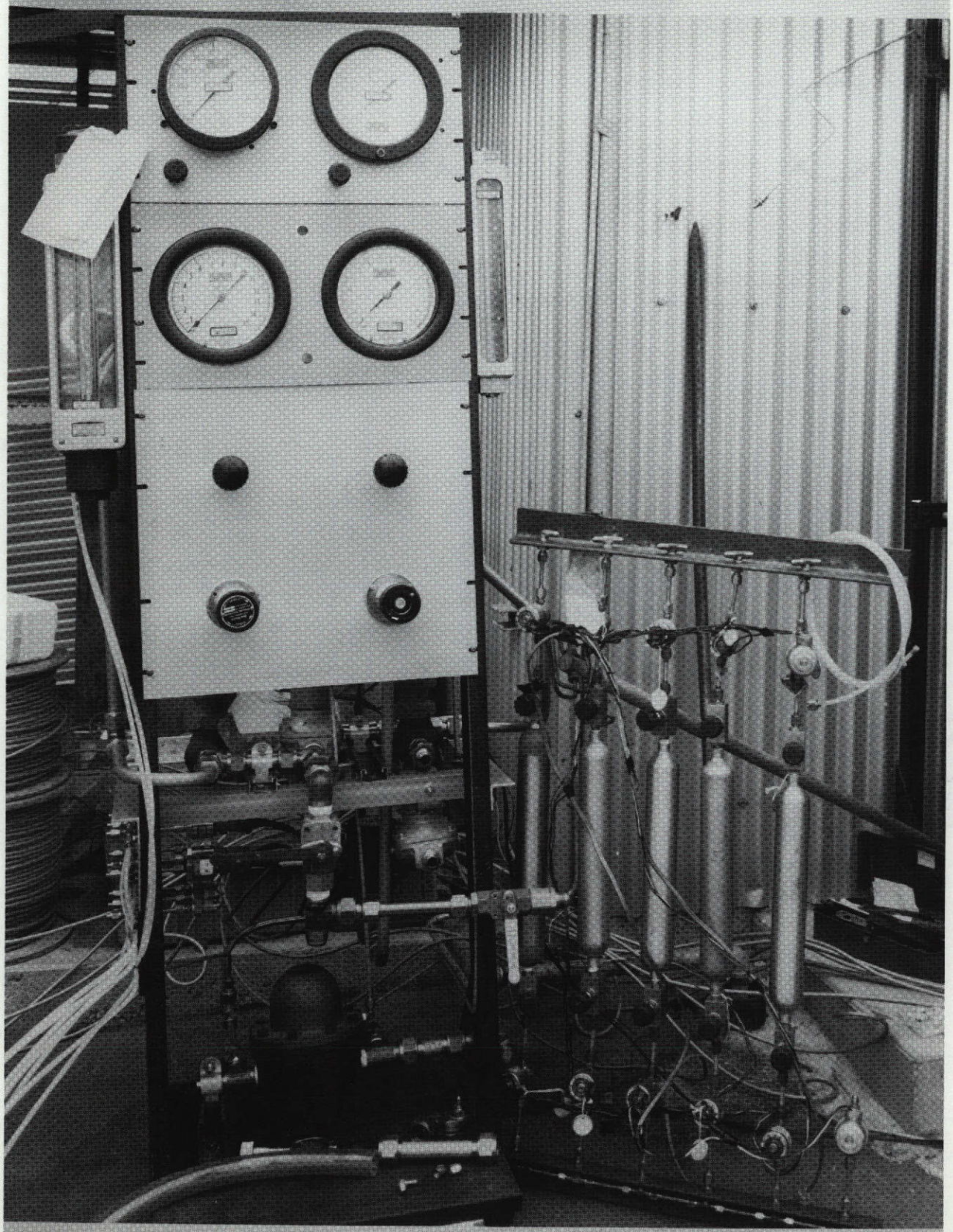

Figure 15.2.2.64-3. Purge Control and Gas Sampling Station

c. Materials Tested: Materials tested include honeycombed, evacuated, and purged insulation and foam insulation system.

d. Reference: LM 311-8002.

15.2.2.65 Cryogenic Test Tank, 2-Foot Diameter

a. Overall Objective: This method covers the procedure for determining the thermal efficiency of insulation systems designed for sidewall application on liquid hydrogen tankage. The test consists of measuring the evaporation rate of liquid hydrogen from the test tankage, the L/D ratio being 2, to determine thermal conductivity.

b. Description:

1. Test Article: The test (insulation) specimen is fabricated on a tank 2 feet in diameter by 4 feet high to appropriate NR process specification (Figure 15.2.2.65-1).

2. Test Conditions: Testing is accomplished by filling the test tank with liquid hydrogen and monitoring volumetric loss of liquid between fixed points within the tank after externally mounted insulation system thermocouples have stabilized. The tankage is maintained in an ambient environment with insulation pressure ranges from 0.1 to 2300 mm Hg.

3. Type of Data: Data include temperature, pressure, time history, and boiloff rates from which thermal conductivity, K, is calculated.

4. Test Equipment: Scale tankage with liquid level sensor rake with associated controls and valving and temperature recording equipment (Figure 15.2.2.65-2).

c. Materials Tested: Honeycombed, evacuated, and purged insulation and foam insulation systems.

d. Reference: LM 311-7002.

15.2.2.66 Flow and Burst Pressure Testing of Polyimide Panels

a. Overall Objective: This method covers the procedure for determining flow and burst pressure characteristics of coated and uncoated polyimide panels designed to protect conventional liquid hydrogen sidewall insulation systems.

b. Description:

1. Test Article: The test panel is a 9-inch diameter disc, whose total thickness is a minimum of 0.50 inch (Figure 15.2.2.66-1).

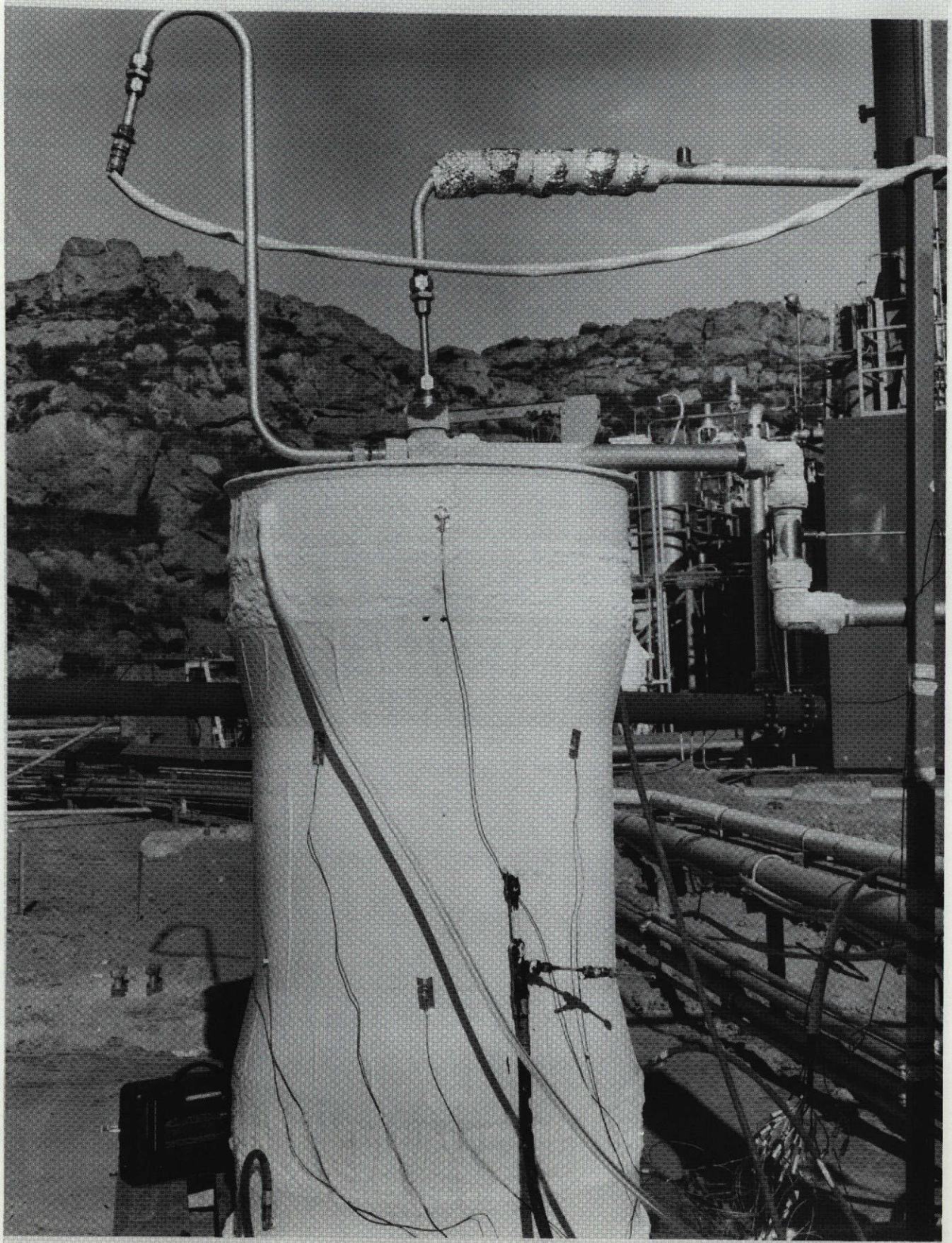

Figure 15.2.2.65-1. 2-Foot Diameter Cryogenic Test Tank

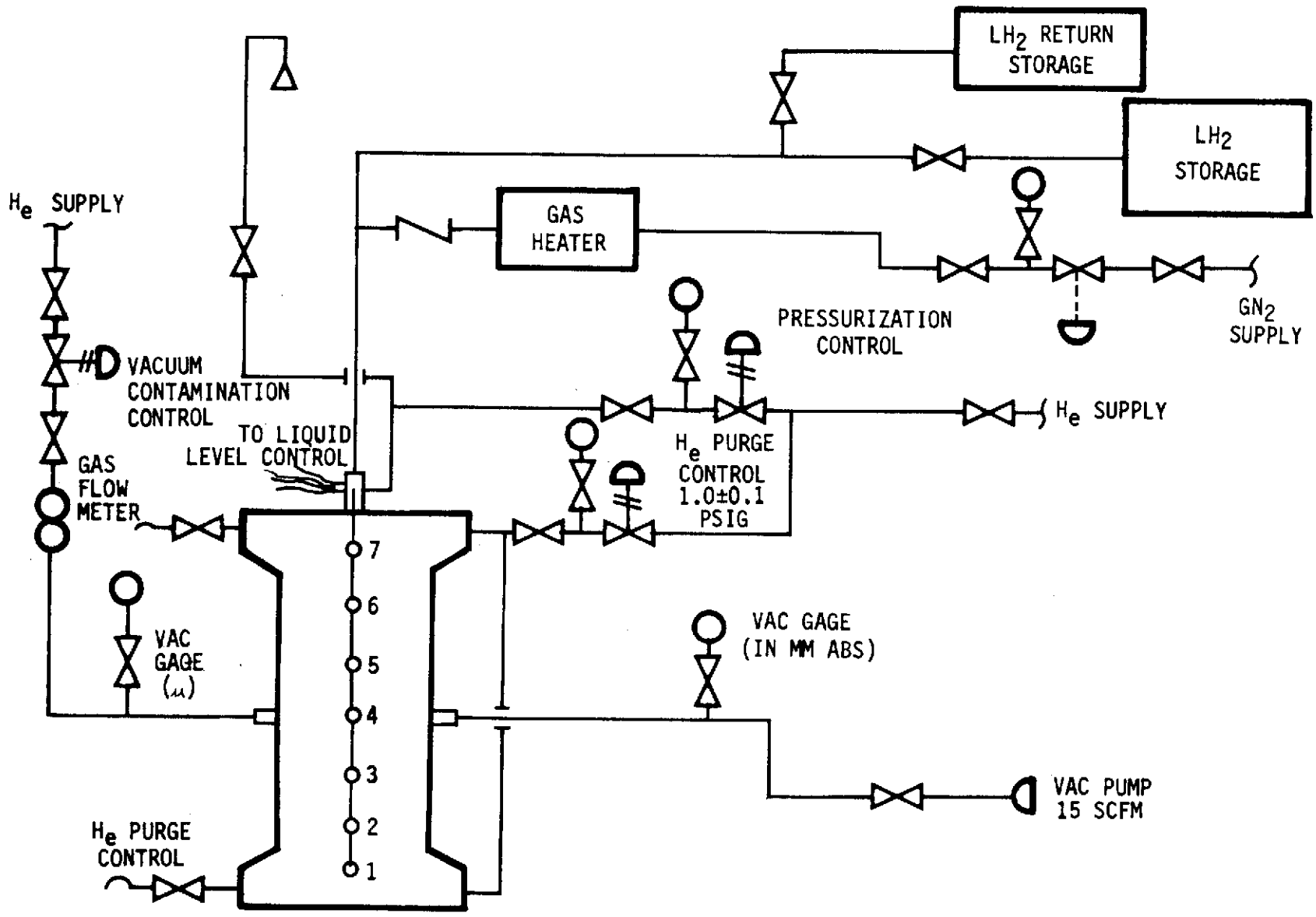

Figure 15.2.2.65-2. Schematic 2-Foot Diameter Cryogenic Test Tank

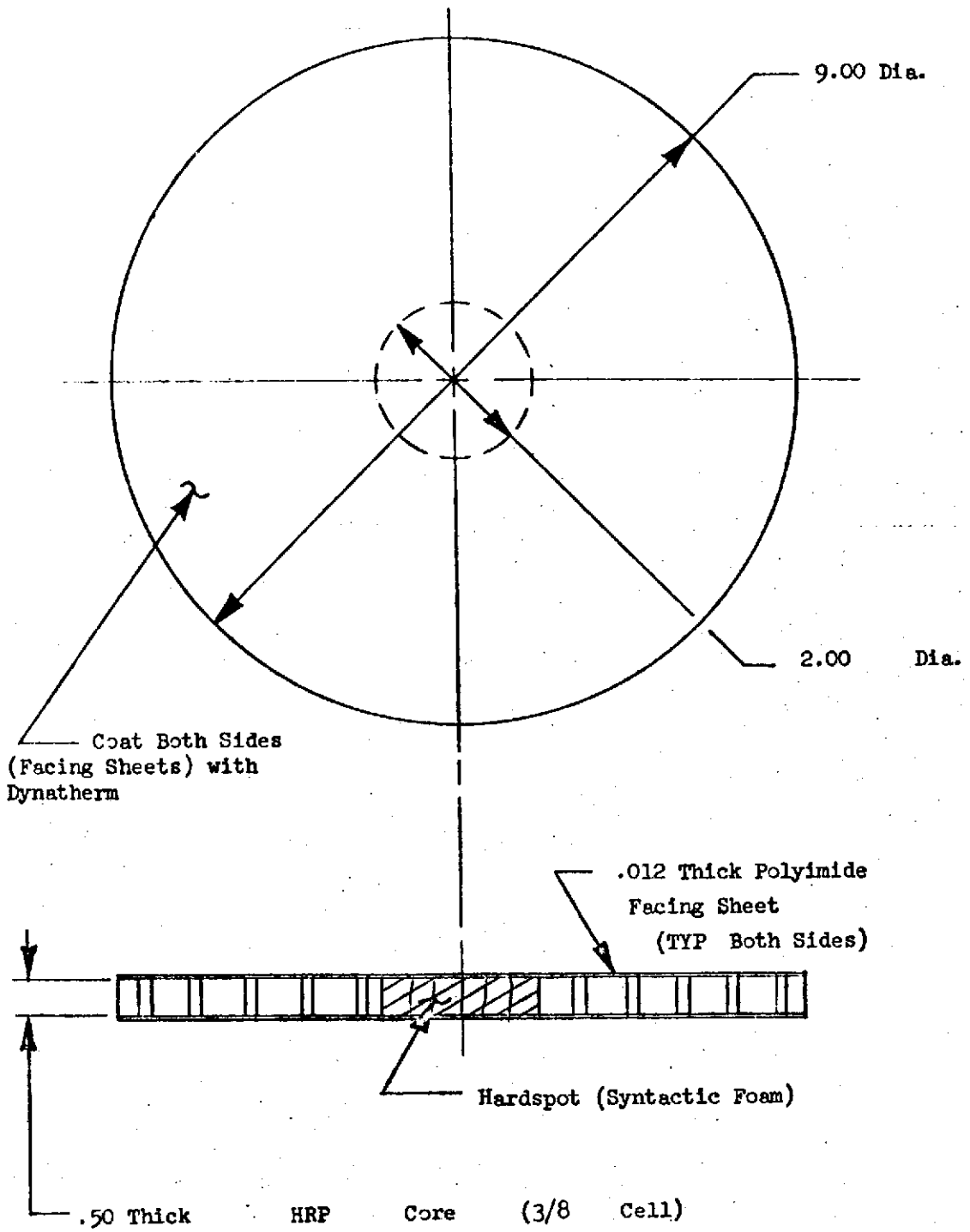

Figure 15.2.2.66-1. Burst Specimen - Hard Spot Configuration

2. Test Conditions: Tests are accomplished in an ambient environment. Internal pressure ranges from ambient to 70 psig, and with flows from 0 to 6 scfm.

3. Type of Data: Data include panel internal pressure and flow.

4. Test Equipment. The panel is restrained in a holding fixture to which flow and pressure controls are attached (Figure 15.2.2.66-2).

c. Material Tested: Materials tested are polyimide panels, both coated and uncoated.

d. Reference: LM 6810-3101.

15.2.2.67 Cryogenic Testing of S-II Feedline Elbow

a. Overall Objective: This method covers the procedure for evaluating the structural and flow characteristics of the configuration for purge and leak detection of liquid hydrogen feed line elbows. The test consists of measuring flow and pressure drop in the purge system with the elbow stabilized at liquid hydrogen temperature.

b. Description:

1. Test Article: The horseshoe purge system is fabricated and installed per applicable NR process specification, followed by application of foam to the elbow.

2. Test Conditions: Testing is accomplished by chilling the feed line elbow and measuring flow through the purge system and leakage through the coils. Test temperatures range from ambient to -423 F and coil pressures range from ambient to 25 psig.

3. Type of Data: Data include temperature, pressure, flow, and leakage values.

4. Test Equipment: Equipment consists of the insulated feed line elbow with associated valves and controls and data recording equipment.

c. Material Tested: Materials tested are the foam on the elbow and the non-metallic elements of the horseshoe purge system.

d. Reference: LM 311-6023.

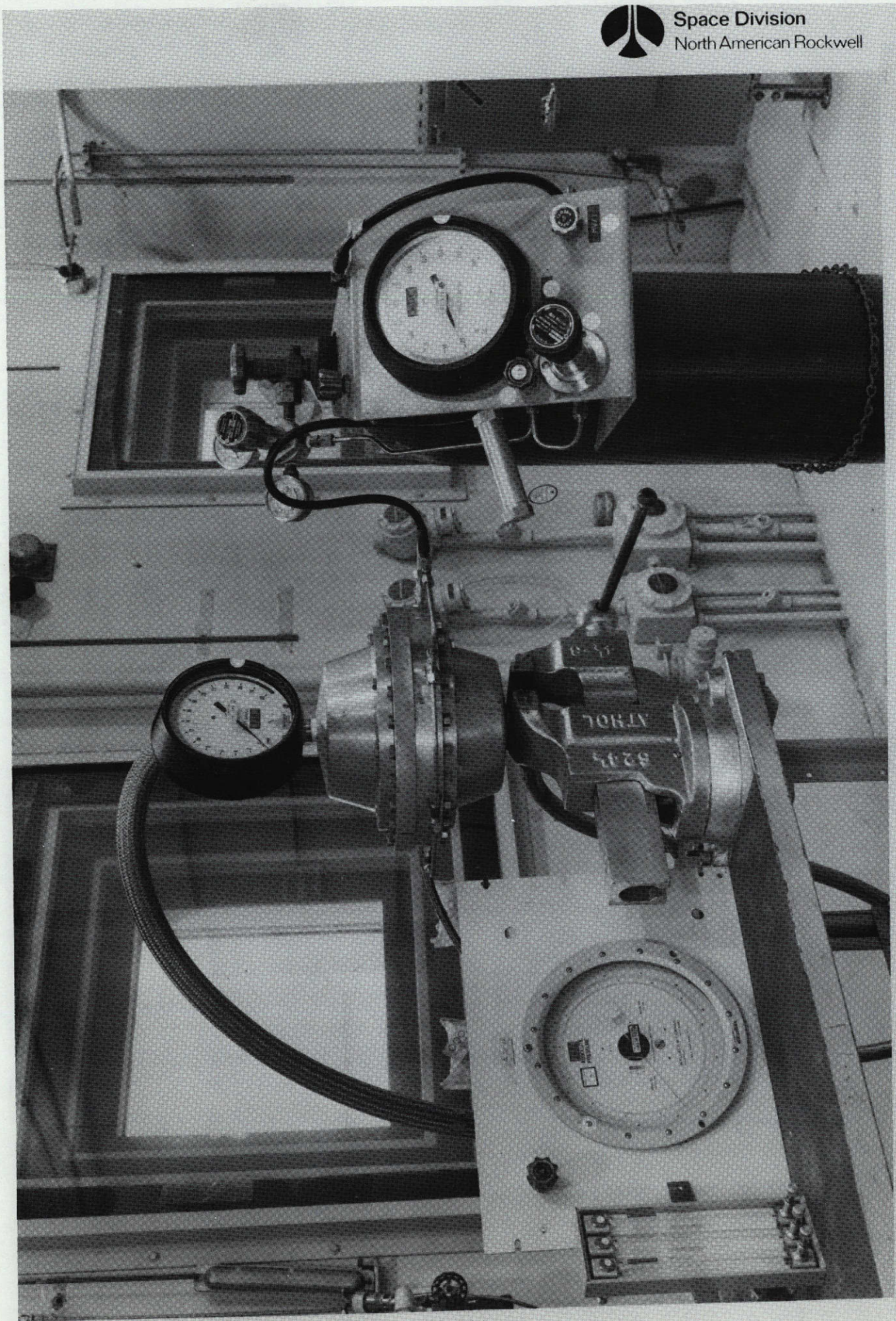

Figure 15.2.2.66-2. Flow Test Set-Up, Burst Test

15.3 QUALITY ASSURANCE PROVISIONS

This report is organized so that the reader may select an insulation design and find in Section 6.0 the significant unique aspects of that design in areas such as application, performance, manufacturing, and quality assurance. In the area of Quality Assurance, however, there are several aspects of quality control that are common to all production operations involving insulation systems. This section deals with those aspects.

15.3.1 Raw Material Control

Prior to receipt in the production area of a raw material to be used in the production of an insulation system, considerable confidence in the quality of that material has been established by prior testing. Significant areas of testing are described in the following paragraphs.

15.3.1.1 Qualification Testing

A Qualified Source List (QSL) is maintained for each raw material procurement specification. The list contains all qualified suppliers to that particular specification along with the commercial designation of the approved product. Prior to addition to the QSL, each material must be successfully tested to all requirements of the specification.

15.3.1.2 Supplier Certification Testing

Certification of materials by suppliers is accomplished through test reports submitted at the time of material delivery. These acceptance tests are the minimum number of tests to be performed by the manufacturer on each shipment and on each batch or lot number within a shipment. Sufficient tests must be performed by the manufacturer or an independent commercial laboratory to assure that the material conforms to all the requirements of the procurement specification.

15.3.1.3 Receiving Inspection Testing

Receiving inspection tests are defined as those necessary to assure that the material received from the supplier conforms to the requirements of the procurement specification. The actual level of testing performed will vary from time to time as well as from material to material and depends on previous receiving history on that particular material.

15.3.1.4 Validation Testing

Validation tests are those tests performed periodically on perishable raw material to assure the material continues to meet specification requirements while in production use.

The normal period for testing is 30 days prior to use. There are two exceptions to the 30-day testing cycle:

a. Foaming adhesives are tested within seven days prior to use.

b. Cryogenic strain compatibility of spray foam insulation is verified within 60 days prior to use.

Table 15.3.1.4-1 tabulates the minimum level of testing performed on applicable materials utilized in the insulation systems presented in Section 6.0. The level of testing was subject to increase at the discretion of Quality Assurance.

15.3.2 Manufacturing Process Controls

In addition to the Quality Assurance provisions established for each design set forth in Section 6.0 certain uniform controls are established throughout the manufacturing area for equipment, facilities, and raw material. Primary areas of control are discussed in the following paragraphs.

15.3.2.1 Equipment Calibration

All instruments used for measurement (dimensions, pressures, temperature, relative humidity, flow rates) are calibrated at scheduled intervals. A tab run is maintained on all calibrated devices employed in the production departments for notification of the using department and tracking purposes. Prior to commencement of all production operations, Inspection verifies that all applicable equipment bears physical evidence (decals) indicating current calibration.

15.3.2.2 Special Equipment Control

Special processing equipment such as autoclaves, curing presses, and ovens are verified operable and functional by performing a dry run in which thermocouples are placed throughout the equipment. Temperature variables within the equipment are verified and documented for a typical cure cycle.

15.3.2.3 Facility Environmental Monitoring and Control

The majority of bonding operations are required by specification to be conducted in a temperature range of 60 F to 90 F with a maximum relative humidity of 70 percent. If automatic recording equipment is not employed, temperature and humidity readings are recorded every four hours.

15.3.2.4 Control of Processing Tanks and Solutions

Processing tank solutions employed for the surface preparation of large subassemblies such as quarter panels and bulkhead facing sheets are analyzed daily for proper chemical composition.

Table 15.3.1.4-1. Raw Material Validation

Specification	Document Title	Testing Performed*
MB0120-008	Adhesive, Room Temperature Curing for Use From -250 F to 500 F	1, 7
MB0120-014	Adhesive, Elevated Cryogenic Temperature-Resistant, Foaming Type, -423 F to 500 F	6
MB0120-023	Adhesive, Modified Epoxy, Low-Temperature Curing, for Cryogenic Usage	1, 2
MB0120-024	Resin, Polyurethane, Low-Temperature Curing for Cryogenic Usage	1
MB0120-026	Adhesive, Elevated Cryogenic Temperature-Resistant, -423 F to 500 F, Thixotropic Paste Type	1
MB0120-032	Adhesive, Primer, Pre-Cured Type, for Use From -423 F to 300 F	1, 2
MB0120-034	Adhesive, Modified Epoxy, Room Temperature Curing, for Usage From -423 F to 425 F	1
MB0120-042	Primer, Room-Temperature Curing, for Usage From -423 F to 120 F	1
MB0120-043	Coating, Elastomeric, Fluorocarbon, Room-Temperature Curing, for Cryogenic Application	1, 12
MB0120-047	Adhesive Primer, -423 F to 500 F Service	1
MB0120-048	Adhesive, Tape, Cryogenic and Heat-Resistant	1, 2
MB0125-006	Primer, Epoxy-Polyimide, Air-Drying	8
MB0125-036	Coating, Synthetic Elastomer Base, External Insulation	12, 13
MB0125-038	Primer, Silicone, Room-Temperature Curing	1
MB01250045	Coating, Polyurethane, for Foam Insulation	10,11,12,13
MB0125-046	Coating, Vinyl, Top Coat for Foam Insulation	10, 12
MB0125-047	Primer, Epoxy, Amine, Corrosion Preventive, Cryogenically Compatible	8, 9, 12
MB0130-019	Silicone Rubber, Low-Temperature Resistant, Room-Temperature Curing	1, 7
MB0130-034	Silicone Rubber, Paste, Room-Temperature Vulcanizing	7, 11
MB0130-069	Foam-In-Place Material, Low-Density, Rigid, Polyurethane, for Cryogenic Application	3, 4, 6
MB0130-077	Foam, Polyurethane, Flame-Retardant, Two-Pound Density, for Spray Application	4, 5, 6
MIL-A-24179	Adhesive, Flexible Unicellular - Plastic Thermal Insulation.	12

*Test designation:

1. Room Temperature Lap Shear
2. Room Temperature Honeycomb Peel
3. Room Temperature Compression
4. Room Temperature Tensile
5. Cryogenic Strain Compatibility
6. Density
7. Shore Hardness
8. Adhesion
9. Drying Time
10. Tack Free Time
11. Pot Life
12. Viscosity
13. Weight Per Gallon

15.3.2.5 Cure Cycle Monitoring

If automatic recording equipment is not employed, temperature and pressure are recorded at 15-minute intervals throughout the cure cycle.

15.3.2.6 Storage and Issuance of Production Adhesives

All production adhesives are withdrawn from a central mix crib. Catalyst addition and mixing are accomplished in the mix crib. Date, mix time, material, and pot life expiration are noted on the container and verified by Inspection.

15.3.2.7 Chemical Solution Control and Issuance

All chemical solutions judged hazardous to personnel and production hardware, such as acid etch and strippers, are controlled, mixed, and issued by the Product Support Laboratory.

16.0 DESIGN EFFECTIVENESS

This section provides a method of evaluating various insulation designs and selecting an optimum system. A trade table method is used. It should be noted that this technique was not used on S-II design but is proposed for use on future designs.

16.1 METHOD

Values are to be determined for the trade factors using the curves given in this subsection. Those values are to be inserted in the proper place in the trade table and added for a total value. An X inserted for any factor indicates an unacceptable condition. N/A indicates not applicable. The highest total value indicates the most desirable rating.

16.1.1 Trade Table Format

The trade table (Figure 16.1.1-1) will be the basis of the insulation system evaluation. Four major categories of trade factors are utilized: technical, producibility, operations, and cost/schedule.

16.1.2 Trade Factor Weighting

The rating is based on a system of 1000 points maximum for all factors. The major categories are weighted by assignment of points as follows:

1. Technical 300
2. Producibility 150
3. Operations 150
4. Cost/Schedule 400

The distribution of major category points to subordinate trade factors may be varied for special cases but are generally as follows:

1. Technical (300)

Performance	100
Reliability	50
Safety	50
State of the art	10
Weight/size	50
Qualification/verification	50
Impact on other systems	10
Growth potential	10
Anticipated problems	10

S-II DERIVATIVES -
SYSTEM EVALUATION
TRADE TABLE

DATE:

MAX RATINGS	TRADE FACTORS / CANDIDATES							
(300)	TECHNICAL							
(100)	PERFORMANCE							
(50)	RELIABILITY							
(50)	SAFETY							
(10)	STATE-OF-THE-ART							
(50)	WEIGHT/SIZE							
(10)	QUAL/CERIF TESTING							
(10)	IMPACT ON OTHER SYS							
(10)	GROWTH POTENTIAL							
(10)	ANTICIPATED PROBLEMS							
( )								
( )								
	SUB-TOTAL							
(150)	PRODUCIBILITY							
(70)	EASE OF MANUFACTURE							
(10)	FAB STATE-OF-THE-ART							
(40)	INSPECTION CAPABILITY							
(10)	FACILITIES IMPACT							
(10)	HARDWARE AVAILABILITY							
(10)	KITABILITY							
( )								
	SUB-TOTAL							
(150)	OPERATIONS							
(10)	GSE IMPACT							
(80)	MAINTAINABILITY							
(40)	C/O IMPACT							
(20)	LAUNCH FACILITIES IMPACT							
( )								
	SUB-TOTAL							
(400)	COST/SCHEDULE							
(150)	NON-RECURRING COSTS							
(150)	RECURRING COSTS							
( )								
(100)	SCHEDULE COMPATIBILITY							
	SUB-TOTAL							
(1000)	TOTAL SCORE							

Figure 16.1.1-1. Trade Table

2. Producibility (150)

Ease of manufacture	70
Fabrication state of art	10
Inspection capability	40
Facility impact	10
Hardware availability	15
Kitability	5

3. Operations (150)

GSE impact	10
Maintainability	80
Checkout impact	40
Launch facilities impact	20

4. Cost Schedule (400)

Nonrecurring costs	150
Recurring costs	150
Schedule compatibility	100

16.1.3 Trade Factor Value Determination

The rating curves for each factor are given in Figures 16.1.3-1 through 16.1.3-22.

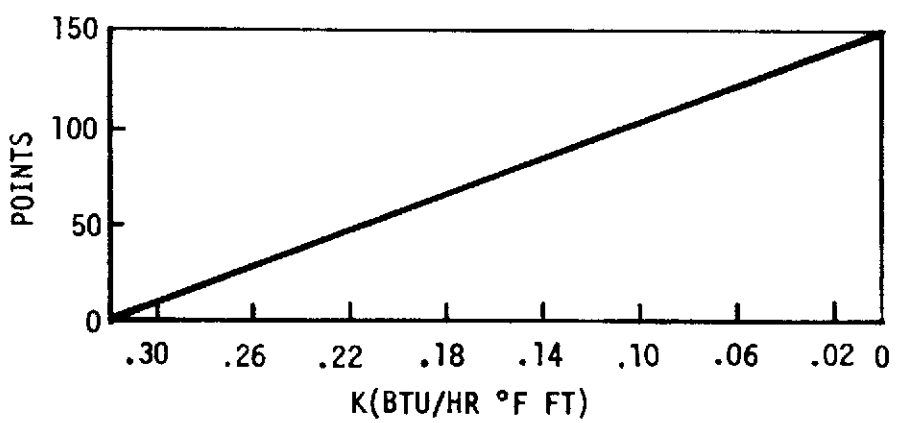

Figure 16.1.3-1. Performance Factor

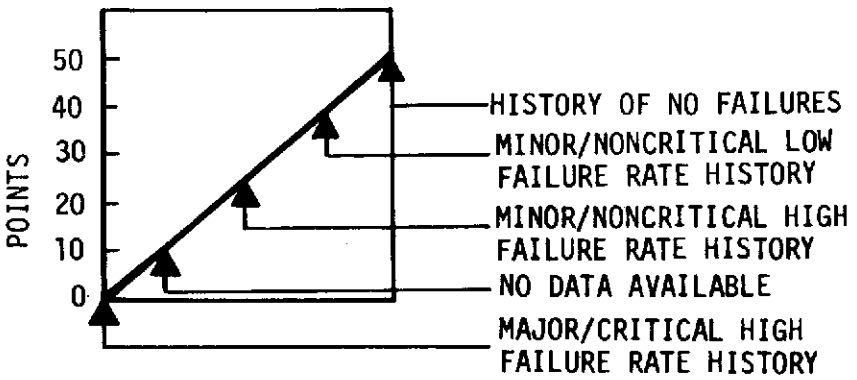

Figure 16.1.3-2. Reliability Factor

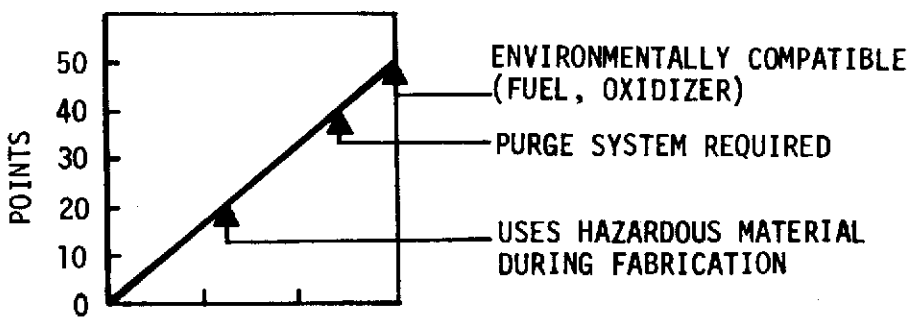

Figure 16.1.3-3. Safety Factor

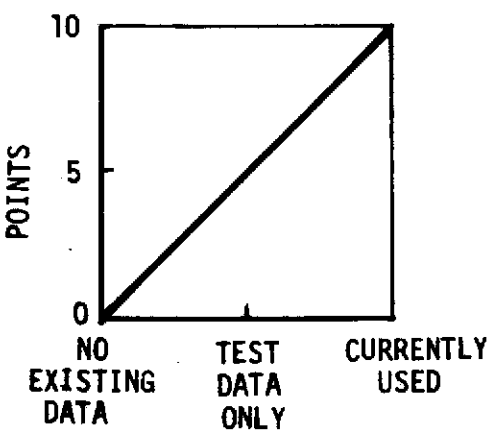

Figure 16.1.3-4. State-of-Art Factor

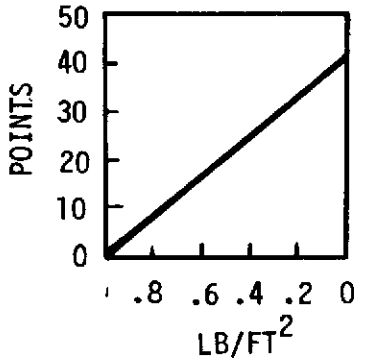

Figure 16.1.3-5. Weight/Size Factor

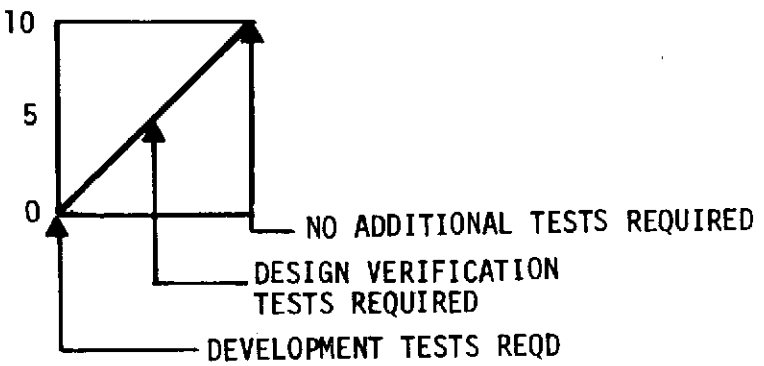

Figure 16.1.3-6. Qualification/Verification Testing Factor

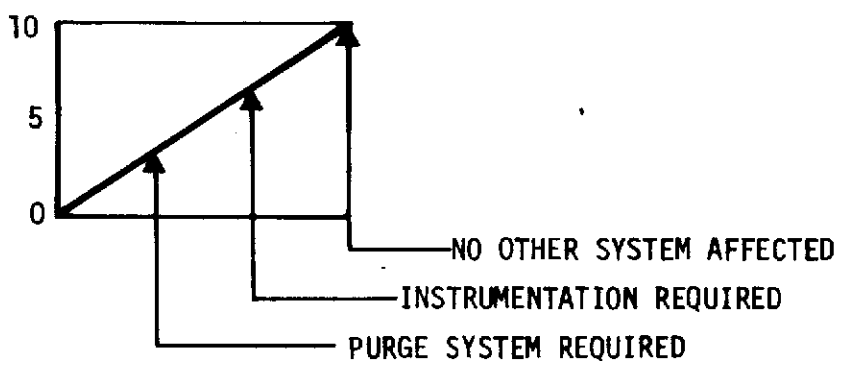

Figure 16.1.3-7. Impact on Other Systems Factor

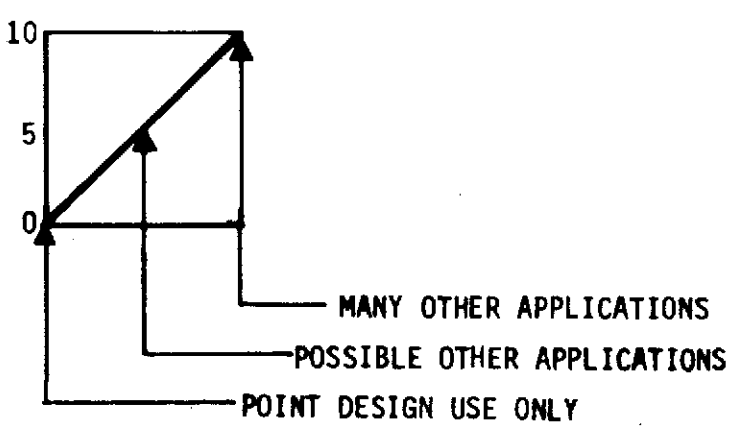

Figure 16.1.3-8. Growth Potential Factor

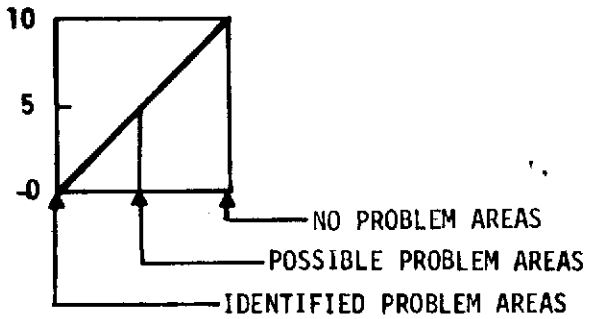

Figure 16.1.3-9. Anticipated Problems Factor

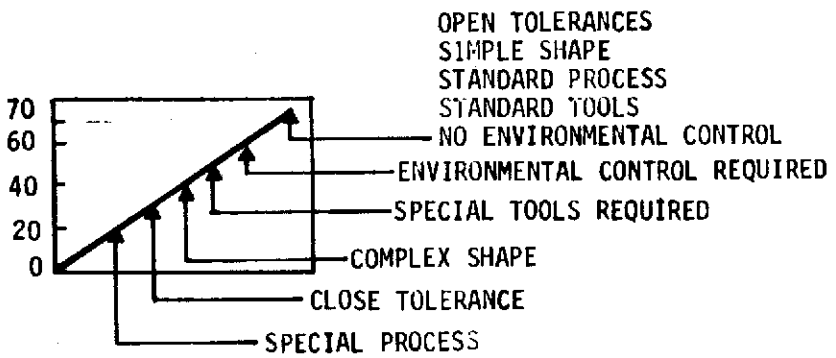

Figure 16.1.3-10. Ease of Manufacture Factor

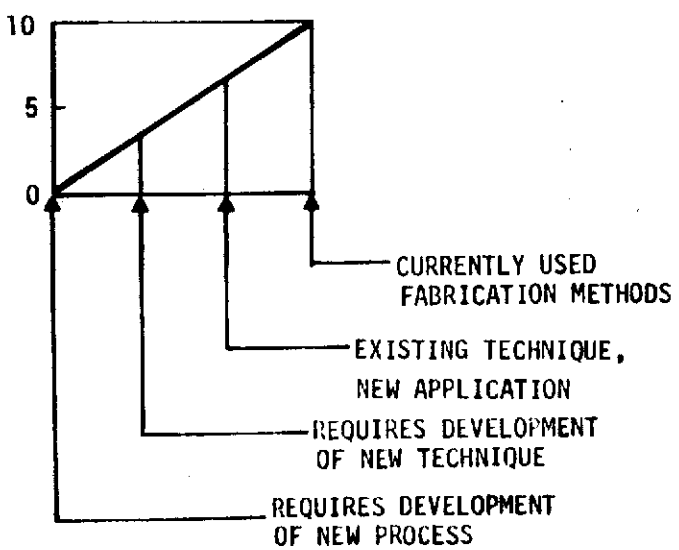

Figure 16.1.3-11. Fabrication State-of-Art Factor

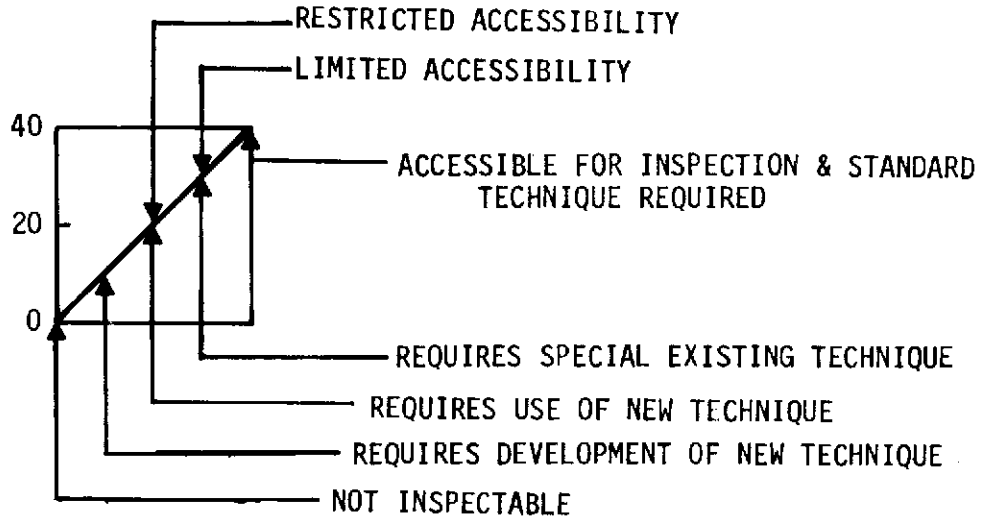

Figure 16.1.3-12. Inspection Capability Factor

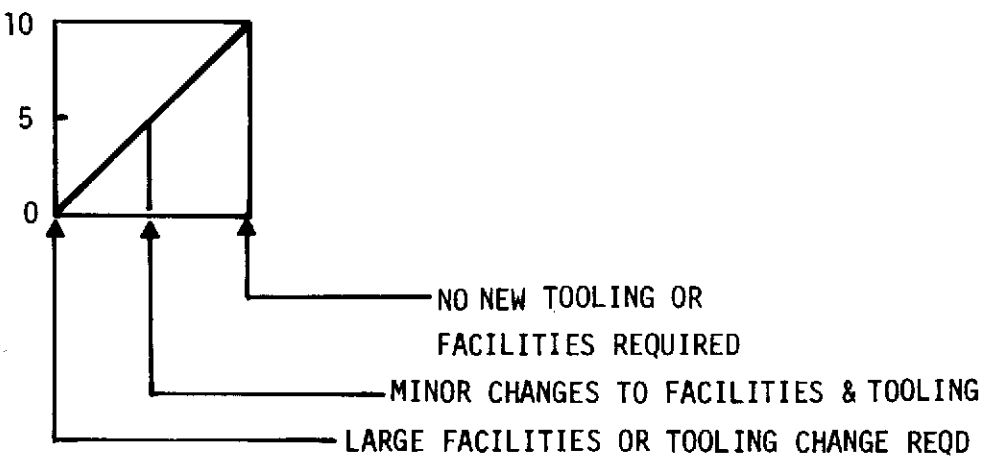

Figure 16.1.3-13. Facilities Impact Factor

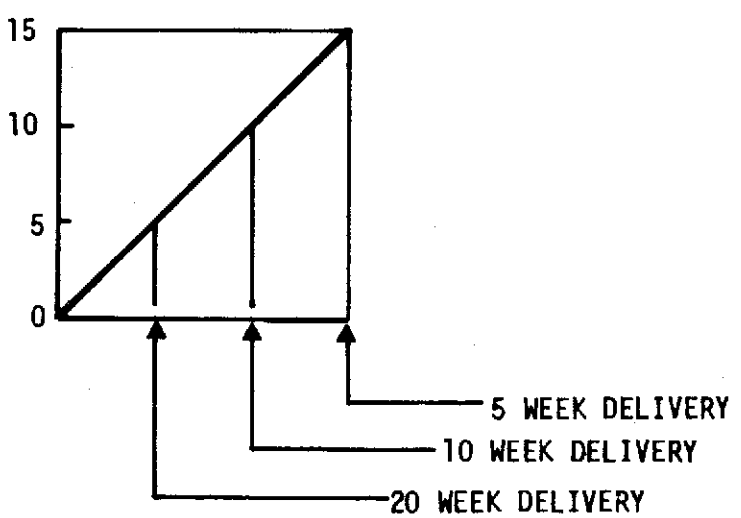

Figure 16.1.3-14. Hardware Availability Factor

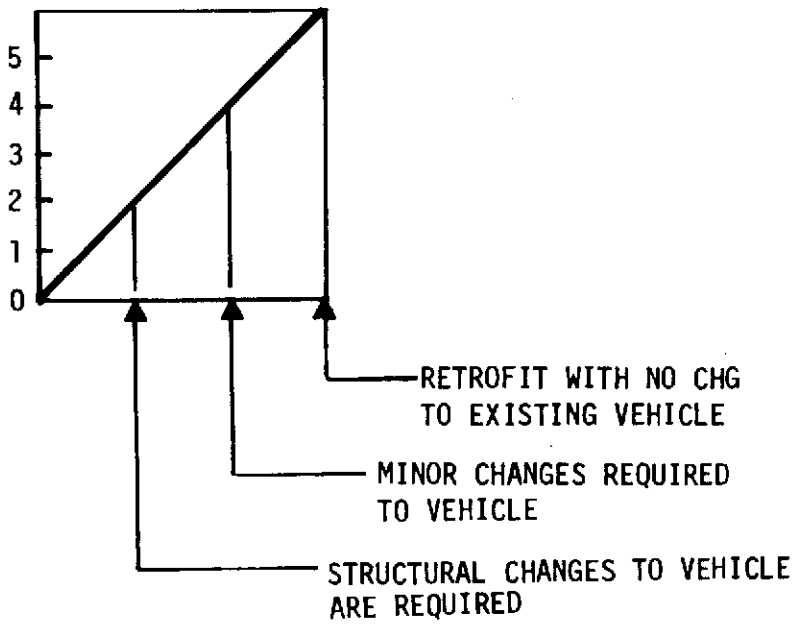

Figure 16.1.3-15. Kitability Factor

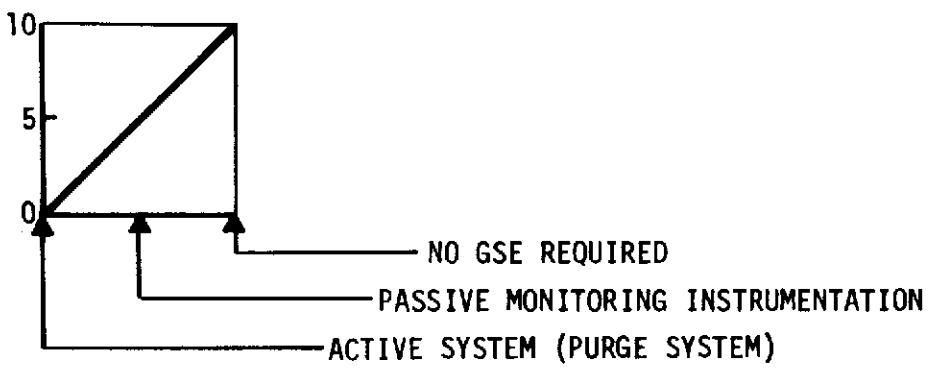

Figure 16.1.3-16. GSE Impact Factor

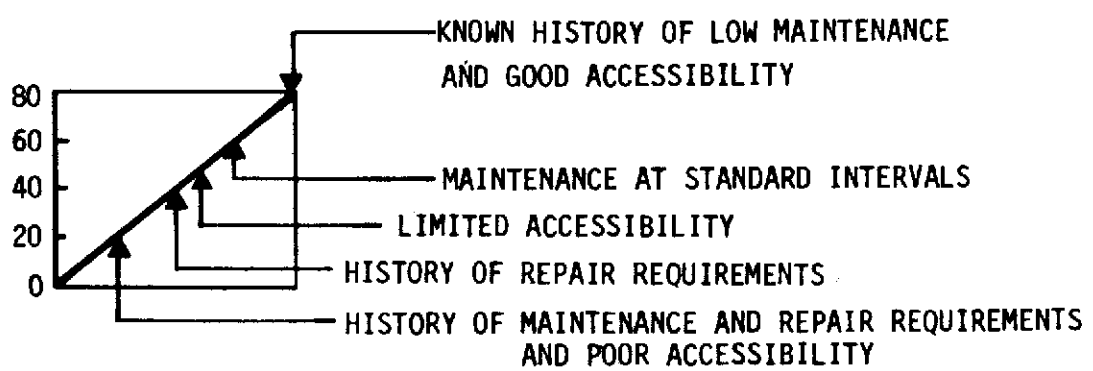

Figure 16.1.3-17. Maintainability Factor

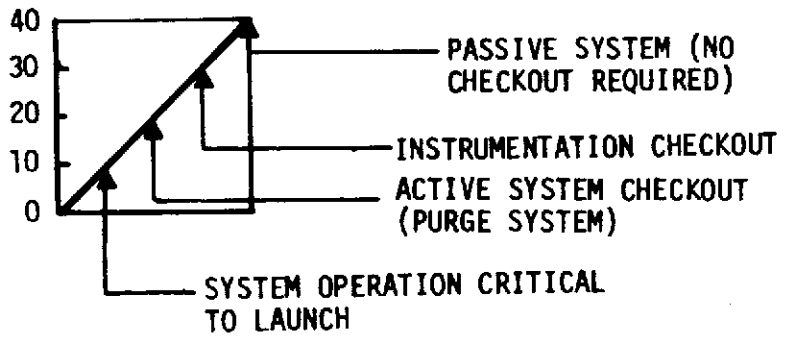

Figure 16.1.3-18. Checkout Impact Factor

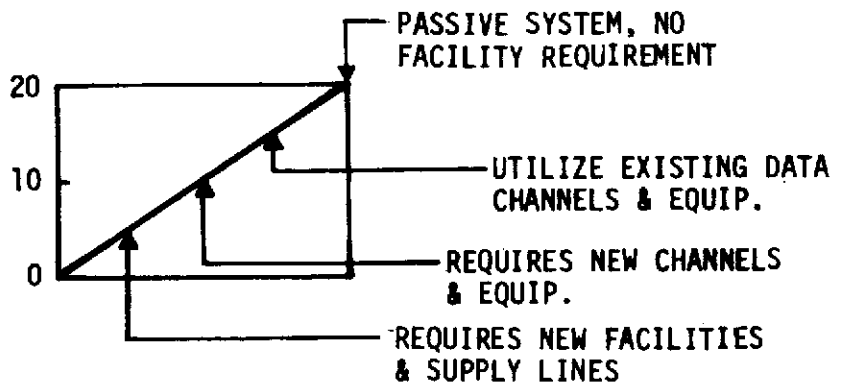

Figure 16.1.3-19. Launch Facility Impact Factor

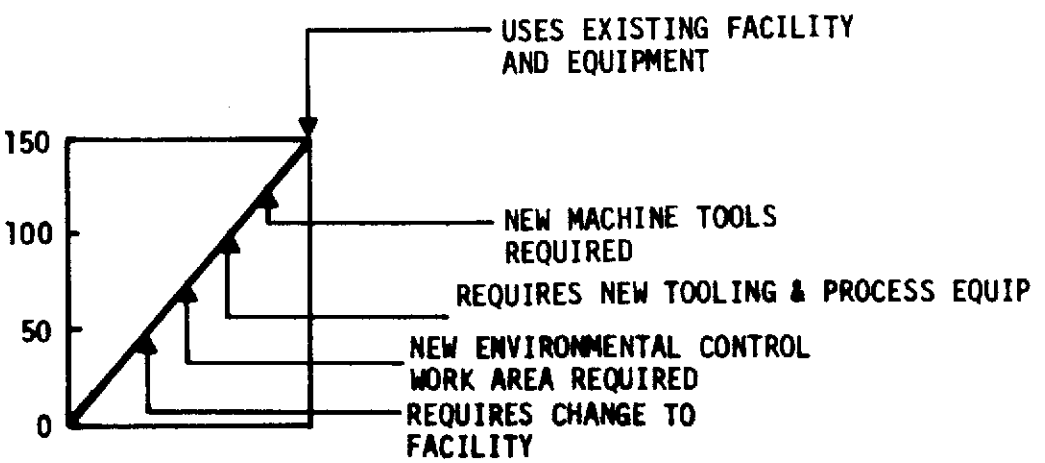

Figure 16.1.3-20. Nonrecurring Costs Factor

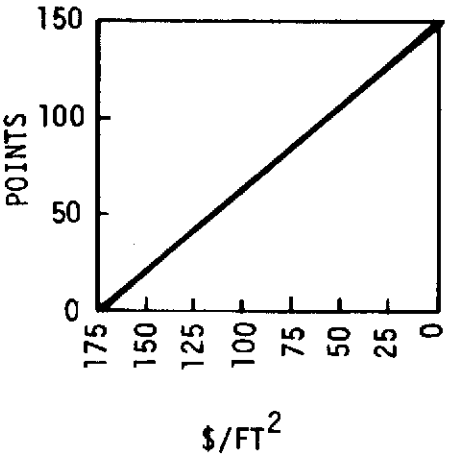

Figure 16.1.3-21. Recurring Costs Factor

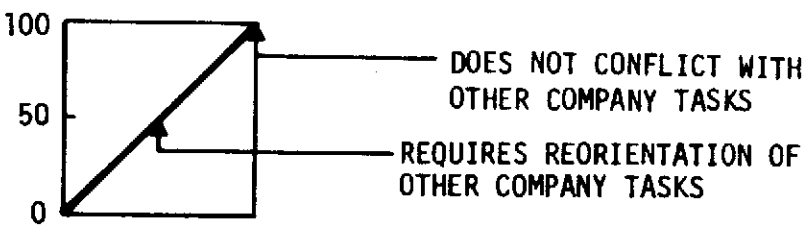

Figure 16.1.3-22. Schedule Compatibility Factor

16.2 SAMPLE EVALUATION

A sample evaluation of a honeycomb insulation system (see Paragraph 6.1.1) is presented in this section to illustrate the method of evaluation. The curves for each factor are given with the rating of the sample system overlaid on them (Figures 16.2-1 through 16.2-22). The rating from each factor are then entered on the trade table (Figure 16.2-23) and summed to yield an overall system rating.

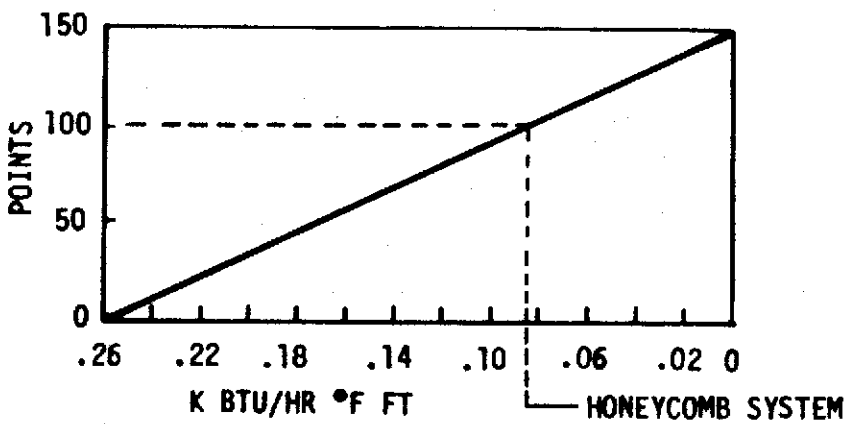

Figure 16.2-1. Performance Factor - Honeycomb System

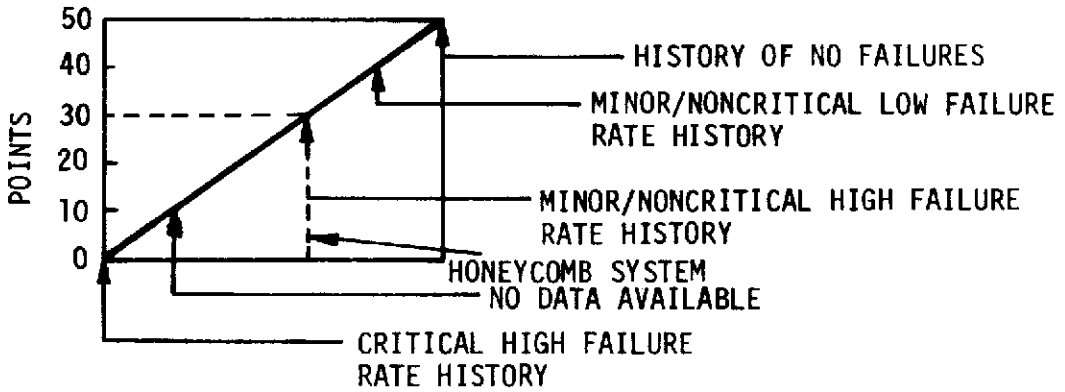

Figure 16.2-2. Reliability Factor - Honeycomb System

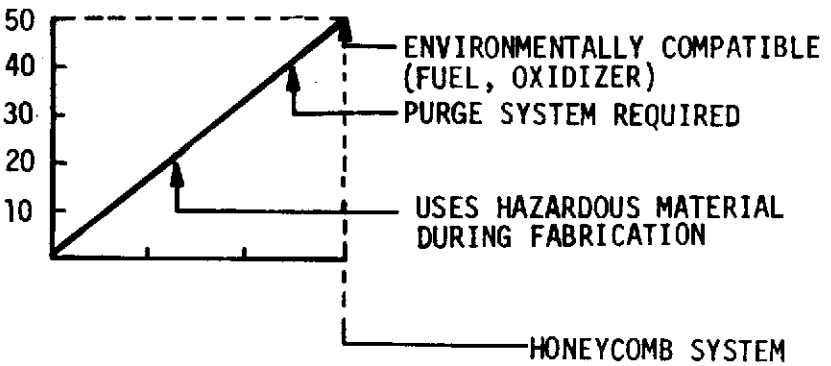

Figure 16.2-3. Safety Factor - Honeycomb System

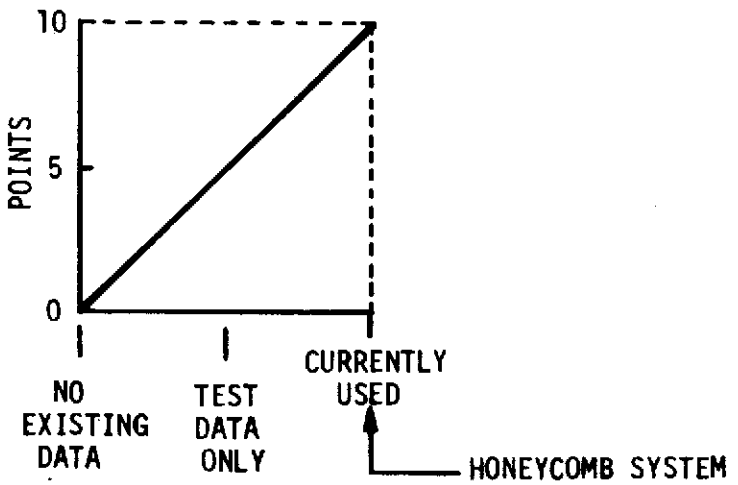

Figure 16.2-4. State-of-Art Factor - Honeycomb System

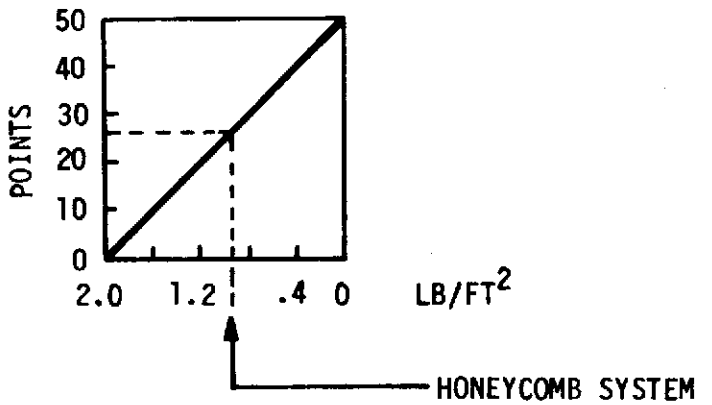

Figure 16.2-5. Weight/Size Factor - Honeycomb System

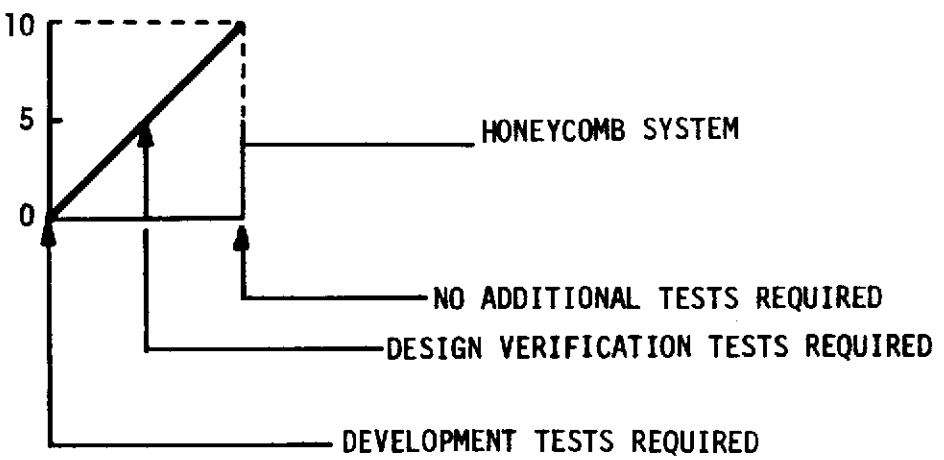

Figure 16.2-6. Qualification/Verification Testing - Honeycomb System

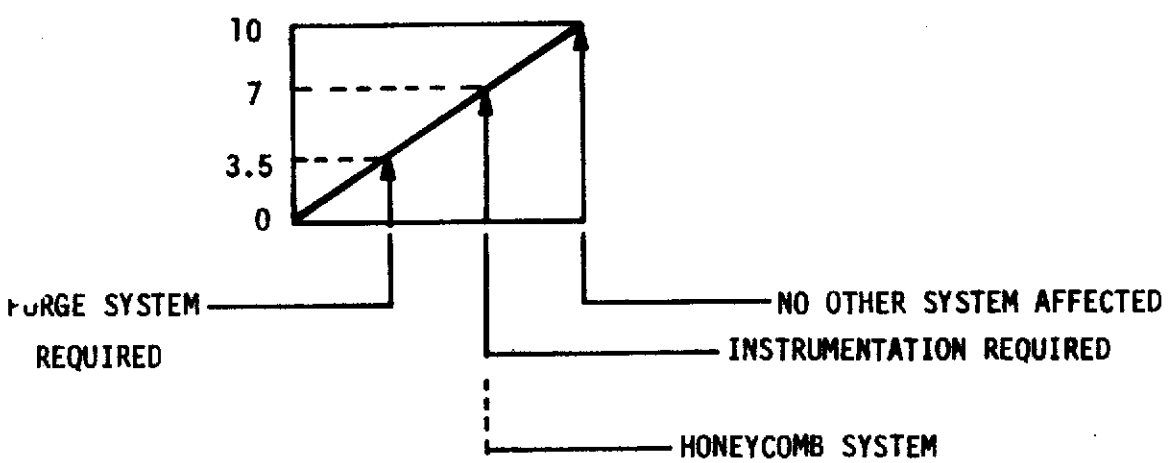

Figure 16.2-7. Impact on Other Systems Factor - Honeycomb System

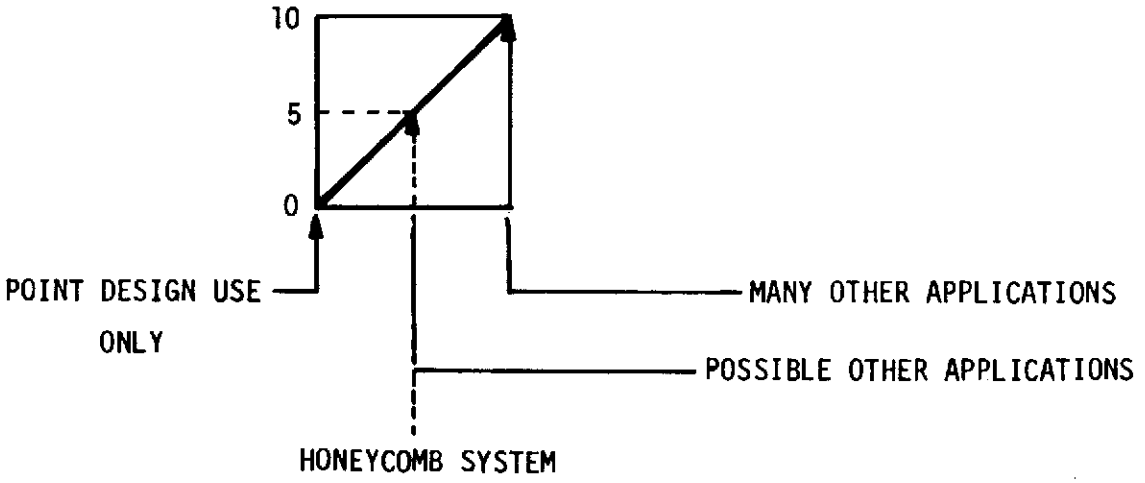

Figure 16.2-8. Growth Potential Factor - Honeycomb System

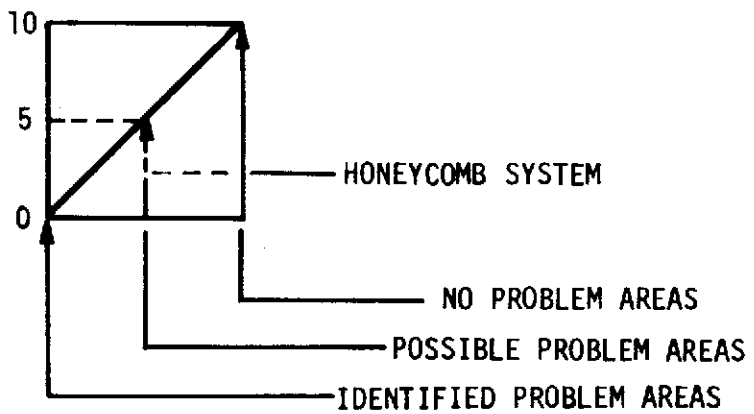

Figure 16.2-9. Anticipated Problems Factor - Honeycomb System

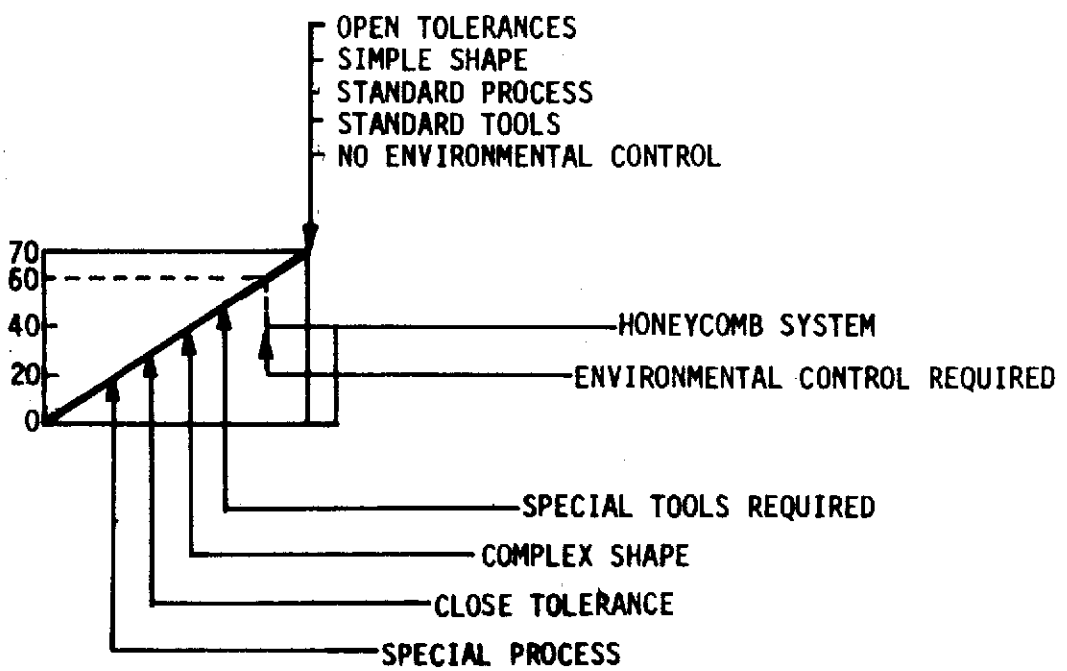

Figure 16.2-10. Ease of Manufacture Factor - Honeycomb System

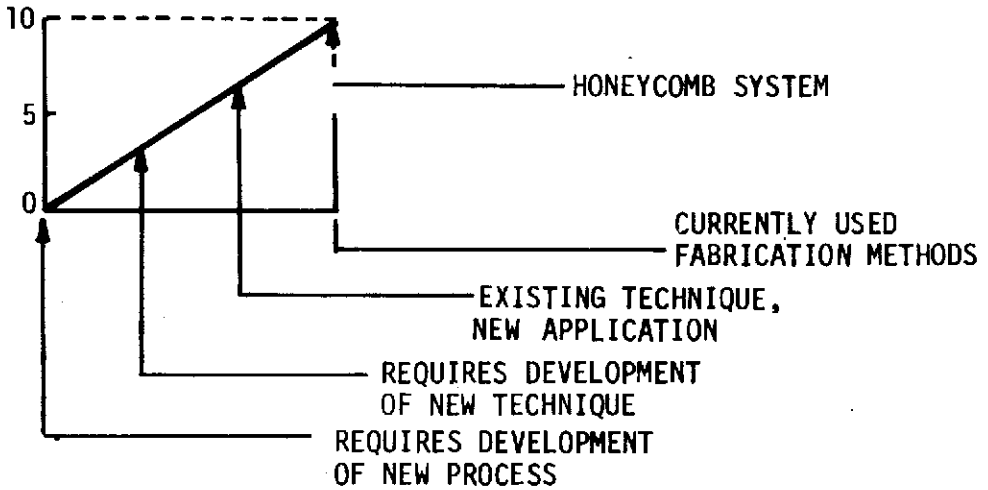

Figure 16.2-11. Fabrication State-of-Art Factor - Honeycomb System

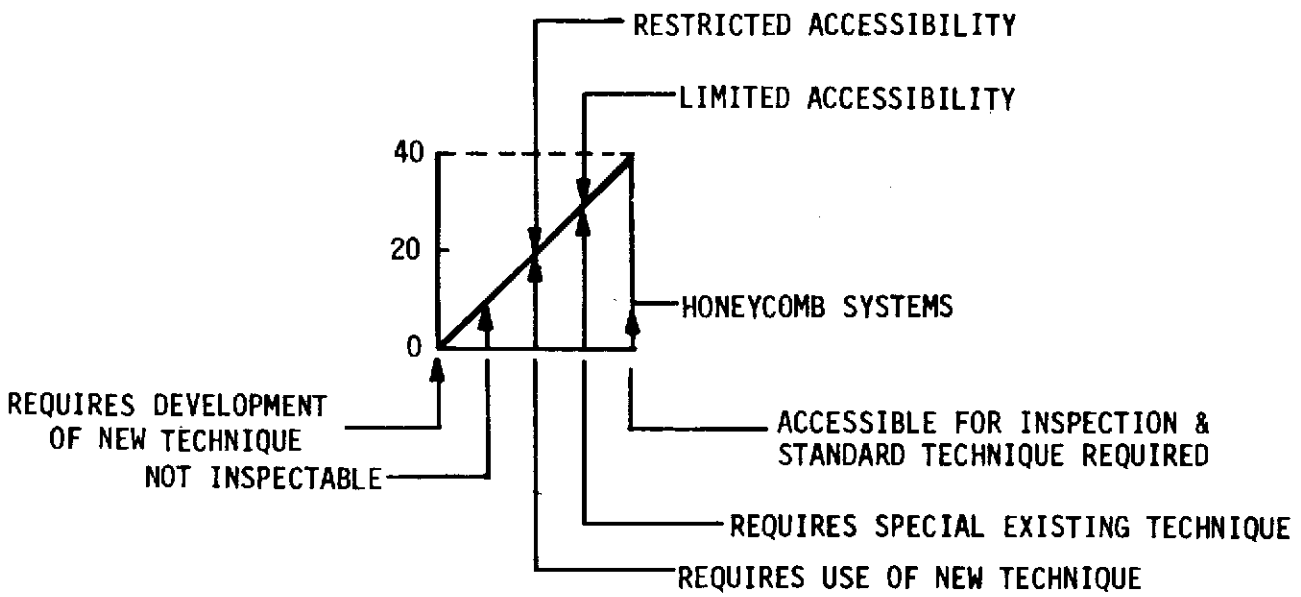

Figure 16.2-12. Inspection Capability Factor - Honeycomb System

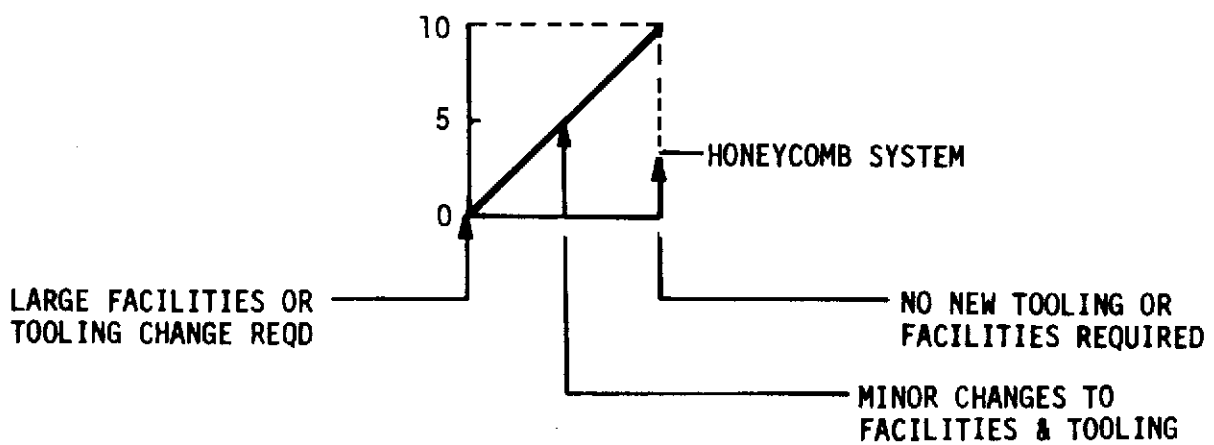

Figure 16.2-13. Facilities Impact Factor - Honeycomb System

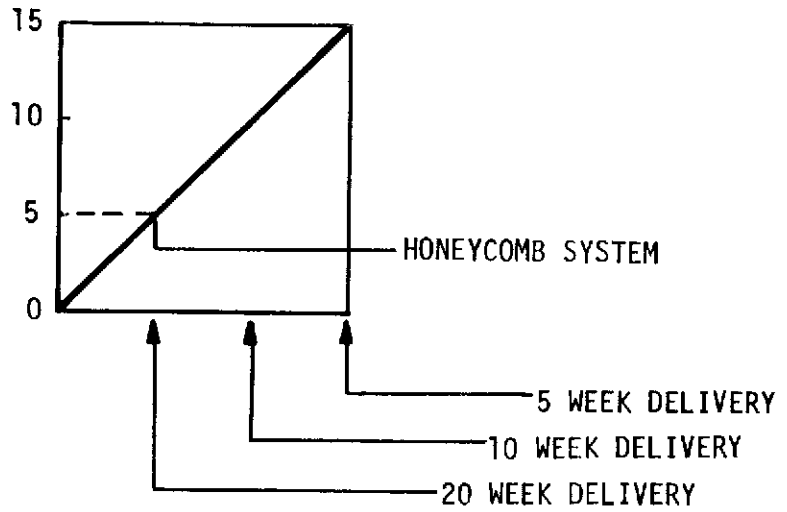

Figure 16.2-14. Hardware Availability Factor - Honeycomb System

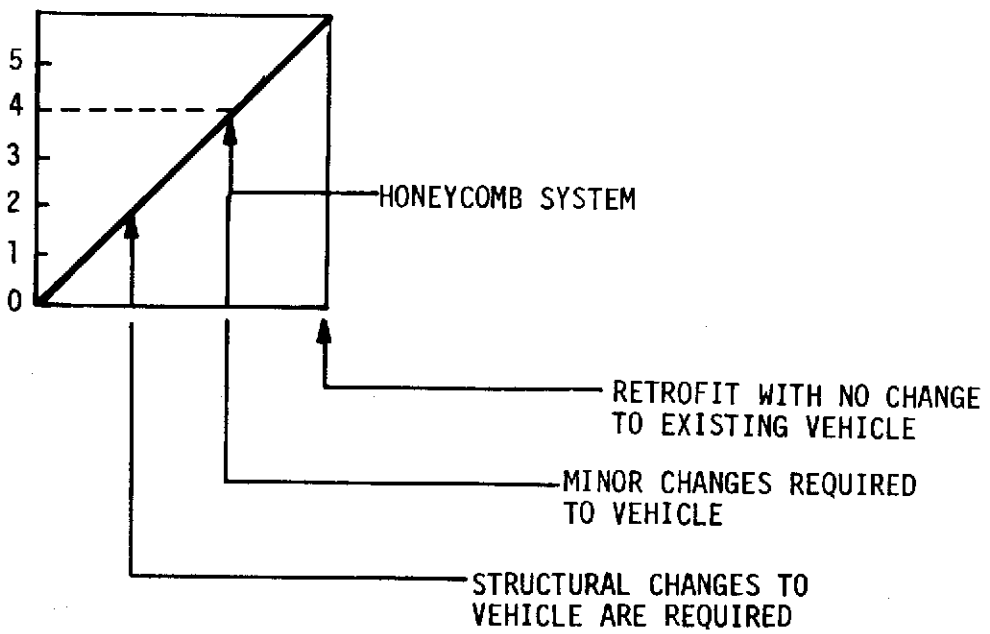

Figure 16.2-15. Kitability Factor - Honeycomb System

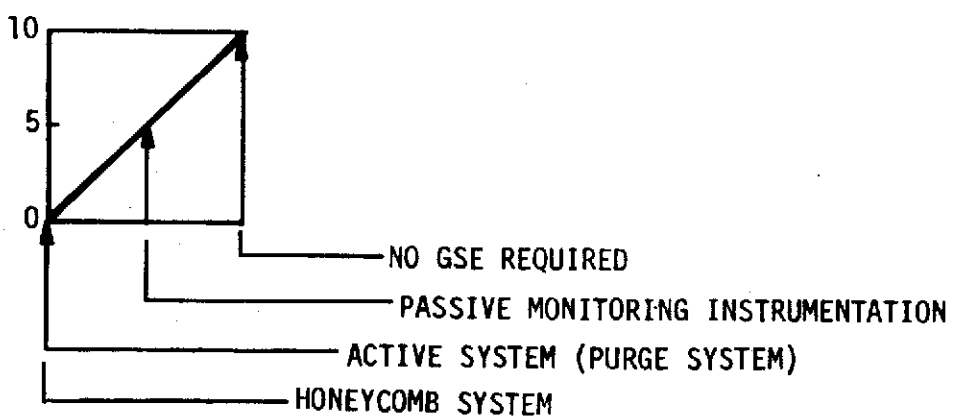

Figure 16.2-16. GSE Impact Factor - Honeycomb System

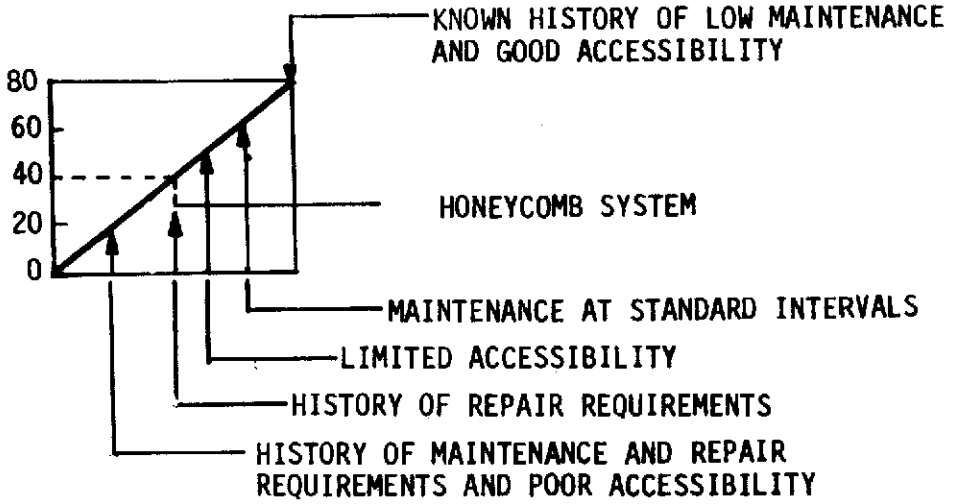

Figure 16.2-17. Maintainability Factor - Honeycomb System

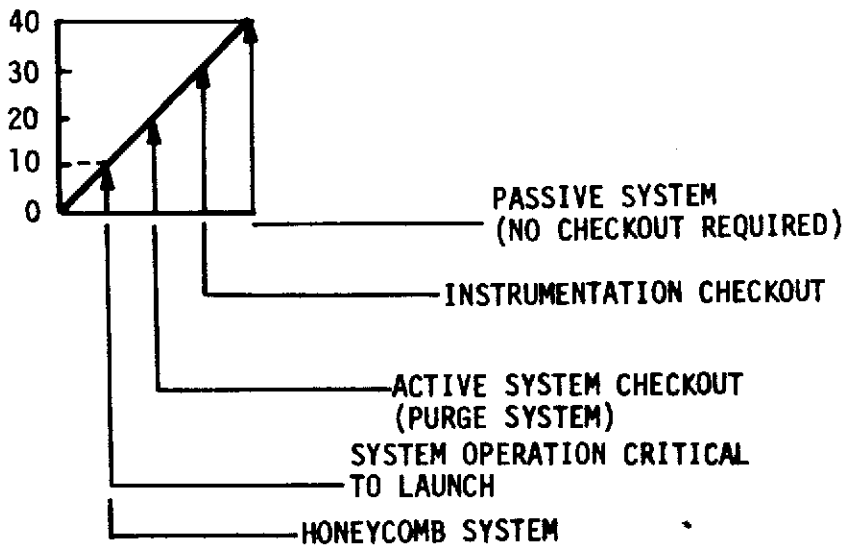

Figure 16.2-18. Checkout Impact Factor - Honeycomb System

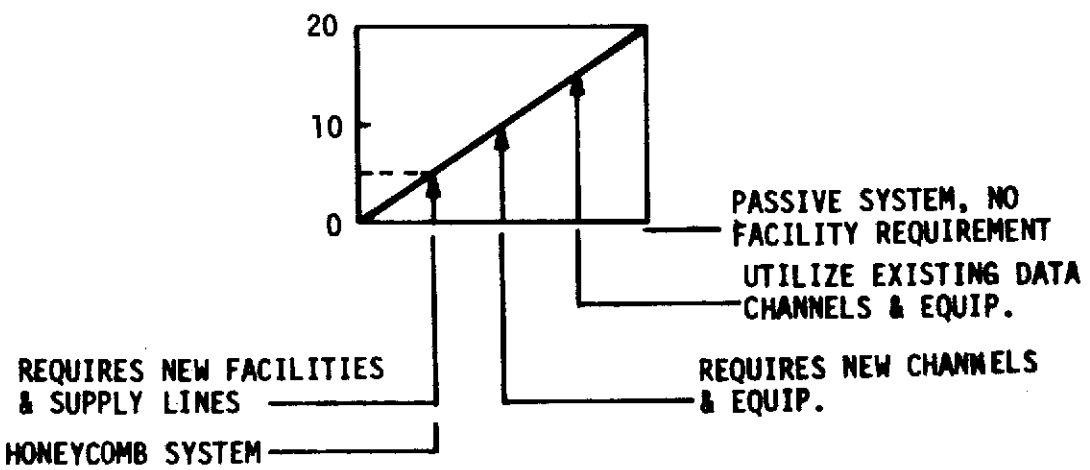

Figure 16.2-19. Launch Facility Impact Factor - Honeycomb System

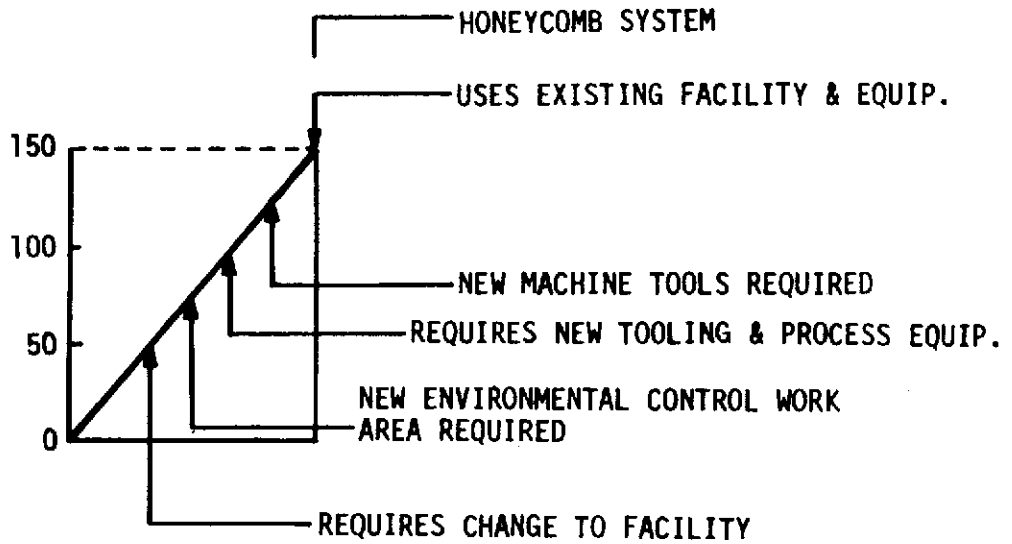

Figure 16.2-20. Nonrecurring Costs Factor - Honeycomb System

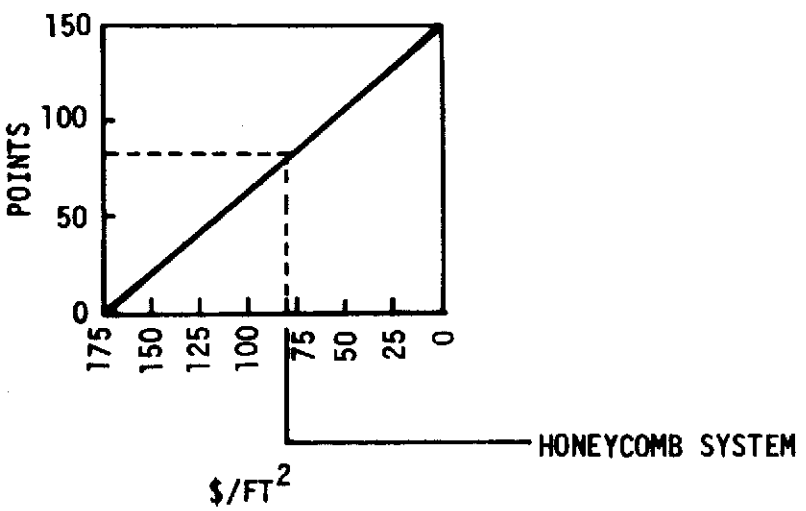

Figure 16.2-21. Recurring Costs Factor - Honeycomb System

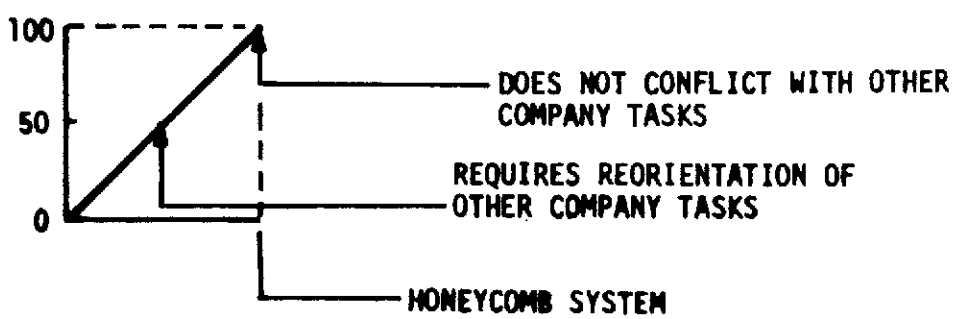

Figure 16.2-22. Schedule Compatibility Factor - Honeycomb System

S-II DERIVATIVES - SYSTEM EVALUATION TRADE TABLE

TITLE: HONEYCOMB INSULATION PARA. 6.1-1

DATE:

MAX RATINGS	TRADE FACTORS \ CANDIDATES	HONEYCOMB INSULATION 6.1.1						
(300)	TECHNICAL							
(100)	PERFORMANCE	100						
(50)	RELIABILITY	30						
(50)	SAFETY	50						
(10)	STATE-OF-THE-ART	10						
(50)	WEIGHT/SIZE	28						
(10)	QUAL/CERIF TESTING	10						
(10)	IMPACT ON OTHER SYS	7						
(10)	GROWTH POTENTIAL	5						
(10)	ANTICIPATED PROBLEMS	5						
( )								
( )								
	SUB-TOTAL	245						
(150)	PRODUCIBILITY							
(70)	EASE OF MANUFACTURE	60						
(10)	FAB STATE-OF-THE-ART	10						
(40)	INSPECTION CAPABILITY	40						
(10)	FACILITIES IMPACT	10						
(10)	HARDWARE AVAILABILITY	5						
(10)	KITABILITY	4						
( )								
	SUB-TOTAL	129						
(150)	OPERATIONS							
(10)	GSE IMPACT	0						
(80)	MAINTAINABILITY	40						
(40)	C/O IMPACT	10						
(20)	LAUNCH FACILITIES IMPACT	5						
( )								
	SUB-TOTAL	55						
(400)	COST/SCHEDULE							
(150)	NON-RECURRING COSTS	150						
(150)	RECURRING COSTS	80						
( )								
(100)	SCHEDULE COMPATIBILITY	100						
	SUB-TOTAL	330						
(1000)	TOTAL SCORE	759						

Figure 16.2-23. Sample Trade Table - Honeycomb System

APPENDIX. REFERENCES AND APPLICABLE DOCUMENTS

REFERENCES

1. Saturn V AS-511 Launch Vehicle Operational Flight Trajectory - April 16, 1972 Launch Window. The Boeing Co., D5-15551(F)-11A (Feb. 10, 1972).

2. Skylab I (SA-513) Launch Vehicle Reference Trajectory. MSFC S&E-AERO-MFT-59-71 (June 3, 1971).

3. Performance Characteristics of the INT-21 Launch Vehicle. Boeing OFA-H-760 (Oct. 20, 1970).

4. Saturn V Maximum Aerodynamic Heating Trajectory. Boeing D5-15250 (Feb. 5, 1965).

5. Saturn V/DWS Launch Vehicle Preliminary Trajectory and Dispersion Analysis. Boeing 5-9400-H-445 (March 11, 1970).

6. Terrestrial Environment (Climatic) Criteria, Guidelines for Use in Space Vehicle Development, 1969 Revision. NASA/MSFC Technical Memorandum Report No. 53872 (March 15, 1970).

7. U.S. Standard Atmosphere, 1962. Superintendent of Documents, U.S. Government Printing Office, Washington, D.C.

8. U.S. Standard Atmosphere Supplements, 1966. Superintendent of Documents, U.S. Government Printing Office, Washington, D.C.

9. A Reference Atmosphere for Patrick AFB, Florida, (1963 Revision). NASA TMX-53139.

10. Space and Planetary Environment Criteria Guidelines for Use in Space Vehicle Development, 1971 Revision. NASA/MSFC, NASA TMX 64677.

11. NASA Space Vehicle Design Criteria (Structures) - Acoustic Loads Generated by the Propulsion System. NASA SP-8072 (June 1971).

12. NASA Space Vehicle Design Criteria (Structures) - Compartment Venting. NASA SP-8060 (November 1970).

13. Saturn V Launch Vehicle Thermal Design Environment AS-513 (Update). 5-9410-H-262 (May 2, 1972).

14. NASA Space Vehicle Design Criteria (Structures) - Buffeting During Atmospheric Ascent. NASA SP-8001 (November 1970).

15. Launch Vehicle Final Thermal Design Environment SA-504, Revision B. Boeing D5-15513-2 (Dec. 9, 1968).

16. Lay, B. Jr., Earthbound Astronauts - The Builders of Apollo - Saturn. Prentice Hall (1971).

17. Terrestrial Environment (Climatic) Criteria, Guidelines for Use in Space Vehicle Development. NASA TMX-64589 (May 10, 1971).

18. Terrestrial Environment (Climatic) Criteria, Guidelines for Use in Space Vehicle Development, 1969 Revision. NASA TMX-53872.

19. Space Environment Criteria, Guidelines for Use in Space Vehicle Development, Second Edition. NASA TMX-53957 (Aug. 26, 1970).

20. Qualification of Helium Purge, Foam-Filled Insulation, 1.6-Inch, 0.8-Inch, and 0.5-Inch. NR Letter 65MA12261, Contract NAS7-200 (Oct. 18, 1965).

21. Elevated Temperature Test of LH_2 Tank Sidewall Insulation Closeouts. NR/NASA/MSFC Letter 66MA7240, Contract NAS-7200 (June 20, 1966).

22. Ignition Tests on 1.6-Inch Foam-Filled Insulation. NR/NASA/MSFC Letter 66MA10142, Contract NAS7-200 (Aug. 11, 1966).

23. NASA Letter R-AERO-F-191-67, from Assistant Chairman, Saturn V Flight Evaluation Working Group, R-AERO-F to Addresses, Minutes of AS-501 7 Day Flight Review Meeting (Nov. 22, 1967).

24. Qualification of Foam Block Insulation for Application on Saturn S-II LH_2 Tank Cylinder No. 1 and Bolting Ring. NR Letter 66MA10141, Contract NAS7-200.

25. Schaaf, S.A., and Chambre, P.L. "Flow of Rarefied Gases, Section H," Fundamentals of Gas Dynamics, Volume III, High-Speed Aerodynamics and Jet Propulsion. Princeton University (1958).

26. Hoerner, S.F., Fluid Dynamics Drag. (1965).

27. Schlichting, H., Boundary Layer Theory. McGraw-Hill (1960).

28. Wind-Induced Loads on a Dynamically Scaled Model of a Large Missile in Launching Position. NASA-Technical Mem. X-109.

29. "Space Radiation: A Compilation and Discussion." NASA TMX-53018 (March 5, 1964).

30. Atmospheric Electricity Criteria, Guidelines for Use in Space Vehicle Development. NASA TMX-64549 (Aug. 25, 1970).

31. "Spray Foam Insulation Test X-15, Final Report." NR Letter 69MA5502 to W.F. LaHatte from W.F. Ezell, Contract NAS7-200 (June 10, 1969).

32. Experimental Determination of the Effective Thermal Conductivity of Honeycomb-Foam Composite Insulation for LH_2 Tankage. Martin Co. report (Sept. 1963).

33. Handbook of Thermophysical Properties of Solid Materials. Wright Air Development Division Report (5 Volumes). MacMillan and Co.

34. A Compendium of the Properties of Materials at Low Temperatures. Wright Air Development Division, Report 60-56.

35. Kreith, F., Principles of Heat Transfer, Second Edition. Internation Textbook Co. (1965).

36. Buckling of Thin-Walled Cylinders. NASA SP-8007 (Rev. August 1968).

37. A Compendium of the Properties of Materials at Low Temperatures. NBS-CEL, WADD Technical Report 60-56, Part IV, Phase II.

38. Athey, R.J., DiPinto, J.G., and Keegan, J.M., "Adiprene L-100, A Liquid Urethane Elastomer," DuPont Bulletin 7, Table II (Oct. 1965).

39. Cuddihy, E.F., and Moacanin, J., Outgassing Rates in Polymeric Foams. JPL Space Programs Summary, No. 37-34, Vol. IV, pp. 137 - 142 (1965).

40. Carslaw, H.S., and Jaeger, J.C. Conduction of Heat in Solids. Oxford University Press, 2nd Edition, (1959) pp. 96-102, 309.

41. Holland, W.D. and J. Hulsebos, "Hydrogen Permeation Measurements on Vapor-Barrier Materials for Cryogenic Insulations," SAE Paper 746D, National Aeronautics and Space Engineering and Manufacturing Meeting, Los Angeles, California (Oct. 1963).

42. Adler, B.K., and R.B. Anderson, Transport Properties of Polar and Polymeric Gas Mixtures. North American Rockwell Corp. Space Division (NR/SD) SID 67-490 (June 1967).

43. Essenhigh, R.A., "On Radiative Heat Transfer in Solids," AIAA Paper 67-287, 2nd AIAA Thermophysics Specialists Conference, New Orleans, La. (April 1967).

44. Personal Communication, F. Stuckenberg to M.B. Hammond.

45. Barron, R., Cryogenic Systems. McGraw-Hill, New York (1966).

46. Tye, R.P., The Thermal Conductivity of Two Thermal Insulating Materials. Dynatech Report No. 798 (Ref. NAS-23) (July 22, 1968).

47. "Coating of Debris Barrier Fabric with Polyurethane for Saturn S-II Program," Letter 7572-4545 (23 March 1970).

48. Richardson, A.J., and V.S. Treppo, Sizing Single and Double Structure for Meteroid Protection. STR242 (June 1970).

49. Richardson, A.J., and L.P. Sanders, "Development of Dual Bumper Wall Constructure for Advanced Spacecraft," Journal of Spacecraft and Rockets, Vol. 9 No. 6 (June 1972), p 448.

50. Ballistic Limit of Double-Walled Meteroid Bumper Systems. NASA Technical Note TN D-3916 (April 1967).

51. Nazarova, T.N., Solid Component of Interplanetary Matter From Vehicle Observations. Space Science Reviews, Vol. 8, No. 3 (July 1968).

52. Zook, H.A., R.E. Flaherty, and D.J. Kessler, "Meteoroid Impact on the Gemini Windows," Planetary and Space Science, Vol.18 Pergamon Press, (1970) pp 953 to 964.

53. Stevenson, J.A., and J.C. Grafton, Radiation Heat Transfer Analysis for Space Vehicles. ASD TR61-119 Part I. (Dec. 1961).

NR REPORTS

1. SID 61-361, Model Specification.

2. SID 61-367, Applicable Specification and Deviations for Saturn S-II Stage and Ground Support Equipment.

3. SID 61-473-1, S-II Environmental Data for S-II Stage.

4. SID 62-137, Subsystem Report for Saturn S-II Thermal Control.

5. SID 62-138, Saturn Stage S-II Thermal Data, Volume I.

6. SID 62-141, Saturn S-II Engine Systems Report.

7. SID 63-498, S-II Aerodynamic Loads Data Manual II.

8. SID 63-600-7, Saturn S-II Materials and Processes Development (Last Half of 1966).

9. SID 63-600-8, Saturn S-II Materials and Processes Development During First Half of 1967.

10. SID 63-600-9, Saturn S-II Materials and Processes Development During Last Half of 1967.

11. SID 63-1042, S-II Performance Data Manual II.

12. SID 63-1397, CONFAC II - A General Computer Program for the Determination of Radiant-Interchange Configuration and Form Factors (January 1964).

13. SID STR123, General Equilibrium Equations for Three-Layered Shells of Revolution, A.P. Capelli, (March 1965).

14. SID STR 124, Axisymmetric Deformations of Three-Layered Shells of Revolution. A.P. Capelli, (March 1965).

15. SID 65-1043-1, A General Computer Program for the Determination of Radiant-Interchange Configuration and Form Factors - CONFAC I (October 1965).

16. SID 66-44, Saturn S-II Stage Common Bulkhead Test.

17. SID 66-138, Saturn Stage S-II Thermal Data, Volume I.

18. SID 66-361, Verification Testing of S-II Helium-Purged, 1.6-Inch Thick Insulation Panels.

19. SID 66-674, Structural Analysis of Saturn S-II Stage Insulation.

20. SID 66-1217, Structural Analysis of the Saturn S-II Stage Heat Shield.

21. SID 66-1465-7, Saturn V S-II Stage Test and Checkout Requirements, Specifications and Criteria for Use at KSC, S-II-7 and Subs.

22. SID 66-1468, Development of an Insulation System for the Thermal Protection of Exterior Surfaces of Saturn S-II Interstage and Aft Skirt (May 13, 1967).

23. SD-IL-67-32, Design Certification Report, Insulation Purge and Leak Detection System, Saturn S-II.

24. SD-IL-67-152, S-II Insulation Contingency Investigation - Summary Report.

25. SD 68-125 (B), Saturn S-II-3 Stage Design Certification Review Report Volume 5 (Revised 23 March 1968).

26. SID 68-394, Spray Foam Insulation Test with MDC (THOR) Tank 2 (31 July 1968).

27. SD 68-760, General Thermal Analyzer Program XF0014 (Dec. 1968).

28. SD 69-96, Structural Verification of Cork Over Spray Foam in Hot-Spot Areas of Saturn S-II Stage (July 15, 1970).

29. SD 69-98, S-II-4 Flight Final Test Report.

30. SD 69-734, Flight Performance Spray Foam Insulation for Application on Saturn S-II Stage.

31. SD 70-446, NARSAMS User's Manual.

32. SD 70-684, Saturn INT-21 Launch Vehicle Task 10 Insulation and System Development (March 31, 1971).

33. SD 70-687, Saturn INT-21 Launch Vehicle, Task 13, Thermal Control System Modification for Existing Avionics.

34. SD 71-245-4, S-II Stage Interorbital Shuttle Capability Analysis, Volume 4, (April 24, 1971).

35. SD 71-263, Saturn S-II Advanced Technology Studies, Study 3 Cryo-Storage Thermal Improvement (Feb. 15, 1972).

36. SD 72-SA-0027, Delta Test Effort to Complement S-II-13 Skylab Flex Curtain Tests - Final Report.

37. SD 72-SA-0042-3, Design and Systems Analysis of a Chemical Interorbital Shuttle, Volume III (May 1972).

NR SPECIFICATIONS

1. MA0105-049, Fabrication and Installation of Organic Edge Seals on Cryogenic Tankage Insulation.

2. MA0106-036, General-Purpose Mechanical Potting and Sealing Service -225 F to 600 F.

3. MA0106-045, Application of Adhesive Primer for Usage from -423 F to 300 F.

4. MA0106-065, Foaming of Multi-Component Rigid or Flexible Polyurethane Material.

5. MA0107-002, Resistance Welding.

6. MA0110-010, General Cleaning Methods.

7. MA0117-001, Handling of Dangerous and Flammable Liquids and Chemicals.

8. MA0201-1837, Purge Flow Characteristics and Checkout of Common Bulkhead Saturn S-II Stage.

9. MA0201-1930, Insulated LH_2 Tank Quarter Panel Leak Check and Proof Pressure.

10. MA0201-4264, LH_2 Tank, Forward Skirt Insulation, Forward Bulkhead Insulation, Check and Gross Leak Test S-II.

11. MA0201-4265, LH_2 Tank Sidewall Insulation, Proof Pressure Check, Gross Leak Test, Saturn S-II.

12. MA0201-4266, LH_2 Tank Lower Cylinder and Bolting Ring Insulation, Bubble Leak Test, Proof-Pressure Test, and Gross Leak Test; J-Ring Flow Check and Leak Tests for Saturn S-II Stages.

13. MA0308-1018, Assembly and Installation of the S-II Base Heat Shield.

14. MA0308-1033, Application of Maskant for Etching and Priming S-II LH_2 Tank Weld Closeouts.

15. MA0601-002, Installation of Threaded/Collared Fasteners for S-II.

16. MA0605-001, Fabrication of Multicore Sandwich Base Heat Shields for S-II.

17. MA0605-002, Fabrication of Base Heat Shield Flexible Curtains for Use on Saturn S-II.

18. MA0605-003, Fabrication of Nylon-Faced Insulation Details for S-II.

19. MA0605-006, Fabrication of Glass Phenolic Laminate Faced Honeycomb Panels and Details.

20. MA0605-014, Fabrication of Nylon-Reinforced Polyurethane Laminates for Sealing Applications - Saturn S-II Program.

21. MA0605-016, Fabrication and Application of LOX-Compatible Cryogenic Insulation System - Saturn S-II.

22. MA0605-017, Fabrication and Installation of LOX-Compatible Insulation for Cryogenic Surfaces.

23. MA0605-022, Fabrication of Temperature-Resistant Flexible Curtains - Saturn S-II.

24. MA0605-024, Procedures for Field Repair of the Temperature-Resistant Heat Shield Curtain, Saturn S-II.

25. MA0606-013, Adhesive Bonding on the Saturn S-II Common Bulkhead.

26. MA0606-027, Application of Cryogenic Insulation on Saturn S-II.

27. MA0606-033, Fabrication of S-II Bolting Ring Thermal Insulation.

28. MA0606-039, Installation of Inserts in Cryogenic Insulation - S-II.

29. MA0606-040, Repair Procedures for Foam-Filled and Helium-Purged Honeycomb Insulation.

30. MA0606-043, Foam-in-Place Insulation of LH_2 System Components - Saturn S-II.

31. MA0606-044, Installation of Saturn S-II Forward Skirt Insulation.

32. MA0606-048, Repair Procedures for the Rigid Panel of the Base Heat Shield.

33. MA0606-049, Emergency Repair Procedures for Sidewall Honeycomb Insulation.

34. MA0606-050, Spray Application of Two-Pound Density Polyurethane Foam Material.

35. MA0606-053, Appliation of Cork Insulation on Exterior Surfaces of Saturn-S-II Aft Skirt and Interstage.

36. MA0606-057, Repair Procedures for Saturn S-II Foam Insulation at Field Sites.

37. MA0606-061, Application of Cork Composite Sheet on Foam Insulation of Saturn S-II.

38. MA0608-015, Application of Coatings to Saturn S-II Foam Insulation.

39. MA0609-007, Corrosion Control of Aluminum Alloy Components of S-II Stage.

40. MA0610-002, Surface Preparation for Adhesive Bond and Application for Adhesive Bond and Application of Chem Films for Detail.

41. MA0610-022, Stripping Organic Coatings from Metals - Saturn S-II.

42. MA0610-023, Surface Preparation of Metals/Non-Metals for Adhesive Bonding - Saturn S-II.

43. MA0615-003, Leak Detection - Saturn S-II Bulkhead and Equipment.

44. MA0616-002, Intra/Interplant Parts Protection Requirements for Saturn S-II.

45. MB0115-003 Filler-Inorganic, Glass Microsphere Particles.

46. MB0120-008, Adhesive, Room-Temperature Curing, for Use From -250 F to 500 F.

47. MB0120-014, Adhesive, Elevated and Cryogenic Temperature - Resistant, Foaming Type, -423 F to 500 F.

48. MB0120-023, Adhesive, Modified Epoxy, Low-Temperature Curing for Cryogenic Usage.

49. MB0120-024, Resin, Polyurethane, Low-Temperature Curing for Cryogenic Usage.

50. MB0120-026, Adhesive, Elevated and Cryogenic Temperature Resistant, -423 F to 500 F, Thixotropic Paste Type.

51. MB0120-030, Adhesive, Paste, Foam Type, Elevated Temperature-Resistant, 300 F to 500 F.

52. MB0120-032, Adhesive, Primer, Pre-Cured Type, for Use From -423 F to 300 F.

53. MB0120-034, Adhesive, Modified Epoxy, Room-Temperature Curing, for Usage From -423 F to 425 F.

54. MB0120-042, Primer, Room-Temperature Curing, for Usage from -423 F to 120 F.

55. MB0120-043, Coating, Elastomeric, Fluorocarbon, Room-Temperature Curing, for Cryogenic Application.

56. MB0120-047, Adhesive Primer, -423 F to 500 F Service.

57. MB0120-048, Adhesive Tape, Cryogenic and Heat-Resistant.

58. MB0125-006, Primer, Epoxy-Polyamide, Air Drying.

59. MB0125-036, Coating, Synthetic Elastomer Base, External Insulation.

60. MB0125-038, Primer, Silicone, Room-Temperature Curing.

61. MB0125-045, Polyurethane Coating, for Foam Insulation.

62. MB0125-046, Coating, Vinyl, Top Coat for Foam Insulation.

63. MB0125-047, Primer, Epoxy, Amine, Corrosion Preventive, Cryogenically Compatible.

64. MB0130-004, Glass Fabric, Elevated Temperature Resistance, Phenolic Resin Impregnated.

65. MB0130-014, Core, Honeycomb, Glass Fabric, Heat-Resistant, Non-Vented and Vented.

66. MB0130-015, Low-Density Rigid Foam for Thermal Insulation.

67. MB0130-018, Core, Honeycomb, Vented, Glass Fabric.

68. MB0130-019, Silicone Rubber, Low-Temperature Resistant, Room-Temperature Curing.

69. MB0130-020, Resin Bonded Cork Insulation,

70. MB0130-023, Nylon Fabric, Phenolic Resin Pre-impregnated.

71. MB0130-024, Film, Plastic, Gas Permeability Barrier.

72. MB0130-034 Silicone Rubber, Paste, Room-Temperature Vulcanizing.

73. MB0130-058, Fabric - High-Temperature Glass Phenolic Resin Pre-Impregnated.

74. MB0130-069, Low-Density, Rigid Polyurethane, Foam-in-Place, Material for Cryogenic Insulation.

75. MB0130-077, Flame-Retardant Polyurethane Foam, Two-Pound Density, for Spray Application.

76. MB0135-008, Glass Fabric, Scrim Type.

77. MB0135-009, Fabric, Glass, Finished, for Plastic Laminates.

78. MB0135-012, Insulation, Thermal, Fibrous, High-Temperature.

79. MB0135-014, Fabric and Tape, High Silica Content (98 percent SiO_2).

80. MB0135-015, Reinforced Mat, High Silica, Woven Construction.

81. MB0135-018, Fabric, Glass, High-Temperature-Resistant.

82. MB0135-019, Thread-Glass, Temperature-Resistant.

83. MB0135-021, Fabric, Woven Nylon.

84. MB0135-022, Thread, Glass, Temperature-Resistant, Polytetrafluoroethylene Coated.

85. MB0135-028, Fabric, Amorphous Silica, Chromium Treated Polytetrafluoroethylene Coated.

86. MB0135-029, Thread, Quartz, Temperature-Resistant, Polytetrafluoroethylene Coated.

87. MB0135-030, Rope, Braided, High Silica.

88. MB0135-034, Film, Aluminized Polyester, Embossed.

89. MB0150-025, Sleeving, Electrical Insulating, Heat Shrinkable, Teflon.

90. MB0170-027, Core Material - Aluminum Honeycomb, 5052-H39.

91. CP621M0014A Contract End Item Detail Specification (Prime Equipment), Performance/Design and Product Configuration Requirements, V7-1 No. 7 and Subsequent for Saturn V Booster, Saturn/Apollo.

92. MC271-0010, Line Assembly, Engine Feed, Liquid Oxygen.

93. MC271-0011, Line Assembly, Engine Feed, Liquid Hydrogen.

94. MQ0501-010, Inspection, Ultrasonic.

95. MQ0501-034, PQV Test of Organic Material Used on S-II Vehicles/ Subassemblies.

96. MQ0501-035, Inspection, Acoustic Brush.

97. ST0105GA0001, Sleeving, Electrical Insulation, Heat Shrinkable, Installation of.

98. Pub. 543-G-35, -36, -37 and -38, Space Division Safety Standards.

99. Pub. 2546-N, NR Space Division Structures Manual (Oct. 1969).

NR DRAWINGS

1. V7-313102, Bulkhead - Common LOX Tank, Assy of.

2. V7-313106, Bulkhead - Common LOX Tank, Assy of.

3. V7-313128, Core - Common Bulkhead, LOX Tank, Assy of.

4. V7-315005, Installation - Insulation Thermal, X_B 196.0 Frame Structures.

5. V7-315007 Installation - External Thermal Insulation, Aft Skirt.

6. V7-530049, Seal Installation - Membrane, Forward Bulkhead, Forward Skirt.

7. V7-530401, Heat Shield Installation - Engine Base.

8. V7-531001, Installation - Insulation, Cylinder No. 1 and Bolting Ring, Complete.

9. V7-531104, Installations Internal Thermal Insulation, Interstage.

10. V7-531120, Insulation Installation - Field, Engine LOX Feed System (KSC-Hi Bay).

11. V7-531122 Debris Barrier Installation. Forward Bulkhead and Forward Skirt.

12. V7-531237, Insulation Installation - Polyurethane Foam, Forward Bulkhead.

13. V7-531240, Insulation Installation - Stage.

14. V7-531247, Insulation Installation - Stage Cork.

15. V7-531250, Insulation Installation - Spray-on Foam, Forward Skirt.

16. V7-531300, Insulation Installation - Lower Cylinder and Bolting Ring, Polyurethane Foam.

17. V7-531320, Installation, External Thermal Insulation, Interstage.

18. V7-531325, Installation, Insulation, LH_2 Feedline Flanges.

19. V7-531370, Preparation, Insulation, Installation, Cork and Anchor Blocks.

20. V7-532001, Insulation Installation - Complete Booster.

21. V7-532196, Insulation Installation - Forward Skirt.

22. V7-532400, Installation - Insulation, Cylinder No. 1 and Bolting Ring, Complete.

23. V7-540803 Container Assembly, Electric Power and Control Center Unit No. 207.

24. V7-953550, Installation, MLI, 105 Inch Diameter Tank.

25. V7-953551, Installation, Inner Purge System.

26. V7-953570, Process Plan - 105-Inch Diameter Tank.

27. V7-953595, Concept - Insulation, Multi-Layer, CIS.

28. V7-953596, Concept - Insulation, Multi-Layer, Drop Tank.

29. ICD 65 ICD 9001, Interface Control Document, Saturn - Skylab Space Vehicle Protuberances.

30. ICD 65 ICD 9000, Interface Control Document, Apollo-Saturn V Space Vehicle Protuberances.